Proceedings of a Symposium on

COMMERCIAL VEHICLE BRAKING and HANDLING

May 5-7, 1975

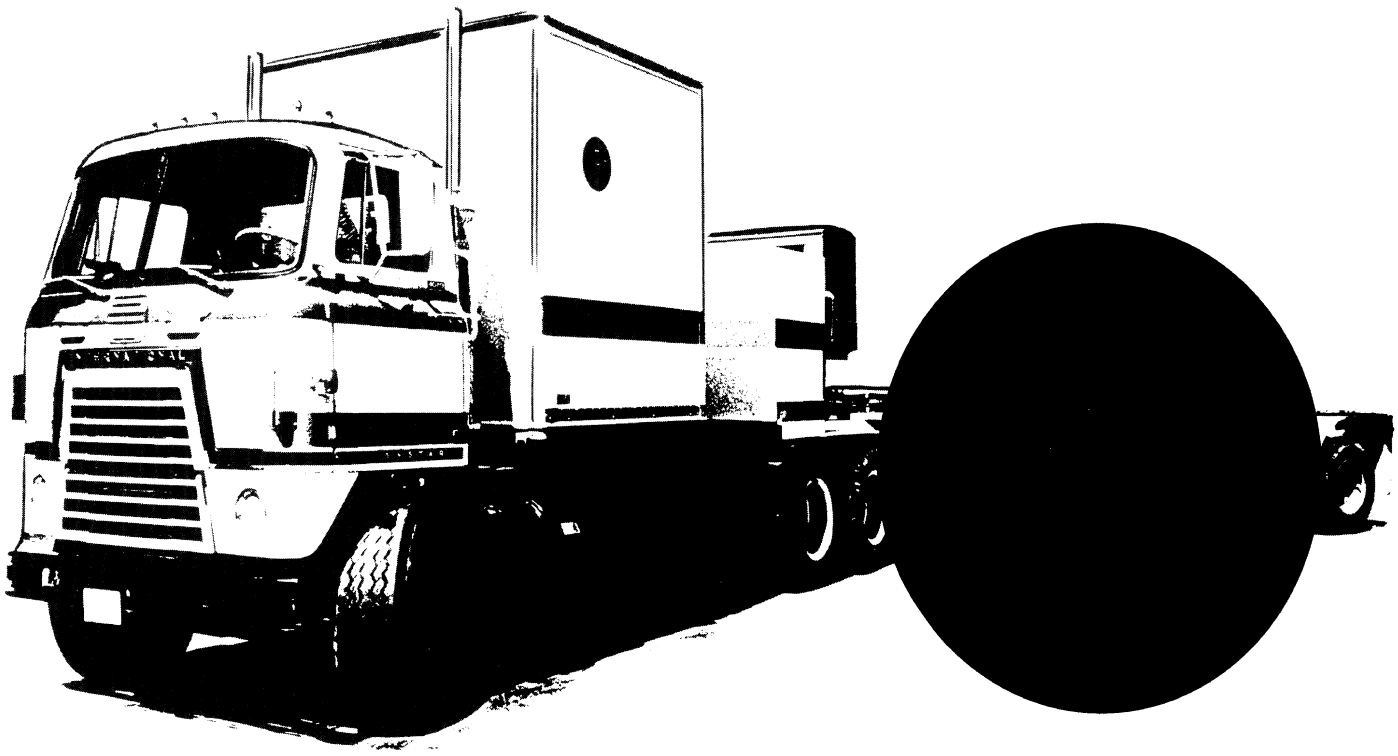

HIGHWAY SAFETY RESEARCH INSTITUTE THE UNIVERSITY OF MICHIGAN

UM-HSRI-PF-75-6

Proceedings of a Symposium on
COMMERCIAL VEHICLE BRAKING AND HANDLING

Sponsored by:

The University of Michigan
Highway Safety Research Institute

in cooperation with the
University of Michigan Extension Service

Chairmen:

Paul S. Fancher
James E. Bernard

Ann Arbor, Michigan
May 5-7, 1975

ACKNOWLEDGEMENTS

This symposium was made possible through the support of the Motor Vehicle Manufacturers Association.

The chairmen would like to express their thanks to those individuals who accepted our invitation to make a presentation at this symposium.

DISCLAIMER

The opinions and conclusions expressed or implied in these proceedings are those of the authors. They are not necessarily those of the Highway Safety Research Institute or The University of Michigan.

TABLE OF CONTENTS

TABLE OF CONTENTS (Cont.)

INTRODUCTION

This symposium on commercial vehicle braking and handling was sponsored by the Highway Safety Research Institute of The University of Michigan. The purpose of the symposium was to provide a review of the state of the art in commercial vehicle braking and handling. It was also designed to provide a forum in which members of various research organizations, industrial operations, and government agencies involved with the topic could communicate ideas and concerns over problems related to measuring and/or simulating the braking and directional response of commercial vehicles.

The symposium had four technical sessions, entitled "The Measurement of Commercial Vehicle Tire Properties," "Brake and Antilock System Performance," "Topics in Computer Simulation," and "An Overview of Simulation and Testing." The symposium closed with a panel discussion on "The Effects of Government Standards on Commercial Vehicle Braking and Handling."

These proceedings contain papers and formal remarks from those speakers who submitted a written version of their presentation. By prior agreement with the authors, these papers and remarks were not edited or changed without their permission. All art work and graphic material was supplied by the individual authors. Each author is responsible for the content and validity of his own work.

Neither the discussions following the papers nor the comments of the panel members were transcribed for inclusion in these proceedings.

The technical papers are presented herein in the order given in the program. After the technical papers the following items are presented:

(1) A copy of the luncheon speech by W. D. Eberle, President and Chief Executive Officer, Motor Vehicle Manufacturers Association

(2) Formal opening statements from several of the panelists

(3) A list of symposium attendees

(4) A copy of the program.

SYMPOSIUM ON COMMERCIAL VEHICLE BRAKING AND HANDLING

Technical Papers

May 5-7, 1975

TRUCK TIRE TESTING ON TIRF

K. D. Bird
and
D. J. Schuring
Calspan Corporation

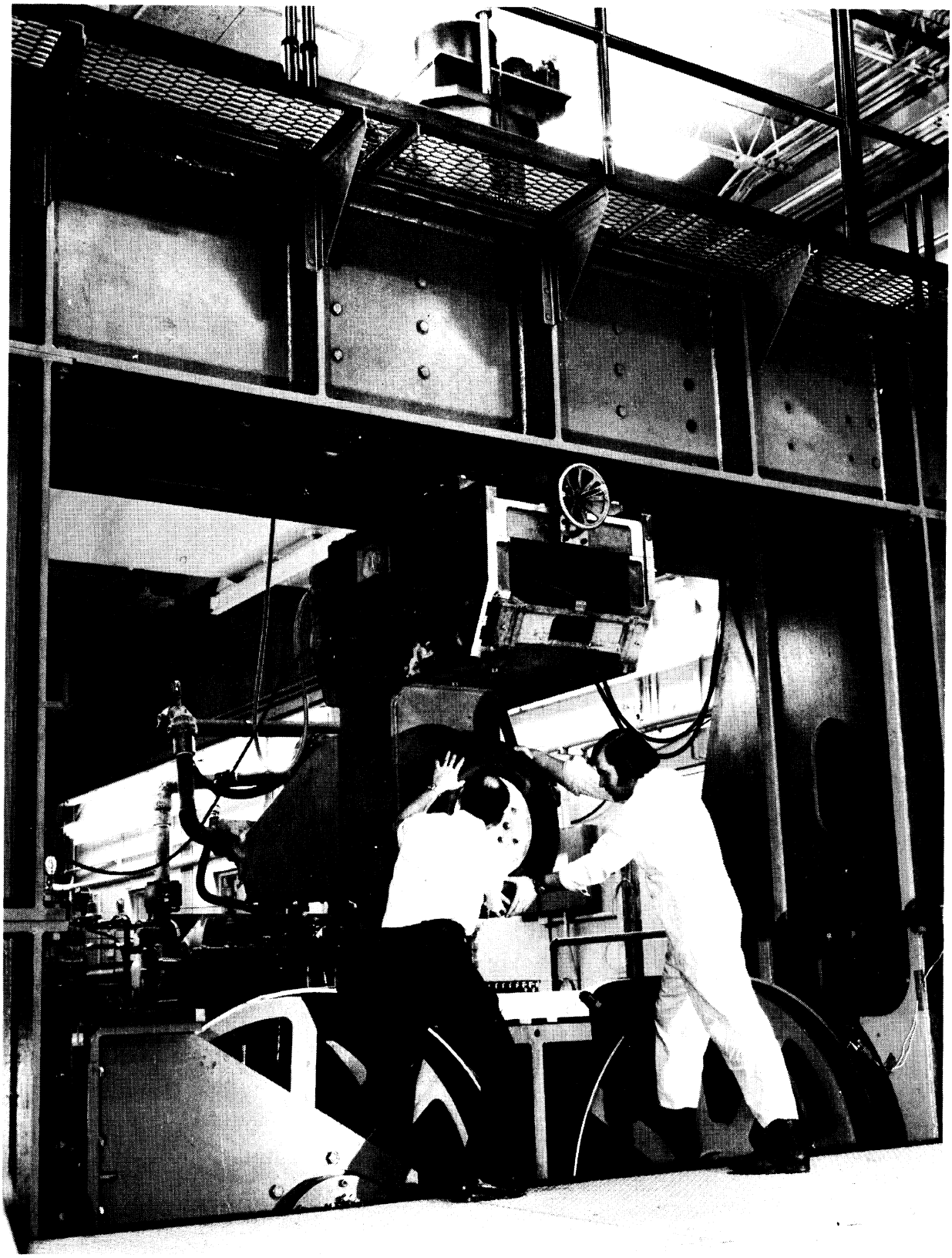

Calspan Tire Research Facility (TIRF)

INTRODUCTION

The prediction and understanding of the directional stability, control, and braking characteristics of commercial vehicles is no less dependent on a knowledge of the general tire tractive properties than it is for passenger cars. It is most appropriate then that the opening session of this conference be concerned with the measurement of commercial vehicle tire properties. This paper deals with that subject by presenting truck tire testing results from the Calspan Tire Research Facility which has come to be known as "TIRF." The overall operational features of TIRF are described in some detail in Reference 1 and will be indicated only very briefly here.

In their recent paper on the longitudinal traction properties of truck tires, Ervin and Fancher [2] have pointed out that very few devices are available for measuring the shear performance of truck tires and only a small number of studies dealing with such measurements have been reported. They point out the difficulties of constructing test facilities for measurement of shear forces and moment properties of truck tires—difficulties arising from the requirements for a large loading system and wheel support assembly and for an adequate multi-component force and moment balance system. We would add that the problems associated with handling loads up to 10,000 pounds or more carry through the construction, calibration, day-to-day operation and maintenance.

The Ervin-Fancher paper contains a review of the very sparse literature on truck tire test facilities; this will not be repeated here except to underscore the observation that in the United States the laboratory

facilities currently in existence which can perform even limited truck tire force and moment tests are confined to two very-low-speed flat plank machines (one with a 5,000-pound side force capability [3], the other with a 10,000-pound load capacity) and the Calspan TIRF whose capabilities are discussed herein.

Tielking, Fancher and Wild presented a cross-section of cornering data on a free-rolling tire on dry surfaces at low speed in Reference 4. At the SAE Troy Truck Meeting in 1974, Bickerstaff and Hartley [5] reported information on light truck tire traction (braking) properties taken from the Calspan TIRF and also from trailer tests and demonstrated the major influence of tire load on dry pavement longitudinal traction performance. In this paper, the TIRF truck tire testing capability beyond either pure cornering (no braking or driving torque application) or straight braking (zero slip angle) on dry roads will be illustrated by some results of combined cornering and braking tests on dry roads, by braking and cornering data measured on wet roads, and by some dual tire test results. It is hoped that these data will be useful in indicating the capability of the facility as well as in adding to the very sparse literature on the general shear performance of truck tires. The authors will indicate current limits of TIRF as regards truck tires and discuss prospects for elimination of some of these limits.

TEST FACILITY

A photograph of TIRF is shown in Figure 1 (frontispiece). The primary features of the machine are:

TIRE POSITIONING SYSTEM

The tire, wheel, force sensing balance, friction brake, and hydraulic motor (to drive or brake the tire) are mounted in the movable upper head. The head provides steer, camber, and vertical motions to the tire. These motions (as well as vertical loading) are servo controlled and programmable. The ranges of the position variables, the rates at which they may be adjusted, and other information are shown in Table I.

Table I

TIRF CAPABILITIES

CHARACTERISTIC	RANGE
TIRE SLIP ANGLE (α)	$\pm 30^{o}$
TIRE CAMBER ANGLE (γ)	$\pm 30^{o}$
TIRE SLIP ANGLE RATE ($\dot{\alpha}$)	10^{o}/SEC
TIRE CAMBER ANGLE RATE ($\dot{\gamma}$)	7^{o}/SEC
TIRE LOAD RATE ($\dot{F}_z$) (TYPICAL)	2000 LB/SEC
TIRE VERTICAL POSITIONING ($\dot{Z}$)	2 IN/SEC
ROAD SPEED (V)	0-200 MPH
TIRE OUTSIDE DIAMETER	18.5 IN TO 46 IN
TIRE TREAD WIDTH	24 IN MAX.
BELT WIDTH	28 IN

ROADWAY

The 28-inch wide roadway is made up of a stainless steel belt covered with material that simulates the surface texture and frictional properties of actual road surfaces. The belt is maintained flat to within 1 to 2 mils under the tire patch by the restraint provided by an air bearing pad which is beneath the belt in the tire patch region. The roadway is driven by one of the two 67-inch diameter drums over which it runs. The road speed is servo controlled; it may be programmed to be constant or varied.

The surfaces usually used are "Safety Walk."* These surfaces have excellent microtexture giving a wet skid number+ of about 60 in the untreated condition. The surfaces are honed to reduce the wet skid number to lower values (typically surfaces of skid number 50 and 30 are used).

A unique feature of TIRF is the ability to carry out tests under wet road conditions. A two-dimensional water nozzle spans the roadway. This nozzle has an adjustable throat which can be set to the desired water depth. The flow through the nozzle is then varied by controlling the water pressure. At each test condition the water film is laid on tangential to the belt at belt velocity. The film thickness may be varied from as low as 0.005 inches up to 0.5 inches.

---

*Manufactured by the 3M Company

+At 40 mph and 0.020 inches water depth using the ASTM E-501 Standard Pavement Traction Tire.

TIRE-WHEEL DRIVE

A drive system which is independent of the roadway drive is attached to the tire-wheel shaft. This separate drive allows variation of tire slip both in the braking and driving modes. The tire slip ratio, referenced to road speed, is under servo control.

BALANCE SYSTEM

Either of two six-component strain gage balances surrounding the wheel drive shaft may be used. Three orthogonal forces and three corresponding moments are measured through this system. A fourth moment, torque, is sensed by a torque link in the wheel drive shaft. The load ranges of the basic passenger car and truck tire balances are shown in Table II. Transfer of forces and moments from the balance axis-system to the conventional SAE reference system at the tire-roadway interface is implemented in the data reduction computer program.

Table II

BALANCE SYSTEM CAPABILITIES

COMPONENT	PASSENGER CAR TIRE BALANCE	TRUCK TIRE BALANCE
LOAD	4000 LB	12,000 LB
LONGITUDINAL FORCE	± 4000 LB	± 8000 LB
LATERAL FORCE	±4000 LB	±8000 LB
SELF ALIGNING TORQUE	±500 FT LB	±1000 FT LB
OVERTURNING MOMENT	±1000 FT LB	±2000 FT LB
ROLLING RESISTANCE MOMENT	±200 FT LB	±400 FT LB

FACILITY VALIDATION

It has generally become accepted by industry and government that passenger car tire data taken on TIRF are valid, in the sense that forces, moments, power losses measured on the facility, are the same as would be experienced on the road under similar conditions. In 1973, a round-robin validation program was sponsored by the Motor Vehicle Manufacturers Association and the Rubber Manufacturers Association in which identical bias-belted and radial-ply tires were run at various test conditions on the Calspan TIRF and eight other car and tire industry facilities. Three of these facilities were road testers (trailers or truck bed), two were circular drums (external) and three (in addition to TIRF) were flat-bed laboratory machines. Typical results are shown in Figure 2.

It may be seen that the road test data show significant spread, with the TIRF data falling near the center of this spread. The single drum data (120 in diameter) are in good agreement as are most of the flat-bed data. One set of the outlying data from a flat-bed plank machine was found to be too low due to insufficient rolling length to obviate tire relaxation effects; when the rolling distance was extended, agreement was improved. The remaining outlier data are also from a plank machine—shorter than the first—so these data are also suspect. Taking these factors into account, plus the acquisition of an extensive body of test data over the past two years, the TIRF passenger car tire results have come to be accepted as representing the actual forces and moments produced under steady-state operating conditions.

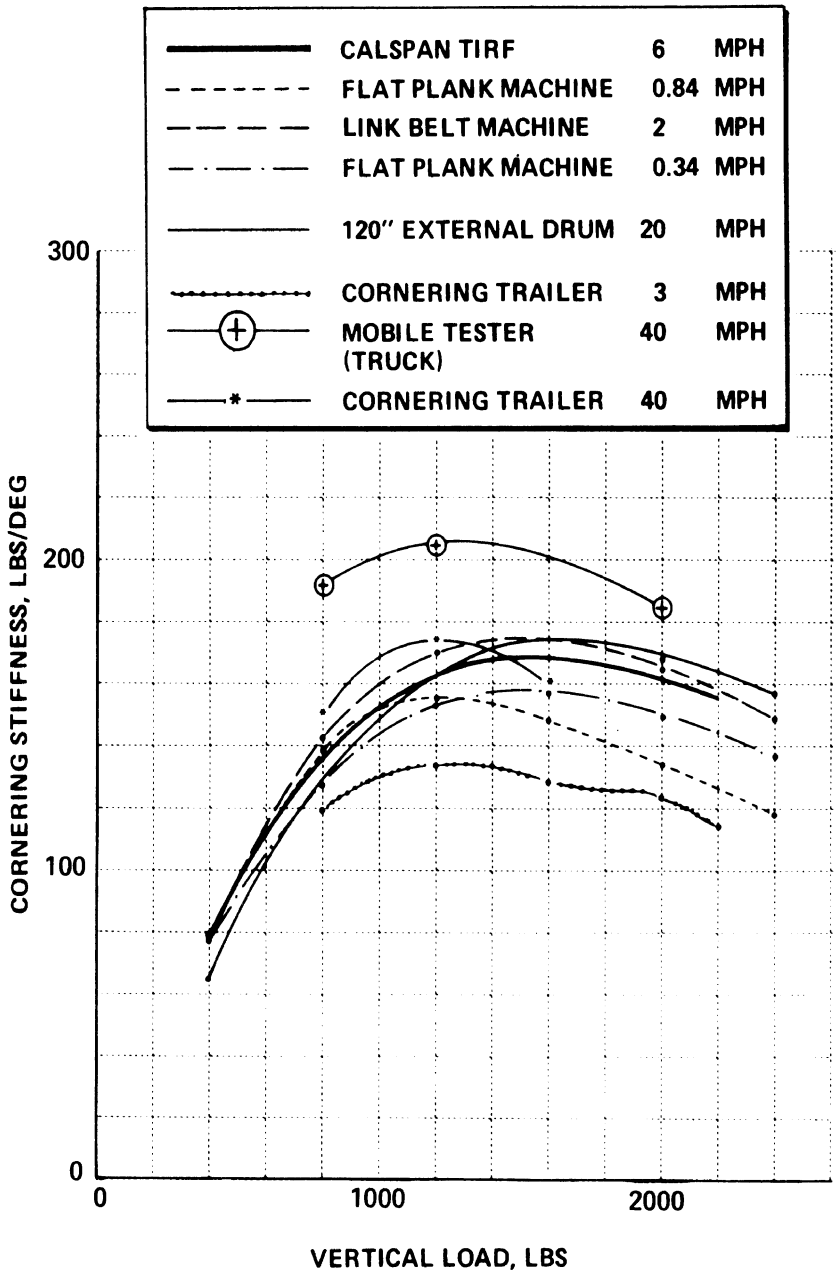

Figure 2a FACILITY VALIDATION RESULTS: G78-15 TIRE AT 28 PSI

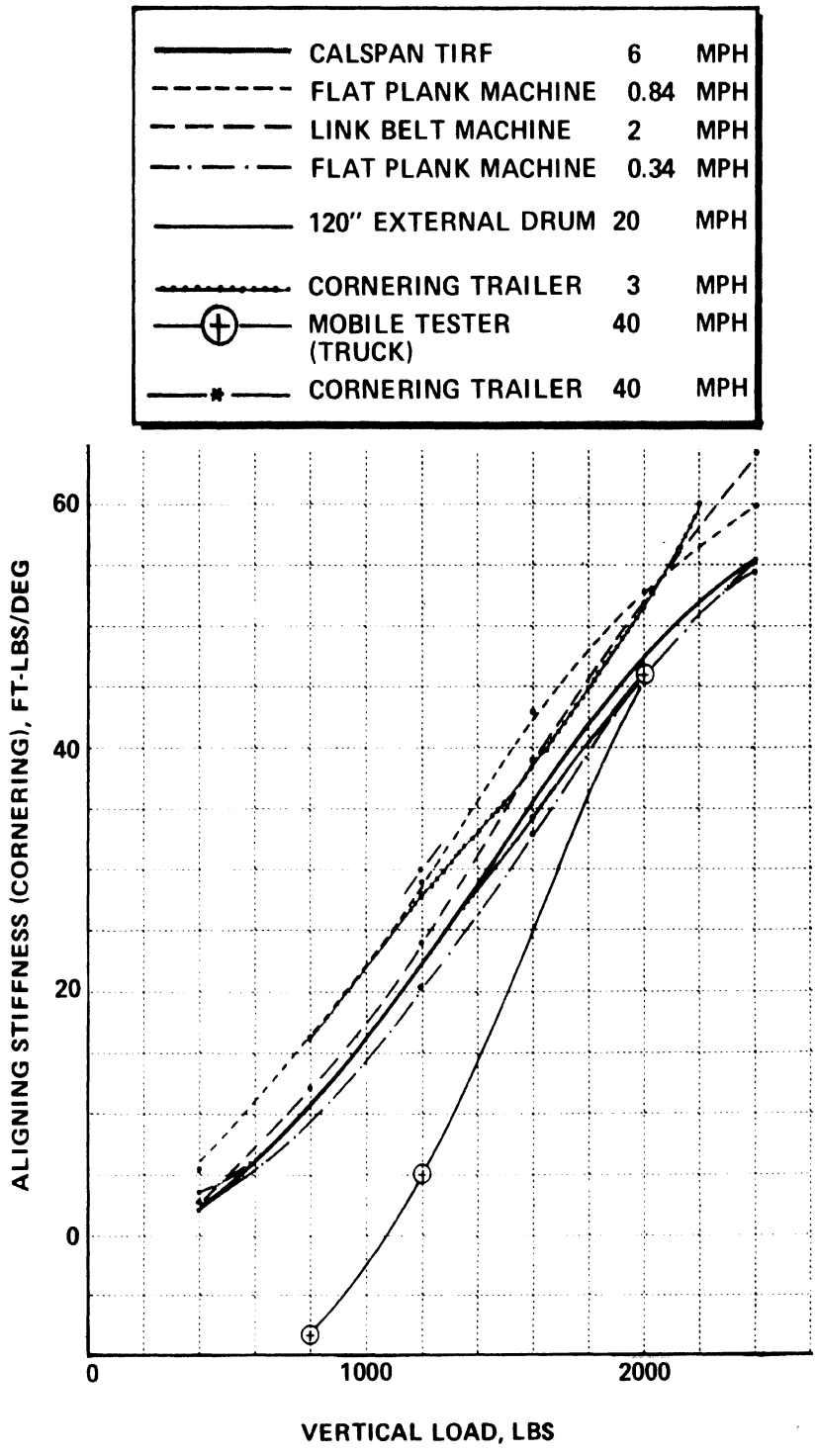

Figure 2b FACILITY VALIDATION RESULTS: G78-15 TIRE AT 28 PSI

Formal correlation tests have not been run on truck tires. As pointed out above, test facilities that are capable of handling truck tires are very limited. The data comparisons of Bickerstaff [5] are the only published comparisons with on-the-road data. A number of braking tests are being initiated at Calspan and it is hoped that in the coming months more direct comparisons with road test can be made.

TRACTION FIELD DEVELOPMENT ON DRY PAVEMENT

On TIRF, truck tires are usually braked by a disc brake mounted on the wheel axle shaft. The free-rolling tire is set to the wanted slip angle and load at the proper road speed. It is then braked at the desired rate until the wheel is brought to a stop. During this period, six-component force and moment data are recorded by the data system at a sampling rate of up to 100 samples per second (the so-called continuous sampling mode). As soon as the tire reaches lock-up, the brake is released, the tire taken to the next operating condition and the process repeated. This procedure is continued until all data are secured or until the data storage capacity of the computer is reached. At this point the run is stopped, data are computed, processed, and put into disc and/or tape storage and a new run is started.

The reduced data of a bias-ply 10.00-20 truck tire braked at a road speed of 40 mph and a load of 4,500 pounds are shown in Figures 3, 4, and 5. The longitudinal and lateral forces (F_x and F_y) have been nondimensionalized by dividing them by F_z. In Figure 3, the longitudinal force coefficient is plotted against slip ratio at slip

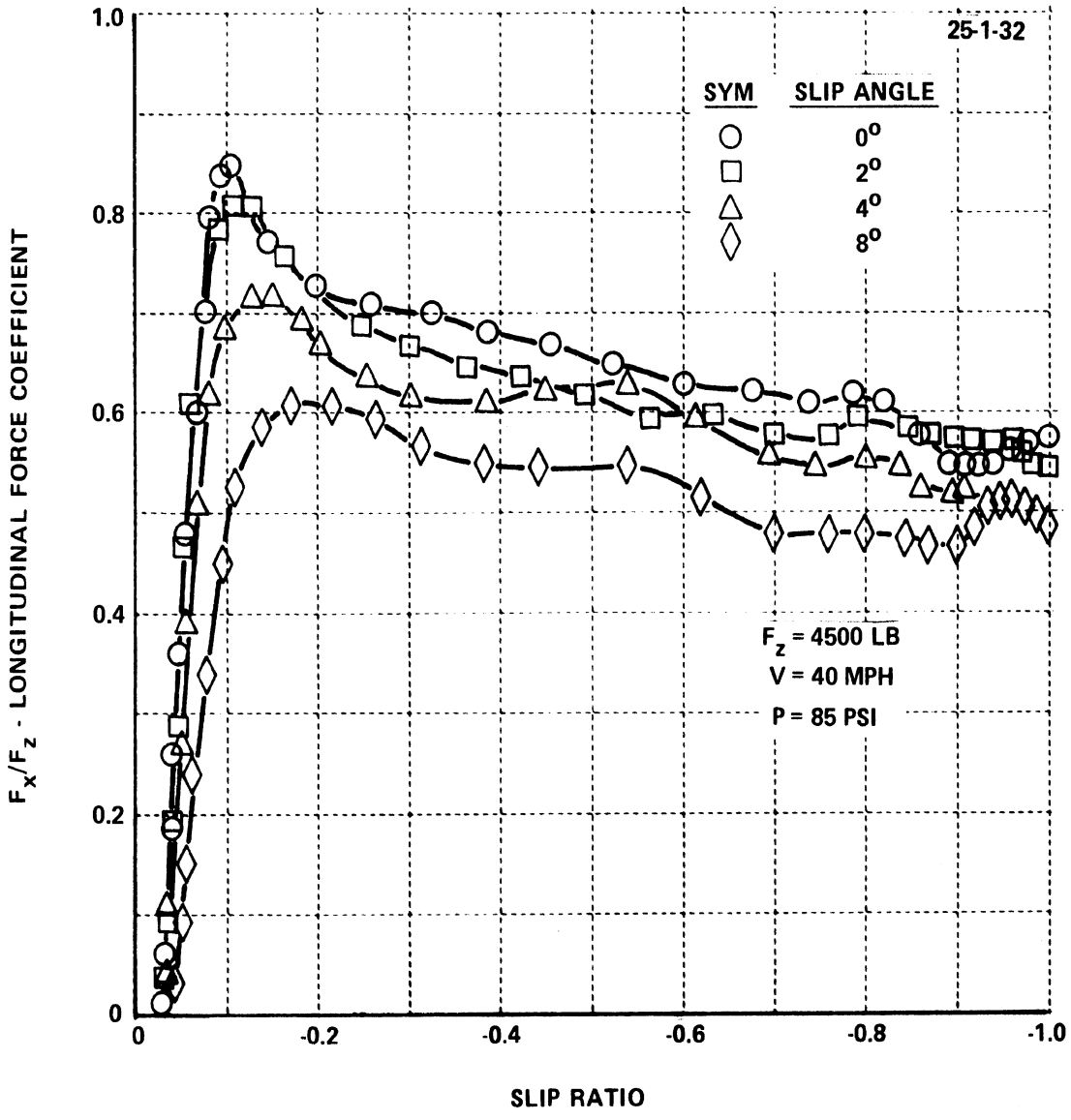

Figure 3 LONGITUDINAL FORCE COEFFICIENT VERSUS SLIP RATIO (BRAKING) OF 10.00-20 (F) BIAS PLY TRUCK TIRE

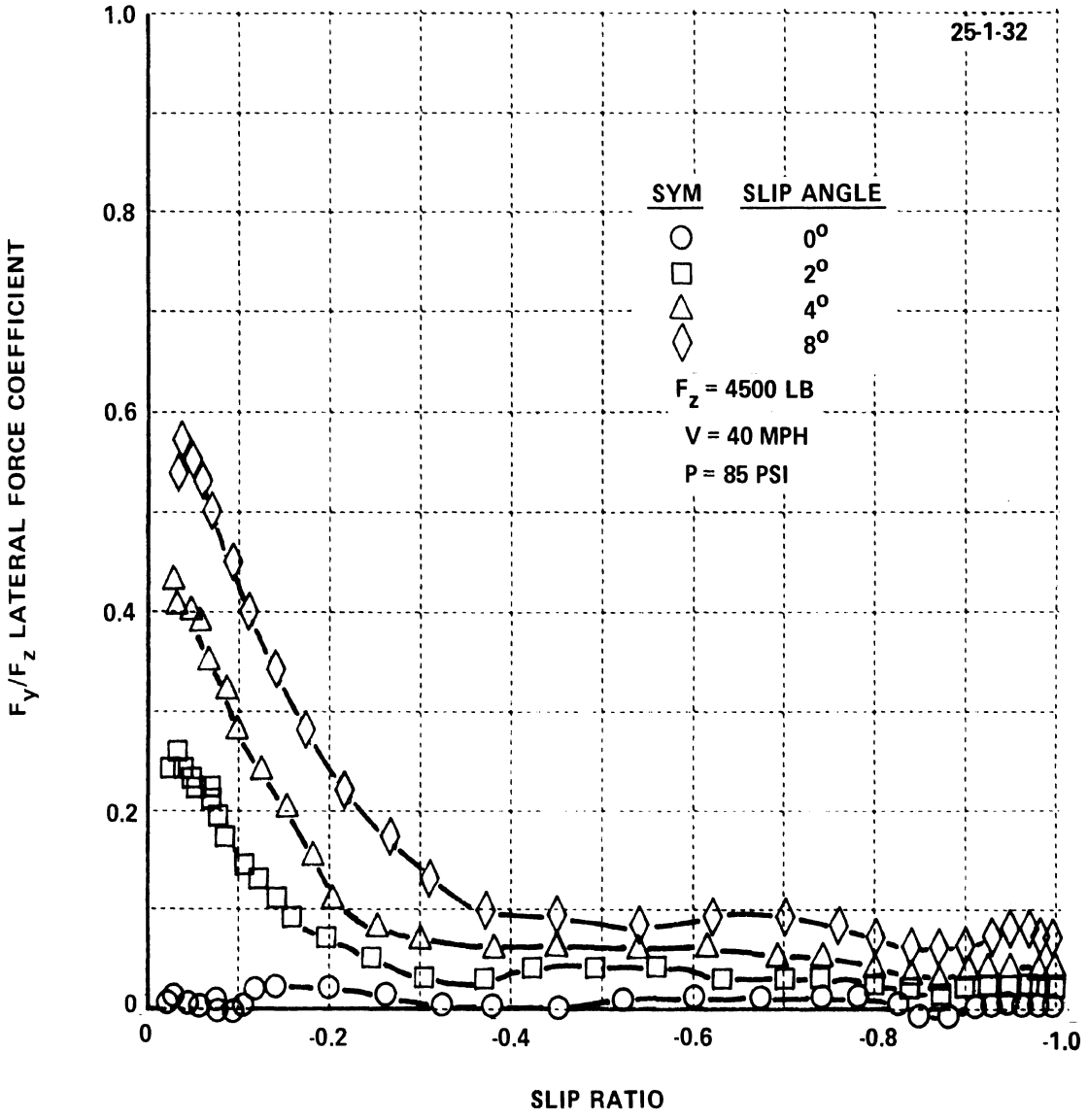

Figure 4 LATERAL FORCE COEFFICIENT VERSUS SLIP RATIO (BRAKING) OF 10.00-20 (F) BIAS PLY TRUCK TIRE

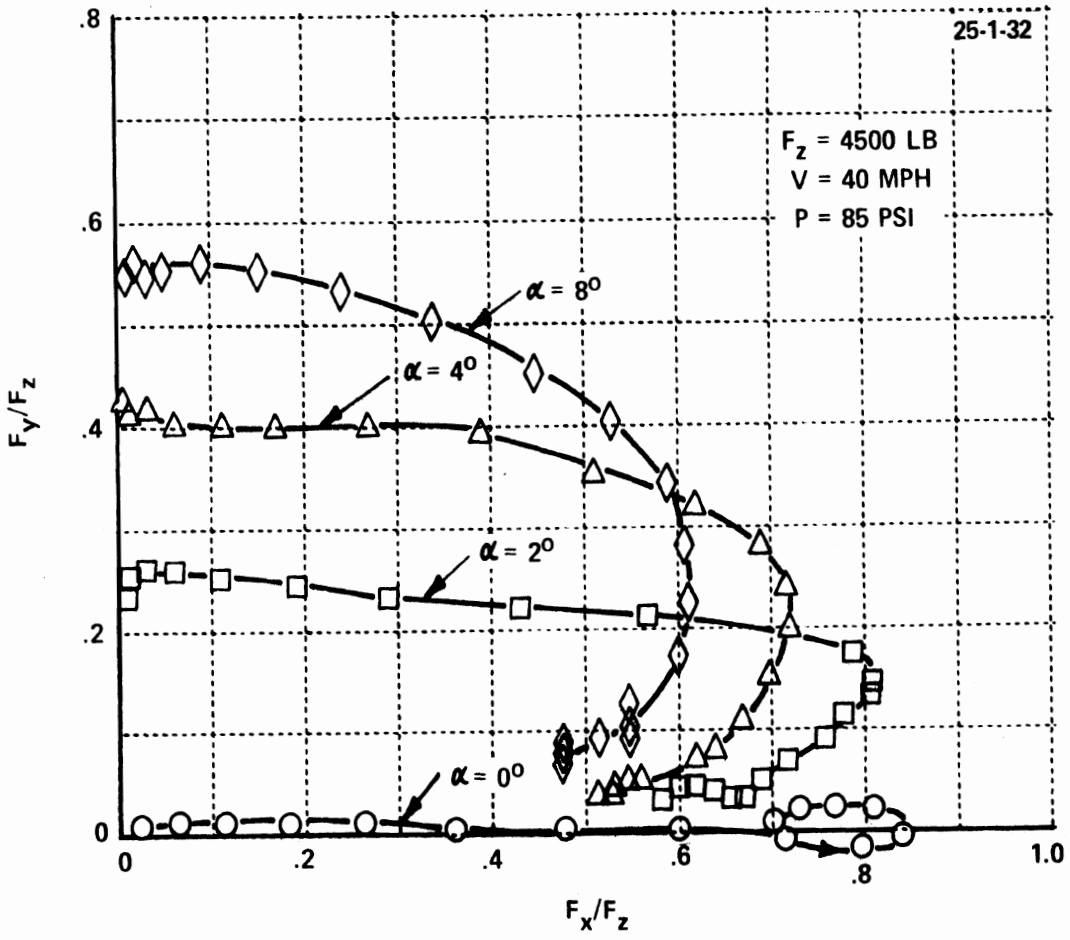

Figure 5 TRACTION FIELD (FY/FZ VS FX/FZ) OF 10.00-20 (F) TRUCK TIRE

angles of 0, 2, 4, and 8°; in Figure 4, the lateral force coefficient is similarly plotted against slip ratio. The traction field for the braking quadrant is constructed by plotting the lateral force coefficient vs. the longitudinal force coefficient as in Figure 5. To achieve good definition of the field, it is important to generate numerous data points up to slip ratios of about 15%, that is, between the free-rolling condition and the peak of the longitudinal force, as demonstrated in Figure 5. The interval from the time of brake application to lock-up was only about 0.5 seconds. Recently, much larger rates of brake application have been accomplished so that an even denser, almost continuous distribution of points is obtained.

The aligning torque (M_Z) is plotted against longitudinal force coefficient in Figure 6. At positive slip angle with no braking ($F_X \approx 0$), the aligning torque is positive, which in the SAE convention* means that the torque is self-"aligning" (tends to turn the tire toward zero slip angle). Application of the brakes and development of braking force, however, leads to large negative aligning torques which tend to increase the slip angle; this has been likened to a "negative caster angle effect" [6]. With the compliances inevitably present in truck steering systems, this sign reversal could have significant implications in truck handling and be a matter of concern in connection with meeting FMVSS 121.

The authors had hoped to be able to present aligning torque data for a radial-ply truck tire which were expected to exhibit quite different aligning torque behavior than the bias-ply truck tires. This expectation was based on characteristics measured on passenger

*SAE J670-C, Vehicle Dynamics Terminology

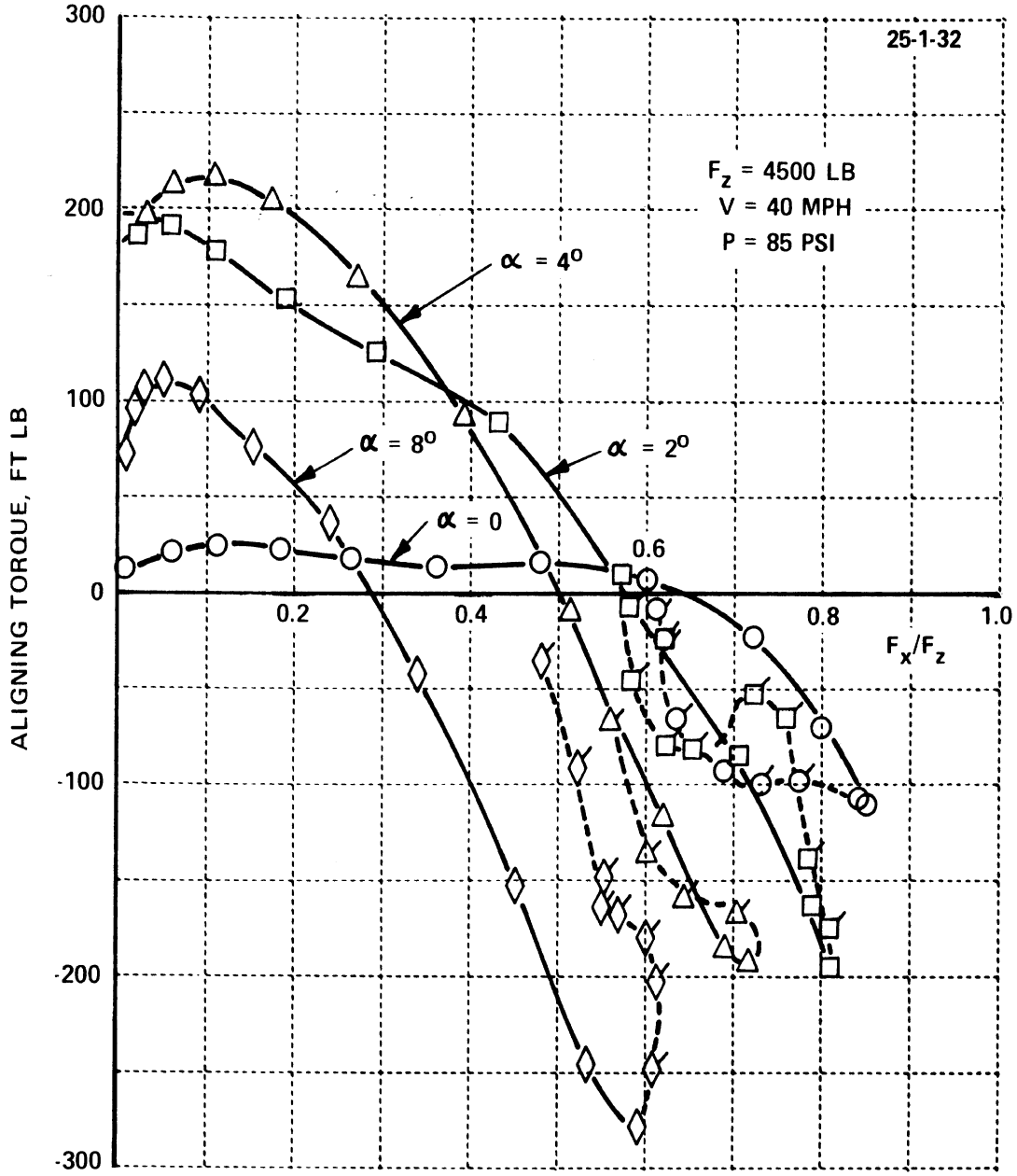

Figure 6 ALIGNING TORQUE VS BRAKING TRACTION COEFFICIENT OF 10.00-20 (F) TRUCK TIRE

car tires (Reference 7). A faulty strain gage (a manufacturer's quality control problem) on one of the beams of the truck tire balance, however, necessitated curtailment of tests so that these data are not available for this paper. It is suggested, however, that differences in bias-ply and radial-ply tires under combined cornering and braking may be important in some FMVSS 121 considerations.

WET ROAD PERFORMANCE

It is curious that the National Highway Traffic Safety Program as regards vehicle stability and control has been concerned with dry road* rather than wet road vehicle performance since it has been well established that most loss-of-control accidents take place on wet roads [8]. On TIRF, truck tire tests performed under wet-road conditions show marked differences between tires in both their cornering and braking capabilities and suggest, therefore, opportunities to improve vehicle lateral and longitudinal response under hazardous (slippery) road conditions.

Two surfaces were used with nominal skid numbers of 30 and 60. Whereas passenger car tire testing is usually done with 0.020 inch of water on the surface to conform with ASTM skid trailer practice, these tests used 0.060 inch of water in view of the larger drainage grooves in the truck tire treads. Although both ribbed and lugged tires were tested, only some of the grooved tire results will be reported here.

---

*Unlike the highway counterpart wherein the primary effort is directed toward improved wet road performance.

ASTM standard pavement tires* were used as reference tires to "calibrate" the surfaces. Runs were made with both 0.020 inch and 0.060 inch of water; the measured skid numbers are shown in Figure 7. At 20 mph, the circumferential grooves in the ASTM tires were able to provide the necessary drainage. As the speed increased to 40 and 60 mph, drainage was increasingly inadequate with the tires reaching near hydoplaning conditions on both surfaces with 0.060 inch of water at 60 mph. At 40 mph and 0.060 inch water depth, the skid numbers of the two surfaces were 30 and 50.

Figure 8 is a lateral force-slip angle-road speed carpet plot of a "control" tire with superior wet road performance as compared to two other tires shown in subsequent figures. In Figure 8, the vertical axis is lateral force and the horizontal axis slip angle. The nearly vertical curve on the left of the carpet plot is thus a plot of lateral force versus slip angle at 20 mph. For 40 and 60 mph, the zero slip angle origin is shifted to the right—generating two more curves. The points of constant slip angle are connected to produce the carpet plot. The slopes of the load curve at zero slip are the cornering stiffnesses. The slopes of constant slip angle lines show the sensitivity of the tire to speed.

In Figure 9, the control tire is compared with two other tires on the two surfaces (nominal skid numbers of 30 and 50 at 0.060 inch water depth). These other tires differ from the control tire in compound and tread pattern. In Figure 10, the tires are "rated" by using the ratio of two lateral forces at 10° slip angle—the

*ASTM E-501-74

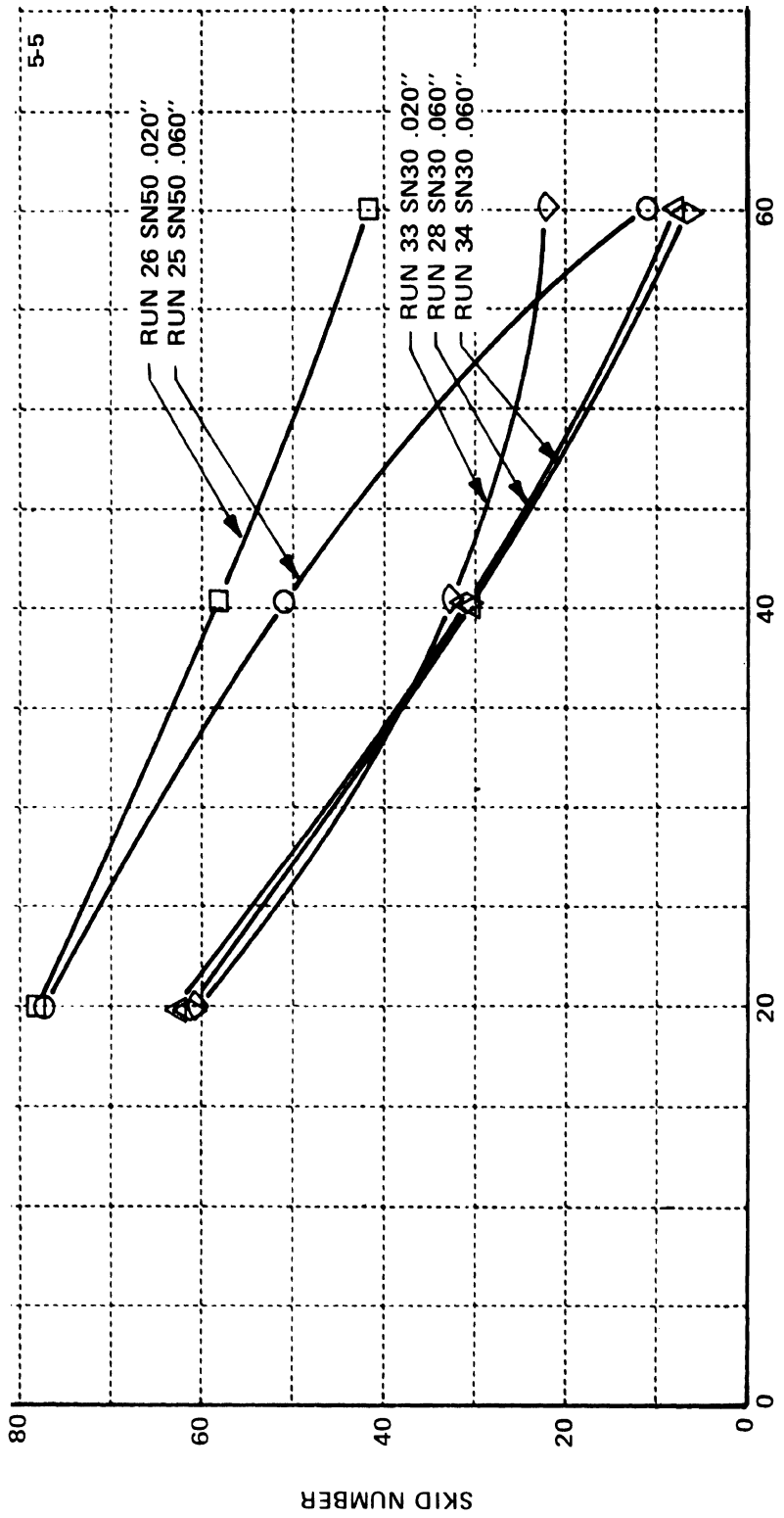

Figure 7 ASTM E-501-74 TIRE DATA

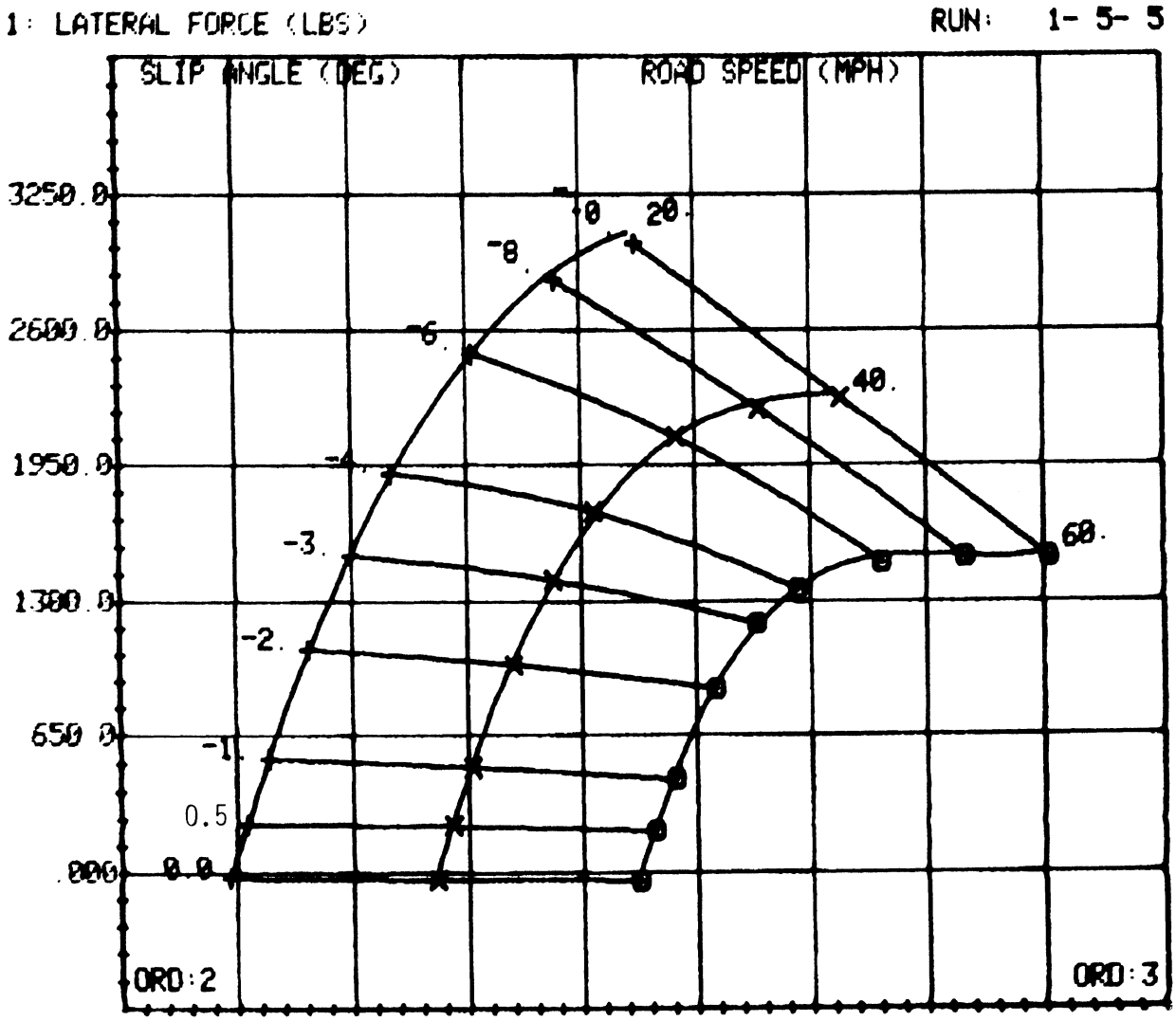

0.060 IN WATER DEPTH
85 PSI
5430 LB LOAD

Figure 8 LATERAL FORCE - SLIP ANGLE - ROAD SPEED CARPET COMPUTER PLOT: CONTROL TRUCK TIRE (10.00-20)

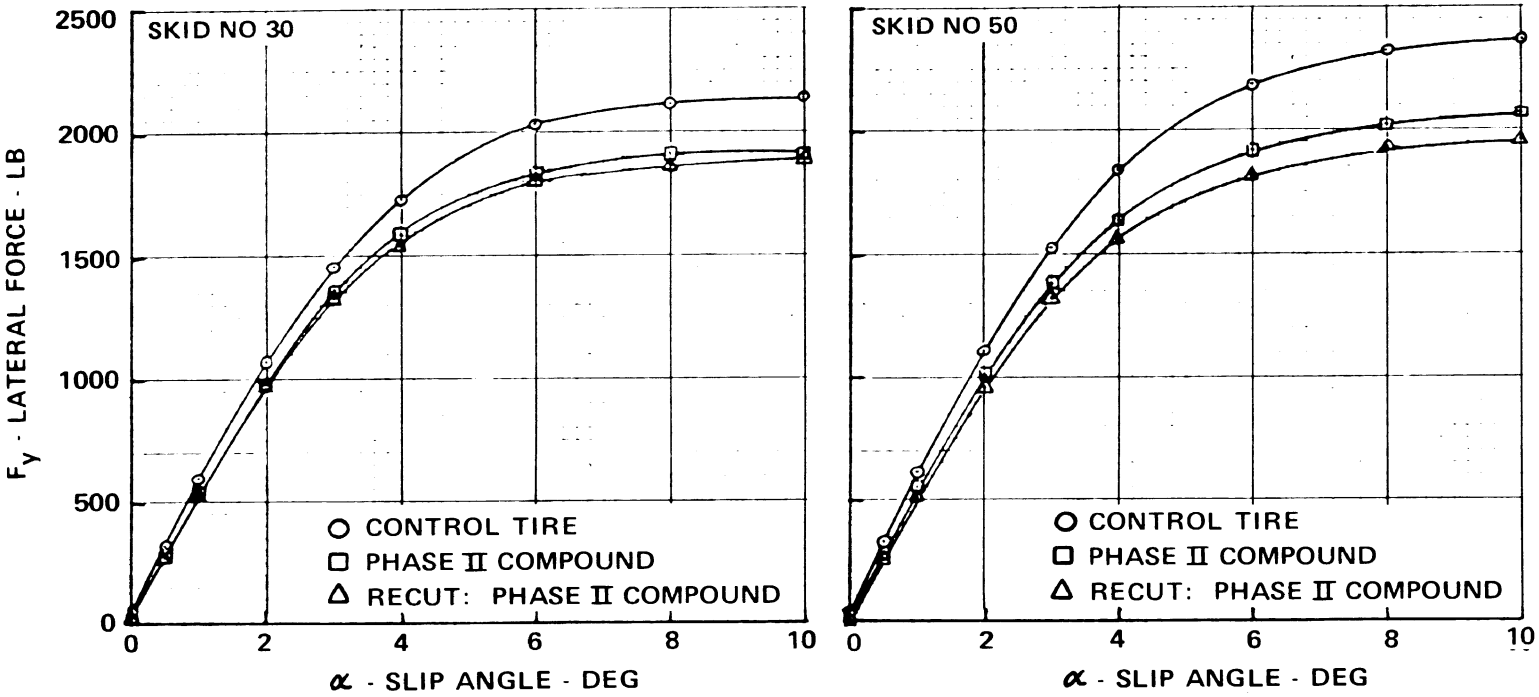

Figure 9 COMPARISON OF WET CORNERING PERFORMANCE OF DIFFERENT TRUCK TIRES (10.00-20)

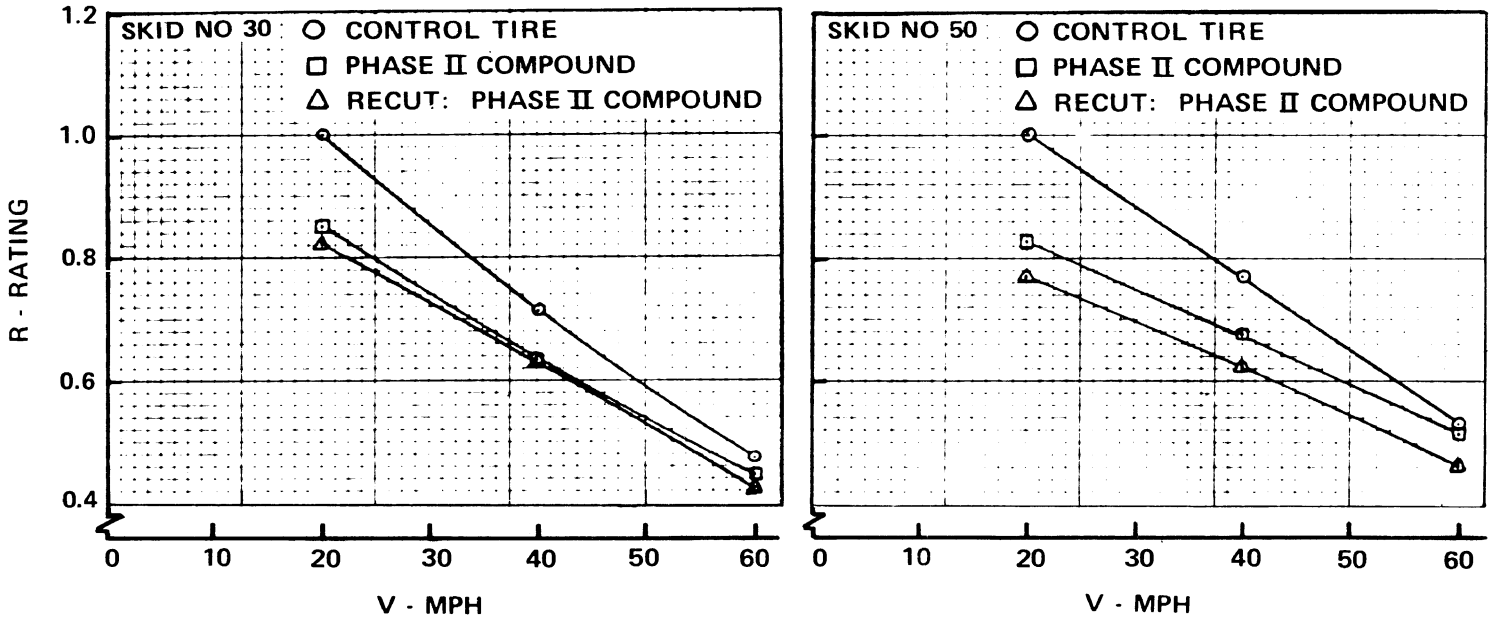

Figure 10 CORNERING PERFORMANCE RATINGS OF 3 10.00-20 TRUCK TIRES

lateral force of the candidate tires at given speeds and the lateral force developed by the control tire at 20 mph. It may be seen that significant differences exist between the tires on both surfaces although it appears that they may come together at sufficiently high speeds.

Straight braking comparisons were also made of these tires. Figure 11 is a computer generated plot of the normalized tractive force (F_x/F_z) versus slip ratio. From plots such as these, the peak and slide coefficients were determined and plotted as in Figure 12. Again it is apparent that significant differences are present among these three tires.

DUAL TIRE RESULTS

Dual truck tires are tested on TIRF in essentially the same fashion as single tires. Figure 13 shows a set of dual 8.00-16.5 (C) light truck tires mounted on TIRF. Their (free-rolling) cornering test results are shown in Figures 14 through 19, with single-tire test results added for comparison. Figure 14 indicates that the lateral force coefficients of both single and dual tires, compared at the same vertical load per tire (here 1,800 pounds), are virtually identical for all slip angles tested. One would therefore expect corresponding cornering coefficients to be identical, too, which is very nearly true as Figure 15 demonstrates.

Lateral forces of the single and dual tires, however, are not identical if they are generated by tire cambering rather than side-slipping. Figure 16 suggests that in this case the two footprints of the dual tires act as parallel individual units, each contributing to the

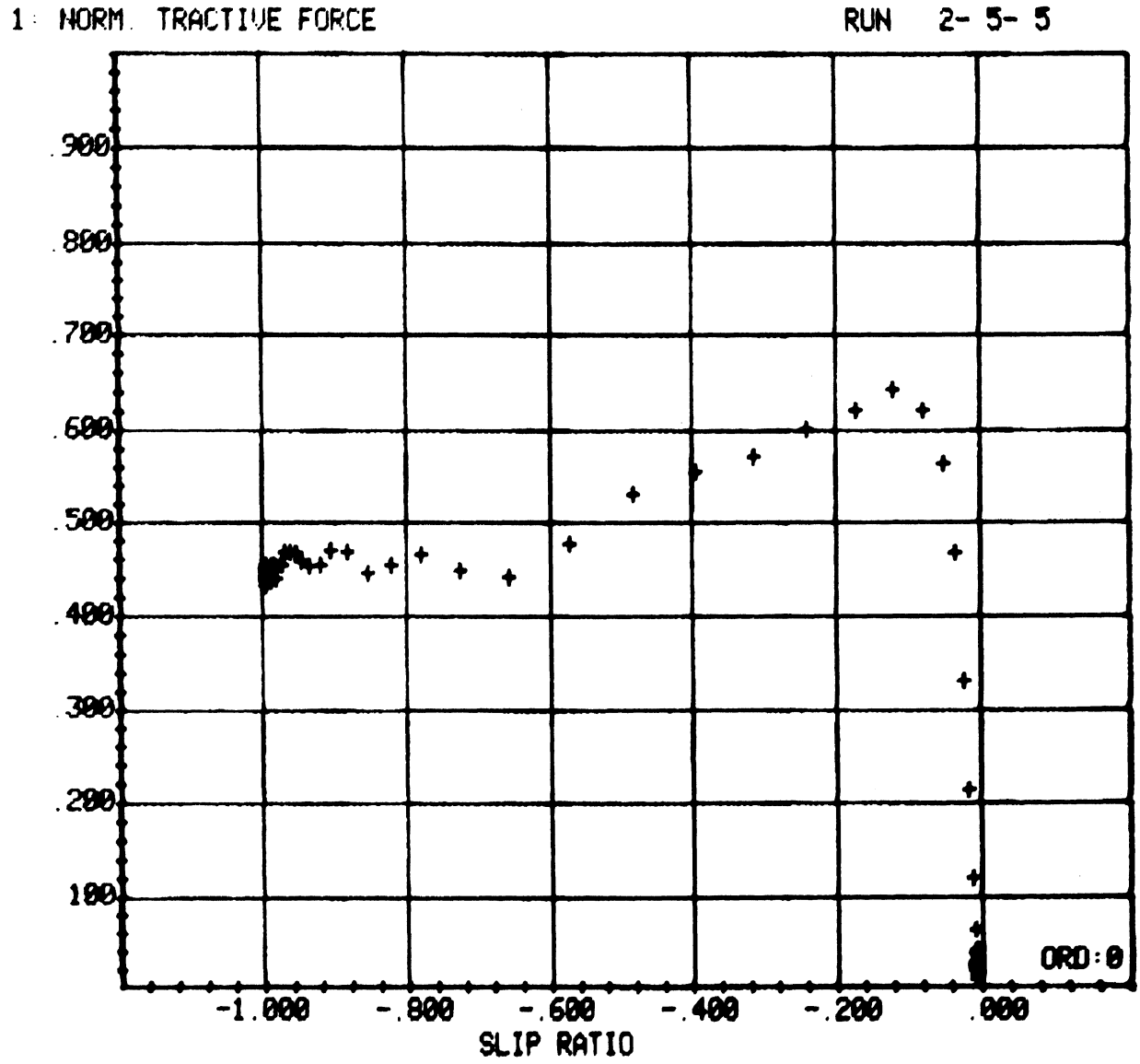

40 MPH
4340 LB LOAD
85 PSI

Figure 11 NORMALIZED TRACTIVE FORCE (TRACTION COEFFICIENT) VS SLIP RATIO: COMPUTER PLOT.CONTROL TRUCK TIRE (10.00-20)

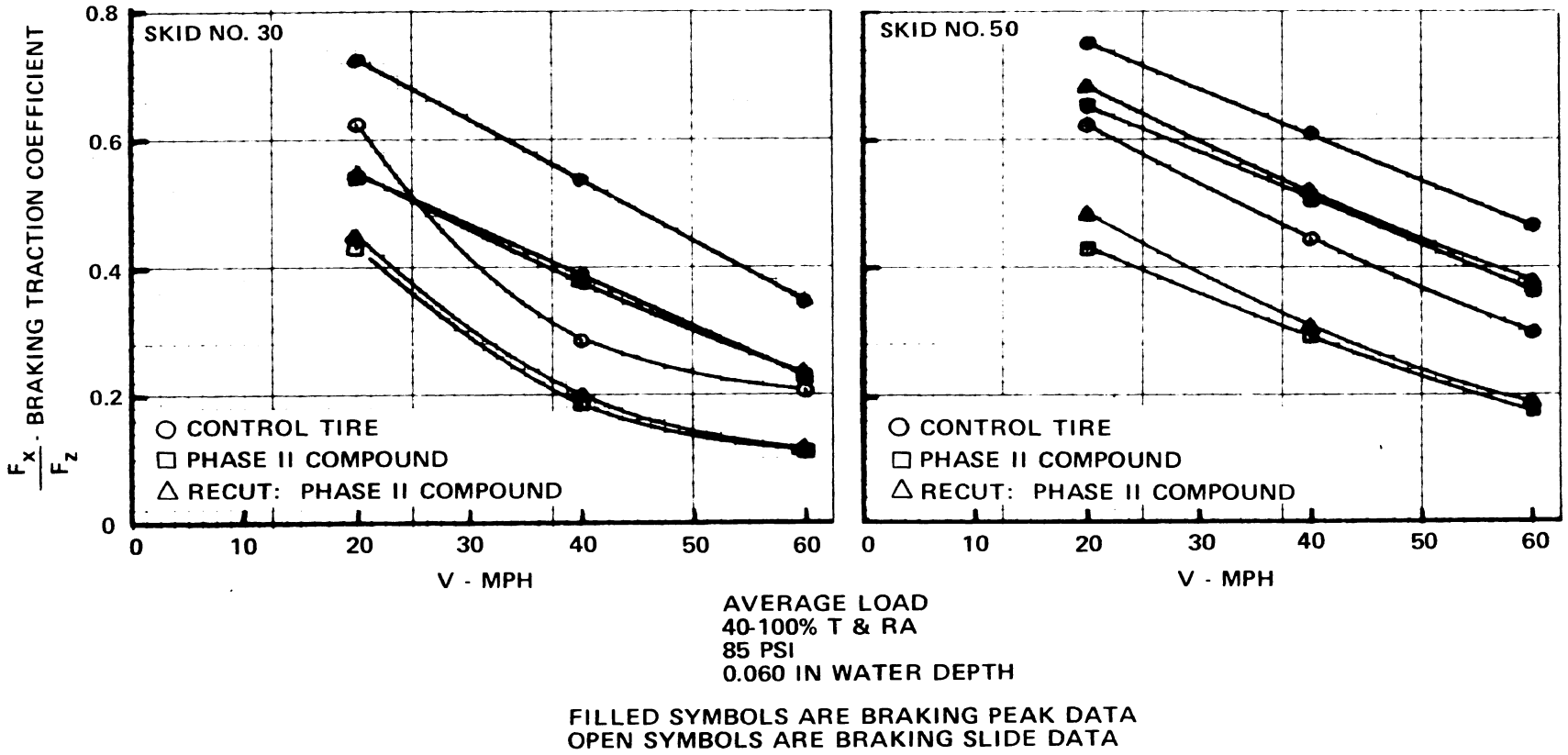

Figure 12 BRAKING TRACTION PERFORMANCE OF 10.00-20 TRUCK TIRES

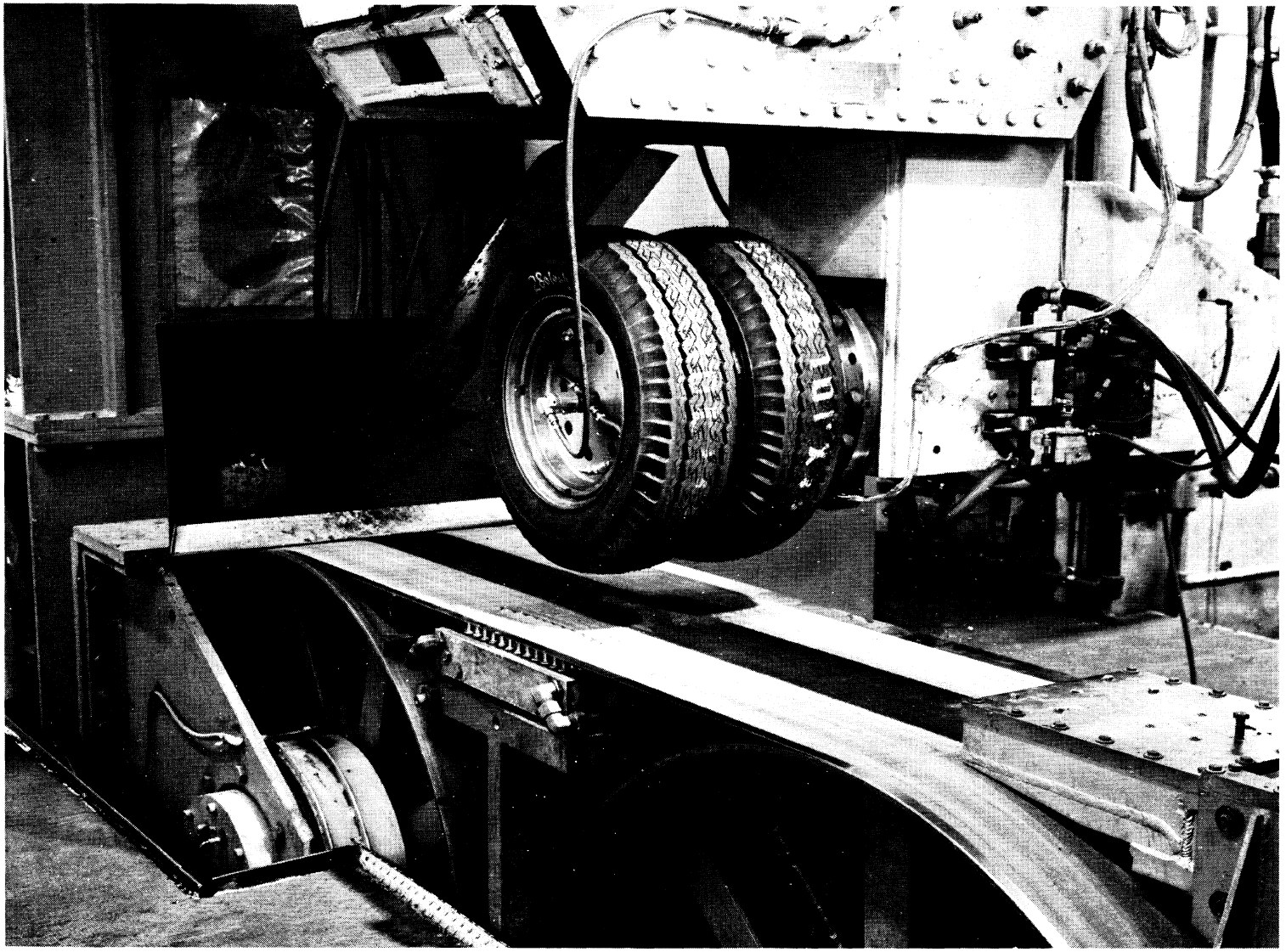

Figure 13 DUAL TIRE CONFIGURATION ON TIRF 8.00-16.5 (C) WIDE BASE

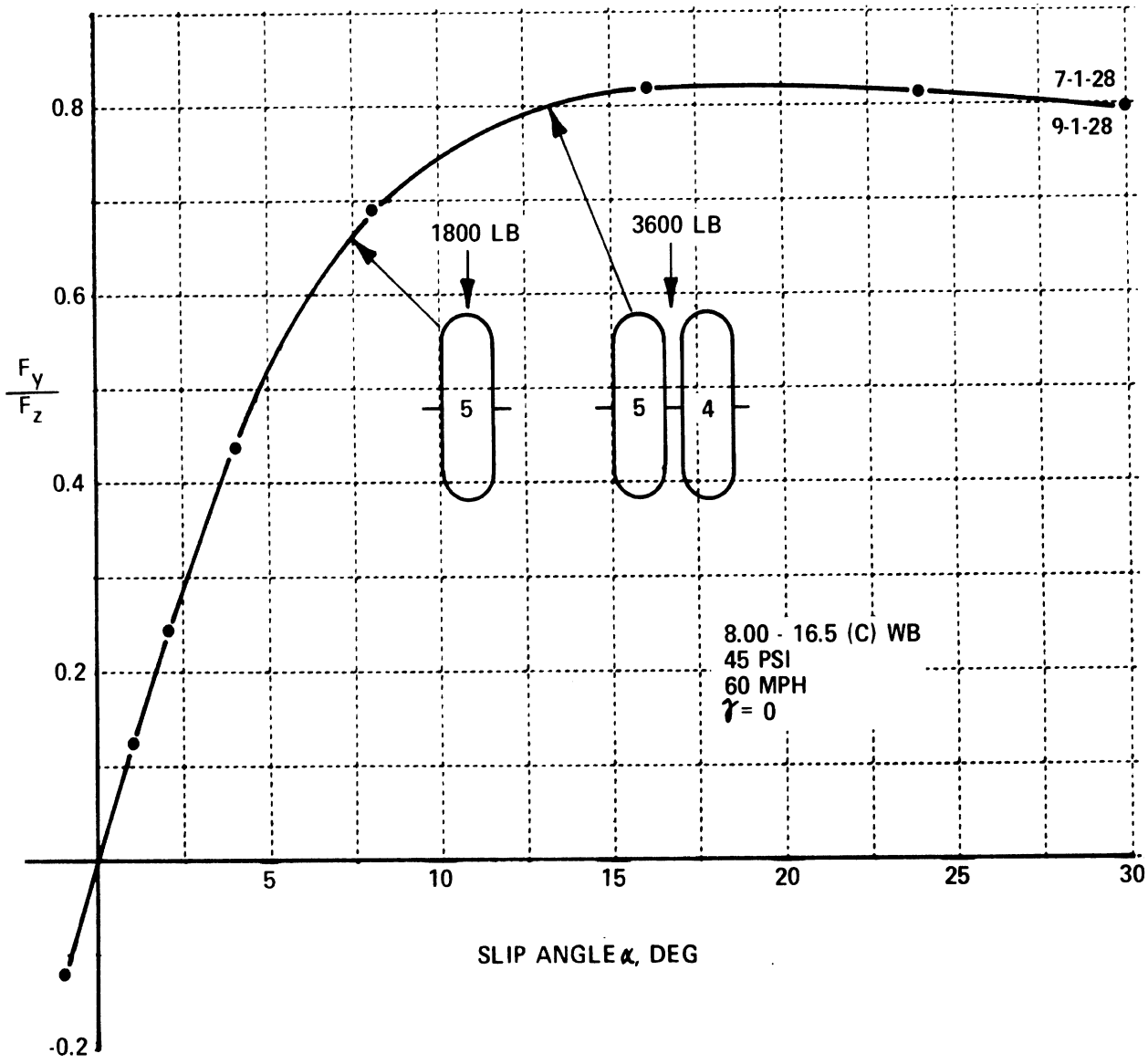

Figure 14 LATERAL FORCE COEFFICIENT OF SINGLE AND DUAL TRUCK TIRES

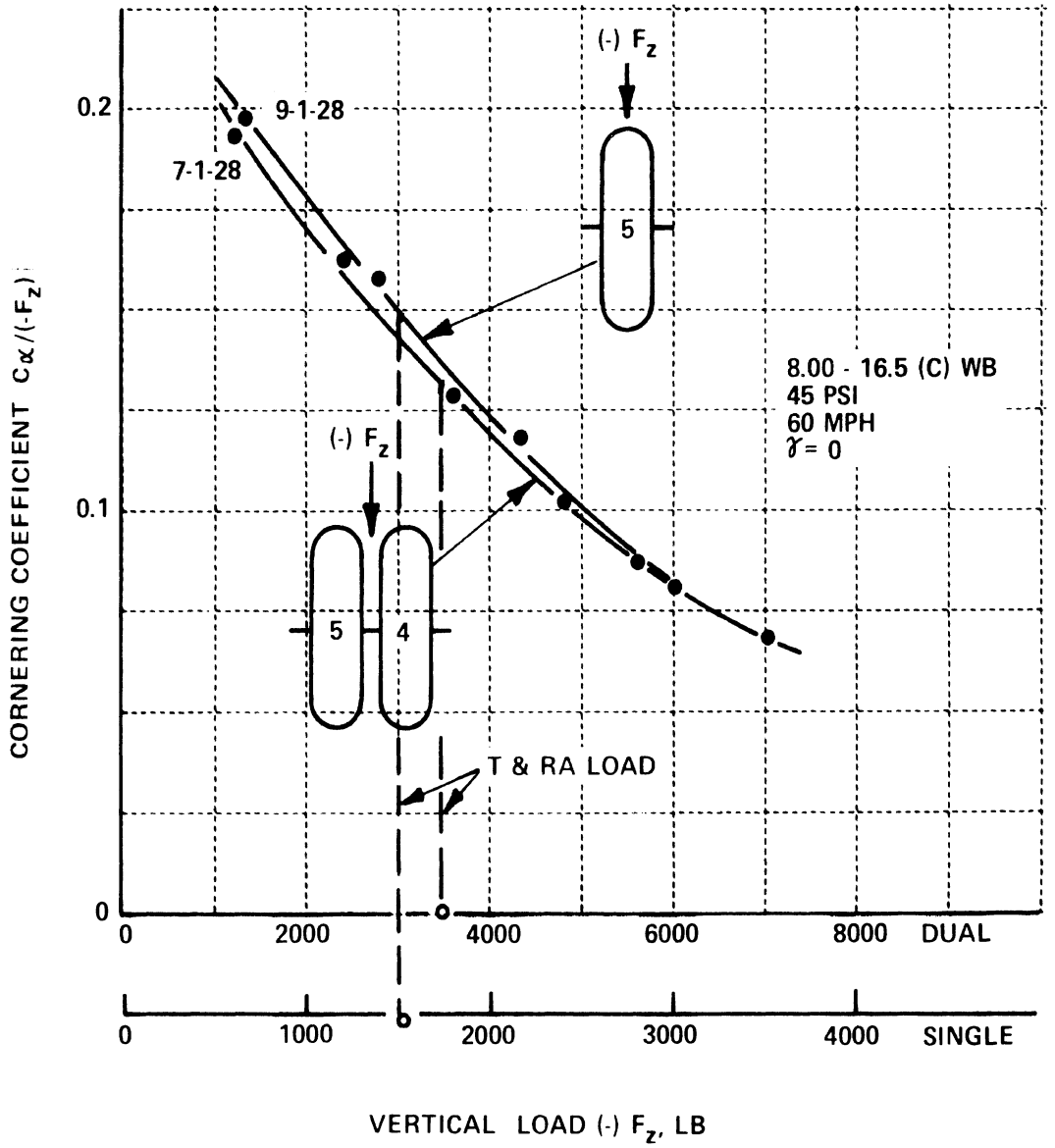

Figure 15 CORNERING COEFFICIENT OF SINGLE AND DUAL TRUCK TIRES

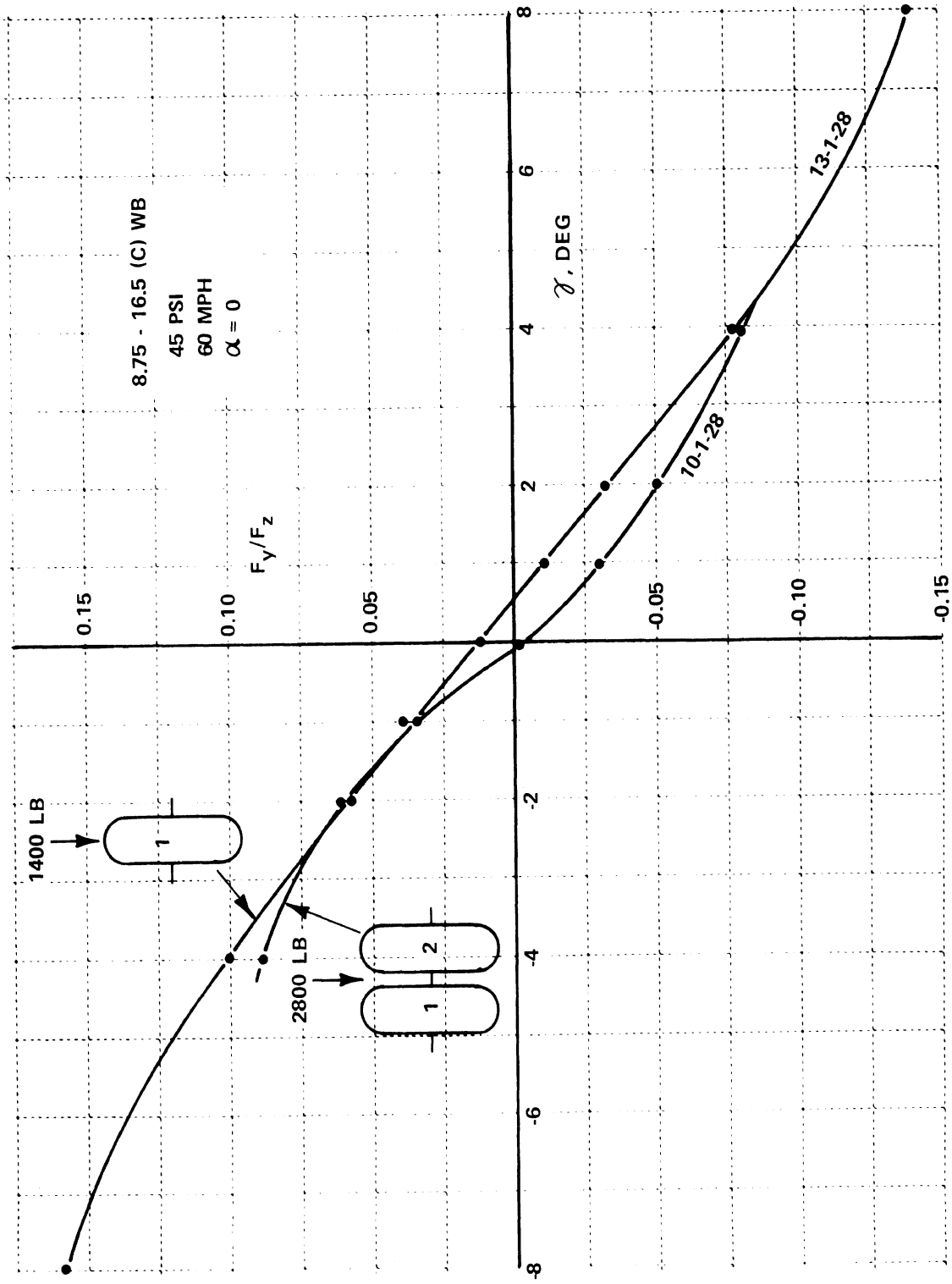

Figure 16 LATERAL FORCE COEFFICIENT OF SINGLE AND DUAL TRUCK TIRES

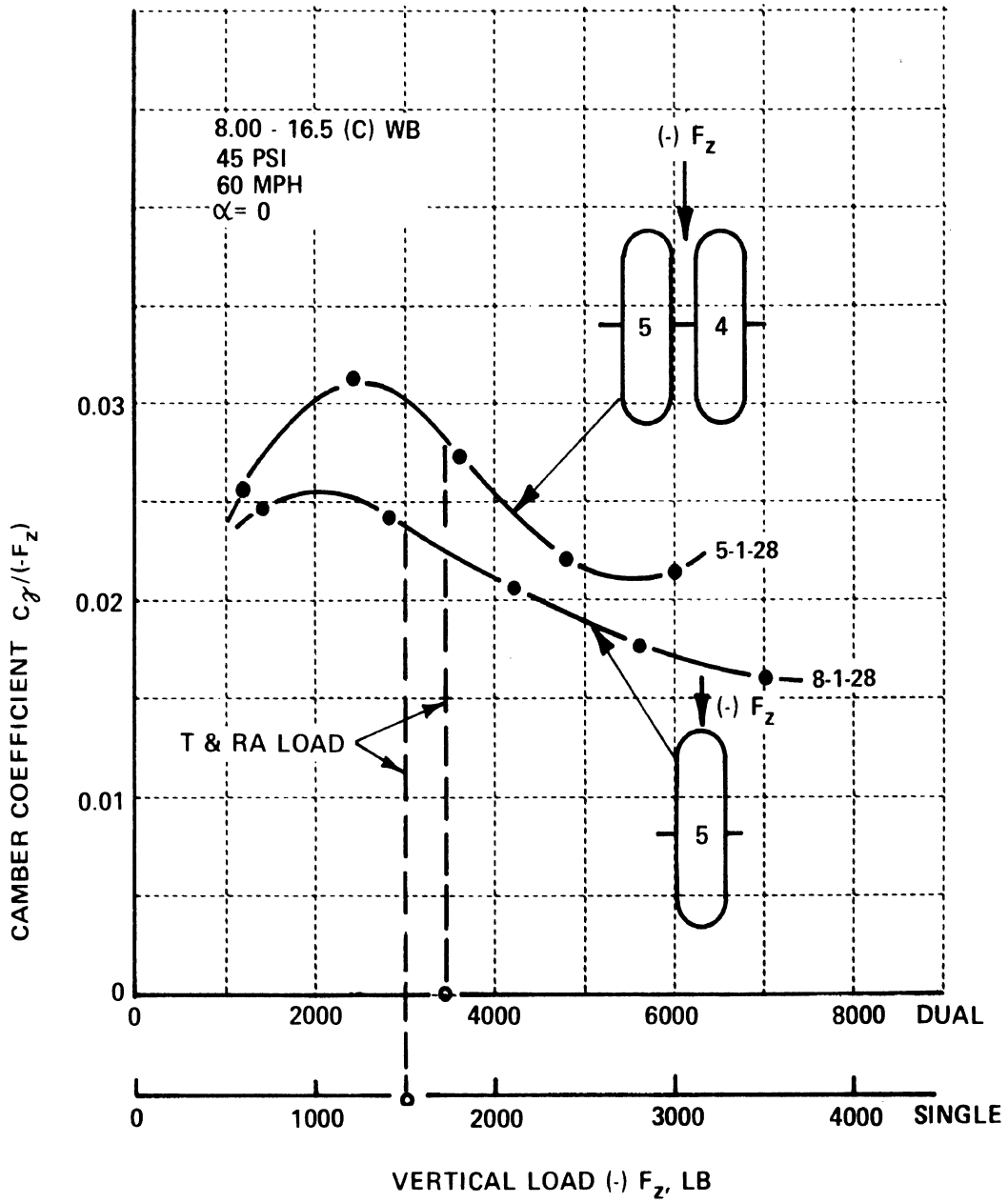

Figure 17 CAMBER COEFFICIENT OF SINGLE AND DUAL TRUCK TIRES

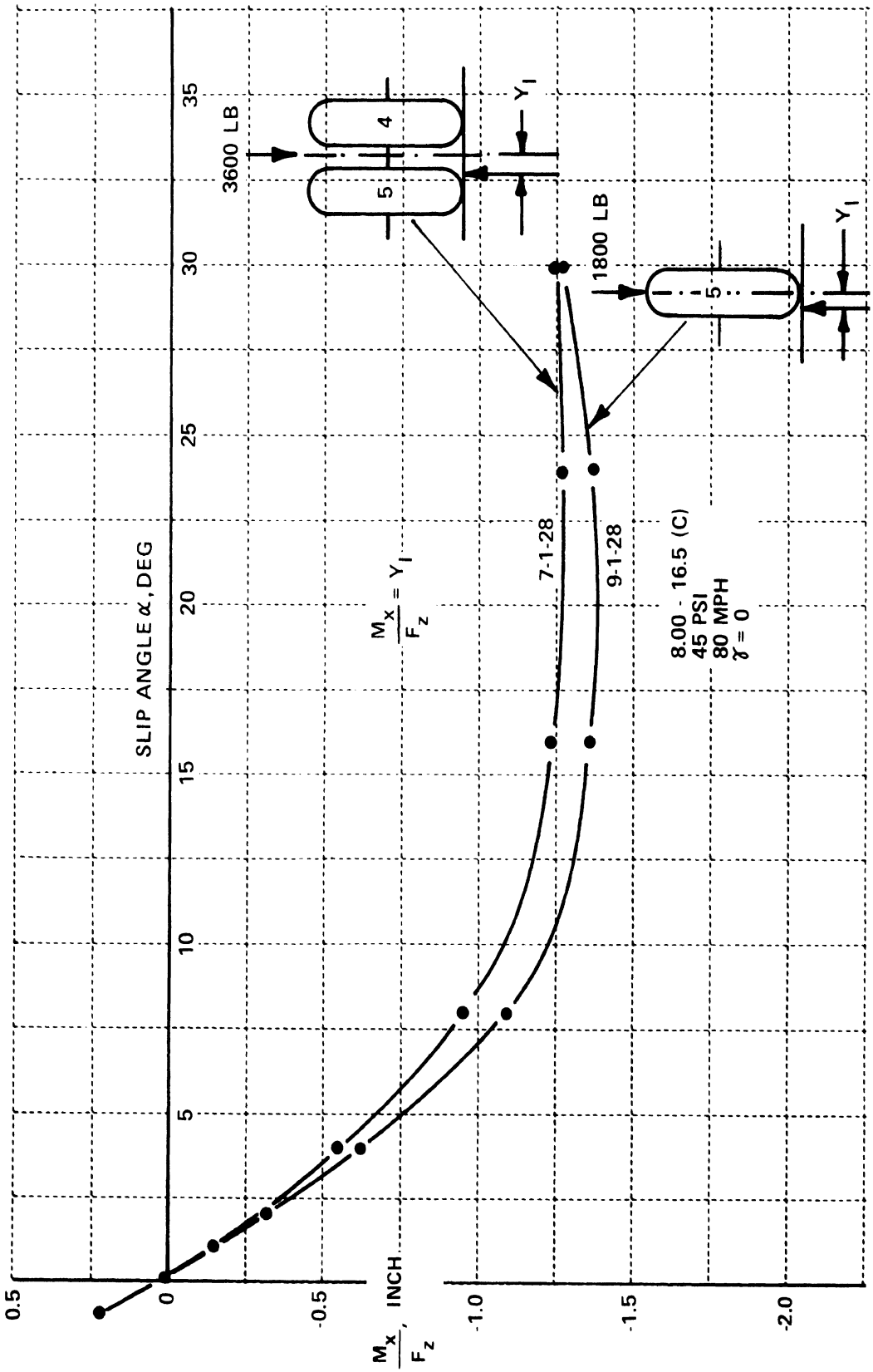

Figure 18 OVERTURNING MOMENT COEFFICIENT OF SINGLE AND DUAL TRUCK TIRES

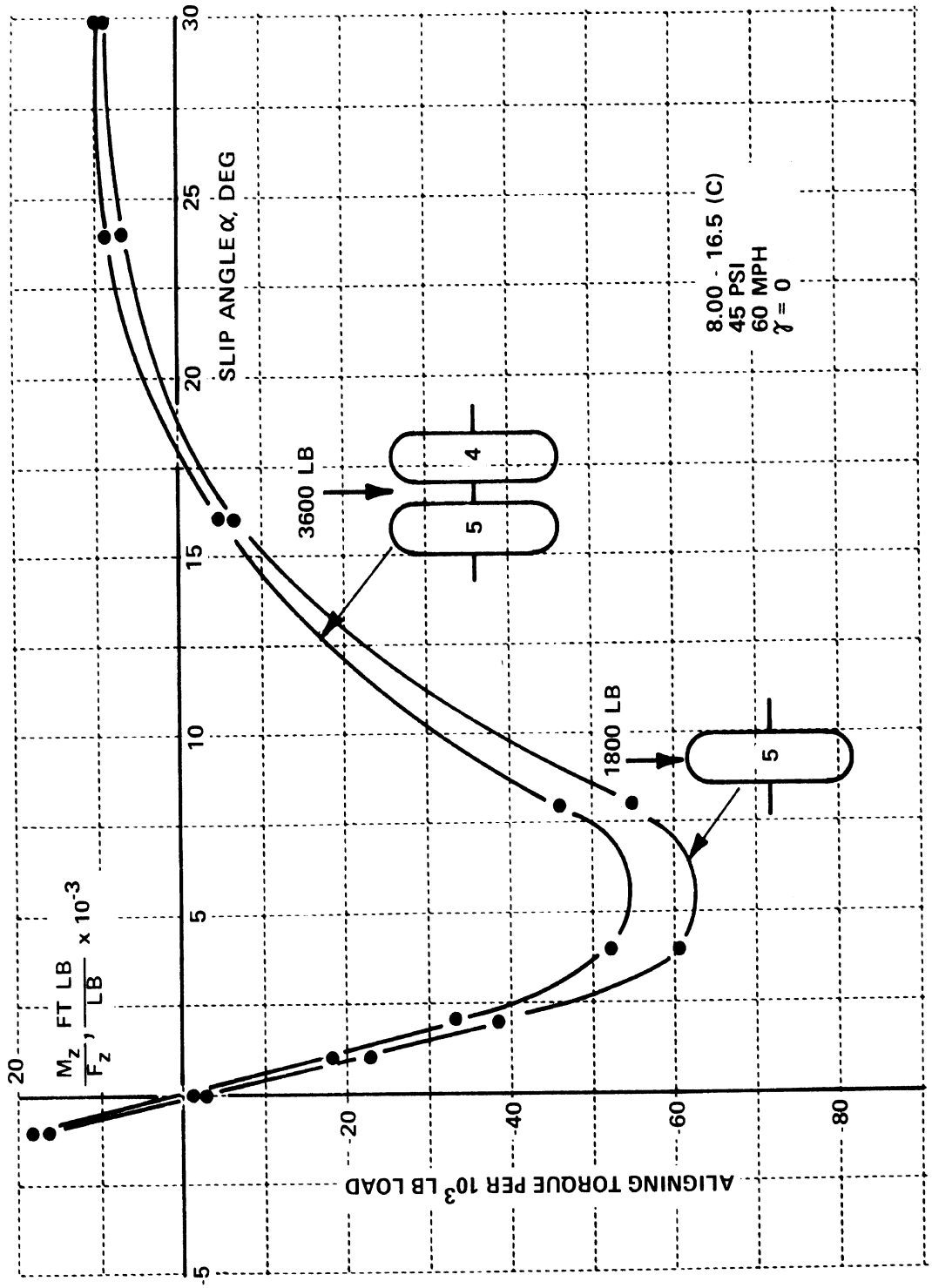

Figure 19 ALIGNING TORQUE COEFFICIENT OF SINGLE AND DUAL TRUCK TIRES

total lateral force according to its share of vertical load. Consequently, the camber coefficients of the dual and single tires are different, as illustrated in Figure 17.

The overturning moment coefficients, Figure 18, are not very different, which is perhaps surprising since M_x/F_z represents the lateral offset of the center of pressure, y_1—a quantity one would expect to be longer for dual than for single tires. Similarly, the aligning torque coefficients of both configurations do not show significant differences (Figure 19). With the exception of camber effects, these results are in agreement with data reported by Tielking, Fancher, and Wild [4] who found that for 8-22.5 (D) tires, the traction force and the aligning torque generated by the dual configuration are nearly twice as large as corresponding values generated by a single tire.

FACILITY LIMITATIONS

TIRF was initially designed to serve as a test facility for passenger car tires. At the conclusion of the preliminary design phase, Calspan was asked by the Motor Vehicle Manufacturers Association, one of the primary sponsors of the facility,* to make provisions for testing truck tires without materially changing the concept or cost of the facility. Hence, the design was modified so that the tire positioning and loading systems would accommodate truck tire sizes and loads. It was also found necessary to construct a separate truck tire balance system for loads up to 12,000 pounds (Table II). It was known, however, that a maximum load of 12,000 pounds was inconsistent with the capacities of both the braking and the air bearing systems.

*Along with the Rubber Manufacturers Association

Testing experience to date has shown the air bearing upper load to be 8,000 pounds or just under 150% of the T&RA load for a 10.00-20(E) tire at 85 psi. At this load, slip angles have been run up to at least 16°. Studies are now underway on the replacement of the air bearing with a water bearing. The system appears to be completely practical and the performance should be adequate up to 12,000 pounds tire load.

Current braking capability limits maximum load to 6,000 pounds or less if the full range of slip ratios from free-rolling to locked-wheel is to be covered. The exact upper load depends upon the peak and sliding traction coefficients for the particular tire. (Obviously, higher loads can be run on wet roads than on dry roads.) Extension of the braking performance to higher loads is difficult. The roadway itself is driven by an hydraulic drive with an installed power of 450 hp. When a tire is braked, the braking force on the belt results in a torque on the driving drum. If this torque exceeds the drive capability, the roadway will be rapidly decelerated—rapidly because the inertia of the roadway system is quite low (low inertia is a requirement for good speed control). With large braking loads it is not uncommon to bring the roadway completely to rest in a few seconds. Increasing the drive horsepower to be able to maintain constant speed, and a dry traction coefficient of 0.8, approximately 850 hp are dissipated in the contact patch of a sliding tire. It would be practical, however, to couple inertia to the simulated roadway so that the rate of slow-down would match that of commercial vehicles being braked.

While truck tire power consumption is not a specific subject of this meeting, it is a topic of high national priority at this time. TIRF, as it stands, has the capability for steady-state measurements of tire rolling resistance or power consumption at loads, slip angles, and torques up to the maximum values of interest. TIRF appears to be the only facility in the U.S. with this capability, and truck tire power consumption tests are being initiated.

SUMMARY

The Calspan Tire Research Facility (TIRF) as a laboratory apparatus for testing truck tires is described and typical truck tire test results are presented. Test results are shown for a combined lateral slip (slip angle) and longitudinal slip (braking) operations of a 10.00 x 20 truck tire on a dry road surface. The measured lateral and longitudinal forces and aligning torques are used to portray the "traction field" for this tire. The aligning torque behavior possibly has important implications on the handling characteristics of a truck under heavy braking.

Wet road cornering and braking characteristics of three different 10.00 x 20 truck tires measured on TIRF show significant differences. It is noted that wet road handling and braking performance of trucks (as well as passenger cars) has received very little attention in the National Highway Traffic Safety Program in spite of the fact that the majority of skidding accidents occur on wet roads. The presented results show the practicability of wet-road testing of truck tires on TIRF.

Comparisons are made of single versus dual tire performance. The presented results indicate that for equivalent loads, little differences exist in cornering, aligning torque, and overturning moment coefficients. The camber coefficients of dual tires, however, appear to be different from corresponding values of single tires.

TIRF's upper limits of load and brake forces are certainly below those desirable to evaluate tire-vehicle systems with respect to proposed FMVSS 121. The current limit on tire load is extended fairly readily and, in fact, steps are being taken that are expected to extend the load up to at least 12,000 pounds. Increasing the braking capability would involve more expensive modifications of the facility. These modifications appear to be practical; their implementation, however, is contingent upon justification of the additional capital investment required.

REFERENCES

1. Bird, K.D. and Martin, J.F., "The Calspan Tire Research Facility: Design, Development and Initial Test Results," presented at Automobile Engineering Meeting, Detroit, Michigan, SAE Paper No. 730582, May 14-18, 1973.

2. Ervin, R.D. and Fancher, P.S., "Preliminary Measurements of Longitudinal Traction Properties of Truck Tires," presented at SAE Truck Meeting, Troy, Michigan, SAE Paper # 741139, November 4-7, 1974.

3. Ginn, J.L and Marlowe, "Road Contact Forces of Truck Tires as Measured in the Laboratory," SAE Transactions, Vol. 76 (1967), Paper No. 670493.

4. Tielking, J.T., Fancher, P.S., and Wild, R.E., "Mechanical Properties of Truck Tires," presented at SAE International Automotive Engineering Congress and Exposition, Detroit, Michigan, Paper No. 730183, January 1973.

5. Bickerstaff, D.J. and Hartley, G., "Light Truck Tire Traction Properties and Their Effect on Braking Performance," SAE Truck Meeting, Troy, Michigan, SAE Paper No. 741137, November 4-7, 1974.

6. Gillespie, T., Ford Motor Company, Personal Communication with the Authors.

7. "Mechanics of Pneumatic Tires," S. K. Clark, Ed., National Bureau of Standards Monograph 122, 1971.

8. Dunlap, D.F., et al., "Passenger Car Skidding as Influenced by Roadway Design, Tire Tread Depth, and Pavement Conditions," Highway Safety Research Institute, HIT Lab Report, Vol. 5, No. 4, December 1974.

MOBILE MEASUREMENT OF TRUCK TIRE TRACTION

R. D. Ervin
Highway Safety Research Institute
The University of Michigan

ABSTRACT

A mobile dynamometer system has been developed for use in measuring the lateral and longitudinal traction properties of truck tires on actual paved surfaces. The apparatus is described, together with certain practices which are employed in its use. Data are presented covering basic characteristics measured with the longitudinal-testing portion of this apparatus. The data describe those sensitivities of truck tire traction which are of first-order relevance to the limit braking behavior of heavy trucks on dry pavements.

INTRODUCTION

The technical literature is virtually devoid of experimental measurements describing the traction properties of commercial vehicle tires. Indeed, only very recently has the technical capability been developed for conducting measurements of the friction-limited shear force properties of such tires. Notable reportings of this capability have been made by the Goodyear Tire and Rubber Company (1), the Highway Safety Research Institute (HSRI) (2, 3, 4), and the Calspan Corporation (5). While the latter reporting describes a high-speed laboratory machine, the preceding publications describe devices for conducting over-the-road measurements. This paper supplements HSRI's previous publications, presenting a total truck tire traction measurement system, heretofore presented only in part, and providing data concerning longitudinal traction which has been documented in detail within the technical report of Reference 4.

MOBILE TRACTION MEASUREMENT APPARATUS

The HSRI mobile dynamometer in its current stage of development consists of a tractor, semi-trailer vehicle which permits investigation of either longitudinal or lateral traction characteristics of heavy truck tires. The system, shown in Figure 1, permits measurement of longitudinal properties by way of the trailer-configured dynamometer as it is towed and serviced by the instrumented tractor. Mounted on the same tractor is a structure supporting a lateral traction measurement system, as diagrammed in the plan view of Figure 2. Each test system is basically designed to expose a truck tire

Figure 1. The HSRI Mobile Truck Tire Dynamometer consisting of service tractor and longitudinal traction measurement trailer.

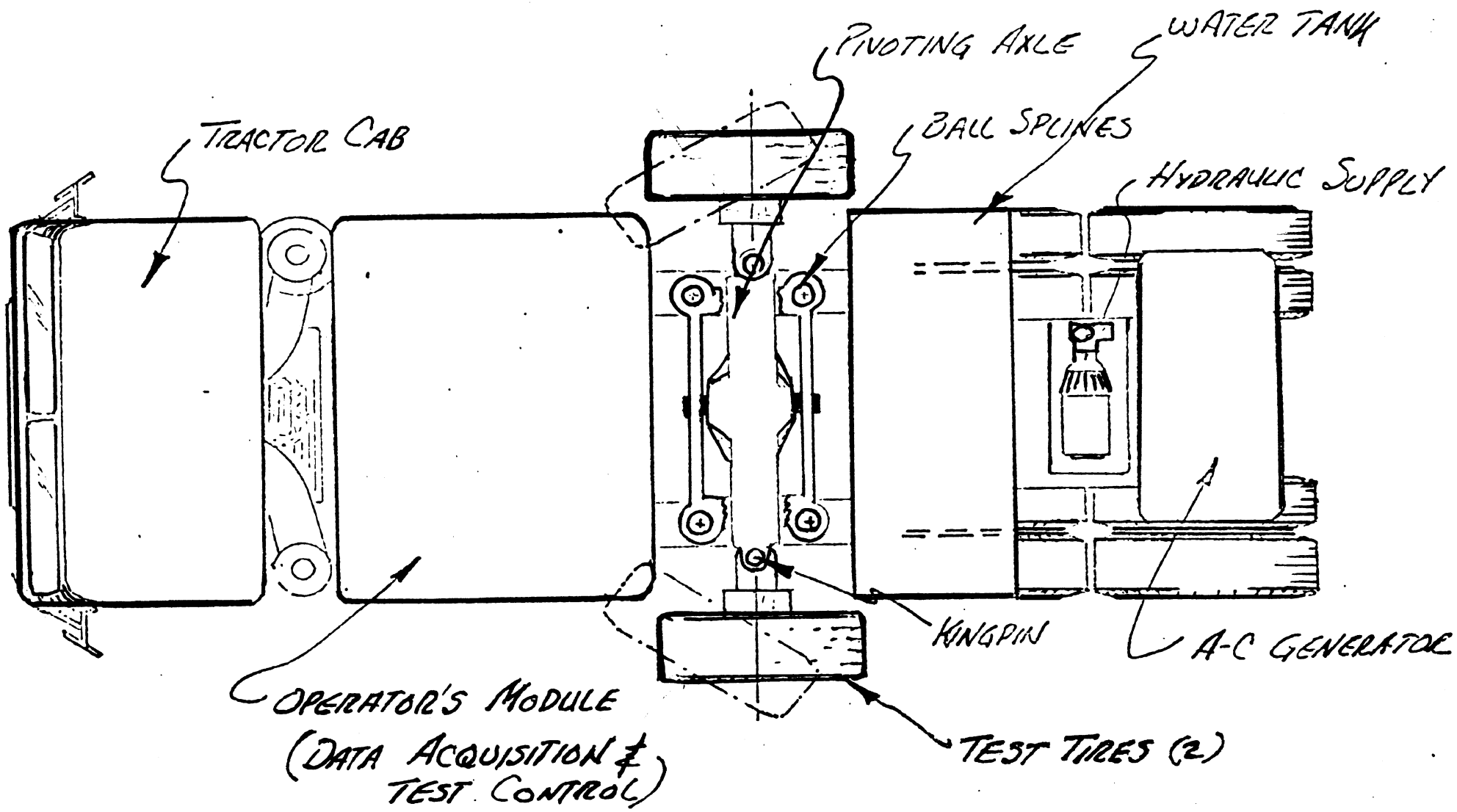

Figure 2. Plan View of Mobile Truck Tire Side Force Dynamometer

specimen to a set of operating conditions which cover the full range of possible loads, velocities, longitudinal or angular slip, and pavements such as can be encountered under either normal or emergency situations on the highway.

The longitudinal traction dynamometer, shown in Figure 3, is a welded trailer structure of pipe and plate sections, designed for economy of construction and for stiffness. The test wheel is situated approximately at the trailer c.g. position and is supported by a parallelogram suspension. This suspension configuration, shown in Figure 4, derives from attempts to achieve three fundamental qualities in a mobile traction measurement machine, viz.,

1) The elimination of kinematic interactions between the loads applied to the test wheel and resulting shear forces and moments.

2) The employment of a low-spring rate loading mechanism (an air spring), to assure the attainment of the desired load levels while neither (a) sacrificing frequency response in the vertical degree of freedom of the test wheel, nor (b) imposing a significant through-coupling of the vibrations of the foundation vehicle to the test wheel.

3) The minimization of the value of the "unsprung" mass, i.e., the mass which is displaced with the vertical motion of the test wheel spin axis.

The parallelogram linkage suspension is thus provided to assure kinematic isolation of forces while assuring a zero inclination (camber) of the test wheel plane.

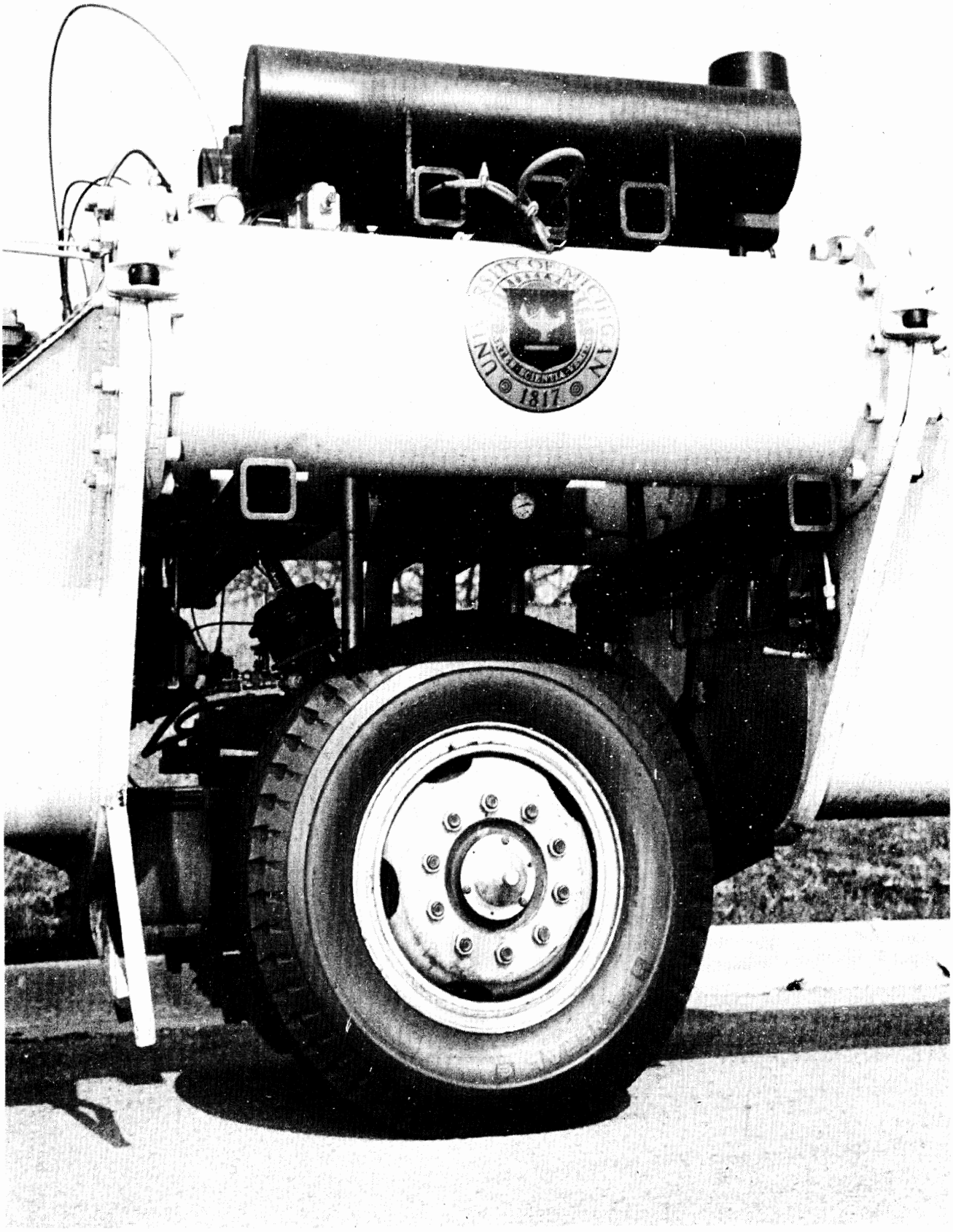

Figure 3. Test Wheel Mounted on the Longitudinal Force Trailer.

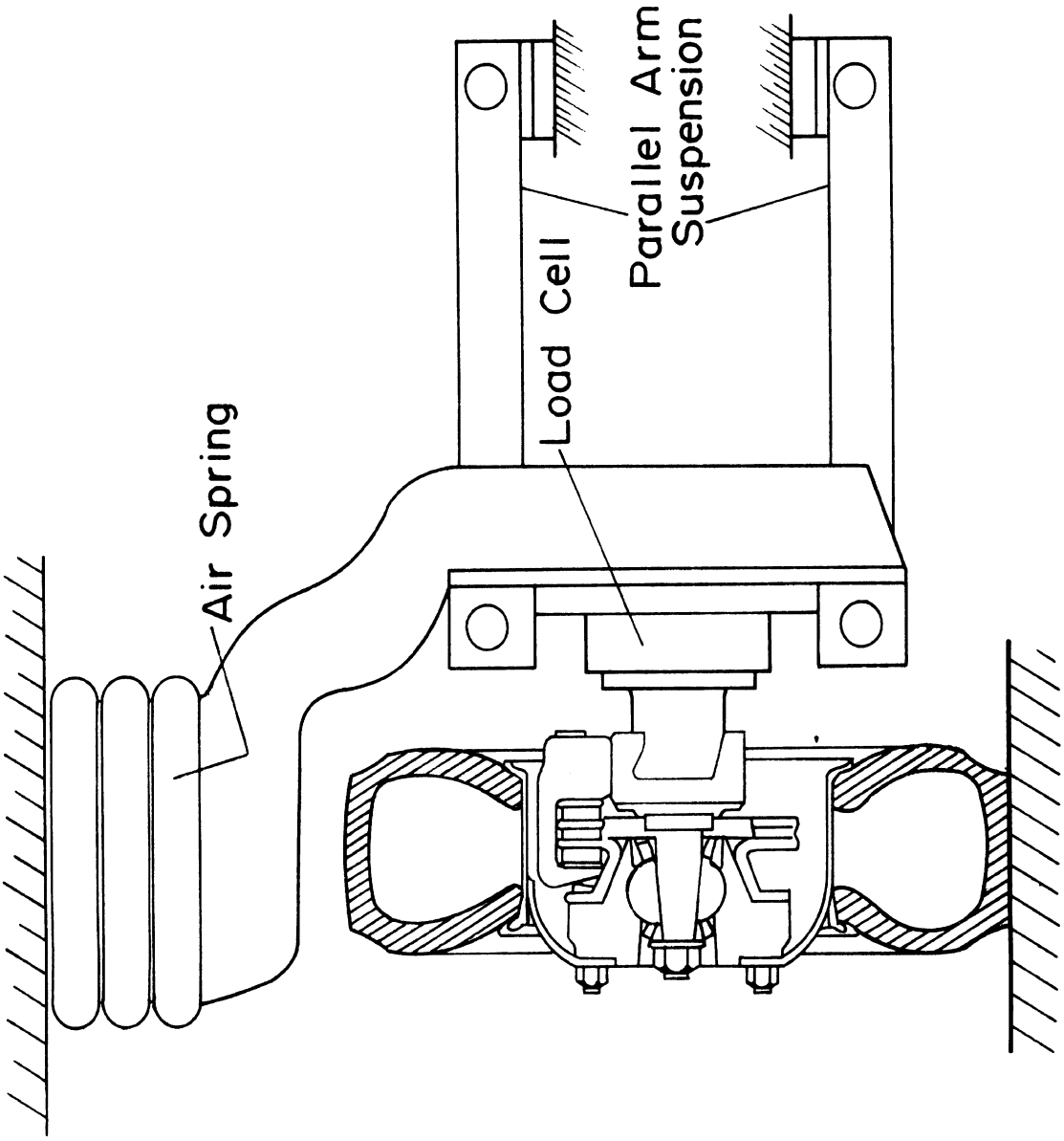

Figure 4. Test wheel suspension.

The use of an air spring loading mechanism permits a controllable vertical load condition and, in the case of the HSRI machine, imposes a nominally 350 lb/in coupling between the trailer and the test wheel—while operating at a common mid-range load of 5000 lb., F_z. At higher loads, the spring rate rises to a maximum value of 1000 lb/in at a load of 20,000 lbs., while the spring rate, of course, diminishes to zero at zero inflation of the air spring. These spring rates contrast with corresponding leaf suspension rates of trucks which are five to eight times stiffer at comparable rated wheel loads.

The basic design principle behind air spring loading, then, is that the machine incorporates a relatively "soft" loading member (which is also virtually frictionless) and thereby attains features which serve to enhance the quality of the vertical load condition which is imposed upon the test tire. With such a mechanism, it is then straightforward to obtain precision selections of vertical load through the use of commercially available precision regulators.

The unsprung mass which is associated with the vertical degree of freedom of the test wheel on the HSRI machine weighs 1850 lbs., when outfitted with a 10.00 x 20/F tire and the corresponding 20 x 7.50 disc wheel rim. By such a configuration, the "wheel hop" system indicates a natural frequency of approximately 5 Hz (for an effective radial spring rate of the tire of 5000 lb/in). In general, a high frequency wheel hop system permits a minimal vertical load fluctuation as the tire follows the varying profile of the test surface. In the design of HSRI's longitudinal force

dynamometer, the "quality" deriving from a reduced size of the unsprung mass was compromised with the obvious needs of strength, stiffness, and economy of construction of the wheel support assembly. The longitudinal force, F_x, vertical load, F_z, and brake torque, T_b, are transduced by way of a serial-mounted load cell. These signals, together with wheel angular velocity and vehicle velocity, constitute the primary data channels for the machine.

The nominal pitch and jounce trim of the HSRI trailer are controlled through the use of self-leveling air suspensions on both the trailer rear axle and the tractor rear tandem. Thus, as a given vertical load is transferred from the two respective axle sets to the test wheel, through inflation of the test wheel air spring, the tractor and trailer leveling systems adjust to a running equilibrium at which the trailer assumes its design trim attitude. The use of air suspensions on both ends of the trailer also contributes to attenuation of ride motions, thus further assuring quality in the vertical load condition.

The test trailer is capable of mounting any tire in the 20-inch rim size, and above, which is:

a) less than 46 inches in free diameter, and

b) 18 inches or less in maximum section width.

Tires can be loaded to a maximum level of 20,000 lb., although, to date, brake torque limitations have prevented the lockup of tires on high friction surfaces at loads exceeding about 15,500 lbs.

The lateral traction dynamometer shown schematically in Figure 5, mounts two tire samples on opposing steerable spindles outboard of the tractor's wheel

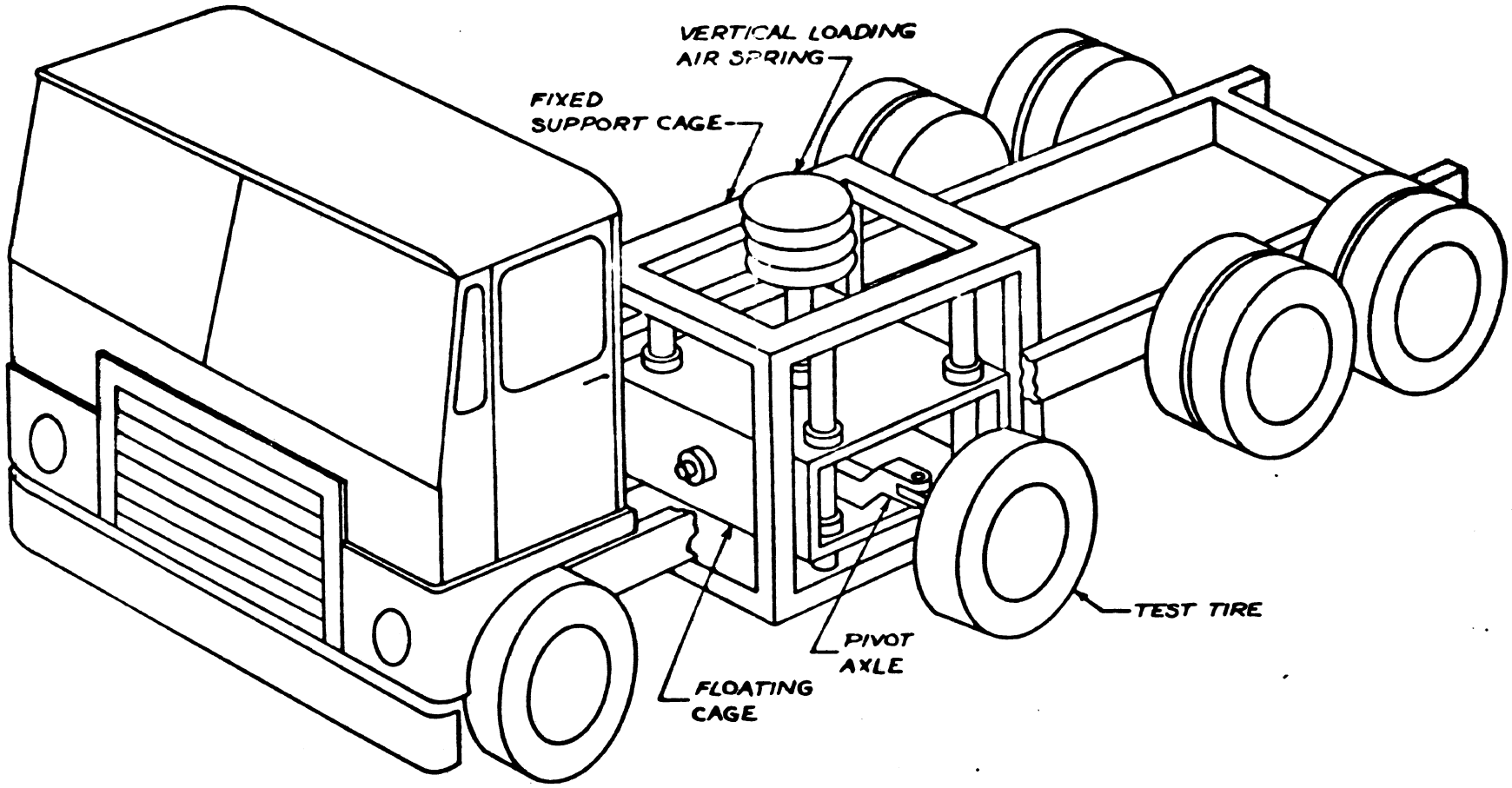

Figure 5. Major Components of the Side Force Dynamometer Assembly.

tracks. The two tires are "toed-in" together by an electrohydraulic servo system covering a slip angle range from -1° to +30°. The test wheel spindles are mounted upon a solid cross-axle which is constrained by a single longitudinal pivot pin.

The pin itself is fastened within a cage which can move only vertically, as constrained by a set of four ball-spline bearings. The vertically-"floating" cage is then loaded through inflation of a set of air springs. This machine thus incorporates a suspension designed to maximize the three "fundamental virtues" of mobile measurement described earlier—but for the more complicated case in which two tires are needed to achieve a side force equilibrium on the foundation vehicle. Clearly, the "pivot axle" arrangement provides for a load equalization between both tires while also providing a higher frequency response to road profile irregularities which are uncorrelated, side-to-side. The "floating cage" provides the needed kinematic isolation of the vertical load from forces in the ground plane by virtue of its rectilinear antifriction constraints. The air spring loading configuration again provides for precision load selection while incorporating a low spring rate coupling between the unsprung mass(es) and the foundation vehicle.

The two wheel spindles are "steered" to equal but opposing slip angles by an electrohydraulic servo system which incorporates two sets of actuating cylinders as shown in Figure 6. The linkage arrangement which mechanically couples both spindles together permits the use of a single control loop, operating on the feedback signal from the one instrumented wheel while assuring common slip angles, side to side, even in the event of a servo power failure.

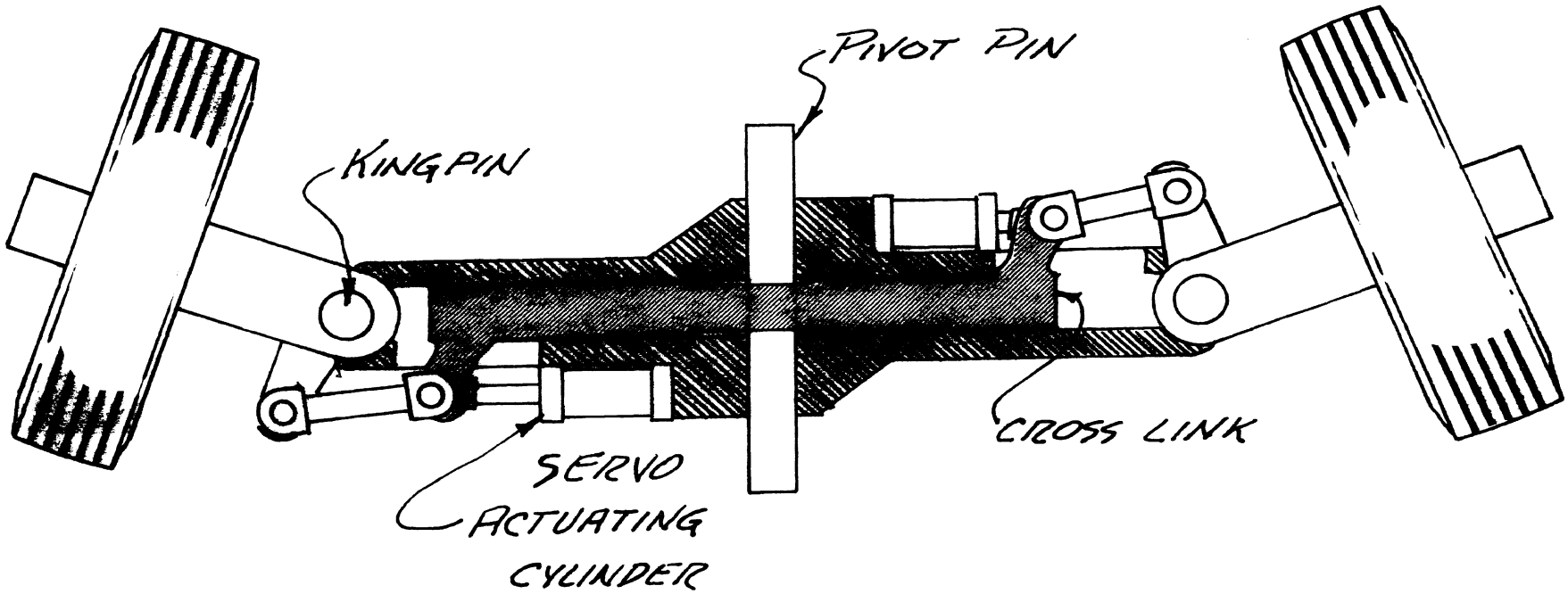

Figure 6. Section View of Pivot Axle with Steering Servo Linkage.

The system permits mounting of any tire within the 30" to 48" range of free diameters and which is less than 18" in cross-section width. The measurement of tire force and moment conditions is achieved by way of a serial multicomponent load cell which transduces lateral and vertical force components as well as aligning moment.

Data signals from either the longitudinal or lateral test apparatuses are conditioned and recorded within a tractor-mounted module. The module serves as a self-contained data acquisition laboratory as well as the operator's station for selecting and initiating test control functions. As shown in Figure 7, the operator's module provides an array of hard-wired electrical controls in addition to certain pneumatic and hydraulic control elements.

MEASUREMENT PRACTICES AND EXPERIENCE

While the total mobile test system described here is currently operational, the lateral force dynamometer is only beginning its initial program of experiments and is cited in this paper merely as an up-to-date reporting of HSRI test capabilities. The longitudinal force trailer has been utilized in a program of baseline experiments, providing data which is presented in the remainder of this paper. For a detailed discussion of the data presented here, the reader should consult Reference (4).

The measurement of longitudinal traction properties has involved the repeated execution of a basic test cycle over a range of loads, velocities, pavements, and

Figure 7. Data Acquisition Module on Tractor.

tire samples. The test cycle incorporates the wheel spin-down transient shown in Figure 8. This time history derives from a controlled-onset brake torque application followed by an automatic brake release. By means of an appropriate throttling valve setting, the flow of air into the chambers of a dual-wedge drum brake is controlled to provide a gradual approach toward the peak force condition, thus increasing the quantity of data gathered in the vicinity of the peak longitudinal force. The locked-wheel condition is constrained to approximately 150 milliseconds duration to minimize the load variations that derive from "flat-spotting," as reported previously (2, 3).

In preparation of a new sample for testing, a tire is "broken-in," on the test machine, for a distance of approximately 10 miles, and at a velocity of 40 mph, followed by the execution of six preliminary "lockup cycles" for purposes of removing any surface contaminants remaining from the tire molding process.

It has been rationalized that customary preparations employed in passenger car tire testing, such as utilization of a 100-mile free-rolling break-in practice, are most likely inappropriate for preparation of heavy truck tire samples, given that the slip energy experienced in a single lockup far exceeds the accumulated work history encountered during the free-rolling practice. Accordingly, the initial application of six lockup cycles is seen by HSRI as a more satisfactory method for assuring that the sample experiences the necessary transition in tread surface conditions prior to data-taking. It would appear from data which are presented later that the tires examined in HSRI's initial test sample did indeed exhibit a quite stable

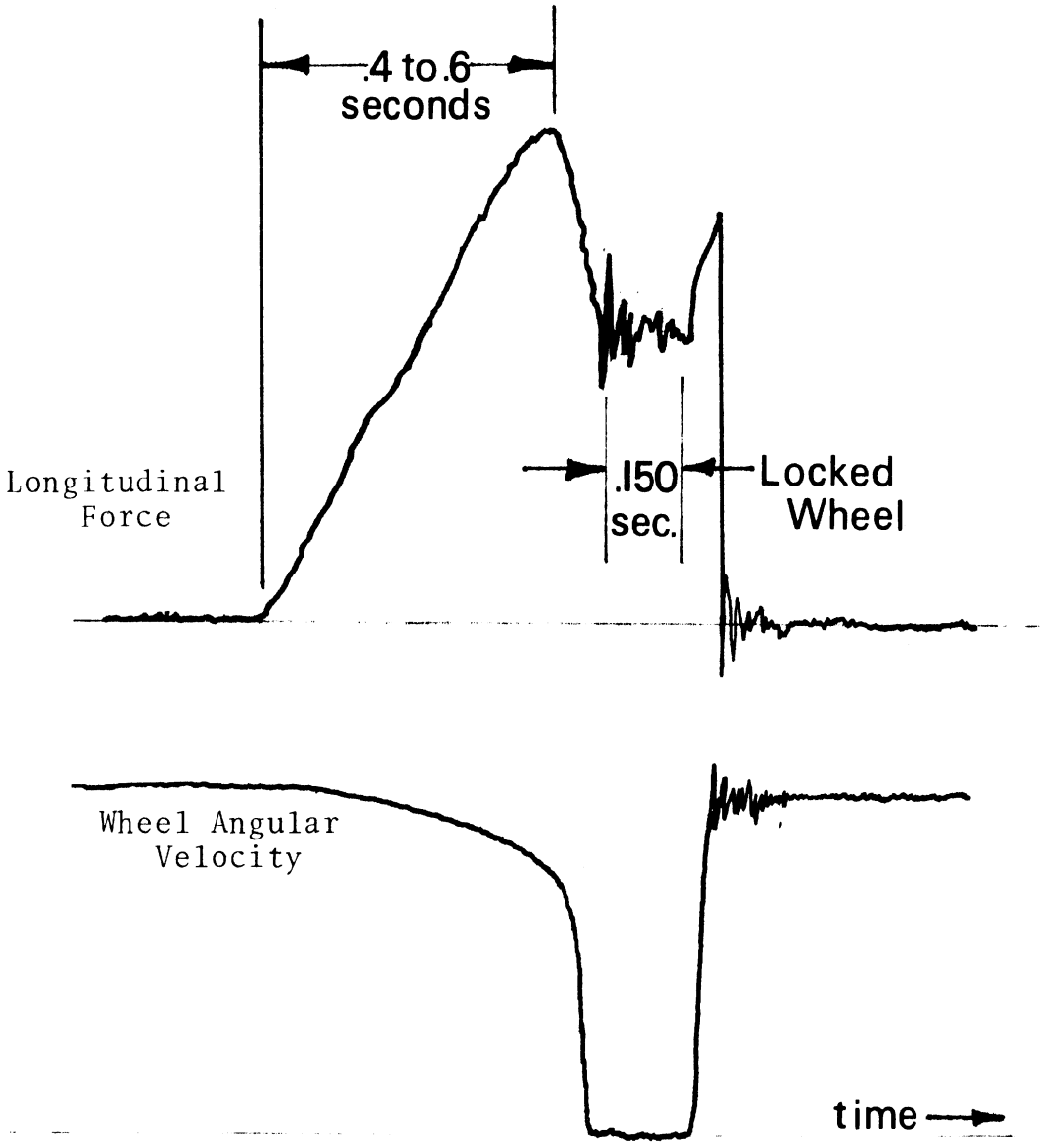

Figure 8. Approximate time scale of the basic "lockup cycle."

traction performance over the sequence of test runs, following the indicated break-in procedure. The need for such a break-in practice, however, has not been explored.

In HSRI's mobile experiments, raw data has been recorded directly on FM analog tape and subsequently processed through a hybrid computer system. Final calculations of averaged traction performance have been performed digitally and all filtering has incorporated no-phase-lag digital techniques.

In processing the data gathered at low test velocities in HSRI studies, it was observed that the longitudinal traction force which accrues at the locked-wheel condition can involve a transient process, probably thermal in nature, which spans a significant range of F_x values. As shown in Figure 9a, the F_x time history for a lockup cycle at 3 mph indicates a time-dependency in the F_x response, following achievement of 100% slip. (The locked-wheel value is sustained here through manual override of the automatic brake release circuit.) The non-single-value relationship between F_x and slip causes the "slide" value of F_x (such as was calculated during processing) to assume a value which is somewhat below the initial value of F_x at 100% slip and above the "steady-state" value. The implications of this F_x time-decay phenomenon are illustrated in Figure 9b in which are plotted the "μ-slip" (that is, normalized longitudinal force, F_x/F_z versus longitudinal slip, s), curves obtained for a single 10.00 x 20/F tire over the examined range of velocities. The time-dependent "tails" are manifested visibly on the 3-mph and 10-mph curves but are indistinguishable at higher velocities. In the processing of data presented in this paper, the F_x/F_z value at 100% slip was determined

Figure 9a. Time dependence of locked-wheel value of F_x - at a test speed of 3 mph.

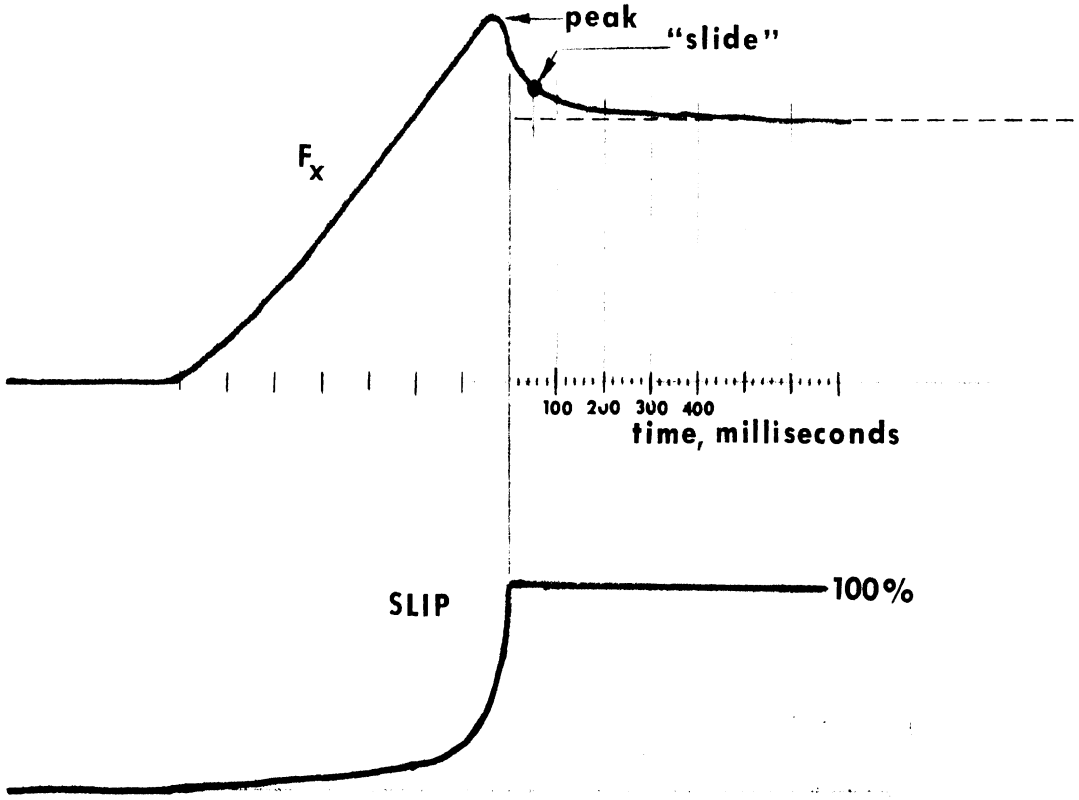

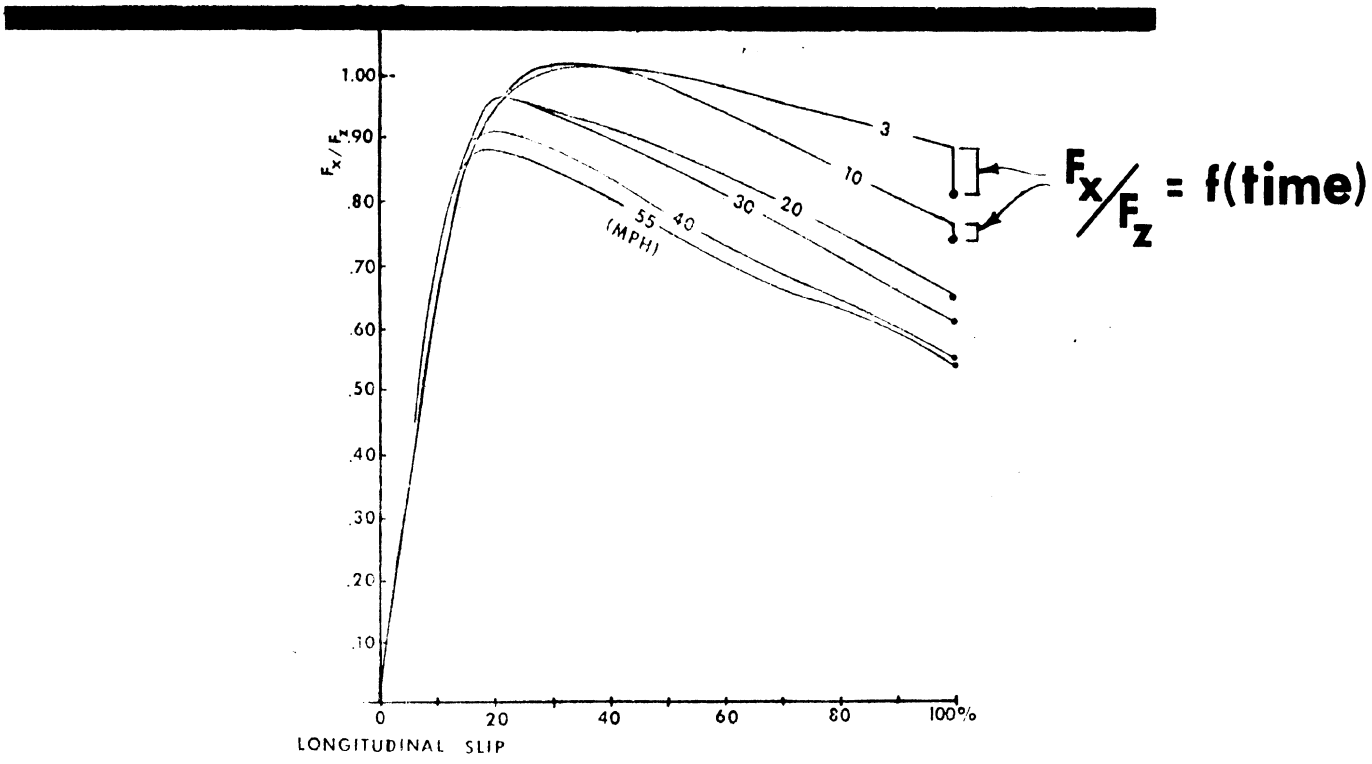

Figure 9b. Implication of locked-wheel time dependency on an array of "μ-slip" curves.

by averaging the digital samples accumulated over the first 100 msec. following the detection of 100% slip. Thus the time-dependent behavior at low velocities has not been routinely characterized in the data which are to follow.

DATA DESCRIBING BASIC LONGITUDINAL TRACTION SENSITIVITIES

In Figure 10, a typical summary of μ-slip curve-shapes is shown, indicating load sensitivity on the left and velocity sensitivity on the right. All load-sensitivity runs were made at a nominal velocity value of 40 mph; all velocity-sensitivity runs were made at a vertical load value nominally equal to the Tire and Rim Association load rating for each respective tire.

In terms of overall curve shapes, the data in Figure 10 confirm the large fall-off in F_X/F_Z from the peak to the 100% slip condition, as was reported in previous work (2, 3)—a dry pavement traction characteristic whose proportions clearly distinguish heavy truck tires from passenger car tires. It is significant to note also that the μ-slip curves representing differing load conditions are virtual scale models of one another throughout the slip range, while gross changes in curve shape are seen to accompany the differing velocity conditions. In terms of the mechanisms of longitudinal force production, it appears that a linear sensitivity of tread rubber friction to the relative velocity in the contact patch accounts for the bulk of the observed velocity influence on traction performance in the high-slip regime.

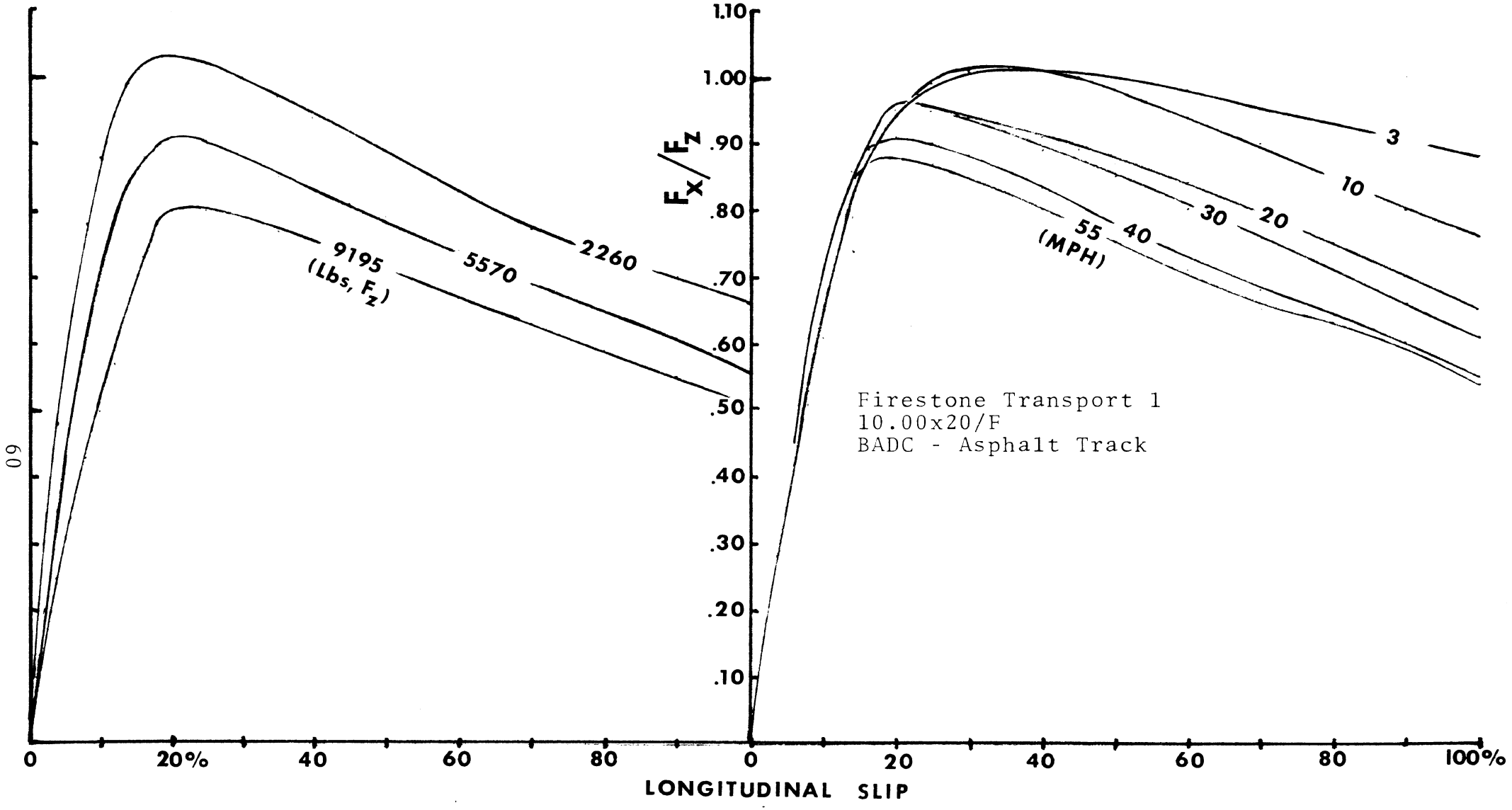

Figure 10. Typical load and velocity influences on the F_x/F_z versus slip behavior of a 10.00x20/F tire.

As shown in Figure 11, the non-normalized F_x versus slip curves verify a first-order dependency of so-called longitudinal stiffness (C_S) on vertical load where

$$C_S = \left.\frac{\partial F_x}{\partial s}\right|_{s=0}$$

The C_S parameter is characteristically influenced by vertical load because of the increasing length of the tire-road contact patch with increased load. In the data presented, the load range is sufficiently broad that the C_S versus F_Z relationship is seen to stiffen markedly at the higher load level. As expected, however, C_S has been found to be unaffected by variations in velocity as was illustrated in the normalized data curves of Figure 10.

The "μ-slip" data (such as shown in Figure 10) has been reduced further to yield numeric characterization of F_X/F_Z at the peak of the curve and at the 100% slip (or "slide") point. These peak and slide characterizations are utilized here to illustrate a variety of basic findings.

Let us examine, first, the variation in performance measured for a six-tire sample on an asphalt pavement. Figure 12 summarizes the sample's traction sensitivity to normalized vertical load, i.e., $F_Z/F_{Z(rated)}$. On recognizing that the tire sample included four "F"-rated tires (open symbols) and two "H"-rated tires (closed symbols), we note that the traction data produced by the tires having a common load-range rating are rather tightly grouped, especially

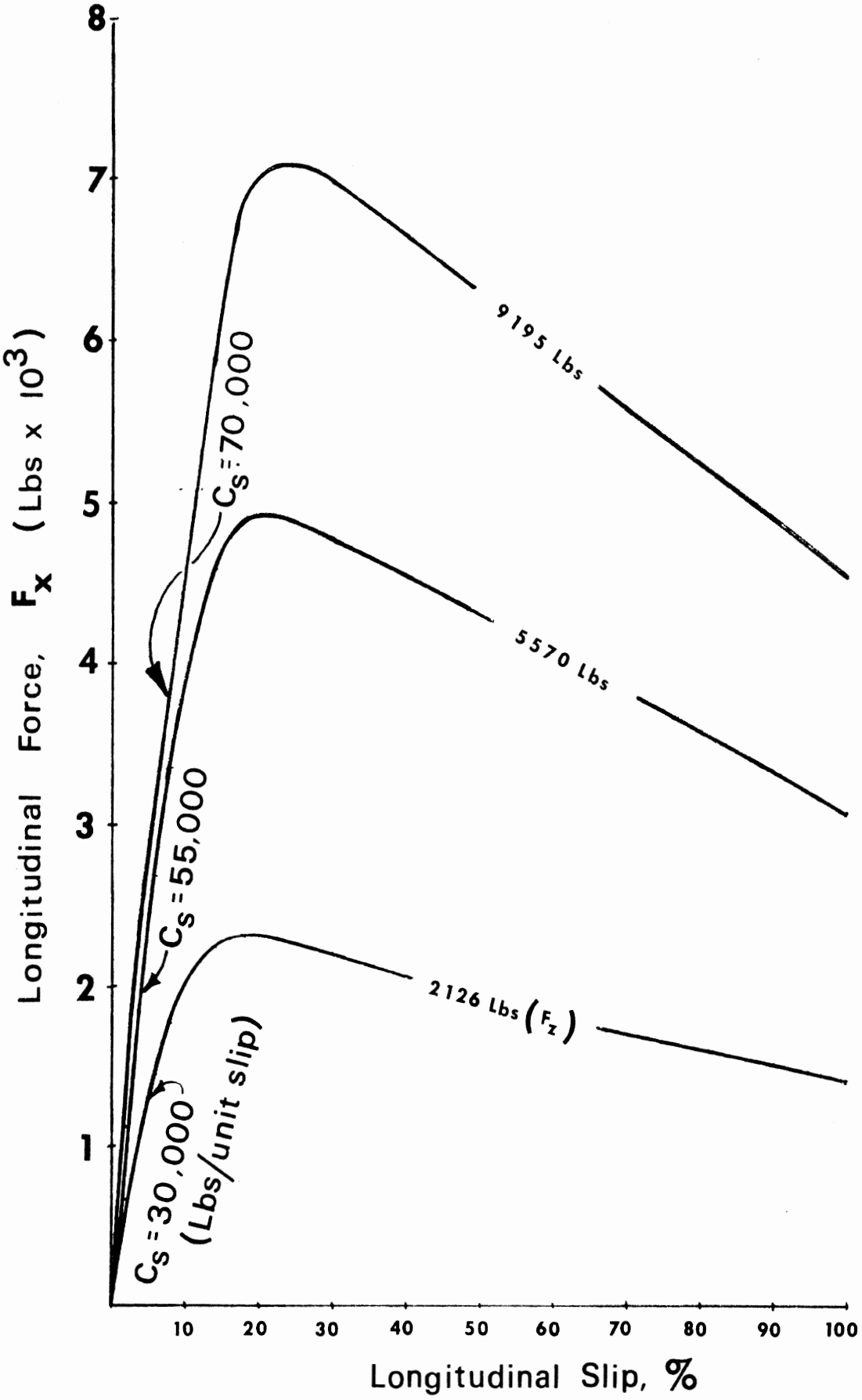

Figure 11. Influence of vertical load on the non-normalized (F_x) versus slip behavior of a Firestone 10.00x20/F on the BADC asphalt surface.

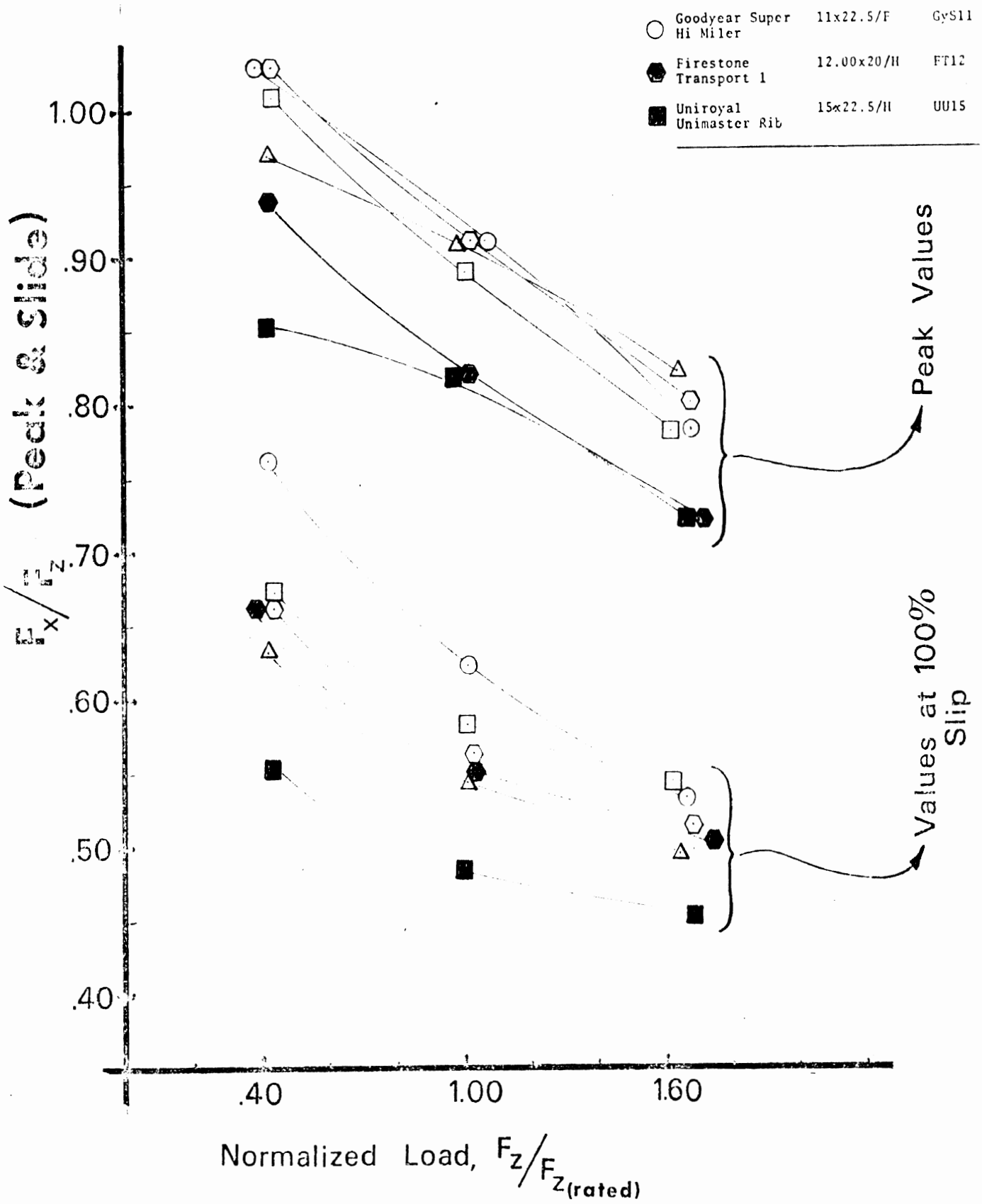

Figure 12. Normalized load sensitivity in the peak and slide traction of the six-tire sample (on BADC's asphalt).

with regard to peak values. It is surprising, however, that the size 15 x 22.5/H wide base single tire (code UU15) provides such a small increment in normalized traction when the load is reduced from the rated value (8460 lbs) to 0.4 of the rated value (3380 lbs). This performance suggests, for example, that the wide base single is less suitable for operation at lower loads than tires which are rated in the lower load range. As shown in Figure 13, with vertical load (non-normalized) plotted on the axis of abscissa, the wide base tire provides a reduced tractive performance (compared to 10.00 x 20/F's) when the value of F_z is below about 8000 lbs. Thus the notion that one can "tire-up" to resolve stopping performance deficiencies in heavy trucks may not be a universal axiom.

Figure 14 illustrates the influence of velocity on the normalized traction behavior of the six-tire sample as measured on the asphalt pavement. The data show a rather narrow band within the respective peak measurements and slide measurements across the tire sample, with consistent gross trends exhibited in all cases. The data in Figure 14 again place the H-rated tires (codes FT12 and UU15) at the lower boundary of performance for these experiments in which each tire was operated at its rated load.

To characterize the repeatability of the data presented in Figures 12 through 14, the data obtained from a set of five repeat runs which were interspersed within data runs for each tire are plotted in Figure 15. Each repeat run represents the average of six locking cycles conducted at 40 mph and the T & RA rated load on each tire. Data points are presented, left to right, in the order in which they were gathered. Below each

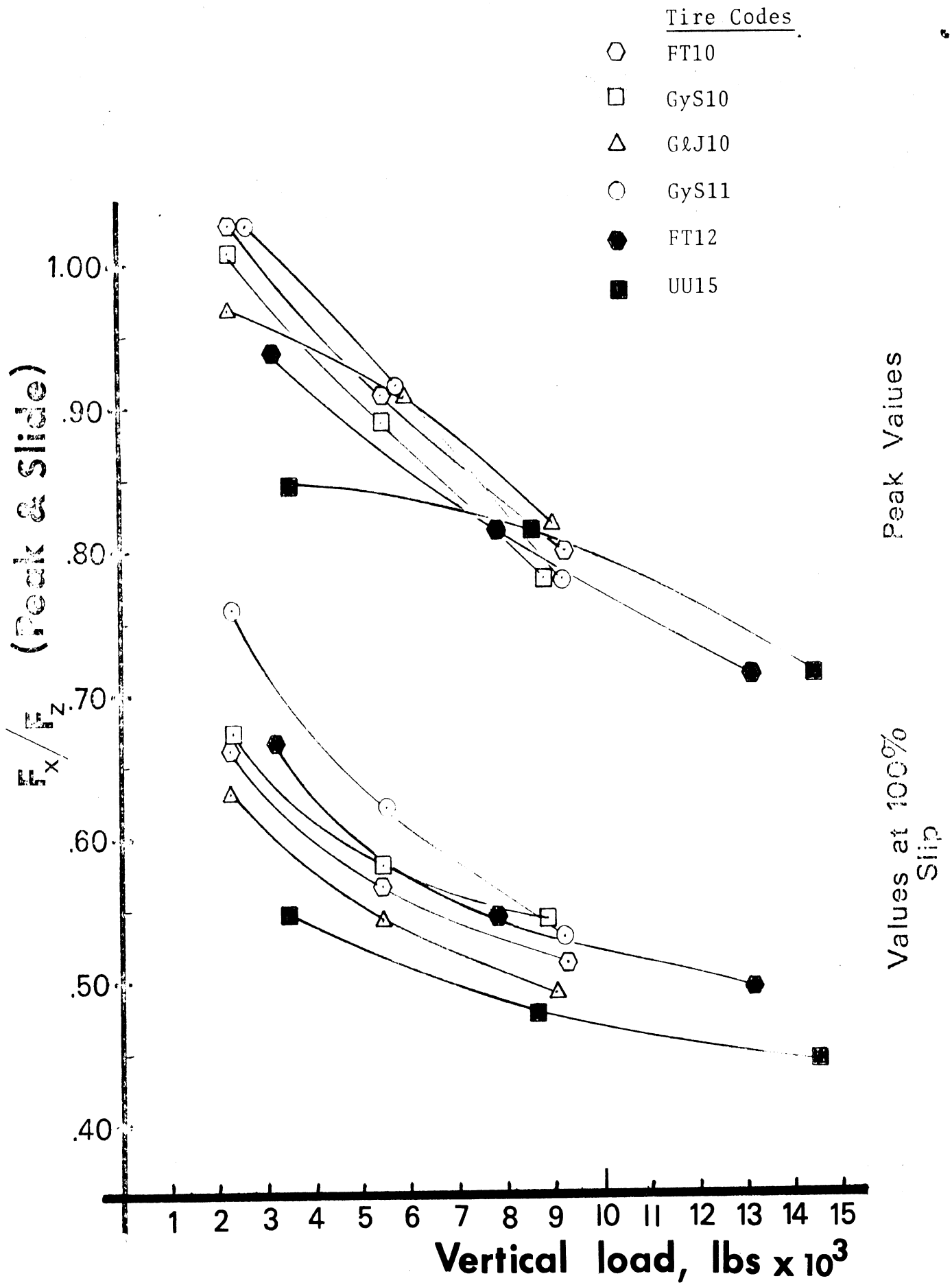

Figure 13. Load sensitivity (non-normalized abscissa) in the peak and slide traction of the six-tire sample (on BADC asphalt).

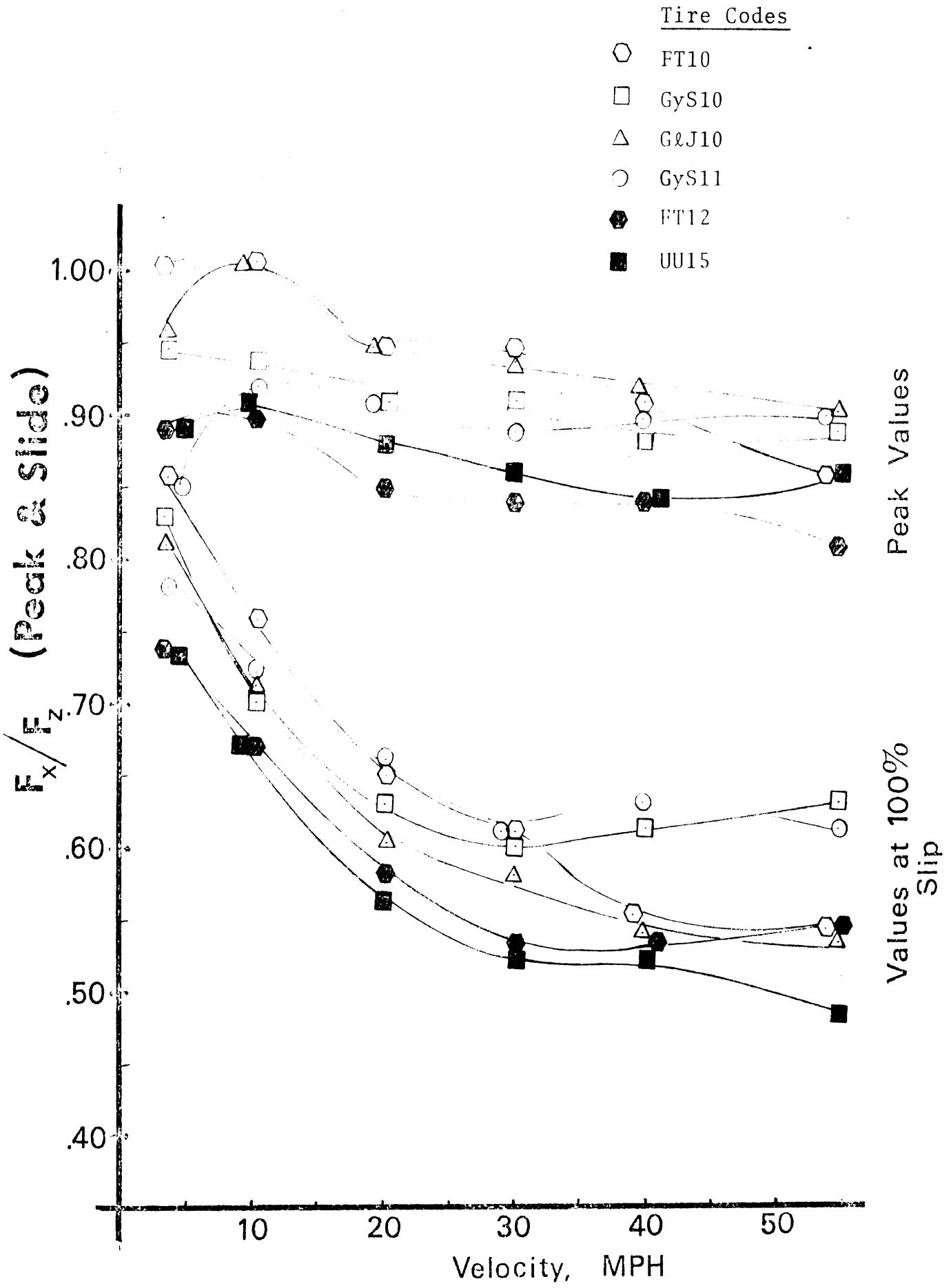

Figure 14. Velocity sensitivity of the peak and slide traction values for the six-tire sample (on BADC asphalt).

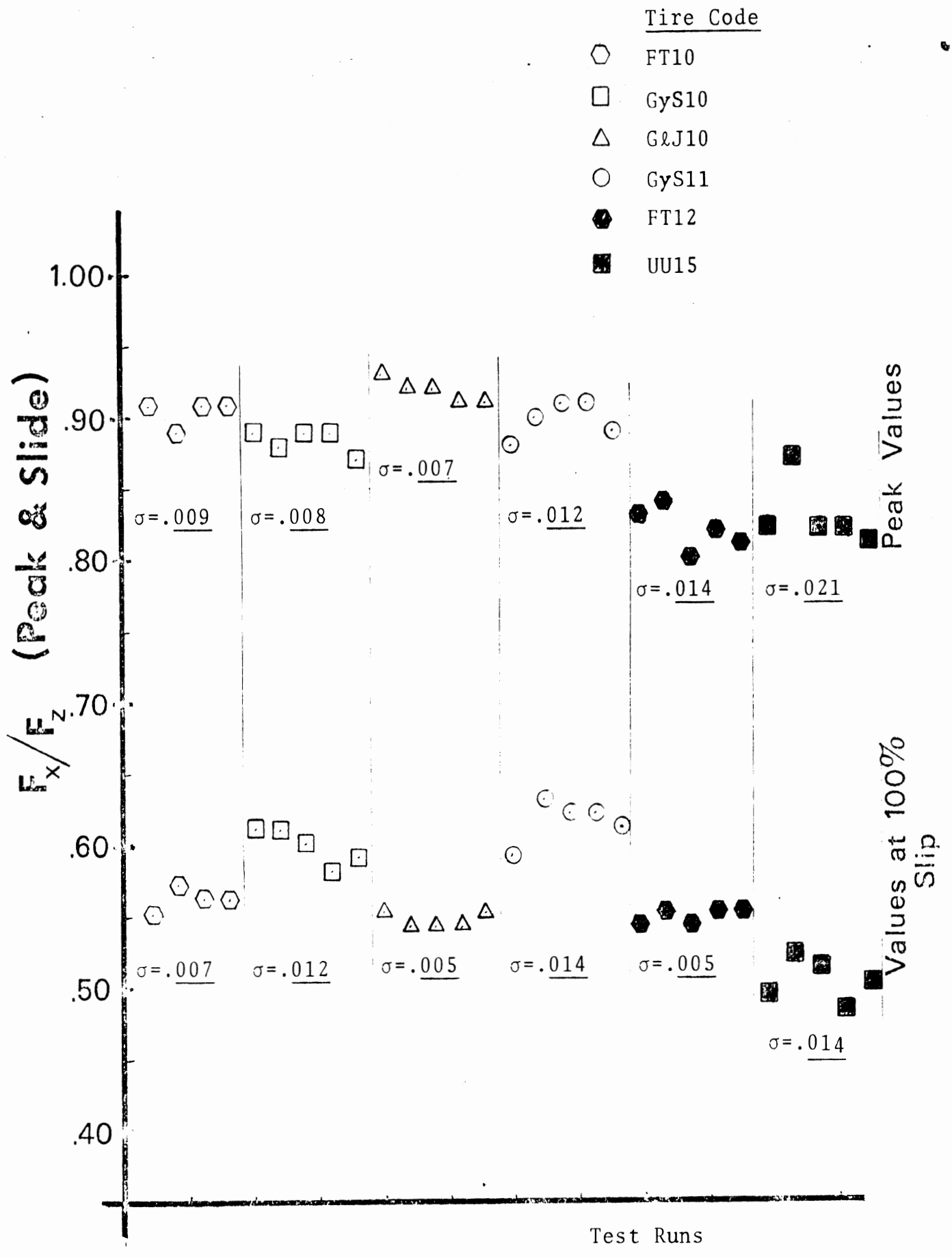

Figure 15. Peak and slide traction measures deriving from repeat runs of each of the six tires tested on the asphalt track at BADC.

group of peak and slide data presented in Figure 15 for each tire, the standard deviation of the measures is printed. In general, the indicated repeatabilities are of considerably higher quality than is observed, say, in peak readings gathered using ASTM skid trailers. In addition to the observed repeatability, it is most significant to note that the test process is causing no monotonic trend in peak/slide characteristics as a function of work history. Thus we have concluded that each tire sample was behaving in a stable fashion throughout the sequence of test runs.

To demonstrate the influence of pavement surface characteristics on peak and slide traction, results have been summarized as load and velocity sensitivities for a baseline tire tested on four different test surfaces. Figure 16 illustrates the extent to which the four pavement selections altered the load sensitivities of this tire. While there appears to be a changing rank among the surfaces in terms of the peak and slide traction values, the two asphalt surfaces which were examined generally provided higher peak traction performances than did two concrete surfaces.

Figure 17 indicates the influence of the pavement differences on velocity sensitivity. Whereas previously reported measurements indicated a profound difference between peak traction performances on concrete and asphalt, these data show basically comparable trends among the two asphalt and two concrete surfaces.

To characterize the statistical repeatability of the data describing pavement influences, the "check run" values of peak and slide traction are plotted for each of two baseline tires in Figures 18 and 19. As before,

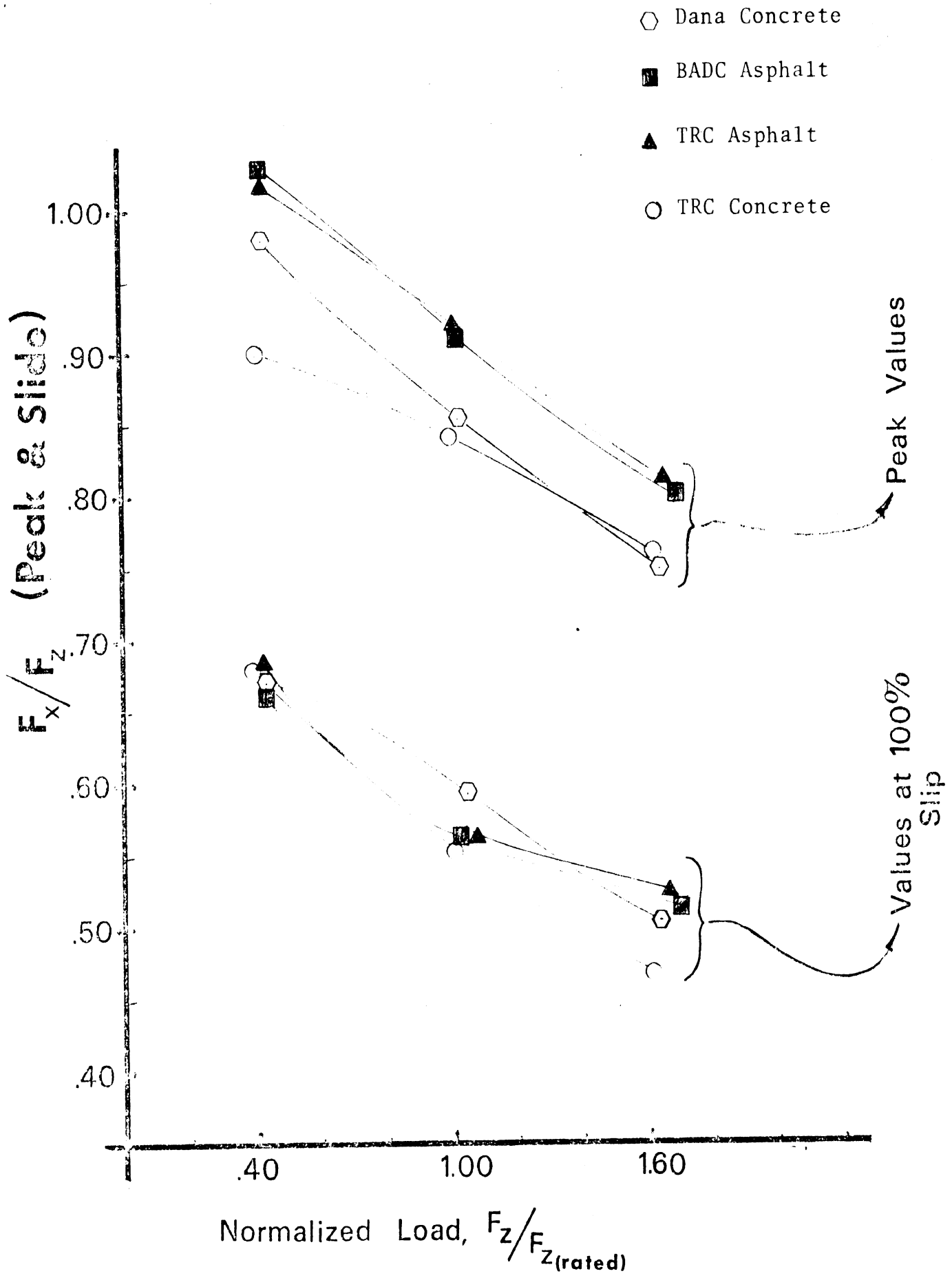

Figure 16. Influence of normalized load on the peak and slide traction of the Firestone Transport 1 (10.00x20/F) on four surfaces.

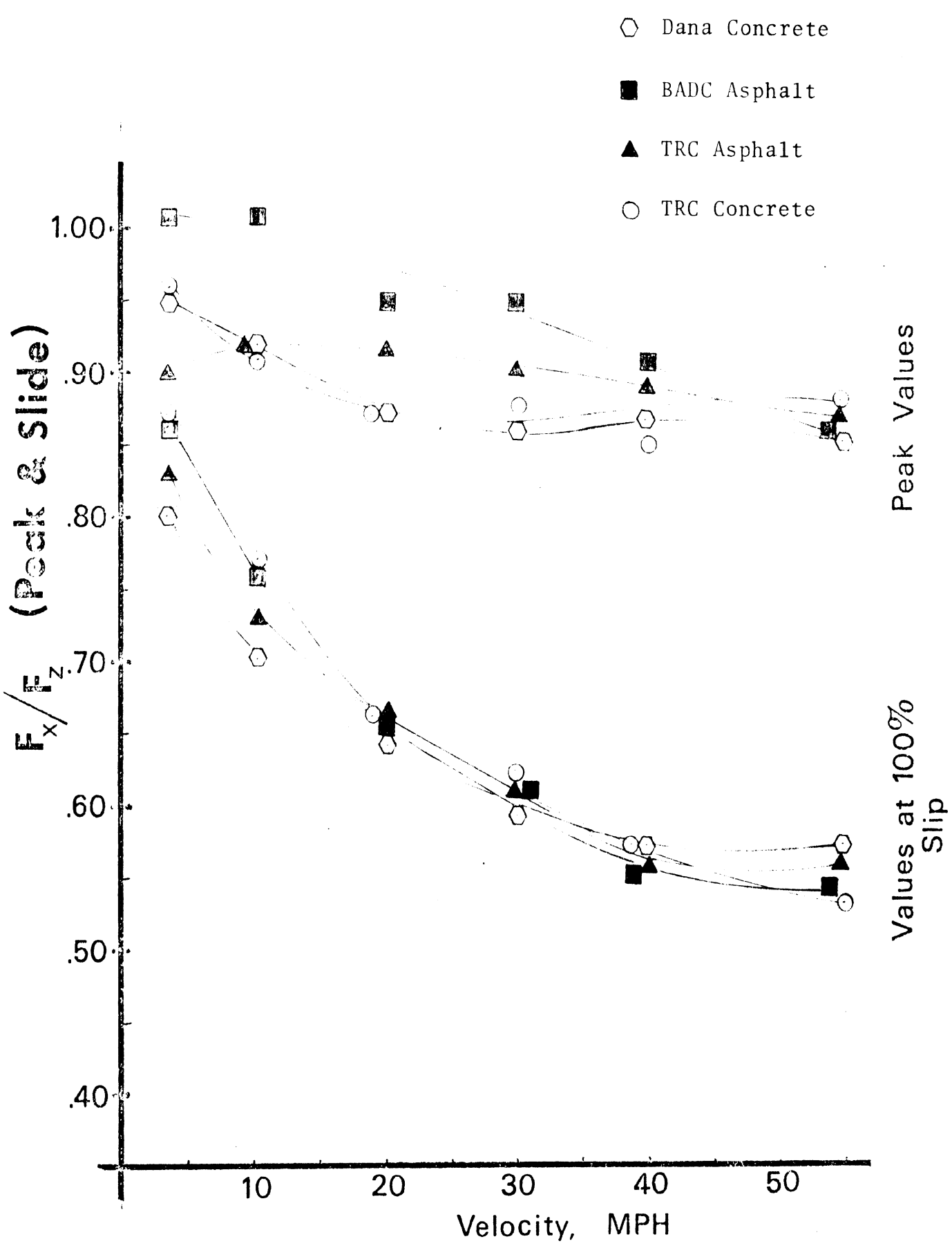

Figure 17. Influence of test velocity on the peak and slide traction of the Firestone Transport 1 (10.00x20/F) on four surfaces.

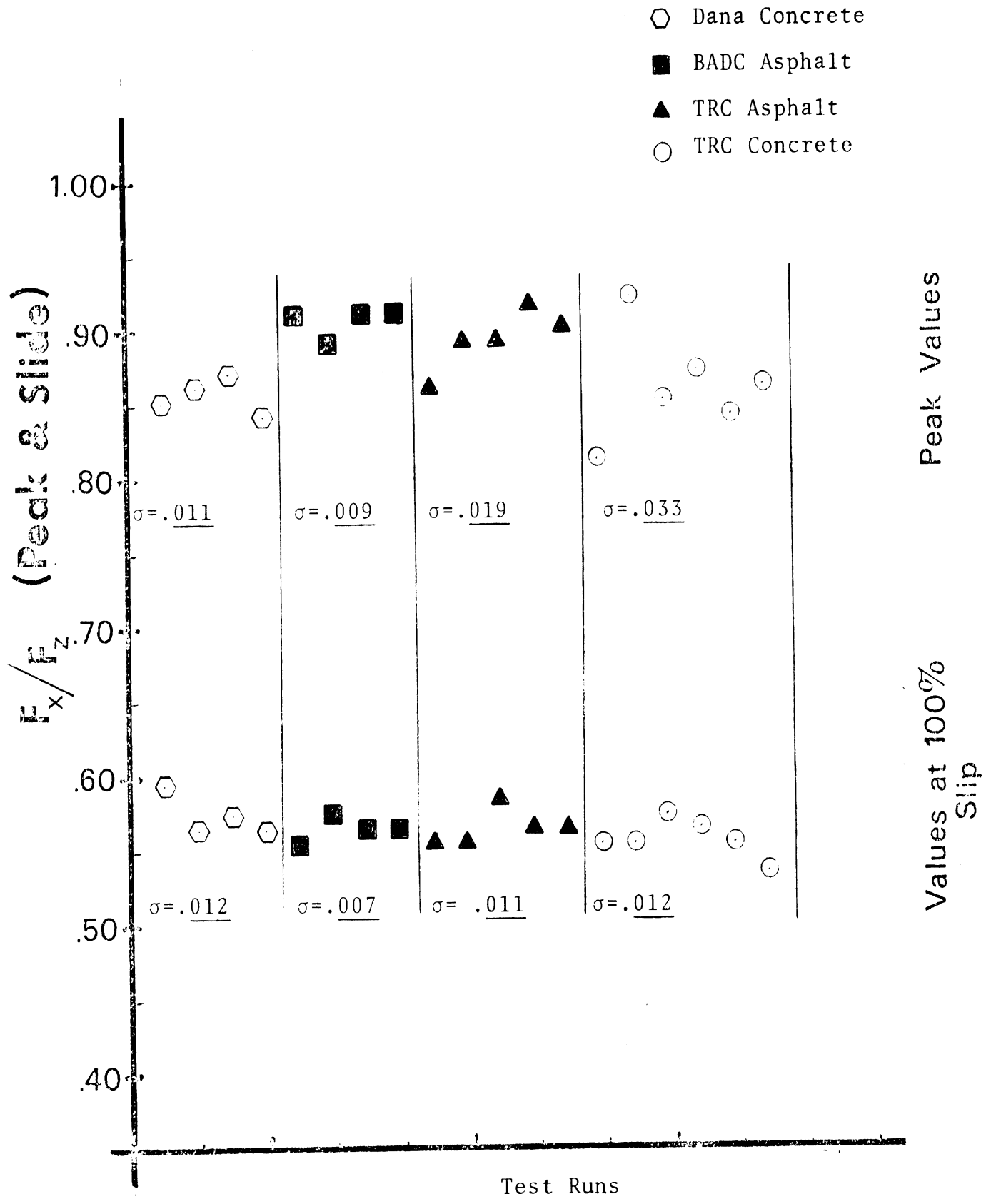

Figure 18. Peak and slide values deriving from repeat runs of the Firestone Transport 1 (10.00x20/F) on four surfaces.

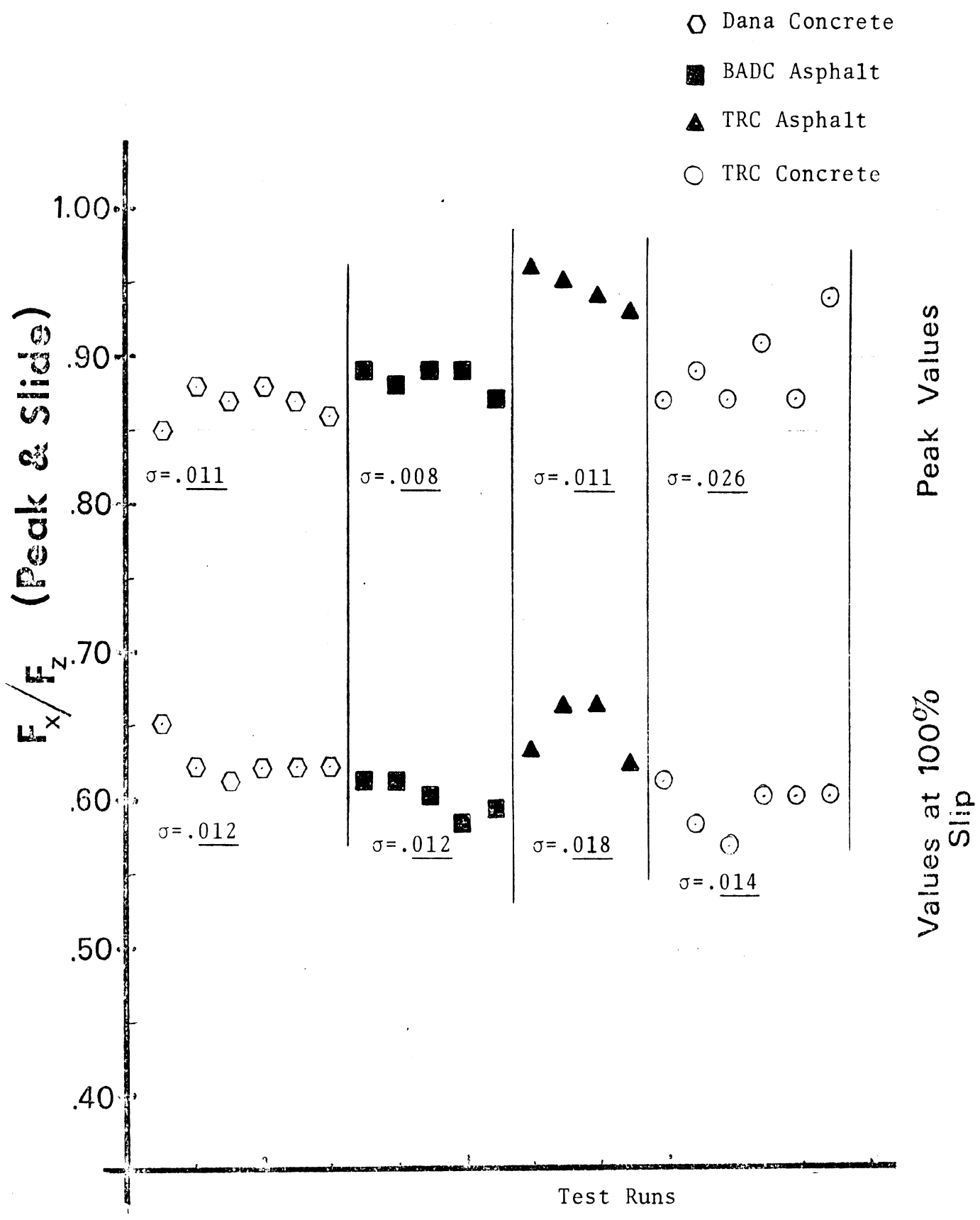

Figure 19. Peak and slide values deriving from repeat runs of the Goodyear Super Hi Miler (10.00x20/F) on four surfaces.

these data points are plotted from left to right as they were acquired. It is significant to note that the higher variability in the repeated check run measurements indicated for the TRC-concrete data is common to both tire samples. It is believed that this variability derives from a spatial inhomogeneity which characterizes the TRC Hi Speed Track facility. As a consequence of a pavement grinding operation which was employed to correct certain "high spots" which ensued from the paving process, there exist areas of differing surface texture (and apparently differing friction potential), among which areas HSRI did not discriminate in conducting its traction experiments.

Comparing the repeatability data presented in Figures 18 and 19 and previously in Figure 13, it would appear that the repeatability of measurements of truck tire longitudinal traction depends more upon pavement uniformity than upon the stationarity of innate tire properties.

CONCLUDING REMARKS

This paper has presented a mobile test system which has recently been developed to permit measurements of truck tire traction behavior. While this apparatus is not totally unique in its capability, it represents the only such hardware outside of private industry. As such it represents a most significant means by which truck tire traction data can and will continue to be presented in the open literature.

Although the data which have been presented herein represent a limited examination of an important group of traction influences, it is believed that they

establish, to first order, the behavioral mechanisms involved in the generation of longitudinal traction by truck tires on dry surfaces.

Clearly, much more experimental work needs to be done, and the results made available, before the general field of truck tire traction mechanics can be called a technology. A broader base of truck tire longitudinal traction data is needed to establish the degree of generality which is applicable to findings presented herein. Experiments should also be designed and conducted to investigate, on an elemental level, the mechanics of dry traction such as applies to the operating conditions and tread materials of heavy truck tires. Insight into the mechanisms involved in the profound peak-to-slide "fall-off" of heavy truck tires operating on dry pavements would be useful to the development of an adequate semi-empirical model of the process and for the design of tires with improved braking performance at high slip.

Efforts should also be directed at the development of a standard practice in truck tire preparation that is both maximally efficient and comprehensively effective in assuring stable, representative samples for testing.

Finally, the work being done at HSRI and elsewhere to investigate the longitudinal traction mechanics of truck tires should be expanded into the angular slip and combined slip portions of the traction field so that a comprehensive understanding of this critical truck component can be developed.

REFERENCES

1. Bradisse, J.L., Ramsey, A.F., and Sacia, S.R., "Truck Tire Traction Trailer," Society of Automotive Engineers Paper No. 741138, November 1974.

2. Ervin, R.D. and MacAdam, C.C., Baseline Tests of the Longitudinal Traction Properties of Truck Tires, Highway Safety Research Institute Report No. UM-HSRI-PF-74-6, April 1974.

3. Ervin, R.D. and Fancher, P.S., "Preliminary Measurements of the Longitudinal Traction Properties of Truck Tires," SAE Paper No. 741139, November 1974.

4. Ervin, R.D., MacAdam, C.C., and Fancher, P.S., The Longitudinal Traction Characteristics of Truck Tires as Measured on Dry Pavements, Highway Safety Research Institute, Univ. of Michigan, Report No. UM-HSRI-PF-75-3, February 1975.

5. Bird, K.D. and Martin, J.F., "The Calspan Tire Research Facility: Design Development and Initial Test Results," SAE Paper No. 730582, 1973.

MEASUREMENT AND PREDICTION OF COMMERCIAL VEHICLE BRAKE TORQUE

T.M. Post
Highway Safety Research Institute
The University of Michigan

ABSTRACT

A new test vehicle has been developed at HSRI to measure time histories of brake torque over-the-road at nearly constant velocity. Four truck air brakes were used in an initial test program which included tests to assess the influence of brake pressure, rubbing speed, and drum temperature on brake torque. Special tests were included to measure hysteretic effects.

The results from the program were used to develop a semi-empirical formula to simulate torque as a function of time during a spin-down process.

INTRODUCTION

The last few years have witnessed the promulgation of government safety standards which have significantly increased the demands to be met by commercial vehicle brakes. The most notable standard is FMVSS 121 (1)*, which stipulates maximum stopping distances for many commercial vehicles, and minimum torque requirements for commercial vehicle brakes. Since this standard requires a significant upgrading of commercial vehicle brakes, much recent interest has been generated in brake testing.

Compliance with the brake torque requirements of FMVSS 121 is based on an inertial dynamometer test, in which time histories of torque are measured as a function of brake line pressure and initial velocity during spin down. Inertial dynamometers suitable for these measurements have for years been a primary test tool used by brake manufacturers to characterize their brakes, usually through an average torque value during the spin-down cycle. However, the current interest in brake fade (particularly with regard to the loaded 60 mph facets of FMVSS 121) and hysteresis during antilock cycling (the wheel lock provisions of the standard have caused the vehicle manufacturers to adopt antiskid braking systems in many cases) have made it desirable to be able to measure torque as a function of time at a constant wheel spin rate. Such a constant speed device has been developed at the Highway Safety Research Institute of The University of Michigan (2). In the present paper, some results from the initial brake test program of this device are reported (3). In addition, some analytic modeling in

---

*Numbers in parentheses designate References at end of paper.

which the brake torque time histories are simulated is presented. The parameters used in the analytic model were chosen to reflect the results and conclusions of the test program.

EXPERIMENTAL APPARATUS

The brake test device makes use of a modified tractor-trailer and associated apparatus (Fig. 1). It is outfitted with modular items which supply electric and hydraulic power, and an operator's station contained in the forward module. The unique feature of this device is that it operates at nearly constant velocity. It can be used as either a truck tire tester or a truck brake tester. It is capable of handling up to 20,000 lbs. of vertical load and 240,000 in-lb. of brake torque. The combined weight of 45,000-50,000 lbs. of tractor-trailer allows quasi-constant speed experiments up to 70 mph.

Figure 2 shows the control and data acquisition equipment located in the operator's station. Here, brake line pressure and vertical tire loads are controlled by the operator. It is instrumented with an FM analog tape recorder which records time histories of brake torque, brake line pressure, vehicle velocity, wheel spin velocity and two drum temperatures. These measurement signals are then transferred to a six-channel pen recorder for a visual confirmation of the test.

Figure 3 shows the mounting and measuring device. The wheel is mounted on a spindle arrangement which, in turn, is fastened to a strain gauge load cell member. The load cell measures longitudinal and vertical tire forces as well as brake torque. The angular velocity of the test wheel is measured by a DC tachometer while a fifth wheel is used to obtain the vehicle's longitudinal velocity. The steady-state drum

Figure 1. Modified Tractor-Trailer.

Figure 2. Control and Data Acquisition Equipment.

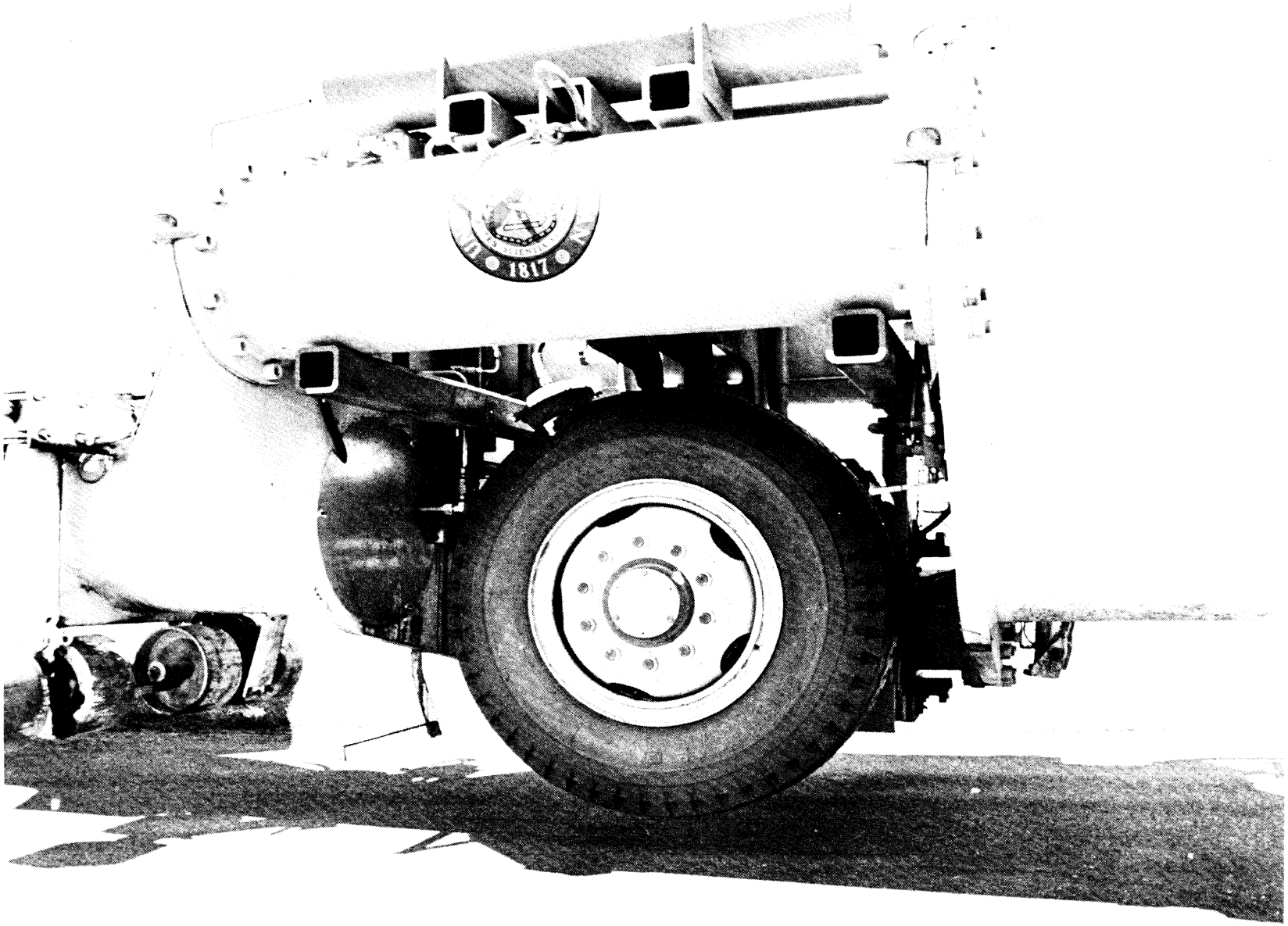

Figure 3. Mounting and Measuring Device

temperature is measured utilizing an iron-constantan thermocouple imbedded in a copper rod which extends through the lining and rubs on the brake drum.

INITIAL TEST PROGRAM

Four commercially available truck air brakes were used in the test program including two S-cam and two dual wedge brakes.

Specifications describing these brakes are given in Table 1. Brakes A and B are S-cam types, while brakes C and D are the dual wedge brakes. Note that brake D was tested with two different types of drums, namely, a cast iron drum and a centrifugally cast drum.

BURNISH

The burnish procedure for each brake consisted of 100 brake applicators at a brake line pressure of 40 psi at vehicle speed 55 mph for a duration of 3-4 seconds. During this procedure, brake information, such as brake line pressure,brake torque, the vehicle and wheel spin velocity and the drum temperature are obtained. The drum temperature is not allowed to exceed 600° F.

A typical set of burnish data is shown in Figure 4 in which brake torque is plotted against burnish test number. The cross-hatched region is enveloped on the top by the peak torque and on the bottom by the torque obtained after three seconds of application. Note that after about 80 burnish runs, the values of both the peak and the 9-second faded torque reach a steady value. A smoothed approximation of the drum temperatures are plotted along the bottom, denoted by the dashed line. The dips in the temperature curve indicate that the burnish procedure was stopped for

Table 1. Brake Specifications

Brake*	Drum Type	Lining ABB-693	Shoe Size	Wedge Angle	Slack Adjusting Length	Air Chamber Type
A	Cast Iron	551-D	16.5" x 7"		6.5 in.	30
B	Cast Iron	551-C	16.5" x 7"		6.5 in.	30
C	Cast Iron	539	15" x 7"	12°		12
D_i	Cast Iron	551-D	15" x 7"	12°		12
D_{ii}	Composite	551-D	15" x 7"	12°		12

*Brakes A and B are S-Cam types from different manufacturers. Both have a leading-trailing shoe configuration. Brakes C and D are dual wedge types from different manufacturers. D_i and D_{ii} indicate the same brake tested with different drums.

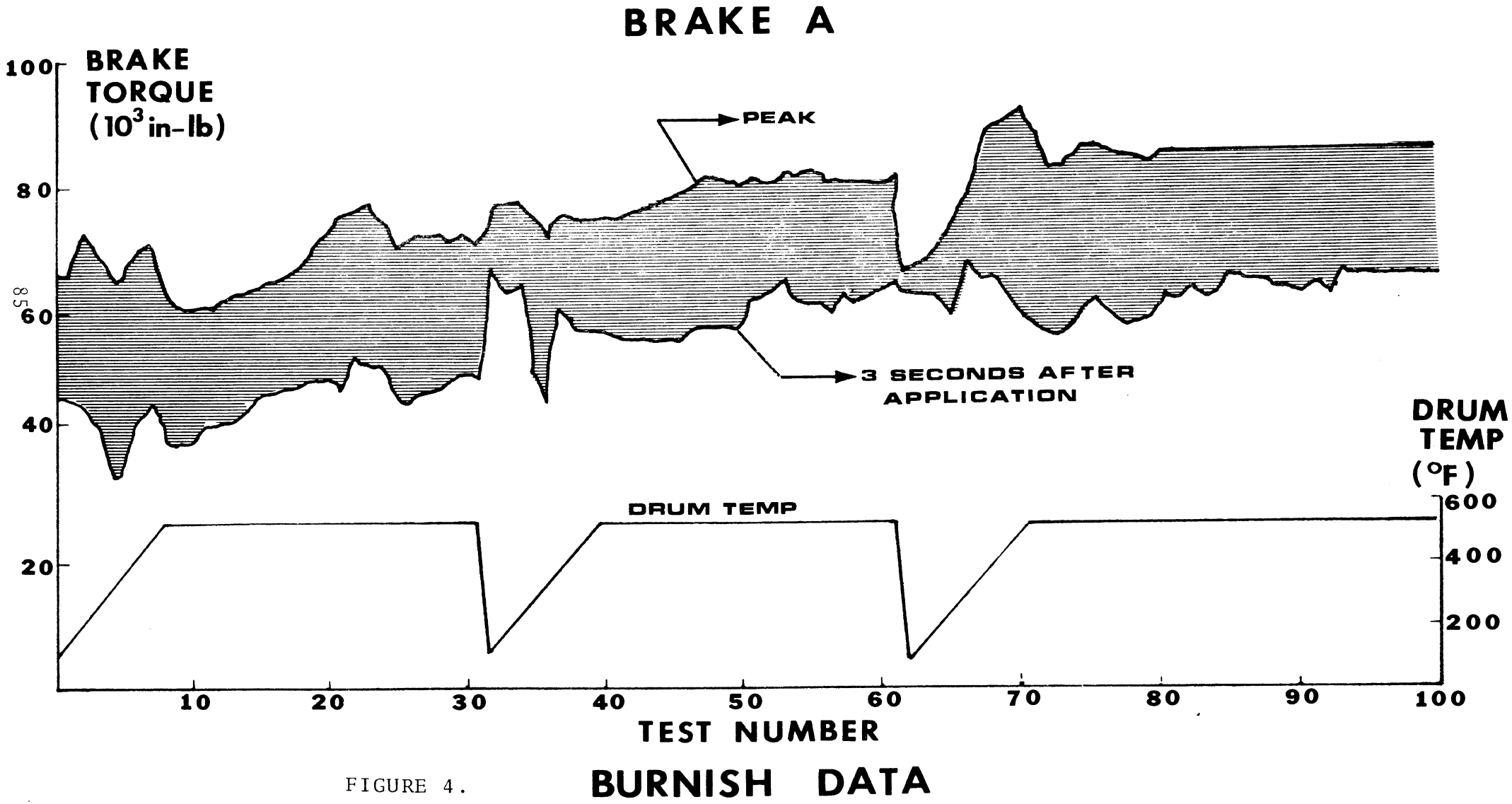

FIGURE 4. BURNISH DATA

extended periods of time. It is interesting to note that these temperature dips at runs 31 and 61 produce corresponding anomalies in the value of the torque.

TEST MATRIX

The initial test program was built around a standard test matrix consisting of brake application runs made at a variety of operating conditions. The nominal values of brake pressure, velocity, and initial drum temperature used in this matrix are:

(1)	Brake Pressures	40, 60, 80 psi
(2)	Vehicle Velocities	20, 40, 55 mph
(3)	Initial Drum Temperatures	200°, 350°, 500° F

The pressure is maintained for at least three seconds. In some cases, lower pressures were used to prevent wheel lock.

Examination of the time histories of the relevant parameters leads to a better understanding of the test process. Recorded data from two consecutive brake applications are shown in Figure 5. In the first run, #38, the pressure reaches 40 psi, the nominal velocity is 55 mph, and the initial drum temperature is 350° F. Inspection of the wheel velocity trace indicates that the test wheel did not lock and the torque reached a maximum of 120K in-lb in less than one second and decreased significantly after that.

Sixty psi was attempted in run #39 in which wheel lock did occur momentarily, as indicated by the wheel velocity trace. An automatic pressure release circuit becomes operative at a preset low value of wheel speed preventing excessive tire wear associated with a prolonged locked wheel condition.

Three torque values have been used to characterize brake performance in this study.

(1) Peak torque
(2) Three-second "faded torque"
(3) Average torque

The peak and the three-second faded torques are as indicated in run #38 of Figure 5. The average torque is defined by the following equation:

$$T_{AVE} = \overline{PT}/\overline{P} \qquad (1)$$

where

P = Pressure
T = Torque

And the bars denote a time average.

BRAKE TEST RESULTS

A typical set of data for one of the brakes tested in the test program is shown in Table 2. These results give rise to an important observation: Initial temperature has neither a consistent nor significant influence on brake torque within the range of temperatures employed. This trend was also found to hold for the other brakes tested. Reflecting this finding, the values of torque used to represent the standard matrix test will be the average torque over the range of initial temperatures employed at each pressure-speed condition.

Figure 6 exhibits a carpet plot of the peak and the three-second faded torque as a function of speed and pressure. The solid lines denote the peak torque while the dotted lines denote the three-second faded torque. Here "fade" is defined as the difference

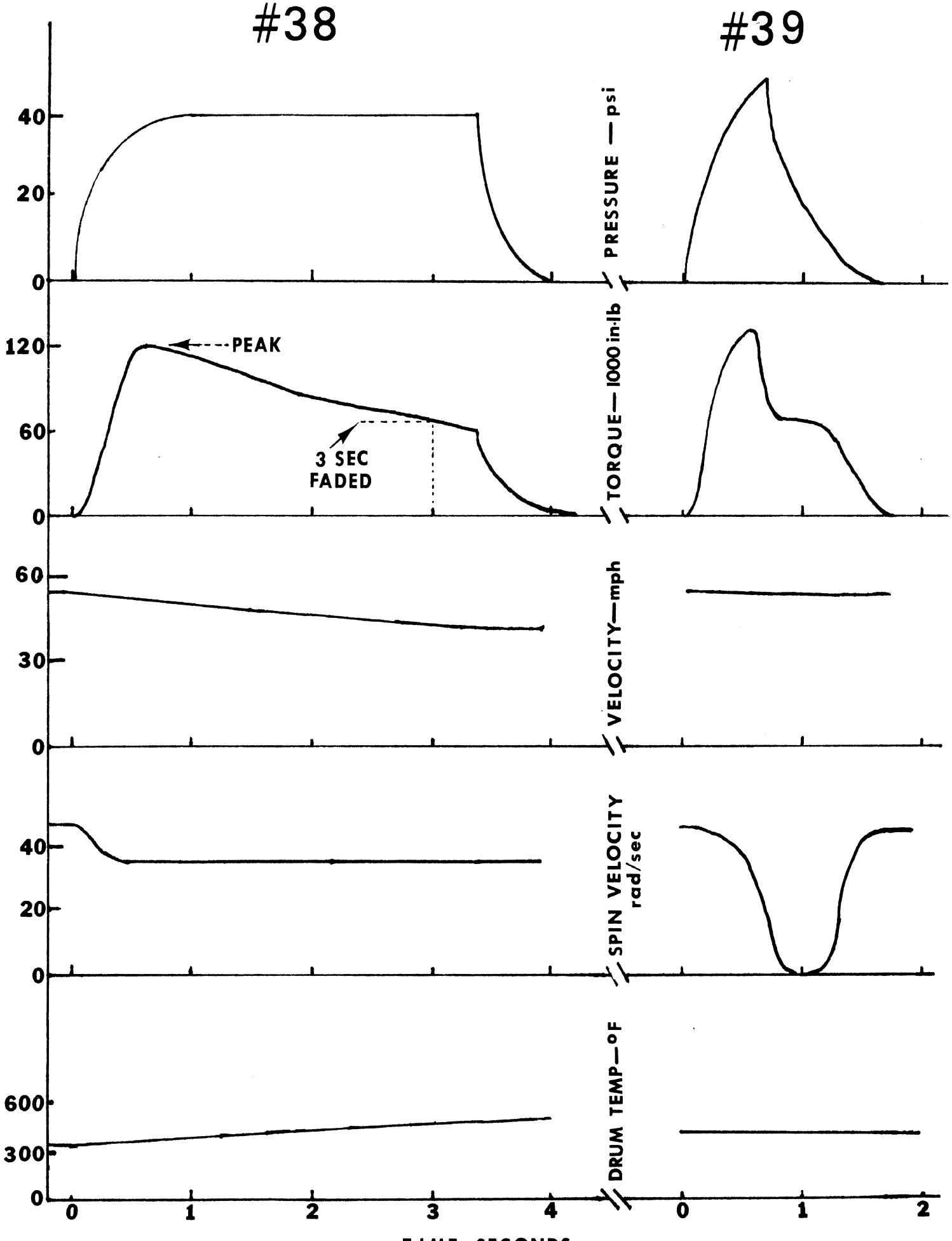
#38
#39
PRESSURE — psi
40
20
0
TORQUE — 1000 in-lb
120
60
0
PEAK
3 SEC
FADED
VELOCITY — mph
60
30
0
SPIN VELOCITY
rad/sec
40
20
0
DRUM TEMP — °F
600
300
0
0
1
2
3
4
0
1
2
TIME SECONDS

FIGURE 5

Table 2. Data from a Standard Test Matrix

Brake D_i - Cast Iron Drum

Pressure psi	Velocity mph	Temperature °F	Peak Torque K in-lb	3-Second K in-lb	Average K in-lb
40	20	200	64	61	62
		350	78	69	74
		500	93	82	87
	40	200	64	64	64
		350	69	53	61
		500	61	56	59
	55	200	63	51	57
		350	61	35	50
		500	53	44	50
60	20	200	104	102	103
		350	Lock		
		500	Lock		
	40	200	108	85	98
		350	106	85	97
		500	98	85	93
	55	200	98	63	80
		350	97	53	75
		500	84	63	74
80	20	200	144	125	135
		350	Lock		
		500	Lock		
	40	200	133	112	123
		350	Lock		
		500	116	93	104.5
	55	200	106	80	93
		350	96	56	85
		500	120	65	93

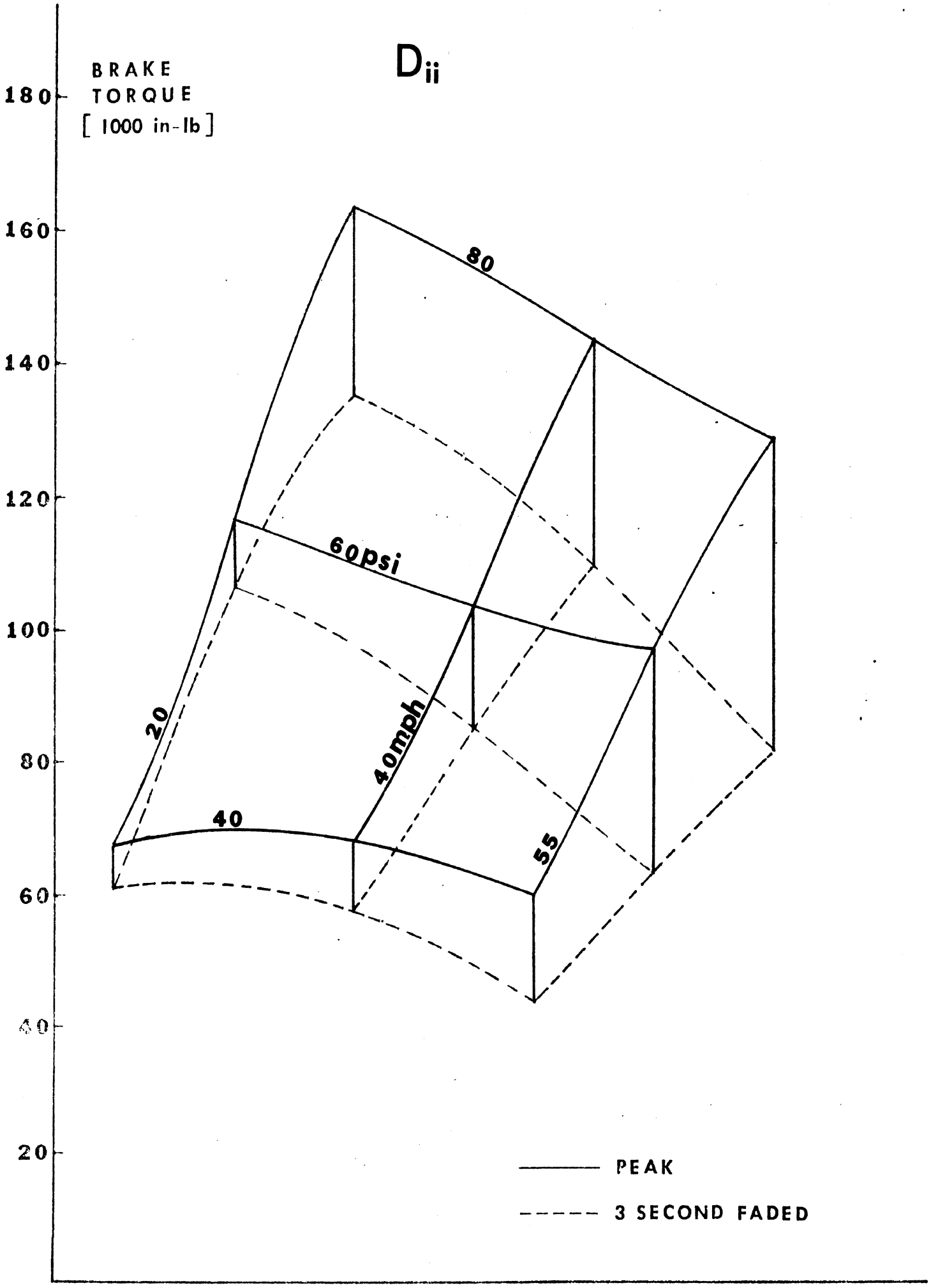
D_{ii}
BRAKE TORQUE [1000 in-lb]
180
160
140
120
100
80
60
40
20
80
60psi
40mph
20
40
55
PEAK
3 SECOND FADED

FIGURE 6

between the peak and the three-second faded torque, shown in the figure as the length of the vertical lines. The wedging shape of these curves indicate that fade increased with increasing speed and/or pressure.

Data from the standard matrix has been used to produce Figure 7. Here, average torque is plotted against brake pressure along lines of constant velocity. This torque-pressure representation looks similar to the conventional results from a spin-down dynamometer. However, it should be emphasized that these results are from constant speed tests while the spin-down dynamometer curves are expressed in terms of initial velocity.

SPECIAL PURPOSE TESTS

The standard matrix was supplemented with two additional tests. The first was designed to measure the hysteresis in the line pressure/brake torque relationship resulting from cyclic braking as in antilock operation. The second, called the drag test, was used to study the effects of quasi-constant temperature levels on brake torque.

In the hysteresis test, the pressure was increased to a preset level and then decreased at a controlled rate. The torque levels achieved during the pressure rise were compared to those obtained during the pressure release. Tests with and without wheel lock were performed. The dotted line in Figure 7 represents the instantaneous torque level reached during the pressure rise.

Figures 8 and 9 display the complete torque loop associated with the pressure rise and fall. The tests were repeated at two velocities--a low and an intermediate velocity. The arrows indicate the chronology of the pressure history.

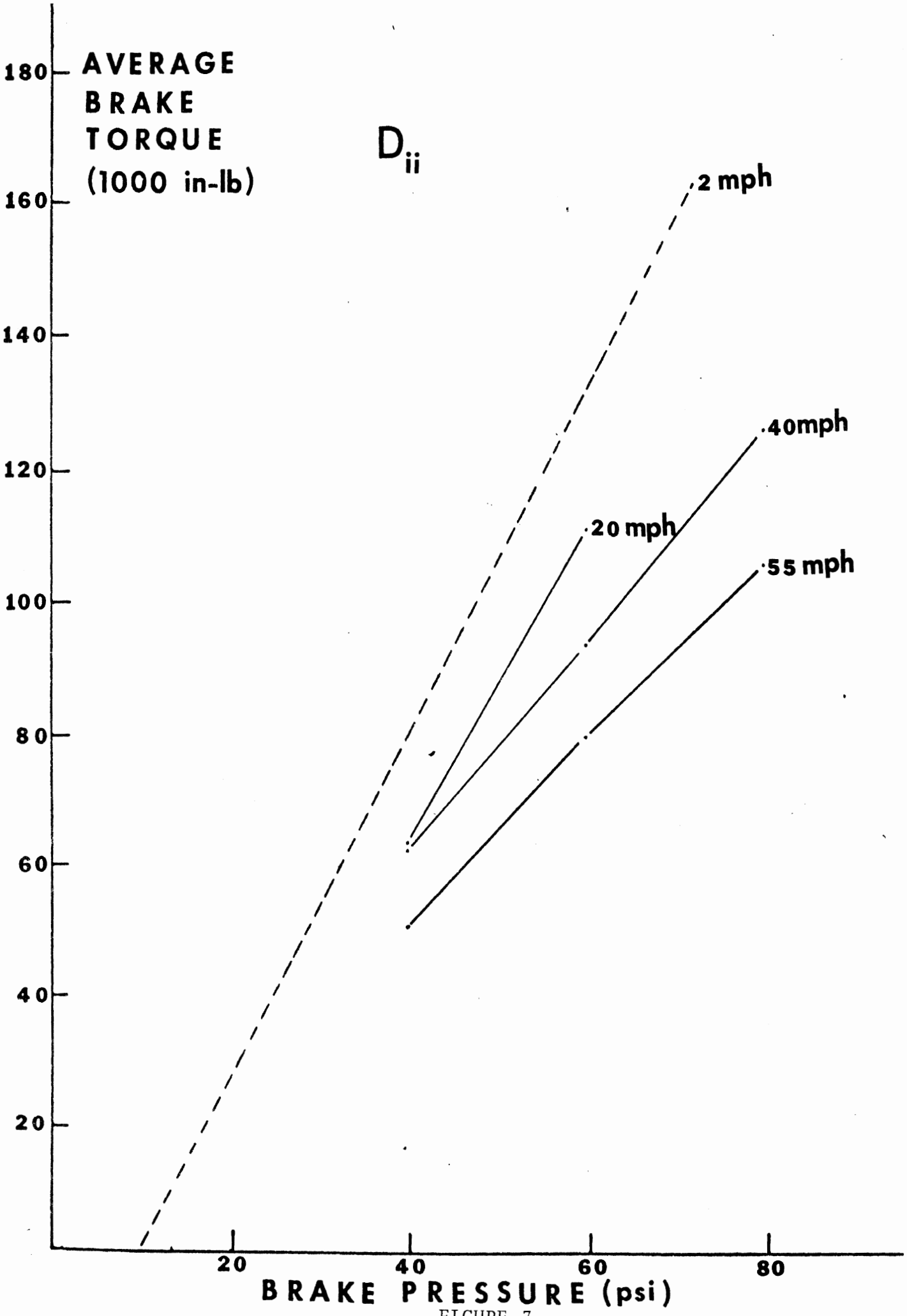
AVERAGE
BRAKE
TORQUE
(1000 in-lb)
D_{ii}
180
160
140
120
100
80
60
40
20
2 mph
40mph
20 mph
55 mph
20
40
60
80
BRAKE PRESSURE (psi)

FIGURE 7

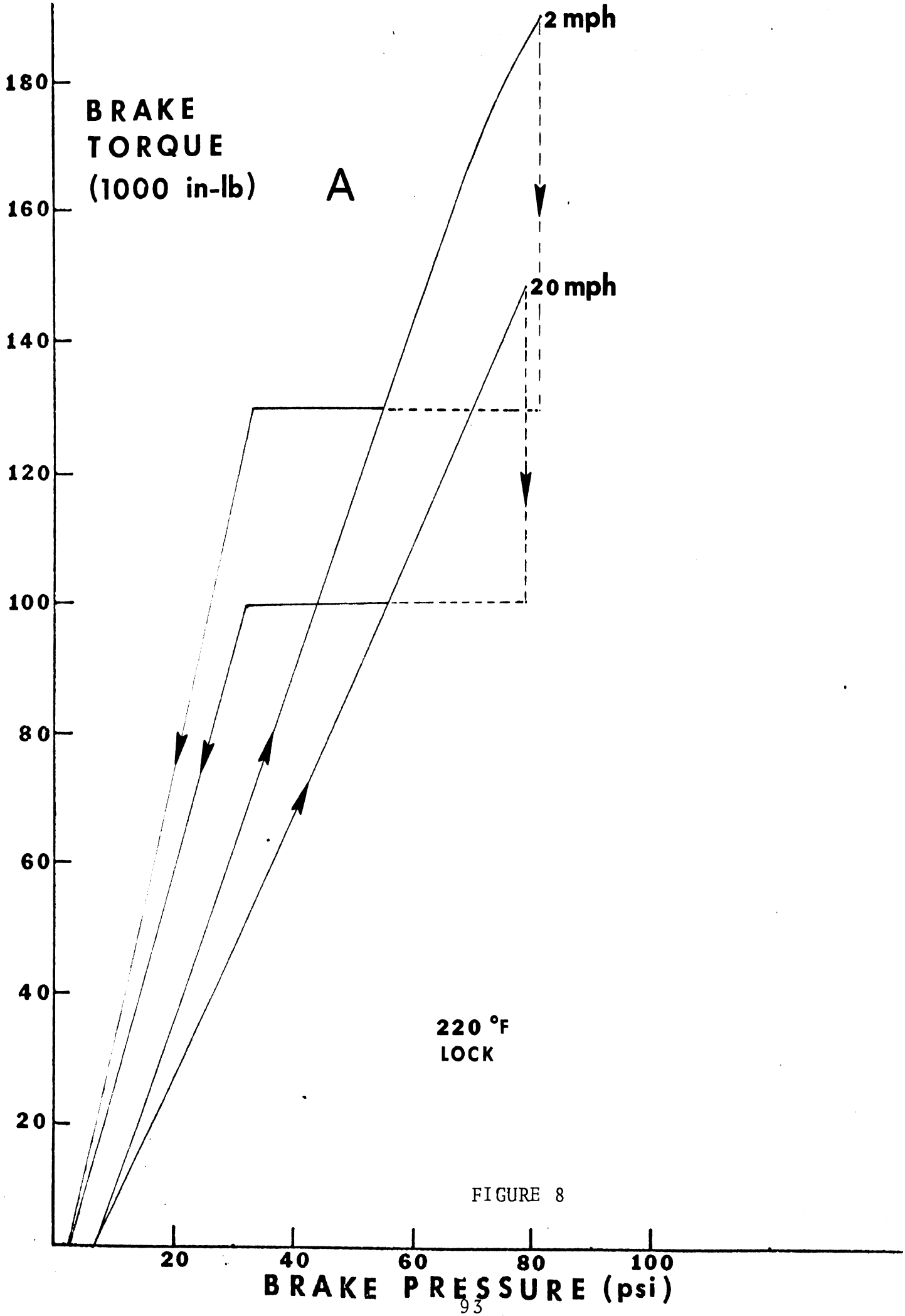
2 mph
20 mph
BRAKE
TORQUE
(1000 in-lb)
A
180
160
140
120
100
80
60
40
20
220 °F
LOCK
20
40
60
80
100
BRAKE PRESSURE (psi)

FIGURE 8

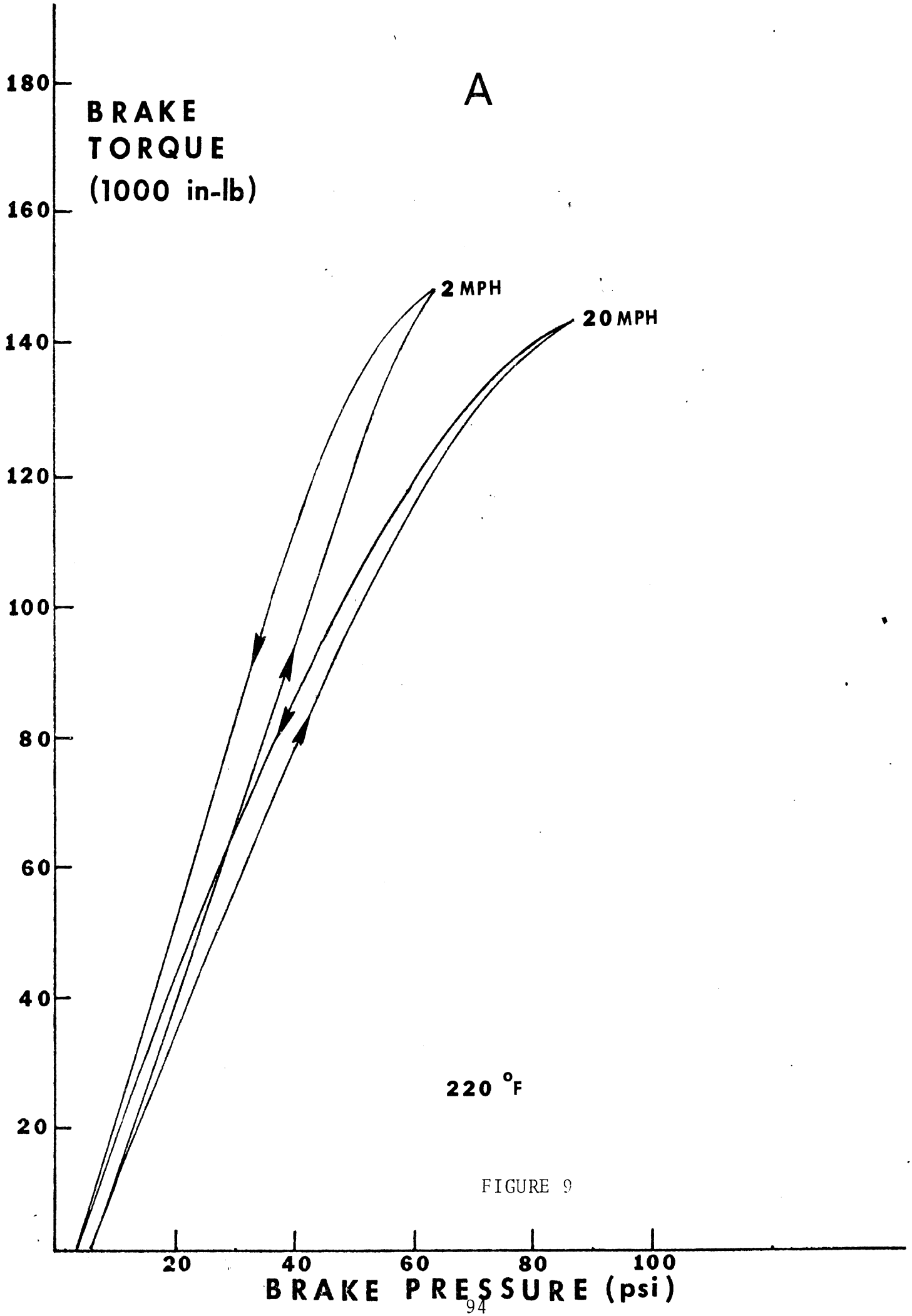
A
BRAKE
TORQUE
(1000 in-lb)
180
160
140
120
100
80
60
40
20
2 MPH
20 MPH
220 °F
20
40
60
80
100
BRAKE PRESSURE (psi)

FIGURE 9

In Figure 8, the torque begins to rise at a push-out pressure of about 10 psi and wheel lock occurs at a pressure of about 70 psi for each velocity, at which point, the brake torque immediately drops to a value indicative of the product of the sliding tire force and the effective tire radius. The pressure is then reduced and the eventual wheel spinup occurs at about 40 psi. Any further reduction in brake pressure reduces the torque level. The length of the solid portion of the horizontal line is a measure of the brake hysteresis.

The same brake tested in which no wheel lock occurs gives results as shown in Figure 9. It was observed for all the brakes tested that hysteresis is greater when wheel lock occurs.

The drag test results are shown in Figure 10, in which brake torque is plotted against time. The brake was operated continuously at 40 psi. The test began with a drum temperature near ambient and terminated when the drum temperature reached 500° F. The test was performed at very low speed (4-6 mph) and again at higher speeds (20-25 mph). While during the lower speed tests the brake torque increased along with increasing drum temperatures, the opposite result was found at the higher speeds, that is, the torque faded with time. This result supports the theory that the energy rate plays an important role in association with brake fade.

ANALYTICAL TECHNIQUES

The commercial vehicle research in progress at HSRI has many facets in addition to the measurement of brake torque. For example, significant effort has been expended to produce a computer simulation

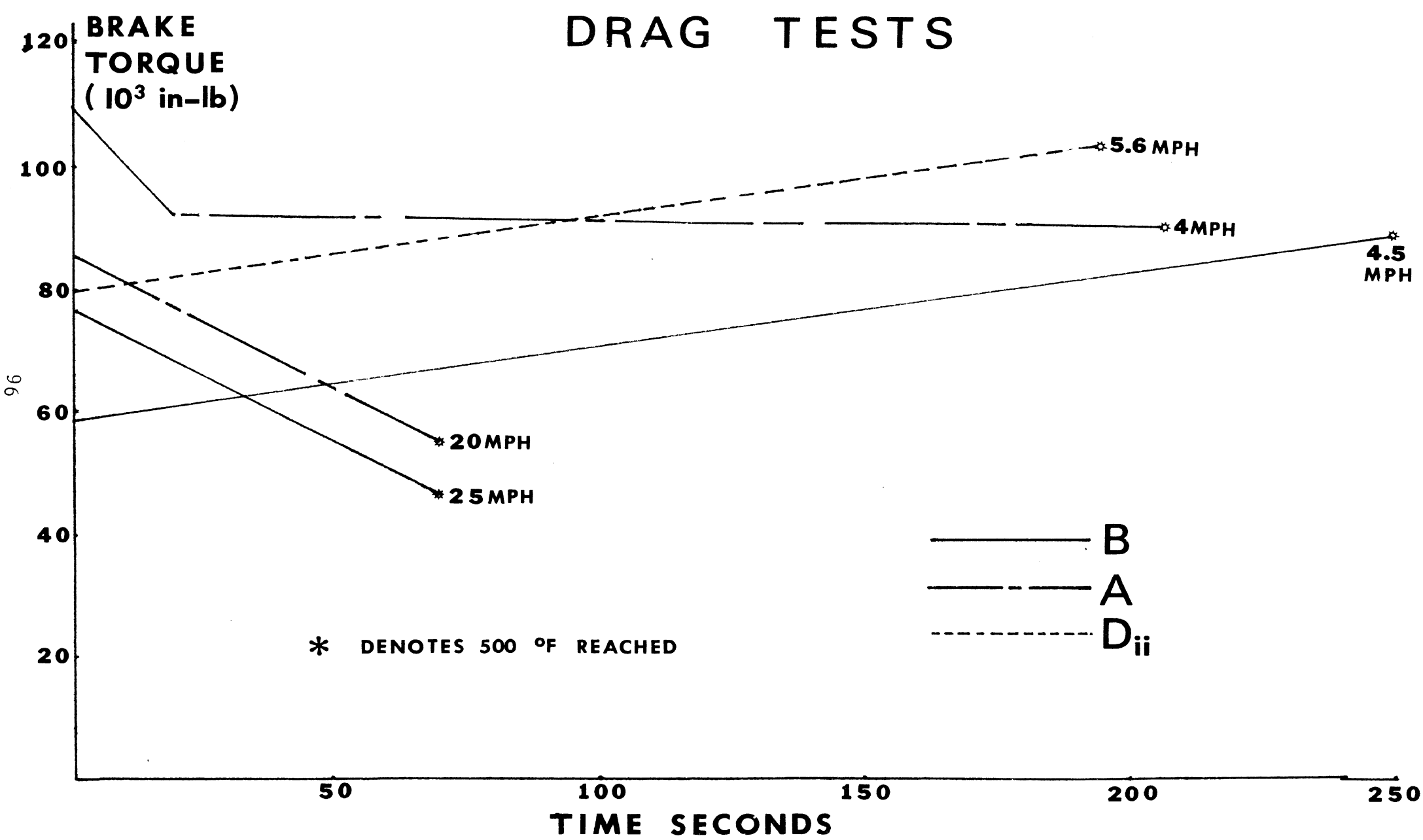
DRAG TESTS
BRAKE TORQUE (10^3 in-lb)
120
100
80
60
40
20
5.6 MPH
4 MPH
4.5 MPH
20 MPH
25 MPH
B
A
D_{ii}
* DENOTES 500 °F REACHED
50
100
150
200
250
TIME SECONDS

FIGURE 10

of commercial vehicle braking (4,5,6). Presently, the simulation is being modified to reflect time varying brake torque to reflect brake fade. The brake fade algorithm is based in large part on empirical results measured using the mobile brake dynamometer.

A semi-empirical relationship in which torque and surface temperature (7) are linearly related has been established with surprisingly good results.

The faded torque is given by the following equation:

$$T_F(t) = T_{UF}(P, V_o) \left\{ 1 - \frac{\theta(t)}{\theta_T(V_o)} \right\} \qquad (2)$$

where:

T_{UF} = the unfaded torque
θ = the drum surface temperature rise
θ_T = the fade parameter
P = brake pressure
V_o = initial velocity
t = time

Thus there are two empirical parameters used in the model, the unfaded torque T_{UF} and the fade parameter θ_T.

Although it is not surprising that the value of the unfaded torque is pressure dependent, both T_{UF} and θ_T may be functions of initial velocity. Each parameter can be chosen to insure that both the average torque and the functional shape of the torque history accurately simulate the experimental results.

There are two types of data to which this semi-empirical relationship can be applied to determine these two quantities:

(1) Conventional spin-down dynamometer representations of either average torque versus brake pressure or torque versus time at a given pressure.

(2) Data from the constant-speed mobile dynamometer.

Spin-down torque-time curves differ in character from resulting constant-speed torque curves, as shown in Figure 11. While during constant speed tests the torque decreases monotonically in time after the peak, the spin-down results show the torque increasing toward the end of the stop.

Examination of the corresponding drum surface temperature histories in Figure 12 shows an analogous trend in the character of these curves. The temperature during the constant speed tests increased monotonically in time while the temperature decreased towards the end of the stop for the spin-down test.

These torque-speed-temperature interdependencies lend credibility to the implications of equation (2) that the transient temperature rise has a first-order effect on the brake torque.

CONCLUDING REMARKS

Data has been presented which was gathered from a test matrix tailored to the capabilities of the apparatus. The findings from the data indicate:

(1) Drum-shoe rubbing speed is an important factor influencing the brake torque obtained at a given pressure.

(2) Initial drum temperatures in the 200-500°F range have little influence on the level of brake torque.

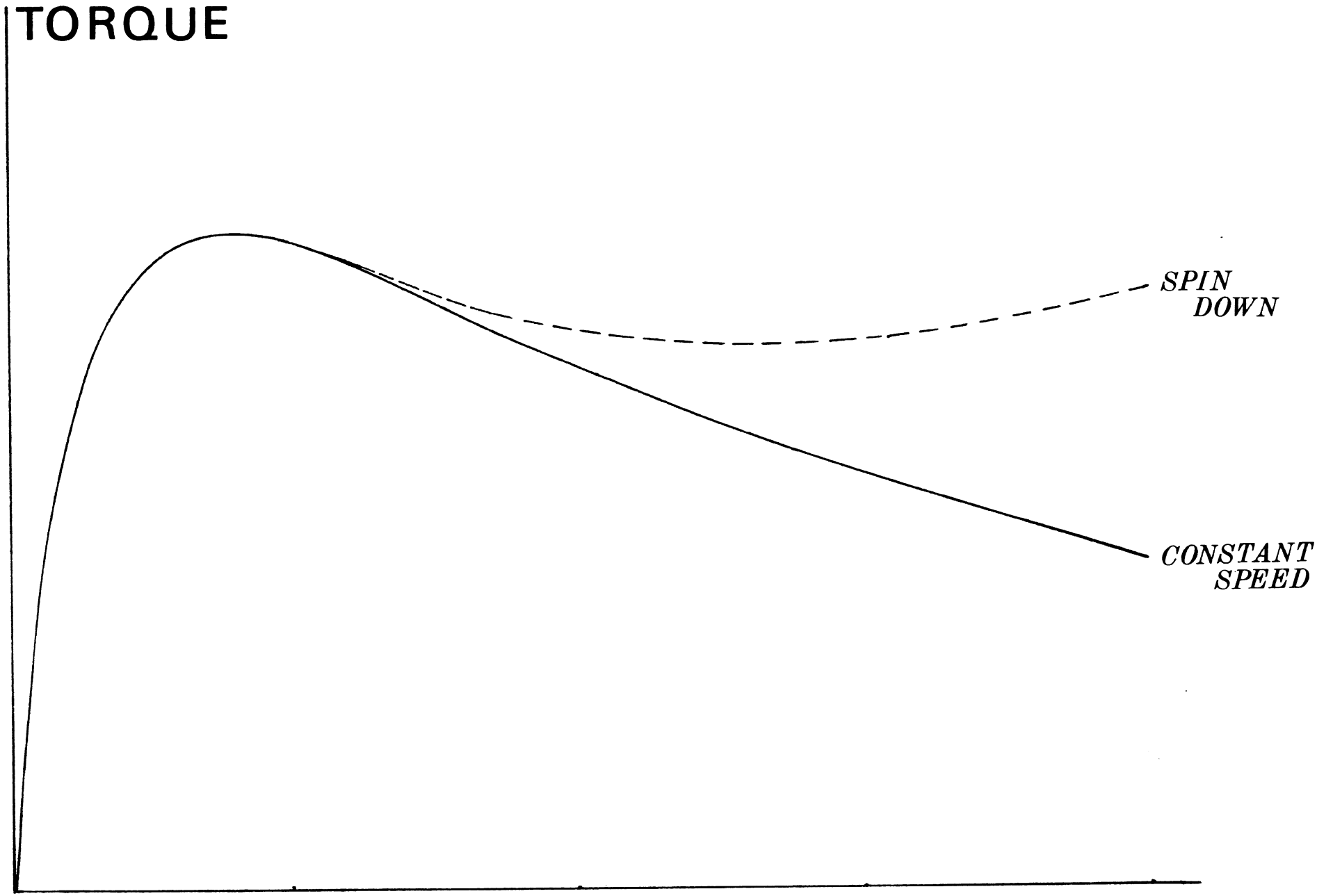

FIGURE 11

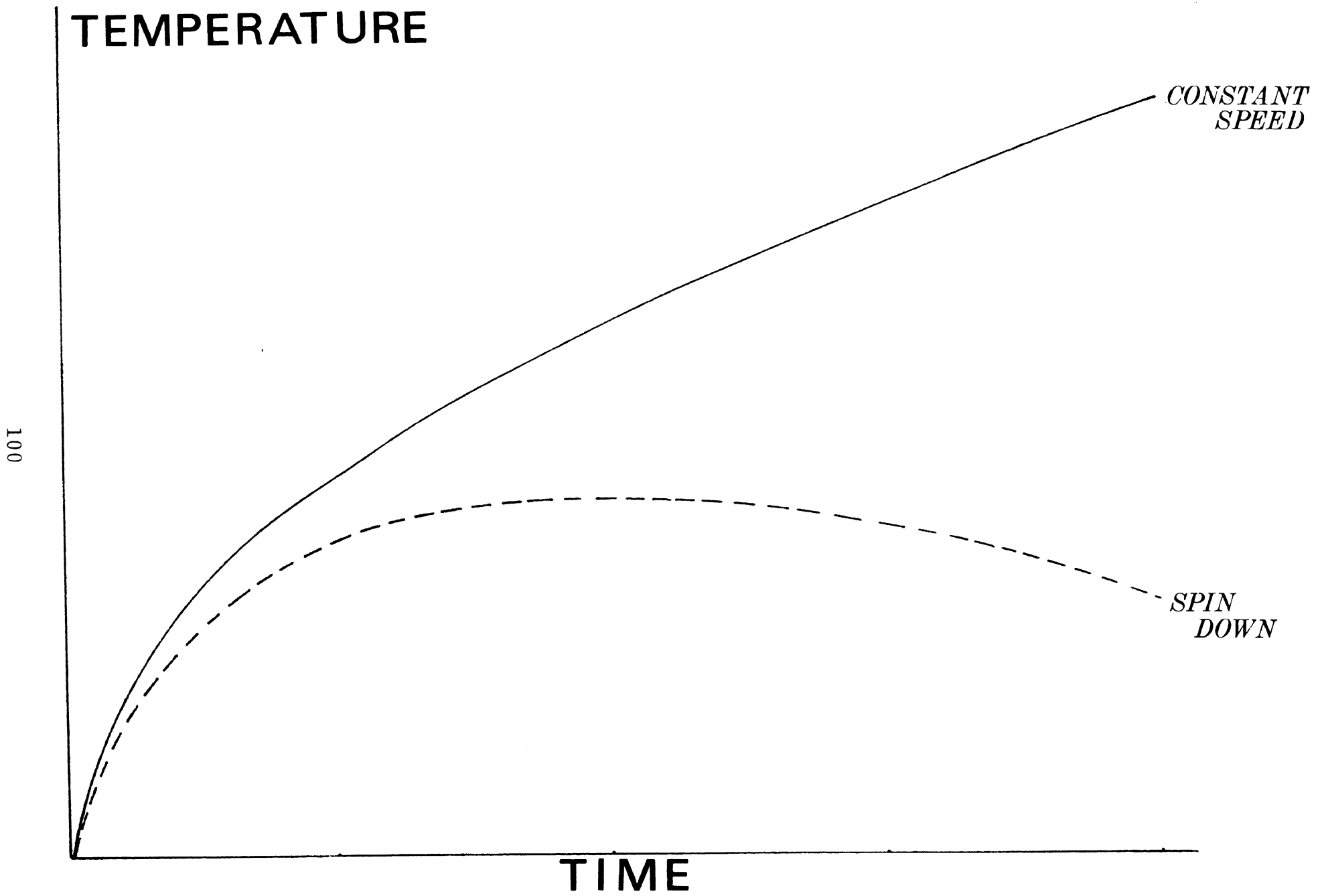

100

FIGURE 12

(3) The data generated in this study indicate that the rate of energy input to the drum is the more pertinent factor, i.e., the time history of the change in temperature is more important than the temperature itself.

Based on these findings, a semi-empirical brake fade model has been developed in which torque is assumed to vary linearly with the temperature change at the lining/drum interface.

REFERENCES

1. Federal Motor Vehicle Safety Standards No. 121, Air Brake Systems: 49CFR571.121.

2. Post, T.M., Fancher, P.S., Bernard, J.E., "Torque Characteristics of Commercial Vehicle Brakes" SAE Paper 750210, presented at the Automotive Engineering Congress and Exposition, Detroit, Michigan, February 1975.

3. Ervin, R.D., and P.S. Fancher, "Preliminary Measurement of Longitudinal Properties of Truck Tires" Paper 741139 presented at SAE National Truck Meeting, Troy, Michigan, November 1974.

4. Murphy, R.W., Bernard, J.B., and Winkler, C.B., A Computer Based Mathematical Method for Predicting the Brake Performance of Trucks and Tractor-Trailers, Phase I Report, Motor Truck Braking and Handling Performance Study, HSRI, The University of Michigan, September 15, 1972.

5. Bernard, J.B., Winkler, C.B., Fancher, P.S., A Computer Based Mathematical Method for Predicting the Directional Response of Trucks and Tractor-Trailers, Phase II Report, Motor Truck Braking and Handling Performance Study, January 1973.

6. Post, T.M., and Bernard, J.E., "Transient Temperature Evaluation in the Mechanical Friction Brake." Third Quarterly Report, HSRI, University of Michigan, June 1973.

SIMULATION IN ANTILOCK SYSTEM DEVELOPMENT

G. A. Cornell
Bendix Research Laboratories
and
B. E. Latvala
Bendix Heavy Vehicle Systems Group

ABSTRACT

This paper discusses the use of computer simulation in the development of antilock systems for air-braked vehicles. The need for such simulations, the parameters significant to antilock development, and discussions concerning physical simulations and vehicle testing are included. Comparisons of simulation and test results are presented.

INTRODUCTION

The development of antilock brake systems for air-braked vehicles has been made necessary by the safety standards established by the National Highway Traffic Safety Administration. This development has proved to be a complex and difficult problem, not only with respect to cost and component design, but also with respect to the system dynamics. Antilock system development has therefore led to the need for computer simulation.

This paper discusses the need for computer simulation and the parameters found to be significant to antilock system performance. Specific simulation models are described briefly. Problems of vehicle testing are noted to justify the emphasis on simulation as a design tool. Finally, a comparison of simulation results and vehicle test data is presented.

NEED FOR SIMULATION

Analysis of the factors involved in the operation of an antilock braking system proved very useful in developing the basic equations and relationship between the brake, wheel, vehicle, and tire-road interface. However, understanding the dynamic interrelationship between the various factors is significantly more difficult, and manually reducing calculated results to meaningful data which can be applied to system development is too time-consuming to be effective. When the large number of factors affecting the antilock system are considered, it is obvious that a great deal of analysis is required to gain a good understanding of

the effects of all parameter variations. Some of these parameters are listed below.

PARAMETERS SIGNIFICANT TO ANTILOCK SYSTEM PERFORMANCE

The components significant to antilock brake system performance are depicted in Figure 1. These components are the brake modulator, brake characteristics, wheel dynamics, vehicle dynamics, speed sensor and control logic.

The brake modulator increases and decreases the brake pressure by means of a solenoid controlled by the control logic. A functional sketch of a modulator is shown in Figure 2. The solenoid is in effect positioned to close off the port to the atmosphere or to the reservoir. Closing off the port to the atmosphere allows pressure to build; closing off the reservoir port allows pressure to decay. The reservoir, delivery, brake chamber volumes, the port areas, brake line sizes and lengths, and the initial brake application rate all affect the dynamics of the brake pressure.

The wheel dynamics are affected by the brake torque, road torque, wheel inertia, weight on the wheel, and the vehicle velocity. The brake torque is, of course, generated as a result of the brake pressure. The gain between the two is highly nonlinear with speed and brake temperature and also varies as a function of lining composition and type of brake.

Wheel inertia affects the wheel dynamics and, for dual wheels, is typically twice that of a single wheel. Road torque is generated from the slippage between the tire and the road. This slippage is defined by

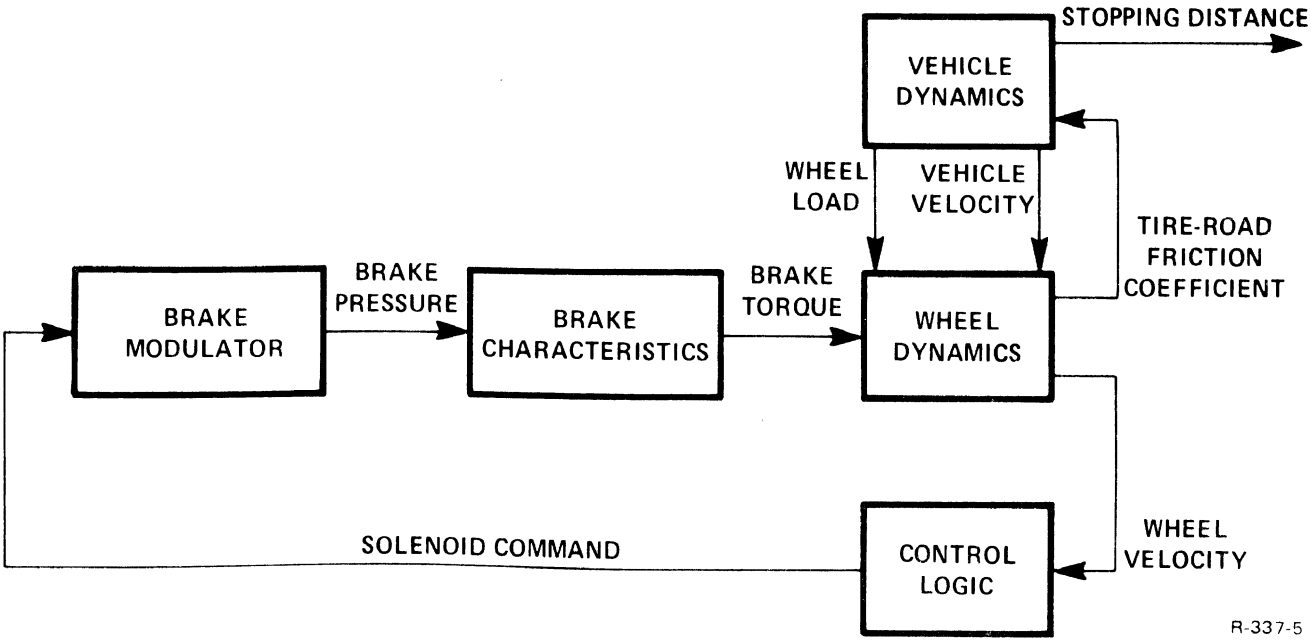

Figure 1. Typical Antilock System

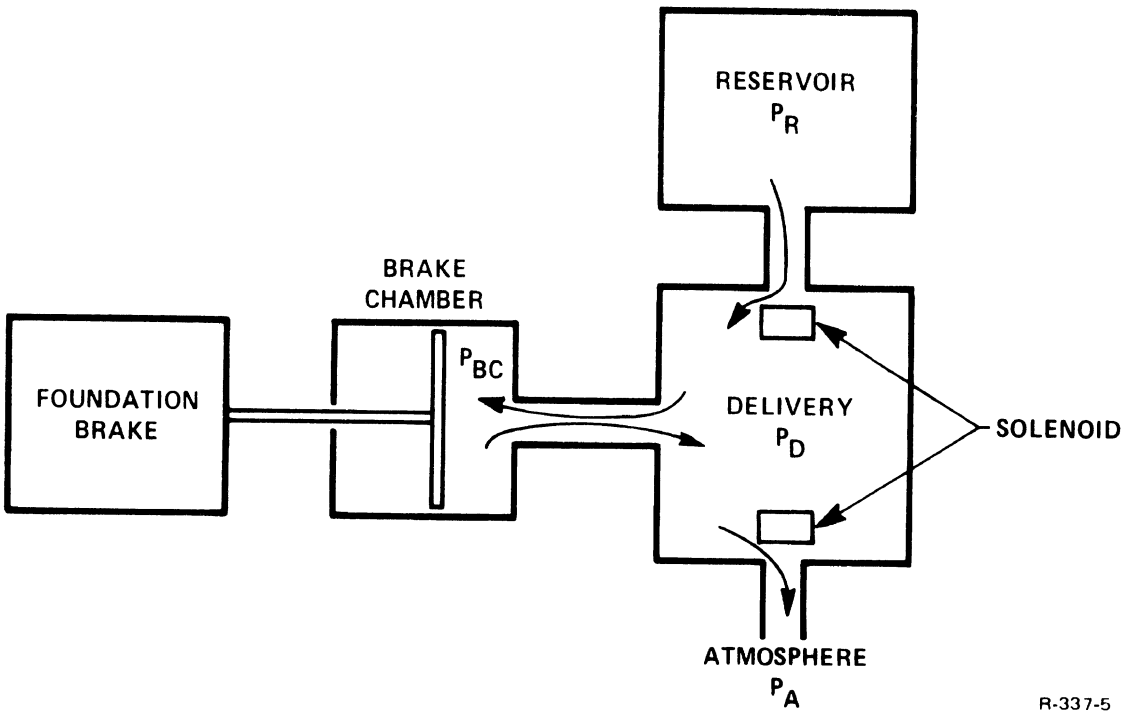

Figure 2. Functional Sketch of Brake Modulator

$$\text{SLIP} = 100 \frac{\text{VEHICLE VELOCITY - WHEEL VELOCITY}}{\text{VEHICLE VELOCITY}}$$

and typically generates a coefficient of friction μ between the tire and road as shown in Figure 3. The road torque, Q_R, is then given by

$$Q_R = R W \mu$$

where R is the wheel radius and W is the weight on the wheel. The maximum road torque is generated on most road surfaces when SLIP equals 10 to 30 percent, i.e., when the wheel velocity is 70 to 90 percent of the vehicle velocity. The weight on the wheel can have a wide range of values since the vehicle can be empty or loaded, and it can be towing a loaded trailer or driven bob-tail without a trailer. The wheel weight is also a dynamic quantity that varies during braking. When the vehicle decelerates, the wheel weight transfers from the rear to the front of the vehicle. The dynamics of the transfer are a function of the vehicle and suspension characteristics.

Wheel load and the tire-road friction coefficient combine to produce the braking force and, in turn, the vehicle deceleration and stopping distance.

The wheel velocity processed from the speed sensor for use in the control logic must be filtered to reduce noise. A compromise must be made between the resulting dynamic lag and the amount of noise that can be tolerated.

Many schemes have been devised for the control logic, but they all either control the wheel velocity

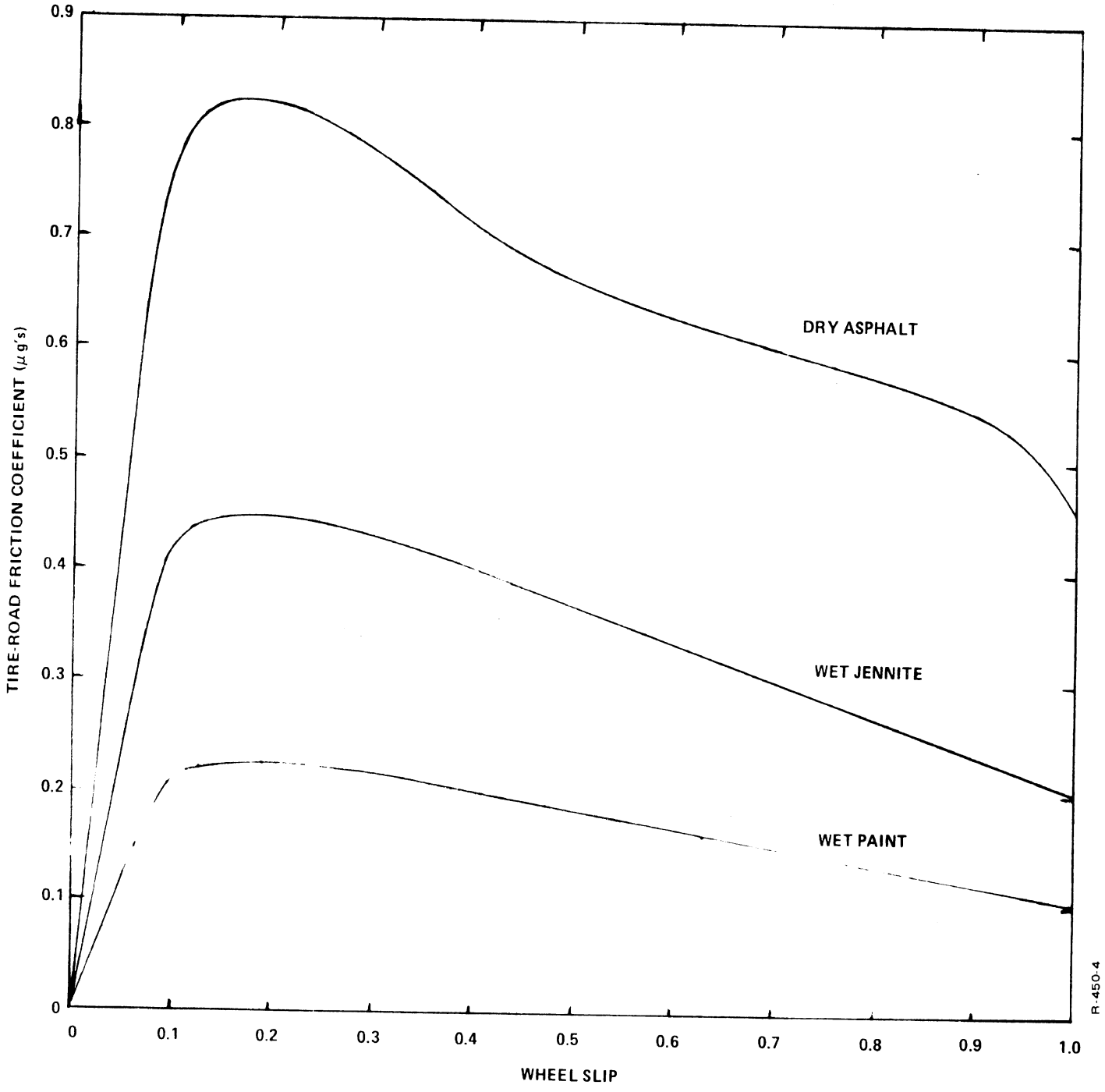

Figure 3. Simulated μ-Slip Curves

by cycling about the peak of the μ-slip curve or they develop a wheel slip that nominally produces the maximum tire-road friction coefficient.

SPECIFIC MODELS FOR SPECIFIC NEEDS

Once the need for simulation has been established, a major step is to determine the model configuration and the level of complexity required. Effort has been made to minimize complexity and to use different models, depending on the requirements of each development phase.

CONCEPT DEVELOPMENT

Generating candidate control concepts requires some means of evaluating performance. This level of development does not require exact answers; often the systems engineer is more interested in the character of control or the significance of a given parameter. Identifying the system components which, if improved, would improve system performance, aids in concentrating effort in the proper areas.

The most basic model will serve this need. A single-wheel model, as shown in Figure 4, has all of the basic elements of the control loop.

VEHICLE CHARACTERISTICS

More sophisticated models are required when studying weight transfer and side-to-side brake and/or road coefficient unbalance. These characteristics are very significant to the antilock system, and both require a minimum of two wheels. For weight transfer,

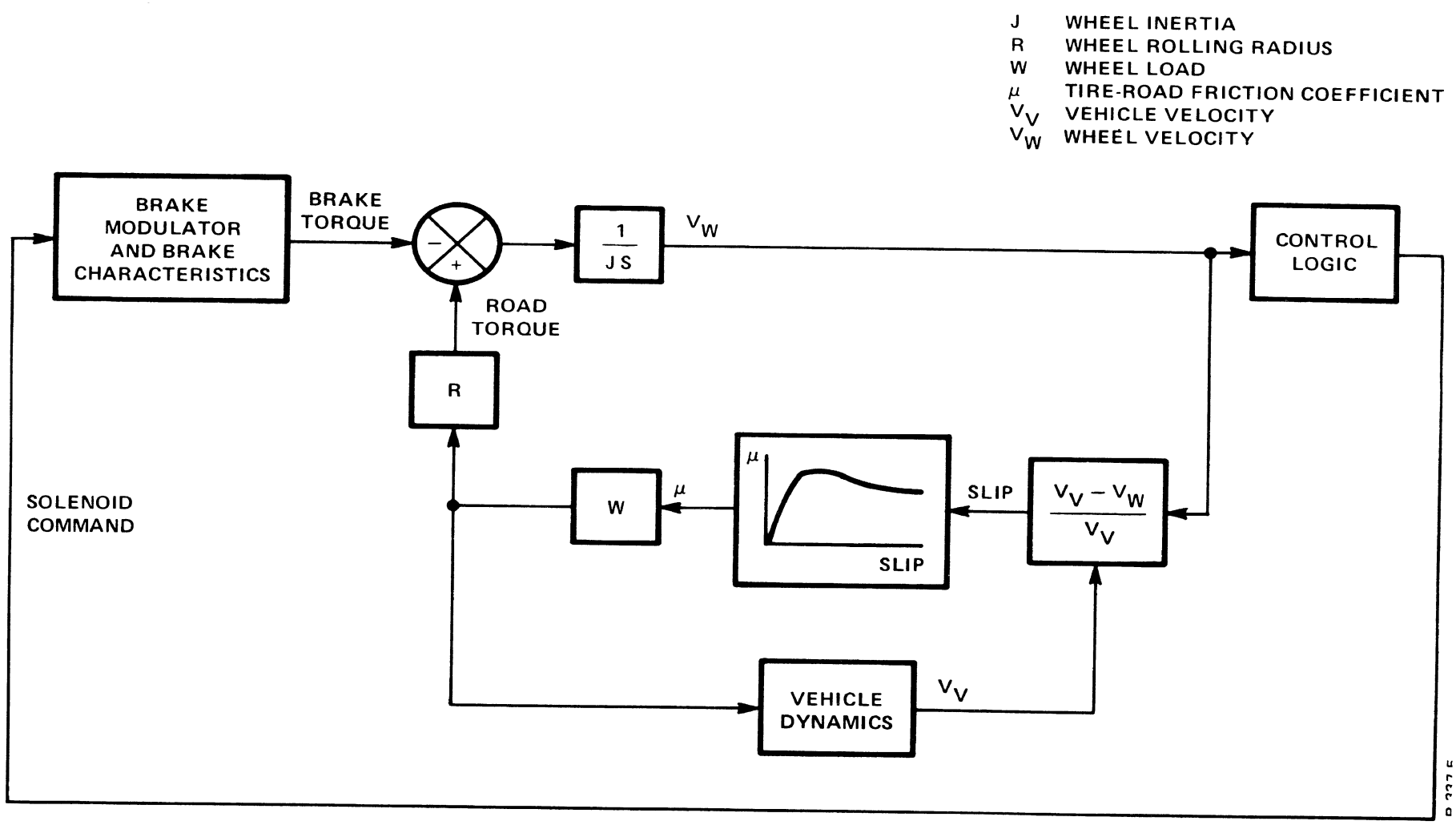

Figure 4. Basic Single-Wheel Model

a bicycle configuration is used. For the other, a two-wheel axle configuration is used. These two models, shown in Figures 5 and 6, permit evaluation of the following variables:

1. Fore and aft weight transfer.
2. Variation in center of gravity location.
3. Variation in wheel base.
4. Side-to-side weight transfer (curve).
5. Brake unbalance.
6. Road coefficient unbalance.
7. Interaction between axles.

COMPONENT DEVELOPMENT

The models described above serve to define desirable component system characteristics or evaluate system performance with existing component performance. Refining or optimizing performance of a particular component, for example the modulator, necessitates defining a detailed model of that component.

A detailed part-by-part mathematical model of the brake modulator was therefore developed for an optimization program. Once defined and optimized, the detailed model was simplified for use in the system simulations.

SIMULATION WITH PROTOTYPE COMPONENTS

Bench testing of individual prototype components is necessary and desirable, but does not test their effect on closed-loop system performance. In addition,

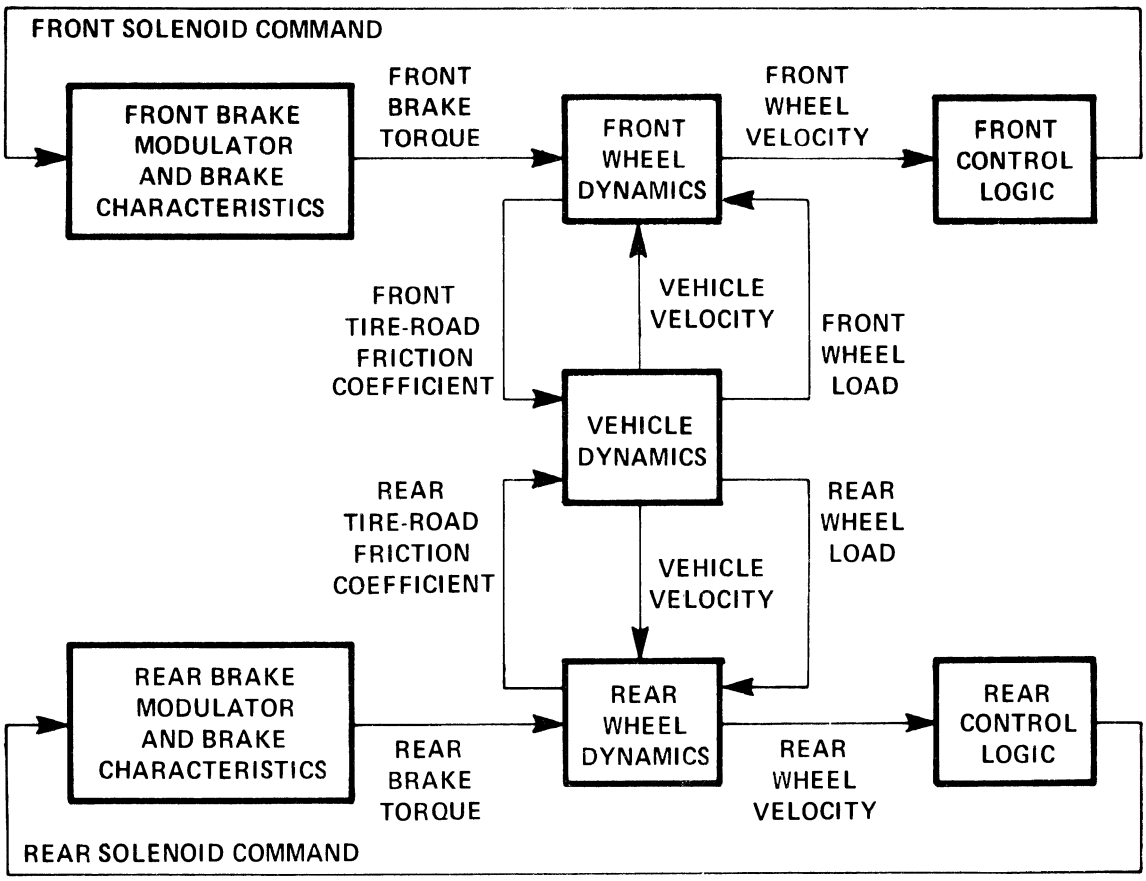

Figure 5. Bicycle Configuration Model

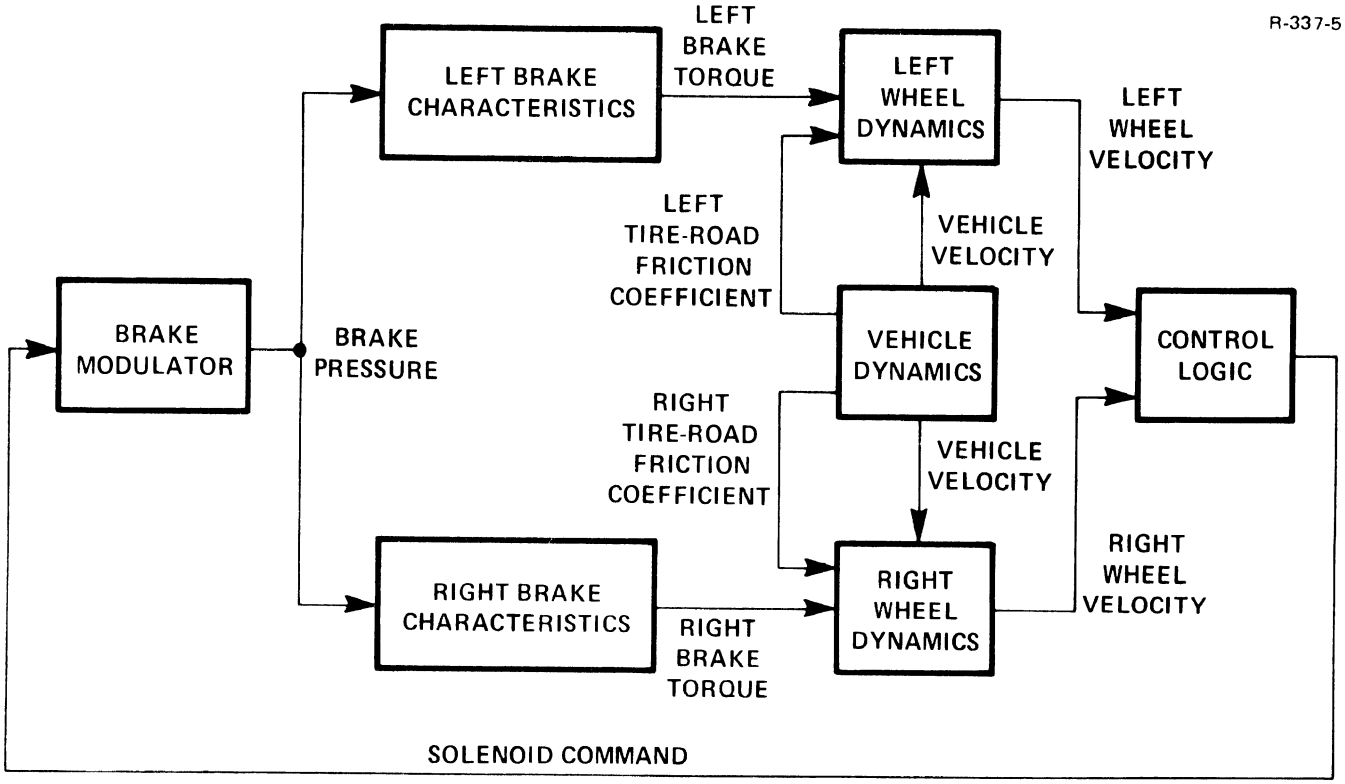

Figure 6. Axle Configuration Model

no prototype performs exactly like the model. It is therefore desirable to test closed loop, in the laboratory, as much of the system hardware as possible prior to vehicle testing.

Operating the actual hardware, including the control logic and the air brake system, as shown in Figure 7, allows convenient prototype testing and parameter optimization for best system performance. In addition, parameters such as percent slip and individual wheel contribution to efficiency can be determined. This approach minimizes problems during vehicle testing because prototype "bugs" have been identified prior to vehicle testing. Because the prototype components have been operated with the model, differences between vehicle test data and simulation results can be attributed to the vehicle and tire-road interface modeling, thus simplifying analysis of the data. It has been found that the time saved in vehicle testing alone is worth this step; the improved confidence in the accuracy of the vehicle data and insight into dynamic component performance have been extremely valuable to the system and component designer.

VEHICLE TESTING

Vehicle testing of an antilock system has several disadvantages:

- A great deal of time, money and effort must be expended for relatively little data.
- Variability of conditions makes quantitative analysis of data very difficult and time-consuming.

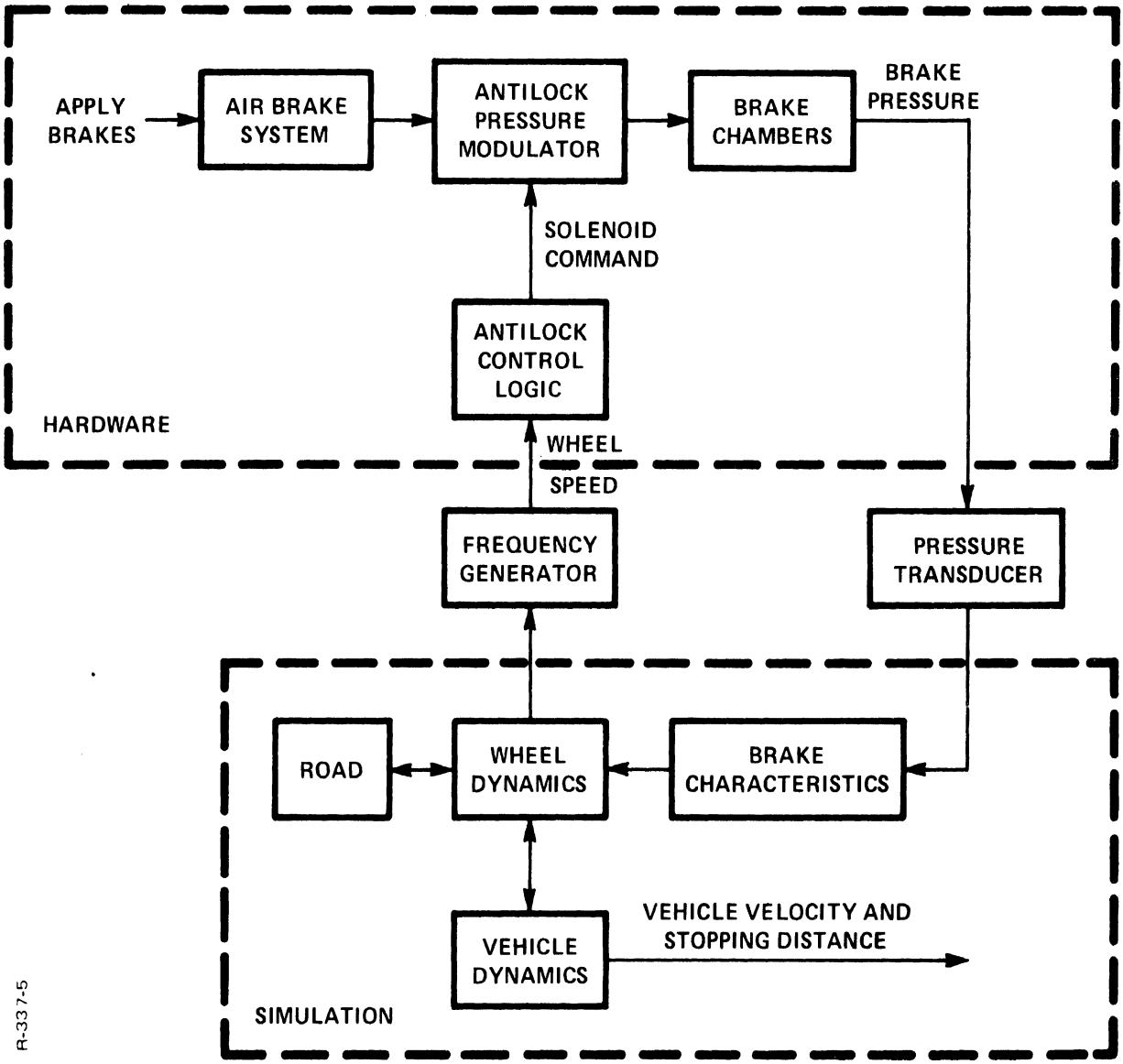

Figure 7. Simulation With Hardware

- Because the vehicle is being operated at the braking performance limit, damage to tires, brakes, and suspension can easily occur, with possible injury to the driver.
- Interaction between the instrumentation and antilock electronics requires special precautions when monitoring the electronics or speed sensors.

These characteristics of vehicle testing justify the emphasis on simulation as a tool in developing and testing antilock systems. If sufficiently high correlation can be developed between the vehicle and simulation performance, vehicle testing need only be used to confirm antilock system performance and certify vehicle performance.

COMPARISON OF SIMULATION AND VEHICLE DATA

To date, four different antilock systems were developed using the simulation models described. These systems were then vehicle tested. The comparison of simulation and test data showed that the simulations were effective in predicting qualitative performance and relative performance levels of the different systems. In addition, optimization of the system parameters during vehicle testing demonstrated that the optimum parameter values selected by simulation were also optimum of the vehicle.

Wheel velocity behavior in the simulation is considered to be in agreement with vehicle test data as shown in Figure 8. Differences that appear are due

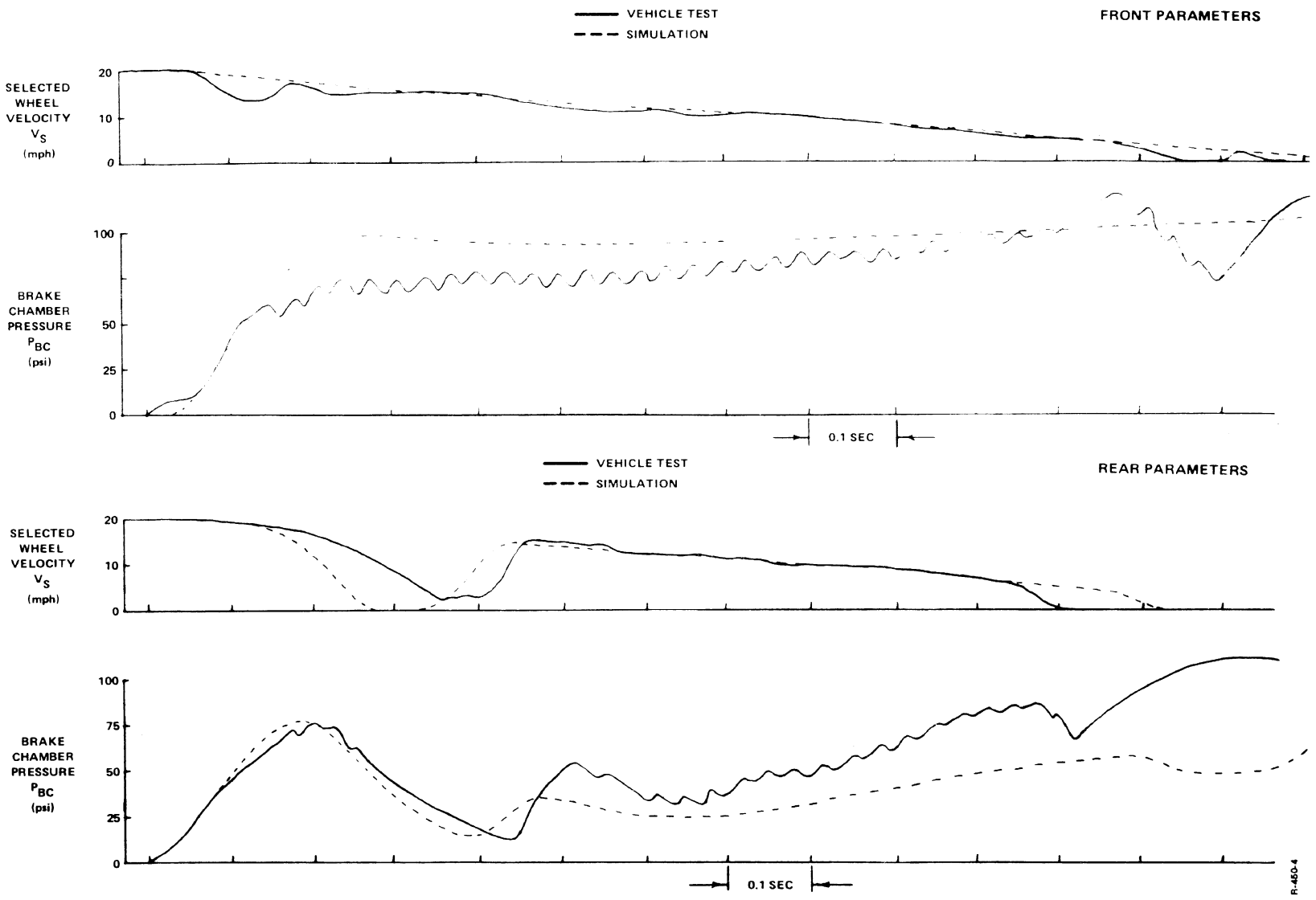

Figure 8. Comparison of Test Data and Simulation Results - Dry Asphalt, Loaded, V = 20 mph.

to the simplified weight transfer simulation model utilized. Weight transfer models that consider the vehicle pitch dynamics should reduce the observed differences.

CONCLUSIONS

Antilock brake systems have been designed using relatively simple simulation models. These models, structured to accommodate different developmental phases, have proven to be effective design tools. Comparison of vehicle and test data has demonstrated that the simulation adequately predicts system behavior. It has also been demonstrated that optimization of the system parameters can be accomplished using these various simulation models.

A GENERAL-PURPOSE SIMULATION FOR ANTISKID BRAKING SYSTEMS

C. C. MacAdam
Highway Safety Research Institute
The University of Michigan

ABSTRACT

A general purpose digital computer program for simulating the wheel sensor, control logic, and pressure modulator characteristics of antiskid systems is presented. The flexibility of the program is demonstrated by simulation results which reproduced the basic features exhibited by three antiskid systems tested in a laboratory setting. A final example showing the simulation result achieved using a proportional controller scheme for pressure modulation is also included.

INTRODUCTION

The antilock simulation presented in this paper is a flexible and general-purpose program which allows for the simulation of the basic features exhibited by many of today's widely varying antilock systems. The program is presently being used in conjunction with the HSRI truck and tractor-trailer digital simulation for the study and prediction of antilock braking performance.

The simulation concentrates on three areas common to most antilock systems: (1) wheel sensor, (2) control logic module, and (3) pressure modulator. Additional features and special options such as general purpose counters and one-shots are included for extended flexibility. Axle-by-axle systems are allowed for as well as three side-to-side options: (1) worst wheel, (2) best wheel, and (3) average wheel. Figure 1 shows the general block structure of the antilock program and its relationship to the main program represented by the "Vehicle Dynamics" block. Wheel speed, ω, is received from the main program and processed by the wheel sensor wherein an effective time delay occurs resulting in delayed wheel speed and acceleration signals, ω_d and $\dot{\omega}_d$. These signals along with $\dot{X}$, vehicle velocity, X, vehicle acceleration, and feedback from the pressure modulator, are input to the control logic module. The control logic outputs an ON/OFF solenoid command signal to the pressure modulator which in turn generates the brake pressure, P, returned to the main program.

The remaining sections of the paper outline and explain each of these areas in more detail. In

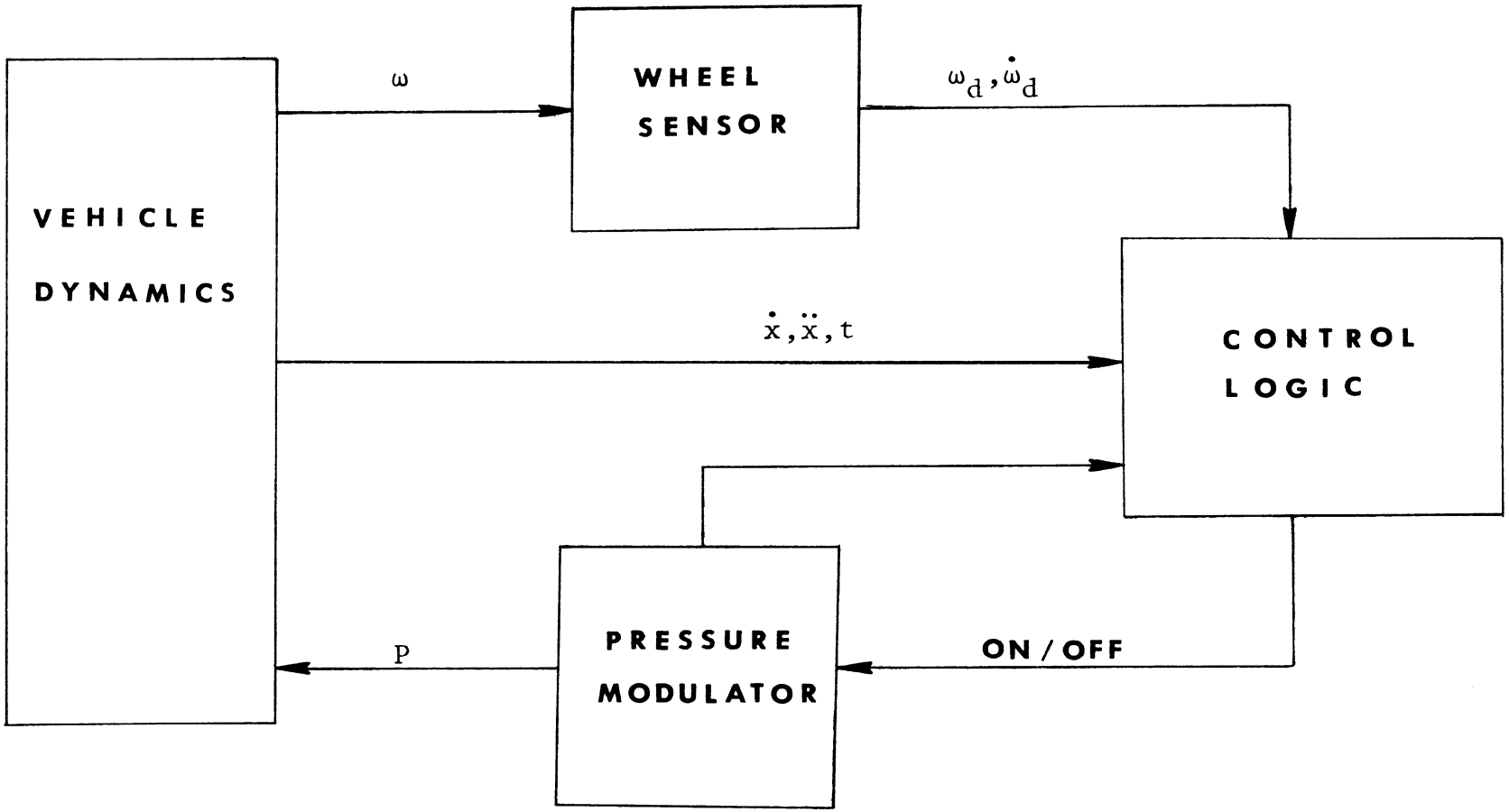

Figure 1
ANTI-LOCK BLOCK DIAGRAM

addition, laboratory test results for three different antilock sytems in use today, and the simulation of the basic features exhibited by these systems, are presented.

USER DICTIONARY OF VARIABLES/PARAMETERS

In order to offer flexibility to the program user as regards variable and parameter programming choices, a table or dictionary of pertinent antilock variables/parameters is included. This table includes such items as maximum and minimum pressure in the last cycle, times of the last ON or OFF solenoid command, maximum and minimum wheel accelerations in the last cycle, and other parameters that might be of special interest to an antilock system. The dictionary, as shown in Figure 2, is simply a listing of such variables and parameters which are available to the user.

The purpose of the dictionary is to allow the program user to select, from a wide variety of possible antilock variables/parameters, only those which are of interest to the particular system he is attempting to simulate.

A user selects, for programming purposes, a particular variable/parameter by referring to its variable I.D. numeral shown in Figure 2. Some of these variables/parameters are defined in Figure 3. (If a user has need for a particular variable or parameter not included in the dictionary, this can be accomplished by rather simple additions to the FORTRAN code.)

HSRI DYNAMIC VEHICLE SIMULATION
UNIT VEHICLE TANDEM AXLE MODEL

DICTIONARY OF ANTI-LOCK VARIABLES/PARAMETERS AVAILABLE TO USER.

VARIABLE I.D.	DESCRIPTION
1	1.0
2	TIME
3	OMEGA
4	OMEGADOT
5	XDOT
6	XDDOT
7	POFF1
8	POFF2
9	PON1
10	PON2
11	TOFF1
12	TON1
13	XDOFF
14	XDON
15	WOFF
16	WON
17	WDOFF
18	WDON
19	WDMAX
20	WDMIN
21	TPMAX1
22	TPMIN1
23	WLOCK
24	TLOCK
25	SLON
26	SLOFF
27	PMAX1
28	PMAX2
29	PMIN1
30	PMIN2
31	PD
32	ON
33	TMOD
34	SLIP
35	P
36	CYCNT
37	SQUARE
38	SQUARN
39	TOFF2
40	TON2
41	FOS1
42	FOS2
43	FOS3
44	GPCNT
45	WMAX1
46	WMAX2
47	TWMAX1
48	TWMAX2
49	WMIN
50	TWMIN
51	TPMAX2
52	TPMIN2

Figure 2

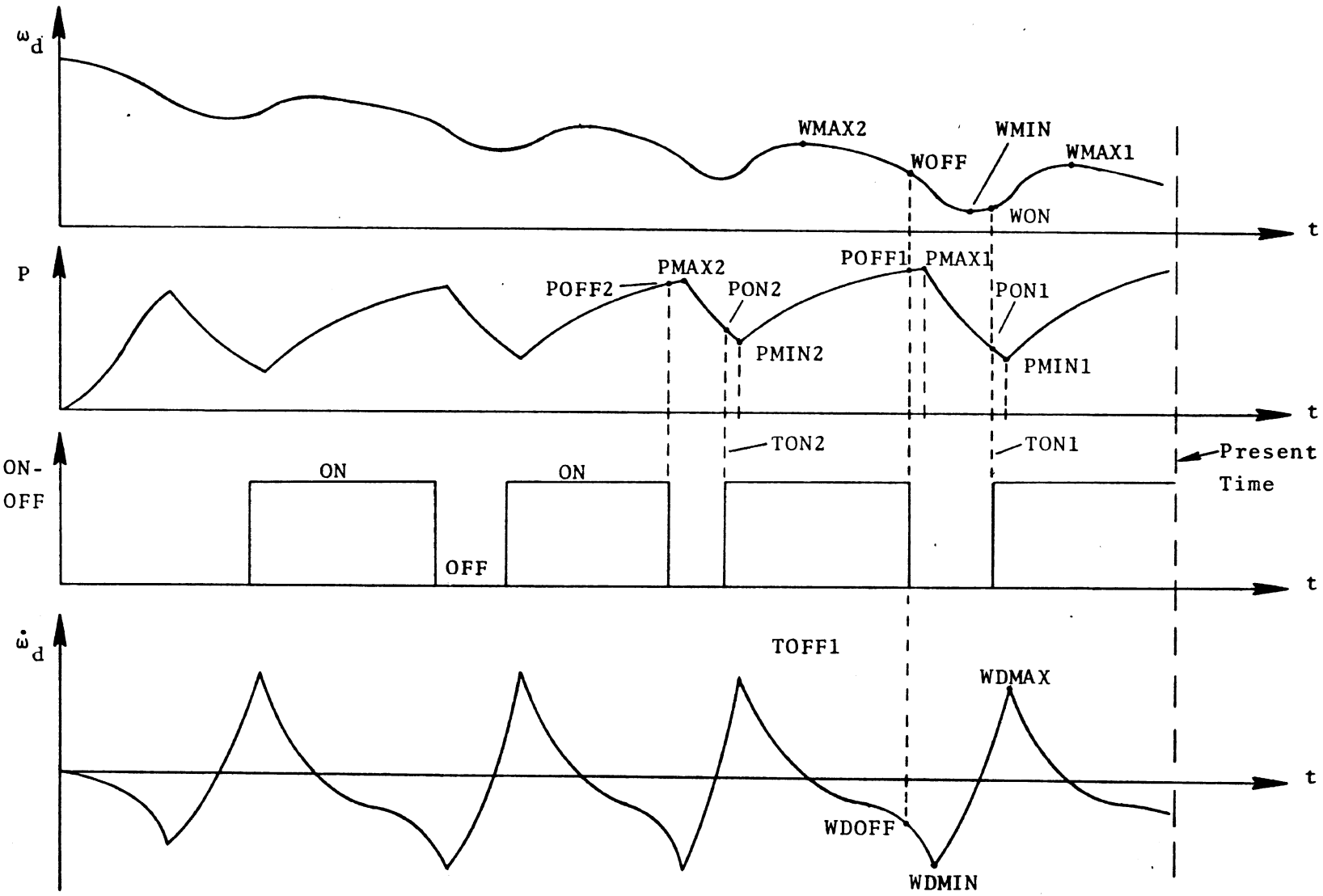

Figure 3. Variable/Parameter Relationships.

WHEEL SENSOR MODULE

The primary effect of a wheel sensor is a phase shift and/or time delay between the actual wheel rate and the derived wheel rate. This input-output relationship can often be described adequately by transfer functions of various order and/or transport time delay expressions. The present version assumes a general first-order filter of the form $\frac{1}{\tau_\omega p + 1}$ relating actual wheel rate and derived wheel rate, where τ_ω is the time constant of the filter and p is an operator-denoting differentiation with respect to time.

Many antilock systems make use of wheel acceleration derived from the output of the wheel sensor. This normally involves additional delays along with a differentiation process. The assumed transfer function here was taken as $\frac{p}{\tau_{\omega d} p + 1}$ relating derived wheel rate to derived wheel acceleration. The derived wheel acceleration calculation normally takes place within the electronic control unit. However, since it, along with wheel rate, is a primary input to the control unit logic, it is included here within the wheel sensor module so that the control unit can be characterized primarily by logical or decision-making processes. The wheel sensor module can then be described by the input-output relationships shown in Figure 4.

ω_d and $\dot{\omega}_d$ are used as the primary inputs to the control logic module. (Other variables are provided as possible inputs to the control logic module, however, no similar operations are attempted on these other input variables.) The assumed wheel sensor and derivative circuit input-output relationships are

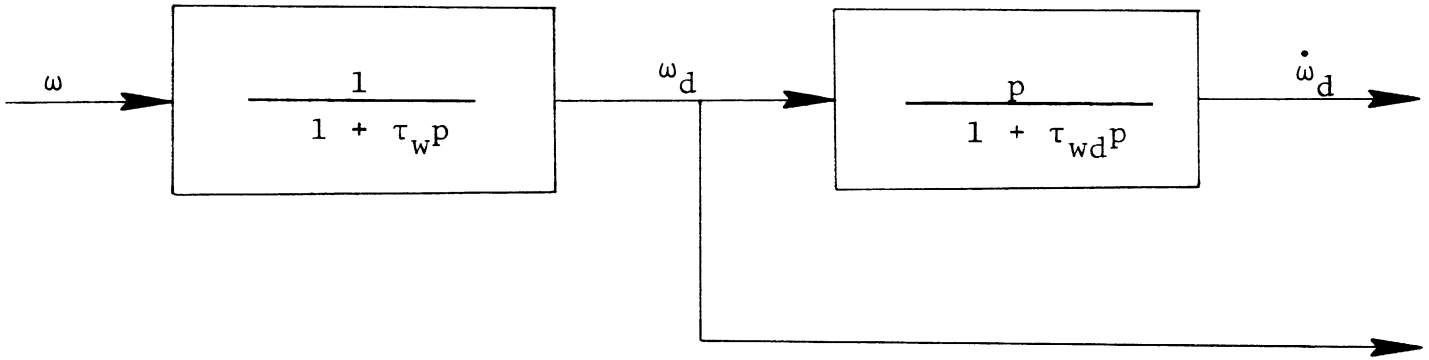

Figure 4
WHEEL SENSOR MODEL

therefore described by two input parameters, τ_{ω} and $\tau_{\omega d}$, which represent the first-order filter time constants of the wheel sensor and its derivative circuit. ω_d and $\dot{\omega}_d$ appear in the user dictionary as OMEGA and OMEGADOT, I.D. codes 3 and 4.

CONTROL LOGIC MODULE

The control logic is characterized by a set of eight inequality expressions which the user forms as necessary conditions for generating 'ON' and 'OFF' signals. Associated with each arithmetic inequality expression is a logical variable. These logical variables, reflecting the state or polarity of the inequality expressions, are logically combined to generate the 'ON' and 'OFF' signals.

Figure 5 summarizes the overall structure of the control logic module, showing the relationships between programmed inequality expressions on the left and the generation of an OFF/ON solenoid command on the right. The inequality expressions listed in column 1 are arithmetic in nature and are the primary means by which the user programs the control logic. Each inequality used would represent a necessary condition for applying or releasing brake pressure. The first four are used for the OFF command; the last four for the ON command. Associated with each is a logical variable, shown in column 2, having either the value TRUE or FALSE depending on whether or not the inequality is satisfied. These logical variables are combined, by the logical operators shown in column 3, to form a final OFF or ON solenoid command. The general forms of the logical equations are given by

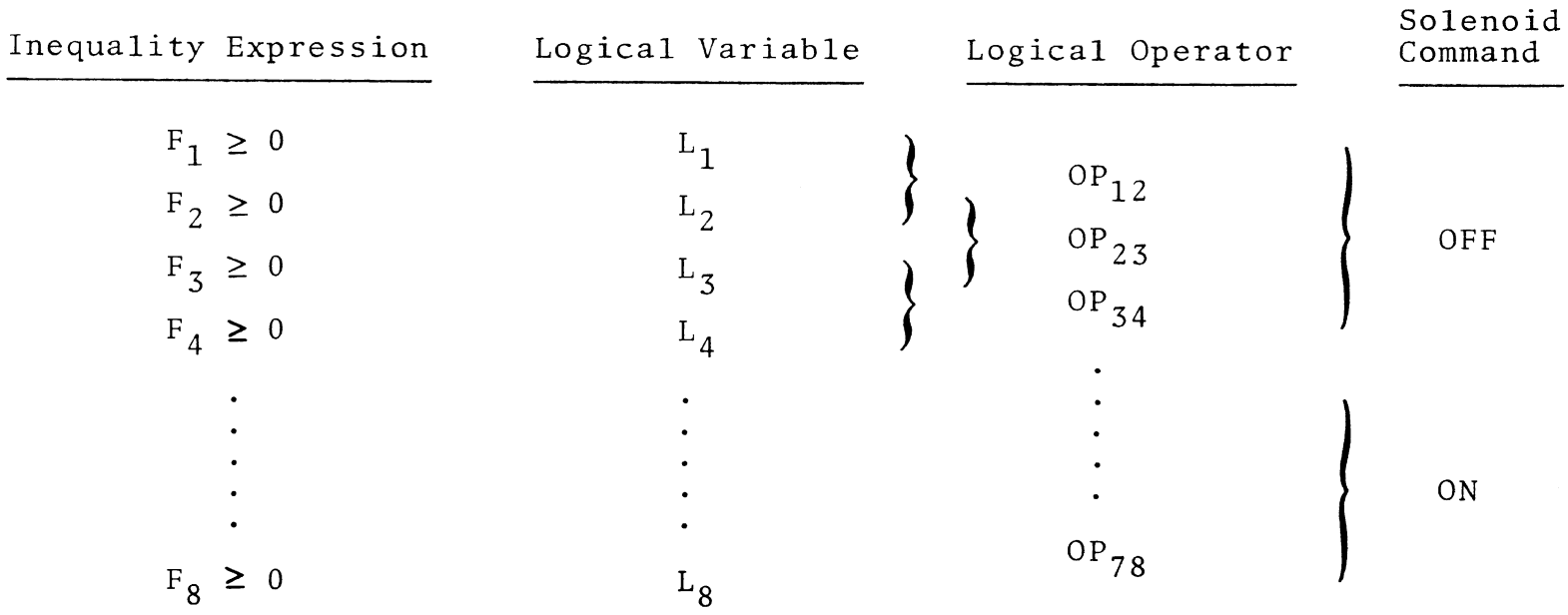

Figure 5
CONTROL LOGIC MODULE

$$OFF = (L_1 \; OP_{12} \; L_2) \; OP_{23} \; (L_3 \; OP_{34} \; L_4)$$

and

$$ON = (L_5 \; OP_{56} \; L_6) \; OP_{67} \; (L_7 \; OP_{78} \; L_8)$$

The user specifies the logical operations between L_1 and L_2, L_3 and L_4, and between the bracketed expressions by means of the three logical operator switches, OP_{12}, OP_{34}, and OP_{23}, respectively. Input values of 0 imply logical 'OR' operations; values of 1 imply logical 'AND' operations. The same rules apply to logical variables L_5, L_6, L_7, L_8 and their logical operator switches OP_{56}, OP_{78}, and OP_{67}.

The eight arithmetic inequality expressions, F_i, are defined by the following general form:

$$F_i \triangleq c_{i1}v_{i1} + c_{i2}v_{i2} + c_{i3}v_{i3} + c_{i4}v_{i4}w_{i4}$$

$$+ c_{i5}v_{i5}w_{i5} \geq 0 \quad , \quad (i=1,8)$$

where

c_{ij} , (j=1,5) are the constant coefficients of each term possessing an adaptive feature.

v_{ij}, w_{ik}, (j=1,5; k=4,5) are the variables/parameters selected from the user dictionary.

A wide variety of necessary conditions can be achieved with the variables/parameters available in the user dictionary and subject to the algebraic form given above.

Time delays within the control logic module can be achieved by means of four time delays provided within the control logic and/or by use of the special option one-shots.

ADAPTIVE COEFFICIENTS

Many antilock systems possess adaptive capabilities for changing coefficients involved in their control logic. For this reason, and increased programming flexibility, an adaptive coefficient feature is provided for in the program. Each coefficient, C_{ij}, involved in the inequality expressions may be allowed to change its value as a function of one or two dictionary variables in the manner shown in Figures 6 and 7.

In Figure 6, the value of C_{ij} is A_o, its initial value, or A_1 if u_{ij}, the adaptive variable, is <u>greater than</u> its break-point value of b_1.

If two adaptive variables, u_{ij} and z_{ij}, are involved as illustrated in Figure 7,

$$C_{ij} = \begin{cases} A_o & \text{if } u_{ij} \leq b_1 \text{ and } z_{ij} \leq b_2 \\ A_1 & \text{if } u_{ij} > b_1 \text{ and } z_{ij} \leq b_2 \\ A_2 & \text{if } z_{ij} > b_2 \end{cases}$$

By including an additional numerical switch in the input, the two adaptive variable case may be altered to:

$$C_{ij} = \begin{cases} A_o & \text{if } u_{ij} \leq b_1 \\ A_1 & \text{if } u_{ij} > B_1 \text{ and } z_{ij} \leq b_2 \\ A_2 & \text{if } u_{ij} > b_1 \text{ } \underline{\text{and}} \text{ } z_{ij} > b_2 \end{cases}$$

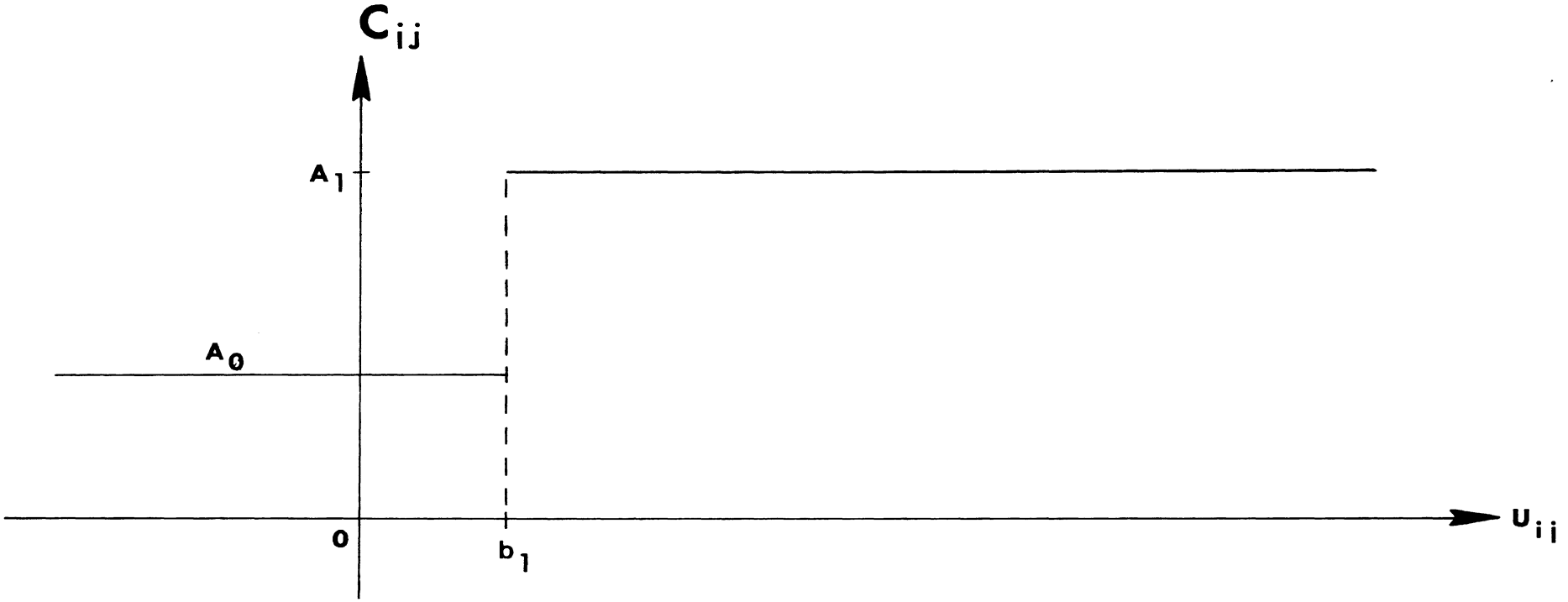

Figure 6. Adaptive Coefficient Feature

$$C_{ij} = \begin{cases} A_0 \text{ , if } u_{ij} \leq b_1 \text{ and } z_{ij} \leq b_2 \\ A_1 \text{ , if } u_{ij} > b_1 \text{ and } z_{ij} \leq b_2 \\ A_2 \text{ , if } z_{ij} > b_2 \end{cases}$$

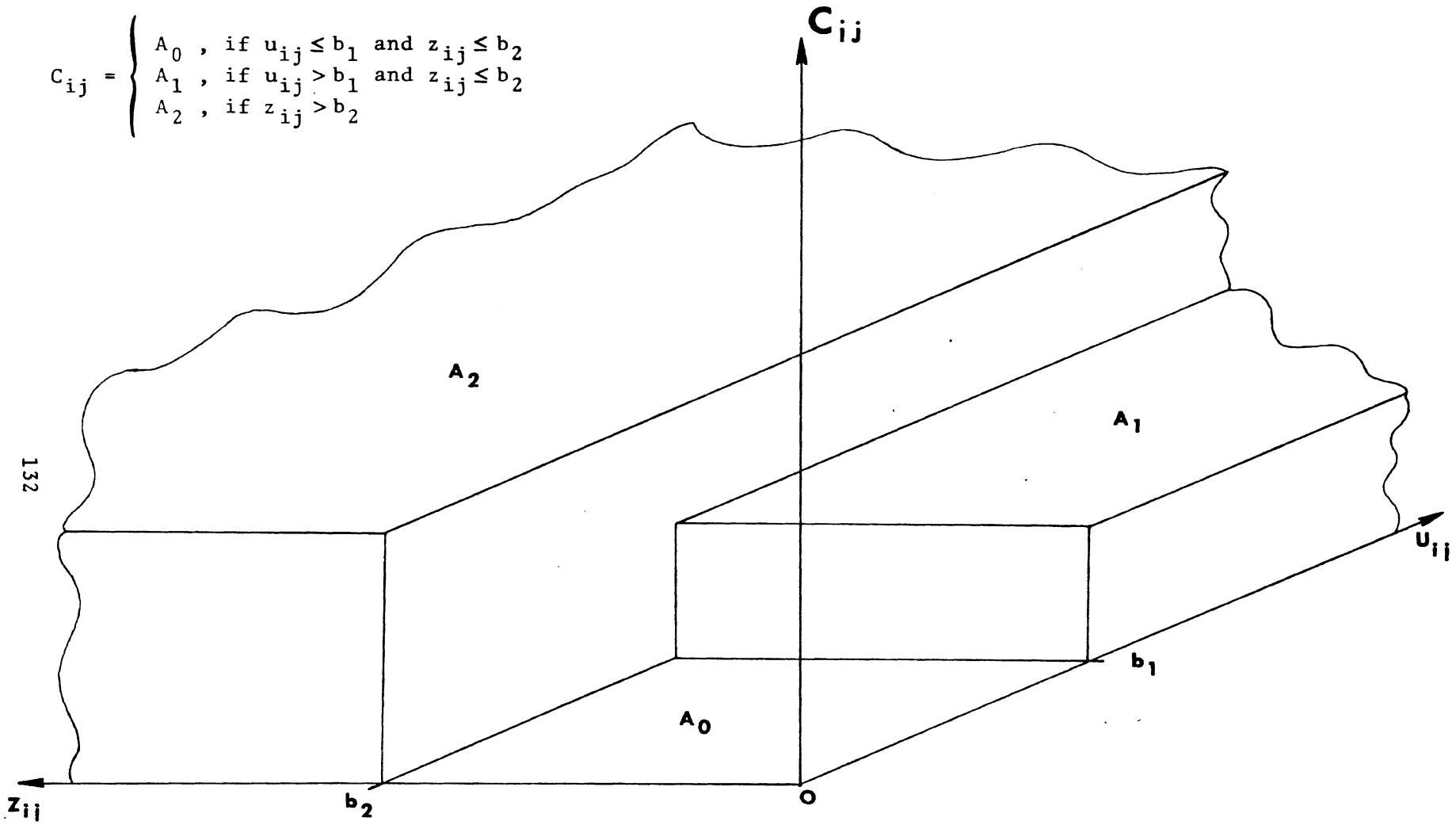

Figure 7.
ADAPTIVE COEFFICIENT FEATURE

SIDE-TO-SIDE OPTIONS

Three different side-to-side options per axle are available. One antilock system is allowed for each axle with the same pressure being returned to both sides for each of the available options. These are summarized below:

OPTION 1 - Worst Wheel. The wheel having the lowest rotational rate for a given axle is selected by the control logic as its input. The same pressure is returned to both sides based on this input.

OPTION 2 - Best Wheel. Same as Option 1 except that the wheel with the highest rotational rate is selected as input.

OPTION 3 - Average Wheel. Both wheel rates are averaged by the control logic module and used as input. The same pressure is returned to both sides.

For vehicle velocities less than 7 ft/sec, the antilock simulation is inactivated and line pressures will follow the treadle pressure.

LOGIC SAMPLING RATE CONTROL

The program user is asked to specify a logic sampling period, TSMPLE, which controls the rate at which the antilock logic is interrogated. If TSMPLE is specified to be less than or equal to the digital simulation time step, then no sampling rate control is in effect. If, however, a logic sampling period greater than the digital simulation time step is called for, all control logic and special option features

pertaining to the control logic module are interrogated at time intervals set by the logic sampling period, TSMPLE. Wheel sensor computations and pressure modulator activities are not affected.

PRESSURE MODULATOR

The pressure modulator valve is simulated by two time delays and several programmable rise and fall rates for both exponential and linear characteristics. The programmable rise and fall rates make possible the simulation of relatively complex pressure modulator activity including designs involving pneumatic logic and pulse-width modulators. See Figure 8.

T_{ON} and T_{OFF} are the time delays between solenoid command signals and the corresponding times of pressure increase or decrease. These are specified as constant inputs for the program.

The manner in which the exponential or linear rise and fall rates are defined is shown in Figures 9 through 12. The rates are programmed as a function of a general form expression (similar to the control logic forms) shown as $\varepsilon_1 \ldots \varepsilon_4$. The breakpoints, $x_1 \ldots x_8$, separate the three rate regions along the respective ε_i axes. The exponential rates are functions of ε_1 and ε_2 defined as

$$\varepsilon_1 \triangleq H_1 v_1 + H_2 v_2 + H_3 v_3 + H_4 v_4 w_4 + H_5 v_5 w_5$$

$$\varepsilon_2 \triangleq G_1 v_1 + G_2 v_2 + G_3 v_3 + G_4 v_4 w_4 + G_5 v_5 w_5$$

a) Time Delays ; T_{on},T_{off}

b) Exponential Pressure Characteristic

c) Linear Pressure Characteristic

d) Programmable Rise and Fall Rates

Figure 8
PRESSURE MODULATOR

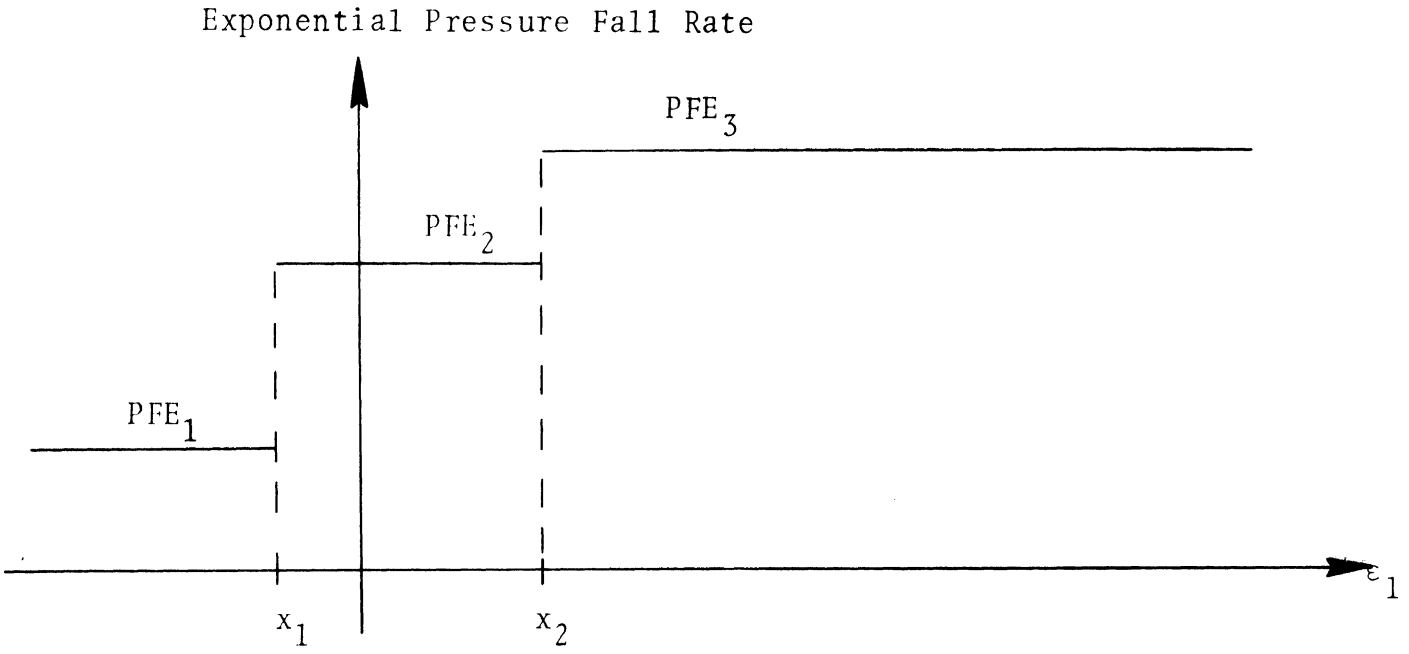

Figure 9.

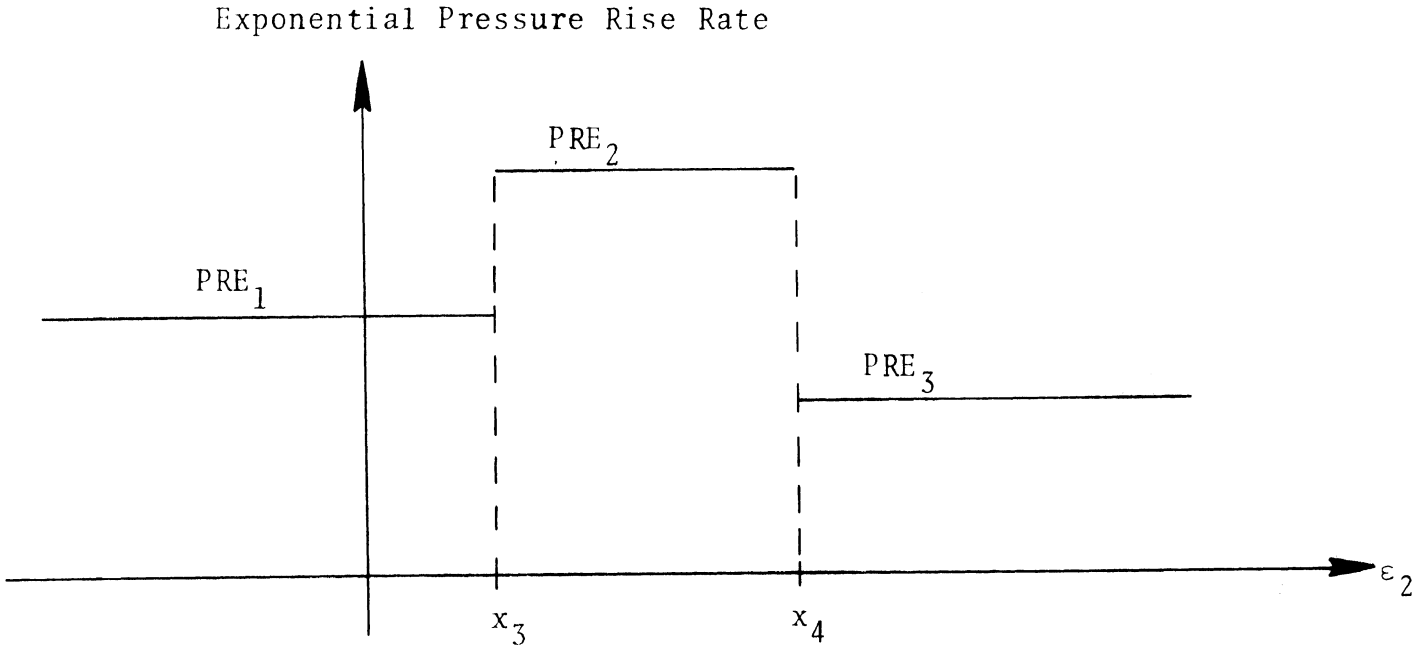

Figure 10.

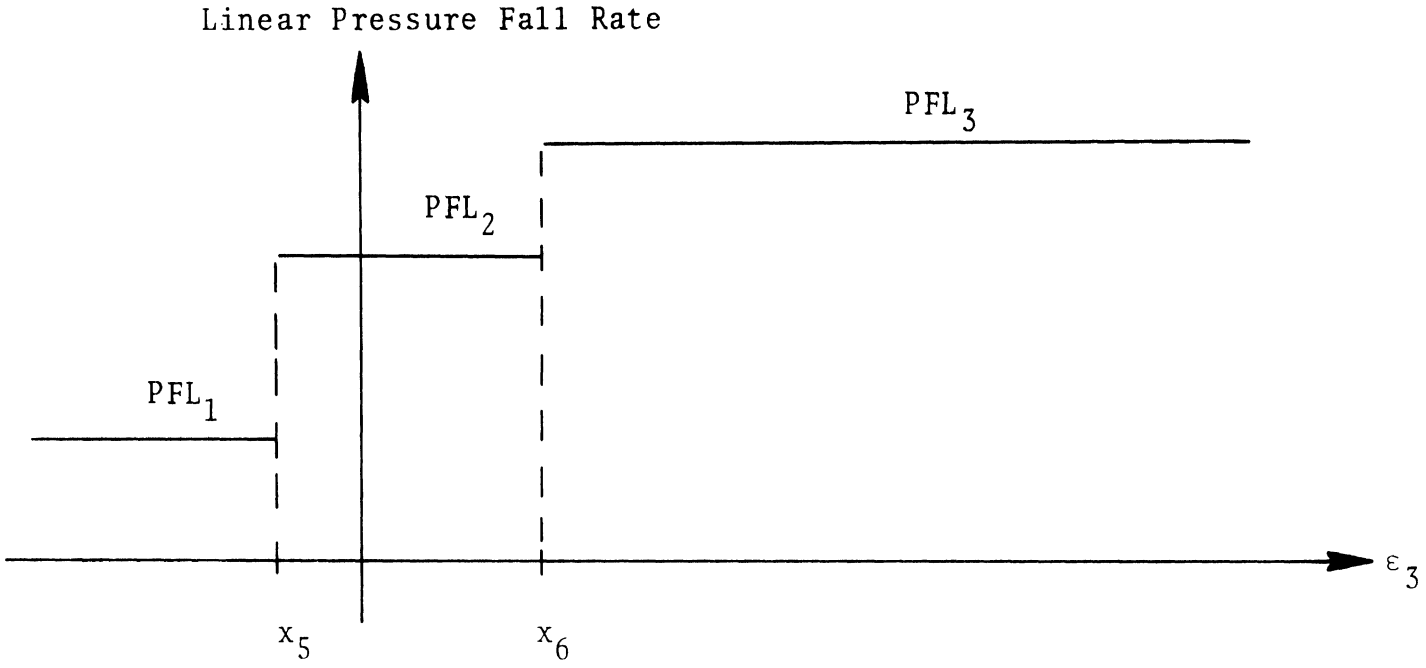

Figure 11.

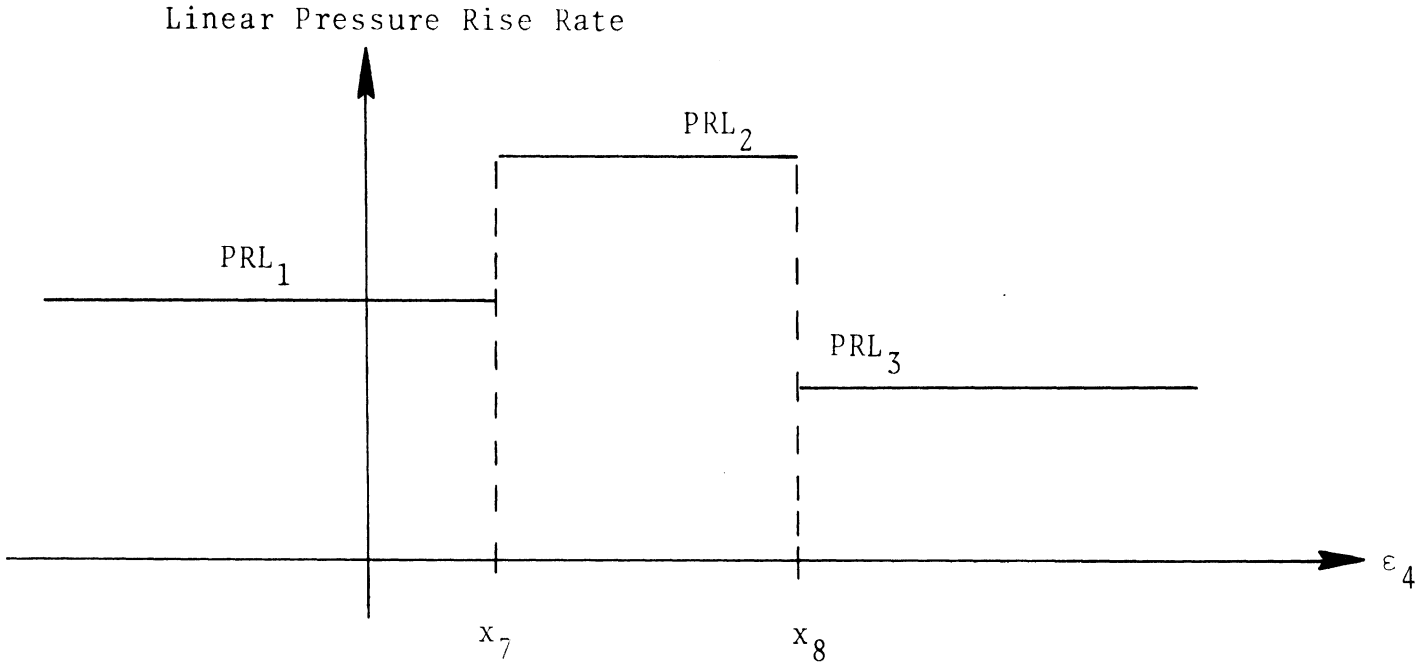

Figure 12.

where H_i and G_i, (i=1,5), are the constant coefficients of each term, and v_j and w_k, (j=1,5; k=4,5), are variables/parameters available in the user dictionary. A similar set of equations define ε_3 and ε_4 for the linear pressure rates. PFE_1, PFE_2, etc., denote the specific rate values.

SPECIAL OPTIONS

Four special options have been included in the model in order to facilitate simulation of certain features displayed in some actual antilock systems while also providing increased programming flexibility. The four options referred to are:

1) Treadle or Demanded Pressure Modulation

2) Pulse-Width-Modulated Square Wave

3) One-Shots

4) General Purpose Counter

TREADLE PRESSURE MODULATION/PROGRAMMING

Most pressure valves operating without antilock interruption, and many under antilock cycling, follow or are limited above by the treadle pressure application; while similarly, fall to treadle pressure or zero pressure when treadle pressure is decreased or removed. However, in some valves, during antilock cycling, pressure may rise to some limiting pressure less than treadle and/or fall to some pressure greater than zero. Such treadle modulation or programming of demanded pressure is a feature which is allowed for under this option.

PULSE-WIDTH MODULATED SQUARE WAVE

A time, or pulse-width, modulated square wave is provided as an option for general use. This option was motivated by a particular antilock system known to possess such a feature for purposes of treadle pressure modulation. The square wave generated under this option can be used in any portion of the program and is available in the user dictionary under the name SQUARE. Figure 13 illustrates the parameter and variable relationships which define the square wave. The period of the square wave, PERIOD, is constant. The amount of time modulation, represented by TMOD, may be variable and programmable. This is accomplished in the program by allowing the ratio, TMOD/PERIOD, to be a tabular function of a variable, ε_5, as shown in Figure 14. ε_5 is defined as a general form expression:

$$\varepsilon_5 = PW_1 v_1 + PW_2 v_2 + PW_3 v_3 + PW_4 v_4 w_4 + PW_5 v_5 w_5$$

where

PW_i , (i=1,5) are constant coefficients for each term. The adaptive coefficient feature is provided for these coefficients.

v_i, w_k , (i=1,5; k=4,5) are variables/parameters selected from the user dictionary.

Note that the FZ_i values in the $\frac{TMOD}{PERIOD}$ table should not be greater than 1.0 or less than 0.0. Values of 1.0 ideally signify 100% modulation; values of 0.0, no modulation. (In actuality, the degree of modulation attainable depends on the simulation time step and the period chosen for the square wave.)

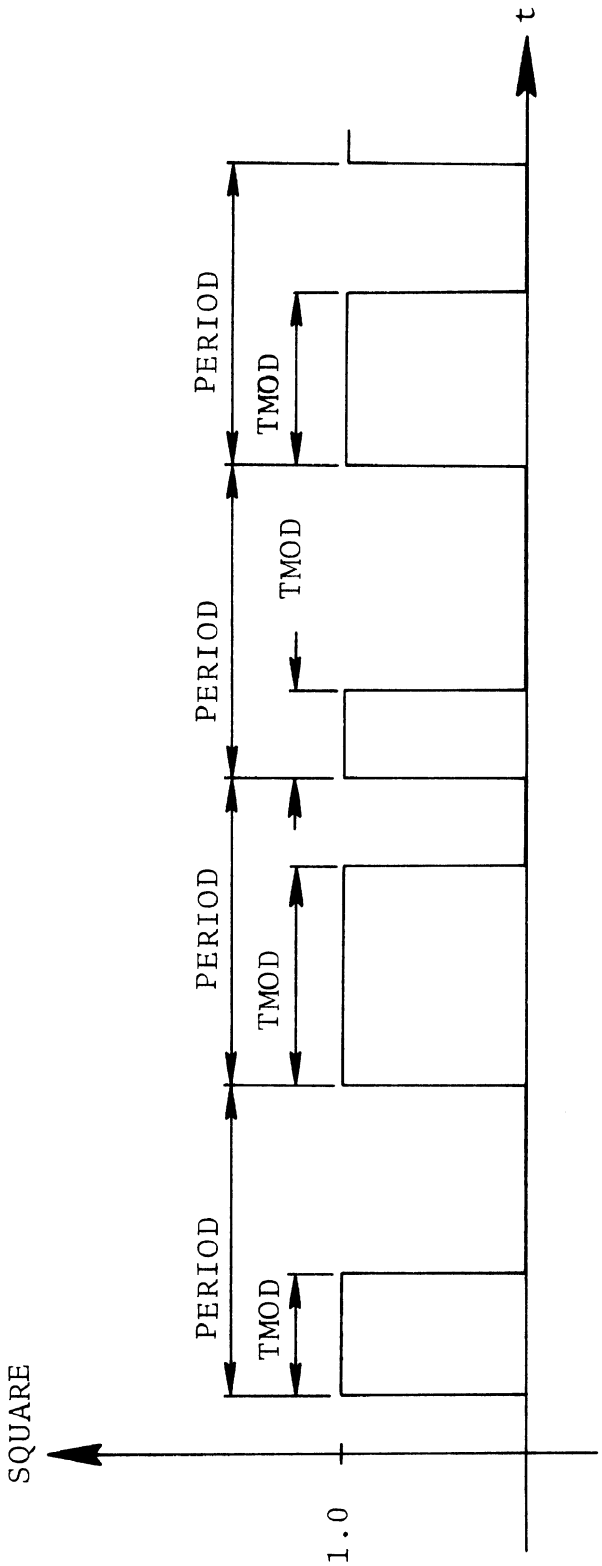

Figure 13. Pulse Width Modulated Square Wave

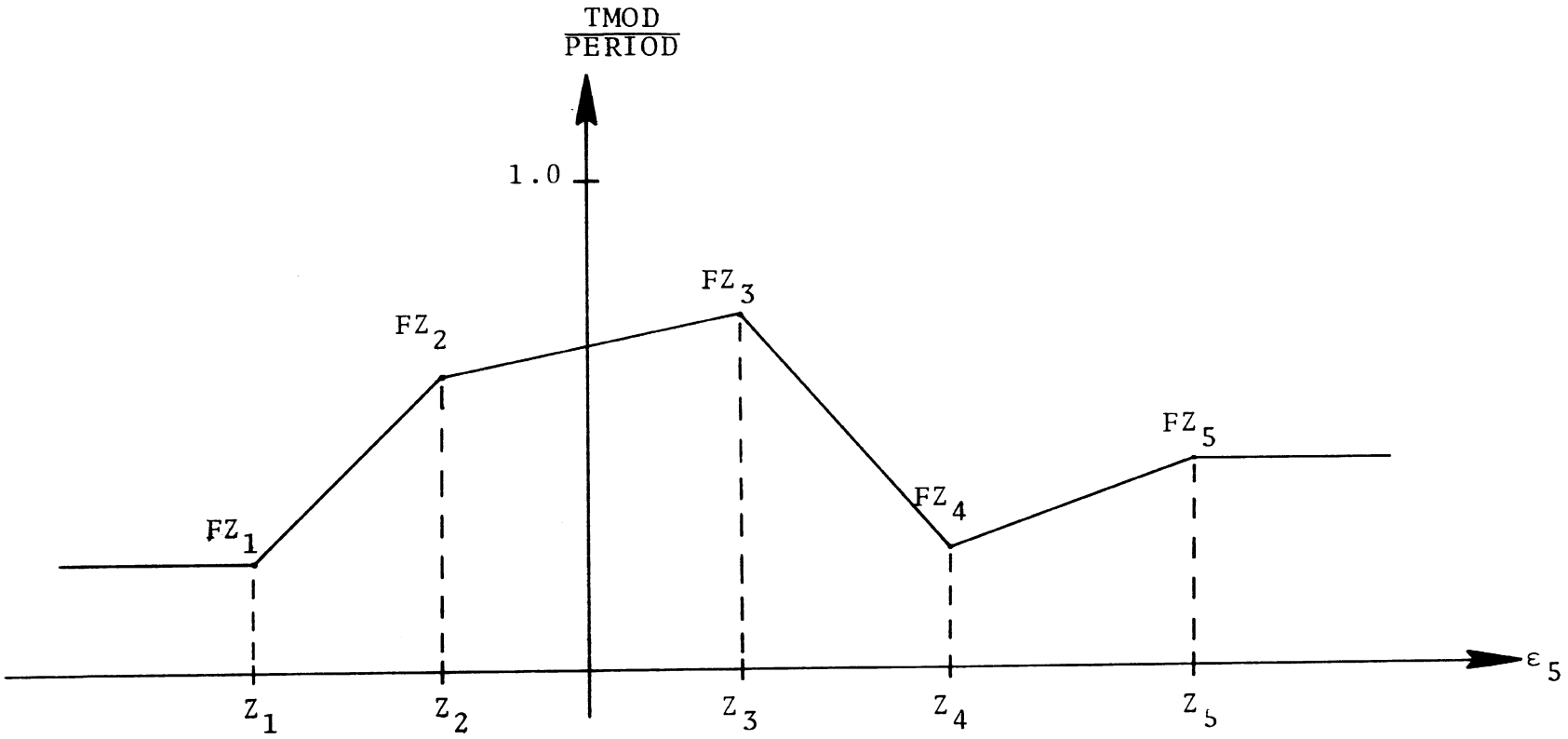

Figure 14. Pulse Width Table

ONE-SHOTS

Three programmable one-shots are provided under this option and can be used for several different purposes. Two common uses would be: (1) time delay effects and (2) as auxiliary binary variables for use in any general purpose expressions. The three one-shots, by definition here, are binary variables having the numerical value of 1.0 or 0.0. These are available in the user dictionary under the names FOS1, FOS2, and FOS3.

The one-shots used in the program operate according to the following rule: If a trigger or input condition (inequality) changes from negative to positive, the one-shot will change its value from 0.0 to 1.0 for a fixed length of time, specified by the user, then return to 0.0. During a one-shot firing (1.0 value), the trigger input is disabled and cannot effect recurrent firings from this state. The one-shot is reset for another firing by two occurrences: (1) the time duration of the present one-shot firing has been exceeded, followed by or concurrent with, (2) the trigger condition being negative. A trigger condition value of 0.0 is interpreted by the program as positive. See Figure 15.

The trigger condition is defined by the general form expression:

$$OS_1 v_1 + OS_2 v_2 + OS_3 v_3 + OS_4 v_4 w_4 + OS_5 v_5 w_5 \geq 0$$

where

OS_i, (i=1,5) are constant coefficients for each term and possess the adaptive coefficient feature.

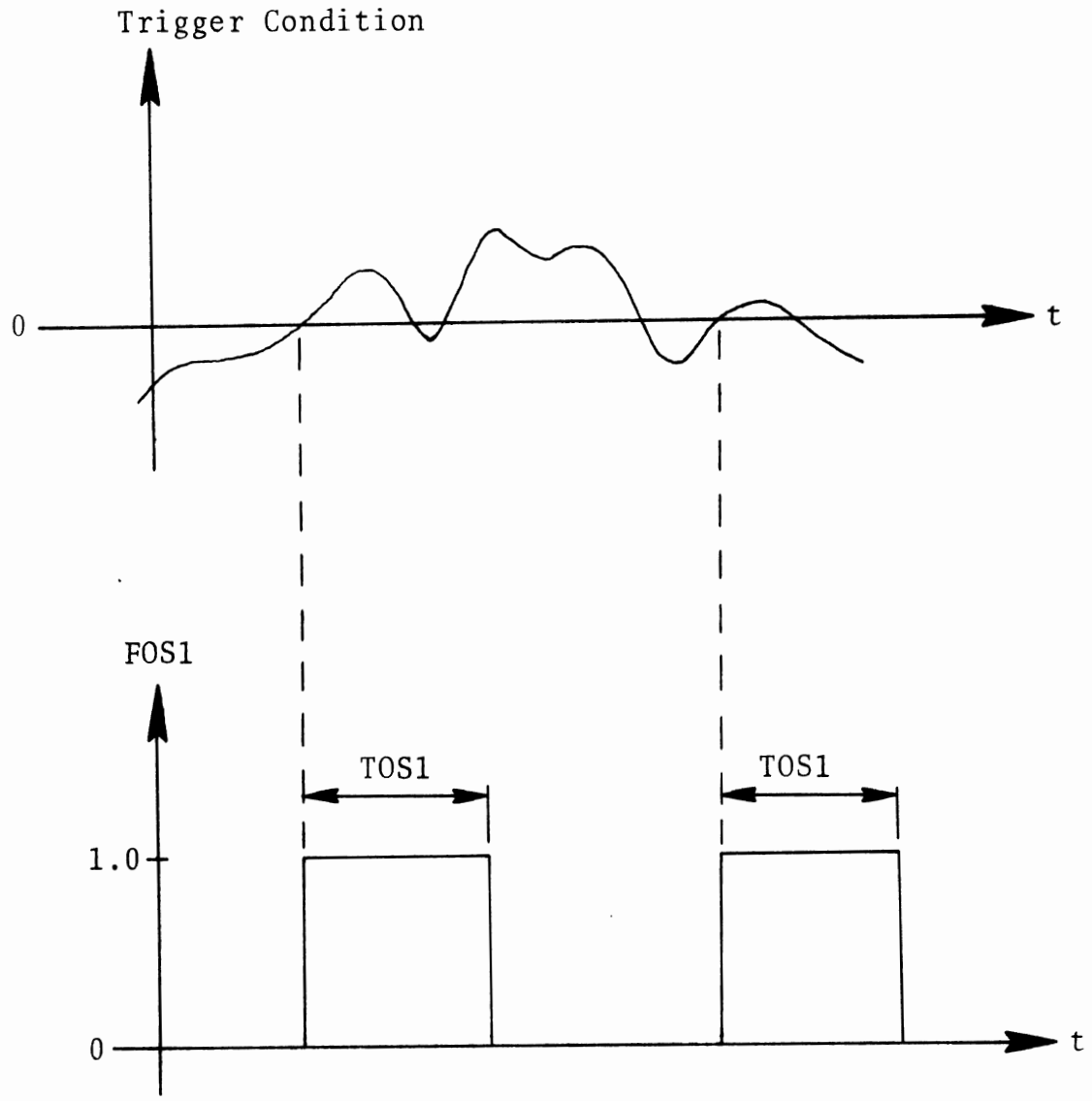

Figure 15. One-Shot Operation

v_i, w_k , (i=1,5; k=4,5) are variables/parameters from the user dictionary.

Each one-shot trigger is programmable by a general form expression as shown above. The one-shot time durations are denoted as TOS1, TOS2, and TOS3 and are required as input for each one-shot used.

GENERAL-PURPOSE COUNTER

This option allows the user to generate a counter sequence by incrementing a counter by 1 every digital time step, if a particular inequality expression is greater than or equal to 0. The variable containing the count is called GPCNT and is in the user dictionary with the I.D. code 44. The general form expression is given by

$$GP_1v_1 + GP_2v_2 + GP_3v_3 + GP_4v_4w_4 + GP_5v_5w_5 \geq 0$$

where

GP_i , (i=1,5) are constant coefficients for each term and can be adaptive.

v_i,w_k , (i=1,5; k=4,5) are variables/parameters from the user dictionary.

If the above inequality is satisfied, the GPCNT count is incremented each time step. If only a one count increment is desired whenever a particular condition is satisfied, then a one-shot could be fired for a time period equal to or less than the digital time step, with the general purpose counter incrementing itself every one-shot firing.

The above discussion applies whenever the logic sampling period is specified as less than or equal to the digital simulation time step. If the user specifies a larger logic sampling period (slower sampling rate), then the general-purpose counter will be incremented only each logic sampling period.

LABORATORY-SIMULATION RESULTS

The flexibility of the antilock program is demonstrated in the following section which contains both laboratory antilock system test results and corresponding simulation results. The basic characteristics which are exhibited in the laboratory test results are reproduced using the antilock program.

Laboratory test data for three different types of antilock braking systems was gathered by means of the arrangement outlined in Figure 16. Left and right wheel dynamics for one axle were simulated on an analog computer supplying a pair of wheel speed signals to a truck's antilock logic module. A pressure transducer, installed on the truck's corresponding brake chamber, returned an electrical signal proportional to brake pressure back to the analog computer, closing the loop. During a typical test, an operator stationed in the truck's cab would fully depress the air brake so as to simulate a panic stop thereby cycling the truck's antilock system. During each test, brush recordings were made of wheel speed, wheel acceleration, brake pressure, and tire force.

The corresponding digital simulation results are for the front tandem axle of a 3-axle straight

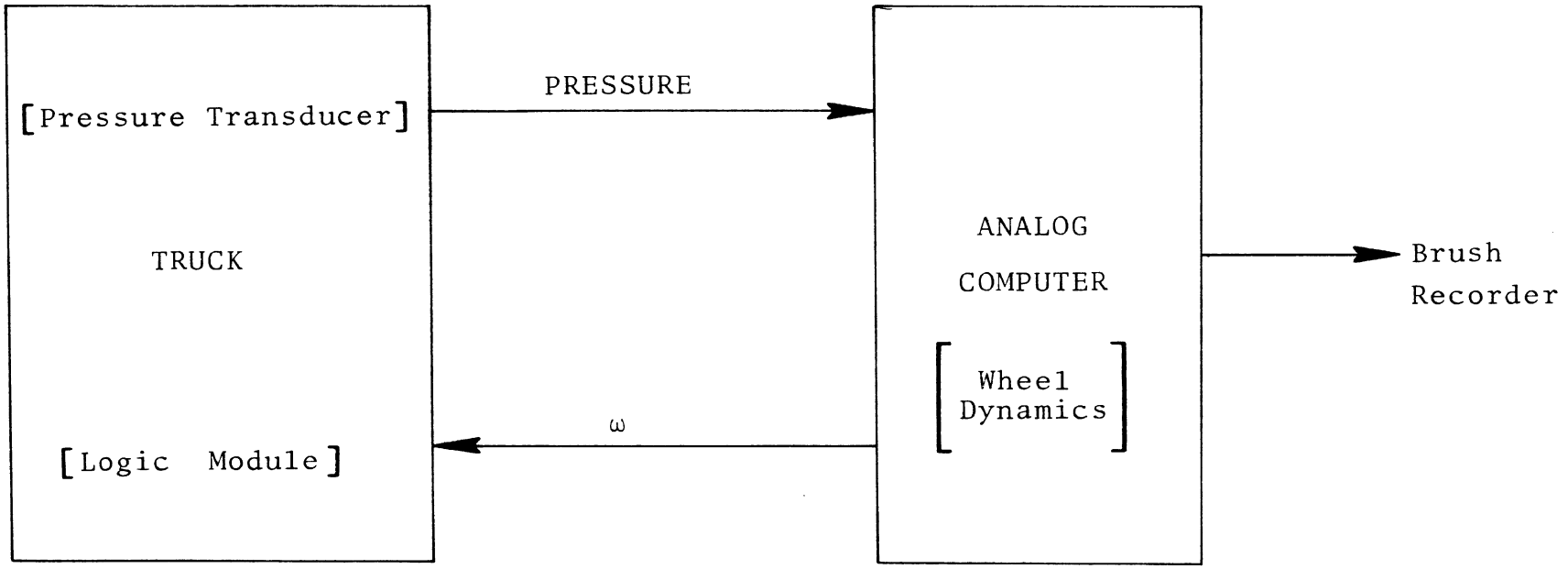

Figure 16

LABORATORY SETUP

truck loaded to 44,000 lbs. The loaded truck had a 62" c.g. height and 165" wheelbase.

Figure 17 shows a brake pressure and wheel slip time history laboratory test result for System #1. The cycling frequency is about 4 Hz with minimum slip values of about 10%. μ_p and μ_s are the peak and locked wheel friction coefficient values for the tire-road interface. G_b is the brake gain factor for the simulated linear torque-pressure relationship (analog computer).

Figure 18 shows the digital simulation result for very similar road and load conditions. The pressure and wheel slip characteristics are in very good agreement with the laboratory result for this case.

Figure 19 shows the laboratory result for System #2 which exhibits a more complicated valve characteristic. The pressure rise contains a knee or breakpoint which separates an exponential-like characteristic from a slow linear-like characteristic. In addition, a certain amount of one-shot activity takes place in the valve represented by the small pressure releases occurring within the first 2 seconds.

Figure 20 shows a simulation result with features very similar to those shown in Figure 19. Even though the load and brake factor are different than those for the lab result, the basic pressure trace and wheel slip characteristics are reproduced rather well.

Figure 21 demonstrates the way in which the valve mechanism for System #2 was simulated. A pressure bleed or time ramp from the maximum pressure in the previous cycle (shown as the dashed line) determined the knee or breakpoint for the pressure rise. Pressure

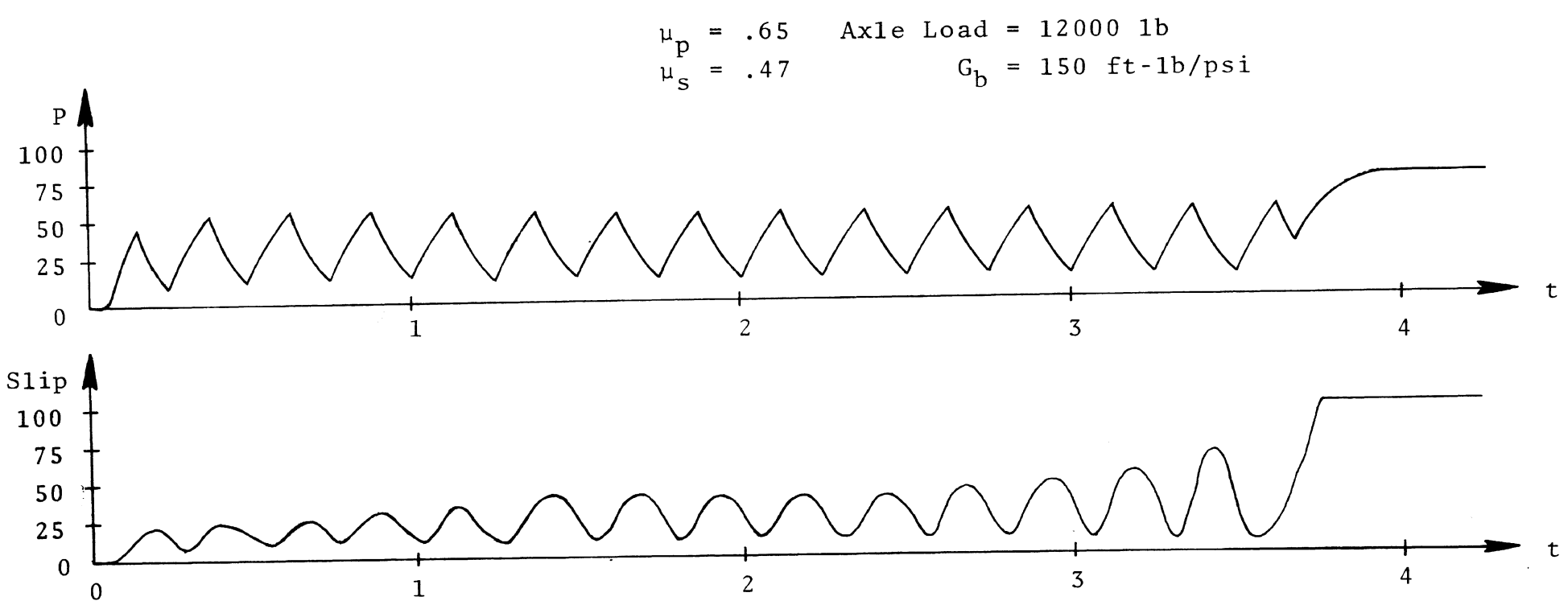

Figure 17

LABORATORY TEST --- SYSTEM #1.

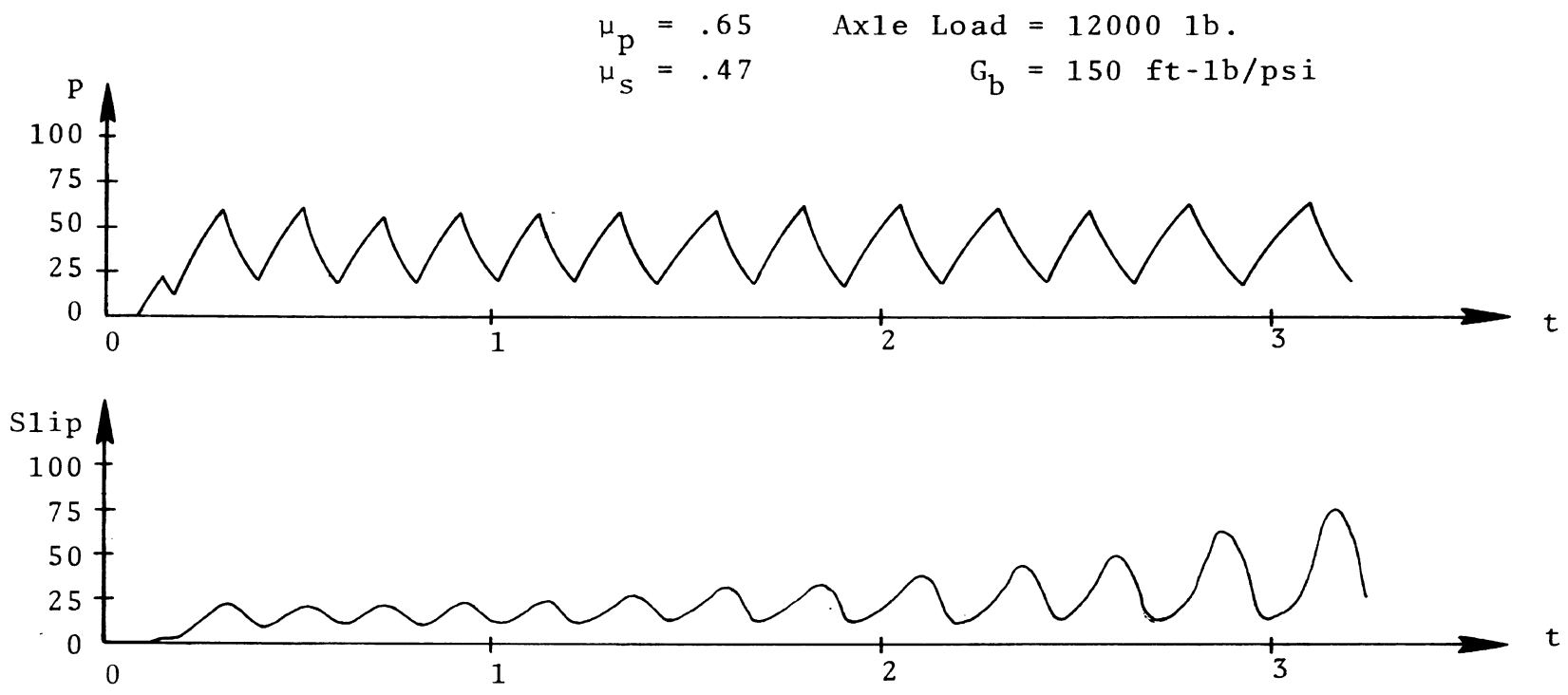

Figure 18
SIMULATION RESULT --- SYSTEM #1.

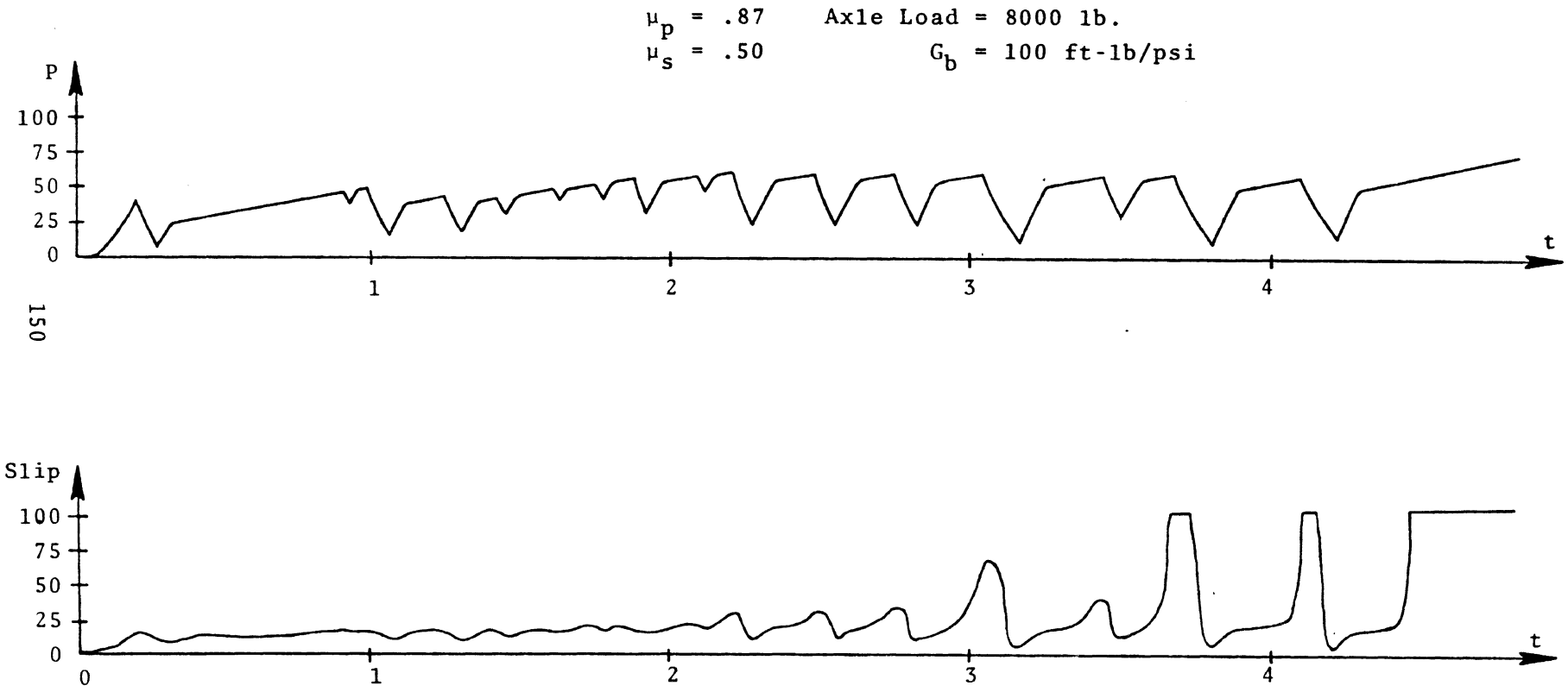

Figure 19
LABORATORY TEST --- SYSTEM #2.

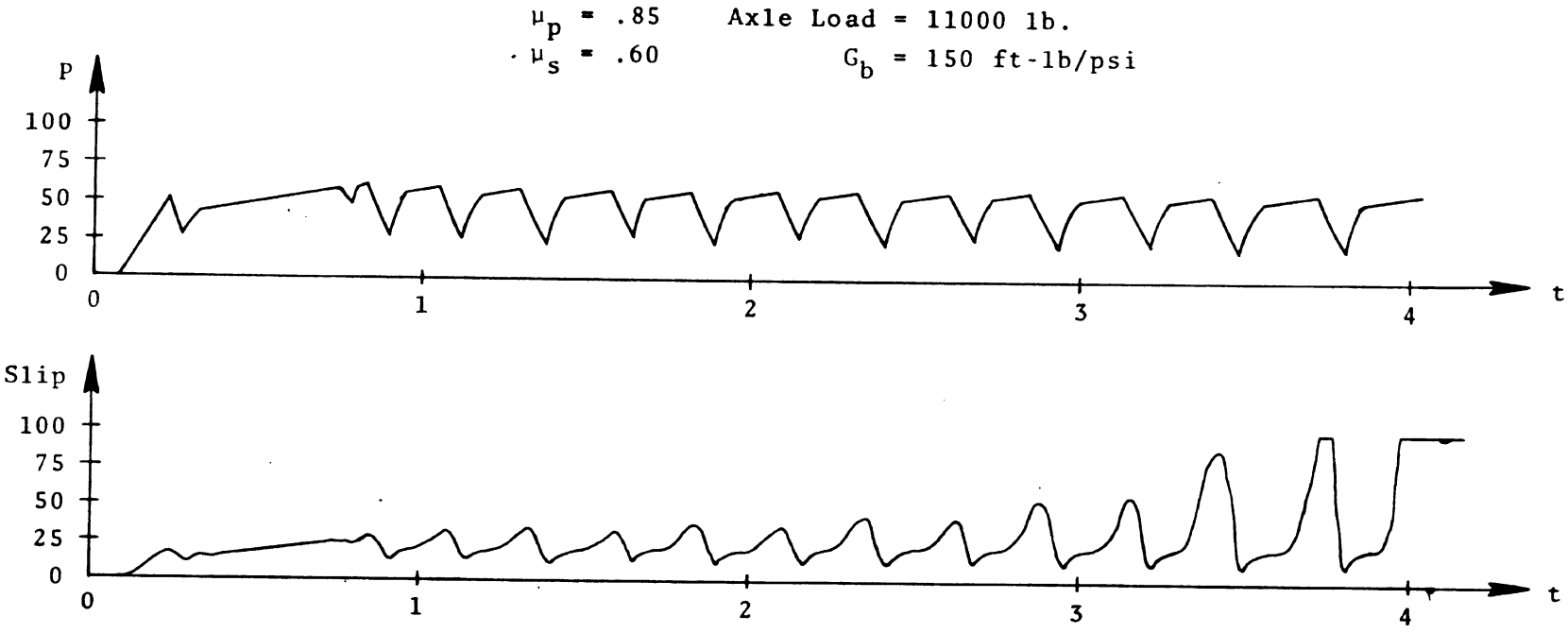

Figure 20
SIMULATION RESULT --- SYSTEM #2.

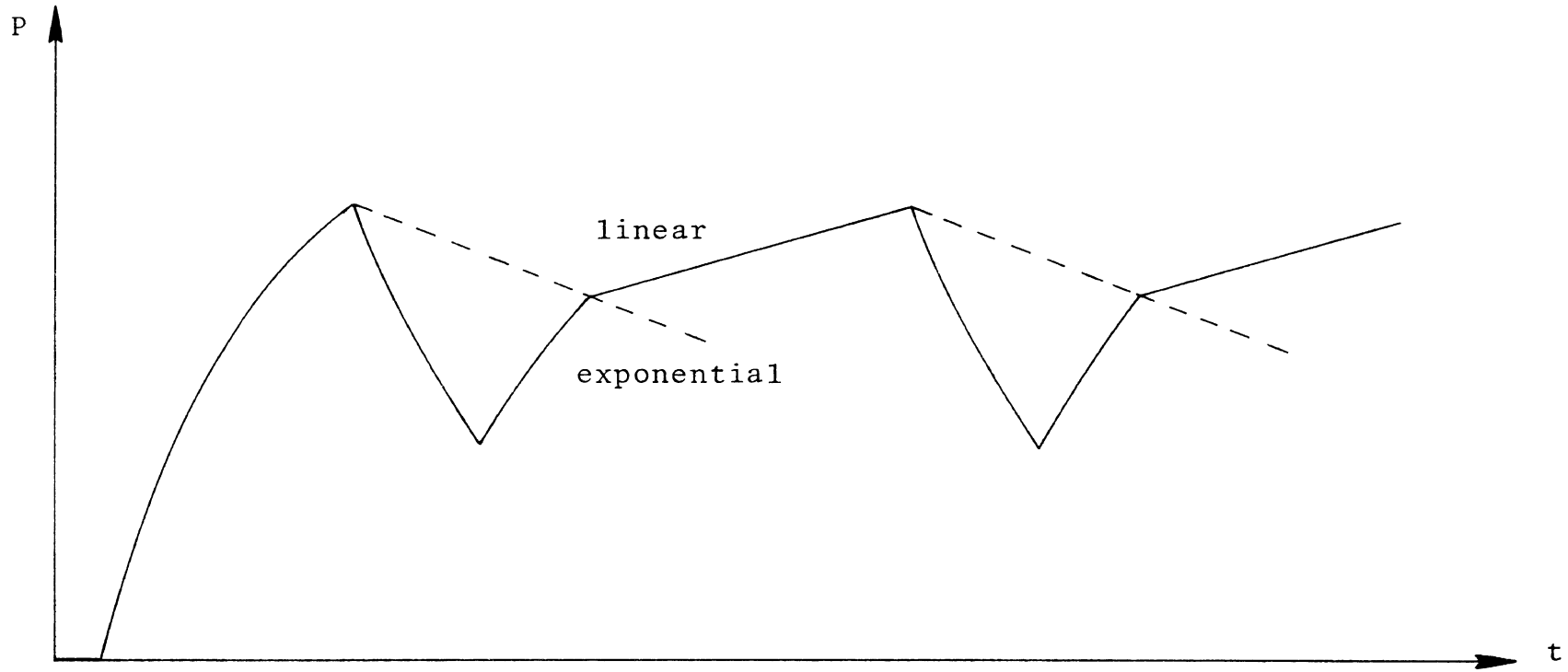

Figure 21. PRESSURE MODULATOR CHARACTERISTIC --- SYSTEM #2.

rates below this time ramp were defined as exponential in nature; those above were linear.

The laboratory test for System #3 is shown in Figure 22. This is a digital system using a pulse-width modulated square wave for pressure modulation. The cycling in the first second is fairly rapid and is gradually reduced to about 2 Hz for subsequent cycles. Note also the level to which pressure rises in the first few cycles is gradually decreased to a relatively constant value.

Figure 23 shows a digital simulation result for this type of system. The initial rapid cycling and gradual reduction in cycling frequency to demanded pressure level is simulated rather well. The simulation used the maximum pressure achieved in the last cycle as means of modulating the demanded pressure for subsequent cycles.

Figures 24 and 25 do not represent any particular antilock system, but are included to demonstrate the type of results possibly achieved using a continuous control. Figure 24 shows the results for a proportional controller wherein the difference between demanded brake pressure, P_d, and the present brake pressure, P, is modulated in direct proportion to the error between the wheel slip and a reference value of 20%. The response is somewhat like a lightly damped second-order system for the selected value of K.

Figure 25 is for the same control scheme but now with rate control, represented by the $L(\dot{\omega} + 40.)$ term, added. The increased damping, due to the rate control, significantly improves the slip time history within the first second.

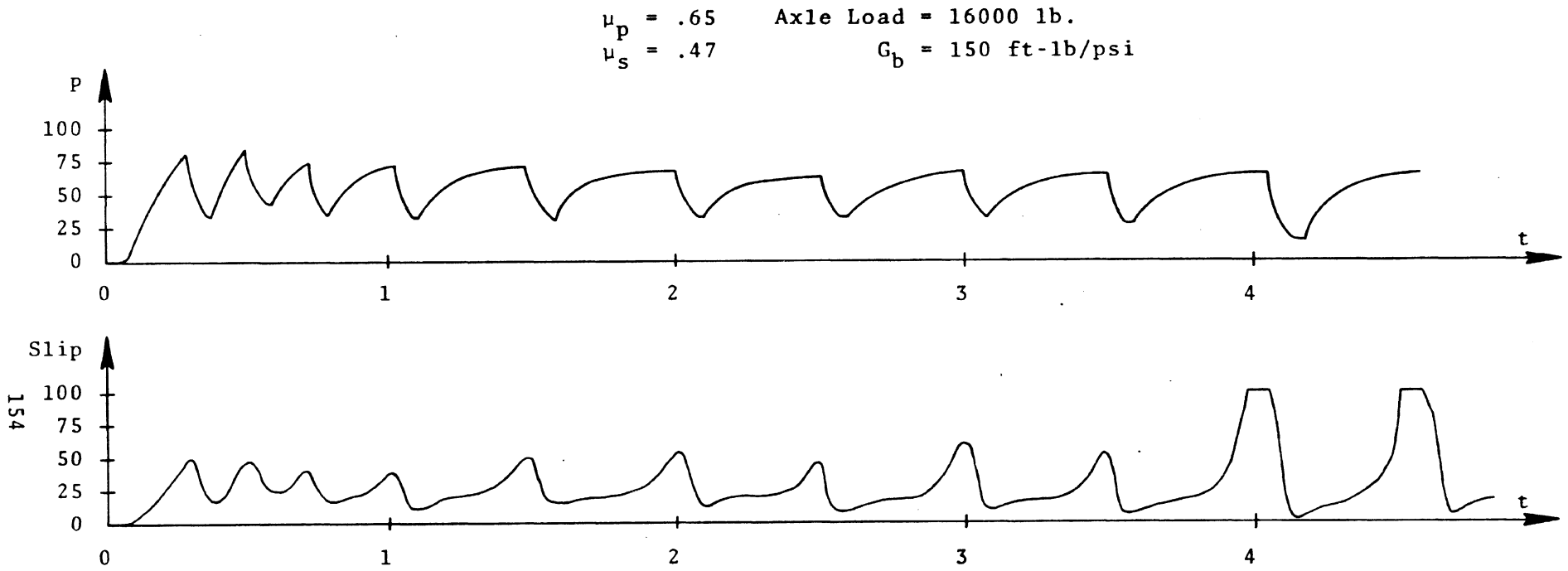

Figure 22
LABORATORY TEST --- SYSTEM #3.

μ_p = .85 Axle Load = 12000 lb.

μ_s = .60 G_b = 150 ft-lb/psi

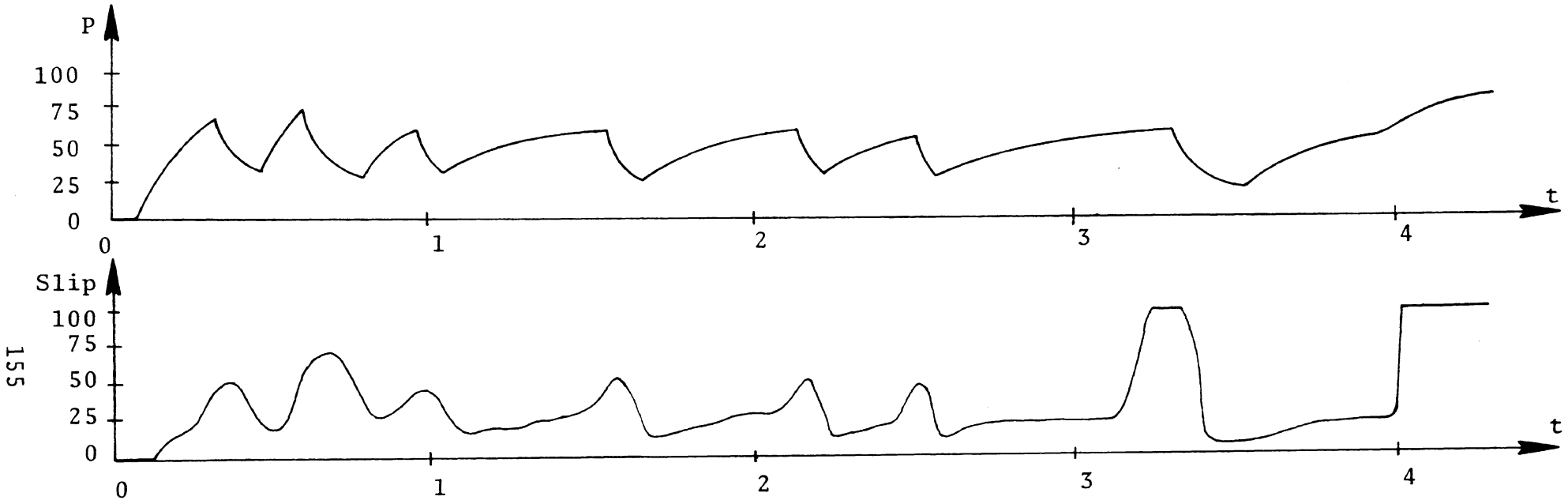

Figure 23

SIMULATION RESULT --- SYSTEM #3.

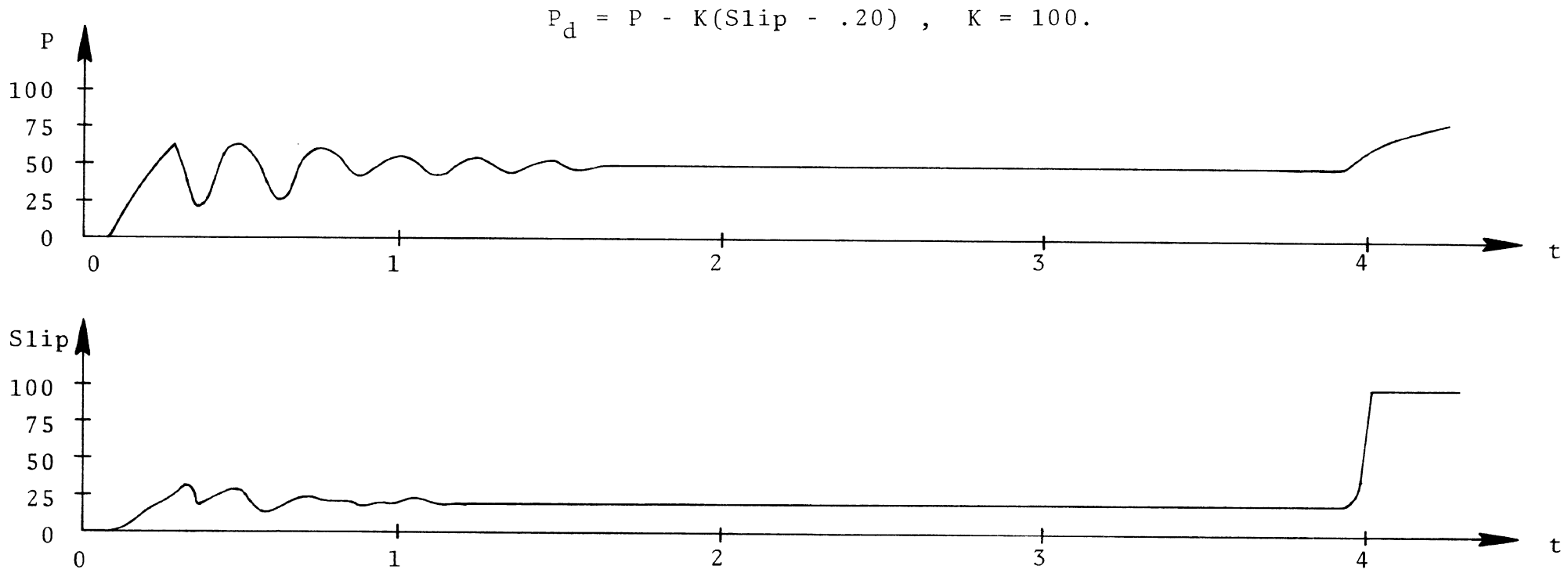

Figure 24. PROPORTIONAL CONTROLLER --- SIMULATION RESULT.

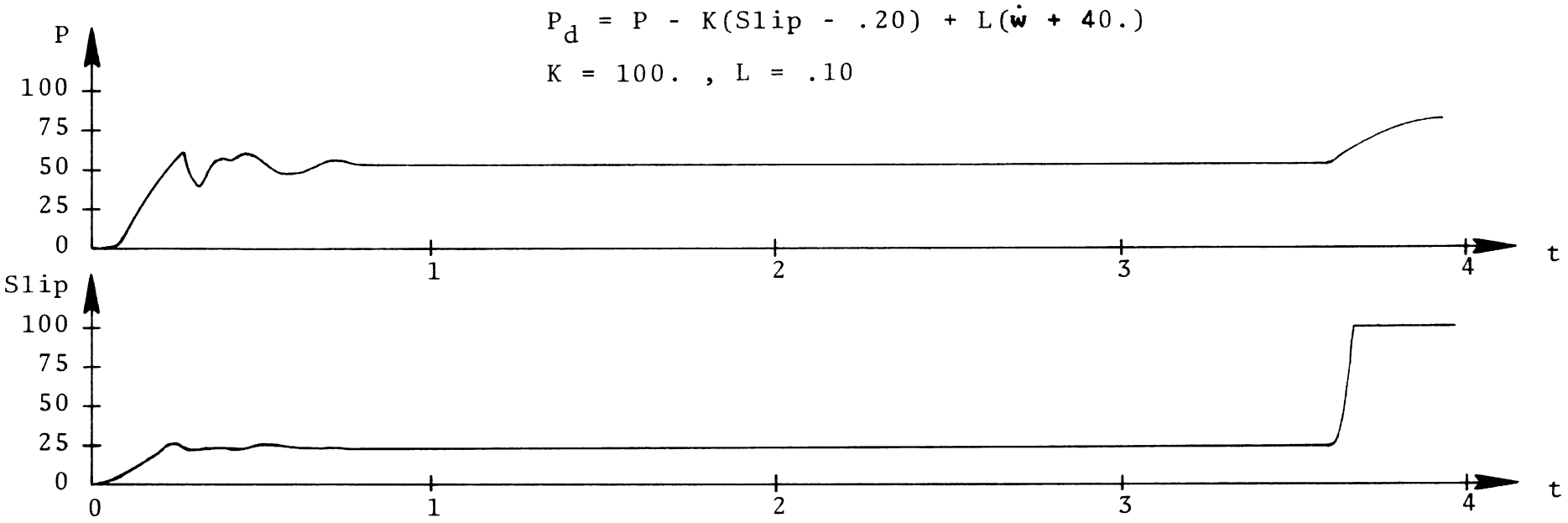

Figure 25. PROPORTIONAL + RATE CONTROLLER --- SIMULATION RESULT.

CONCLUSION

The general-purpose antilock simulation discussed in this paper has been shown to be a flexible tool for simulation and study of the diverse characteristics exhibited by many antilock systems. The laboratory-simulation results presented demonstrate the capability and potential of the program for simulating the various features and behavior associated with different antilock systems.

TESTING FOR FMVSS 121
-A DISCUSSION OF RESULTS-

C.W. Booth
PACCAR, INC.

INTRODUCTION

The Kenworth and Peterbilt Divisons of PACCAR Inc. manufacture over 14% of the Class 8 and above trucks each year. During the past 3 years, a comprehensive test and development program has been implemented at the Corporate Truck R&D Center in Renton, Washington to develop and certify these vehicles in accordance with the requirements of FMVSS No. 121. The object of the following presentation is to show some of the data we have gathered in the course of this program. We think that we are beginning to understand some of the things that take place in the previously unexplored world of anti-lock systems and high torque brakes.

In many instances, we have found that the predictions and design guidelines of "classical" brake theory do not hold true when anti-lock systems and high torque brakes are used. Such effects as increasing brake torque and/or speeding up air timing can result in longer stopping distances and will be discussed in this presentation. FMVSS 121 as currently in effect, does not make proper allowance for effects such as these. For this reason, among others, it does not either objectively or reasonably define vehicle performance requirements as presently written.

We have made 1286 test stops on '121' equipped vehicles to date and are just beginning to understand the data we have gathered. Our primary conclusion is that consistent compliance with the present stringent stopping distance requirements of the Standard is dependent upon factors beyond our control. Additionally, we are highly concerned with the fact that a Federally mandated deadline has left one major question unanswered. How will heavy trucks with both more powerful brakes and anti-lock systems perform outside of a highly contrived and artificial test environment? Here

are some of our test results and our interpretation of them.

VEHICLE TEST RESULTS

Figure 1 illustrates some typical results of one of our stopping distance tests for FMVSS 121. There are two major factors which show up in these results. The first is that the unladen vehicle stops in about 80% of the distance traveled by the same vehicle in a laden configuration. Brake torques were such that the anti-lock systems were cycling in the laden configuration and the cause of this result must lie in some other factor(s). Note that the data are presented on log-log coordinates. This was done to make linear the expected square law relationship between velocity and stopping distance. This brings us to the second major effect shown by this data. This is the fact that the data does not follow the square law relationship and that there is a progressive loss of distance with increasing speed. The convergence between the actual data and the requirements of '121' (square law) at the higher speeds illustrates this very important point. Figure 2 shows similar results from tests on a short 4 x 2 straight truck. These effects are general ones and we have not found them to be very sensitive to vehicle configuration. The next logical question is; What is the cause of these effects?

Figure 3 illustrates the general traction characteristics of a heavy truck tire. This data provides an explanation for the unexpected effects seen in the above results. Figure 3A shows a typical truck tire μ-slip curve. Once a brake has retarded a wheel to the peak of this curve, the wheel decelerates into lockup. The retarding force at the road surface in this region is completely dependent on the action of the anti-lock system and its

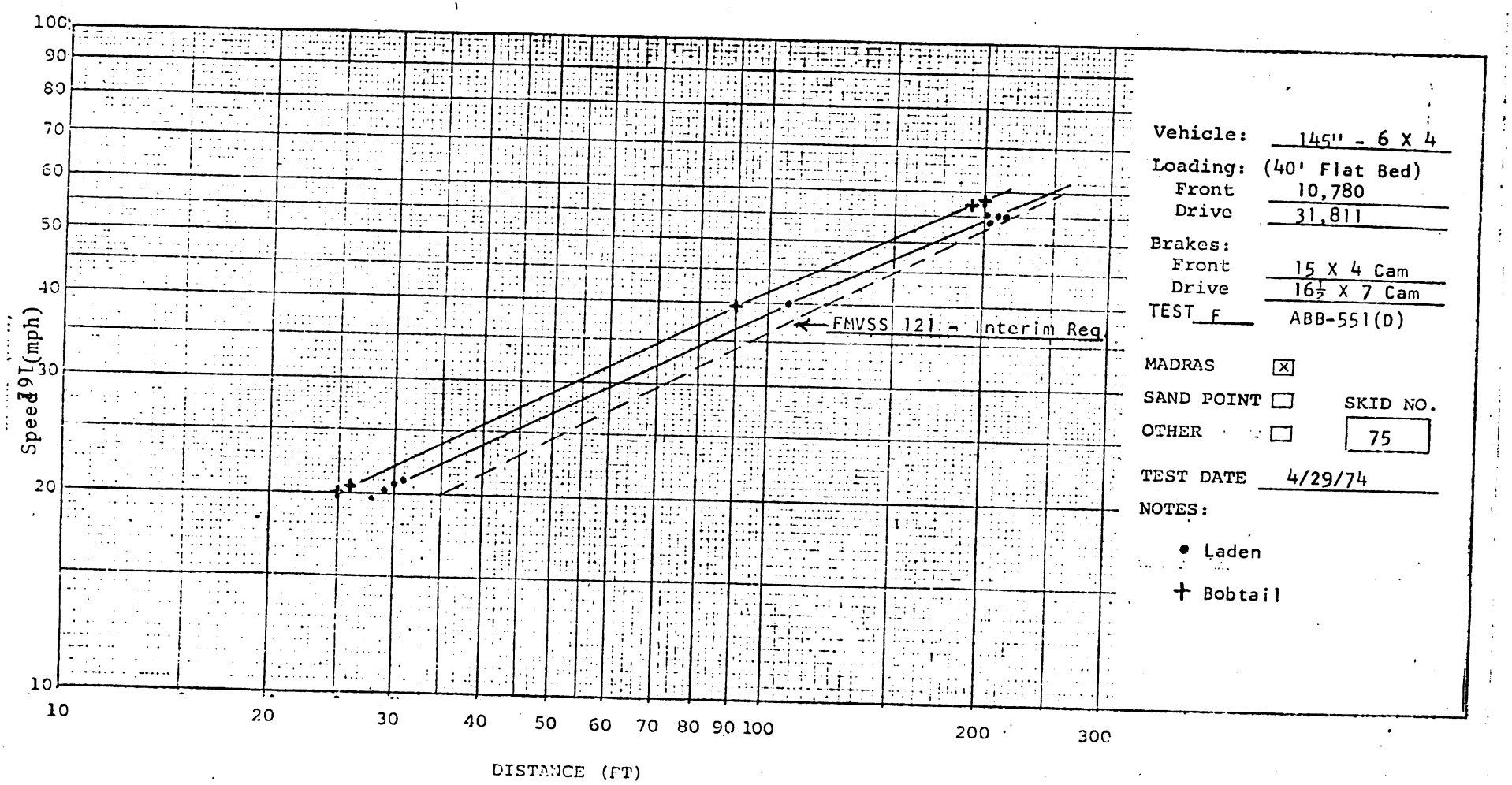
100
90
80
70
60
50
40
30
20
10
Speed (mph)
10
20
30
40
50
60
70
80
90
100
200
300
DISTANCE (FT)
FMVSS 121 - Interim Req.
Vehicle: 145" - 6 X 4
Loading: (40' Flat Bed)
Front 10,780
Drive 31,811
Brakes:
Front 15 X 4 Cam
Drive 16½ X 7 Cam
TEST F ABB-551(D)
MADRAS [X]
SAND POINT [ ]
OTHER [ ]
SKID NO. 75
TEST DATE 4/29/74
NOTES:
• Laden
+ Bobtail

Figure 1

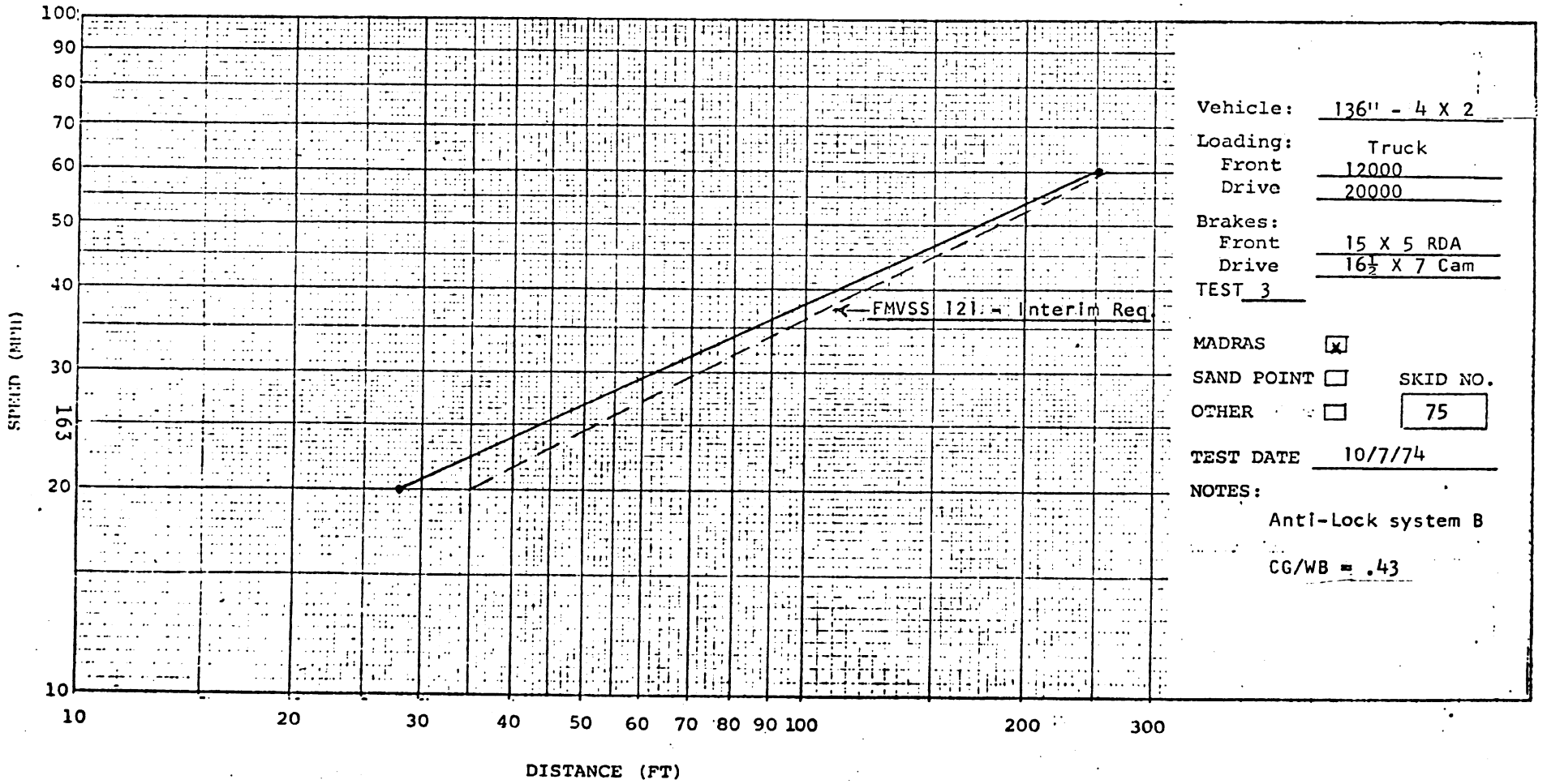
100
90
80
70
60
50
40
30
20
10
SPEED (MPH)
10
20
30
40
50
60
70
80
90
100
200
300
DISTANCE (FT)
FMVSS 121 - Interim Req.
Vehicle: 136" - 4 X 2
Loading: Truck
Front 12000
Drive 20000
Brakes:
Front 15 X 5 RDA
Drive 16½ X 7 Cam
TEST 3
MADRAS [X]
SAND POINT [ ]
OTHER [ ]
SKID NO. 75
TEST DATE 10/7/74
NOTES:
Anti-Lock system B
CG/WB = .43

Figure 2

NOTE: FOR ILLUSTRATIVE PURPOSES ONLY

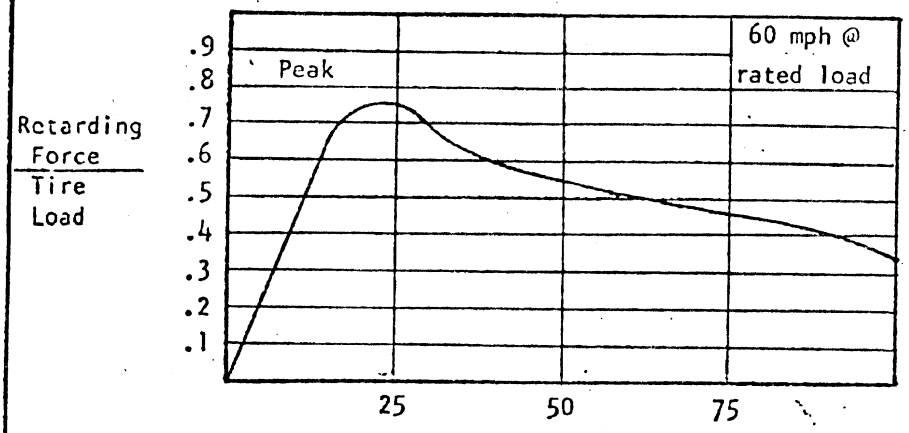

A

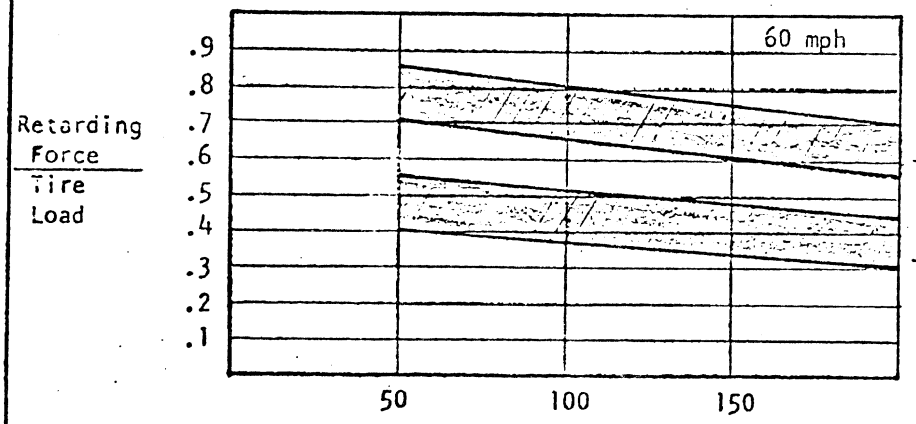

B

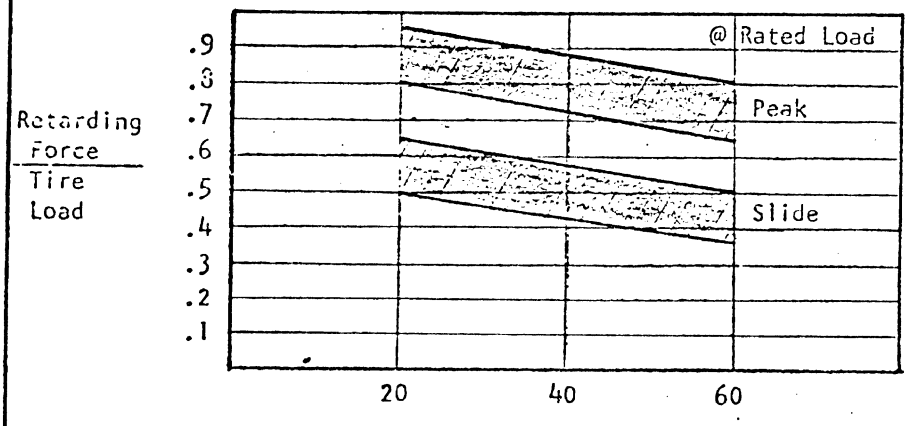

C

NOTE: The ranges sho in Figures 3B and 3C are based on variatio due to tire design.

Truck R & D Center
700 Garden Ave. N., Renton, WA 98055, (206) 235-2815

TYPICAL TRUCK TIRE PERFORMANCE
SKID NUMBER = 75 (DRY)

FIGURE 3

control of slip between peak and full lock. The tire characteristics shown in 3A are not static. They have been found to be significantly dependent on both speed and tire load. These effects are shown in 3B and 3C respectively. These two effects explain the effects seen in the previous data. The decreased friction level at higher loads explains the increase in stopping distance of heavily laden vehicles, and the loss of traction with increasing speed accounts for the disproportionate increase in stopping distance at higher speeds. This form of tire traction information has only recently become available. An excellent presentation of this type of information on a limited cross section of heavy truck tire types is presented in a recently published report from the Highway Safety Research Institute. (1)

Figure 4 illustrates another very significant effect observed during the testing of FMVSS 121 equipped vehicles. The effect shown is that of scatter. Some scatter is to be expected in any physical experiment and vehicle stopping distance tests are no exception. The most important point illustrated in Figure 4 is the fact that the scatter in stopping distance increases with increasing speed. If the scatter in the results increased in direct proportion with speed, it would be a constant percentage effect. This would show up as a scatter band of constant width on the log-log coordinates. This is definitely not the case for the typical results shown. The scatter becomes far more severe at the higher test speeds.

Figures 5 and 6 are another presentation of the scatter in stopping distances for this same vehicle, a short 4 x 2 straight truck. Figure 5 is for tests at a CG/wheelbase ratio of .36 and Figure 6 is for a ratio of .42. The data is shown plotted on Normal Probability coordinates and a

---

(1) R.D. Ervin, C.C. MacAdam, P.S. Fancher; The Longitudinal Traction Characteristics of Truck Tires as Measured on Dry Pavements; H.S.R.I., University of Michigan, Feb. 1975.

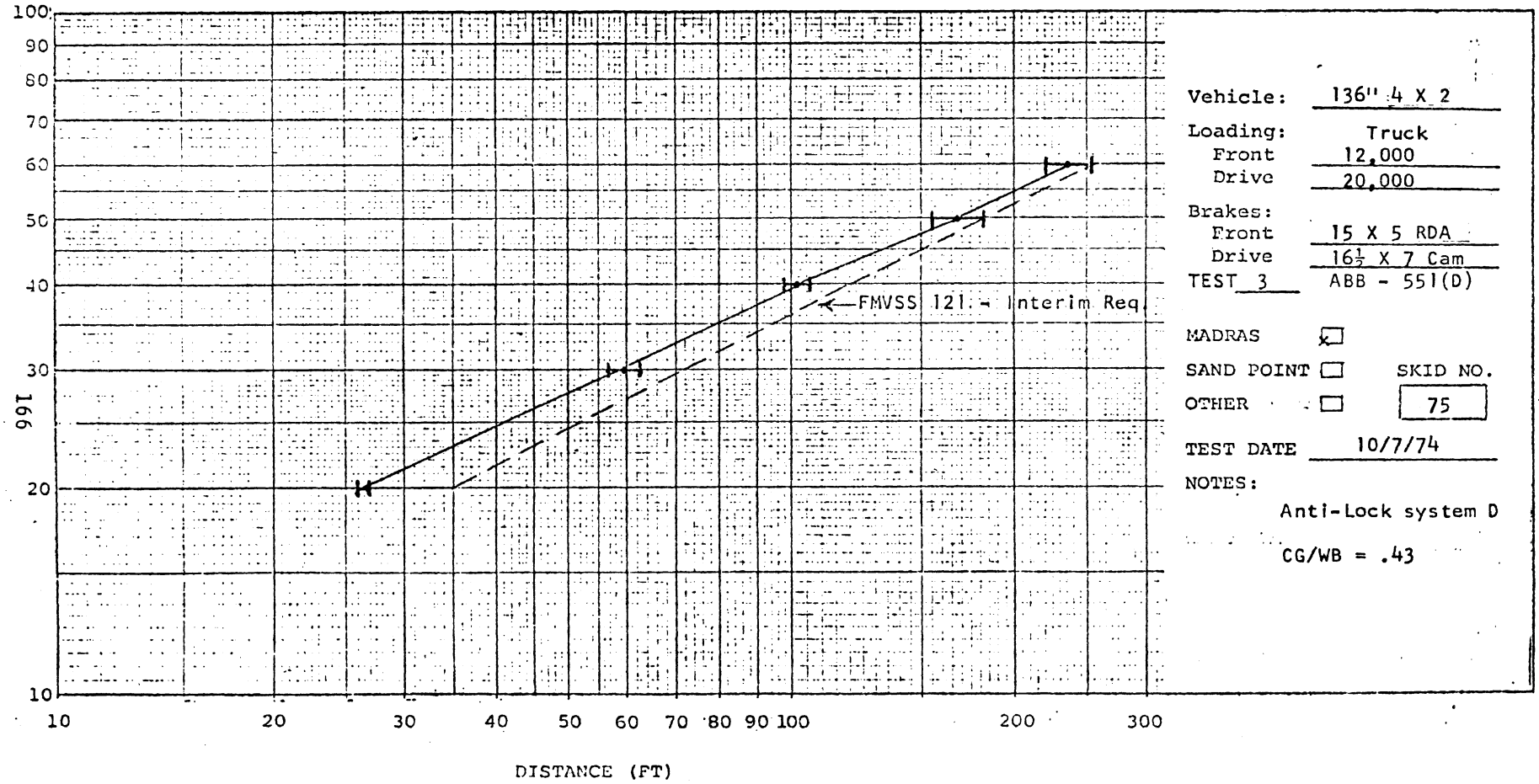
100
90
80
70
60
50
40
30
20
10
166
10
20
30
40
50
60
70
80
90
100
200
300
DISTANCE (FT)
←FMVSS 121 - Interim Req.
Vehicle: 136" 4 X 2
Loading: Truck
Front 12,000
Drive 20,000
Brakes:
Front 15 X 5 RDA
Drive 16½ X 7 Cam
TEST 3 ABB - 551(D)
MADRAS ☒
SAND POINT ☐
OTHER ☐
SKID NO. 75
TEST DATE 10/7/74
NOTES:
Anti-Lock system D
CG/WB = .43

Figure 4

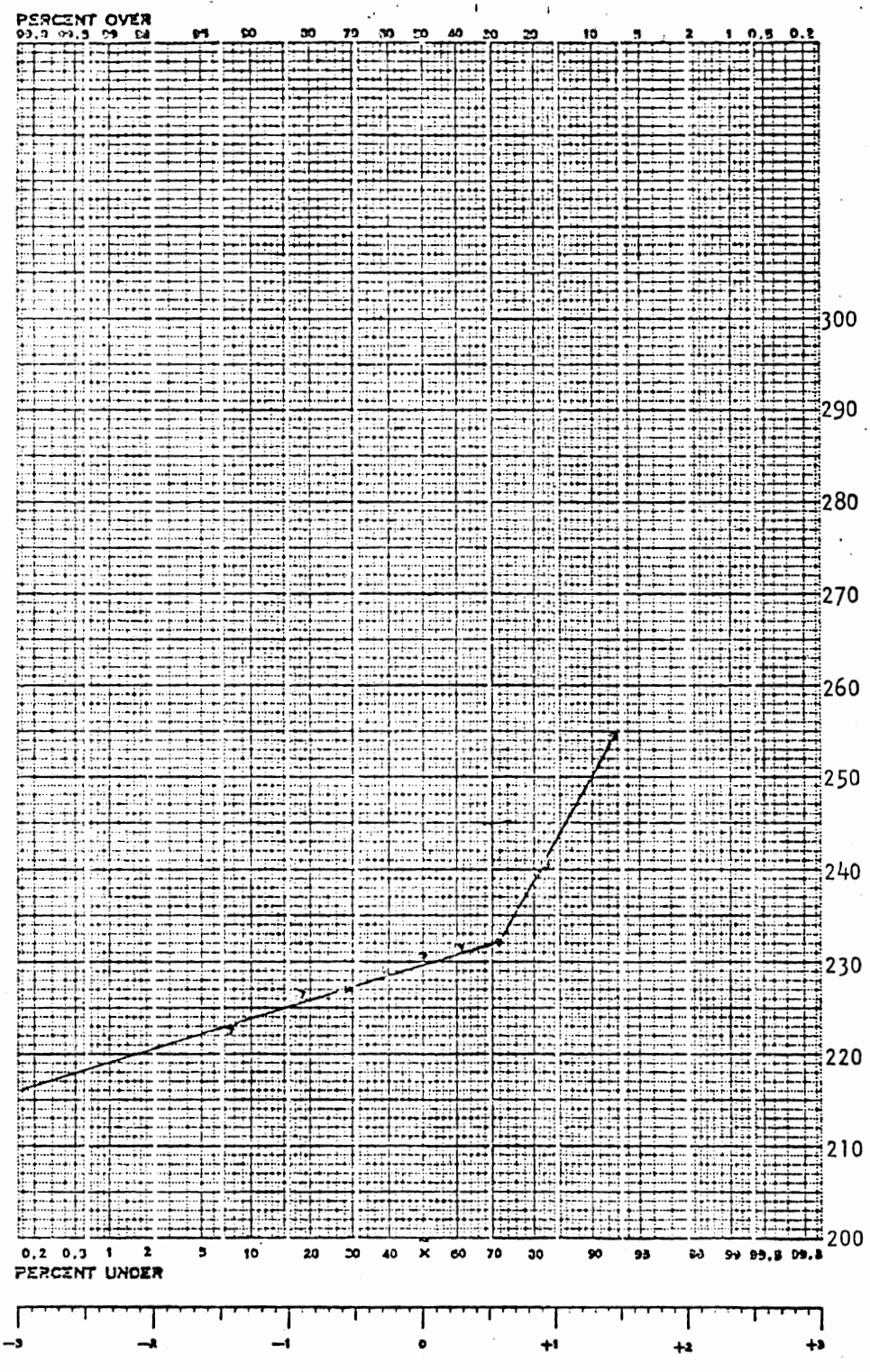

Std. Dev.= N.A.

Mean = N.A.

CG/WB = .36

DATA SOURCE TEST #3

NO. OF SAMPLES 9

TITLE 136" 4 X 2 TRUCK, Front @ 12,000 , Rear @ 20,000 , Anti-Lock System D

NORMAL PROBABLITY PAPER

Figure 5

Analyzed by CWB

Date

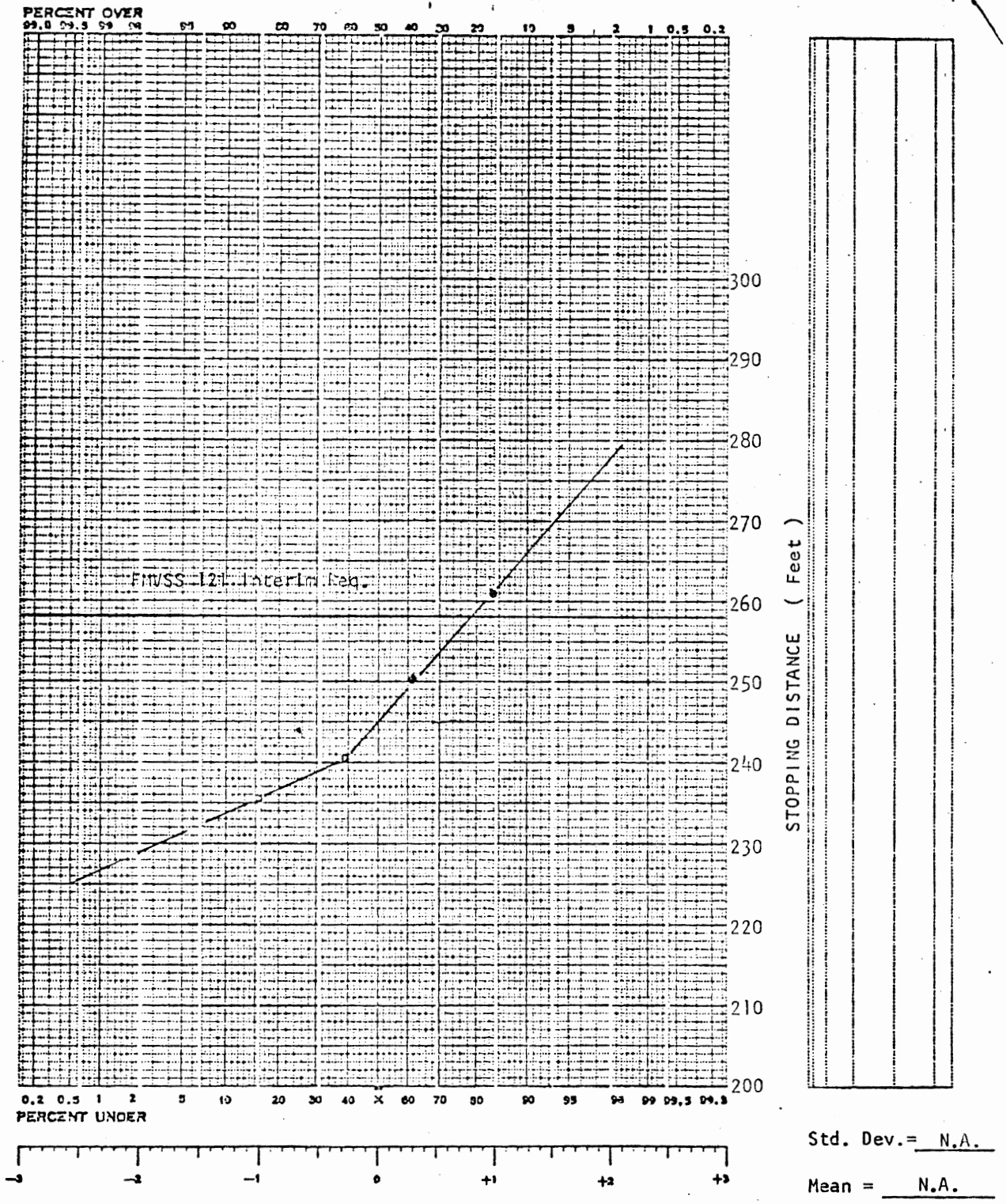

Std. Dev.= N.A.

Mean = N.A.

CG/WB = .43

DATA SOURCE TEST #3

NO. OF SAMPLES 4

TITLE 136" 4 X 2 TRUCK, Front @ 12000, Rear @ 20000, Anti-Lock System D

Analyzed by CWB

Date

NORMAL PROBABILITY PAPER

Figure 6

single straight line relationship would represent a Normal Distribution of results. Some sample sizes are minimal in these figures but do illustrate the trends in the scatter. With reference to Figure 5, which is a larger sample, there appear to be two normally distributed variables affecting the results in a significant manner. The sample size is too small to be very sure of anything but the same 'two distribution' effect seems to be present. Figures 7 and 8 are copies of the strip chart records for the four test stops shown in Figure 6. The strip chart records show the variations in pressure on the front and rear axles during these stops and are a direct indication of the anti-lock system activity during each run. Distances are shown for each run and a direct relationship between anti-lock activity and increased stopping distance is clearly shown. The test conditions under which these stops were made (sequentially) included; full treadle 'panic' application, controlled initial brake temperatures, and constant initial air pressure. Based on this data, and much more just like it, we have concluded that when using brakes with sufficient torque to cycle the anti-lock systems on all axles of a vehicle, stopping distance and scatter are a function of only two primary variables-- tire-to-road friction and the anti-lock system's capability in utilizing the peak friction force available. Having established the fact that the anti-lock system is one of the primary variables governing the stopping distance under these conditions, another answer becomes apparent. The double distribution of the scatter shown in Figures 5 and 6 is probably related to the variable effects of the two individual axles and the performance of their associated anti-lock modulators.

Figure 9 shows the scatter in results for a short wheelbase 6 x 4 straight truck. Once again, the sample size is small, but some interesting trends are apparent.

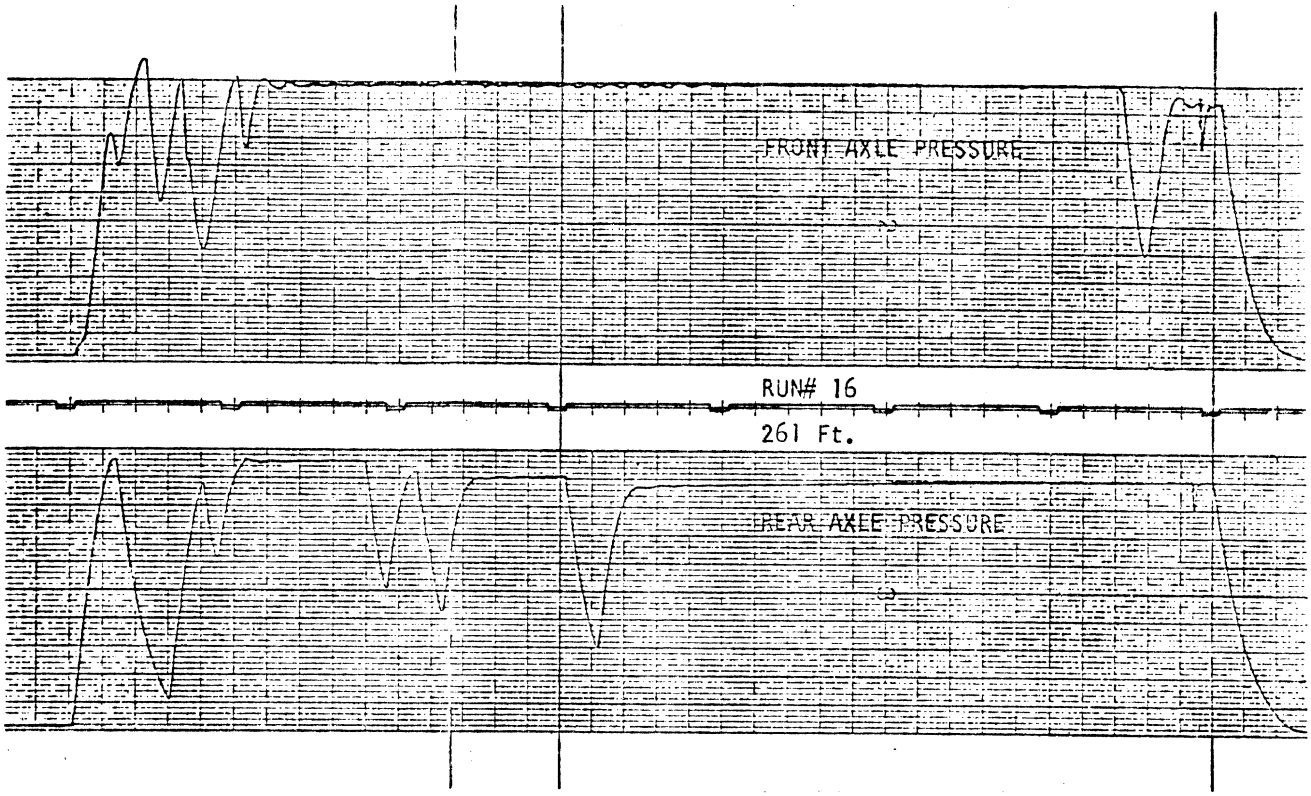

TEST #3 - 136" 4X2 TRUCK - CG/WB= .43 - Anti-Lock System D

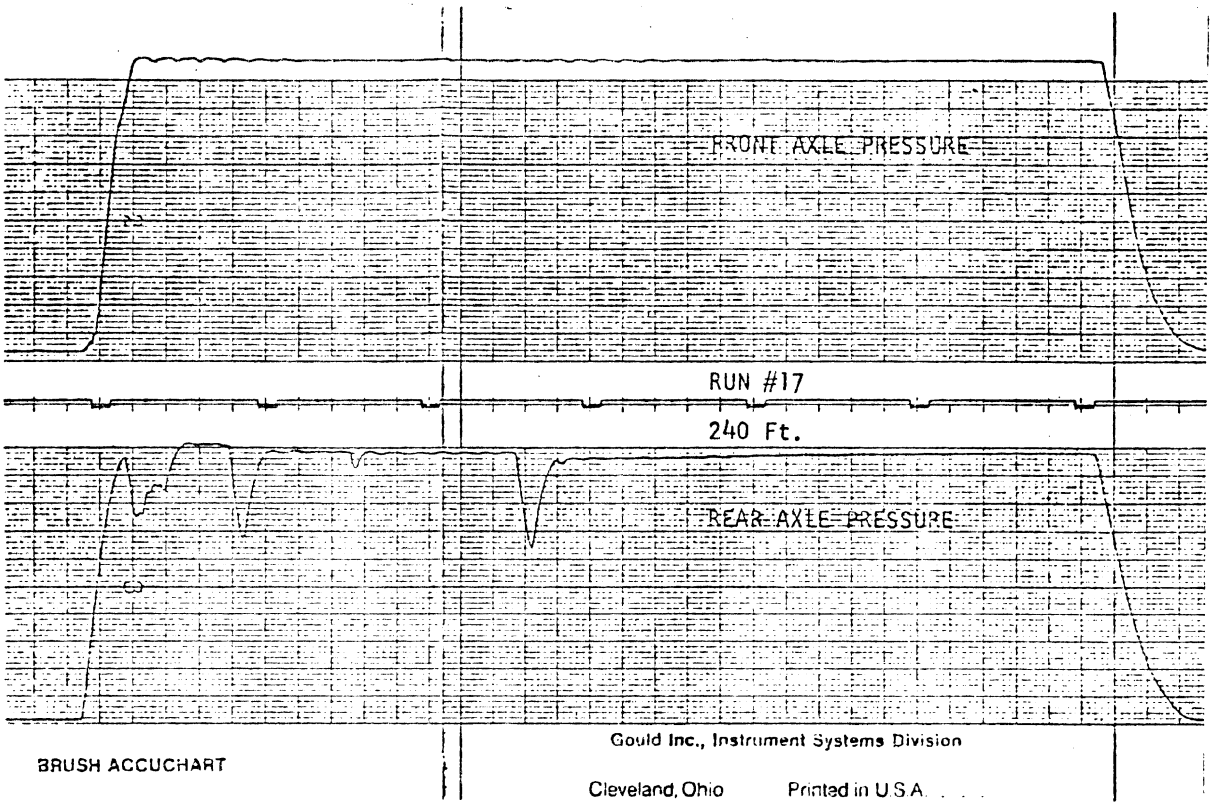

Figure 7

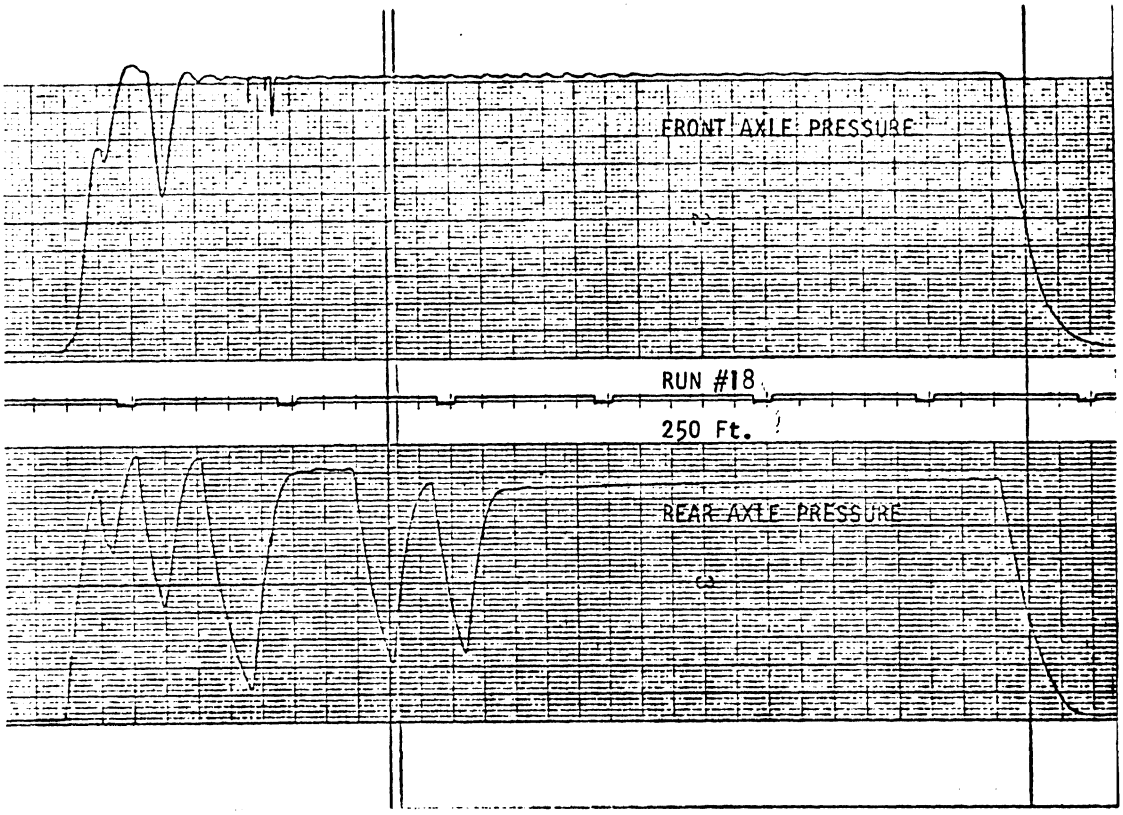

TEST #3 - 136" 4X2 TRUCK - CG/WB= .43 - Anti-Lock System D

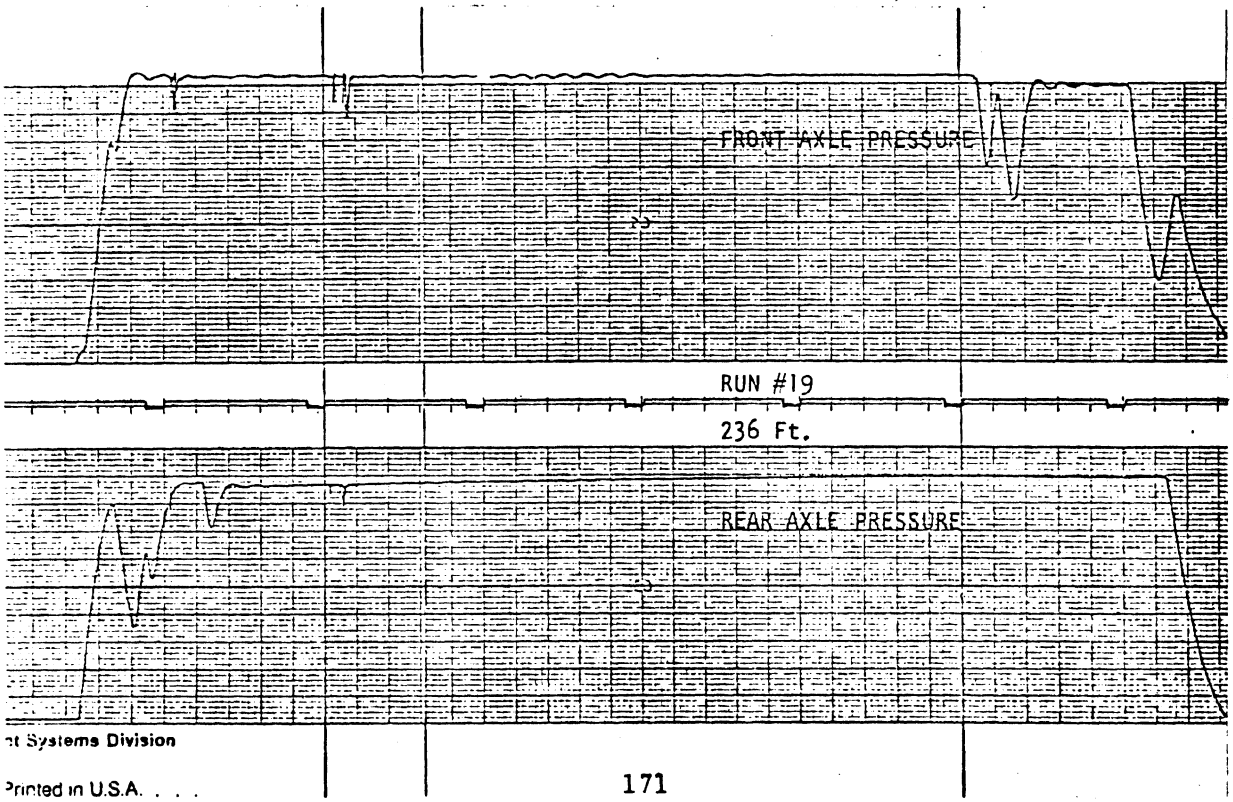

Figure 8

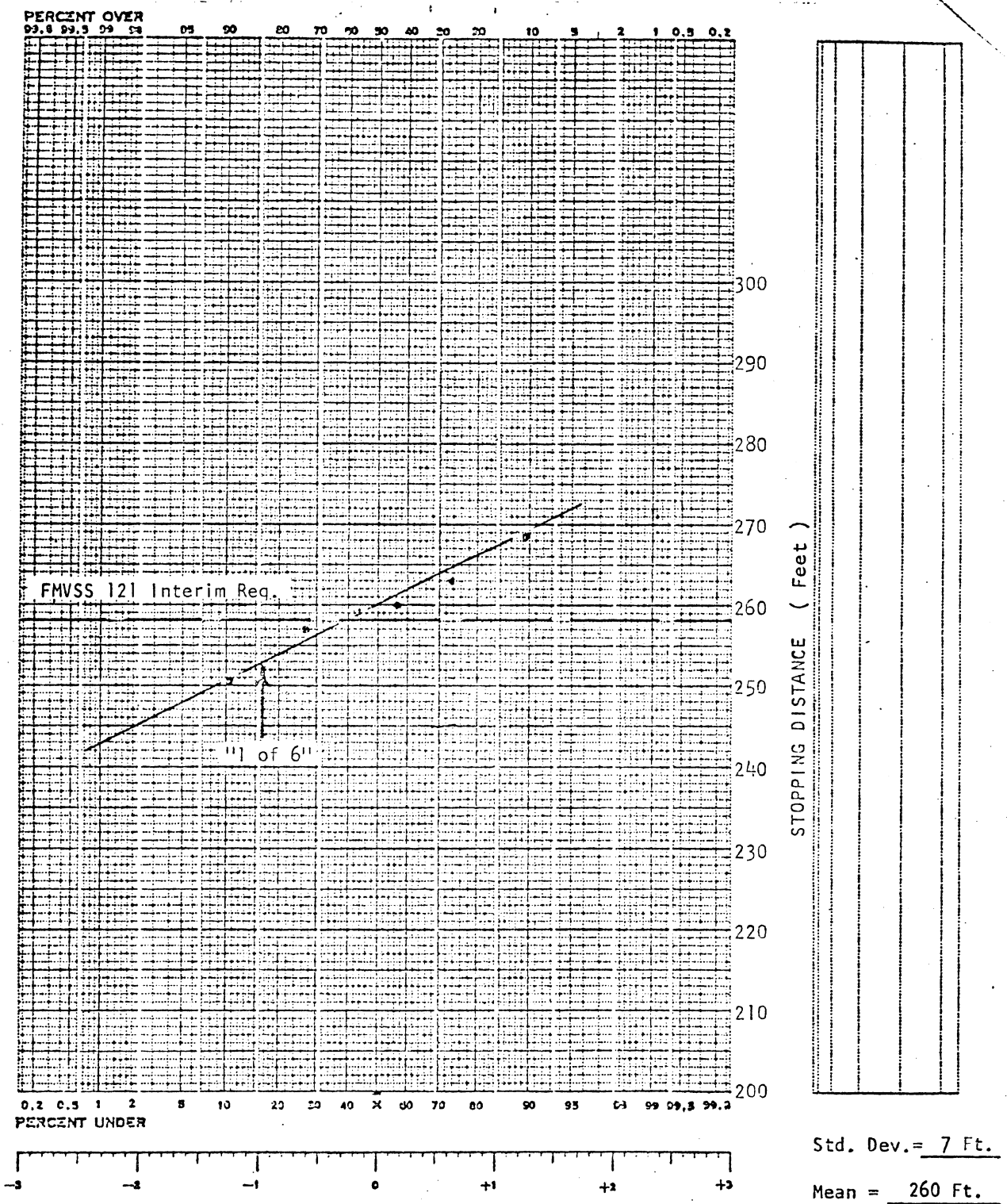

Std. Dev.= 7 Ft.

Mean = 260 Ft.

DATA SOURCE TEST #6

NO. OF SAMPLES 6

CG/WB = .36

TITLE 145" 6 X 4 TRUCK, Front @ 12,000, Rear @ 38,000 , Anti-Lock System A-2

NORMAL PROBABLITY PAPER

Figure 9

Analyzed by _____

Date _____

The "S" format of the data points supports the previous suspicion that the scatter is strongly dependent upon the anti-lock activity on the individual axles of the vehicle. An "S" shaped distribution is a common result of combining the random effects of three independent factors, in this case, three axles. The 258 foot interim distance requirement of '121' and the "1 out of 6" (16.7%) compliance level are shown for reference purposes. It is important to note at this point that, if the 5% and 95% confidence bands were plotted for the required sample size of 6, the 1 out of 6 qualification requirement would be properly shown to be a very unsound basis for establishing the performance capability of the vehicle. Figure 10 shows the results for this same vehicle at a higher CG/WB ratio and indicates a 2 foot increase in mean distance and about the same scatter. This data, along with much more that we have obtained, indicates that when vehicle performance is governed by road friction and anti-lock factors, CG/WB has minimal effect on stopping distance.

Figure 11 is a similar presentation for a tractor-trailer configuration. The vehicle in this case is a short 6 x 4 with a 40' flatbed trailer. We have found that, in general, the stopping distance capability of tractor-trailers is somewhat better than that of straight truck configurations. Scatter in the results is less for the 5-axle combinations due to the "averaging" effect of the larger number of active anti-lock systems on the overall vehicle. This test, along with some others we have run, shows a tendency for the distance to approach some "ultimate value" for each vehicle. In this case, it is about 255 feet. This appears to be due to the fact that the brake sizes and loads on the vehicle limit the anti-lock activity on each axle to some maximum amount. This represents a worst case condition for this vehicle and correlates

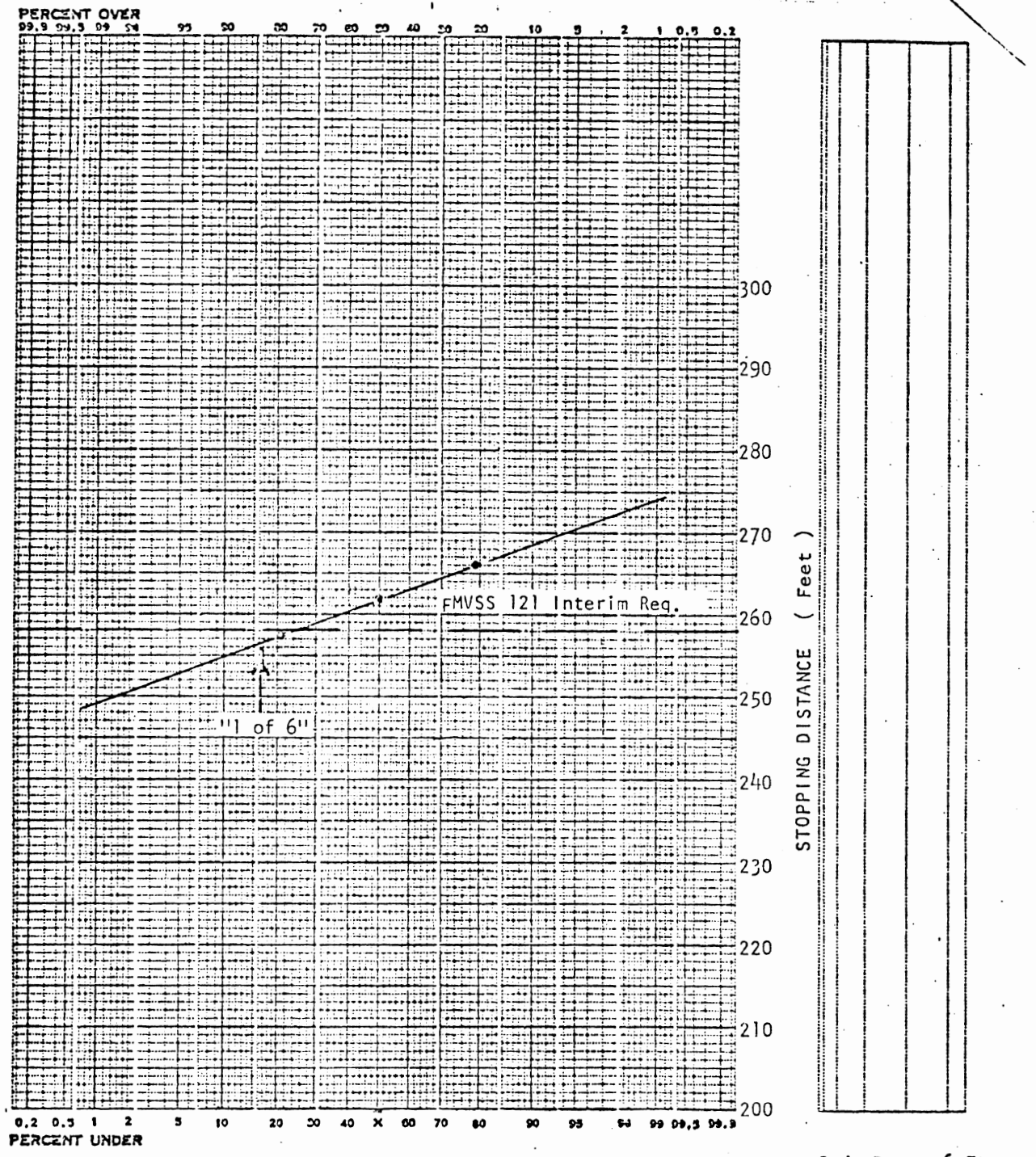

Std. Dev.= 6 Ft.

Mean = 262 Ft.

CG/WB = .42

DATA SOURCE TEST #6

NO. OF SAMPLES 3

TITLE 145" 6 X 4 TRUCK, Front @ 12000, Rear @ 38,000, Anti-Lock System A-2

Analyzed by CWB

Date

NORMAL PROBABLITY PAPER

Figure 10

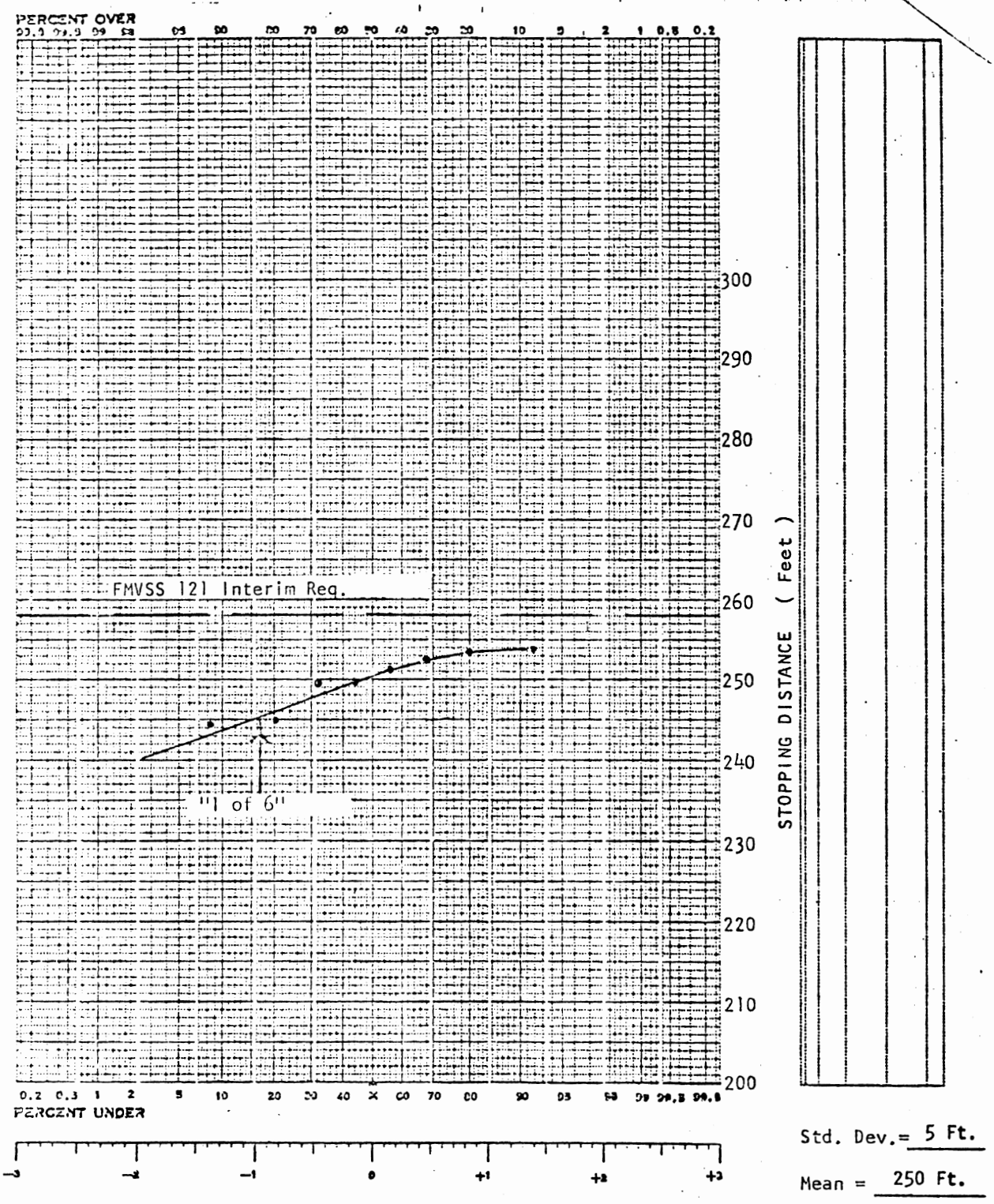

Std. Dev.= 5 Ft.

Mean = 250 Ft.

DATA SOURCE Test #1

NO. OF SAMPLES 8

TITLE 145" 6 X 4 TRACTOR, 38,000 & 34,000 COMBINED, Anti-Lock System A-1

Analyzed by CWB

Date

NORMAL PROBABLITY PAPER

Figure 11

with the maximum expected stopping distance. The anti-lock system on each axle drops out of the picture and stops cycling when a brake becomes torque limited due to a combination of air pressure reduction, brake fade, and tire-to-road friction increase with decreasing speed.

ANTI-LOCK SYSTEM PERFORMANCE

Once we had determined that the anti-lock system on a vehicle was a major variable governing stopping distance, we initiated a series of tests to compare the effectiveness of these systems. One such group of tests was run on the analog vehicle simulation at Rockwell International's Autonetics Division in Anaheim, California. This simulation utilizes an analog computer in conjunction with a dummy axle equipped with an air reservoir, brake chambers, and the anti-lock logic and valve under tests.

Figure 12 is an illustration of some results of these tests. Four different systems are shown under six different conditions. The brake torque simulated for these runs was at a level which ensured cycling of each system for the entire duration of each stop. All data shown represents a front axle simulation. Average deceleration was measured for each stop and the average retarding force delivered by each system computed on this basis. The data is presented as a percentage of the maximum retarding force available, i.e., peak μ. The value of retarding force corresponding to that delivered by a locked wheel is shown as a reference. On the higher coefficient surface, the four systems are seen to deliver significantly different levels of retarding force and the performance of the systems relative to each other is not a significant function of velocity. The relative performance of the four systems tends to become equal as friction coefficient is decreased and they all approach the

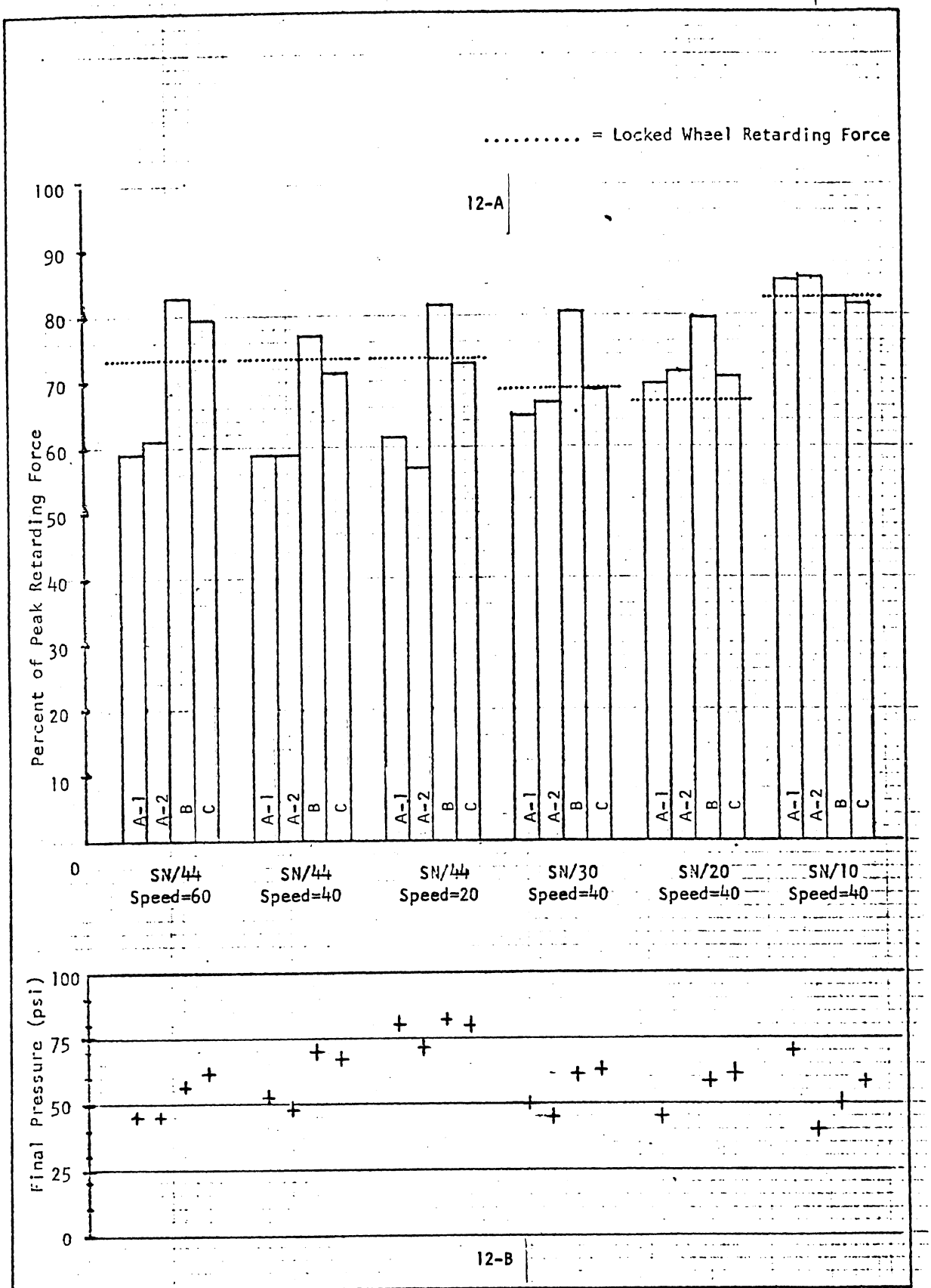

PACCAR Truck R & D Center
790 Garden Ave. N., Renton, WA 98055, (206) 235-2815

ANTILOCK SYSTEM RETARDATION EFFECTIVENESS

FIGURE 12

locked wheel value of retarding force. This is to be expected since all systems that we have evaluated thus far tend to control wheel slip in a deep wheel slip mode on low coefficient surfaces. The most significant fact illustrated by Figure 12 is that the largest difference in retardation effectiveness of the various systems is on the high coefficient surface.

Figure 12B illustrates the large differences in air consumption found during the runs in 12A. Pressures below 50 psi become significant from the standpoint of spring brake actuation.

Figure 13 is another illustration of the anti-lock performance data gathered on the simulator. This figure shows the effect of increasing brake torque on stopping distance using four different anti-lock systems. The solid line in the "torque limited" region represents the classical force-distance relationship up to the point where the brake has just enough output to lock the wheels under the dynamic load present. This torque level was calculated for the vehicle being simulated and is used as an "ideal" torque reference for purposes of comparing the performance of the various systems. In the absence of an anti-lock system, brake torques in excess of the 100% "ideal" cause the wheels to exceed the slip at peak μ and deliver a force corresponding to "slide" μ as shown by the dashed line. A perfect anti-lock system would deliver a retarding force corresponding to that provided by the "peak" μ of the surface as shown by the extension of the solid line in the overtorqued region. From the data shown, it is obvious that, although none of those tested are perfect, some do provide a significant gain in retardation over that of a locked wheel on a high μ surface.

Two very important points are illustrated by the data in Figure 13. The first is that all systems tested showed losses in retardation effectiveness with increasing overtorque,

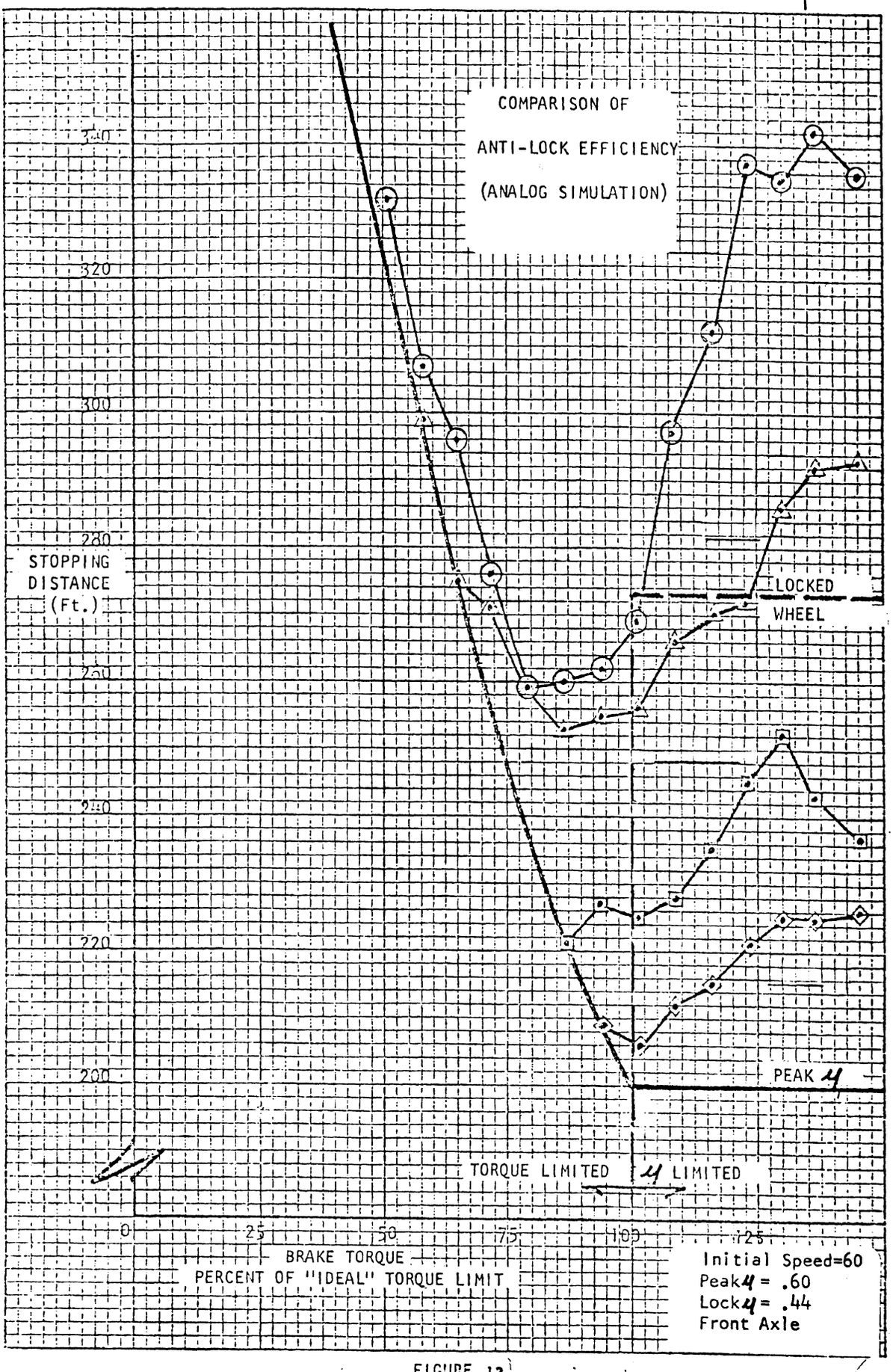
COMPARISON OF
ANTI-LOCK EFFICIENCY
(ANALOG SIMULATION)
340
320
300
280
STOPPING
DISTANCE
(Ft.)
260
240
220
200
LOCKED
WHEEL
PEAK μ
TORQUE LIMITED
μ LIMITED
0
25
50
75
100
125
BRAKE TORQUE
PERCENT OF "IDEAL" TORQUE LIMIT
Initial Speed=60
Peak μ = .60
Lock μ = .44
Front Axle

FIGURE 13

i.e., over 100% of "ideal." The second point is related to the fact that all systems tested began cycling at values of torque less than the "ideal" peak torque. This occurs for two primary reasons. The first is the fact that this was a front axle simulation and the pitch inertia controlled delay in vehicle weight transfer allowed the rapidly energized front brake to lock the wheel before a maximum dynamic load condition could be established. The second factor is that some systems are relatively "soft" and are triggered by lower values of wheel deceleration. In the case of the two systems that resulted in the longest distances shown, the critical value of deceleration was exceeded before the wheels had decelerated to the 20% slip corresponding to the peak of the μ-slip curve. This effect is intimately related to the basic configuration of the vehicle, the "gain"[1] of the brakes, wheel inertia, and to the effect of these basic variables on the anti-lock servo system. In our simulation work, we have dubbed this factor "A/V" (Anti-lock Vehicle) Sensitivity. It is interesting to note that the system showing the best performance did so because of a 'fluke' in the test conditions that minimized its sensitivity. A restriction in the supply line to the modulator valve caused the valve to "knee over" the air pressure at about 60 psi during initial application. This allowed the torque rise rate to be slower, i.e. lower "gain," and more in-phase with the weight transfer.

STOPPING DISTANCE SIMULATION

With our preliminary knowledge of the major variables that control the stopping performance of anti-lock equipped vehicles, we are developing a digital computer model to estimate stopping distance. The model is a simplified single degree of freedom one and will handle both single unit

(1) Brake "gain" = lb-ft/sec = (lb-ft/psi x (psi/sec)

and combination vehicles. Primary inputs are: vehicle configuration, brake characteristics derived from dynamometer data, and peak tire traction as a function of speed and load. Secondary inputs include A/V Sensitivity and retardation effectiveness. We are using the results of all vehicle tests run to date to get an empirical fit between calculated and measured results. Our goal is to achieve a calculated result that is within ± 5% of the measured value under all test conditions required by FMVSS 121. Figure 14 illustrates the present capabilities of our simulation as compared to vehicle test results. The vehicle in this case is a 145" wheelbase 6 x 4 tractor. We have not yet achieved our ± 5% objective but seem to be progressing in this direction.

In the process of testing our vehicles and determining the factors that govern stopping distance, we have necessarily done a good deal of parametric evaluation. Figure 15 shows the effects of reducing both front and rear brake torque on stopping distance for a 6 x 4 tractor. Simulated results are also shown. All brakes had sufficient torque to cycle the anti-lock systems at full pressure. For this vehicle, limiting either front or rear brakes to 50% of their full torque does not change stopping distance significantly. Simulated results are in excellent agreement with these results.

Figure 16 illustrates the effect of reducing front brake torque on the stopping distance of a 4 x 2 tractor. A minimum stopping distance was achieved at the torque level where the anti-lock system ceased to function and torque limited performance resulted below this level. Once again the simulation predicted the results quite accurately.

Figure 17 shows the effect of changing CG/WB ratio for a straight truck configuration. Simulated results are

TYPICAL RESULTS OF PACCAR DIGITAL SIMULATION

DATA SOURCE: Trip #2

VEHICLE: 145" 6X4 Tractor

BRAKES: Front - 15 X 4 RSA, Rear - $16\frac{1}{2}$ X 7 Cam

TEST CONDITION	INITIAL SPEED	MEASURED DISTANCE	SIMULATED DISTANCE	% ERROR
Laden Front - 10,800 Rear - 38,000 Trail.- 34,000				
A Full Service	60	245-254	249	-.2
	40	112	108	-3.6
	20	28	29	+3.6
B No Fronts	20.4	32	35	+9.4
	55.2	235	246	+4.6
C No Rears	19.2	44	44	0
	55.1	407	380	-6.6
"Bobtail" Front - 9740 Rear - 4300				
A Full Service	60	224-226	232	+3.1
	20	24-27	28	+9.8
B No Rears	21.5	48.5	57	+17.5
	58.5	411	442	+7.5
Trailer Only	48.4	393	406	+3.3
Trailer Cal. Weight	60	430	408	-5.1

Figure 14

DATA SOURCE; Test #2

VEHICLE: 145" 6X4 Tractor

BRAKES: Front - 15 X 4 RSA, Rear - 16½ X 7 Cam

AXLE LOADS: Front - 10,700, Rear - 38,000, Trailer - 34,200

A. Effect of reducing FRONT brake torque (pressure limiting) - All other brakes full on - 55 MPH distances.

FRONT PRESS.	MEASURED DISTANCE	SIMULATED DISTANCE
Full	209	206
90	208	206
80	212	205
70	211	208
60	210	211
50	216	215

B. Effect of reducing REAR brake torque (pressure limiting) - All other brakes full on - 55 MPH distances.

REAR PRESS.	MEASURED DISTANCE	SIMULATED DISTANCE
Full	209	206
90	212	206
80	206	205
70	212	204
60	207	209
50	208	225

C. Estimated effects of reduced application at 60 MPH.

BASELINE - Full Application 248-250 Ft. (measured)

SIMULATED

FRONT PRESS.	REAR PRESS.	SIMULATED DISTANCE
50	Full	259
Full	60	252
60	60	259

Figure 15
183
TRACTOR BRAKE TORQUE EFFECTS

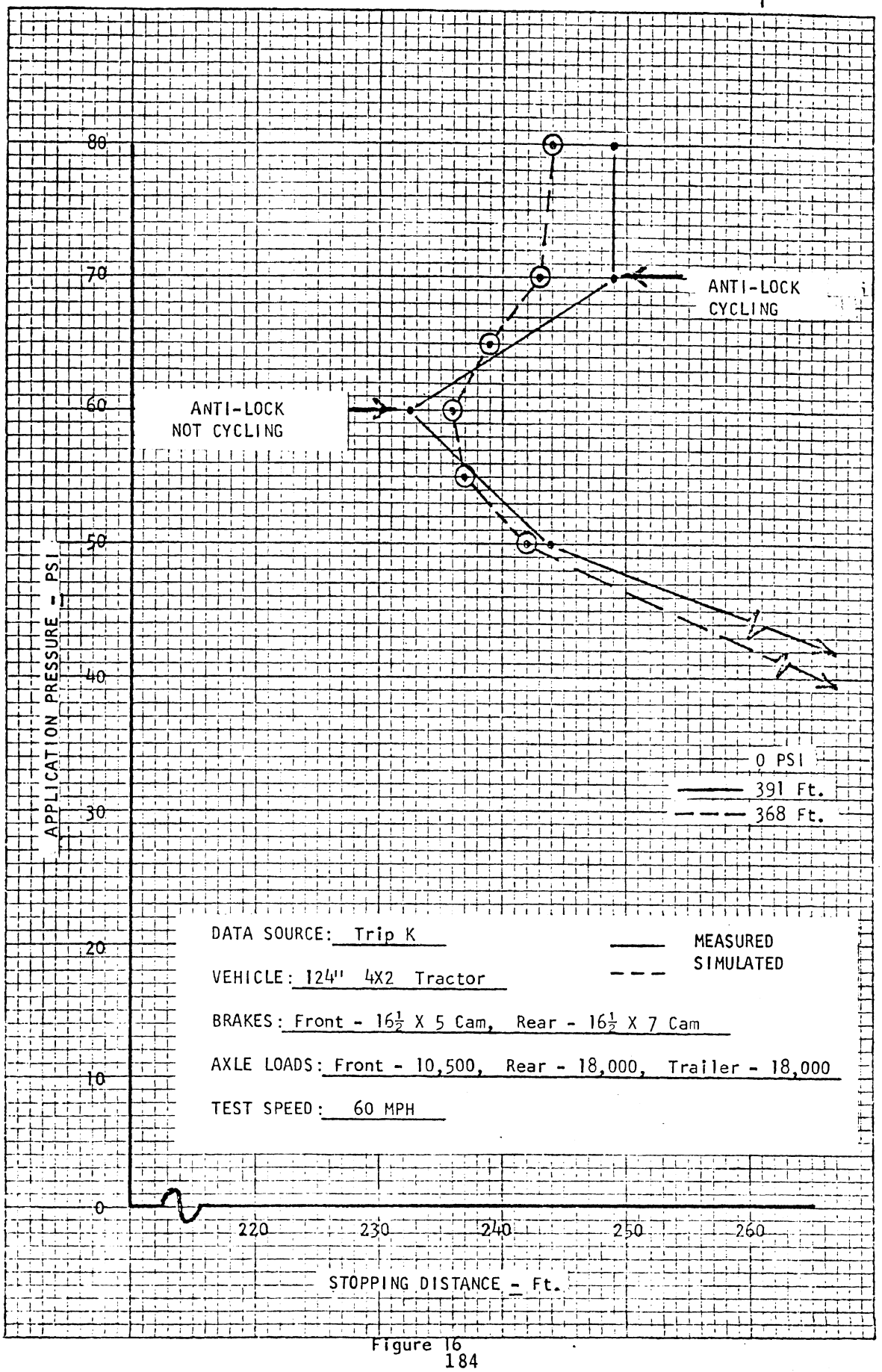
80
70
60
50
40
30
20
10
0
APPLICATION PRESSURE - PSI
ANTI-LOCK
CYCLING
ANTI-LOCK
NOT CYCLING
0 PSI
391 Ft.
368 Ft.
DATA SOURCE: Trip K
VEHICLE: 124" 4X2 Tractor
BRAKES: Front - 16½ X 5 Cam, Rear - 16½ X 7 Cam
AXLE LOADS: Front - 10,500, Rear - 18,000, Trailer - 18,000
TEST SPEED: 60 MPH
MEASURED
SIMULATED
220
230
240
250
260
STOPPING DISTANCE - Ft.

Figure 16

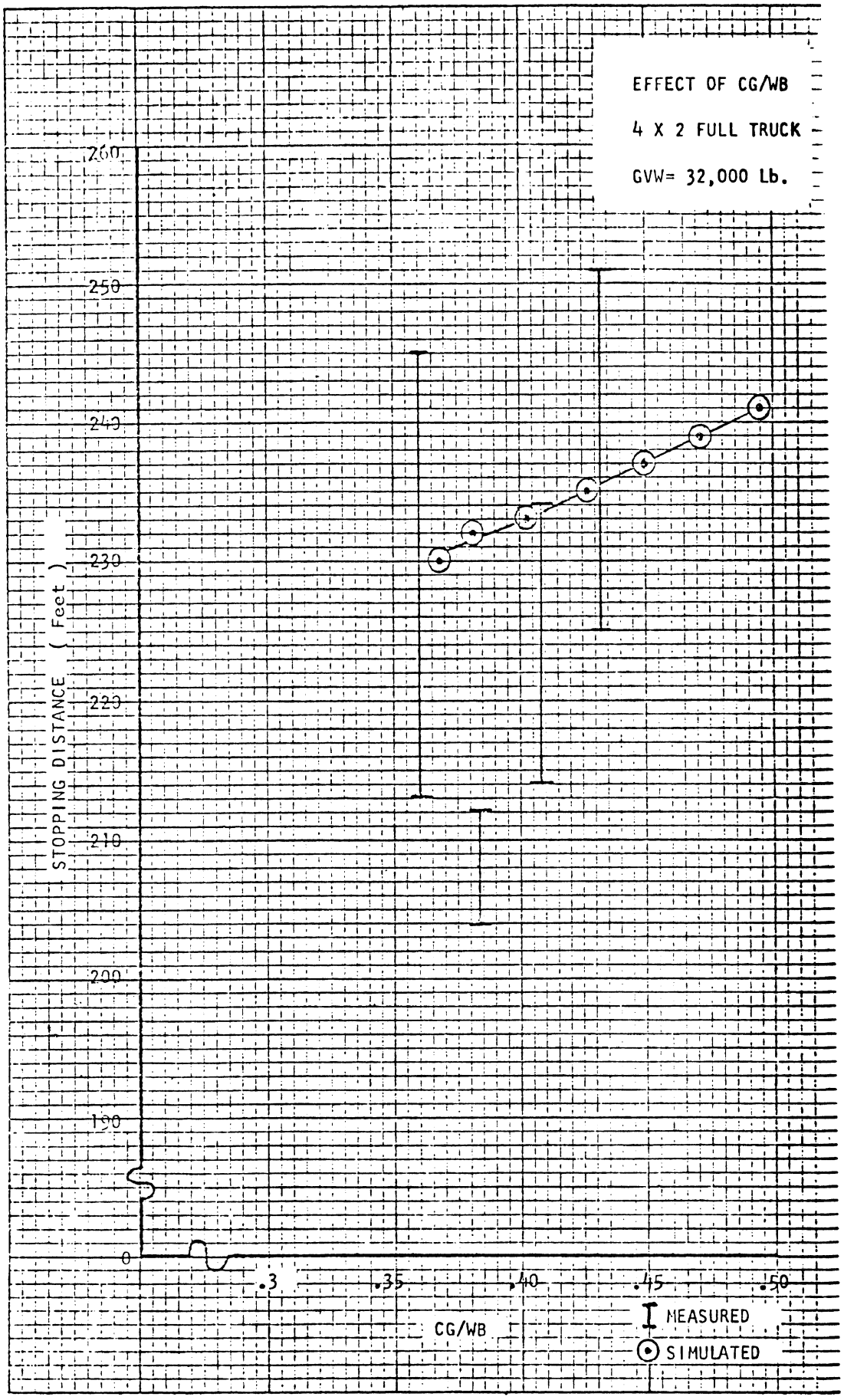

Figure 17 185

also shown and agree with the trend of the actual test data within the large scatter band observed.

Figure 18 presents the results of other parametric variations as calculated by our simulation. Front brakes had sufficient torque to cycle the anti-lock on the vehicle simulated. Significant changes in both axle weights and brake torque on this vehicle will cause minor variations in distance that are well within the scatter band of vehicle test results. The major variables influencing stopping distance under these conditions are related to anti-lock system performance and peak tire traction characteristics. The short stopping distances predicted for the case of highly effective anti-lock systems must be viewed with extreme caution. During the course of our testing, we have generally observed that the vehicle decelerations present during stops of 230 ft. or less (approximate) are at levels which begin to compromise the handling and stability of high CG and/or short wheelbase vehicles.

CONCLUSIONS:

1. On anti-lock equipped vehicles with brakes sized sufficiently to produce wheel lockup, the stopping distance capabilities are primarily controlled by the function of the anti-lock system in use and the peak traction characteristics of the tires. How much tractive force is available and how much of it can the anti-lock deliver?
2. Anti-lock systems tend to deliver lower average retardation and longer stopping distances with increasing brake overtorque and/or faster air timing. Any standard which specifies the required brake torque performance levels and/or arbitrarily fast air timing must either take the

OTHER PARAMETRIC EFFECTS - SIMULATED RESULTS

DATA SOURCE: Simulator

VEHICLE: 136" 4X2 TRUCK

BRAKES: 15 X 5 RDA, 16½ X 7 Cam

AXLE LOADS: Front-12,000, Rear-20000 (baseline)

A. Effect of changing axle weights

FRONT	REAR	60 MPH DISTANCE
12,000	20,000	245'
12,000	23,000	247'
12,000	17,000	247'
10,800	18,000	241'

B. Effect of initial brake torque

Nominal	245'
20% High	247'
20% Low	244'

C. Effect of Anti-Lock Sensitivity

Sensitivity (S)	
1.0	231'
.9	238'
.8	245'
.7	250'
.6	251'

D. Effect of Anti-Lock System Efficiency

Efficiency (%)	
100	182'
90	193'
80	207'
70	225'
60	245'

Figure 18

proper effect of these variables into account or must leave them in the hands of the vehicle manufacturer.

3. The basic factor determining the stopping capabilities of a vehicle is the peak tire traction available from each axle's tires under dynamic load conditions. Peak tire traction of truck tires has been found to decrease significantly with both increasing load and increasing speed. Vehicle stopping distance requirements must take these factors into proper account if they are to be objective requirements. The tire-to-road traction of a locked truck tire, which is coarsely approximated by the ASTM "Skid Number" measurement, has no direct physical bearing on the retardation capabilities of a road surface relative to an anti-lock equipped vehicle.

4. Scatter in stopping distance test results increases with increasing initial speed. This effect has been traced to increasing effect of anti-lock system activity, and variations in this activity, as speed increases. This factor can make compliance with pseudo-statistical, i.e. "1 out of 6," test requirements more difficult at higher speeds.

5. Vehicle simulation using computer techniques shows significant promise as a means of brake sizing and evaluation for compliance with stopping performance requirements of imposed Standards. There are an exceedingly large number of truck configurations required to adequately cover the wide spectrum of productive roles required of these vehicles in our economy. This number of configurations is so large that physically testing all of them is prohibitive. We feel that these simulation techniques can be used to adequately define the stopping capabilities of a wide range of configurations and that use of these techniques represents a responsible

"due care" approach which can be shown to be based on the current "state-of-the-art" of brake technology.

6. In general, we can only conclude that anti-lock systems are a beneficial addition to a truck brake system. The fact that these systems do not deliver maximum peak traction force on a high coefficient surface may be a blessing in disguise. Although this causes a nominal increase in stopping distance, it limits the maximum deceleration of the vehicle to values which do not compromise stability and allow the driver to maintain control, i.e. "soft" anti-lock systems are desirable. We have found that these systems provide substantial gains in lateral tire traction on low coefficient surfaces which is in line with their design objective.

7. The present stopping distance requirements of FMVSS 121 are too stringent with respect to observed variations in test results. These variations occur for reasons that are neither accounted for in the provisions of the Standard, nor controllable by the final manufacturer of the vehicle. We can only conclude that consistent compliance with the stopping distance requirements of FMVSS 121, as it is currently (5-6-75) written, is dependent upon factors beyond our control. Figure 19 presents a simplified approach toward specifying more realistic stopping distance requirements for the vehicles addressed by 121. The approach includes approximate effects of variables which were not known when the Standard was issued. This information was transmitted to The Department of Transportation in PACCAR's petition of 12-10-74.

8. All of our testing has been done under the specific and limited test conditions mandated by the Standard. The performance of FMVSS 121 equipped vehicles outside

These requirements are based on the general formula:

$$S = \frac{3}{8}\frac{V_o^2}{A1} + \frac{1}{8}\frac{V_o^2}{A2} + T\,V_o$$

Where: S = Distance in feet

V_o = Initial velocity in feet per second

A1 = Deceleration with antilock cycling

A2 = Deceleration without antilock cycling

T = Pressure rise delay time in seconds

The equation is based on the assumption that the antilock system cycles until the vehicle has decelerated to a velocity of 1/2 V_o.

A1 is related to an estimate of the effective coefficient of friction of a loaded truck tire when the wheel is being cycled by a "typical" antilock system on a dry high coefficient surface.

A2 is related to the peak coefficient under the above conditions and applies when the antilock stops cycling. When these systems stop cycling it is because the brakes have torque limited and the wheel is operating right at peak coefficient. Some temperature fade occurs after this point.

SPEED	DISTANCE
20	35
25	52
30	73
35	98
40	127
45	159
50	194
55	234
60	277

Estimated values used to calculate the distances shown are:

A1 = .435 x 32.2 = 14 FTPSPS

A2 = .730 x .8 x 32.2 = 18.8 FTPSPS

T = .200 sec.

This equation is a preliminary estimate only.

Figure 19

of this highly simplified and "pure" test environment is a most critical unanswered question. The highly accelerated timetable imposed by the Standard has not allowed sufficient time for both the development of advanced hardware and the preliminary testing of this hardware under actual in-service conditions. The word hardware, in this case, refers to the combination of both anti-lock systems and more aggressive brakes.

One of the cardinal rules governing the process of technological development and advancement is to never change more than one variable if the objective is to accurately evaluate the effect of that change. In the case of FMVSS 121, this rule has been clearly violated. The consequences of this fact are yet to be determined.

AN EVALUATION OF ANTILOCK SYSTEM PERFORMANCE ON HEAVY DUTY AIR BRAKED COMMERCIAL VEHICLES

J. M. Ehlbeck
and
R. W. Murphy
Freightliner Corporation

ABSTRACT

Performance test results of heavy duty air braked vehicles equipped with various wheel antilock control systems are presented. These tests compared both the straight-line stopping capability and the limit of lateral stability of vehicles equipped with antilock systems from six manufacturers. In addition, the effects of increasing brake power and brake response time on the performance of wheel antilock systems are discussed. The importance of the results of these tests are discussed in light of the requirements of FMVSS-121.

INTRODUCTION

The stringent requirements of Federal Motor Vehicle Safety Standard 121 mandate the use of wheel antilock systems on air braked commercial vehicles. However, due to the fact that wheel antilock systems have not been widely used up to this time, very little is known about the comparative performance of these systems. For this reason, tests were conducted to compare relative performance of six different makes of antilock systems. The six systems were tested on two different vehicles: a short wheelbase C.O.E. single-drive tractor, and a typical dual-drive C.O.E. linehaul tractor. Each system on each vehicle was subjected to:

1. Straight-line stopping distance tests on both a dry asphalt and a wet sealed asphalt surface.
2. A split-coefficient test designed to determine braking capability and stability when the wheels on one side of the vehicle are braking in a surface different from that on the other side of the vehicle.
3. A braking-in-a-lane-change test to determine braking and handling characteristics in an avoidance maneuver.

A description of these comparative tests, the test vehicles, and the test results are given in Part I of this paper. In Part II, a second series of tests is described, wherein the effects of brake lining effectiveness, brake power, and brake response time on vehicle braking capability are evaluated. In the

second test series, three different makes of antilock systems were utilized.

The results from both sets of tests form the basis of the discussion given in Part III.

PART I
ANTILOCK SYSTEM PERFORMANCE COMPARISON

DESCRIPTION OF TESTS

Since both straight-line braking and braking combined with steering, such as in an obstacle avoidance maneuver, are important conditions for evaluating vehicle braking and handling performance, two types of tests were employed to provide comparative data for evaluating the six antilock systems selected for testing. First, straight-line stopping distance tests were conducted to compare the efficiency with which each antilock system utilized available traction for braking. Subsequently, lane change tests were conducted to compare the level of lateral stability provided by each antilock system. The geometry and surface specifications of the split coefficient and lane change tests are shown in Figures 1 and 2.

The straight-line braking tests were conducted on a dry asphalt surface having a nominal skid number (as defined in FMVSS-121) of 75, on a wet slippery surface (wet sealed asphalt) having a nominal skid number of 20, and on a split coefficient surface. Both the dry asphalt and wet slippery surface tests were conducted fully loaded and bobtail*, similar to FMVSS-121 test requirements. The split coefficient

*Unladen tractor without trailer.

SPLIT COEFFICIENT TEST

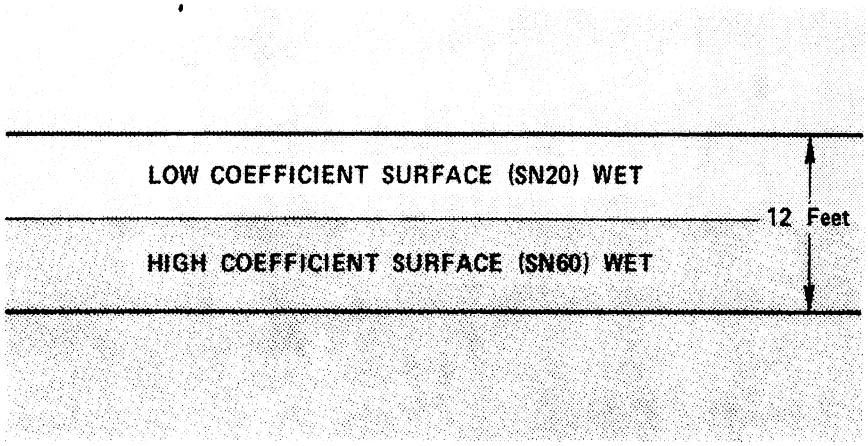

Figure 1.

LANE CHANGE TEST

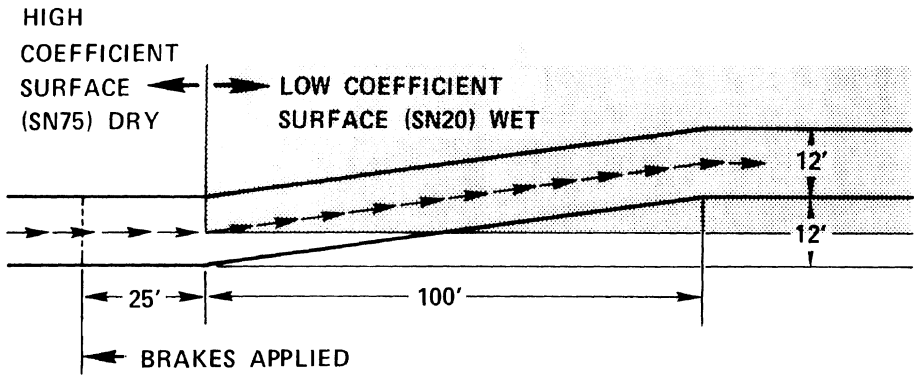

Figure 2.

tests were conducted bobtail only due to space limitations at the test site. The dry asphalt tests were conducted at 20 mph and 60 mph, while the wet slippery and split coefficient tests were conducted at 20 mph and 30 mph, respectively. The measure of performance for all straight-line braking tests was the distance required to stop from the different speeds on the different surfaces under the given load conditions.

The lane change test was used to measure the limit of lateral stability provided by each antilock system under conditions where steering was combined with braking. The surface over which this test was conducted was designed to represent a reasonably adverse real world situation. Combined into this one test were high coefficient, low coefficient, and split coefficient conditions. Due to the complex course over which the lane change test was conducted, considerable driver skill was involved. The brakes had to be applied at the same point each time and the driver had to respond to the effects of the antilock modulated on-off braking forces while steering the vehicle to remain within the 12-ft. wide curved course. The maximum speed at which the vehicle-antilock system could be successfully maneuvered through the curvilinear course was selected as the measure of performance. After some initial testing, a scale of performance employing 5-mph increments was selected. It was judged that ± 2 mph represented test repeatability.

Both the straight-line braking and lane change tests were designed to compare the performance of antilock systems. In order to eliminate driver modulation of the brakes as a test variable, a rapid full service

brake application which was maintained throughout the duration of the stop was employed (provided vehicle directional control could be maintained). Since these tests were designed to compare the relative performance of the antilock systems, each antilock system was tested on the same vehicle under the same test conditions.

DESCRIPTION OF TEST VEHICLES

Two vehicles were selected for testing. A 138-inch wheelbase, three-axle (6x4) tractor (1)* and a 103-inch wheelbase, two-axle (4x2) tractor (2) were used. All axles of each vehicle were equipped with wheel antilock systems. Brake system plumbing and reservoir volumes on both test tractors were modified to meet FMVSS-121 requirements.

The drive axle brakes on both tractors produced wheel lockup on the dry asphalt surface when fully loaded. But since only one pair of steering axle brakes meeting FMVSS-121 requirements were available at the time these tests were conducted (Nov.-Dec., 1973), only the 4x2 tractor was equipped with the more effective front brakes. The steering axle brakes on the 6x4 tractor lacked adequate torque to produce wheel lockup (loaded or bobtail) on the dry asphalt surface.

Loaded vehicle tests were conducted using flat-bed trailers loaded with concrete blocks. The 6x4 tractor was tested with a 40-ft. tandem-axle trailer, while the 4x2 tractor was tested with a 27-ft. single-axle trailer. The brake power and plumbing on both test trailers were modified to meet FMVSS-121

---

*Number in parentheses indicates vehicle-test identification number. For complete vehicle-test specifications, consult appendix.

requirements. Both trailers were equipped with antilock systems. To eliminate trailer performance as a test variable, the antilock systems on the test trailers were not changed during the performance evaluation tests.

TEST RESULTS

A summary of the test results is shown in Table I. This table includes results from the straight-line braking tests, the split coefficient tests, and the lane change tests. The letters "B" and "W" indicate "best" and "worst" performing antilock systems for each test. The variation between the best and worst performing antilock systems is included at the bottom of the table.

It should be emphasized that the stopping distances should not be used as a basis for judging compliance with the stopping distance requirements of FMVSS-121. The drive axle brakes on both test tractors lacked adequate power to meet FMVSS-121 dynamometer test requirements (but did produce wheel lockup), and the brakes on the two test trailers were not calibrated to assure minimum compliance with FMVSS-121 "control trailer" requirements. In addition, the results of the comparative performance tests, shown in Table I, are based upon tests conducted in late 1973. Since that time, numerous design and parameter changes have been made to the various antilock systems tested.

DISCUSSION OF TEST RESULTS

The results of the comparative performance evaluation tests show that no single antilock system performed "best" overall. This can be graphically seen in Table Ia. Significant performance variations

TABLE I

ANTILOCK SYSTEM PERFORMANCE COMPARISON

SUMMARY OF AVERAGE STRAIGHT LINE STOPPING DISTANCES AND MAXIMUM LANE CHANGE SPEED

Antilock System	Test Tractor	Dry Asphalt Test Surface (SN-75) Ave. Stopping Distance In Feet				Split Coefficient Ave. Stopping Distance In Feet	Lane Change	Wet Slippery Test Surface (SN-20) Ave. Stopping Distance In Feet	
		Loaded		Bobtail		From	Max. Speed Mph	From 20 Mph	
		20 Mph	60 Mph	20 Mph	60 Mph	30 Mph	Bobtail	Loaded	Bobtail
A	6 x 4	28.4(B)	248.4(W)	27.7	243.3	103.6(B)	45(B)	64.6	54.9
	4 x 2	29.4	277.0(W)	25.9(W)	213.4	112.9	35	71.8	55.9
B	6 x 4	28.5	219.3(B)	29.0	232.4	117.0	40	68.7	62.3(W)
	4 x 2	29.3	237.8	25.4	95.1 @ 40 mph*(W)	114.4	35	76.5(W)	65.0(W)
C	6 x 4	28.4(B)	231.7	26.8(B)	222.0(B)	110.4	40	69.0(W)	59.9
	4 x 2	29.0(B)	234.8(B)	23.7	166.3 @ 55 mph*	**(W)	30(W)	57.6(B)	48.6(B)
D	6 x 4	30.4(W)	230.5	30.0(W)	265.7(W)	141.9(W)	45(B)	62.6(B)	54.3(B)
	4 x 2	30.7	246.9	23.9	134.8 @ 50 mph*	104.7(B)	40(B)	66.2	50.8
E	6 x 4	29.3	227.3	27.4	238.8	122.5	35(W)	65.1	56.0
	4 x 2	33.7(W)	275.6	23.0(B)	202.7(B)	**(W)	35	60.6	57.2
F	6 x 4	29.8	222.4	28.7	241.4	113.3	45(B)	63.7	56.4
	4 x 2	31.4	259.6	23.5	129.9 @ 50 mph*	113.2	40(B)	66.0	57.3
% Variation Between Best & Worst Systems	6 x 4	7.0	13.3	11.9	19.7	37.0	28.6	10.2	14.7
	4 x 2	16.2	18.0	12.6	--	--	33.3	32.8	33.7

*Stopping distance at maximum speed for which driver could retain vehicle within 12 foot lane.

**Unable to maintain vehicle within 12 foot lane.

TABLE Ia

COMPARATIVE PERFORMANCE EVALUATION OF ANTILOCK SYSTEMS
SUMMARY OF BEST (B) AND WORST (W) SYSTEMS BY TEST

Antilock System	Test Tractor	Dry Asphalt Test				Split Coefficient Test	Lane Change Test	Wet Slippery Test From 20 Mph	
		Loaded		Bobtail					
		20 Mph	60 Mph	20 Mph	60 Mph			Loaded	Bobtail
A	6 x 4	B	W			B	B		
	4 x 2		W	W					
B	6 x 4		B						W
	4 x 2							W	W
C	6 x 4	B		B	B			W	
	4 x 2	B	B			W	W	B	B
D	6 x 4	W		W	W	W	B	B	B
	4 x 2					B	B		
E	6 x 4						W		
	4 x 2	W		B	B	W			
F	6 x 4						B		
	4 x 2						B		

occurred as a result of vehicle configuration, loading, test surface, and test speed. Examples of the performance variations due to each of these factors are:

Configuration - Antilock System "D" which performed best on the 4x2 tractor in the split coefficient test, performed worst in the same test conducted on the 6x4 tractor.

Loading - Antilock System "E" which performed best on the 4x2 tractor in the 20-mph dry asphalt test bobtail, performed worst in the same test conducted with the vehicle loaded.

Surface - Antilock System "C" which performed best on the 6x4 tractor in the 20-mph loaded dry asphalt test, performed worst in the same test conducted on the wet slippery surface.

Speed - Antilock System "A" which performed best on the 6x4 tractor in the 20-mph loaded dry asphalt test, performed worst in the same test conducted at 60 mph.

These performance variations are shown graphically in Figures 3 through 6. As can be seen in these graphs, if the results of one performance comparison test are arranged in descending order, a nearly uniform ascending order is assumed by the results of the second performance comparison test. This demonstrates that

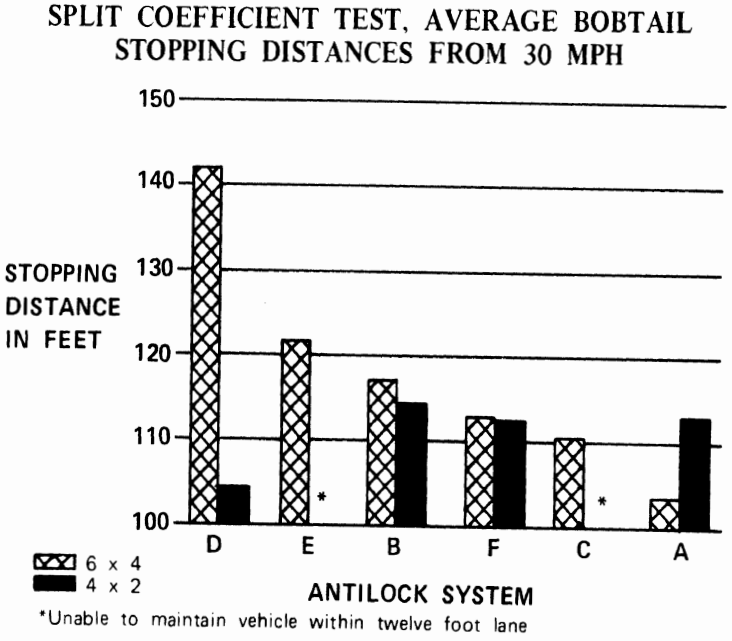

Figure 3.

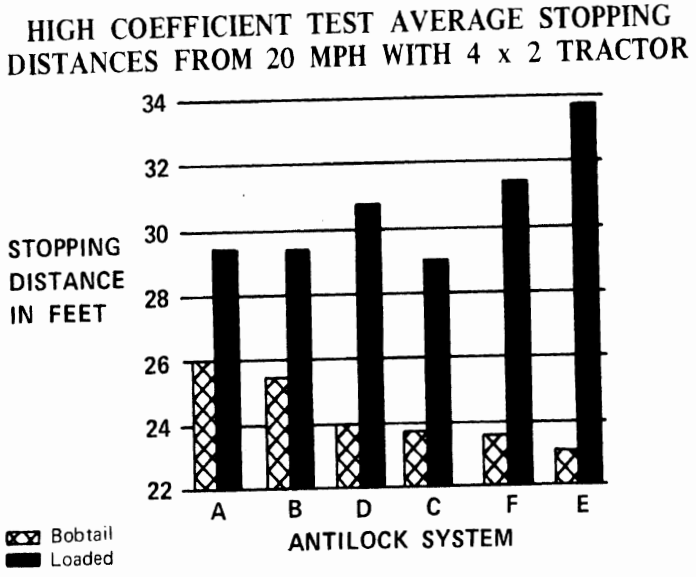

Figure 4.

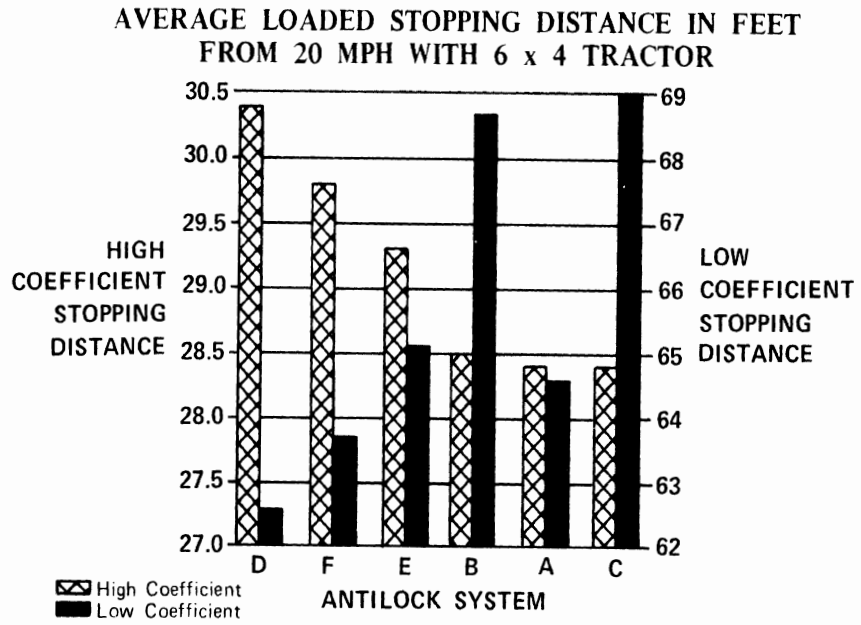

Figure 5.

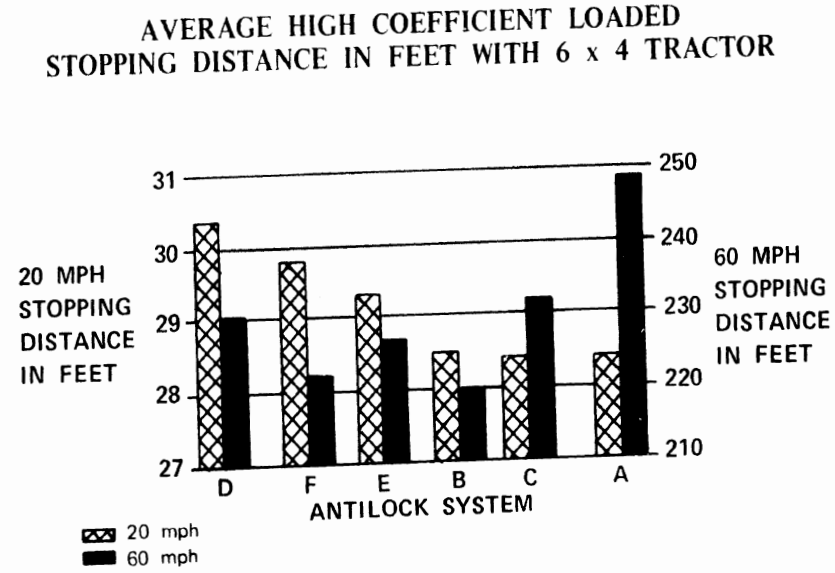

Figure 6.

significant performance trade-offs were made (knowingly or unknowingly) in the choice of wheel control parameters employed in the design of each antilock system. Further, the data demonstrate that none of the antilock control systems were able to adapt to all prevailing vehicle, load, and road conditions by providing maximum utilization of available traction for braking and lateral stability. Finally, these data point up the existence of a significant trade-off between straight-line dry asphalt stopping distance capability and the limit of lateral stability as measured in the lane change test. This trade-off is clearly shown in Figures 7 and 8, wherein stability and stopping distance data are plotted in the same graph for each vehicle.

SUMMARY

The results of the antilock system performance comparison tests show that no single antilock system performed "best" overall. Significant performance variations occurred as a result of vehicle configuration, loading, test surface, and test speed. In addition, these tests showed the existence of a significant performance trade-off between straight line dry asphalt stopping distance and lateral stability provided by each antilock system.

PART II
ADDITIONAL FACTORS AFFECTING ANTILOCK SYSTEM PERFORMANCE

The results of the comparative performance evaluation tests demonstrated that "truly adaptive" wheel antilock systems were not available. Thus, it was decided to investigate the variations in antilock

AVERAGE HIGH COEFFICIENT STOPPING DISTANCE VERSUS STABILITY WITH 6 x 4 TRACTOR

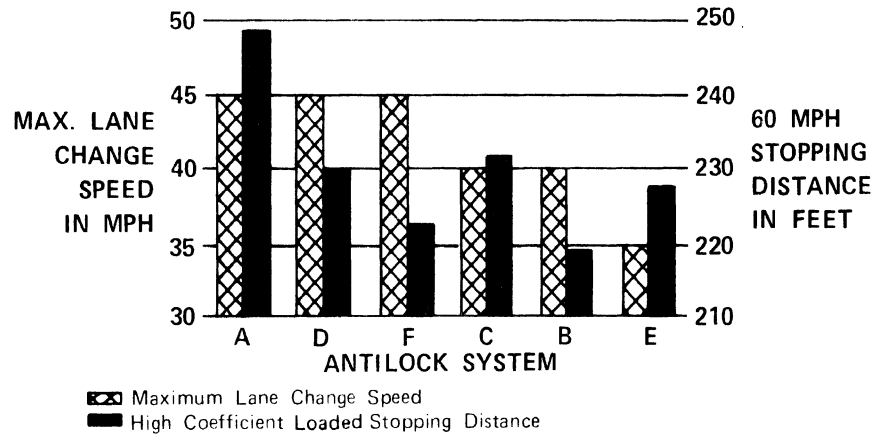

Figure 7.

AVERAGE HIGH COEFFICIENT STOPPING DISTANCE IN FEET VERSUS STABILITY WITH 4 x 2 TRACTOR

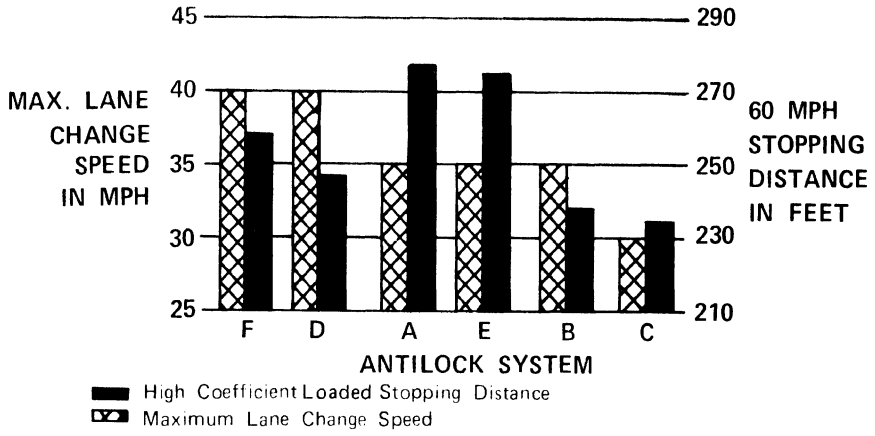

Figure 8.

system performance which result from "other factors" involved in the brake system. A second series of tests were conducted to determine the effect that variations in brake effectiveness, brake power, and brake actuation time has upon the straight-line dry asphalt stopping distance performance of antilock systems.

This second series of tests was conducted in strict accordance with FMVSS-121 requirements—all tests were conducted on a nominal skid number 75 surface and all loaded vehicle tests were conducted with control trailers as specified by the standard. The effect which driver skill has upon vehicle performance in straight-line braking was minimized by conducting all tests using a rapid full service brake application.

BRAKE RETARDATION FORCE

The effect which two brake linings from different suppliers (both of the same friction class) have upon the stopping distance performance of a three-axle tractor (3) is shown in Table II. Although both Linings A and B provided torque adequate to produce wheel lockup (controlled by the antilock system) of the drive axle brakes throughout all stops, average 60 mph stopping distances varied by as much as 6.5% when the tractor was tested with the loaded control trailer and by 15.5% when tested bobtail. The only apparent difference between Lining A and B was that, nominally, Lining B provides 8% (average) higher retardation force than Lining A when tested on an inertial dynamometer.

Based upon the air pressure required to produce wheel lockup, it was determined that Lining B did indeed produce a higher level of brake retardation

TABLE II

BRAKE LINING PERFORMANCE COMPARISON

Brake Lining	Average Stopping Distance In Feet			
	Loaded		Bobtail	
	20 Mph	60 Mph	20 Mph	60 Mph
A	29.3	234.1	25.5	186.1
B	29.8	249.2	26.7	214.9

force. In addition, from an analysis of recorded vehicle dynamic data (wheel speeds, suspension loads and brake chamber air pressure), it was determined that the increased brake retardation force was also the reason for the longer stopping distances recorded with the higher torque "B" lining. The increased brake torque provided by Lining B increased the demand placed upon the antilock system to modulate the brakes which resulted in more violent "on-off" modulation of the brakes. This resulted in lower average utilization of available traction for braking and hence longer stopping distances.

Similarly, the effects which increased steering axle brake retardation force has on stopping distance is shown in Table III. The level of steering axle brake retardation force was varied by increasing the size of the brake chamber used to actuate the brakes. To insure the validity of the test results, all tests were performed using the same two-axle tractor (4) tested on the same SN 75 test surface using the same control trailer. Although all loaded tests were conducted using the same calibrated control trailer, caution should be used in making a direct comparison between the loaded stopping distance performance of Antilock Systems I, II, and III, since the antilock system used on the control trailer was changed between the testing of Antilock Systems II and III.

Based upon elementary vehicle braking theory, up to a 10-ft. reduction in loaded 60 mph stopping distance would be expected when the steering axle brake actuation power was increased. The key to explaining this anomaly lies in the fact that with the 5.5 x 16 actuation power, the steering axle brakes were torque limited (lacked adequate power to produce wheel lockup), but

TABLE III

STEERING AXLE BRAKE ACTUATION POWER
PERFORMANCE COMPARISON

	Average Stopping Distance In Feet					
Antilock System	I		II		III	
Steering Axle Brake Actuation Power*	5.5x16	5.5x20	5.5x16	5.5x20	5.5x16	5.5x20
			Loaded			
20 Mph	29.2	27.3	30.4	28.7	28.8	27.9
60 Mph	239.6	242.4	218.2	236.1	234.2	241.5
			Bobtail			
20 Mph	27.9	24.4	26.1	23.0	23.2	25.2
60 Mph	213.5	204.2	200.5	195.2	192.9	193.4

*Brake actuation power is given by slack adjuster (brake torque arm) length in inches and effective brake chamber area, i.e., 5.5x20 means a slack adjuster length of 5.5 inches and a brake chamber area of 20 sq. in.

with the 5.5 x 20 actuation power, wheel lockup, controlled by the antilock system, occurred. Similar to the data presented in Table II, the effect of increasing the steering axle brake actuation power was to require the antilock system to modulate the steering axle brakes. But, the low utilization of available traction provided by antilock systems resulted in increased stopping distances. The increasing steering axle brake retardation force also produced highly undesirable vehicle pitching and random steering force inputs due to the "on-off" antilock modulation of the steering axle brakes. The tests were repeated with three different antilock systems with identical results. These data unequivocally demonstrate the low efficiency with which currently available antilock systems utilize available traction for braking.

BRAKE ACTUATION TIME*

The effect of brake actuation time on stopping distance performance of a three-axle tractor (3) is shown in Table IV. Increased brake actuation time provided a small but significant reduction in the loaded 60 mph stopping distance. But more significantly, the results from these tests demonstrated that increased brake actuation times improved the ability of the antilock system to control incipient wheel lockup which in turn reduced vehicle pitching and provided smoother stops.

As shown in Table V, increasing the steering axle brake actuation time on a two-axle tractor (4) drastically

---

*Brake actuation time is defined (in accordance with FMVSS-121) as the elapsed time between first movement of the service brake control and the time at which 60 psi is reached at the service brake chamber with an initial supply reservoir pressure of 100 psi.

TABLE IV

BRAKE ACTUATION TIME
PERFORMANCE COMPARISON

Brake Actuation Timing Tractor (Sec.)	Average Stopping Distance In Feet			
	Loaded		Bobtail	
	20 Mph	60 Mph	20 Mph	60 Mph
0.23	29.3	234.1	23.7	186.0
0.28	29.0	227.1	24.5	188.3
0.35	28.1	226.6	24.8	199.6

TABLE V

STEERING AXLE BRAKE ACTUATION TIME
PERFORMANCE COMPARISON BOBTAIL

Steering Axle Brake Actuation Time (Sec.)	Ave. Bobtail Stopping Distance In Feet		Comments
	20 Mph	60 Mph	
0.2	25.2	193.4	Two of the three 60 mph tests conducted resulted in loss of vehicle control (spin out).
0.3	26.1	198.6	All three 60 mph runs resulted in the vehicle remaining within the 12 ft. lane.
0.4	24.9	219.6	All three 60 mph stops were within the 12 ft. lane and control was good.

improved vehicle stability. By increasing the brake actuation times, the high initial torque spike, inherent with drum-type brakes, was reduced. The reduction of this torque spike reduces the spin-down rate of the wheels, allowing the antilock controller adequate time to react and modulate brake pressure, thereby minimizing skidding and improving vehicle control. In addition, increasing the steering axle brake actuation time reduced antilock modulation of the steering axle brakes which provided a marginal improvement in loaded stopping distance as shown in Table VI.

Although these test results indicate significant vehicle performance improvement resulting from increased brake actuation time, it must be emphasized that brake actuation time is composed of the sum of the transmission and pressure rise times (see Figure 9). For these tests, only the pressure rise time was varied. Analysis of the test data shows that reducing the pressure rise rate reduced the spin-down rate of the wheels. But since wheel spin-down rate is a function of the instantaneous brake torque, wheel load, and tire-road interface conditions, it must be concluded that no overall "optimum" brake actuation time exists to cover all possible variations in vehicle-road conditions.

SUMMARY

The results of this second series of tests show that even with antilock systems, when brake retardation force is increased above the level required to produce incipient wheel lockup, stopping distance is also increased. The reason for this increase in stopping distances with increased brake power lies in the low utilization of available braking forces provided by

TABLE VI

STEERING AXLE BRAKE ACTUATION TIME

PERFORMANCE COMPARISON LOADED

Steering Axle Brake Actuation Time (Sec.)	Average Loaded Stopping Distances In Feet	
	20 Mph	60 Mph
0.2	28.8	241.5
0.4	28.9	239.3

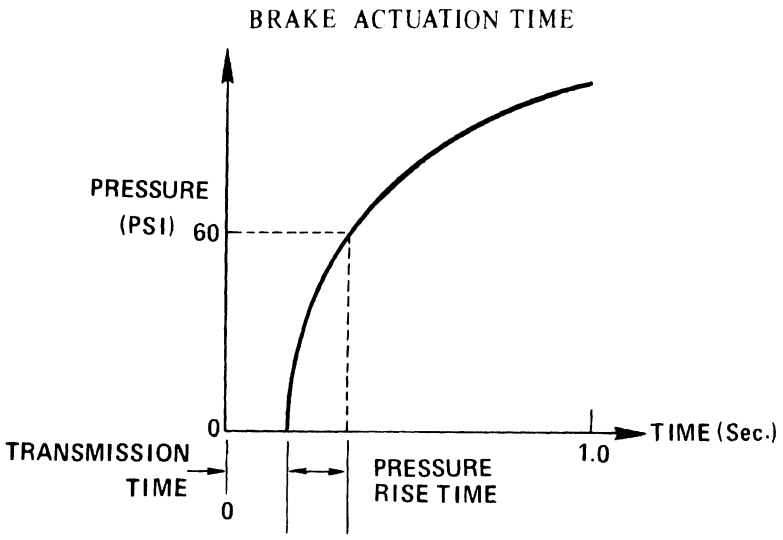
BRAKE ACTUATION TIME
PRESSURE
(PSI)
60
0
TIME (Sec.)
1.0
TRANSMISSION
TIME
0
PRESSURE
RISE TIME

Figure 9.

presently available wheel antilock systems. Further, these tests show that a reduction in loaded vehicle dry asphalt stopping distance and improved vehicle stability can be achieved by increasing brake actuation time beyond current FMVSS-121 limits. This sensitivity of antilock systems to both brake retardation force and actuation time demonstrates that truly adaptive wheel antilock systems, systems which adopt to all prevailing vehicle and road conditions to provide maximum utilization of available traction for braking and lateral stability, are not presently available.

PART III
DISCUSSION

Since the margins between FMVSS-121 stopping distance requirements and actual stopping distances for many classes of vehicle can in certain cases be small, the supposed numerically insignificant effects which brake lining effectiveness, brake power, and actuation time have upon the performance of antilock systems cannot be ignored if consistent compliance with the 60 mph, 245 ft. stopping distance requirement is to be assured. These effects, combined with the sensitivity of antilock systems to vehicle configuration, loading, test surface and test speed, result in a requirement for an inordinate number of vehicle tests to establish the conditions of compliance unless options and alternative sources so vital to the trucking industry are to be eliminated.

Finally, these test results indicate that the employment of currently available technology in the design and manufacture of brake control systems has not produced systems which can allow for significant

variations in vehicle configuration, loading, test surface traction properties, and test speed such that uniform performance is achieved. Thus the following question naturally arises: "Do the test conditions and stopping distance requirements specified by FMVSS-121 necessitate employment of brake control system design configurations and parameters which compromise the full potential safety benefit possible from utilization of such systems?" If vehicle stability and performance on slippery and split coefficient surfaces are sacrificed for an unreasonably stringent straight ahead stopping capability, the answer to the question would seem to be affirmative.

The last testing and analytical program sponsored by the National Highway Traffic Safety Administration (NHTSA) aimed at gathering data upon which a standard for air-braked vehicles may be based was conducted five years ago.* Many changes have occurred in the past five years in vehicle, brake, and brake control system design. Therefore, we strongly recommend that the Department of Transportation immediately undertake to sponsor further studies to specifically address and answer questions raised by us and other contributors to this symposium. We further recommend that an advisory committee be established of representatives of truck, bus, and trailer manufacturers and the major users to advise the NHTSA in establishing and carrying out such a program in order to keep the administration in contact with the "real world."

---

*Murphy, R.W., et al., Bus, Truck, Tractor-Trailer Braking System Performance, Vol. 1 of 2: Research Findings. The Highway Safety Research Institute, March, 1971, PB #201 364.

TEST VEHICLE EQUIPMENT AND LOADINGS

Vehicle Test I.D. No.	Tractor	Wheel Base (Inches)	Axle Weights (lbs.)				Steering Axle		Drive Axle(s)	
			Loaded		Bobtail					
			Steering	Drive	Steering	Drive	Brake Size	Actuation Power	Brake Size	Actuation Power
1	6 x 4	138.00	8,800	34,180	7,650	6,800	16½x3½	5.5x16	16.5x7	5.0x30
2	4 x 2	103.00	8,870	20,080	7,450	4,350	15x4	5.5x20	16.5x7	5.0x30
3	6 x 4	138.00	10,390	34,760	7,650	6,800	15x4	5.5x20	16.5x7	5.5x30
4	4 x 2	115.75	9,240	19,720	7,190	4,160	15x4	5.5x20	16.5x7	5.5x30

NHTSA/APL HYBRID COMPUTER VEHICLE HANDLING PROGRAM

P. F. Bohn
and
R. J. Keenan
Applied Physics Laboratory
The Johns Hopkins University

ABSTRACT

The National Highway Traffic Safety Administration (NHTSA) currently has operational at the Applied Physics Laboratory of The Johns Hopkins University (APL/JHU) a simulation which predicts the dynamic response of motor vehicles to braking and steering commands as well as aerodynamic and road roughness disturbances. The simulation model equations are solved simultaneously on an analog computer and a digital computer yielding a hybrid computer solution to the model. Simulation control is exercised via a CRT and keyboard terminal with complete interactive operation available for data manipulation, data collection, and run control. The interactive terminal need not be located at the hybrid computer and thus remote simulation operation is feasible.

This paper explains the interactive use of the Hybrid Computer Vehicle Handling Program (HVHP), examines the development of the mathematical model, details the types of motor vehicles for which it has been validated, explains the interactive use of the simulation, and discusses the computing system on which the simulation model is solved.

INTRODUCTION

The Applied Physics Laboratory first became involved in the prediction of vehicle dynamic performance via simulation in May of 1972. At that time APL was requested by NHTSA to move to APL an existing vehicle simulation operational on the hybrid computer at the Bendix Research Laboratories [1, 2].* NHTSA's motive in moving the simulation was to make it available to all NHTSA contractors for vehicle research. APL reprogrammed the Bendix simulation for its hybrid computer without change of the model and published the result in Reference [3]. The derivation of the original Bendix model is presented in Reference [4].

Work with NHTSA contractors began in July, 1973, when APL started providing simulation service to the Calspan Corporation on the NHTSA investigation into tire properties' effects on vehicle handling [5]. During the work with Calspan, two primary simulation modifications were completed:

(1) a very flexible user interface for interactive simulation control designed at APL was added by APL

(2) a new tire force and moment model specified by Calspan was added by APL.

Also added to the simulation about this time was the capability to automatically initialize the simulation to perform any of the six Vehicle Handling Test Procedures (VHTP's) and to collect and process the data required to calculate the vehicle performance

*Numbers in brackets refer to references listed at the end of this paper.

comparison variables (CV). These VHTP's and CV's were originally developed by HSRI (Highway Safety Research Institute) in References [6] and [7] and restated for computer implementation by APL in Reference [8]. The result of this work was the HVHP (Hybrid Computer Vehicle Handling Program) documented in Reference [9].

Recent work with NHTSA contractors has led to the simulation additions which extend the types of vehicles for which the simulation is applicable and further refine the tire force and moment model to represent truck as well as passenger car tires. Currently, dynamic performance of vehicles of the following suspension types can be predicted by the HVHP:

(1) independent front and rear,

(2) independent front with solid rear axle,

(3) solid front and rear axles,

(4) solid front and rear axles with dual rear tires.

In its work with NHTSA contractors, APL has added to the simulation model any refinements required by the contractor to successfully complete his research.

The simulation has proven to be economical for vehicle dynamic performance prediction. User experience with the HVHP has shown that while performing parametric runs, 500 seconds of vehicle motion can be simulated in one hour of computer use. This translates to a cost of less than $0.50 per vehicle simulation second and represents a fifty percent utilization of the available computing time. Since this simulation, running at one-fourth of real time, is capable of 900

vehicle simulated seconds per hour, approximately fifty percent of the time is utilized for observing data and changing parameters. The $0.50 per simulated second should be viewed as the current lower cost limit.

For program debugging and model checkout, fewer runs are made in a given time period than when parametric data are being produced. Therefore, the cost per vehicle simulated second would increase. However, general experience has indicated that on-line data observation for debugging decreases the total time required for program checkout. During the debug phase, HVHP cost usually ranges between one and two dollars per vehicle simulated second, with a decreasing trend toward the $0.50 per second figure.

SIMULATION MODEL

The simulated vehicle is represented by a seventeen-degree-of-freedom model which consists of:

(1) A basic ten-degree-of-freedom model of the vehicle body, front wheels, and rear axle.

(2) A three-degree-of-freedom steering system model.

(3) A four-degree-of-freedom wheel rotational dynamics model.

The basic ten-degree-of-freedom model regards the vehicle as an assembly of four rigid masses: the vehicle body, two front wheel masses, and the rear wheel axle combination (solid rear axle). The ten

degrees of freedom consist of the six standard translational and rotational degrees of freedom for the body, two for the vertical motion of each front wheel, and two for the rotation and vertical motion of the rear axle. When the vehicle model includes the independent rear suspension, each rear wheel is considered as an independent mass; and the vertical motion of each rear wheel is a degree of freedom.

The steering system model with three degrees of freedom represents the compliance in each of the front wheels and in the connecting rod. The tire moments about each kingpin axis are functions of the circumferential and side tire forces, tire aligning torque, the inclination and caster of the kingpins, and the caster trail effects of the tires. Steering wheel displacement is the steering system input.

Four additional degrees of freedom (for a total of seventeen) are contained in the rotational equations of motion about the spin axis of each wheel. These equations, which include the differential effects of the rear wheels, yield the wheel rotation rates from which slip and, in turn, the circumferential and lateral friction coefficients are computed. The input to the equations can be either drive torque or brake torque.

The equations of motion of the vehicle body, wheels, and rear axle are perturbed by suspension, gravity, and tire forces and moments. The suspension equations include the effects of the springs, shock absorbers, and front and rear auxiliary roll stiffness. The suspension deflections are calculated relative to the suspension equilibrium position which varies with vehicle weight. Vehicle functions, such as camber, caster, and toe angles, anti-pitch and anti-roll forces, and bump

stop forces are input relative to the unloaded vehicle suspension positions. These functions are then corrected to the equilibrium position for varying vehicle weight when used for calculations within the vehicle model.

The tire forces (radial, circumferential, and lateral) are computed for each wheel. The radial load is proportional to the distance between the wheel center and the road. The circumferential force is the product of the tire radial load and circumferential coefficient of friction which is a function of wheel slip, radial load, and normalized slip angle. The lateral tire force is the product of the tire radial load, lateral friction coefficient, and two shaping functions representing the effects of normalized steer angle and longitudinal slip. Additionally, the lateral friction coefficient is a function of radial load and wheel velocity. Wheel aligning torques and overturning moments are included as functions of wheel radial load, side force, and camber angle.

ALLOCATION OF ANALOG AND DIGITAL COMPUTER TASKS

Since the model is solved on a hybrid computer, it must be subdivided for solution into equations to be solved on the analog computer and those to be solved on the digital computer. The allocation of computing tasks was determined using the following guidelines:

(1) Function generation requiring extensive algebraic calculations or reference to tables of values should be performed in the digital computer.

(2) System variables determined from the solution of differential equations should be graded according to response time (time constant). The differential equations representing the fastest variables should be solved on the analog computer, and the remaining on the digital computer.

Slight compromises to the task allocation determined from the above rules were required due to limitations in digital computer computation speed, numbers of analog computer computation modules, and available analog-to-digital and digital-to-analog data communication modules.

The present allocation of computing tasks between the analog and digital computers is presented in Figure 1. Calculated in the digital portion are the sprung mass equations of motion, wheel orientation angles, and tire force equations. Wheel brake and drive torques, velocities of the tire contact point, and resultant forces and moments are also computed in the digital portion.

The analog computations include the suspension forces, shock absorber and wheel spring functions, longitudinal wheel slip, and circumferential coefficient of friction. In addition, the equations of motion of the unsprung masses and steering system equations are solved on the analog computer.

The hybrid simulation is time scaled to run at one-fourth real time, i.e., twenty seconds of clock-on-the-wall time is required for five seconds of vehicle simulation.

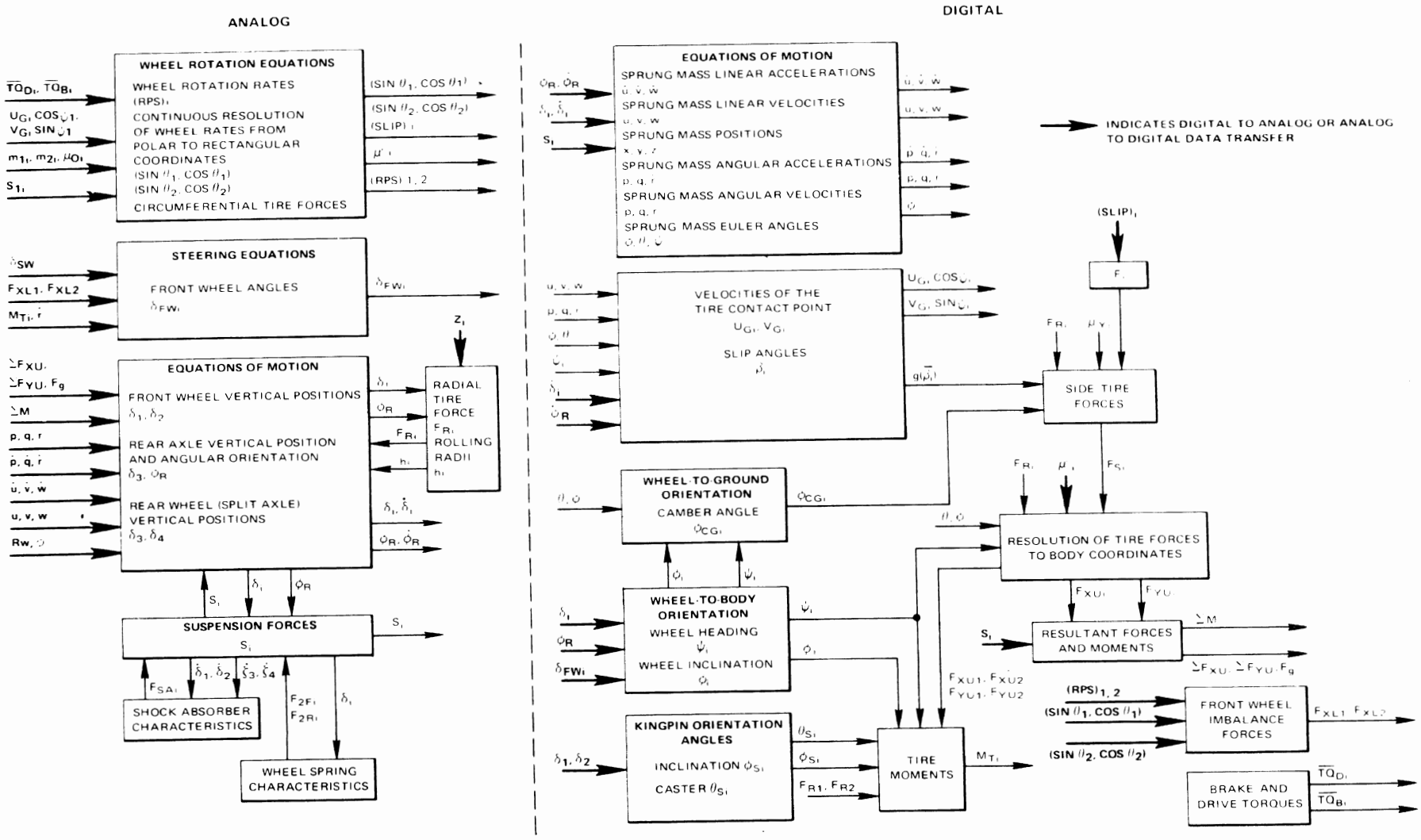

Fig. 1 HYBRID SIMULATION BLOCK DIAGRAM

HYBRID COMPUTER

Figure 2 is a diagram of the APL/JHU hybrid computer system. The primary units are the analog and digital computers, the hybrid control and data interface, the hybrid operators control console, and the remote batch station. Two types of analog computers manufactured by Electronic Associates, Inc., are located in the hybrid laboratory and the portion of the model programmed on the analog computer is divided between them. The entire steering system is contained on an EAI 231-R and the rotational wheel dynamics, circumferential friction coefficient calculation, tire deflection, and suspension dynamics is contained on an EAI 680.

The hybrid data and control interface permits control of the analog computer by the digital computer and exchange of data between the analog and digital computers. Data communication with the digital computer is provided by 24 multiplying digital-to-analog converters (MDAC's), 24 non-multiplying DAC's and 24 channels of analog-to-digital conversion (ADC's). The system contains a control interface which allows complete control of the 680 analog computer and data interface via Fortran IV callable subroutines by the digital computer which is remotely located 1000 feet from the hybrid laboratory. A detailed description of the APL/JHU hybrid facility is presented in Appendix C of Reference [9].

The digital computer is an IBM 360 Model 91. This is one of the largest and fastest computers built by IBM and is characterized by the following:

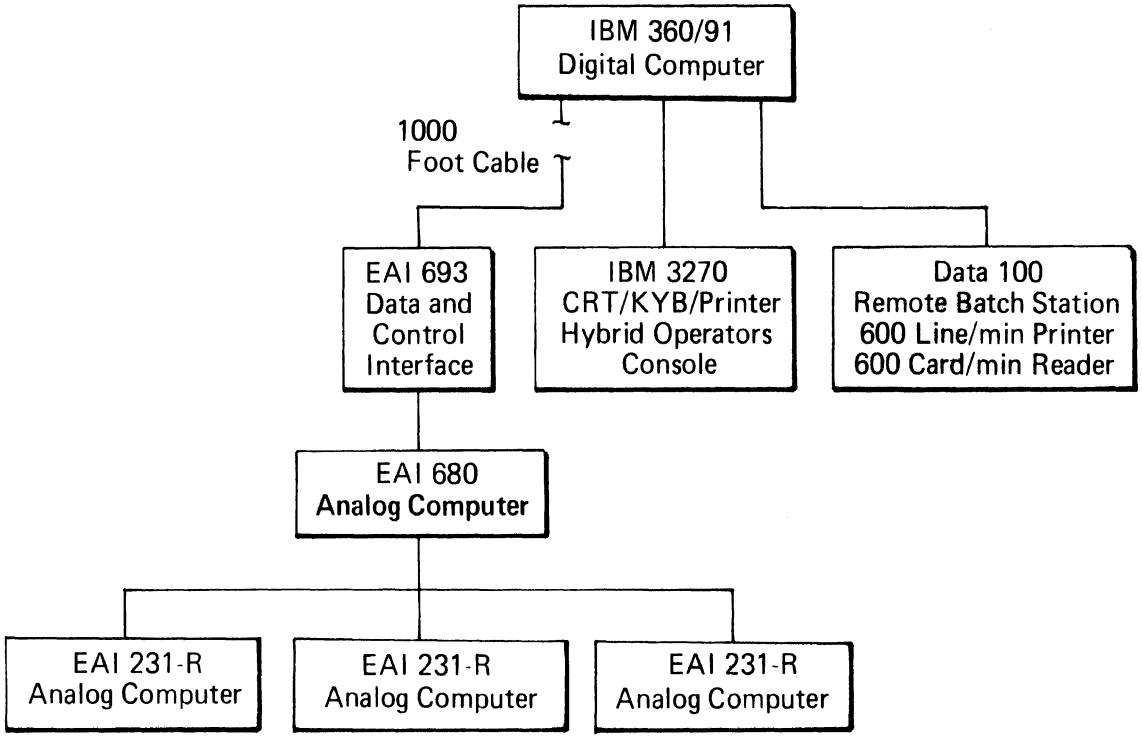

Fig. 2 APL/JHU HYBRID COMPUTER SYSTEM BLOCK DIAGRAM

Third generation hardware

4 million bytes of main core storage

4 billion bytes of random access storage

Minimum instruction execution time of 60 nanoseconds

Use of the Operating System OS/MVT (Multi-programming with a Variable Number of Tasks).

All vehicle model calculations not assigned to the analog computers are performed digitally. Simulation coding is performed in the Fortran IV language.

Since the hybrid computing facility is remotely located from the digital computer, a remote batch terminal is required for program deck submission and printing of digital output. The terminal used in the hybrid laboratory is manufactured by Data 100 and contains a 600 card/minute reader and a 600 line/minute printer.

The hybrid operators control console is an IBM 3270 display system consisting of a CRT, keyboard, and printer. All simulation control is exercised at this station. Simulation directives, user information input via the keyboard and simulation output appear on the CRT. The printer is used to ghost print everything that appears on the CRT so that user/computer transactions are not lost. A very powerful and flexible set of communication routines, designed for simulation use, is available to the user at the hybrid operators console.

USER'S INTERFACE

To increase efficiency and convenience of use, an interface between the engineering user and the computer has been designed and implemented in the HVHP. In this way, user control and information retrieval from the hybrid computer is maximized [10]. The interface has been implemented by a set of generalized input/output subroutines. Using these communication routines, the following necessary tasks can be accomplished interactively at the CRT hybrid control console.

- Interrogation of any digital variable, including arrays, by Fortran name or an alias.
- Assignment of new values to any digital parameter or initial condition.
- Tracking and printing the values of any digital variable as a function of time.
- Printing the end of run values of any digital variable or parameter.
- Performing automatically a group of parametric runs varying one or more parameters or initial conditions by an arbitrary amount.
- Assigning new digital variables to the DAC's (digital-to-analog converters) and ADC's (analog-to-digital converters).
- Rescaling the digital variables output on the DAC's or input on the ADC's.

- Commenting the computer output with observations pertinent to the computer runs.

- Printing the value of all digital variables on command.

The usefulness of these routines is augmented by having the following features:

- The output unit for all digital computer responses is selectable (line printer, CRT, or both).

- Extensive subroutine error recovery which allows operation by untrained personnel.

- Free format input which obviates the need to always insert decimal points, spaces, etc., which would be required by Fortran syntax.

An explanation of the modules which are the building blocks of the routines, as well as a discussion of interaction, is presented in Appendix D of Reference [9].

VHTP MANEUVERS AND COMPARISON VARIABLES

Due to the importance of handling test procedures in vehicle research, the HVHP was programmed to automatically perform those defined for passenger cars by HSRI [8]. The associated comparison variables (CV's) for the VHTP's are also calculated. Since test procedures generally employ the input commands of braking, steering, and combinations of braking and steering,

the HVHP implementation can generally be used to generate test procedures for all types of vehicles. The comparison variables are less general and refer specifically to the HSRI passenger vehicle VHTP's.

VHTP MANEUVERS

The simulation has the capability of self-initializing to perform any of the six passenger car VHTP maneuvers and to calculate the comparison variables appropriate for the selected VHTP. Utilizing the communication routines, a VHTP is selected by addressing the Fortran variable VHTPNO and assigning it a value from 1 to 6. The value of 0 is reserved for a special check run that verifies correct dynamic operation of the simulation. Once a VHTP has been selected, the input command pertinent to the VHTP can be accessed. For all VHTP's the Fortran variable PFL represents brake line pressure. For VHTP's 2 to 6, the steering wheel input has the Fortran name STR2, STR3, etc. The names PFL, STR2, etc., can be used in the multi-run routine to simulate a series of VHTP tests in which the brake line pressure or steering wheel input is incremented. By convention, when a VHTP is selected in which the steering input is normally a parameter (VHTP 2, 4, 5), the STR variable contains the steering wheel rotation required to input 2.0 degrees of normalized steer. Normalized steer is the independent variable required for run series in which the steering is incremented.

VHTP COMPARISON VARIABLES

Comparison variables are output in both the single run and multiple run modes. If a single run is executed, a general comparison variable format is selected in

which all CV's are output. However, only those pertinent to the selected VHTP will be nonzero. If a series of runs is executed, the output is in a tabular format with the input command (steering wheel angle or brake line pressure) starting in the left column followed by the pertinent CV's. An example is presented in Figure 3, in which the following occurs:

(1) VHTP 4 is selected.

(2) The STR4 variable is interrogated to determine the steering wheel rotation for two degrees of normalized steer.

(3) The steering wheel input is set equal to 300 degrees.

(4) A single run is executed.

(5) A run series of four runs is set up with STR4 initialized to two degrees normalized steer (NS) and incremented by two degrees NS in each run.

(6) A multiple run is executed.

A representative parametric run series for each VHTP is presented in Figure 2-2(a) to 2-2(f) of Reference [9].

SIMULATION OUTPUT

In addition to the user/computer transactions printed on the hybrid operator's printer, the simulation has several outputs which are normally available to the user. The output is summarized below:

(1) VHTP comparison variable values

(2) analog strip chart time history recordings (sixteen variables)

```
**********    THIS IS THE FIRST OF TWO SPECIAL CARDS FOR THE 2741 ACM  *********
        VEHICLE HANDLING SIMULATION
ENGAGE PATCH PANEL FOR TEST
TYPE OK WHEN READY
****
MAY        21   1974
TIME   14   0 11.76
OPTION
****  F
ENTER
****  VHTPNO 4
****
OPTION
****  IC
OPTION
****  F
ENTER
****  STR4
   27.90
****  STR4 300.
****
OPTION
****  X
MAY        21   1974
TIME   14   2  7.18
RUN    1 HAS STARTED
OUTPUT BELOW
 AXAV=    0.0    DECL TIME=    0.000 AVCUR=    0.981 BTDMAX=    0.210 BTMAX=    0.126 DELBT=    0.126
AYMAX=    0.945 PHIMAX=    4.101 RMAX=    0.708 LANE CHNG DEL=    0.0    DELPSI=    0.0    MAX STEER= 300.000
TIRQMAX=    0.0    RTRQMAX=    0.0

OPTION
****  F
ENTER
****  VHTPNO
   4.000
****
OPTION
****  MULTI
NUM OF LOOPS/VARS
****  4 1
VAR
****  STR4
LOOP/VAL/INC
****  1 27.9 27.9
****
OPTION
****  XM
MAY        21   1974
TIME   14   4 16.24
RUN    2 HAS STARTED
OUTPUT BELOW
MULTI TOTAL STR4..(    1) BETAMX(    1) BETDMX(    1) CUVRAT(    1) AYMAX.(    1) RMAX..(    1)
  1     2       27.9        0.315E-02     0.208E-01     0.928E-01     0.134         0.694E-01
  2     3       55.8        0.105E-01     0.341E-01     0.260         0.342         0.186
  3     4       83.7        0.219E 01     0.646E-01     0.428         0.539         0.304
  4     5       112.        0.375E-01     0.909E-01     0.573         0.691         0.409
OPTION
```

Fig. 3 HVHP USER'S INTERACTIVE CONTROL

(3) digital printout of variables versus time (up to fifty variables)

(4) comparison variable graphs.

The appropriate VHTP comparison variable values are printed following the execution of a VHTP maneuver. Typical examples are presented in Figure 3.

Sixteen channels of strip chart time history recordings are available. Time histories for the braking in a turn test procedure are presented in Figures 4(a) and 4(b). The variables are defined below:

Figure 4(a) -

(1) longitudinal deceleration in gees (A_x),

(2) lateral acceleration in gees (A_y),

(3) vehicle yaw rate in radians per second (r),

(4) steering wheel input in radians (δ_{sw}),

(5) vehicle forward velocity in feet per second (u),

(6) vehicle side velocity in feet per second (v),

(7) vehicle sideslip angle in radians (β), and

(8) turning radius of curvature in feet^{-1}, (1/R).

Figure 4(b) -

(1-4) the angular velocities of the right front, left front, right rear, and left rear wheels in revolutions per second (ω_1, ω_2, ω_3, ω_4, respectively);

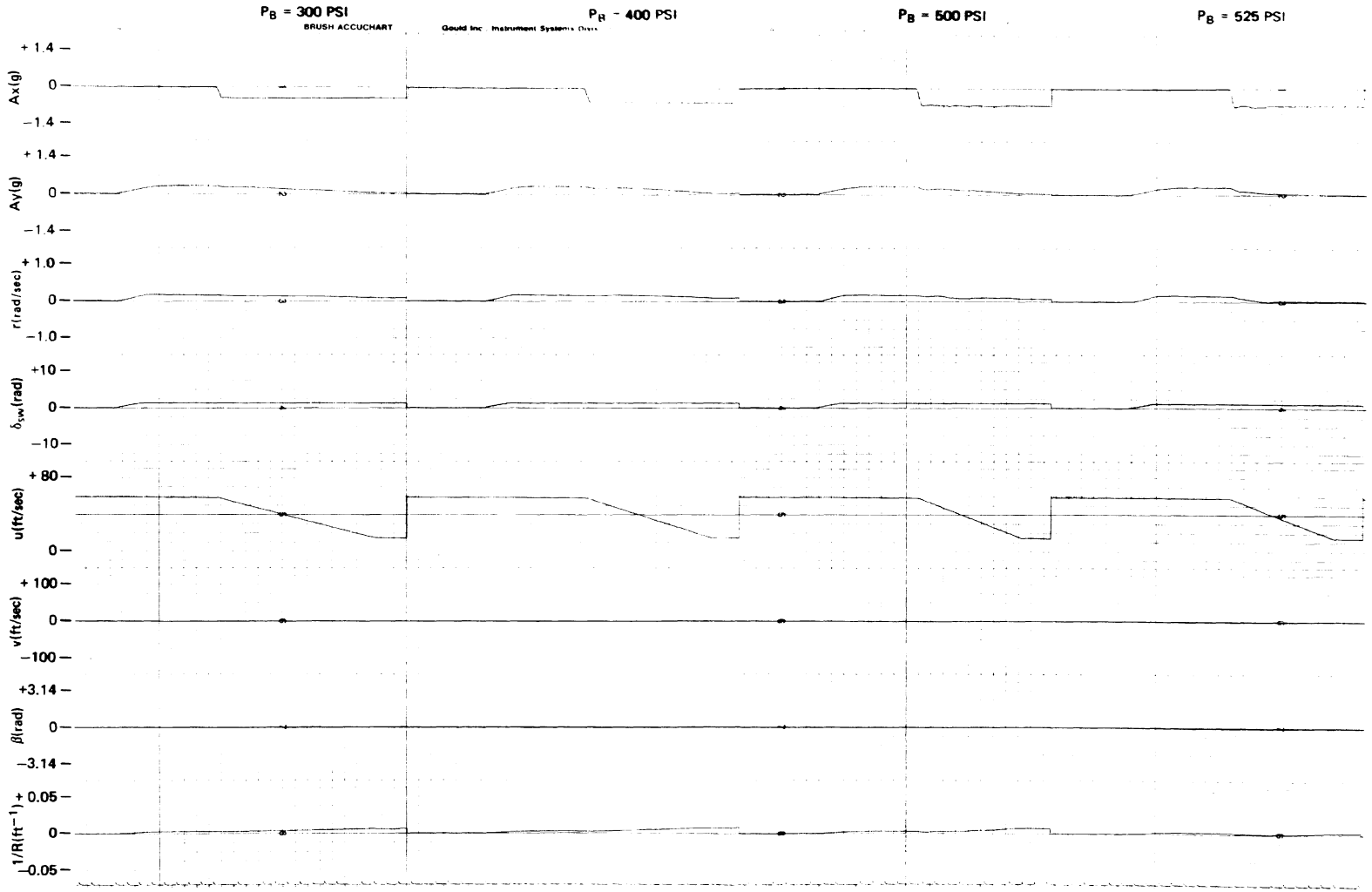

Fig. 4-a TIME HISTORIES - BRAKING IN A TURN

Fig. 4-b TIME HISTORIES - BRAKING IN A TURN

(5-7) the deflection from the equilibrium position of the right front wheel, left front wheel, and rear axle in inches (δ_1, δ_2, δ_3, respectively);

(8) the angular rotation of the rear axle with reference to the sprung mass in radians (ϕ_r).

The digital printout of variables versus time is the typical output associated with digital simulation. The variables to be output can be specified in the program data deck or selected interactively during program execution. The time interval for output is also interactively selected. The interactive selection capability is particularly useful for simulation validation or studying unexpected dynamic phenomena. Any variable within the simulation can be selected for output. An output example is presented in Figure 5.

To aid in quick analysis of vehicle performance, computer generated comparison variable plots are made available. An example plot for a trapezoidal steer test procedure is presented in Figure 6.

CONCLUSION

The Hybrid Computer Vehicle Handling Program (HVHP) has demonstrated realistic dynamic simulations of vehicles with various suspension configurations. The performance of simulation runs, especially those involving the six vehicle handling test procedures (VHTP), is inexpensively and easily performed. In addition, the performance measuring vehicle Comparison Variables (CV) for each VHTP are also provided.

```
OPTION
****  TRACK
UNIT,MODE
****  T A
ENTER TIME ON,OFF,STEP
****  .5 1.1 .1
TYPE RETAIN OR ENTER NEW ARRAY
****  PSIDT PHIDT PHI ZIMX(1) ZIMX(3)
****
```

TIME	PSIDT.(1)	PHIDT.(1)	PHI...(1)	ZIMX..(1)	ZIMX..(3)
0.50	0.43077	0.77597E-02	-0.11728	0.29986E-01	0.10125
0.60	0.35703	0.29683	-0.10414	0.29986E-01	0.10125
0.70	0.28586	0.49151	-0.59047E-01	0.29986E-01	0.10125
0.80	0.28740	0.32454	-0.16426E-01	0.29986E-01	0.10125
0.90	0.30123	0.14344E-02	-0.12279E-03	0.29986E-01	0.10125
1.00	0.28316	-0.14820	-0.90558E-02	0.29986E-01	0.10125
1.10	0.29048	-0.38197	-0.30314E-01	0.29986E-01	0.10125

OPTION

Fig. 5 DIGITAL LINE PRINTER OUTPUT

*** LATERAL ACCECERATION VS. NORM. STEER ANGLE ***

(CALSPAN, O.E. TIRES, TRAPEZOIDAL STEER)

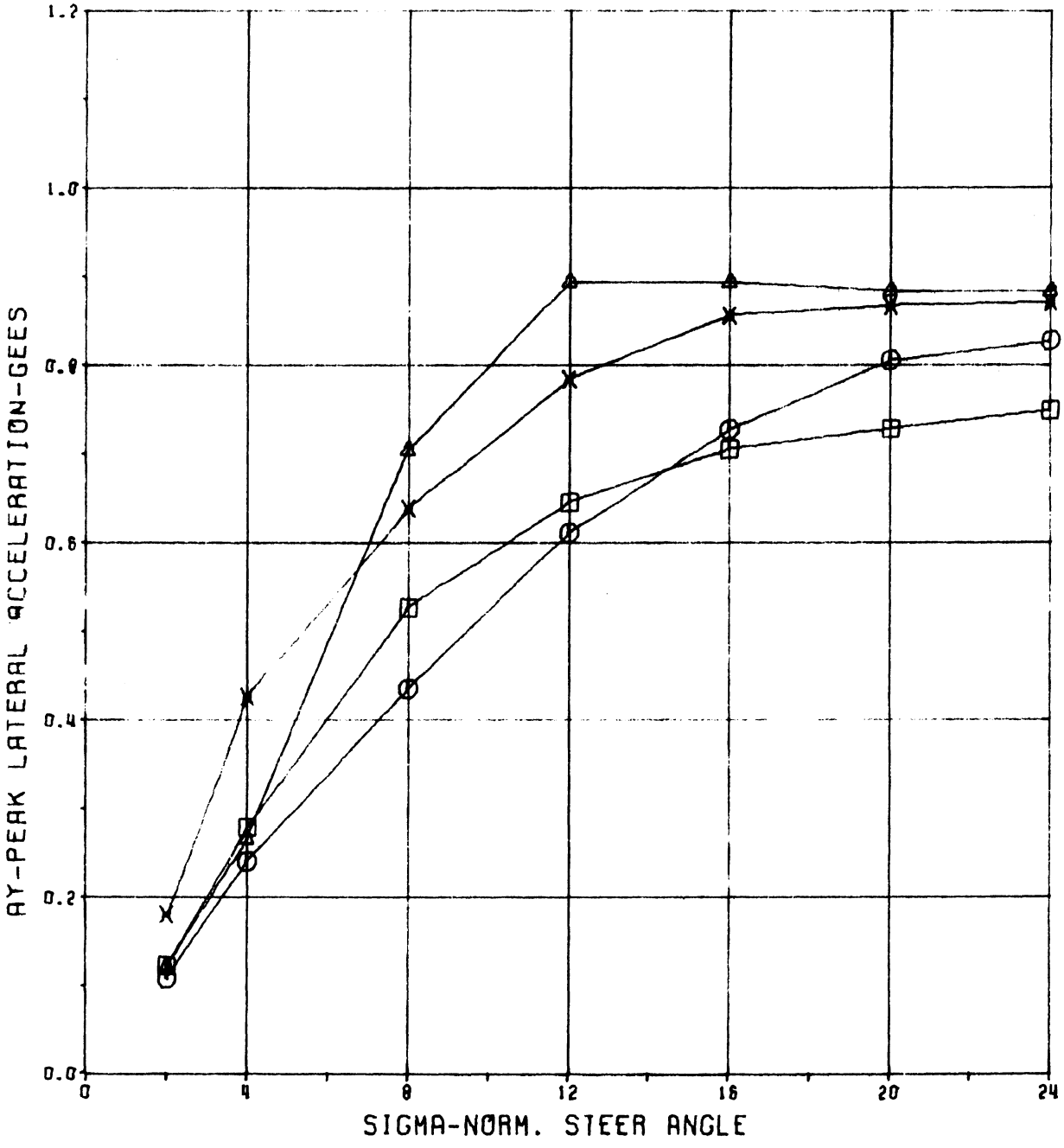

o - DODGE CORONET

□ - CHEVY BROOKWOOD

△ - PONTIAC TRANS AM

× - VW SUPERBEETLE

Fig. 6 COMPARISON VARIABLE PLOT

16 JUL 74

REFERENCES

1. Vehicle Handling, Final Report, Vol. II - Technical Report, Contract DOT-HS-800-282, Bendix Research Laboratories, Southfield, Michigan, April, 1970.

2. Computer Simulation of Vehicle Handling, DOT NHTSA Control FH-11-7563, Bendix Research Laboratories, Southfield, Michigan, September 1972.

3. Bohn, P.F., Keenan, R.J., and Prowznik, J., Operational Hybrid Computer Simulation for Vehicle Handling Studies, Contract DOT-HS-800-764, Applied Physics Laboratory, The Johns Hopkins University, September 1972.

4. Development of Handling Test Procedures for Light Trucks, Vans, and Recreational Vehicles, Final Report, Contract DOT-HS-4-00853, Dynamic Science.

5. Research on the Influence of Tire Properties on Vehicle Handling, Final Report, Contract DOT-HS-053-3-727, Calspan Corporation.

6. Ervin, R.D., Grote, P., Fancher, P.S., MacAdam, C.C., and Segel, L., Vehicle Handling Performance, Contract DOT-HS-800-758, Highway Safety Research Institute, University of Michigan, November, 1972.

7. Fancher, P.S., Ervin, R.D., Grote, P., MacAdam, C.C., and Segel, L., Limit Handling Performance as Influenced by Degradation of Steering and Suspension, Highway Safety Research Institute, University of Michigan, November, 1972.

8. Bohn, P.F., "Modeling and Simulation in Vehicle Handling," DOT HS-82-306, Vehicle Safety Research Integration Symposium, May 30, 1973.

9. Bohn, P.F. and Keenan, R.J., Hybrid Computer Vehicle Handling Program, DOT HS-801-290, Applied Physics Laboratory, The Johns Hopkins University, July, 1974.

10. Colby, K.W. and Bohn, P.F., "Generalized Man/Machine Communication Subroutines for Hybrid Simulation," Proceedings of the Summer Computer Simulation Conference, July, 1974.

TIRE FRICTION MODELS AND THEIR EFFECT ON SIMULATED VEHICLE DYNAMICS

P. K. Nguyen
and
E. R. Case

ABSTRACT

In this paper, various tire friction models are examined and their similarities and differences are pointed out. Emphasis is placed on the tire side force and a numerical comparison is illustrated based on existing experimental data. Different uses of the friction ellipse are discussed. The sensitivity of vehicle response to different tire models is studied using a nonlinear, simplified vehicle model. Three basic maneuvers are simulated: cornering, straight ahead braking and braking in a turn. The simulation results are compared with one particular set of simulations in which the tire forces are specified by tables of experimental tire data. Accuracies and computing times for each tire model are studied.

NOTATIONS

a_i	constants to be determined, i=1,2,...
d_x, d_y	components of the radius vector from vehicle c.g. to the wheel center (ft)
k	"fore and aft" tire spring constant (lbs/ft)
ℓ	half length of tire/ground contact patch (ft)
n	constant defined in Equation (6)
r	tire free radius (ft)
t	time (sec)
t_d	delay time used in modelling brakes (sec)
u, v	forward and lateral velocities (fps)
x, y	coordinates of vehicle c.g. (ft)
C_α	lateral tire stiffness (lbs/rad)
C_s	longitudinal tire stiffness (lbs)
F	resultant friction force (lbs)
F_x	longitudinal force (lbs)
F_y	lateral force (lbs)
G	a function defined in Equation (25)
I	yaw moment of inertia of vehicle (slug-ft^2)
J	wheel polar moment of inertia (slug-ft^2)
M	vehicle mass (slugs)
N	normal load on tire (lbs)
R	tire tread resilience, see Equation (7)
P	constant defined in Equation (7)
S	longitudinal slip ratio

T	braking torque (ft-lbs)
V	vehicle speed (fps)
α	slip angle (rad)
δ	steering angle (rad)
ε	friction reduction parameter
μ	tire/road friction coefficient
ξ	tire coordinate (ft)
τ	rise time used in modelling brakes (sec)
ψ	yaw angle (rad)
Ω	wheel speed (rad/sec)

INTRODUCTION

Since the air-inflated tire was first used by Sir Robert Thompson in England around 1845 [1], extensive research has been conducted on tire friction, particularly in recent years. An excellent collection of tire friction theories has been presented by Kummer [2], and other, more recent research results, are given in Reference [3]. Present literature on the subject is so extensive that a full description of tire friction would require an entire book. Therefore, for the purposes of this paper, it is sufficient to say that tire friction involves much more than the friction of rubber material against a surface; it also depends upon tire construction, tire loading, vehicle velocity, pavement structure, and other environmental factors.

Tire friction has been studied both experimentally and theoretically. Experiments have been conducted [4-12] to determine tire friction in terms of the above factors. Unfortunately, depending on methods of curve fitting and observation, different "empirical" formulas are often presented for the same physical phenomenon. In contrast to the abundance of experimental investigations, there is a scarcity of analytical studies of tire friction [13, 14]. The complexity of tire friction has forced the analyst to idealize the tire elasticity, to assume a pressure distribution over the contact patch and to lump tire/road interface friction, tread pattern and weather conditions into one coefficient usually referred to as the "tire/road friction coefficient, μ." The outcome of such a study will be referred to in this paper as "analytical" formulas.

Tire friction forces (and moments) play a very important role in vehicle dynamics as they determine the stability and control of the vehicle. Some factors that influence the vehicle response are: suspension system characteristics, brake system response, inertia distribution, aerodynamic forces, etc. To make the problem more complicated, a tire behaves differently in transient and steady-state responses [4]. In most practical cases, the side slip angle varies slowly (except in violent maneuvers) so that the tire transient response can be justifiably neglected in vehicle simulations. As a consequence, the discussion in this paper is limited to the role of steady-state tire frictional forces in vehicle dynamics. The question now arises: which empirical or analytical tire friction formulas should be used in vehicle simulations to obtain a reasonable result? The purpose of this study was to find an answer to this question.

A number of analytical and empirical formulas are examined and compared. For this purpose, these formulas are first rewritten in a unified notation and are applied to the same operating condition, i.e., same tire loading, vehicle speed, etc. The discussion is confined to tire frictional forces on dry or wet pavements, with emphasis on lateral force properties. Tire traction on snow covered pavements, tire aligning torque, etc., are therefore beyond the scope of this paper. To find the sensitivity of vehicle motions to the friction formulas, a simplified, nonlinear vehicle model is used to compare the vehicle motions as predicted by different friction formulas.

TIRE FRICTION MODELS

The tire friction, F, is considered as a function of five of the most important variables:

$$F = F(\mu, \alpha, S, N, V) \qquad (1)$$

where

μ = tire/road friction coefficient

α = slip angle

S = slip (ratio)

N = normal load on tire

V = tire translational speed

Tire camber angle is considered to be zero in this discussion. Figure 1 illustrates the longitudinal component, F_x, and the lateral component, F_y, of the frictional force, F. Figure 2 shows typical experimentally-determined variations of F_x and F_y with S, α, V and pavement conditions. Figure 3 depicts the distribution of F_x and F_y when both of them exist simultaneously.

LATERAL FORCE FORMULAS FOR ZERO SLIP CONDITIONS

Under normal operating conditions (i.e., excluding spin-out and drift-out), the slip angle is usually within the range of 20°, as shown in Figure 2. The "simple" behaviour of the F_y vs. α curve, as compared with the F_x vs. S curve, has attracted more attention and as a result a number of empirical lateral force formulas have been proposed. For the zero-slip case, most investigators assume a cubic polynomial relationship between F_y and α under a given load, vehicle speed

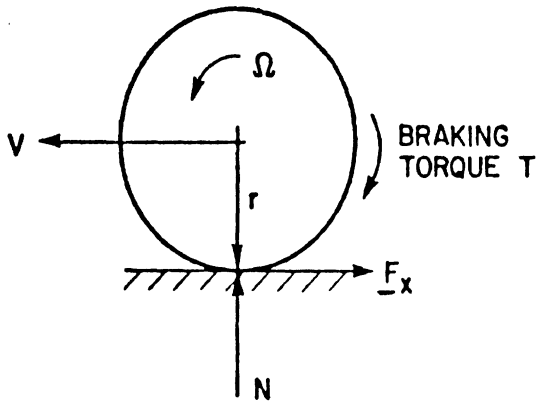

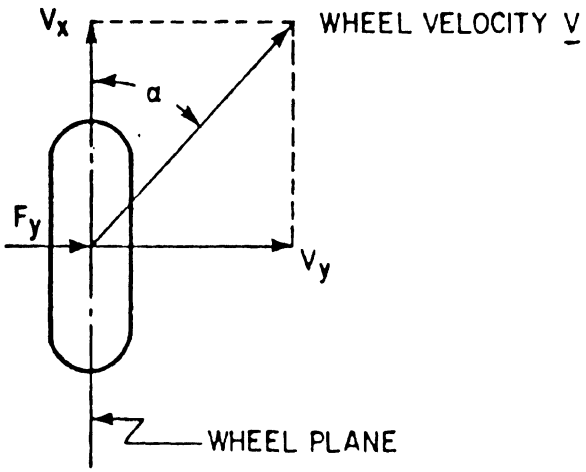

$$S = \text{SLIP} = 1 - \frac{r\Omega}{V}$$

$$\alpha = \text{SIDE SLIP} = \tan^{-1}\frac{V_y}{V_x}$$

Figure 1, Longitudinal and Lateral Frictional Forces

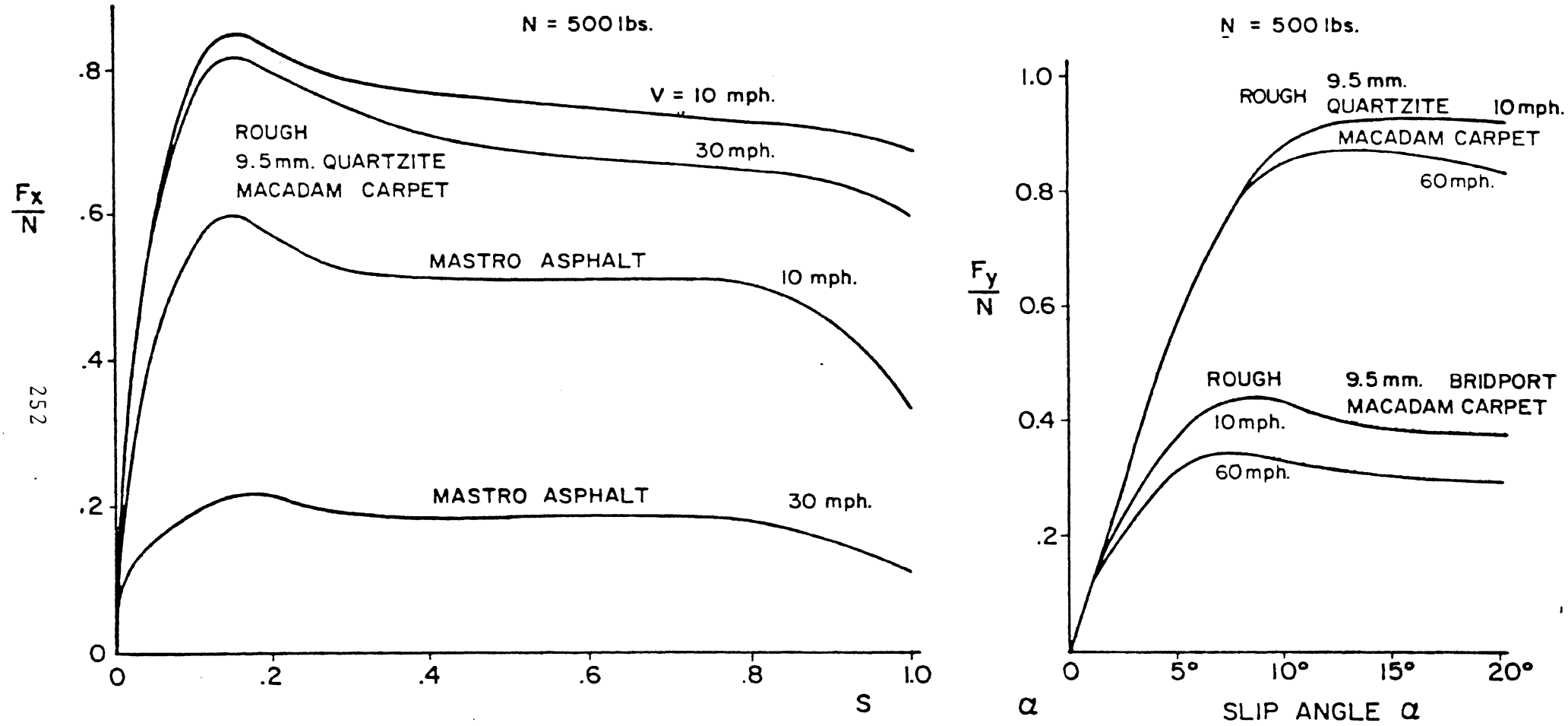

Figure 2, Typical Variations of Longitudinal and Lateral Forces

(After Beauregard and McNall [4] and Holmes and Stone [5]

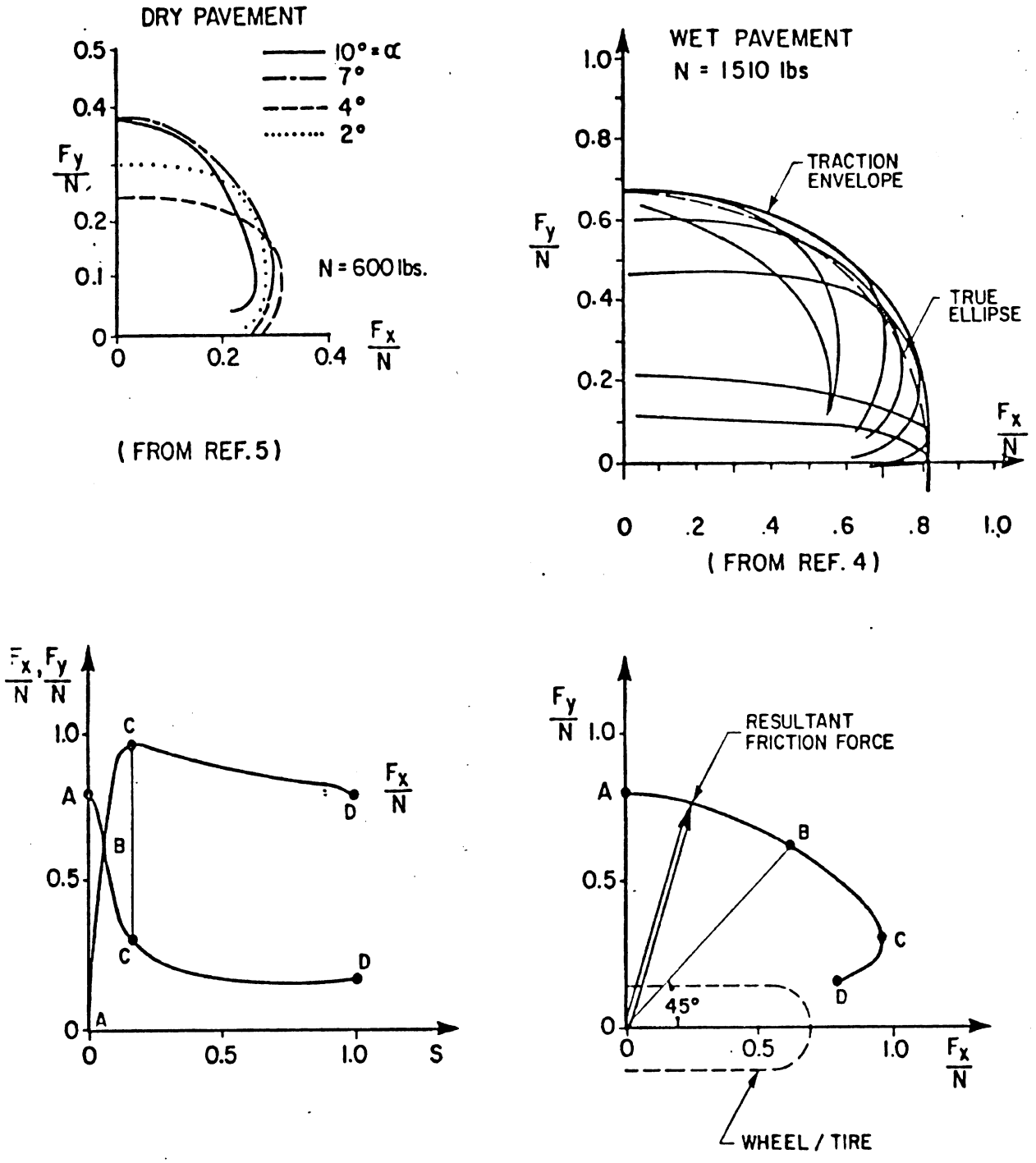

Figure 3, Combined Longitudinal and Lateral Friction

and road surface conditions [5-11]. Nicolas and Comstock [12] viewed the same curve as an exponential function. Some typical empirical formulas are now presented. They appear in a unified notation and in chronological order.

In 1958, from an extensive study of pneumatic aircraft tires, Smiley and Horne [6] established the following relationship

$$F_{ySmiley} = \begin{cases} C_\alpha \alpha \left(1 - \dfrac{\alpha^2}{3\alpha_m^2}\right) & \alpha \leq \alpha_m \\ \dfrac{2}{3} C_\alpha \alpha_m & \alpha > \alpha_m \end{cases} \qquad (2)$$

where

C_α = lateral stiffness (or cornering power)
= $\partial F_y / \partial \alpha$ evaluated at $\alpha = 0$

α_m = value of α at which F_y is maximum
= $1.5\ \mu\ N/C_\alpha$

The subscripted name indicates the investigator associated with the formula. Figure 4 shows the variation of $F_{ySmiley}$ with α.

In 1960, Radt and Milliken [7] employed the following formula in their simulation of skidding automobiles:

$$F_{yRadt} = \begin{cases} C_\alpha \alpha \left(1 - \dfrac{\alpha}{\alpha_m} + \dfrac{\alpha^2}{3\alpha_m^2}\right) & \alpha \leq \alpha_m \\ C_\alpha\ \alpha_m/3 & \alpha > \alpha_m \end{cases} \qquad (3)$$

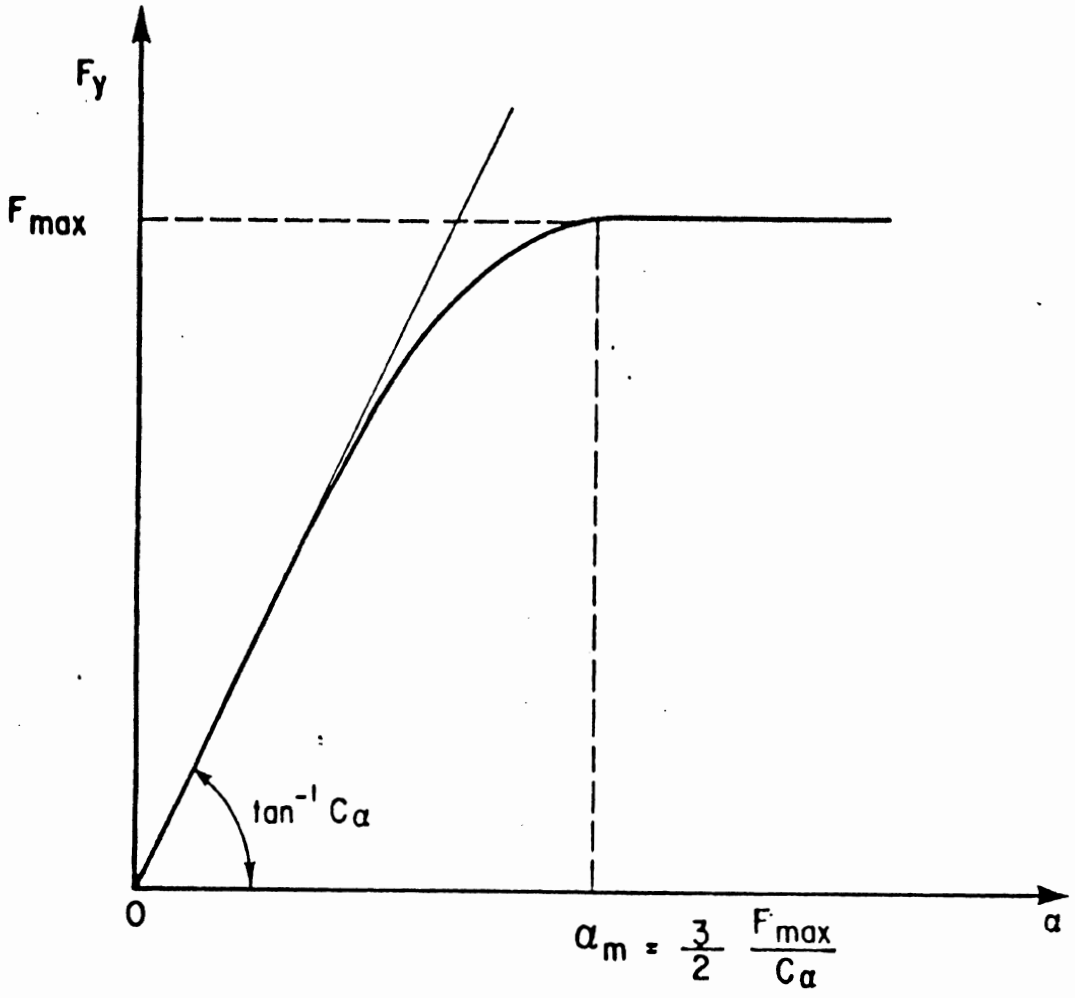

Figure 4, Variation of $F_{y\ Smiley}$ ($\equiv F_{y\ Ellis}$) with α

It is observed that both $F_{ySmiley}$ and F_{yRadt} are odd functions of α. A comparison with $F_{ySmiley}$ for the same values of C_α and F_{max} in Figure 5 shows a similarity between the two curves although they attain their maxima at different slip angles. Equation (3) has been used by other researchers, for example, McHenry [15] and Piziali [16] who both also used the following curve fitting:

$$C_\alpha = a_0 + a_1 N - a_1 N^2/a_2$$

$$\frac{C_\alpha \alpha_m}{3N} = a_3 + a_4 N + a_5 N^2 \qquad (4)$$

where $a_0,\ldots,a_5$ are constants to be determined by curve fitting.

In 1964, when discussing the problem of tractor and semi-trailer handling with F. Jindra, Ellis [8] proposed a formula of the form:

$$F_y = c_1\alpha + c_2\alpha^3$$

where c_1 and c_2 are two constants chosen to satisfy the following conditions:

$$\frac{dF_y}{d\alpha} = 0 \qquad \text{at} \qquad \alpha = \alpha_m$$

$$F_y = \sqrt{\mu^2 N^2 - F_x^2} \qquad \alpha \geq \alpha_m$$

The result is what is now known as the Ellis formula:

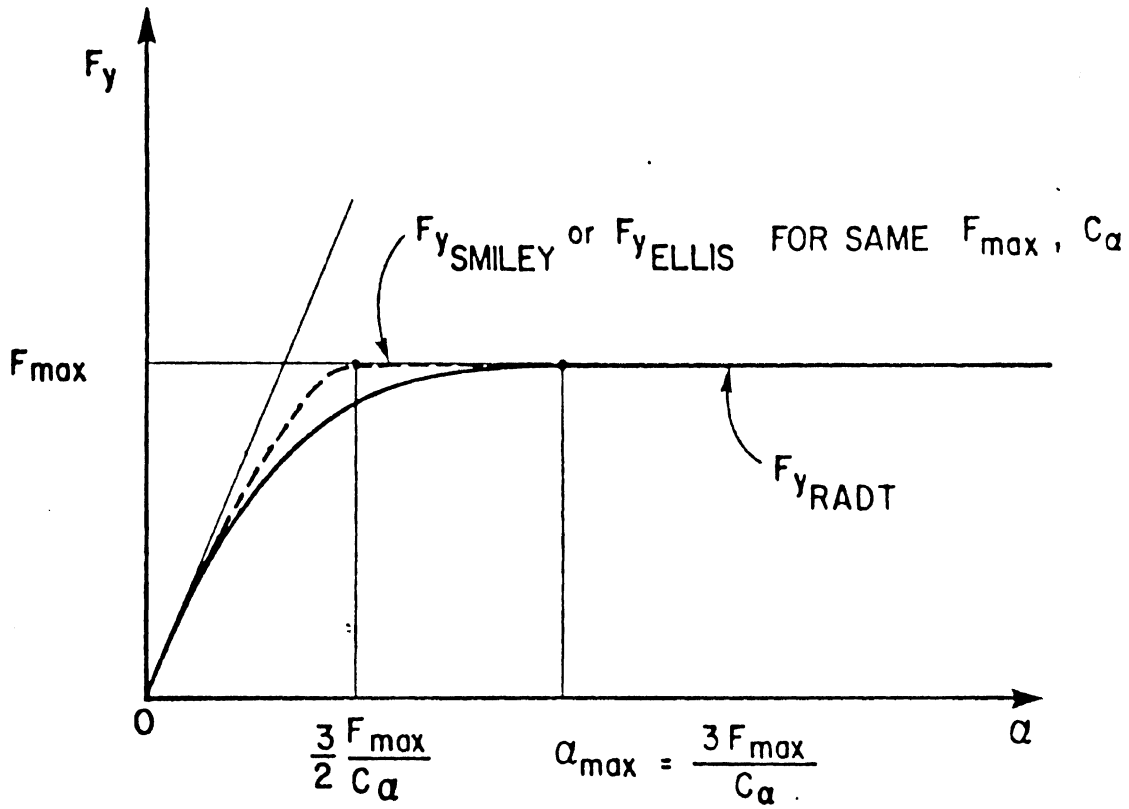

Figure 5, Variation of $F_{y\ Radt}$ with α

$$F_{yEllis} = \begin{cases} 1.5\ \mu_y N \dfrac{\alpha}{\alpha_m}\left(1 - \dfrac{\alpha^2}{3\alpha_m^2}\right) & \alpha \leq \alpha_m \\ \mu_y N & \alpha > \alpha_m \end{cases} \qquad (5)$$

where

$$\mu_y = \sqrt{\mu^2 - F_x^2/N^2}$$

Equation (5) is exactly the same as $F_{ySmiley}$ given by (2). The advancement here is the use of the friction circle concept to determine μ_y.

In 1967, Chiesa and Rinonapoli [9] used a nonlinear vehicle model simulation. They proposed a curve fitting scheme in which F_y is given by

$$F_{yChiesa} = \left(1 - \left[\frac{F_x}{2\mu N}\right]^n\right)^{1/2} N[(a_1 + a_2 N)\alpha + (a_3 + a_4 N)\alpha^2 + (a_5 + a_6 N)\alpha^3 + (a_7 + a_8 N)\alpha^4 + \ldots] \qquad (6)$$

where n, a_1, a_2... = constants to be determined for the tire in consideration. It is interesting to note that in Equation (6):

(i) $F_{yChiesa}$ is not an odd function of α

(ii) the tire lateral stiffness varies with N^2

(iii) the friction envelope is a parabola if n=1 and an ellipse if n=2

(iv) the polynomial can be truncated at the α^3 or α^4 terms depending on the case investigated [9]

(v) at least six data points are required to determine the constants a_1, a_2,...

In 1969, through extensive testing of different tires on various surfaces at varying speeds, Holmes and Stone [5] attempted to establish a formula for each pavement condition:

$$F_{yHolmes} = (a_0 + a_1V + a_2V^2 + a_3\alpha + a_4\alpha^2 + a_5\alpha^3 + a_6R + a_7P) \quad (7)$$

where $a_0,\ldots,a_7$ = constants to be determined experimentally

R = tire tread resilience

$$P = \begin{cases} 0 & \text{smooth tire} \\ 1 & \text{patterned tire} \end{cases}$$

Unfortunately, the variance from their statistical analysis is rather large and they admitted that it "discourages the use of the equation as a direct substitute for experimental results." Perhaps, the peculiarity of Equation (7) is the linear combination of functions of V, α,... This point contrasts with what other researchers believe, namely, that F_y is a product of functions of V, α,...

In 1973*, Okada et al. [10] discussed vehicle handling and stability in terms of their simulation of a nonlinear mathematical model in which the following formula was used:

$$F_{yOkada} = \left[1 - a_0 \frac{F_x}{N}\right] N[(a_1 + a_2N + a_3N^2 + a_4N^3)\alpha + (a_5 + a_6N + a_yN^2)\alpha|\alpha| + (a_8 + a_9N)\alpha^3 + a_{10}\alpha^3|\alpha|] \quad (8)$$

where $a_0,\ldots,a_{10}$ = constants to be determined by the least squares method. It is evident that (8) is similar to $F_{yChiesa}$ in (6) except for the following differences:

(i) F_{yOkada} is an odd function of α.

(ii) F_{yOkada} varies with $\alpha^m N^n$, $m+n \leq 5$.

(iii) a linear relationship exists between F_x and F_y.

As was the case with Chiesa's paper, no discussion on typical values of $a_0,\ldots$ was given by Okada et al. [10].

---

*At the time this paper was edited, the following formula by T. Nakatsuka and K. Takanami was discovered:

$$F_{yNakatsuka} = \begin{cases} C_\alpha \alpha\left(1 - 1.10648 \frac{\alpha}{\alpha_{1im}} \text{ sign } \alpha - 0.26221 \frac{\alpha^2}{\alpha_{1im}^2}\right) & \alpha \leq \alpha_{1im} \\ 1.006\mu N \text{ sign } \alpha & \alpha > \alpha_{1im} \end{cases}$$

where $\alpha_{1im} = 1.594\mu N/C_\alpha$ (cf. α_m in Equation (2))

$$\mu = a_0 + a_1N + a_2N^2$$

$$C_\alpha = a_3 + a_4N + a_5N^2 + a_6N^3$$

This expression is contained in their paper, "Cornering Ability Analysis Based on Vehicle Dynamics System," SAE Paper No. 700368, 1970 International Automobile Safety Conference Compendium.

In 1973, Eshleman et al. [11] developed a simulation program for articulated vehicles in which, among other tire models, they used the empirical formula (for tractor (trailer) tires):

$$F_{yEshleman} = \begin{cases} C_\alpha \alpha \left(1 - \frac{10}{11} \left|\frac{\alpha}{\alpha_m}\right| + \frac{3}{11} \frac{\alpha^2}{\alpha_m^2}\right) & \alpha < \alpha_m \\ \\ \frac{4}{11} C_\alpha \alpha_m (0.786 - \alpha)/(0.786 - \alpha_m) & \alpha \geq \alpha_m \end{cases} \tag{9}$$

where $C_\alpha = \frac{11}{4} \mu_{Eshleman} N/\alpha_m$

$$\mu_{Eshleman} = \begin{cases} 1 - \frac{.35N}{6800} \mu & N \leq 6800 \text{ lbs.} \\ \\ .65 \mu & N > 6800 \text{ lbs.} \end{cases}$$

$$\alpha_m = 9(1 + N/6800)/57.27 \qquad N \text{ in lbs.}$$

Figure 6 depicts the variation of $F_{yEshleman}$ with α where a discontinuity in slope at α_m can be readily observed. A scrutiny of (3) and (9) reveals that for the same C_α and α_m, $F_{yEshleman}$ is always greater than F_{yRadt} for $0 < \alpha \leq \alpha_m$. Note that $C_{\alpha Eshleman}$ can be rewritten as

$$C_{\alpha Eshleman} = \frac{11}{4} \mu \frac{N}{\alpha_m} \left(1 - \frac{35N}{6800}\right) \tag{10}$$

which is similar to the expressions in (4) used by McHenry and Piziali.

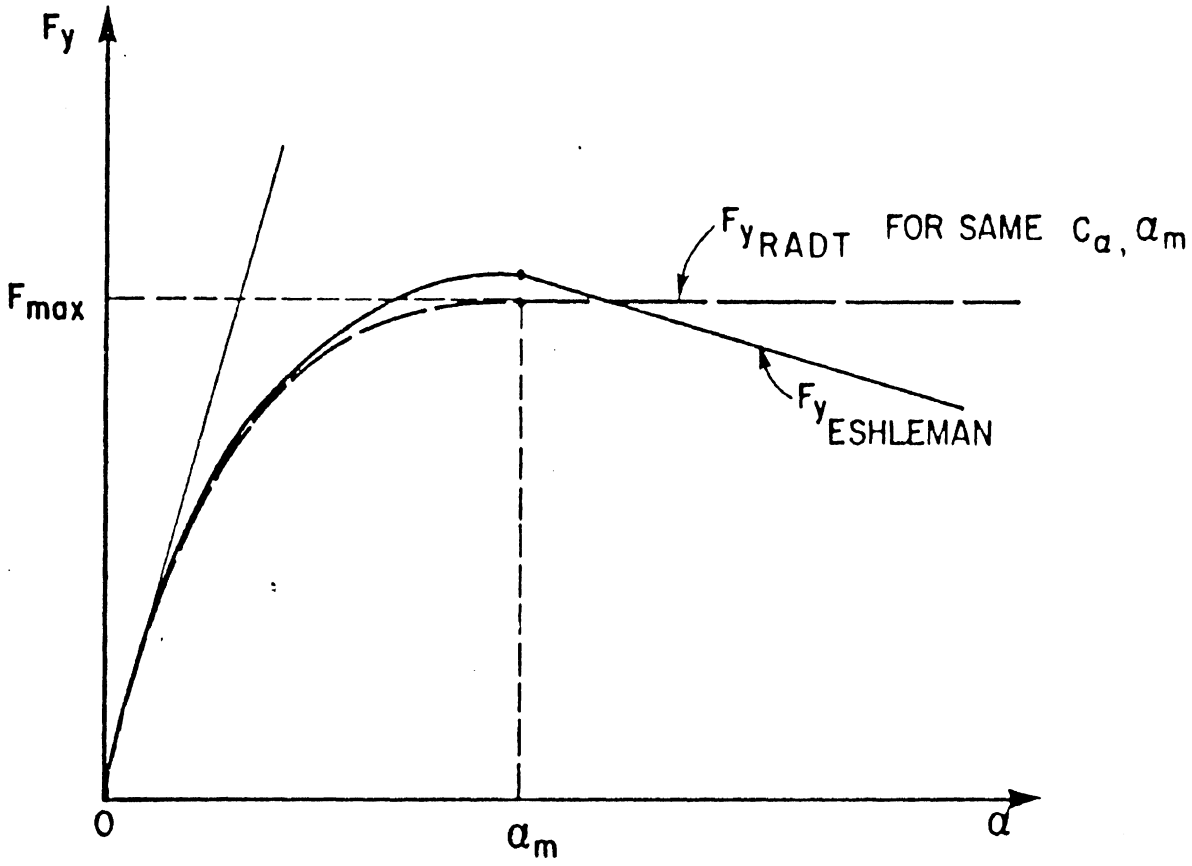

Figure 6, Variation of $F_{y\ Eshleman}$ with α

A distinct side force formula was employed by Nicolas and Comstock [12] in their simulation program of tractor-semi-trailers performing a combination braking and cornering maneuver with anti-skid brake systems. Admitting a "limiting" side force and an infinitely large "limiting" slip angle, their formula, written in the "unified" notation, is

$$F_{yNicolas} = \mu_{1im} N[1 - \exp(-C_\alpha \alpha/\mu_{1im} N)] \qquad (11)$$

where $\mu_{1im} = a_0 \mu_x$

$C_\alpha = a_1 N e^{a_2 N}$

a_0, a_1, a_2, = constants to be determined

It is important to note that $F_{yNicolas}$ is not an odd function of α. If $F_{max} = \mu_{1im} N$, then for the same C_α and F_{max}, $F_{yNicolas}$ is always smaller than F_{yEllis}, F_{yRadt}, and the others, which have their maxima at a finite α_m. To compare (11) with Radt's and Eshleman's formulas, the following parameter is defined

$$\alpha_{1im} = \frac{2\mu_{1im} N}{C_\alpha} \qquad (12)$$

so that (11) can be written:

$$F_{yNicolas} = C_\alpha \alpha \left(1 - \frac{\alpha}{\alpha_{1im}} + \frac{2}{3} \frac{\alpha^2}{\alpha_{1im}^2} - \ldots\right)$$

$$C_{\alpha Nicholas} = a_1 N \left(1 + a_2 N + a_2^2 \frac{N^2}{2} + \ldots\right) \qquad (13)$$

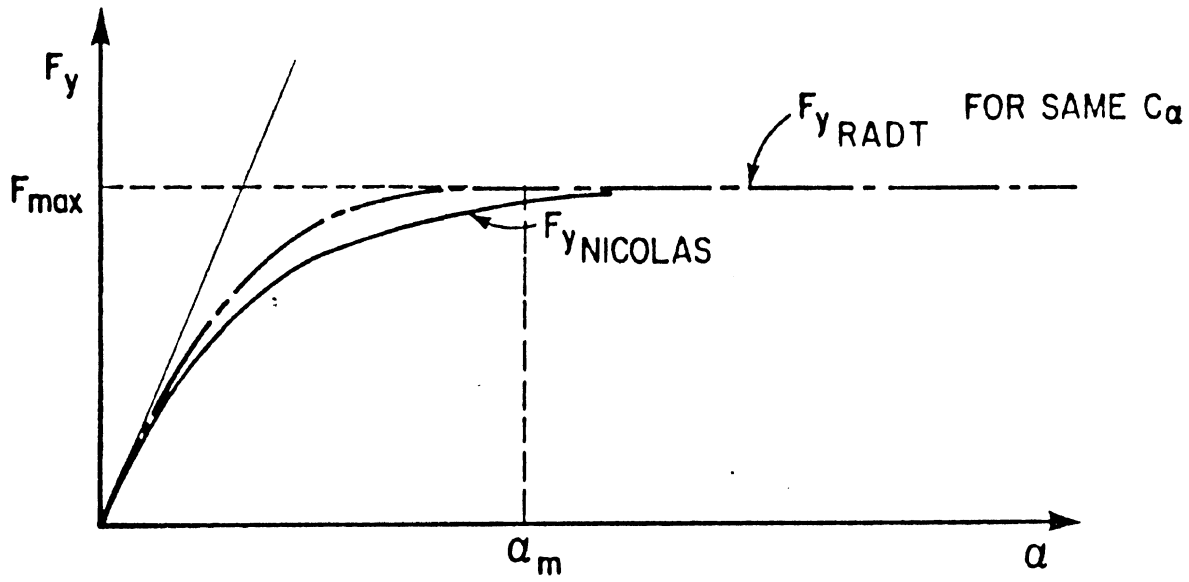

Figure 7, Variation of $F_{y\ Nicolas}$ with α

The similarity between Nicolas and Comstock's formula [12] and Radt and Milliken's and Eshleman et al.'s formulas [7, 11] can be readily recognized from the form of (13).

This section presents the analytical result established by Dugoff et al. [13] who derived the closed form expressions for the lateral and longitudinal forces F_y and F_x, respectively, containing both α and S. Formulas only are quoted here; the derivations may be found in their report [13]. At this point, only the simplified version of Dugoff et al.'s formula in which S has been set to zero will be considered.

$$F_{yDugoff} = \begin{cases} C_\alpha \tan \alpha & \alpha \leq \alpha_0 \\ \mu N \left(1 - \dfrac{\mu N}{4C_\alpha \tan \alpha}\right) & \alpha > \alpha_0 \end{cases} \tag{14}$$

where $\alpha_0 = \tan^{-1}[\mu_0 N/(2C_\alpha + \varepsilon V \mu_0 N)]$

$\mu = \mu_0 (1 - \varepsilon V \tan \alpha)$

μ_0 = "nominal" friction coefficient

ε = tire reduction parameter

It should be noted that, in practice, the angle α_0 is usually small, e.g., $\doteqdot 3°$. It can readily be observed that for small α, $F_{yDugoff} = C_\alpha \tan \alpha \geq C_\alpha \alpha$. However, since α is small, the difference between tan α and α is too small to be noticeable. For $\alpha > \alpha_0$ $F_{yDugoff}$ has its maximum at α_{max} where α_{max} is given by the following quadratic equation:

$$-\varepsilon V(4C_\alpha + \mu_0 N\varepsilon V)(\tan^2 \alpha_{max})^2 + (\mu_0 N - \varepsilon V[4C_\alpha + \mu_0 N\varepsilon V]) \tan^2 \alpha_{max} + \mu_0 N = 0 \quad (15)$$

The variation of $F_{yDugoff}$ with α is depicted in Figure 8.

Observe that all formulas above reduce to the basic form

$$F_y \doteqdot C_\alpha \alpha \quad (16)$$

for small α, i.e., the differences between the formulas really exist only for large values of α. Unfortunately, however, a single relationship cannot be established between C_α, α_{max} and F_{max} where α_{max} is the value of α at which F_y attains its maximum F_{max}. Table 1 illustrates the points discussed above in terms of the numerical values of F_y. In particular, Table 1 shows the input parameters which are used to compute F_y. These input parameters are chosen from the three available values of C_α, α_{max} and F_{max} such that the computed values of F_y are in good agreement with experimental data. The numerical values of F_y obtained from either a quartic or a cubic fit are very sensitive to the data points chosen. However, a good choice of data points leads to fairly good values of F_y. The lateral forces predicted by the Dugoff et al. formula agree well with experimental data.

LONGITUDINAL FORCE FORMULAS

In contrast to the abundance of empirical formulas for the lateral force $F_y(\alpha)$, few empirical

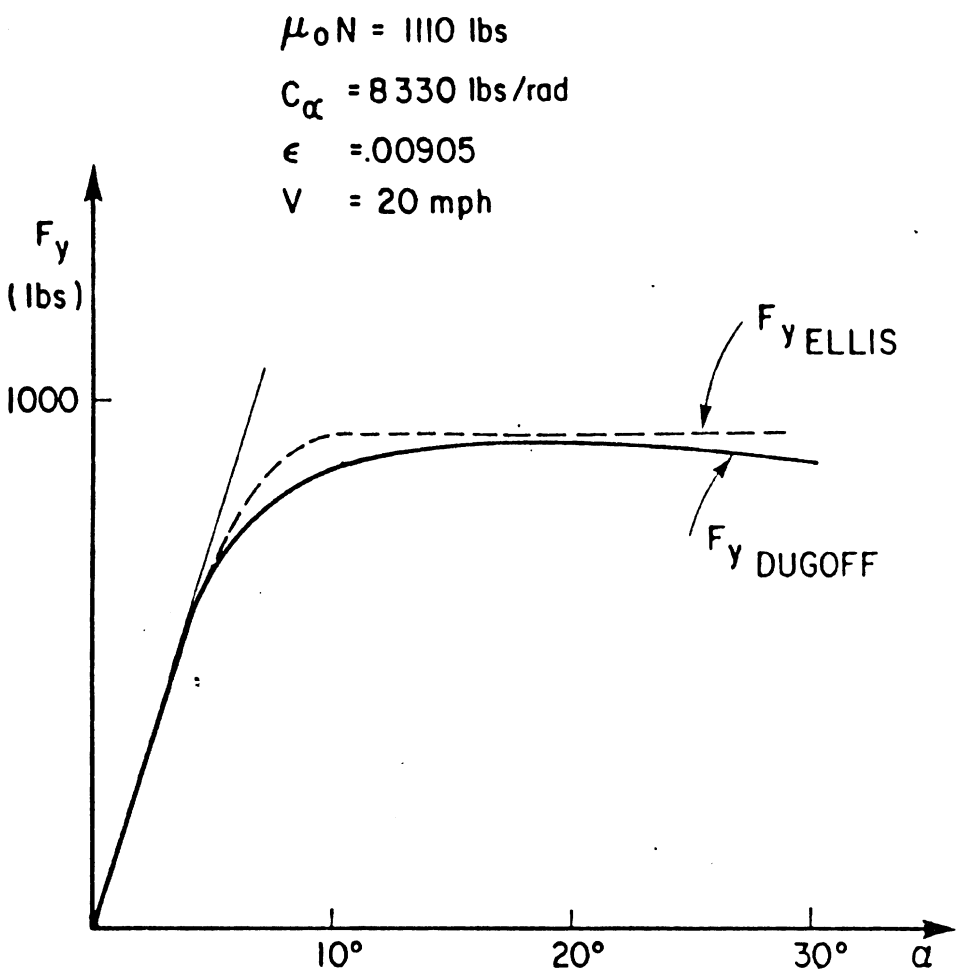

Figure 8, Variation of $F_{y\ Dugoff}$ with α

TABLE 1

Variation of Lateral Force With Slip Angle Under Zero Slip Conditions

($C\alpha$ =8330 lbs./rad, F_{max} = 935 lbs., α_m = 15.3°, N = 800 lbs., Ref. 17)

α	2° (.03491)	4° (.06981)	6° (.10472)	8° (.13963)	10° (.17453)	12° (.20944)	14° (.24435)	16° (.27925)	18° (.31416)	Calculated Lateral Stiffness C_α	Input parameters used to calculate F_y
tan α	0.03492	0.06993	0.10510	0.14054	0.17633	0.21256	0.24933	0.28675	0.32492		
Smiley & Horne (Ellis)	182.	357.	521.	665.	785.	873.	925.	935.	935.	5238.	$\alpha_{m'}$, F_{max}
Radt & Milliken	262.	469.	629.	747.	831.	884.	916	930.	935.	8330.**	$C_{\alpha'}^{**}$, F_{max}
Chiesa & Rinonapoli	279.	518.	700.	819.	880.	902.	913.	955.	1081.	8309.	4 pairs of (α, F_y) at α =2°, 8°, 12°, α_m
Holmes & Stone	279.	507.	687.	819.	907.	951.	955.	919.	846.	8739.	3 pairs of (α, F_y) at α =2°, 8°, α_{max}
Okada* et al	279.	518.	700.	819.	880.	902.	913.	955.	1081.	8309.	Same as in Chiesa & Rinonapoli
Eshleman et al	424.	697.	851.	919.	935.	921.	865.	809.	754.	14646.	$C_\alpha = \frac{4}{11} F_{max}/\alpha_m$ N
Nicolas & Comstock	250.	433.	567.	665.	738.	790.	829.	857.	878.	8330.**	$C_{\alpha'}^{**}$, F_{max}
Equation (42)	263.	475.	641.	764.	850.	904.	930.	–	–	8330.**	$C_{\alpha'}$, $\alpha_{m'}$, F_{max}
Dugoff et al	291.	580.	747.	825.	868.	892.	907.	915.	919.	8330.**	$\in$ = .00905, C_α* $\mu_0 n$ =1110 lbs.*** V = 20 mph.

* Same as in Chiesa & Rinonapoli

** Measured from Figure 18 in Reference [17]

*** Measured from Figure 3 in Reference [17]

formulas have been developed for the longitudinal force $F_x(S)$. Also, the variation of F_x with S is normally specified at discrete points rather than continuously as was the case for both the empirical and analytical expressions for the F_y vs. α curve. Linear interpolation is used to determine F_x for points in between.

A simple scheme was used by Nicolas and Comstock [12] where the function $F_x(S)$ for a given speed V, load N, and zero slip angle α is specified by only five points, as illustrated in Figure 9. The two empirical formulas by Smiley and Horne [6] and Holmes and Stone [5] are, unfortunately, not generally useful. Smiley and Horne [6] found that for small S

$$F_{xSmiley} \doteqdot rk\ S \tag{17}$$

where

r = tire free radius

k = "fore and aft" tire spring constant

Equation (17) was verified for $S \leq 0.1$ and found good for $S \leq 0.04$, which is quite small under normal braking conditions. As in (17), Holmes and Stone [5] tried the following curve fitting expression:

$$F_{xHolmes} = N(a_0 + a_1 V + a_2 V^2 + a_3 S + a_4 S^2 + a_5 S^3 + a_6 R + a_7 P) \tag{18}$$

where = $a_0, \ldots, a_7$ are constants to be determined

Their statistical analysis shows a large variance which, they believe, is due to the inadequacy of the number

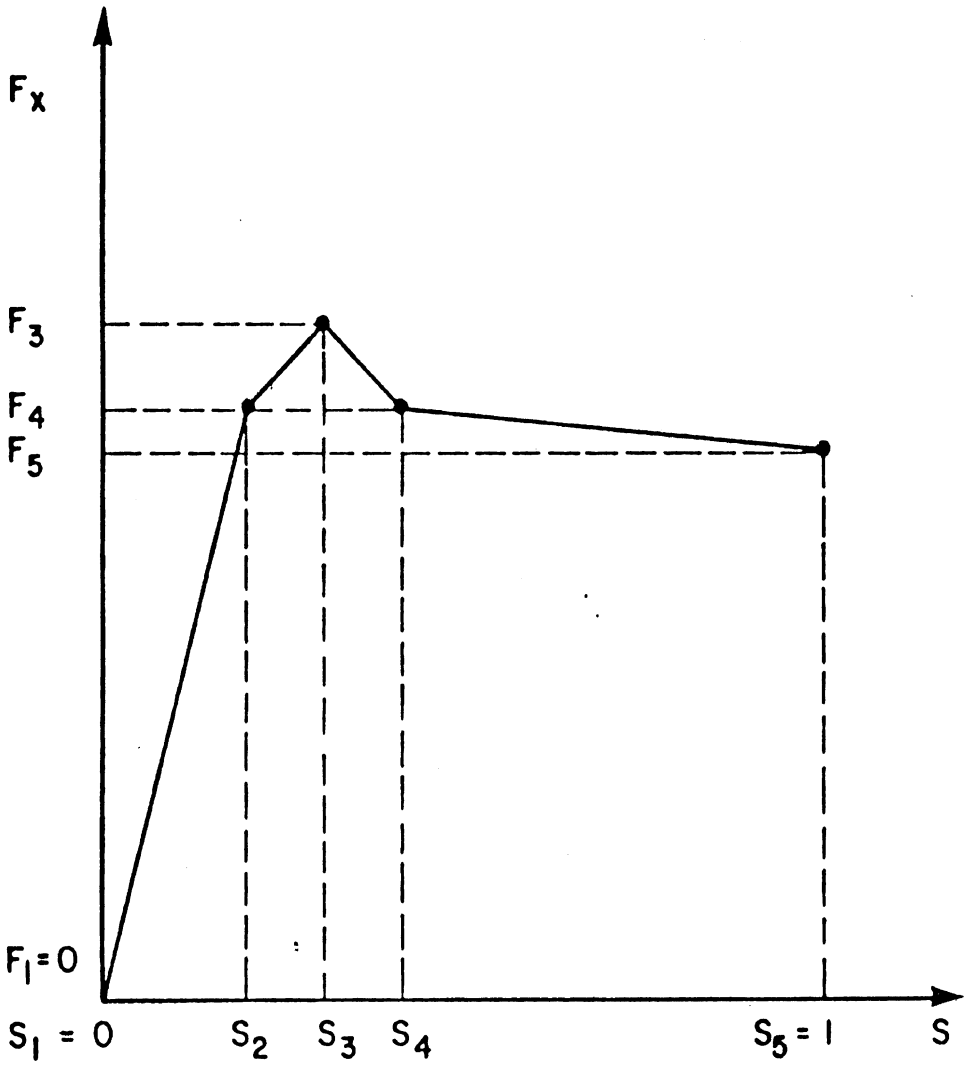

Figure 9, Nicolas and Comstock's Longitudinal Force F_x (O,S)

of terms in S. In other simulations or friction studies, most authors did not mention how they specified the function $F_x(S)$; presumably the function was specified by more than five points for $0 \leq S \leq 1$.

The simplified version of the theoretically derived formula by Dugoff et al. [13] follows. For $\alpha = 0$, their formula is

$$F_{xDugoff} = \begin{cases} \dfrac{C_s S}{1-S} & S \leq S_0 \\ \mu N \left(1 - \dfrac{\mu N(1-S)}{4C_s S}\right) & S > S_0 \end{cases} \tag{19}$$

where

$$S_0 = \frac{2C_s + \mu_0 N(1+\varepsilon) - \sqrt{(2C_s + \mu_0 N(1+\varepsilon))^2 - 4\varepsilon V \mu_0^2 N^2}}{2 \varepsilon V \mu_0 N}$$

$$\mu = \mu_0 N(1 - \varepsilon VS)$$

ε and μ_0 are as defined in (14)

As pointed out to the authors by Ewald Schroeder, Project Research Engineer, Ministry of Transportation and Communications, Dugoff et al., in deriving (14) integrated the tire shear stress over the "tire carcass region" instead of over the "ground contact patch." More precisely, in Dugoff et al.'s notation, the integration was carried out over $0 \leq \xi_s' \leq 2\ell$ instead of $0 \leq \xi_s \leq 2\ell$ where ξ_s' = tire carcass centerline coordinate,

ξ_s = ground contact patch coordinate, 2ℓ = length of contact patch. (Dugoff et al. did not discuss why the integration was carried out over this interval instead of the interval $0 \leq \xi_s \leq 2\ell$.) The two above coordinates are related to each other by

$$\xi_s' = (1 - S)\ \xi_s \tag{20}$$

By integrating Dugoff et al.'s stress over ξ_s from 0 to 2ℓ it is found that

$$F_{xDugoff,modified} = \begin{cases} C_s S & S \leq S_1 \\ \\ \mu N \left(1 - \dfrac{\mu N}{4 C_s S}\right) & S > S_1 \end{cases} \tag{21}$$

where $S_1 = \mu_0 N/(\mu_0 N + 2C_s)$

μ is as in (19)

Figure 10 illustrates the similarity between $F_{xDugoff}$ and $F_{xDugoff,\ modified}$. From Equations (19) and (21), it is evident that

$$F_{xDugoff} > F_{xDugoff,\ modified} \qquad 0 \leq S \leq 1 \tag{22}$$

and $S_0 < S_1$

It is obvious from (21) that the anomalous concavity in (19) for small S has been removed.

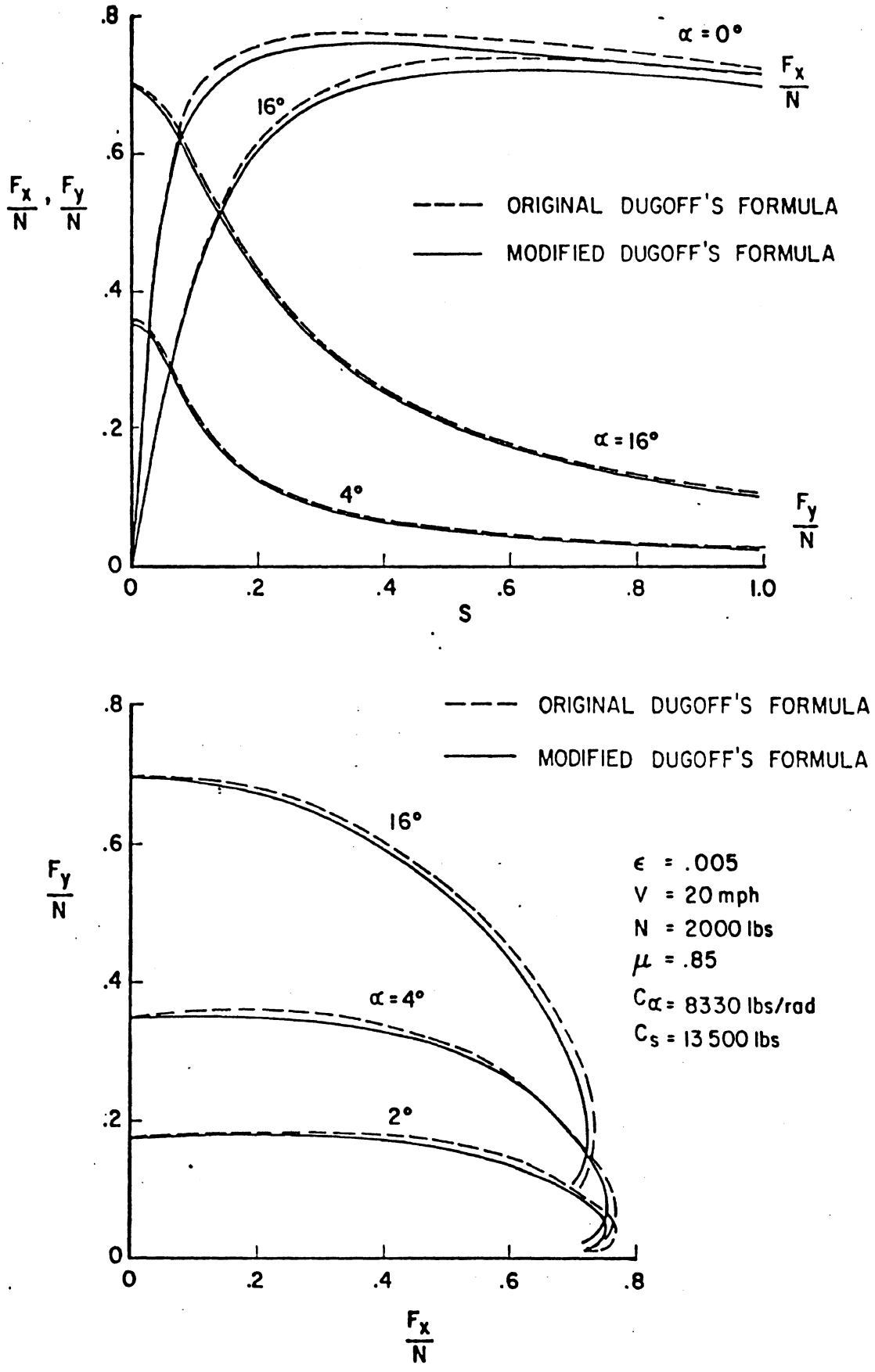

Figure 10, Differences Between Dugoff's Original and Modified Formulas

DISTRIBUTION OF F_x AND F_y AND THE FRICTION ELLIPSE

The preceding sections emphasized the variation of one component of the tire friction when the other component was absent. This section discusses the interaction between F_x and F_y. Experimental evidence, such as that shown in Figure 5, has brought into the literature the friction ellipse concept. According to this concept, the "traction envelope" [4] looks almost like an ellipse whose semi-axes are the maximum values of F_x and F_y. For purposes of illustration, a true ellipse has been superimposed in Figure 3 and is shown passing through the two points $(F_{xmax}, 0)$ and $(0, F_{ymax})$. Although the friction ellipse is not quite an accurate representation of F_x, F_y distribution, it seems to be more realistic than the friction circle theory and the distributions used by Chiesa and Rinonapoli [9] and Okada et al. [10].

Within the limitation of the friction ellipse theory, there is more than one approach and the ratio of semi-axes varies from one study to another. In Eshleman's report [11], for example, the ratio of major to minor axes is 1.5; the semi-major axis represents the "braking" force F_x. Nicolas and Comstock [12] derived their expressions for $F_x(\alpha, S)$ and $F_y(\alpha, S)$ based on the following two assumptions:

(i) the resultant friction force $\underline{F}$ is co-linear with and opposite to the relative velocity vector of the tire footprint with respect to the ground

(ii) for a constant wheel speed V the friction force vector $\underline{F}$ describes an ellipse whose semi-axes are $F_x(0, S)$ and $F_y(\alpha, 0)$ where $F_y(\alpha, 0)$ is given by (11) and $F_x(0, S)$ is specified as in Figure 9. Their expressions are:

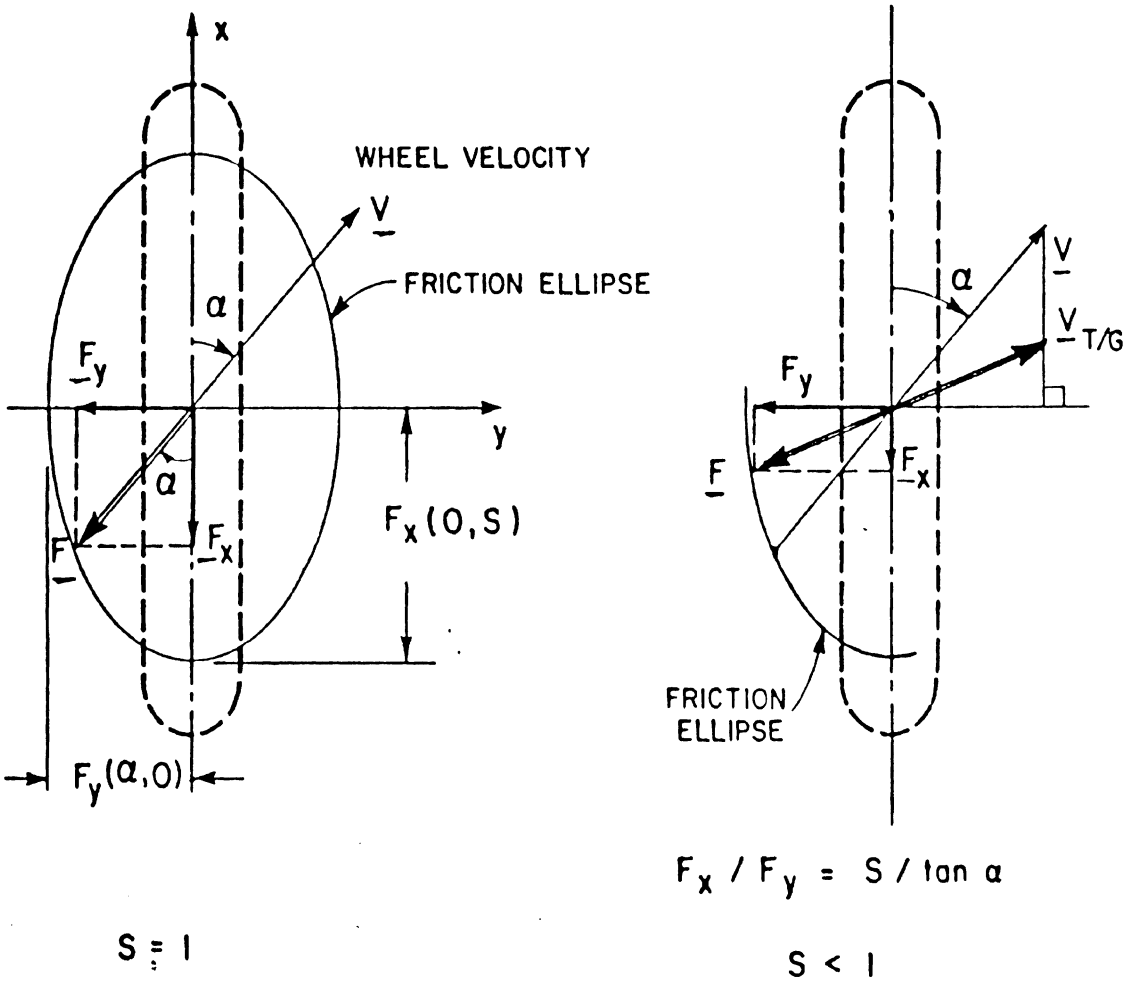

Figure 11, Nicolas and Comstock's Friction Distribution

$$F_{yNicolas}(\alpha, S) = \frac{F_x(0, S)F_y(\alpha, 0)\tan \alpha}{[S^2F_y^2(\alpha, 0) + F_x^2(0, S)\tan^2 \alpha]^{1/2}} \tag{23}$$

$$F_{xNicolas}(\alpha, S) = \frac{F_x(0, S)F_y(\alpha, 0)\, S}{[S^2F_y^2(\alpha, 0) + F_x^2(0, S)\tan^2 \alpha]^{1/2}}$$

Since $F_y(\alpha, S)$ and $F_x(0, S)$ varies with α and S, respectively, the friction ellipse shrinks or expands when α or S varies. Viewed from a different point of view, (23) means

(i) the reduction factor for F_y due to a non-zero S is

$$[1 + S^2F_y^2(\alpha, 0)/(F_x^2(0, S)\tan^2 \alpha)]^{1/2}$$

(ii) similarly, the reduction factor for F_x due to a non-zero α is

$$[1 + F_x^2(0, S)\tan^2 \alpha/(F_y^2(\alpha, 0)\, S^2)]^{-1/2}$$

A more usual approach is typified by McHenry's description [15]. In this approach, the longitudinal force F_x is "given first priority in utilization of the available friction." F_x is determined in terms of the instantaneous values of V, N, and S via tables and interpolations. Whether or not the dependence of F_x on α is taken into account is usually not made clear. The bounding "friction ellipse" is then used to determine the saturation value $F_{ymax}(\alpha_{max}, S)$ by

$$\frac{F^2_{ymax}(\alpha_{max},\ S)}{F^2_{ymax}(\alpha_{max},\ 0)} + \frac{F^2_x(0,\ S)}{F^2_x(0,\ S_{max})} = 1 \qquad (24)$$

where

S_{max} = value of S at which F_x is maximum

α_{max} = value of α at which F_y is maximum

$F_{ymax}\ (\alpha_{max},\ 0)$ is computed as in the previous section

In particular, McHenry [15] used the following algorithm:

$$F_x(0,\ S) = \min \left\{ \mu_x(S)N,\ \frac{F^2_y(\alpha_{max},\ 0)}{\sqrt{\tan^2\ \alpha + F^2_y(\alpha_{max},\ 0)/G^2}} \right\} \qquad (25)$$

where $G = \begin{cases} F_x(0,\ S_{max}) & S \leq S_{max} \\ \mu_x(S)N & S > S_{max} \end{cases}$

According to McHenry [15], the above choice of G "prevents a recovery of side force capability at $S > S_{max}$" and the algorithm for $F_x(0,\ S)$ is necessary to treat "traction" or "braking" appropriately.

In another approach, used by Eshleman et al. [11], the bounding ellipse is used merely as a check to find out whether the resultant friction force lies within the limit of the friction ellipse. In this case, the

semi-major axes of the bounding ellipse are $F_x(0, S_{max})$ and $F_y(\alpha_{max}, 0)$ and the effect of S on F_y is not taken into account when computing F_y.

The complete form of the theoretically-derived formulas of Dugoff et al. [13] are presented below:

$$F_{xDugoff} = \frac{C_s S}{1-S} f(\lambda)$$

$$F_{xDugoff} = \frac{C_\alpha \tan \alpha}{1-S} f(\lambda) \qquad (26)$$

$$f(\lambda) = \begin{cases} \lambda(2-\lambda) & \lambda \leq 1 \\ 1 & \lambda > 1 \end{cases}$$

$$\lambda = \frac{\mu_0 N[1 - \varepsilon V \sqrt{S^2 + \tan^2 \alpha}] (1-S)}{\sqrt{2 \; C_s^2 S^2 + C_\alpha^2 \tan^2 \alpha}}$$

As in (21), when the factor (1-S) in Equation (26) is replaced by 1, the modified Dugoff et al. formulas are obtained. Both original and modified formulas are illustrated by Figure 10. The factor (1-S) in $F_{yDugoff}$ causes a local maximum of $F_{yDugoff}$ at $S \doteqdot .025$ for small α. This maximum is removed in the modified formula and the F_x, F_y distribution then agrees more closely with experimental results as shown in Figure 3.

It is an interesting point that according to (26), if $C_s = C_\alpha$, then $F_{xDugoff}$ varies with S in exactly the same way as $F_{yDugoff}$ does with $\tan \alpha$. In this case, $(F_x/F_y)_{Dugoff} = S/\tan \alpha$ and $(F_x/F_y)_{Dugoff} = (F_x/F_y)_{Nicolas}$. The physical significance and similarity of S and $\tan \alpha$ are, perhaps, best illustrated in Segel's paper [17],

from which his illustration is reproduced in this paper as Figure 12. Experimental evidence confirms this similarity when Holmes and Stone [5] plotted F_x vs. S and F_y vs. sin α in the same graph and Segel [17] superimposed the F_x vs. S curve on the graph of F_y vs. tan α (for the range of α under consideration, tan $\alpha \doteqdot$ sin $\alpha \doteqdot \alpha$). This seems to indicate that tan α is the parameter of importance rather than the angle α itself.

VEHICLE MOTIONS AS PREDICTED BY A SIMPLIFIED MODEL AND FRICTION FORMULAS

To study the sensitivity of vehicle motion to different friction formulas, a simplified vehicle model was chosen (Figure 13). The vehicle is assumed to be basically a rigid sprung mass mounted on four wheels, running on a smooth, horizontal, unbounded road. The tires and suspension systems are considered rigid bodies. The vehicle motion, therefore, consists only of the forward, lateral, and yawing motions. A body-fixed frame (x_B, y_B) was chosen with the origin at the vehicle C.G.; x_B is the vehicle longitudinal axis and y_B is the vehicle lateral axis. Initially, (x_B, y_B) coincides with the inertially-fixed frame (x_1, y_1).

EQUATIONS OF MOTION

Within the above assumptions and without the driving torque, the vehicle motion equations are:

$\underline{V}$ = wheel velocity = $\underline{V}_r + \underline{V}_s$

$\underline{u}$ = in-plane wheel velocity = $\underline{V} \cos \alpha$

$\underline{V}_r$ = rolling velocity

$\underline{V}_s$ = slip velocity = $\underline{V}_{s_x} + \underline{V}_{s_y}$

$S_x = S$ = longitudinal slip = $\dfrac{V_{s_x}}{u}$

$S_y = \dfrac{V_{s_y}}{u} = \tan \alpha$

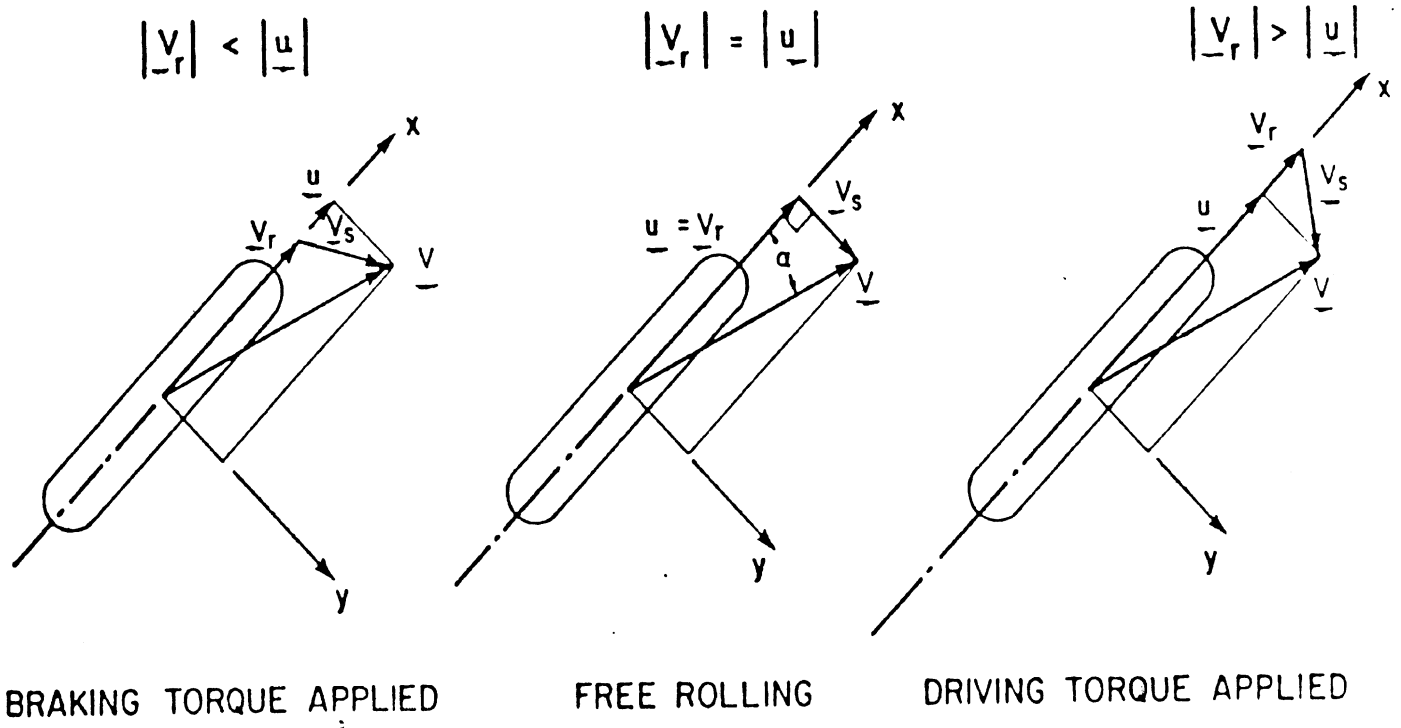

Figure 12, Translational Slip Velocity V_s (after Segel [17])

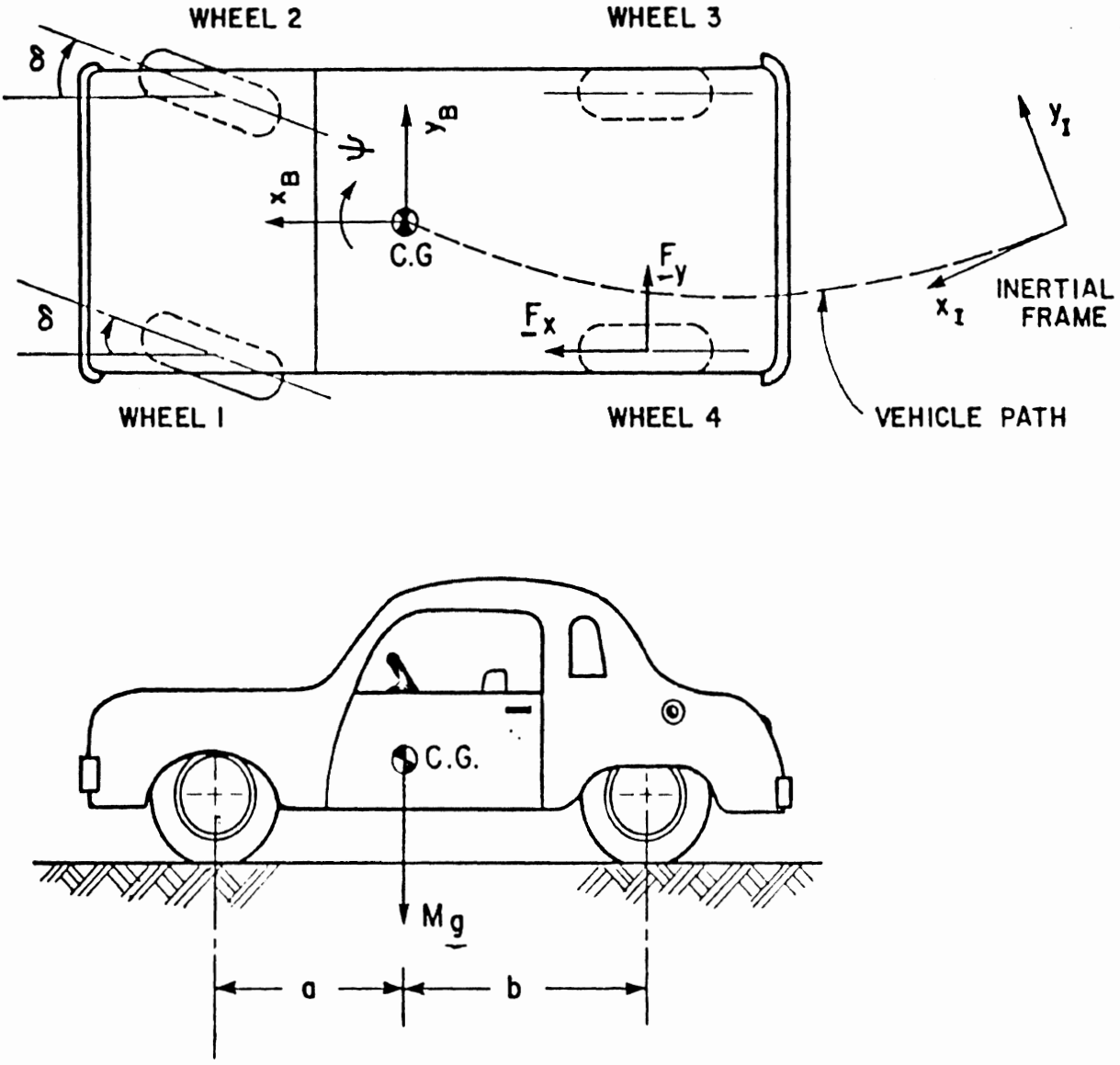

Figure 13, Simplified Vehicle Model

$$M\begin{pmatrix}\ddot{x}\\ \ddot{y}\end{pmatrix} = -\begin{bmatrix}\cos\psi & -\sin\psi\\ \sin\psi & \cos\psi\end{bmatrix}\sum_{i=1}^{4}\begin{pmatrix}F_{x_i}\cos\delta_i - F_{y_i}\sin\delta_i\\ F_{x_i}\sin\delta_i + F_{y_i}\cos\delta_i\end{pmatrix} \tag{27}$$

$$I\ddot{\psi} = -\sum_{i=1}^{4} d_{x_i}(F_{x_i}\sin\delta_i + F_{y_i}\cos\delta_i) - d_{y_i}(F_{x_i}\cos\delta_i - F_{y_i}\sin\delta_i)$$

where

M = vehicle mass

I = yaw principal moment of inertia

x,y = coordinates of the vehicle C.G. in inertial frame

ψ = yaw angle (see Figure 14)

d_{x_i}, d_{y_i} = components of radius vector $\underline{d}_i$ from vehicle C.G. to the centre of wheel i in body-fixed frame

δ_i = steer angle of wheel i

$(\dot{})$ = $\frac{d}{dt}(\ )$, t=time

F_{x_i}, F_{y_i} = as described in Section 2

and the subscript i denotes the wheel number (see Figure 13). To specify F_{x_i} and F_{y_i}, the wheel velocity, $\underline{V}_i$ must be expressed in the wheel reference frame:

$$\underline{V}_i = \begin{pmatrix}u_i\\ v_i\end{pmatrix} = \begin{bmatrix}\cos(\psi+\delta_i) & \sin(\psi+\delta_i)\\ -\sin(\psi+\delta_i) & \cos(\psi+\delta_i)\end{bmatrix}\begin{pmatrix}\dot{x}\\ \dot{y}\end{pmatrix} + \dot{\psi}\begin{bmatrix}\cos\delta_i & \sin\delta_i\\ -\sin\delta_i & \cos\delta_i\end{bmatrix}\begin{pmatrix}-d_{y_i}\\ d_{x_i}\end{pmatrix} \tag{28}$$

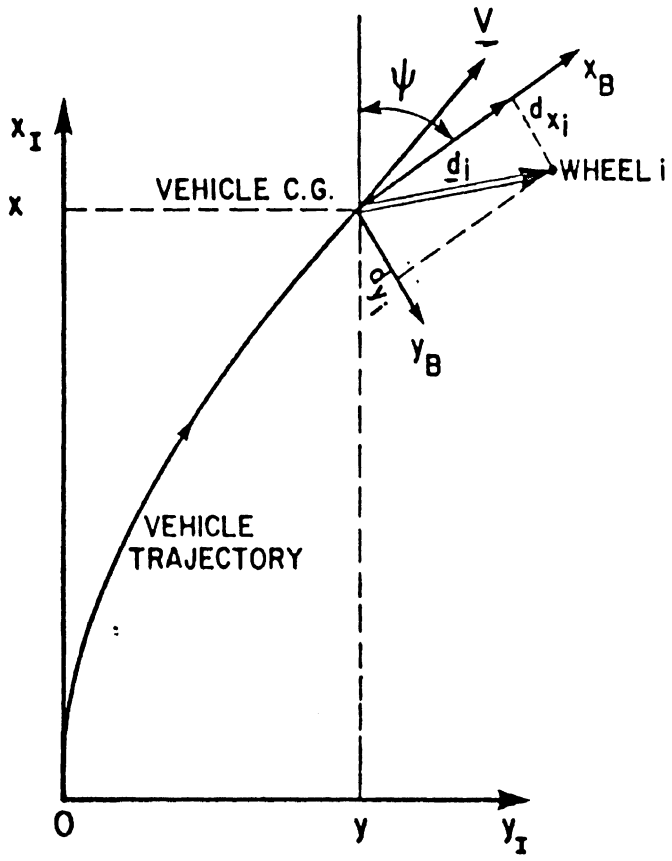

Figure 14, Vehicle Trajectory

and the slip angle α_i:

$$\alpha_i = \tan^{-1}(v_i/u_i) \tag{29}$$

of the wheel under consideration has to be computed.

For the wheel dynamics, it was assumed that all four wheels have the same rolling radius r and polar moment of inertia J so that the motion equation of wheel no. i can be written as

$$J\dot{\Omega}_i = \begin{cases} r F_{x_i} - T_i & S_i < 1 \\ 0 & S_i = 1 \end{cases} \tag{30}$$

where Ω_i = angular speed of wheel i

T_i = braking torque (see Figure 1. The same braking torque T is assumed at all four wheels.)

The longitudinal force F_{x_i} is related to the wheel speed Ω_i via the longitudinal slip S_i:

$$S_i = 1 - r\,\Omega_i/u_i \tag{31}$$

The brake systems are idealized such that the braking torque T_i can be expressed as

$$T_i = T_{max}(1 - \exp[-(t-t_d)/\zeta]) \tag{32}$$

where

T_{max} = maximum value of T

t_d = delay time

ζ = rise time

(This idealization was used by Bernard [19].)

The lack of experimental data, which is required to determine the dependence of the friction force on the tire normal load for all tire friction models, has led to the assumption that all four tires have the same constant load. This assumption is naturally not valid since the loads on the tires depend on the static load distribution and the vehicle inertia force (zero aerodynamic forces and no pitch or roll load transfers were assumed) does contribute to the dynamic loads on the tires. However, it is acceptable in this study because it underlies all tire friction models and merely eliminates the contribution of varying normal loads to the vehicle motion.

SIMULATION

The differences between tire friction models and the vehicle motion equations have been discussed. The simulations will now be discussed with emphasis on how the tire friction models were implemented in the computer programs.

Vehicle Data

In the simulations employed in this study, typical dimensions for passenger cars [7] were used:

$$M = 4000 \text{ lbs}, \; I = 4000 \text{ slug-ft}^2, \; J = 1.5 \text{ slug-ft}^2$$

$$d_{x_i} = d_{x_2} = 4.5 \text{ ft}, \; d_{x_3} = d_{x_4} = -6 \text{ ft} \qquad (33)$$

$$-d_{y_i} = d_{y_2} = d_{y_3} = -d_{y_4} = 3 \text{ ft}, \; r = 1.25 \text{ ft}$$

The tire data are as specified in Table 2 showing the experimental data on $F_x(\alpha,S)$ and $F_y(\alpha,S)$ [17]. From Reference [17], it is found that

$$C_\alpha = 8330 \text{ lbs/rad}, \quad C_s = 13500 \text{ lbs}. \qquad (34)$$

for the tire under consideration, at V = 20 mph.

Of the five variables, μ, α, S, N, V, in Equation (1), more emphasis is placed on S and α, partly because of the lack of data for different N, μ, V and partly because S and α are believed to be the more important variables. In what follows, assumptions regarding the dependencies of F_x, F_y on N, μ, V will be discussed. These assumptions are applied to all models so that any difference in the vehicle response will be entirely due to the dependencies of F_x, F_y on S and α.

a) Choice of Tire Data for Normal Load N

As mentioned previously, the assumption is made that F_x and F_y do not vary with N. Using the data in (33), the normal load on the left (or right) front tire is found to be equal to 1143 lbs. and 857 lbs. for the left (or right) rear tire. These loads are close to 800 lbs., the load used in establishing the experimental data in Table 2. It is therefore believed that the experimental data in Table 2 are appropriate for this vehicle model.

TABLE 2

Tire Friction Experimental Data (after Segel [17]

(B170A Bias Ply Tire, Dry Asphalt, Pressure = 28 psi, N = 800 lbs., V = 20 mph

F_x (lbs.)

α \ S	0.	.025	.05	.075	.1	.125	.15	.175	.2	.225
0°	0.	312.	497.	633.	721.	778.	813.	831.	844.	857.
8°	0.	174.	310.	413.	505.	578.	633.	670.	703.	734.
12°	0.	110.	206.	284.	374.	442.	501.	541.	587.	620.
16°	0.	83.	134.	205.	275.	332.	385.	429.	475.	514.

α \ S	.25	.275	.3	.4	.5	.6	.7	.8	.9•	1.•
0°	862.	866.	864.	862.	844.	822.	793.	769.	730.	688.
8°	758.	778.	789.	809.	808.	806.	790.	772.	752.	724.
12°	644.	670.	692.	750.	771.	780.	776.	772.	756.	748.
16°	541.	572.	596.	679.	716.	743.	760.	772.	774.	774.

• extrapolated

TABLE 2 (C'td.)

F_y (lbs.)

α \ S	0.	.025	.05	.075	.1	.125	.15	.175	.2	.225
2°	279.	271.••	262.••	253.••	244.	231.••	217.••	204.••	190.	181.••
4°	551.	533.••	515.••	496.••	478.	452.••	426.••	400.••	374.	356.••
8°	819.	813.	785.	758.	730.	703.	670.	629.	587.	556.
12°	902.	903.	888.	864.	839.	813.	783.	752.	718.	683.
16°	935.	928.	917.	899.	877.	859.	835.	809.	779.	750.

α \ S	.25	.275	.3	.4	.5	.6	.7	.8	.9	1.0
2°	172.••	163.••	154.	127.	114.••	100.	92.••	83.	73.••	62.•
4°	338.••	319.••	301.	249.	216.••	182.	167.••	151.	138.••	125.•
8°	514.	488.	460.	374.	309.	271.	231.	197.	167.•	145.•
12°	644.	609.	572.	488.	409.	354.	296.	262.	211.•	198.•
16°	725.	692.	667.	582.	499.	440.	385.	342.	292.•	272.•

• extrapolated
•• interpolated

b) Simulated Friction Coefficient

From Table 2, at V = 20 mph, N = 800 lbs.

$$\mu_x = \frac{F_x(0,S)}{N} \begin{cases} \leq 1.085 \\ = .86 \end{cases} \quad \text{at } S = 1 \tag{35}$$

$$\mu_y = \frac{F_y(\alpha,0)}{N} \leq 1.168$$

The unusually large (> 1) values of μ may be due to the contamination of experimental data (N was not kept constant) as explained by Segel [17]. To eliminate the uncertainty of the numerical values of μ, the use of μ in the tire friction models is avoided. Instead, the unnormalized forces F_x, F_y are used.

c) Dependence of μ on V

Following the common practice (for example, see Nicolas and Comstock [12], McHenry [15]), the following linear relationship is considered

$$\mu = \mu_0 \ (1 - \varepsilon V) \tag{36}$$

where ε = friction reduction parameter > 0.

For the tire in consideration, ε = 0.00217 sec/ft. This value of ε is based on the values of $F_x(0,S_{max})$ at V = 20 mph and 40 mph as given in Reference [17]. However, since it is decided to abandon the use of μ and to use data at V = 20 mph, (36) is rewritten in the following form

$$F = F_0 [1 - 0.00217(V - 29.33)] \quad (37)$$

where F_0 = 935 lbs. = friction force at V = 29.33 fps.

For Dugoff et al.'s model, however, their equation is used

$$\mu = \mu_0 (1 - \varepsilon V \sqrt{S^2 + \tan^2 \alpha}) \quad (38)$$

From the experimental data in Reference [17], it is found that unfortunately ε varies greatly depending on which data points are chosen. To be consistent with the determination of ε above, the same two data points are used. This results in ε = 0.00905 sec/ft. The difference in the above two values of ε is due to the fact that $F_x(0,S)$ attains its maximum at different S_{max} for different V. Using Dugoff et al.'s formula for $\alpha = 0, S = 1$, μ_0 N = 937 lbs. is obtained which is too low for $F_y(\alpha,0)$ to reach its maximum at 935 lbs. For this reason, it is decided to use $F_{yDugoff}(\alpha_{max},0)$ = 935 lbs. and it is found that μ_0 N = 1110 lbs. which is then used in the simulations.

Algorithms

Due to the assumptions made above and some ambiguity present in the tire models, it is necessary to describe the algorithms used in this study and show how they are implemented in the simulations.

a) Tire Models

Holmes and Stone [5], Chiesa and Rinonapoli [9] and Nicolas and Comstock [12] presented their formulas

of $F_y(\alpha)$ for $\alpha > 0$ without mentioning a validity for $\alpha < 0$. Due to the property $F_y(-\alpha,0) = -F_y(\alpha, 0)$, their formulas have been changed to:

$$F_{yHolmes}{}^{2} = \text{sign}(\alpha)\ (a_1|\alpha| + a_2\alpha^2 + a_3|\alpha|^3)$$

$$F_{yChiesa}{}^{3} = \text{sign}(\alpha)\left[1 - \left(\frac{F_x}{2\mu N}\right)^2\right]^{1/2} N\left[(a_4 + a_5 N)|\alpha| + \ldots\right] \quad (39)$$

$$F_{yNicolas} = \text{sign}(\alpha)\ F_{max}(1 - \exp(-C_\alpha|\alpha|/F_{max})$$

where the constants $a_1, \ldots$ are determined by a curve-fitting scheme (see Table 1). Also, $F_x(\alpha,-S) = -F_x(\alpha,S)$ was set for small S in all models, except in Dugoff et al.'s model. It is noted that this condition is, however, satisfied by the modified Dugoff et al. formula.

For Nicolas and Comstock's model [12], $F_x(0,S)$ is specified at the following five points: S = 0.0, 0.1, 0.275, 0.5, 1.0. The frictional forces are then computed according to (23). For other models, except Dugoff et al.'s model, $F_x(\alpha,S)$ is specified as shown in Table 2 and F_x is "given first priority in utilization of the available friction." The reason why it is decided to specify $F_x(\alpha,S)$ instead of $F_x(0,S)$ will be explained later.

---

[2] In the simulations, the dependence of $F_{yHolmes}$ on V, R, P is ignored.

[3] An elliptical force distribution for Chiesa and Rinonapoli's model is assumed.

Regarding the F_x, F_y distribution, the following are chosen:

- a friction circle for Smiley and Horn's model
- a friction ellipse for Radt and Milliken's model (McHenry's algorithm is used here)
- a friction ellipse for Chiesa and Rinonapoli's model
- a friction ellipse for Holmes and Stone's model (the same ellipse as in Chiesa and Rinonapoli's model is used for comparison purpose)
- a friction ellipse for Eshelman's model (major axis/minor axis = 1.5)

Finally, there is one particular set of simulations in which the forces $F_x(\alpha,S)$ and $F_y(\alpha,S)$ are specified in tabular forms as shown in Table 2. To obtain those points (α,S) not shown in the Table, linear interpolations are used.

b) Maneuvers

Three maneuvers are simulated, namely, cornering, braking-in-a-straight-line and braking-in-a-turn. The steering angle is specified according to

$$\delta(t) = \begin{cases} 8°/\text{sec} \cdot t & t \leq 1 \text{ sec} \\ 8° & t > 1 \text{ sec} \end{cases} \qquad (40)$$

The brake characteristics are defined by

$$t_d = \text{delay time} = .1 \text{ sec}$$

$$\zeta = \text{rise time} = .25 \text{ sec} \qquad (41)$$

$$T_{max} = \text{maximum braking torque} = 1500 \text{ ft-lbs.}$$

For simplicity, it is assumed that all four wheels have the same brake characteristics and the same braking torque. For braking-in-a-turn maneuvers, both (40) and (41) are used with the exception that t_d is now set equal to 1.1 secs at which time $\delta(t) = 8° =$ constant. The condition for terminating the simulation is $t \geq 5$ seconds or the vehicle forward velocity ≤ 0, whichever occurs first.

NUMERICAL RESULTS AND DISCUSSIONS

This section describes the numerical technique used and discusses the simulation results.

Numerical Method/Programming

The system of Equations (27) to (30) is solved numerically using Hamming's modified predictor-corrector method[4]. The integration step size and the error bound are set at 0.002 seconds and 0.001, respectively. The error weight is carefully chosen to avoid excessive integration time. The initial conditions for the motion equations are:

$$x(0) = y(0) = \dot{y}(0) = \psi(0) = \dot{\psi}(0) = S_i(0) = 0;$$

$$i=1,..,4$$

$$\dot{x}(0) = 60 \text{ fps}$$

[4]This is available in the IBM SCIENTIFIC SUBROUTINE PACKAGE under the name SUBROUTINE HPCG. In HPCG, the integration step size is automatically doubled or halved depending on whether the local error is less or greater than the error bound.

These conditions are used in all simulations. The frictional forces F_x, F_y are defined in SUBROUTINE FORCE so that this subroutine only needs to be changed for different tire models.

Discussions

To better understand these simulation results, it should be kept in mind that they all contain errors when compared with experimental vehicle response. The common error arises from over-simplifying the vehicle dynamics; other errors are from modelling the tire friction, as discussed in Section 2. In particular, the tabular-data-model results contain the experimental error in measuring tire forces and the numerical error associated with linear interpolations. Without experimental data on the vehicle response, the tabular-data-model results will be used simply as a baseline to judge the responses predicted by other tire models. It is not implied, however, that the tabular-data-model results would be in best agreement with experimental data. Whether errors in modelling the vehicle dynamics and the tire friction accumulate or cancel each other is not known at present. Future investigations will be aimed at finding an answer to this problem.

The simulation results are presented in Tables 3 to 5 and Figures 15 to 19. In order to keep the graphs uncluttered, only the tabular-data-model results are shown as continuous curves; other results are shown at time t = 1,2,3,... seconds for the purpose of comparison.

TABLE 3

Simulation of Vehicle Dynamics

Maneuver : Cornering

TIME (Sec.)	1			2			3			4			5			COMPUTING (Exec.) TIME (Sec.)
MODEL	χ	y	Ψ	χ	y	Ψ	χ	y	Ψ	χ	y	Ψ	χ	y	Ψ	
Tabular data	59.68	2.90	10.36	114.15	21.95	33.56	155.07	58.40	55.40	177.36	105.62	78.68	178.51	155.42	102.44	44.57
Dugoff et al	59.64	3.21	11.16	113.54	23.70	33.96	153.62	61.60	56.52	174.55	110.12	79.89	173.95	160.77	103.97	41.12
Nicolas	59.81	1.90	7.90	116.23	15.66	28.80	162.53	44.97	47.07	194.72	85.70	65.62	210.63	132.13	85.12	45.07
Smiley	59.79	2.02	8.52	115.22	17.88	32.65	157.32	51.47	54.87	181.07	96.04	77.70	184.66	143.48	101.00	62.92
Radt	59.72	2.68	9.68	114.64	20.48	32.72	156.58	55.54	54.08	180.70	101.50	76.37	184.73	150.77	99.22	47.75
Eshleman	59.57	3.87	11.77	112.86	26.00	35.88	150.92	66.08	59.68	168.12	116.25	84.38	162.45	166.87	109.68	56.12
Holmes	59.69	2.85	10.15	114.03	21.89	34.48	153.95	58.91	57.51	174.22	106.41	81.41	172.94	155.54	105.77	42.33
Chiesa	59.66	3.05	10.93	112.75	24.62	39.19	146.80	65.88	66.92	156.68	115.50	94.63	142.67	161.47	122.15	57.49

χ y, are in feet, Ψ is in degrees

TABLE 4

Simulation of Vehicle Dynamics

Maneuver : Braking-in-a-straight line

MODEL	STOPPING DISTANCE (ft)	TIME REQUIRED TO STOP (sec.)	COMPUTING (EXECUTION) TIME (sec.)
Dugoff et al	81.75* (96.87)**	2.391* (2.849)**	19.88* (28.6)**
Nicolas & Comstock	92.06	2.858	31.01
Tabular data	85.57	2.748	34.29

NOTE: It is recalled that the Nicolas & Comstock's model [12] requires 5 pairs of S and F_x and in the tabular data model, F_x (S) is specified at 20 different values of S.

* $\mu_0 N$ = 1110 lbs

** $\mu_0 N$ = 937 lbs

TABLE 5

Simulation of Vehicle Dynamics

Maneuver : Braking-in-a-turn

TIME (Sec.)	1			2			3			STOPPING POSITION				COMPUTING (Exec.)
MODEL	χ	y	Ψ	χ	y	Ψ	χ	y	Ψ	time	χ	y	Ψ	TIME (Sec.)
Tabular data	59.68	2.90	10.36	109.05	16.25	28.74	133.70	24.80	34.70	3.4557	136.25	25.87	34.44	32.89
Dugoff et al	59.64	3.22	11.16	108.40	17.42	28.66	134.60	24.68	32.84	3.4149	137.45	24.86	31.09	28.54
Nicolas	59.81	1.90	7.90	110.95	10.90	25.11	140.40	16.81	31.08	3.7728	147.44	18.21	29.60	33.37
Smiley	59.79	2.02	8.52	109.50	13.38	27.65	132.61	25.25	34.67	3.602	135.87	27.94	37.70	62.47
Radt	59.72	2.68	9.68	109.03	15.98	25.94	132.98	29.52	35.42	3.6912	137.11	33.2	39.64	58.54
Eshleman	59.57	3.87	11.77	106.56	22.63	33.84	126.00	42.25	52.48	3.7097	129.00	47.27	56.97	36.31
Holmes	59.69	2.85	10.15	107.81	18.48	31.11	128.55	35.63	47.10	3.6686	131.64	39.78	51.09	40.63
Chiesa	59.66	3.05	10.93	106.49	20.85	35.71	125.01	39.63	53.00	3.6482	127.52	43.83	56.74	92.68

χ, y are in feet, Ψ is in degrees

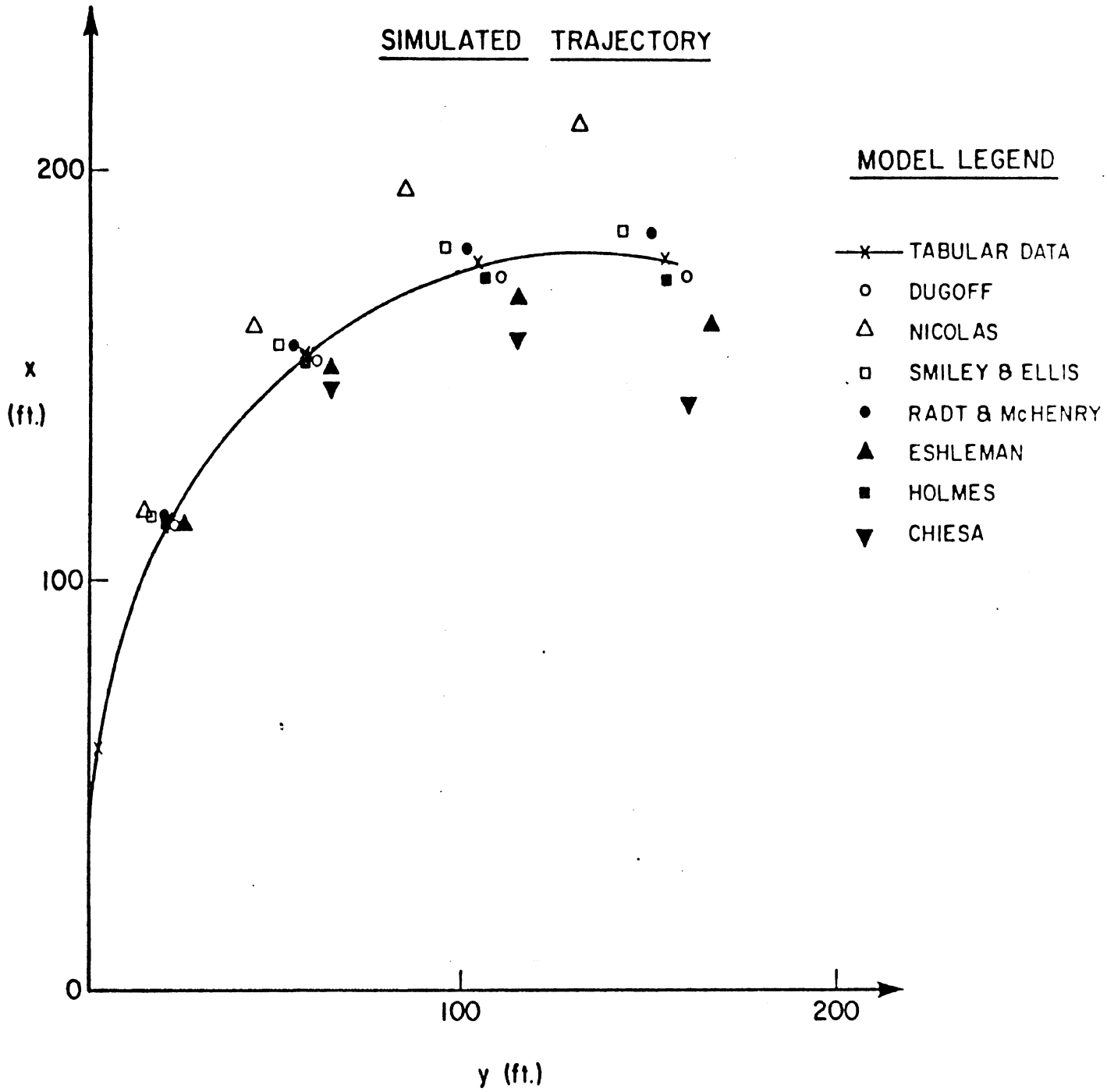

Figure 15, Vehicle Trajectory as Predicted By Different Tire Models (Cornering Maneuver). Data points shown are at t = 2,3,4,5 seconds.

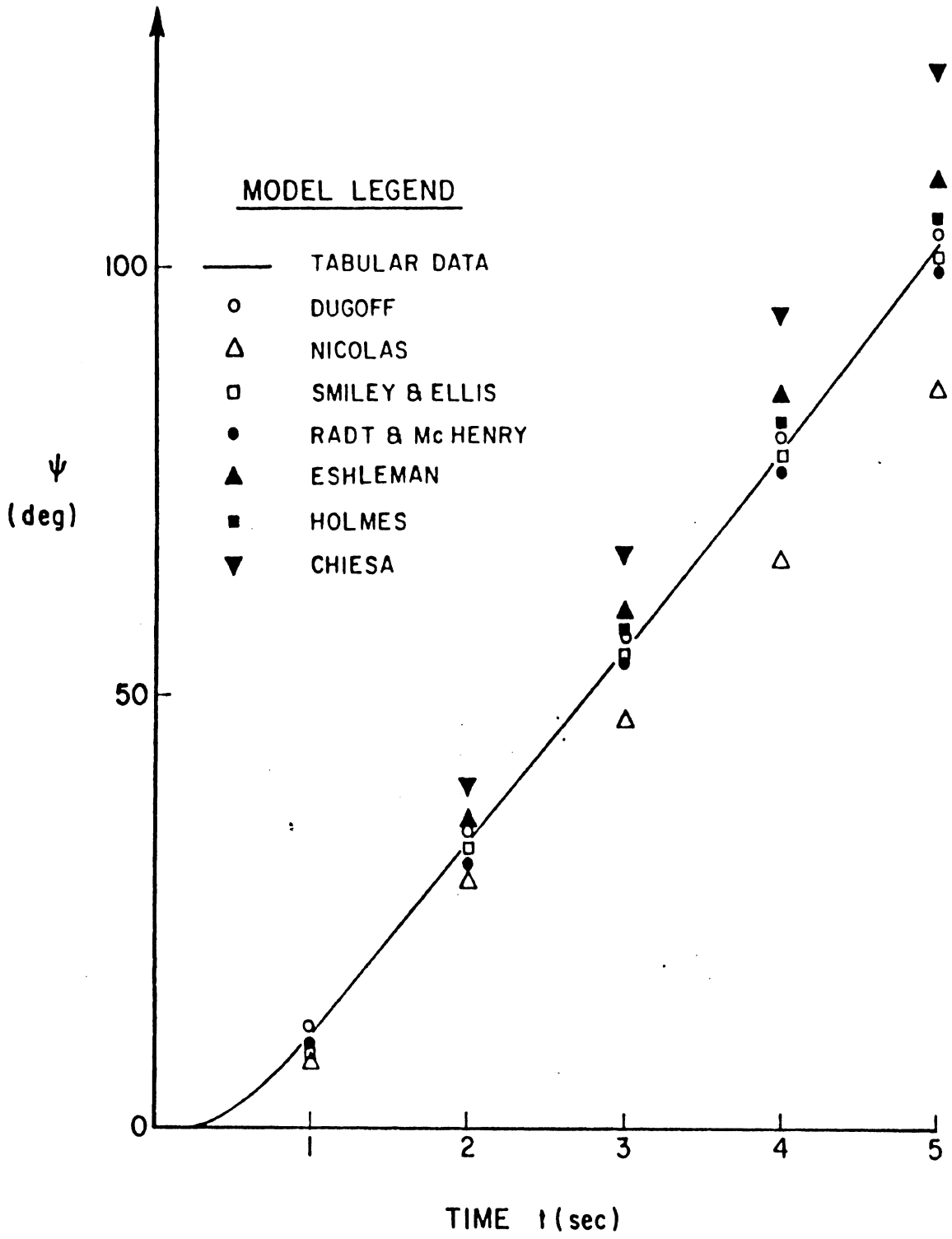

Figure 16, Yaw Angle as Predicted by Different Tire Models
(Cornering Maneuver)

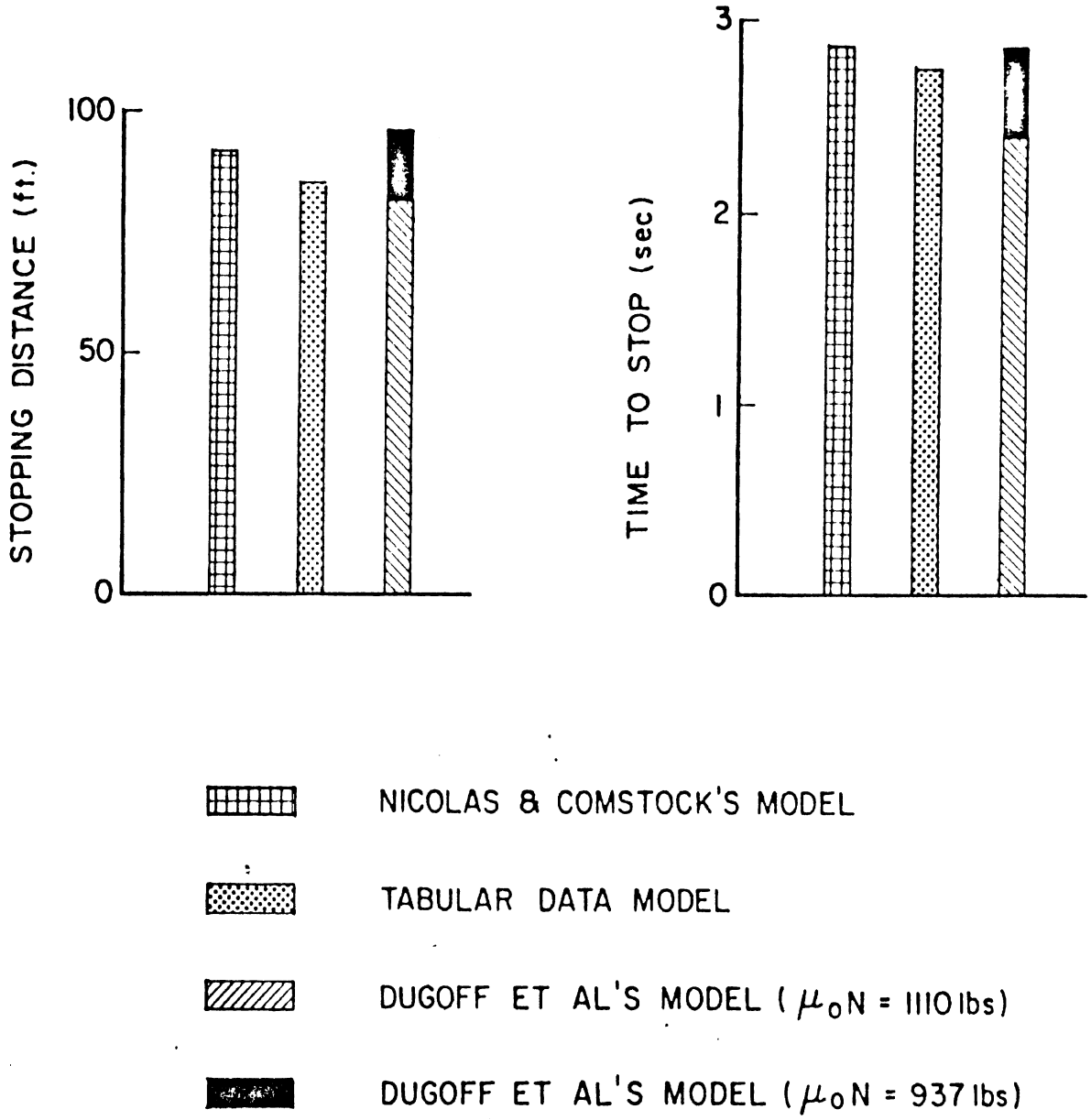

Figure 17, Braking Performance as Predicted by Different Tire Models

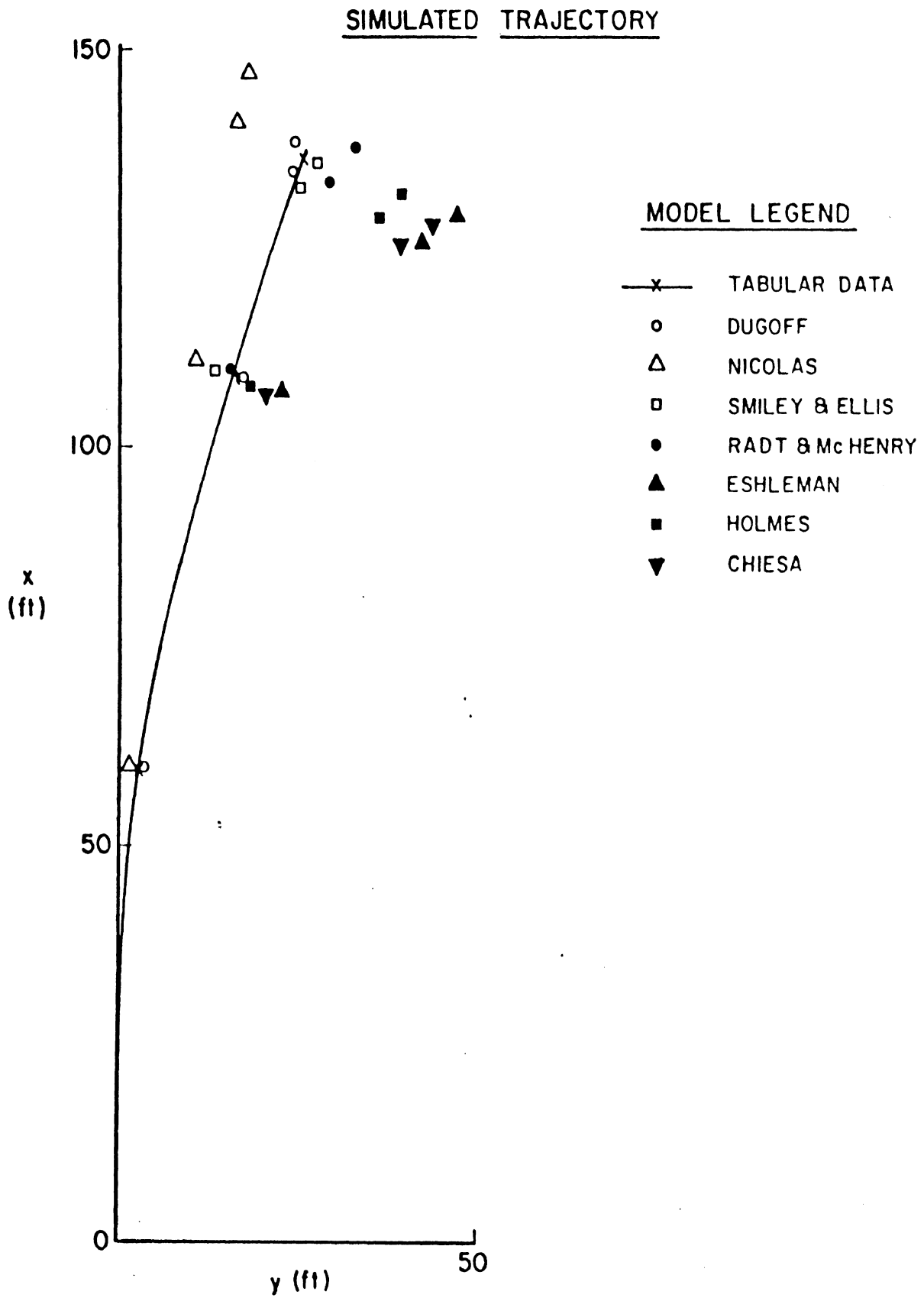

Figure 18, Vehicle Trajectory as Predicted by Different Tire Models (Braking-in-a-turn Maneuver). Data points shown are at t = 1,2,3 seconds and at stopping distance.

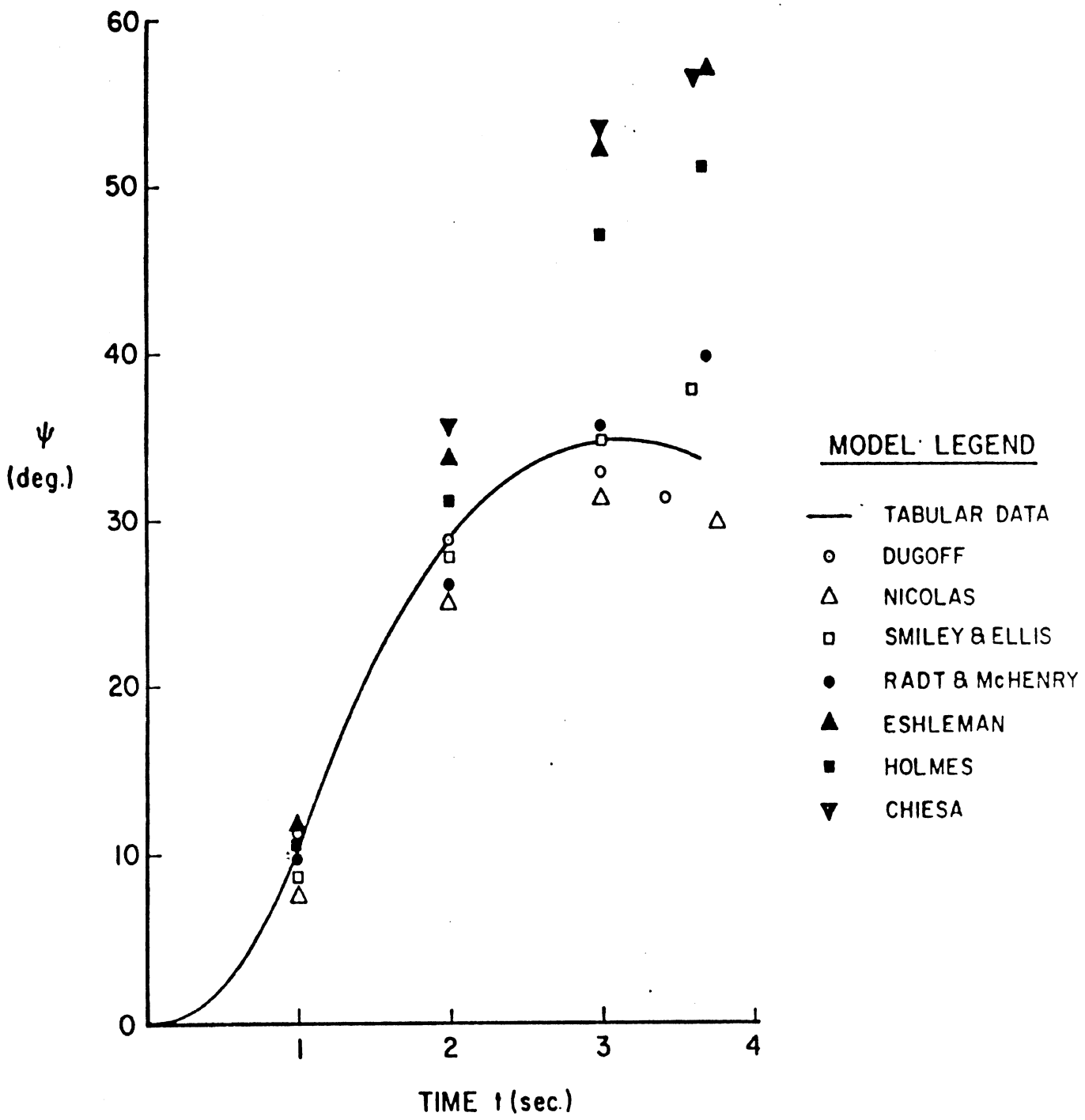

Figure 19, Yaw Angle as Predicted by Different Tire Models

(Braking-in-a-turn Maneuver)

a) Cornering Maneuver

Most x-y trajectories and yaw angle histories $\psi(t)$ are within approximately seven percent of the tabular-data-model results, e.g., 8 ft. in trajectory and 4° in $\psi(t)$, except for the responses predicted by Nicolas and Comstock's and Chiesa and Rinonapoli's models. The instantaneous positions of the vehicle, however, vary more significantly from one model to another. Therefore, if the course of the vehicle is the only concern, most tire friction models will be suitable since most predict practically the same trajectory.

The large radius of curvature and the small yaw angle in the Nicolas and Comstock trajectory show an inadequacy of tire lateral forces, which might be due to the specification used in this study, $\mu_{lim}N = F_{max}$. (Nicolas and Comstock [12] did not discuss in detail how they chose μ_{lim} except by saying that μ_{lim} = a factor multiplied by μ_x.) A better use of $F_{yNicolas}$ in Equation (11) can be made by solving for μ_{lim} from the following nonlinear algebraic equation:

$$F_{max} = \mu_{lim}N(1 - \exp(-C_\alpha \alpha_{max}/[\mu_{lim}N])) \qquad (42)$$

where F_{max}, α_{max}, and C_α are specified according to tire experimental data. Equation (42) essentially fits the $F_y(\alpha)$ curve to the point (α_{max}, F_{max}).

To understand other vehicle responses, it is recalled that, generally speaking, the yaw acceleration varies with the difference between the tire lateral forces at the front and rear wheels, whereas the

y-coordinate of vehicle C.G. varies with the sum of these forces. In the simulations used in this study, the steering angle $\delta = 8°$ for $t \geq 1$ sec., during which time the slip angles are approximately 12° and 4° for the front and rear wheels, respectively. As a consequence, it is found from Table 1 that the Chiesa and Rinonapoli model would produce a large yaw rate $\dot{\psi}$, whereas the Eshleman model would predict a large y-coordinate of the vehicle C.G. These facts are verified in Figures 15 and 16. It is interesting to observe from Figure 16 that the yaw rate $\dot{\psi}$ remains practically constant for a constant steering angle.

b) Braking-in-a-Straight-Line Maneuver

Due to the scarcity of $F_x(S)$ formulas, only three models for this maneuver are used, namely, the Dugoff model, the Nicolas model and the tabular-data-model. The simulation results are summarized in Table 4. Note that the only difference between the Nicolas model and the tabular-data-model is that in the former $F_x(S)$ is specified at five different values of S, whereas the same function is defined at 20 values of S in the latter. It is observed that in the simulations, $F_{xNicolas} \leq F_{xTabular}$ for $0 \leq S \leq 1$, the equality holds only at the points where $F_{xNicolas}$ and $F_{xTabular}$ are defined identically. Consequently, a longer stopping distance is required in the Nicolas model. The difference of 6.5 feet in the stopping distances predicted by the two models above merely represents the accumulated error in inaccurately defining $F_x(S)$.

The comparison of the stopping distances predicted by the Dugoff and tabular-data-models is more significant.

The following differences between the two models should be kept in mind:

- The Dugoff longitudinal stiffness $C_{sDugoff}$ is unaltered by the wheel speed V and at $S > S_0$ (see Equation (19)), the longitudinal force $F_{xDugoff}$ is quadratic in $(1-\varepsilon VS)^2$. The $C_{sTabular}$ and $F_{xTabular}$ are simply proportional to V (see Equation (37)).

- S_{max}, the value of S at which F_x is maximum, varies with V in Dugoff's model. In the tabular-data-model, S_{max} is stationary with respect to V.

- At V = 20 mph, the longitudinal force $F_{xDugoff}$ has its maximum at 935 lbs. for $\mu_0 N$ = 1110 lbs. and 866 lbs. at $\mu_0 N$ = 937 lbs. The experimental data used in the tabular-data-model is $F_{xTabular} \leq$ 866 lbs.

For comparison purposes, the Dugoff model results are used for $\mu_0 N$ = 937 lbs. The stopping times predicted by the two models agree with each other within four percent. The Dugoff model stopping distance is approximately 11 ft. longer than the distance predicted by the tabular-data-model. However, this comparison does not lead to an affirmative conclusion regarding the accuracy of the Dugoff model since Bernard [19], who used the Dugoff model, showed that the accuracy of his simulations depends on the applied braking torque. In the study presented in this paper, only one value (1500 ft-lbs) of the braking torque is used.

c) Braking-in-a-Turn Maneuver

The widely known braking stiffening effect can be readily observed in Figures 18 and 19: the trajectory curvature and the yaw angle are both reduced by braking. An interesting feature is displayed by the results obtained from the tabular-data-model, the Dugoff model, and the Nicolas model, namely that the yaw angle $\psi(t)$ attains its local maximum shortly before the vehicle comes to a full stop. The simulation results are more scattered in this maneuver than in the cornering maneuver, showing the importance of an accurate representation of the F_x, F_y force distribution.

In general, the results from the Dugoff model are in best agreement with the tabular-data-model results and the results from the Eshleman model deviate the most from the tabular-data-model results. It is recalled that in Eshleman's model [11], $F_y(\alpha,0)$ is used as the true lateral force even when F_x = the longitudinal force is nonzero. As a result, Eshleman's lateral force is overestimated for this braking-in-a-turn maneuver. (The same algorithm employed in this paper's simulations was used for Eshleman's model.) The trajectory predicted by the Nicolas model has the same trend as in the cornering maneuver which, it is felt, could be improved by the use of Equation (42).

In the models by Smiley and Ellis, Radt and McHenry, Eshleman, Holmes and Chiesa, the "braking" force $F_x(\alpha,S)$ is given the first priority and $F_x(\alpha,S)$ is specified instead of $F_x(0,S)$ so that the effect of slip angle α on F_x is taken into account. The difference between these models and the tabular-data-model is then simply the determinations of

$F_y(\alpha,S)$. The fact that the Holmes model trajectory deviates from the tabular-data-model trajectory more in this maneuver than in the cornering maneuver shows that the reduction factor $\sqrt{1-F_x^2/\mu^2N^2}$ (in Chiesa's model) is not accurate enough. On the other hand, it is observed that the trajectories predicted by these models have larger curvatures when compared with those given by the Dugoff model, the Nicolas model, and the tabular-data-model. The yaw angles predicted by these models do not have local maxima before the vehicle comes to a full stop. These characteristics are thought to be associated with the use of the friction ellipse. Finally, as in the case of the cornering maneuver, the Holmes model trajectory is closer to the tabular-data-model trajectory than the Chiesa model trajectory. This indicates that a cubic representation of F_y is superior to a quartic one.

CONCLUDING REMARKS

Several tire friction models and their influences on vehicle responses have been presented. A number of conclusions have been drawn.

(i) There are significant differences in vehicle motions predicted by different models. The fact that two "similar" models might lead to significantly different vehicle motions strongly proves the necessity for an accurate model over the entire operating regions of slip angle α, slip ratio S, vehicle speed, V, etc.

(ii) Generally speaking, the vehicle yaw acceleration varies with the difference between the tire lateral forces at the front and rear wheels. The translational, lateral acceleration of the vehicle, however, varies with the sum of these forces.

(iii) The tabular-data-model is expected to give a representative vehicle response, although not necessarily the most realistic one when compared with actual vehicle response. Other models which predict similar vehicle motions are considered "acceptable." A future report will present a study which examines whether the tire friction modelling error cancels or adds to the vehicle modelling error.

(iv) For small slip angles α, all formulas in this study reduce to the basic form

$$F_y = C_\alpha \alpha$$

and the difference between various formulas only exists at large values of α. From experimental and theoretical considerations, tan α appears to be the parameter of importance rather than the angle α itself.

(v) There is no unique relationship between the "maximum" angle α_{max}, the maximum side force F_{ymax}, and the lateral stiffness C_α that can be established.

(vi) A cubic fit for the F_y vs. α curve is found to be superior over a quartic one. Following the ideas in the formulas by Ellis, Radt and Eshleman, the following empirical formula is proposed:

$$F_y = C_\alpha \alpha \left(1 + a_1 \frac{\alpha}{\alpha_m} + a_2 \frac{\alpha^2}{\alpha_m^2}\right) \quad \alpha \leq \alpha_m \qquad (43)$$

where a_1, a_2 satisfy the conditions below:

$$1 + a_1 + a_2 = F_{ymax}/(C_\alpha \alpha_m) \qquad (44)$$

$$1 + 2a_1 + 3a_2 = 0$$

$C_\alpha \alpha_m$, F_{ymax} are determined from experimental data. Equation (44) simply ensures the maximum of F_y at α_m. Indeed, it is very important since without it the slope of F_y vs. α curve is nonzero at α_m and a significant error is introduced in the neighborhood of α_m as in the case of Holmes and Stone's (three point) curve fitting [5]. It is evident that the three formulas by Ellis, Radt and Eshleman all satisfy (43) and (44). Equation (42) is a slight improvement over the Radt formula as illustrated in Table 1.

(vii) The use of the friction ellipse concept is critical for braking-in-a-turn maneuvers. An improper distribution of longitudinal and lateral frictional forces causes significant errors in vehicle simulations.

(viii) Dugoff's model is remarkably good. The computing time for this model is the shortest used in the simulations. This proves the advantage of the closed-form formulas for tire frictional forces.

ACKNOWLEDGEMENTS

The authors are grateful to Mr. Ewald Schroeder, Project Research Engineer, Ministry of Transportation and Communications, for reviewing the paper and to Mr. Alan Billing, Research Officer, Ministry of Transportation and Communications for helpful discussion and comment.

REFERENCES

1. Ludema, K.C., "Tires and Roads," Mechanical Engineering, December 1970, pp. 8-14.

2. Kummer, H.W., "Unified Theory of Rubber and Tire Friction," Engineering Research Bulletin B-94, The Pennsylvania State University, College of Engineering, July 1966.

3. Hays, D.F. and Browne, A.L. (Eds.), The Physics of Tire Traction—Theory and Experiment, Plenum Press, New York, 1974.

4. Beauregard, C. and McNall, R.G., "Tire/Cornering/Traction Test Methods," Paper No. 730147, International Automotive Engineering Congress, Detroit, Mich., January 8-12, 1973.

5. Holmes, K.E. and Stone, R.D., Tyre Forces as Functions of Cornering and Braking Slip on Wet Road Surfaces, Road Research Laboratory Report LR 254, 1969.

6. Smiley, R.F. and Horne, W.B., "Mechanical Properties of Pneumatic Tires with Special Reference to Modern Aircraft Tires," NACA Technical Note 4110, January 1958.

7. Radt, H.S., Jr. and Milliken, W.F., Jr., "Motions of Skidding Automobiles," SAE Paper No. 205A, Summer Meeting, Chicago, Illinois, June 5-10, 1960.

8. Ellis, J.R., "Tractor and Semi-Trailer Handling," International Forum, Automobile Engineer, March 1964, pp. 94-97.

9. Chiesa, A. and Rinonapoli, L., "Vehicle Stability Studied with a Non-Linear Seven Degree Model," SAE Paper No. 670476, 1967, pp. 1708-1724.

10. Okada, T., Takiguchi, T., Nishioka, M., and Utsunomiya, G., "Evaluation of Vehicle Handling and Stability by Computer Simulation at the First Stage of Vehicle Planning," SAE Paper No. 730525, Automobile Engineering Meeting, Detroit, Mich., May 14-18, 1973.

11. Eshleman, R.L., Desai, S.D., and D'Souza, A.F., Stability and Handling Criteria of Articulated Vehicles, Part 2, AVDS3 User's Manual, Report No. DOT-HS-500-916, August 1973.

12. Nicolas, V.T. and Comstock, T.R., "Predicting Directional Behavior of Tractor Semitrailers When Wheel Anti-Skid Brake Systems Are Used," Paper No. 72-WA/Aut-16, ASME Winter Annual Meeting, New York, November 26-30, 1972.

13. Dugoff, H., Fancher, P.S., and Segel, L., Tire Performance Characteristics Affecting Vehicle Response to Steering and Braking Control Inputs, Final Report for Period May 1968-August 1969, Contract No. CST-460, Office of Vehicle Systems Research, National Bureau of Standards, Aug. 1969.

14. Tielking, J.T. and Mital, N.K., A Comparative Evaluation of Five Tire Traction Models, Univ. of Michigan, Ann Arbor, Report No. UM-HSRI-PF-74-2 (PB-229 707), January 1974.

15. McHenry, R.R., "Research in Automobile Dynamics—A Computer Simulation of General Three Dimensional Motions," SAE Paper 710361, Mid Year Meeting, Montreal, June 7-11, 1971.

16. Piziali, R.A., Dynamics of Automobiles During Brake Applications—Validation of a Computer Simulation, Cornell Aeronautical Laboratory, Report VJ-2251-V-9, PB 204 533, July 1971.

17. Segel, L., "Tire Traction on Dry, Uncontaminated Surfaces," The Physics of Tire Traction—Theory and Experiment, Plenum Press, New York, 1974, pp. 65-98.

18. Bernard, J.E., Winkler, C.B., and Fancher, P.S., A Computer Based Mathematical Method for Predicting the Directional Response of Trucks and Tractor-Trailers, Phase II Technical Report UM-HSRI-PF-73-1, Highway Safety Research Institute, Univ. of Michigan, June 1973.

19. Bernard, J.E., "A Digital Computer Method for the Prediction of Braking Performance of Trucks and Tractor-Trailers," SAE Paper No. 730181, International Automotive Engineering Congress, Detroit, Mich., January 8-12, 1973.

APPLICATION OF GENERAL RIGID BODY DYNAMICS TO VEHICLE BEHAVIOR

A. I. Krauter
Shaker Research Corporation
and
W. E. Tobler
Sibley School of Mechanical and Aerospace Engineering
Cornell University

ABSTRACT

This paper is concerned with the application of a 4×4 matrix method to simulating the behavior of articulated highway vehicles. The method requires only that a model of the vehicle be adopted and that data concerning the characteristics of the model be specified—the digital computer is used to represent numerically and to solve exactly the differential equations that govern the behavior of the vehicle model.

The method is applied to simulating the behavior of several articulated vehicles. Results are first given for the predicted behavior of a tractor-semi-trailer truck. These results are compared with those obtained from a previously developed tractor-semitrailer model. The comparison leads to the discovery of an error in the previously developed model. When the effects of this error are eliminated, the results obtained from both models are nearly identical. The method is then used to obtain the predicted behavior of several different articulated vehicles for a cornering maneuver with and without braking. Results of a no-braking case and of a braking case for a triple (tractor with three trailers) are given.

The results illustrate the ease with which the method can be applied to the complex, nonlinear vehicle system. If these results were obtained using conventional methods, many man-years of effort would have been required.

ACKNOWLEDGEMENT

This work was part of a program supported by the Department of Transportation (Contract No. DOT-OS-40015) and by the Eaton Corporation, Cleveland, Ohio.

DISCLAIMER

The paper presents the position of the authors and not necessarily that of the Department of Transportation.

INTRODUCTION

Computer simulation has recently become a widely-used tool for studying the handling behavior of highway vehicles. The conventional process used to produce such a simulation starts with the adoption of an idealized physical model of the vehicle. Analytical differential equations are then obtained to describe the behavior of this model. Finally, the differential equations are solved by the computer to produce the simulation. Typical examples of the procedure are in [1] - [5].*

Unfortunately, obtaining the analytical differential equations for a particular vehicle requires the expenditure of much time and effort. In addition, these equations are not easily modified. Such modification becomes necessary when the vehicle model is changed significantly or when its assumed operational environment is altered substantially.

This paper presents the application to vehicle dynamics of a numerical method recently developed for kinematics. With this numerical method, the second step of the vehicle simulation process—obtaining the differential equations which describe the motion of the vehicle—is eliminated. Instead, these equations are both formulated and solved numerically by the computer.

The method used is based on the 4×4 transformation matrices originated by Denavit and Hartenberg [6]. The method was developed in large part by Uicker and was presented in 1969 [7] for application to closed-loop mechanisms. Tobler [8] generalized the method to

---

*Numbers in brackets refer to references listed at the end of this paper.

include both open- and closed-loop mechanisms and applied it to the dynamics of vehicles. The reader is referred to [8] for a review of the literature pertaining to the method and for a complete description of its application to vehicle modeling. That description presents many details which cannot be included in the present paper.

THE METHOD

The 4×4 matrix method requires that the vehicle being modeled be represented as a system of interconnected rigid elements. These elements have coordinate systems attached to them. Certain 4×4 matrices, called "A" matrices, are used both to transform vectors between the coordinate systems and to reference points in any of the coordinate systems. The "A" matrix for adjacent coordinate systems (systems attached to elements on either side of a kinematic joint or connection point) incorporates the kinematic constraints imposed on the vehicle by the joint. In addition, this "A" matrix contains part of the information necessary to describe the geometry of the vehicles.

Variables of motion are associated with most of the "A" matrices. (For an articulated vehicle, many of these variables are state variables since such a vehicle can generally be modeled as an open chain of connected rigid bodies; i.e., an open loop.) The values of these variables and of their derivatives determine the velocities of all points in the vehicle. Consequently, a Lagrangian approach can be used to obtain the equations which describe the motion of the vehicle. The analytical development is as follows: The position equation

for an arbitrary point on the vehicle is written and then differentiated to determine its velocity. An expression for the kinetic energy associated with this velocity is then obtained. Integration over the vehicle yields the total kinetic energy. Differentiation with respect to time results in the Lagrange equations which describe the motion.

The Lagrange equations require expressions for generalized forces. These expressions can be obtained using the principle of virtual work and are developed and cataloged for common components such as linear springs and dampers. Expressions for the generalized forces due to special components must be developed individually for their use with the method. Such expressions are required, for example, for the generalized forces due to road loads on the tires.

Implementation of the method to simulate the motion of a vehicle (or of any system composed of interconnected rigid elements) proceeds as follows: Information sufficient to characterize the geometry, kinematics, dynamic characteristics, and external forces is provided to the computer. Additional information concerning the manner in which the simulation is to be carried out numerically, the known initial conditions of motions, etc., is also provided. The Lagrange equations are then constructed numerically for the initial time (including the numerical determination of the generalized forces). These equations are manipulated numerically such that the rate of change of each motion variable (e.g., position, speed, angular velocity) is a function of all the other motion variables and of time. A standard numerical integration procedure is then used to determine the values of the motion

variables at the next instant of time. At this new time the process is repeated (the Lagrange equations are reformulated, etc.), the result being a printout—a simulation—of each motion variable as a function of time.

APPLICATION OF THE METHOD FOR A TRACTOR-DOUBLE TRAILER COMBINATION

A tractor-double trailer combination is used to illustrate the manner in which the method is used to simulate vehicle behavior. The double was chosen because the procedure used for it is representative of that used for a single (tractor-semitrailer) or for a triple (tractor and three trailers).

The double is shown schematically in Figure 1. It consists of a tractor, two semitrailers, a dolly, two fifth wheels, and five beam-axle suspension systems. Each of these elements is described briefly below.

The tractor, Figure 2, was modeled as a rigid body having mass. Guides were provided for attaching two idealized beam-axle suspension systems to the tractor. Also a fifth wheel (hitch) pin was provided for attaching an idealized fifth wheel, Figure 3, to the tractor. Two coordinate systems, denoted $X_6Y_6Z_6$ and $X_7Y_7Z_7$, are body-fixed to the tractor. These coordinate systems, along with appropriate dimensions of the tractor, are shown in Figure 2.

The tractor fifth wheel was modeled as a massless rigid body. Two revolute joints for attachment of the fifth wheel to the tractor and to the first semitrailer are included in the model. A single coordinate system, denoted $X_8Y_8Z_8$, is body-fixed to the fifth wheel. This

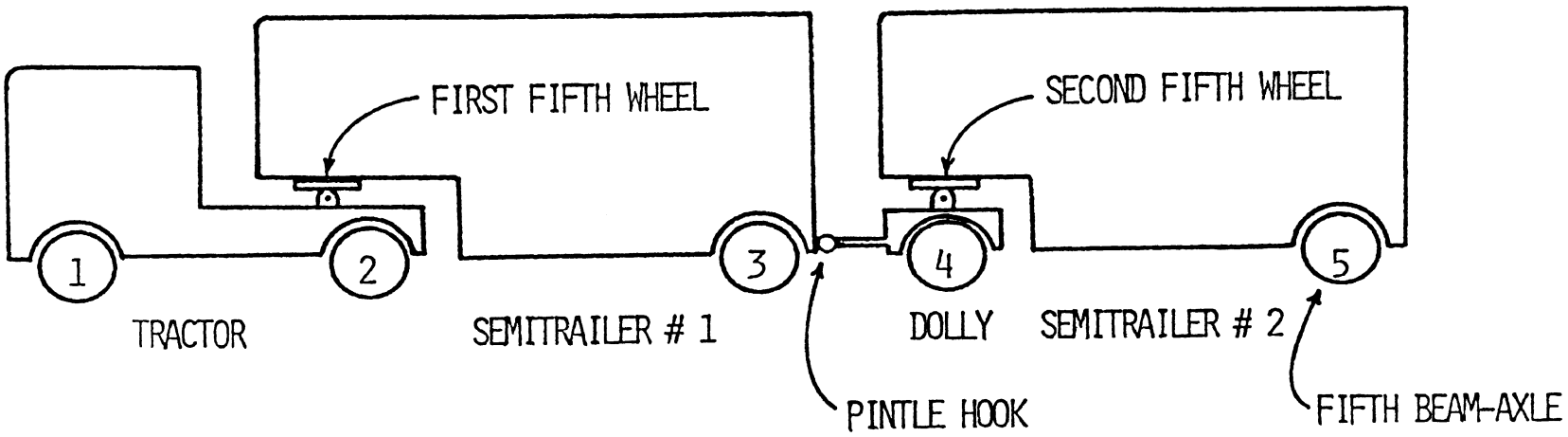

Figure 1. A Tractor-Double Trailer Combination.

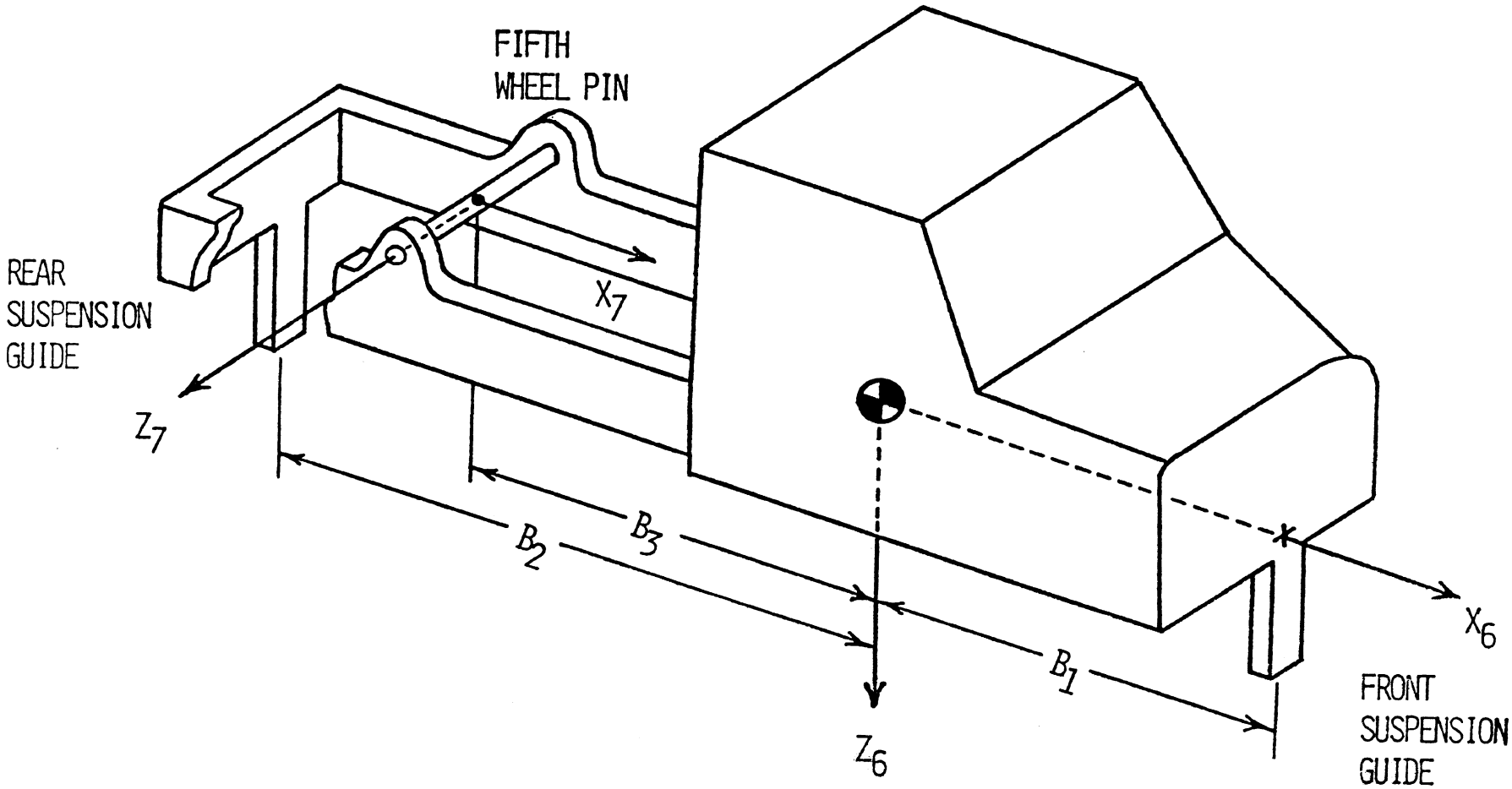

Figure 2. The Tractor

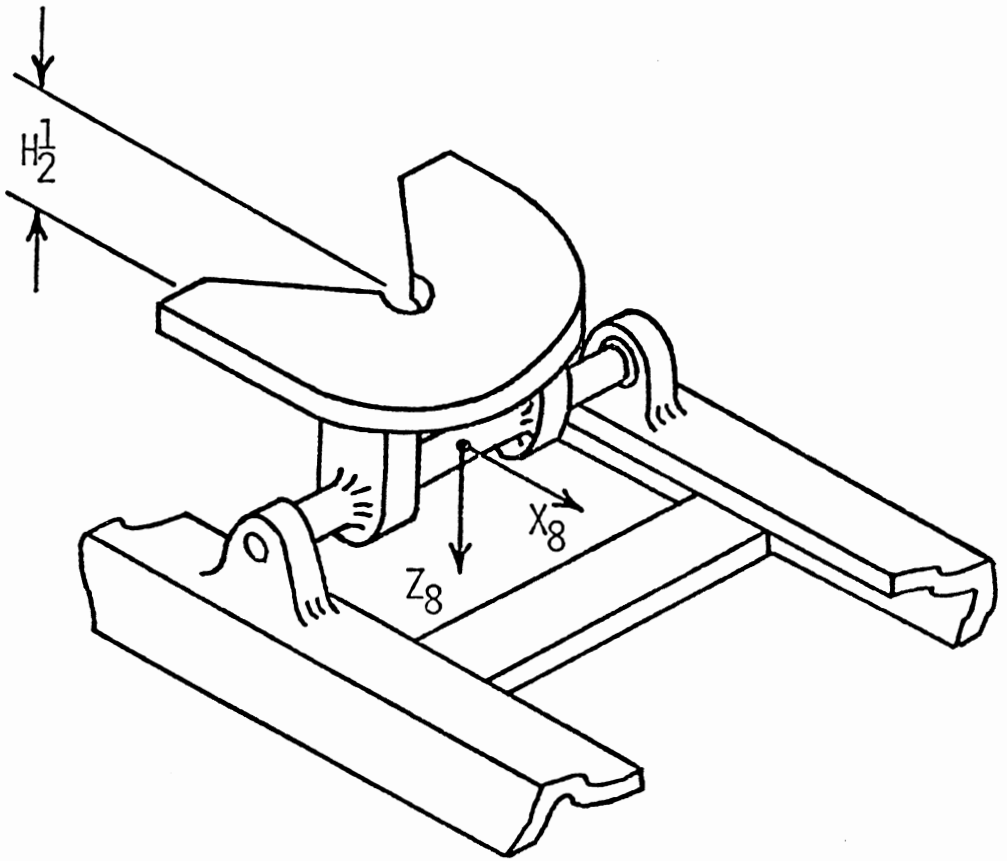

Figure 3. The Tractor Fifth Wheel - Fifth Wheel #1

coordinate system has the same origin as that of $X_7Y_7Z_7$ attached to the tractor. The characteristic dimension of the fifth wheel is shown in Figure 3.*

The second fifth wheel connects the first semitrailer to the second semitrailer. This second fifth wheel is similar to that described above. Its body-fixed coordinate system, denoted $X_{14}Y_{14}Z_{14}$, is analogous to $X_8Y_8Z_8$.

The beam-axle suspension system attached to the front of the tractor is shown in Figure 4. Springs and dampers having linear characteristics are contained within the prismatic and revolute joints. The beam-axle is modeled either as being massless or as having mass. When the beam-axle is modeled as massless, forces and moments which act on the tractor suspension guide are determined by an equilibrium analysis of the wheel-axle assembly. When the beam-axle is modeled as having mass, forces and moments which act on the wheel hubs are determined. Three body-fixed coordinate systems are attached to the suspension system. Two of these coordinate systems, denoted $X_{16}Y_{16}Z_{16}$ and $X_{17}Y_{17}Z_{17}$, are attached to the massless link containing the prismatic joint. The origins of these coordinate systems are located at the revolute joint and have the orientations shown in Figure 4. The origin of the third coordinate system, denoted $X_{18}Y_{18}Z_{18}$, is fixed to the center mass of the beam-axle. The axes of this coordinate system have the orientations shown in the same figure.

---

*This dimension is denoted H_2^1. The superscript 1 indicates that the dimension is that of the first fifth wheel. The corresponding dimension of the second fifth wheel is denoted H_2^2.

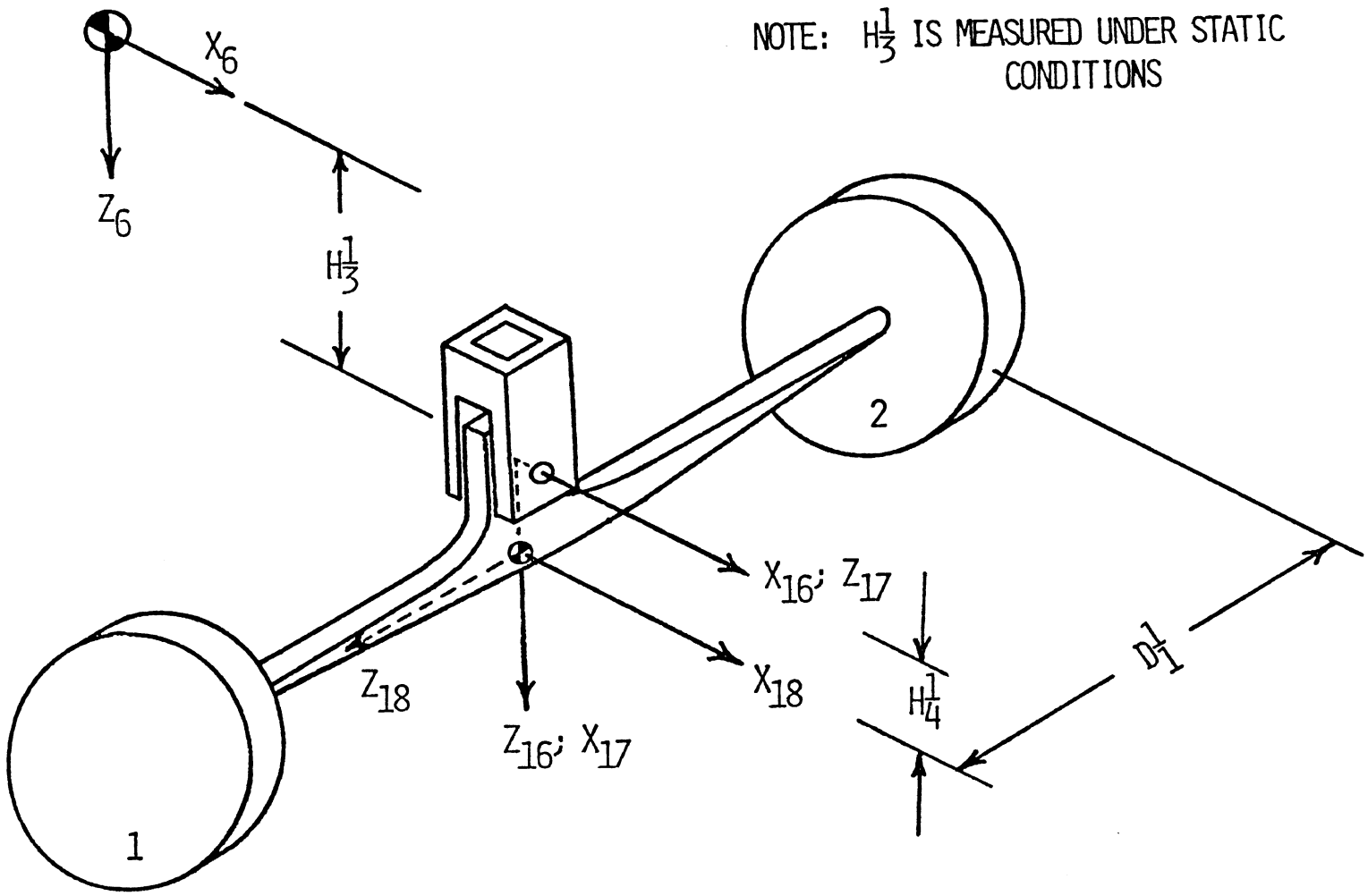

Figure 4. Beam-Axle Suspension System #1

Four additional beam-axle suspension systems are required in modeling the double. These suspension systems are similar to the one described above. Coordinate systems corresponding to those described above are defined for each suspension system.

The first semitrailer, Figure 5, of the double is modeled as a rigid body having mass. A guide is provided for attaching a suspension system similar to the one shown in Figure 4. A fifth wheel pin is provided for attachment of the semitrailer to the tractor fifth wheel, Figure 3. In addition, a pintle hook (modeled as a ball joint) is provided for attaching the dolly, Figure 6, to the semitrailer. Two body-fixed coordinate systems are used for the semitrailer. The origin of the first coordinate system, denoted $X_9Y_9Z_9$, is fixed to the semitrailer mass center. The origin of the second coordinate system, denoted $X_{10}Y_{10}Z_{10}$, is fixed to the pintle hook. These coordinate systems, along with the appropriate dimensions of semitrailer #1, are shown in Figure 5.

The second semitrailer of the double is similar to the one described above. The coordinate system corresponding to $X_9Y_9Z_9$ is $X_{15}Y_{15}Z_{15}$. A coordinate system corresponding to $X_{10}Y_{10}Z_{10}$ is not needed for modeling the double.

The dolly is modeled as a massless rigid body. A guide is provided for attaching a suspension system similar to the one shown in Figure 4. A fifth wheel pin is provided for attaching fifth wheel #2. This fifth wheel is similar to the one shown in Figure 3. In addition, the socket portion of the pintle hook is provided for attachment of the dolly to semitrailer #1. Two coordinate systems, denoted $X_{13}Y_{13}Z_{13}$ and $X_{25}Y_{25}Z_{25}$,

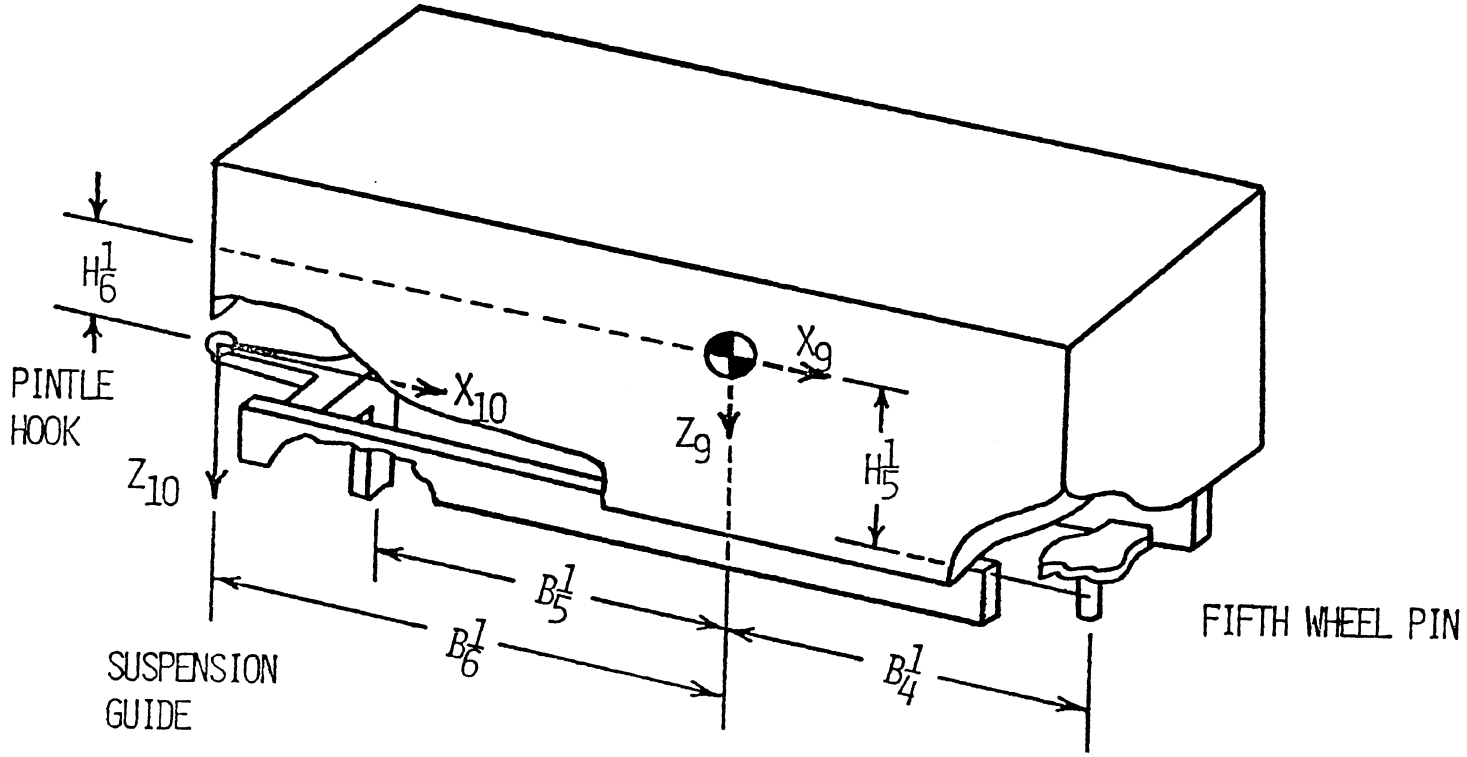

Figure 5. Semitrailer #1

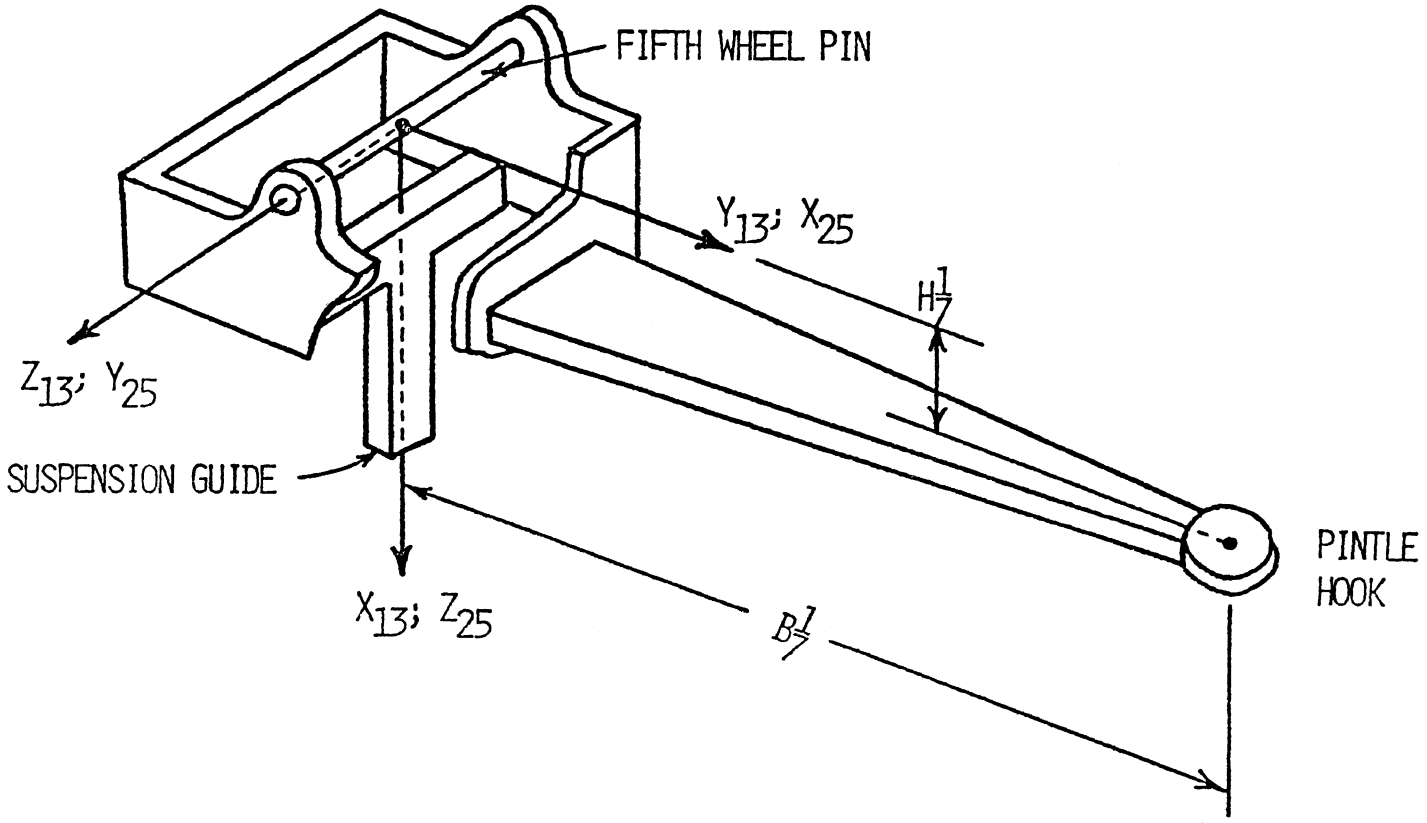

Figure 6. The Dolly

are fixed to the dolly fifth wheel pin. These coordinate systems and the dimensions of the dolly are shown in Figure 6.

Six additional coordinate systems are required to describe the double. The first coordinate system is the inertial coordinate system, denoted $X_0Y_0Z_0$. The origin of this coordinate system is located at the road surface. The X_0 axis is taken to be parallel to the longitudinal centerline of the tractor when the tractor is in its initial position at the beginning of a simulation. The Z_0 axis is directed vertically down. The remaining five coordinate systems are denoted $X_1Y_1Z_1$ - $X_5Y_5Z_5$. These coordinate systems are used to describe the translation and rotation of the tractor.

To complete the description of the vehicle for the computer, data on the dynamic characteristics of the elements and information on the external forces and moments which act on the vehicle must be provided. The dynamic characteristics are provided by means of "J" matrices. A "J" matrix for an element takes the form

$$J = \begin{Bmatrix} m & m\bar{x} & m\bar{y} & m\bar{z} \\ m\bar{x} & \frac{1}{2}(-I_{xx}+I_{yy}+I_{zz}) & I_{xy} & I_{xz} \\ m\bar{y} & I_{xy} & \frac{1}{2}(I_{xx}-I_{yy}+I_{zz}) & I_{yz} \\ m\bar{z} & I_{xz} & I_{yz} & \frac{1}{2}(I_{xx}+I_{yy}-I_{zz}) \end{Bmatrix}$$

where m is the mass element, $\bar{x}$, $\bar{y}$, $\bar{z}$ are the coordinates of the mass center of the element in its coordinate system, and I_{xx}, I_{xy}, etc., are the moments and products of inertia with respect to the same coordinate system.

The external forces and moments in the absence of aerodynamic effects consist of the gravitational forces, forces due to the tires, and moments due to the gyroscopic effects of the wheels. The gravitational forces are considered to be known external forces. The gyroscopic moments are determined from the spin speeds of the wheels. The spin speed of each wheel is computed using an analytical solution to the linearized equation for the angular acceleration of the wheel. The method used is taken from that of Bernard [5].

Evaluation of the spin speed for each wheel and determination of the forces due to the tires require the adoption of a tire-road interaction model. The model used is a modified form of that presented in [9]. The model gives the ratios of the lateral force to normal load and of the braking force to normal load as nonlinear functions of the tire slip and tire slip angle. Curves which show functional dependencies provided by the model and used for the work are given in Figures 7 and 8.

RESULTS

The method was used for comparing simulations of tractor-semitrailer behavior as given by three mathematical models. The first mathematical model was an existing modified Mikulcik model [1] (referred to as model 1) having massless beam-axle suspension systems. The second mathematical model (model 2) was that obtained using the subject method with massless beam-axle suspension systems. Each of these models had fourteen degrees of freedom (including the wheel spin degree of

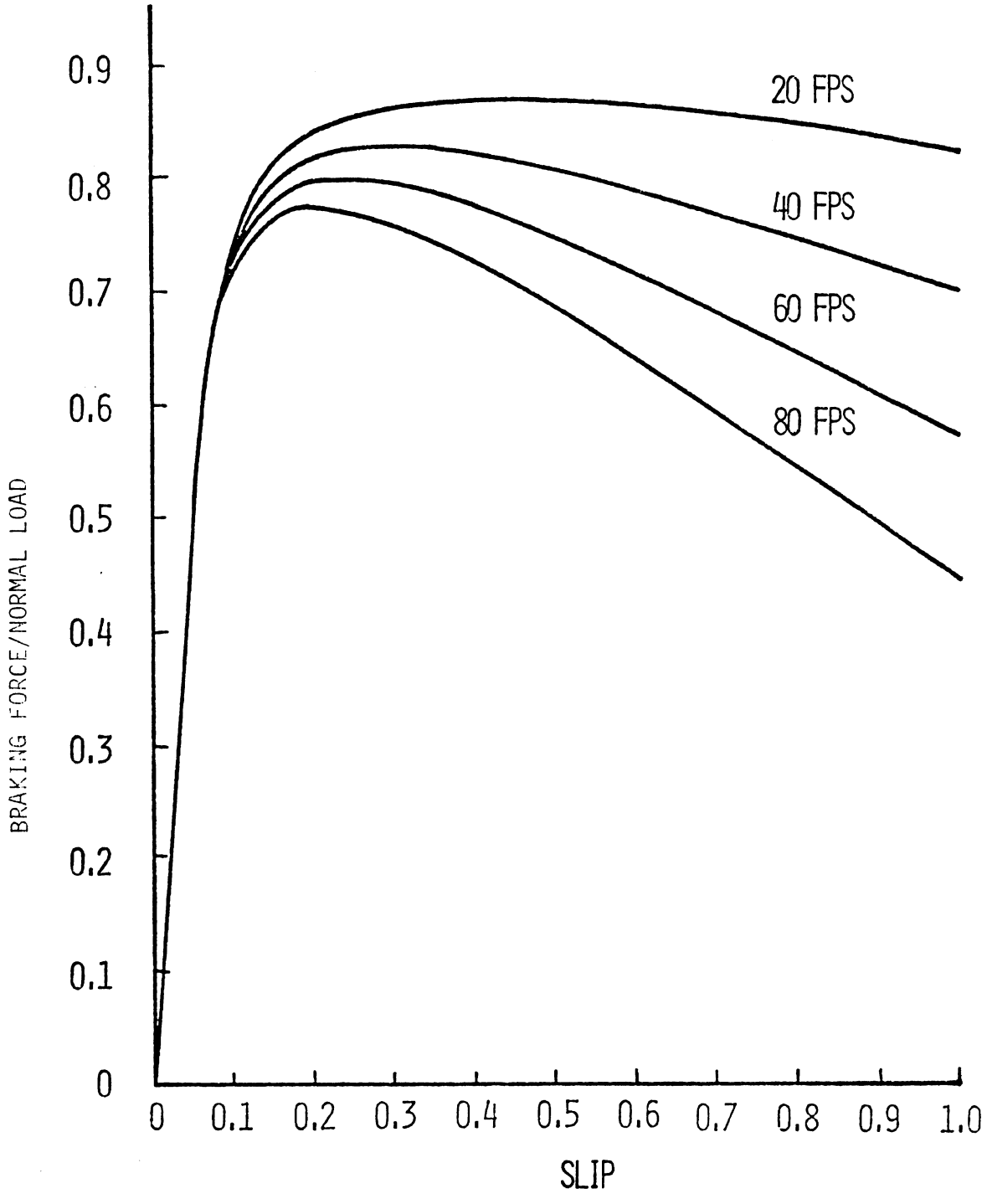

Figure 7. Truck Tire Mu-Slip Curves

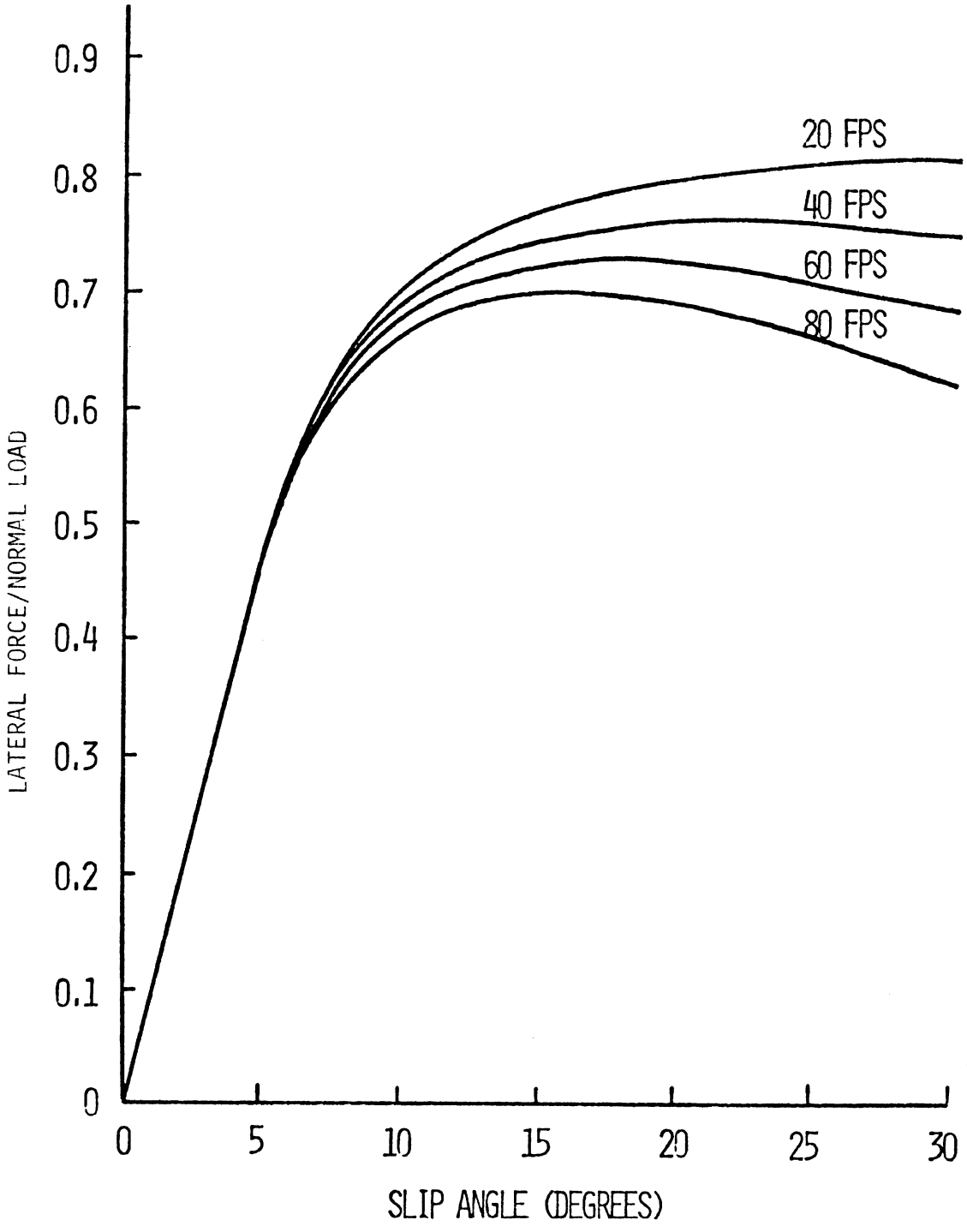

Figure 8. Truck Tire Mu-Slip Angle Curves

freedom). The third model (model 3) was that obtained using the subject method with beam-axles having mass. Model 3 had twenty degrees of freedom. The parameters for all three models are given in Table I. The values of these parameters were chosen to make models 2 and 3 as similar to model 1 as possible.

Each test started with the vehicle moving at a constant forward velocity of 88 fps. All other state variables were initially zero; i.e., the vehicle was moving in a steady state down a straight, level road. At time equal to zero seconds, a step steering angle of 0.01 radians was applied to the front wheels. No braking was applied.

The roll angle behavior versus time of the tractor as predicted by each of the three mathematical models is shown in Figure 9. Each model predicts that the tractor will roll to the outside of the turn. After 3.0 seconds, a nearly steady state value of roll angle has been reached. However, the roll angles predicted by models 2 and 3 are considerably greater than that predicted by model 1.

It can be shown with a static analysis that the steady state roll angle predicted by model 2 is correct (for a massless axle model). This indicates a previously undiscovered error in the Mikulcik analysis (model 1). The error is associated with neglecting gravitational terms in the equations of motion. Once a roll angle has developed, the gravitational force tends to increase the roll angle. For the vehicle and the maneuver considered, the roll angle produced by the gravitational force is approximately equal to that produced by lateral acceleration.

Table I

Vehicle Parameters for Model 1, Model 2, and Model 3

Note: Dimensions and characteristics are common to the three mathematical models except where noted. Exceptions are for Model 3 and are necessary to describe the mass distribution and tire model used.

Dimensions

B_1 = 4.15 ft.	H_1 = 1.00 ft.
B_2 = 6.65 ft.	H_2^1 = 0.25 ft.
B_3 = 4.55 ft.	H_3^1 = 0.03 ft. (.132133 for Model 3)
B_4^1 = 13.4 ft.	H_3^2 = 0.03 ft. (.129491 for Model 3)
B_5^1 = 11.6 ft.	H_3^3 = 4.38 ft. (4.48491 for Model 3)
	H_4^1 = 0.98 ft.
D_1^1 = 3.13 ft.	H_4^2 = 0.98 ft.
D_1^2 = 3.00 ft.	H_4^3 = 0.98 ft.
D_1^3 = 3.00 ft.	H_5^1 = 3.10 ft.

Suspension Dampers and Springs

c^1 = 800 lb. sec./ft.	k^1 = 24480 lb./ft.
c^2 = 2000 lb. sec./ft.	k^2 = 43200 lb./ft.
c^3 = 2000 lb. sec./ft.	k^3 = 43200 lb./ft.
C^1 = 2000 ft. lb. sec./rad.	K^1 = 61200 ft. lb./rad.
C^2 = 5480 ft. lb. sec./rad.	K^2 = 126000 ft. lb./rad.
C^3 = 5000 ft. lb. sec./rad.	K^3 = 108000 ft. lb./rad.

Tire Radius - 1.7 ft. front tires; 1.64 ft. all others

Tire Inertia (spin) - 7.81 slug-ft.^{2} axle 1
16.2 slug-ft.^{2} axle 2
15.6 slug-ft.^{2} axle 3

Tire Stiffness Model 3 - 53400 lb/ft. front tires; 90000 lb./ft. all others

Table I (Cont.)

Mass and Inertia - "J" Matrices (slugs or slug-ft.^{2})

Tractor Models 1 and 2

$$\begin{bmatrix} 442 & 0 & 0 & 0 \\ 0 & 4600 & 0 & -200 \\ 0 & 0 & 2900 & 0 \\ 0 & -200 & 0 & -2100 \end{bmatrix}$$

Tractor Model 3

$$\begin{bmatrix} 367 & 0 & 0 & 0 \\ 0 & 3285 & 0 & -200 \\ 0 & 0 & 1585 & 0 \\ 0 & -200 & 0 & -785 \end{bmatrix}$$

Semitrailer Models 1 and 2

$$\begin{bmatrix} 1041 & 0 & 0 & 0 \\ 0 & 111800 & 0 & -2100 \\ 0 & 0 & 8200 & 0 \\ 0 & -2100 & 0 & 200 \end{bmatrix}$$

Semitrailer Model 3

$$\begin{bmatrix} 979 & 0 & 0 & 0 \\ 0 & 107615 & 0 & -2100 \\ 0 & 0 & 4015 & 0 \\ 0 & -2100 & 0 & 4384 \end{bmatrix}$$

Axle 1 Model 3

$$\begin{bmatrix} 24.9 & 0 & 0 & 0 \\ 0 & -70.6 & 0 & 0 \\ 0 & 0 & 73.4 & 0 \\ 0 & 0 & 0 & 70.6 \end{bmatrix}$$

Axle 2 Model 3

$$\begin{bmatrix} 49.8 & 0 & 0 & 0 \\ 0 & -133 & 0 & 0 \\ 0 & 0 & 137 & 0 \\ 0 & 0 & 0 & 133 \end{bmatrix}$$

Axle 3 Model 3

$$\begin{bmatrix} 62.2 & 0 & 0 & 0 \\ 0 & -167 & 0 & 0 \\ 0 & 0 & 171 & 0 \\ 0 & 0 & 0 & 167 \end{bmatrix}$$

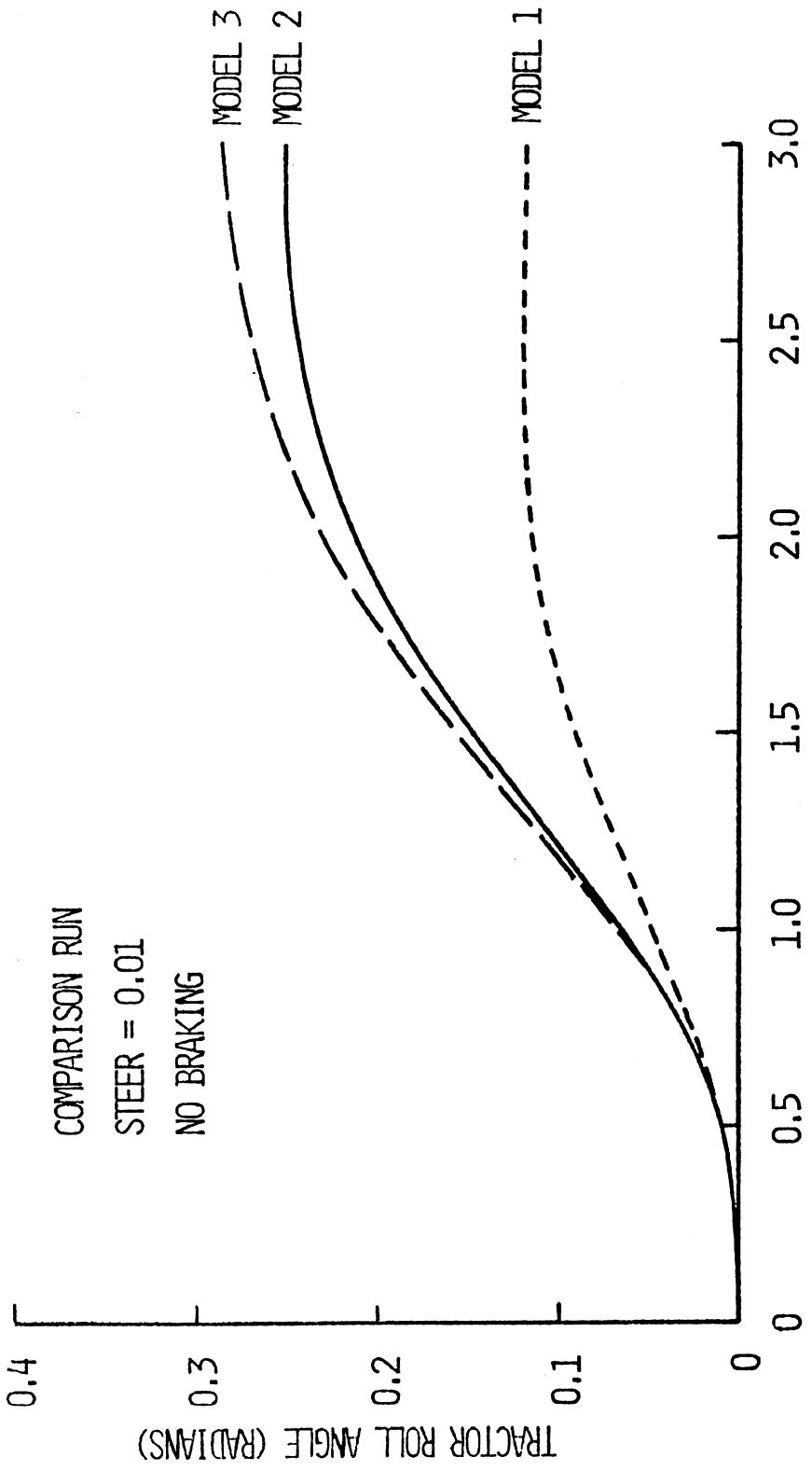

Figure 9. Comparison Run with No Braking: Tractor Roll Angle

The difference in roll angle behavior for models 2 and 3 is associated primarily with the tire stiffness necessary for a suspension system having mass. The effect of the tire stiffness is a decrease in roll stiffness of the vehicle. Hence, a higher roll angle is expected with model 3.

The tractor yaw rate versus time is shown in Figure 10. Tractor yaw rates rather than yaw angles are shown in order to better illustrate the differences between the responses predicted by the three models. The yaw rates attain nearly steady state values after 3 seconds. The difference among the transient responses shown can be explained as follows. The behavior of the semitrailer results in lateral forces acting at the tractor fifth wheel pin. These forces are directed to the outside of the turn and produce a corresponding clockwise yaw rate of the tractor. It can be shown that these forces decrease in magnitude as the vehicle accelerates in roll to the outside of the turn. Since the roll acceleration predicted by model 2 is initially greater than that for model 1, it is expected that the yaw rate of the tractor predicted by model 2 will be initially less than that predicted by model 1. This is shown to be true by Figure 10 at time equal to 1.0 second. At time equal to 2.0 seconds, the roll acceleration predicted by model 2 is less (i.e., it is more negative) than that predicted by model 1. Therefore, it is expected that the yaw rate of the tractor predicted by model 2 will be greater than that predicted by model 1. This is also shown to be true by Figure 10.

The effects of roll angle can be essentially eliminated by increasing the roll stiffness sufficiently. The roll stiffness used in models 1 and 2 was increased forty times—the roll damping rate was increased to

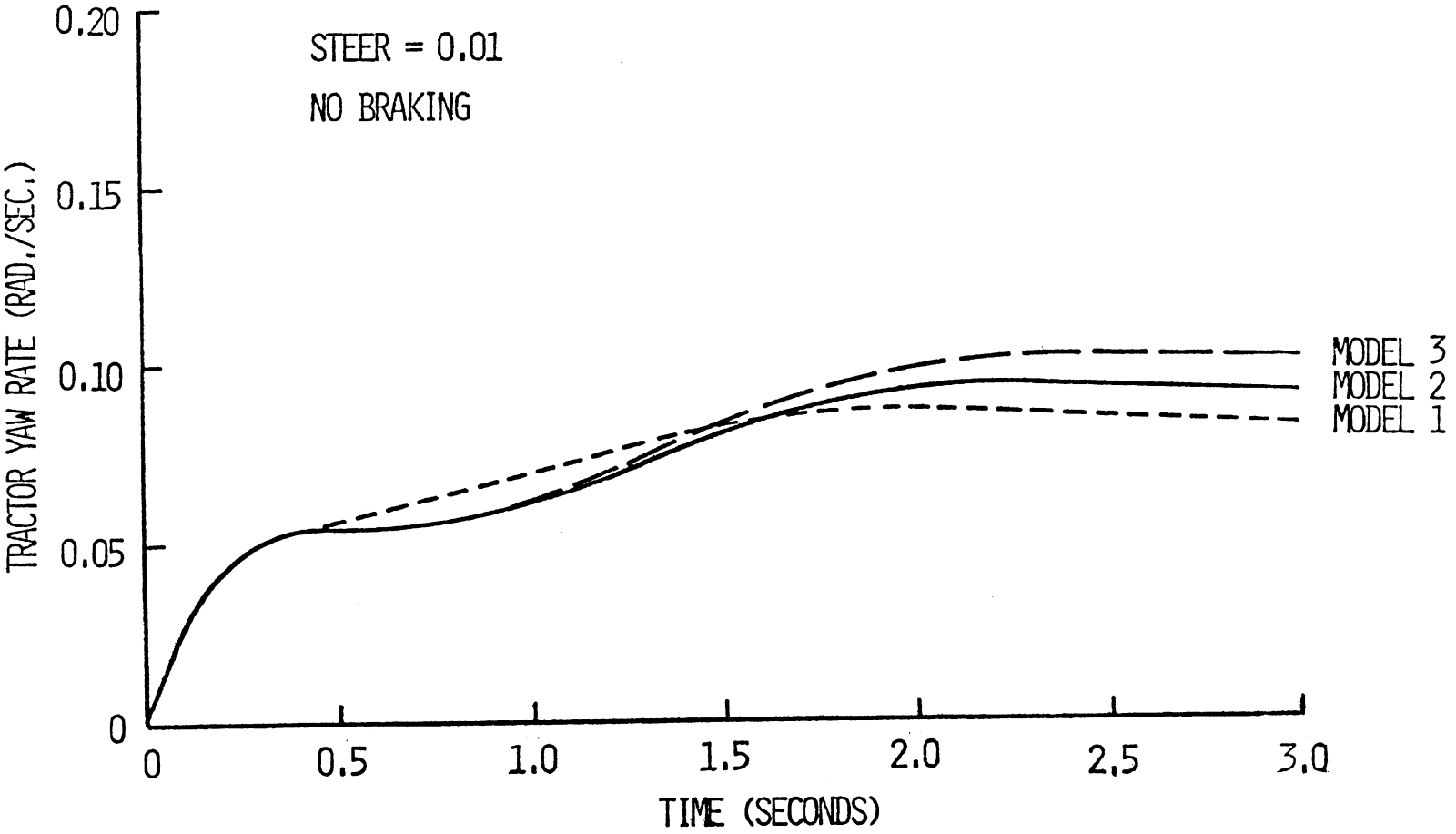

Figure 10. Comparison Run with No Braking: Tractor Yaw Rate

maintain a constant damping ratio. The resulting tractor roll angles of both models are similar to that shown for model 1 in Figure 9 except that they are approximately 40 times smaller. The tractor yaw rate response for both models is shown in Figure 11. The figure illustrates that the yaw rates predicted by models 1 and 2 are nearly identical. Similar statements can be made for the other quantities (articulation angle, etc.) that describe the behavior of the vehicle.

Braking comparison tests were also made. The conditions at the beginning of each test were similar to those before except that braking, increasing at a constant rate and proportional to the static wheel loads, was started at time equal to zero seconds. Results similar to those above were obtained [8]. Increasing the roll stiffness by a factor of 40 caused the behavior of models 1 and 2 to compare closely (small differences in behavior still existed because of simplifying assumptions made in the suspension analysis for model 1).

The results obtained above indicated that the method produced simulations which compared well with those from an accepted vehicle model. In addition, the differences obtained could be justified. As a result, it appeared useful to use the method for additional simulations of articulated highway vehicle behavior. A single, double, and triple were considered in the original work [8]—no-braking and braking cases were run. The results of the no-braking case and of the braking case for the triple are given below.

The model of the single used in [8] was the same as model 2 (above). This model had fourteen degrees of freedom. The model of the double was obtained by combining the model of the single with the model of the

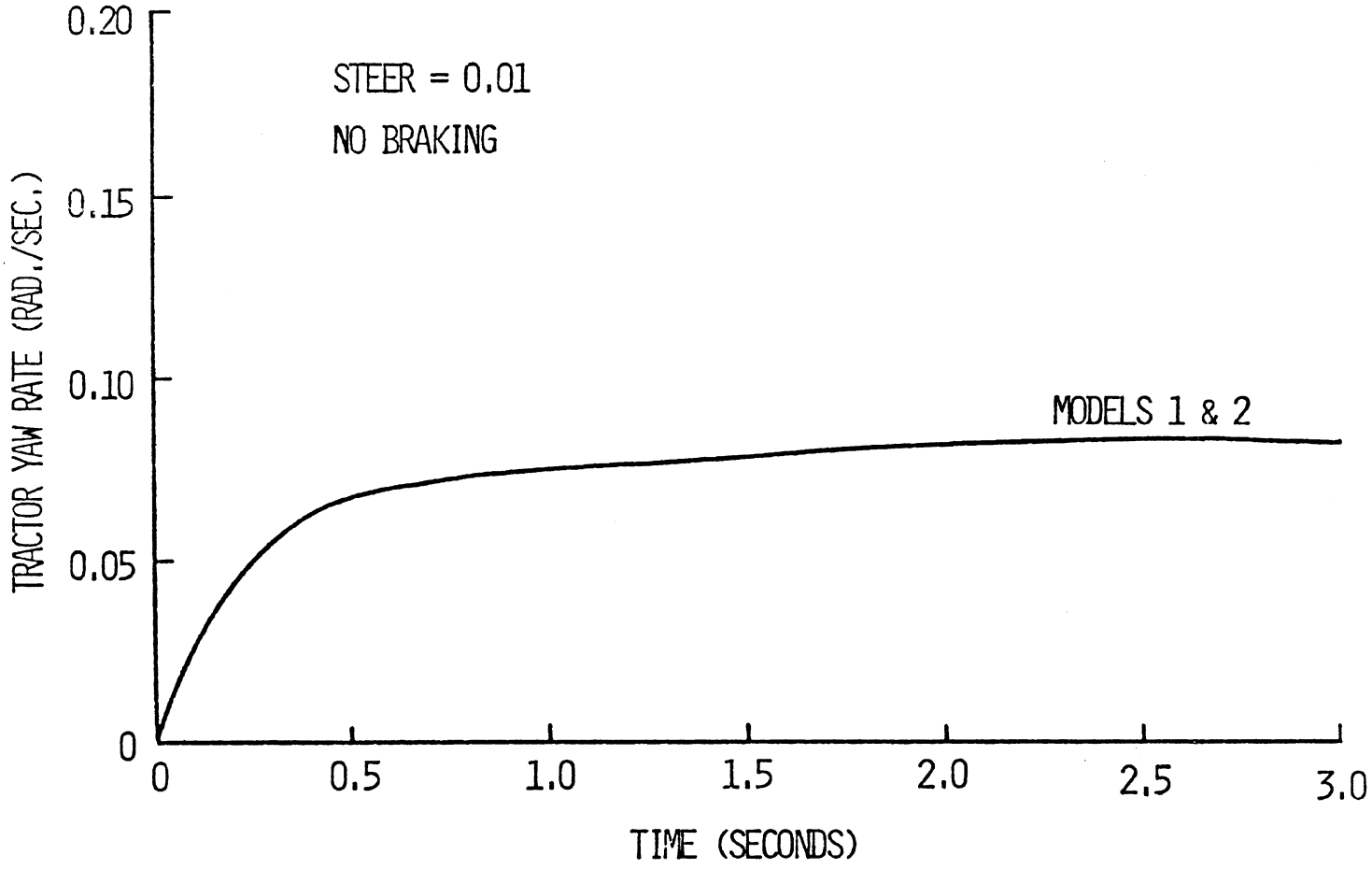

Figure 11. Comparison Run with No Braking and with High Roll Stiffness: Tractor Yaw Rate

massless dolly, Figure 6, and with the model of a second semitrailer identical to that of the first semitrailer. The model of the double had twenty-three degrees of freedom. The model of the triple was obtained by combining the model of the double with the model of a second dolly (identical to the first dolly) and with the model of a third semitrailer identical to that of the first semitrailer. The model of the triple had thirty-two degrees of freedom. Massless beam-axle suspensions were used on each vehicle. The three vehicles are quantitatively described in Table II.

The response of the triple to a step steering output of 0.004 radians at 88 fps is given in Figures 12 through 14. These figures also describe the behavior of the single and the behavior of the double; that is, the tractors of the three vehicles behaved nearly identically. Similar statements can be made for semitrailer #1 of each vehicle and for dolly 1 and semitrailer #2 of the double and of the triple. This situation appears to be due to the manner in which the dollies were modeled; i.e., they were modeled as being massless and as having their fifth wheels located directly over their beam-axle suspension systems. As a result, only small reaction forces existed at the pintle hooks of the double and triple. These reaction forces had an insignificant effect on the behavior of the semitrailers.

The yaw angles of the tractor and of the three semitrailers comprising the triple are shown in Figure 12. It can be seen from the figure that the tractor quickly assumes a nearly steady state (right) turn. The yaw angle behavior of each semitrailer is delayed when compared to that of the tractor. Also, decaying oscillations in the yaw angle behavior of each semitrailer are

Table II

Vehicle Parameters for the Single, Double, and Triple Dimensions

B_1	= 4.15 ft.	H_1	= 1.00 ft.
B_2	= 6.65 ft.	H_2^1	= 0.25 ft.
B_3	= 4.55 ft.	H_3^1	= 0.03 ft.
B_4^1	= 13.4 ft.	H_3^2	= 0.03 ft.
B_4^2	= 13.4 ft.	H_3^3	= 4.38 ft.
B_4^3	= 13.4 ft.	H_3^4	= 1.03 ft.
B_5^1	= 11.6 ft.	H_3^5	= 4.38 ft.
B_5^2	= 11.6 ft.	H_3^6	= 1.03 ft.
B_5^3	= 11.6 ft.	H_3^7	= 4.38 ft.
B_6^1	= 14.6 ft.	H_4^1	= 0.98 ft.
B_6^2	= 14.6 ft.	H_4^2	= 0.98 ft.
B_7^1	= 6.00 ft.	H_4^3	= 0.98 ft.
B_7^2	= 6.00 ft.	H_4^4	= 0.98 ft.
D_1^1	= 3.13 ft.	H_4^5	= 0.98 ft.
D_1^2	= 3.00 ft.	H_4^6	= 0.98 ft.
D_1^3	= 3.00 ft.	H_4^7	= 0.98 ft.
D_1^4	= 3.00 ft.	H_5^1	= 3.10 ft.
D_1^5	= 3.00 ft.	H_5^2	= 3.10 ft.
D_1^6	= 3.00 ft.	H_5^3	= 3.10 ft.
D_1^7	= 3.00 ft.	H_6^1	= 4.38 ft.
		H_6^2	= 4.38 ft.
		H_7^1	= 1.03 ft.
		H_7^2	= 1.03 ft.

Table II (Cont.)

Suspension Dampers and Springs

c^1 =	800 lb.-sec./ft.	k^1 =	24480 lb./ft.
c^2 =	2000 lb.-sec./ft.	k^2 =	43200 lb./ft.
c^3 =	2000 lb.-sec./ft.	k^3 =	43200 lb./ft.
c^4 =	2000 lb.-sec./ft.	k^4 =	43200 lb./ft.
c^5 =	2000 lb.-sec./ft.	k^5 =	43200 lb./ft.
c^6 =	2000 lb.-sec./ft.	k^6 =	43200 lb./ft.
c^7 =	2000 lb.-sec./ft.	k^7 =	43200 lb./ft.
C^1 =	2000 lb.-sec./rad.	K^1 =	61200 ft.-lb./rad.
C^2 =	5840 lb.-sec./rad.	K^2 =	126000 ft.-lb./rad.
C^3 =	5000 lb.-sec./rad.	K^3 =	108000 ft.-lb./rad.
C^4 =	5000 lb.-sec./rad.	K^4 =	108000 ft.-lb./rad.
C^5 =	5000 lb.-sec./rad.	K^5 =	108000 ft.-lb./rad.
C^6 =	5000 lb.-sec./rad.	K^6 =	108000 ft.-lb./rad.
C^7 =	5000 lb.-sec./rad.	K^7 =	108000 ft.-lb./rad.

Tire Radius - 1.7 ft. front tires; 1.64 ft. all others

Tire Inertia (spin) - 7.81 slug-ft.^{2} axle 1

16.2 slug-ft.^{2} axle 2

15.6 slug-ft.^{2} axle 3

Mass and Inertia - "J" Matrices (slugs or slug-ft.^{2})

Tractor

$$\begin{bmatrix} 442 & 0 & 0 & 0 \\ 0 & 4600 & 0 & -200 \\ 0 & 0 & 2900 & 0 \\ 0 & -200 & 0 & -2100 \end{bmatrix}$$

Semitrailers

$$\begin{bmatrix} 1041 & 0 & 0 & 0 \\ 0 & 111800 & 0 & -2100 \\ 0 & 0 & 8200 & 0 \\ 0 & -2100 & 0 & 200 \end{bmatrix}$$

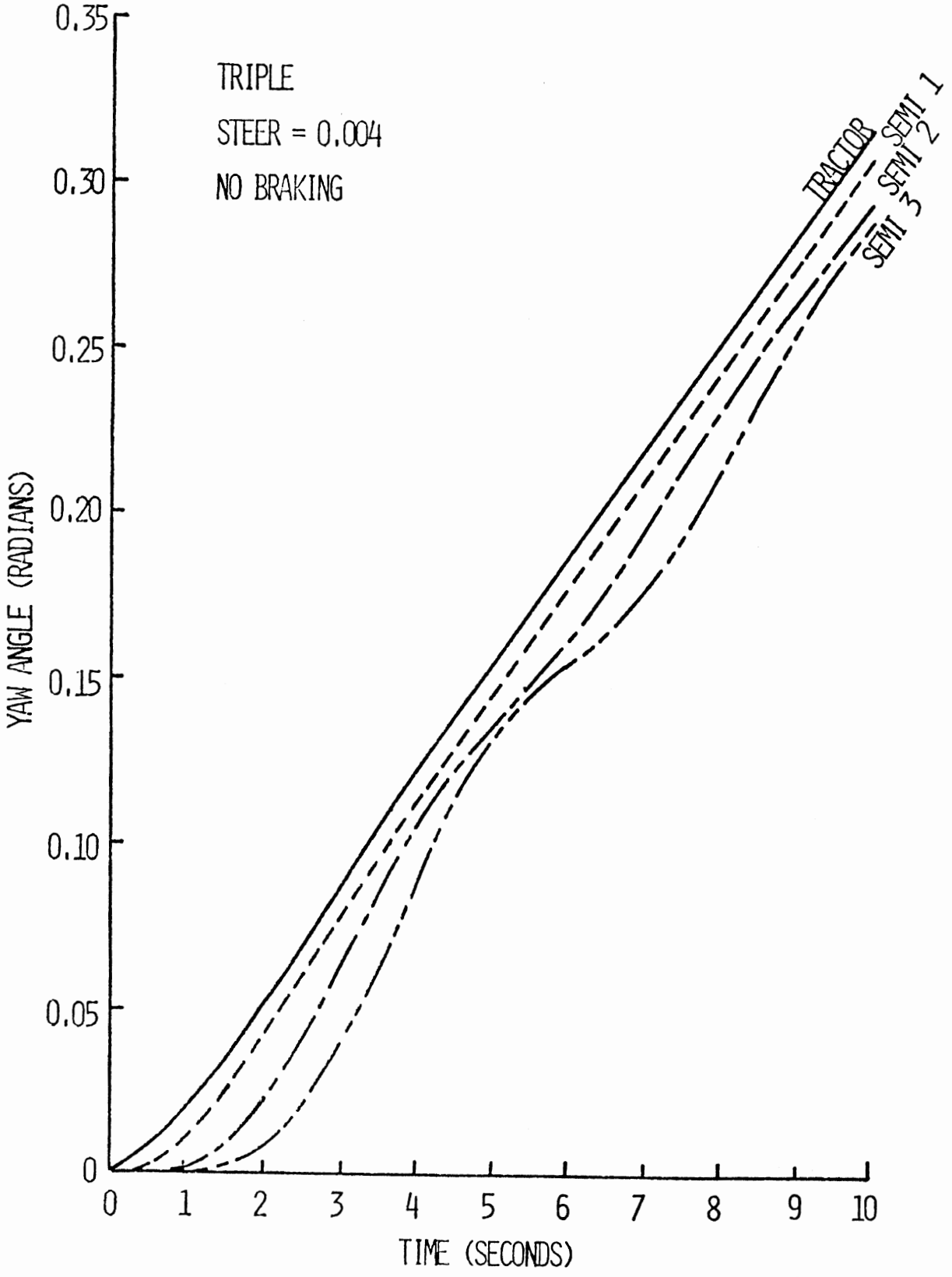

Figure 12. Triple with No Braking: Yaw Angles

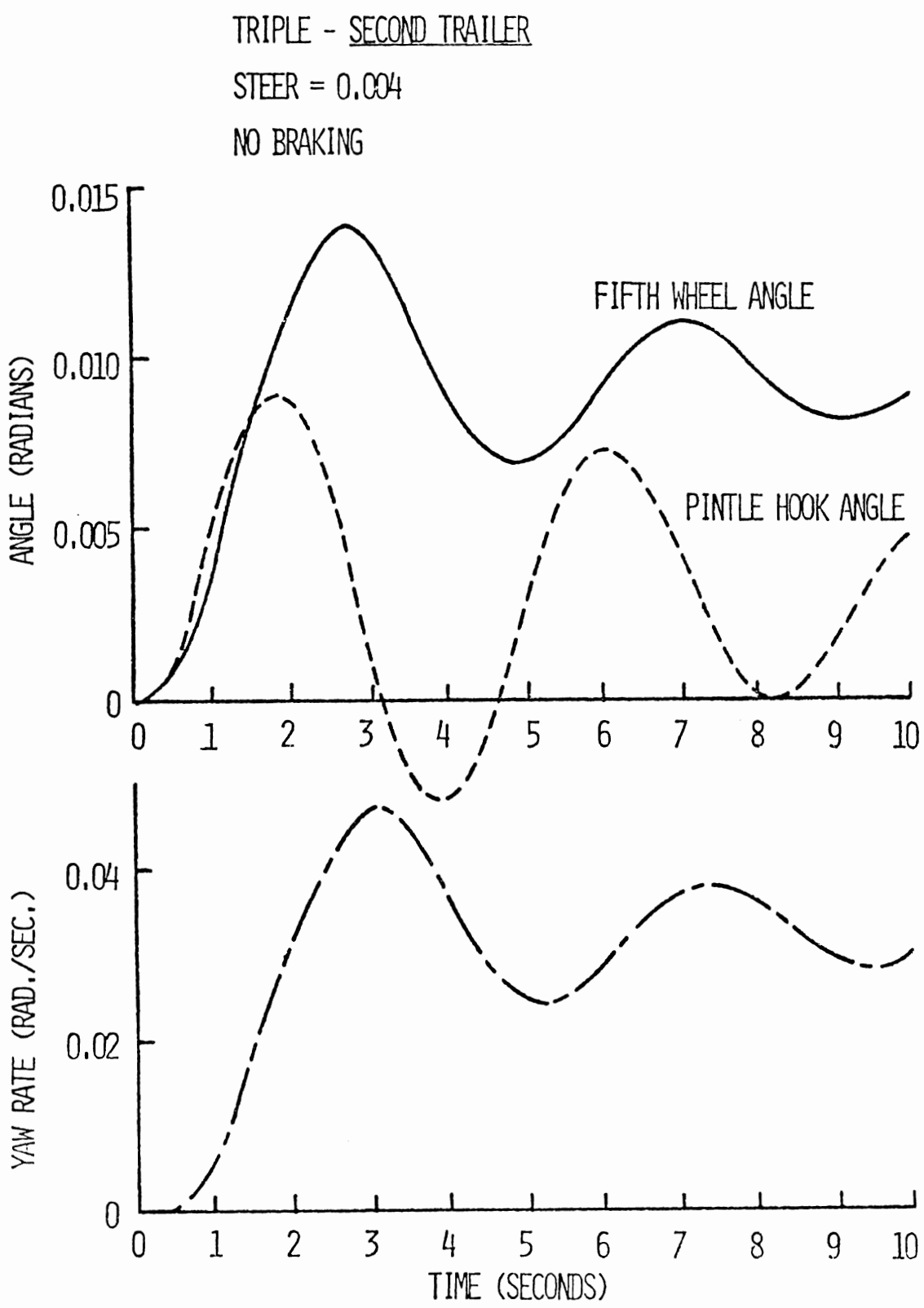

Figure 13. Triple with No Braking: Fifth Wheel Angle, Pintle Hook Angle and Yaw Rate for Trailer #2

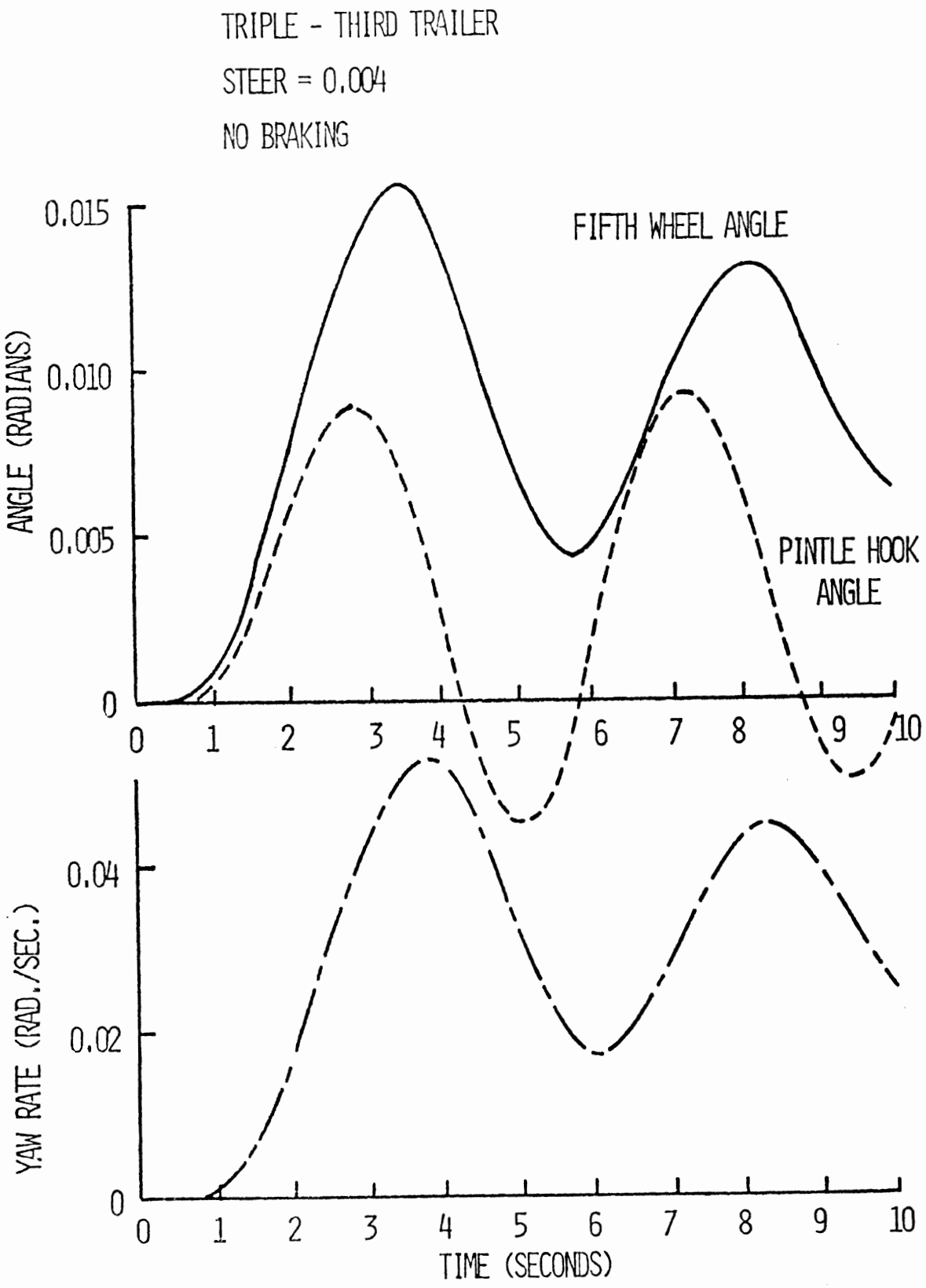

Figure 14. Triple with No Braking: Fifth Wheel Angle, Pintle Hook Angle and Yaw Rate for Trailer #3

apparent. The amplitude of these oscillations is greater and the decaying rate is smaller for the third semitrailer when compared to those for the second semitrailer (and to those for the second semitrailer when compared to those for the first).

The fifth wheel angle, the pintle hook angle, and the yaw rate of the second semitrailer are shown in Figure 13. The pintle hook angle is that associated with articulation of the dolly #1 with respect to semitrailer #1 (this angle is measured about axis Z_{10}, Figure 5). The fifth wheel angle is the angle of rotation of semitrailer #2 with respect to the fifth wheel of dolly #1. The curves in Figure 13 show that the pintle hook angle, the fifth wheel angle, and the yaw rate of semitrailer #2 have an oscillatory behavior. This behavior is explained as follows.

The pintle hook angle must result from the behavior of the dolly and/or from the behavior of semitrailer #1. The behavior of semitrailer #1 (after time equal to 4.0 seconds) is not oscillatory. Consequently, the behavior of the dolly is oscillatory; and since the dolly is massless, this oscillatory behavior must be due primarily to semitrailer #2. However, motion of the dolly due to the semitrailer #2 provides steering for this semitrailer. The interaction between the motion of the dolly and the motion of the semitrailer results in the oscillatory behavior of both.

The pintle hook angle, fifth wheel angle, and yaw rate of the third semitrailer versus time are shown in Figure 14. The curves show that the behavior associated with semitrailer #3 is similar to that associated with semitrailer #2. The frequencies of the oscillations

shown in Figures 13 and 14 are approximately the same. However, the amplitude of the behavior shown in Figure 14 is greater than that shown in Figure 13. This may be due to the effect that the motion of semitrailer #2 has on the motion of dolly #2.

The response of the triple when braking is applied along with the step steering is shown in Figures 15 through 17. The braking torque (ft-lbs) at each wheel is given by

$$T = R * (0.075 * P - 0.05) * W$$

where R is the wheel radius (ft), P is the brake line pressure (psi), and W is the static tire load (lbs). The pressure, P, was applied as a ramp input saturating at 100 psi at 1.0 seconds (a severe braking effort).

The yaw angle behavior of the triple is shown in Figure 15. The yaw angle curves of the tractor and of semitrailer #1 were found to be similar to corresponding curves obtained for a double having the same parameter values and inputs. The yaw behavior given for semitrailer #2 shows little tendency for semitrailer swing. Semitrailer #3 shows an unexpected tendency to yaw in a counterclockwise direction.

The fifth wheel angle for semitrailer #1, the pintle hook angle for dolly #1, and the fifth wheel angle for semitrailer #2 are shown in Figure 16. The curves in this figure were also found to be similar to those obtained for the corresponding double.

The pintle hook angle for dolly #2 and the fifth wheel angle for semitrailer #3 are shown in Figure 17. These curves indicate a severe clockwise buckling or jackknife of dolly #2.

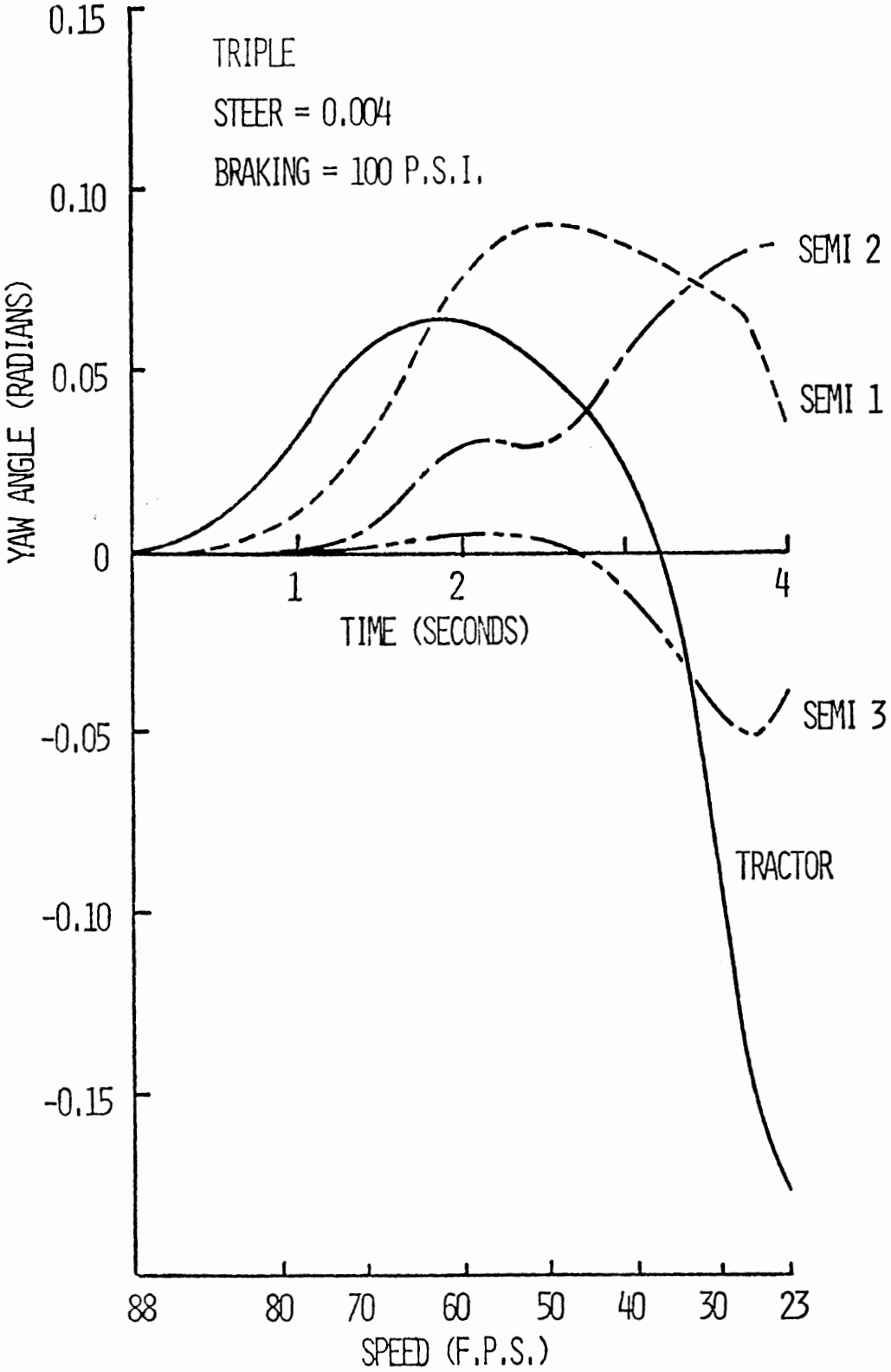

Figure 15. Triple with Braking: Yaw Angles

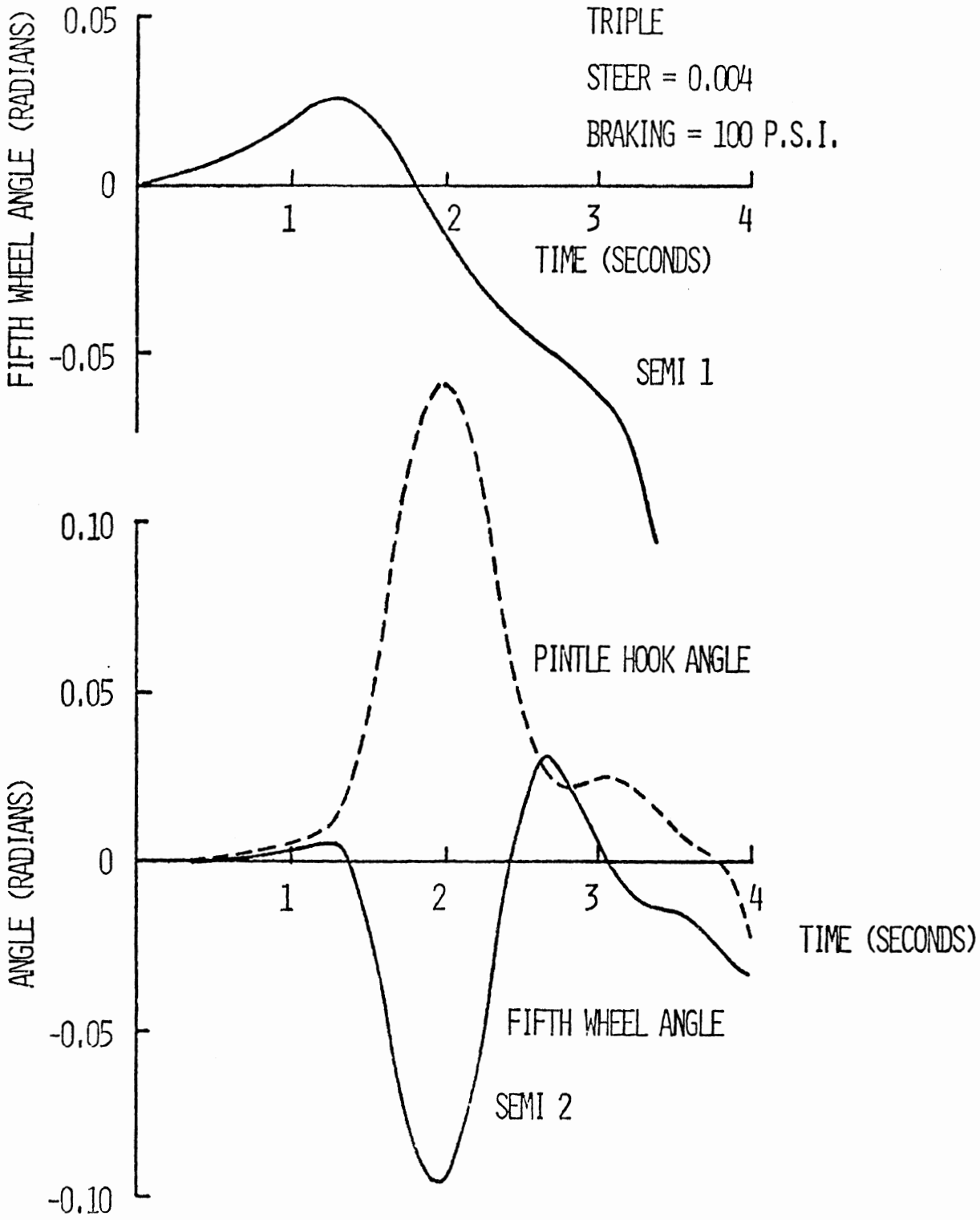

Figure 16. Triple with Braking: Fifth Wheel Angle for Trailer #1, and Fifth Wheel Angle and Pintle Hook Angle for Trailer #2

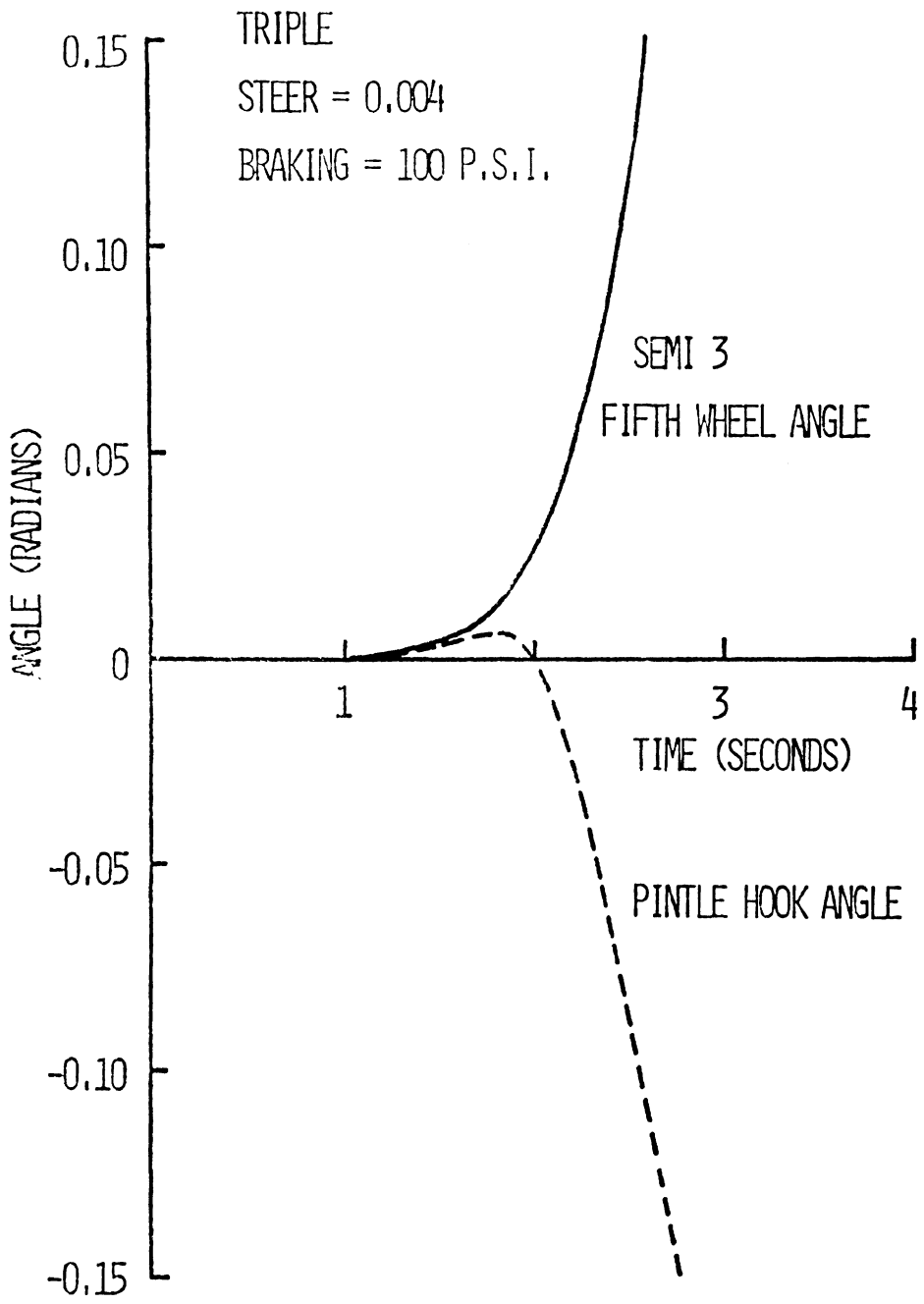

Figure 17. Triple with Braking: Fifth Wheel Angle and Pintle Hook Angle for Trailer #3

The behavior of the triple is explained as follows. In the beginning of the test, the applied braking effort is small and the vehicle has just entered the turn. Therefore, the lateral tire forces required for a stable vehicle behavior are within the capabilities of the tires. After 1.0 second, the maximum braking effort is attained. Forward weight shifts occur from semitrailer #3 to dolly #2 and from dolly #2 to the pintle hook of semitrailer #2. These weight shifts permit all wheels of semitrailer #3 and of dolly #2 to lock up.* The associated loss in dolly tire side forces allows the dolly to jackknife. The jackknifing tendency results from semitrailer #3 overrunning semitrailer #2. There is no semitrailer swing since the lateral acceleration of semitrailer #3 is small during the duration of the test.

The weight shifts from semitrailer #3 to semitrailer #2 increase the vertical tire loads of semitrailer #2. This is a stabilizing condition for semitrailer #2; hence, there is little tendency for swing of that semitrailer. The weight shifts from semitrailer #2 to semitrailer #1 increase the vertical tire loads of semitrailer #1. This is a stabilizing condition for the lateral behavior of semitrailer #1. The unusual tractor behavior is explained by the loss of braking effort (due to wheel lockup) on semitrailer #2. This loss in braking effort results in the overrunning of the tractor by the semitrailers. Hence, the vehicle train is susceptible to buckling. Also, the tractor right rear wheel is locked up (resulting from weight shifts due to tractor roll). The loss in braking effort at this wheel causes a tendency of the tractor to yaw in a counterclockwise direction.

---

*This situation did not occur for the corresponding double. For the double only one dolly tire locked up.

Once this yaw has begun, the vehicle train buckles at the tractor fifth wheel. This buckling is indicated by the large negative fifth wheel angle for semitrailer #1 shown in Figure 17.

CONCLUSIONS

The results illustrate the ease with which the method can be applied to the complex, nonlinear vehicle system. If the above results were obtained using conventional methods, many man-years of effort would have been required. The results given do not represent an exhaustive investigation of the behavior of articulated vehicles. Rather, the results show how a vehicle having multiple trailers could behave under a specific set of conditions. In addition, the results demonstrate the ease in obtaining the simulated behavior of many different types (configurations) of vehicles.

REFERENCES

1. Mikulcik, E.C., "The Dynamics of Tractor-Semi-trailer Vehicles: The Jackknifing Problem," Ph.D. Dissertation, Cornell University, 1968, Condensed Version in SAE Transactions, Paper No. 700371.

2. Tobler, W.E. and Krauter, A.I., "Tractor-Semi-trailer Dynamics: Design of the Fifth Wheel," Vehicle Systems Dynamics, International Journal of Vehicle Mechanics and Mobility, Vol. 1, No. 2, November 1972.

3. Vincent, R.J. and Krauter, A.I., "Tractor-Semi-trailer Handling: A Dynamic Tractor Suspension Model," Commercial Vehicle Engineering and Operations Meeting, Chicago, Illinois, June 1973, SAE Paper 730653.

4. Eshleman, R.L. and Desai, S.D., Articulated Vehicle Handling, I.I.T. Research Institute, Final Report for Period July 1971-March 1972, April 1972.

5. Bernard, J.E., "A Digital Computer Method for the Prediction of Braking Performance of Trucks and Tractor-Trailers," SAE Paper No. 730181, January 1973, SAE Transactions, 1973.

6. Denavit, J. and Hartenberg, R.S., "A Kinematic Notation for Lower-Pair Mechanisms Based on Matrices," Journal of Applied Mechanics: Transactions of the ASME, June 1955, pp. 215-221.

7. Uicker, J.J., Jr., "Dynamic Behavior of Spatial Linkages Part 1 - Exact Equations of Motion; Part 2 - Small Oscillations About Equilibrium," Journal of Engineering for Industry: Transactions of the ASME, February 1969, pp. 251-265.

8. Tobler, W.E., "General Rigid Body Dynamics and Application to Vehicle Behavior," Ph.D. Dissertation, Cornell University, 1974.

9. Dugoff, et al., "Tire Performance Characteristics Affecting Vehicle Response to Steering and Braking Control Inputs," Highway Safety Research Institute, University of Michigan, August 1969.

THE INFLUENCE OF TIRE MODELING IN COMMERCIAL VEHICLE SIMULATION

C.G. Shapley
The Firestone Tire & Rubber Company

NOTATION

D	Differential operator
DEL	Tire lateral deflection
F_Y	Side force produced at tire
H	Height from roll center to vehicle c.g.
I_X	Roll inertia
K_Y	Lateral tire stiffness
$K\alpha$	Change in preferred direction of rolling with lateral deflection
$K\theta$	Suspension roll stiffness
$K\phi$	Roll steer coefficient
M	Vehicle mass
P	Roll velocity
U	Forward velocity
V	Lateral velocity
V_{AX}	Axle lateral velocity
θ	Roll angle
α	Angle between wheel plane and preferred direction of rolling

INTRODUCTION

Over the years a considerable amount of time and money has been spent on preparing mathematical models of road vehicles. These models were generally developed by applying techniques employed in the aerospace industry for the predictions of motions of aircraft, etc.

Some of the models produced have been extremely elaborate, involving the motions of many masses coupled in a complex fashion. In addition to representing the motion of the vehicle efforts have also been made to include complex subsystems such as antilock brakes, and even humans.

Reference 1 summarizes the mathematical models of articulated vehicles which were available a few years ago and describes their complexity.

Such complex models can predict accurately the effect of applying a known force or couple to the vehicle and their accuracy rests primarily upon the precision with which the external forces are represented.

External forces upon road vehicles are of two sorts:

Aerodynamic loadings

Tire forces

Depending upon the operating conditions the aerodynamic loads may or may not be significant. There can be little doubt however that the tire forces are dominant. Consequently any failure to accurately represent the tires will be reflected in unreliable predictions by the mathematical models.

Shortcomings in the representation of tires may be either quantitative or qualitative. In the first case a computed force may be in error by some percentage. The sensitivity of the model to such errors may be

checked and the consequences of such errors predicted and allowed for. Erroneous analysis involving qualitative errors, on the other hand, can affect the predications in a much more serious way. The errors produced may be such that the nature of the prediction is wrong. Such an analysis may predict a damped oscillatory motion when a more accurate analysis predicts an unstable motion. Unfortunately there is no simple technique for investigating the effects of qualitative errors. Therefore it is essential that the mathematical representation of tires should reflect the various processes in a tire which leads to the generation of lateral forces.

Traditionally the generation of lateral forces in tires has been attributed solely to slip angles. Using this approach the tires were assumed to produce lateral forces "instantaneously" upon application of a slip angle. Additionally the tire is assumed to be infinitely "stiff" in the lateral sense. Such models of tires have been employed with some success in predicting the motions of automobiles. Reference 2 describes a vehicle simulation employing a "slip angle" tire model and experiments designed to validate this simulation.

However, automobiles and trucks are different and the approximations which work for an automobile may not work for a truck.

It is the objective of this paper to determine whether or not a form of tire representation based solely on "slip angles" is valid for commercial vehicles.

TIRE MECHANICS

In order to examine the effects of the approximation involved in the "slip angle" tire model, it is necessary to have a tire model which does not contain these approximations.

In addition the tire model should reflect the processes in a tire that determine its behavior.

With the qualifications that the tire is freely rotating at a frequency well below any of its resonant frequencies, two main processes may be identified in the tire:

a) the production of forces by deformation of the structure of the tire
b) the modification of lateral distortion due to changes in preferred direction of rolling, produced by lateral deflection of the tire

Restricting these effects to small amplitudes allows them to be treated as linear relationships, with the following constants.

1. K_Y - the lateral tire stiffness in units of force per unit lateral deflection
2. $K\alpha$ - the change in preferred direction of rolling in radians per unit lateral deflection

Implicit in the small amplitude assumption is that the tire is not sliding. In addition it is assumed that the vertical compliance of the tire is lumped in with the suspension stiffness and that coupling between vertical deflection and lateral characteristics is "small".

These parameters may be related to the traditional cornering force coefficient (C_F) as

$$C_F = \frac{-K_Y}{K\alpha} \qquad (1)$$

Figure 1 shows the geometrical features of the rolling tire where DEL is the lateral deflection and α gives the preferred direction of rolling. Given a forward velocity of the wheel plane the front edge of the contact patch moves towards the wheel plane as

$$\dot{DEL} = -U \cdot \alpha \tag{2}$$

But the direction of rolling is related to lateral deflection, therefore

$$\dot{DEL} = -U \cdot DEL \cdot K\alpha \tag{3}$$

If the wheel plane is allowed to move lateral with velocity (V) then

$$\dot{DEL} = V - U \cdot DEL \cdot K\alpha \tag{4}$$

Equation (4) shows that at zero forward velocity the tire will deform laterally as a consequence of sideways motions of the rim and that at a steady state condition ($\dot{DEL} = 0$)

$$DEL \cdot K\alpha \tag{5}$$

or

$$\alpha = \frac{V}{U} \tag{6}$$

The relationship between lateral deflection and side force completes the time varying description of the tire. It is:

$$F_Y = K_Y \cdot DEL \tag{7}$$

Although equations (4) and (7) are limited by the assumptions described above they do embody the original observations made about the rolling tire and are qualitatively different to the more usual slip angle approach.

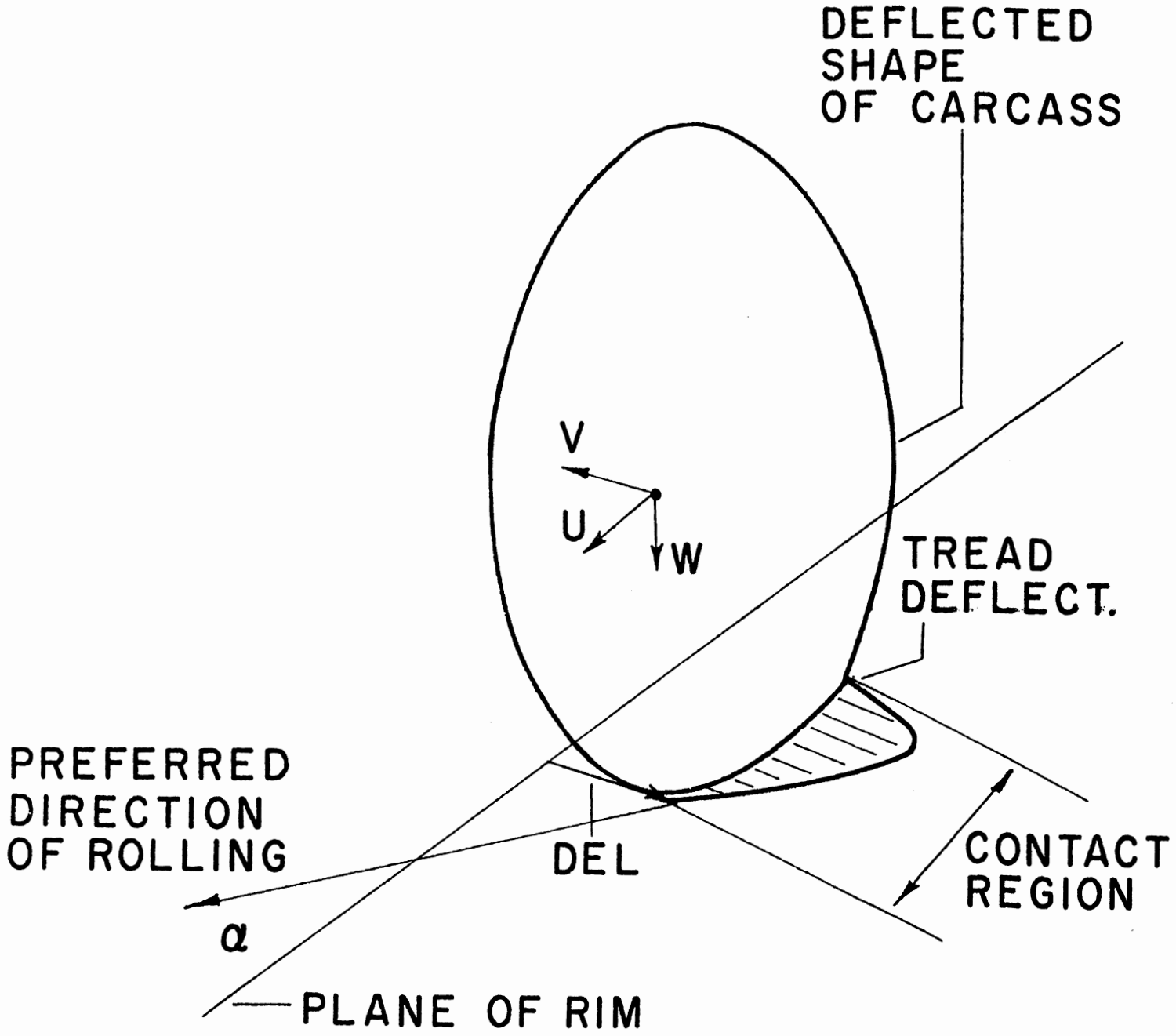

FIGURE I
GEOMETRY OF ROLLING TIRE

SUSPENSION EFFECTS

The tires of the vehicle are attached via the suspension. As the vehicle rolls and moves the geometry of the suspension changes. This changing suspension geometry has the effect of converting any one vehicle motion into a variety of effects at the tires. For example as the vehicle rolls this produces a sideways motion of the axle and a steering of the axle.

This steering of the axle in response to vehicle roll is referred to as "Roll Steer" and is produced by the suspension and the inclination of the vehicle roll axis as in Figure 2.

In the vehicle shown in Figure 3 the rotation and sideways velocity of the center of gravity combine to produce a lateral axle motion (V_{AX}) where

$$V_{AX} = V - P \cdot H \tag{8}$$

Since the roll of the body steers the axle there is also a component of forward velocity present due to roll steer

$$V_{AX} = V - P \cdot H + U \cdot K\phi \cdot \theta \tag{9}$$

To examine the importance of tire mechanisms in vehicle dynamics the rolling motion of the vehicle in Figure 3 will be analyzed.

Equations (1) - (9) describe the tire and suspension effects present in the road vehicle. In addition equations are needed relating the tire forces to the vehicles acceleration. They are:

$$I_X \cdot \dot{P} = K\theta \cdot \theta - H \cdot K_Y \cdot DEL \tag{10}$$

$$M\dot{V} = K_Y \cdot DEL \tag{11}$$

Combining (10) and (11) with (3) and (7) allows the equation to be assembled in matrix form:

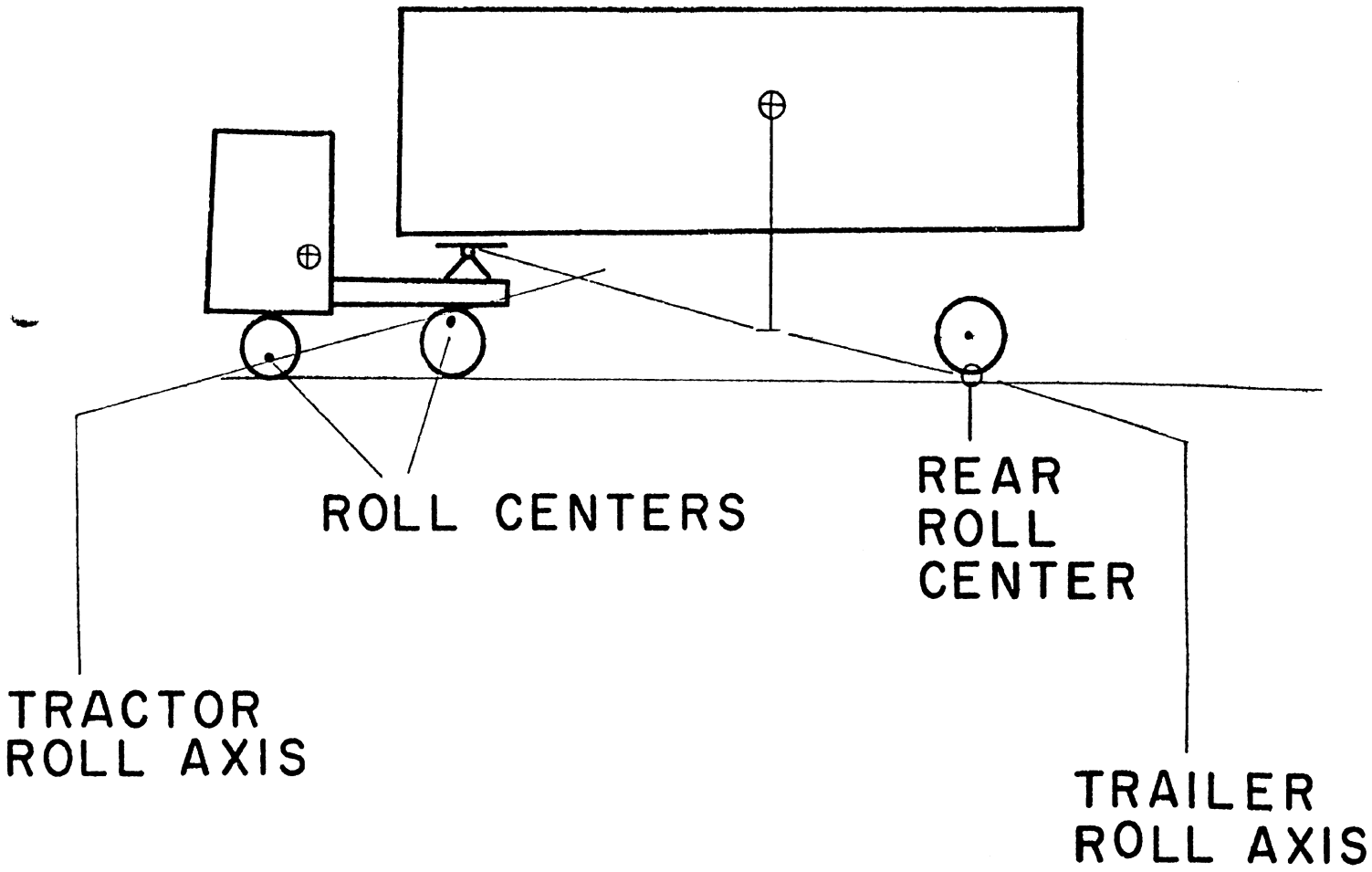

FIGURE 2
ROLL AXES OF AN
ARTICULATED VEHICLE

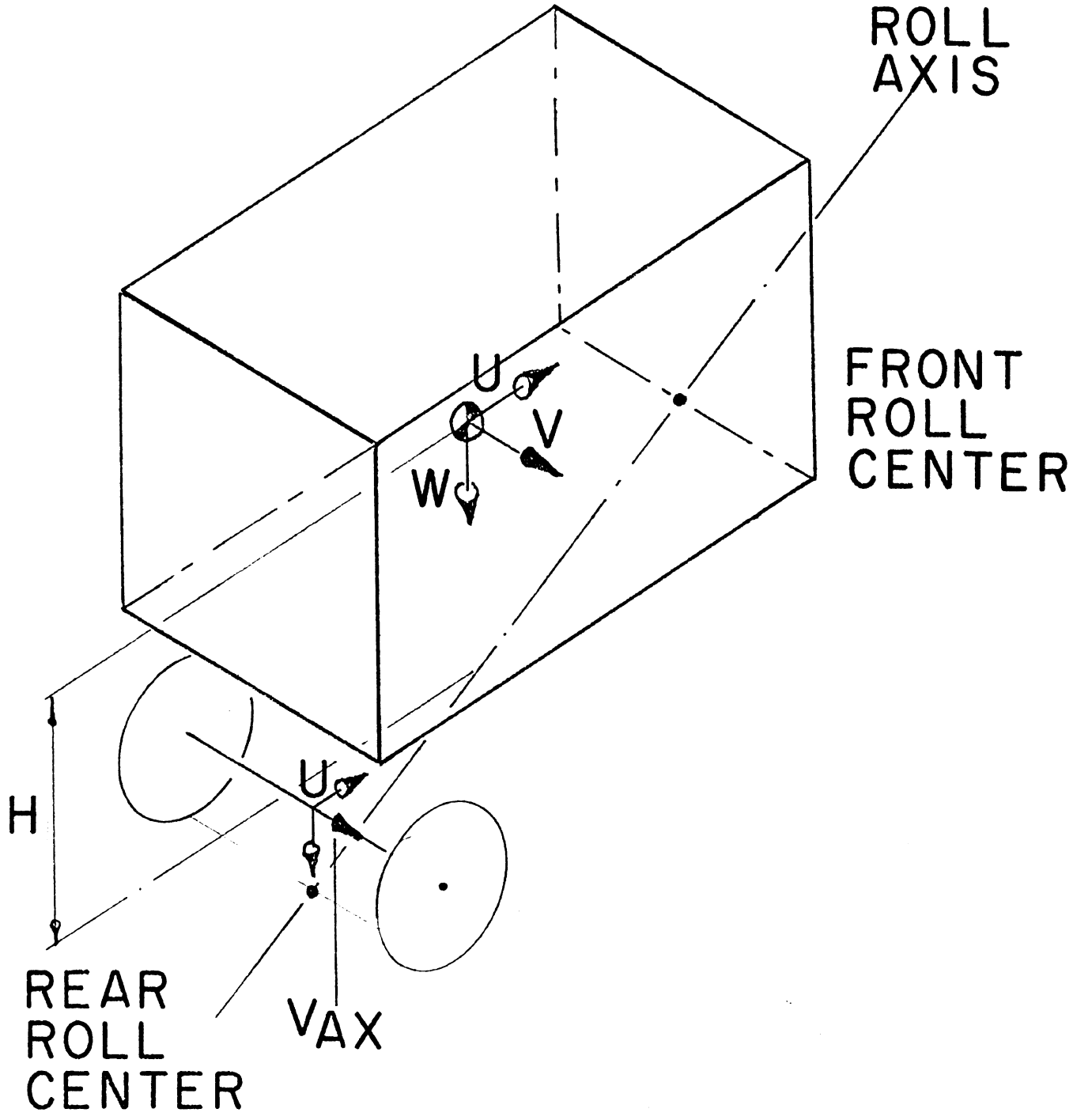

FIGURE 3

AXES USED IN TRAILER ANALYSIS

$$\begin{vmatrix} D + UK_\alpha & DH - UK\phi & -1 \\ \frac{K_Y \cdot H}{I_X} & D^2 - \frac{K\theta}{I_X} & 0 \\ \frac{-K_Y}{M} & 0 & 0 \end{vmatrix} \cdot \begin{vmatrix} DEL \\ \theta \\ V \end{vmatrix} = 0 \qquad (12)$$

where D is the differential operator. Equation (12) may be expanded as:

$$D^4 + U \cdot K\alpha D^3 - \left[+ \frac{K\theta}{I_X} + \frac{K_Y}{I_X} \cdot H^2 + \frac{K_Y}{M} \right] \cdot D^2$$

$$- \left[\frac{K\alpha \cdot K\theta}{I_X} - \frac{K\phi K_Y}{I_X} \cdot H \right] U \cdot D + \frac{K\theta \cdot K_Y}{M \cdot I_X} = 0 \qquad (13)$$

The equivalent expression for the slip angle based analysis is given by dividing (13) by K_Y then using the equation (1) and letting K_Y become infinite. This yields:

$$\frac{-U \cdot D^3}{CF} - \left[\frac{H^2}{I_X} + \frac{1}{M} \right] \cdot D^2 + \left[\frac{K\theta}{CF \cdot I_X} + \frac{K\phi \cdot H}{I_X} \right] U \cdot D + \frac{K\theta}{M \cdot I_X} = 0 \qquad (14)$$

Tabulating the coefficients of the two characteristic equations gives Table I.

In Table I it can be seen that the two series differ in coefficients of the fourth and second powers of the differential operator. With the highest order operator in the slip angle based analysis being three this means that it has only one mode of oscillation where the laterally flexible tire model has two.

The difference in the second power coefficient means that the predictions of stability will be different.

TABLE I

COEFFICIENT OF CHARACTERISTIC EQUATIONS

ORDER OF OPERATOR	FLEXIBLE TIRE MODEL	SLIP ANGLE MODEL
4	1	0
3	UK_α	$\frac{-U}{CF}$
2	$\frac{-K_\theta}{I_X} - \frac{K_\gamma \cdot H^2}{I_X} - \frac{K_\gamma}{M}$	$-\frac{H^2}{I_X} - \frac{1}{M}$
1	$-U\left[\frac{K_\alpha K_\theta}{I_X} - \frac{K_\phi \cdot K_\gamma}{I_X} \cdot H\right]$	$U\left[\frac{K\theta}{CF \cdot I_X} + \frac{K\phi H}{I_X}\right]$
0	$\frac{K_\theta \cdot K_\gamma}{M \cdot I_X}$	$\frac{K_\theta}{M \cdot I_X}$

In addition to these gross differences there will also be changes in the indicated values of roll frequency and damping.

These differences are illustrated by an example.

SPECIMEN VEHICLE

Figure 2 shows a semitrailer which has the dimensions given in Table II. The roll axis inclination is due to the difference in height between the rear roll center and the fifth wheel coupling. It should be noted that the tire lateral stiffnesses relate to the lumped values for all of the tires on one axle. Although the data used in these calculations are not meant to represent a specific vehicle, they are within the bounds of current design practice.

Table III contains the roots for the system at different values of tire lateral stiffness.

DISCUSSION

Table III shows that including various amounts of tire lateral flexibility affects both the predicted roll frequency and damping.

Reducing tire lateral stiffness reduces the predicted roll frequency. Omitting the tire lateral flexibility introduces a 10% error into the roll frequency and 20% in the damping.

Similarly increasing the lateral flexibility ten fold, approximately halves the roll frequency and damping.

TABLE II

ESTIMATED DATA FOR TRAILER

	Symbol	Value	Units
Mass	M	1000	Slug.
Inertia	I_X	9000	Slug·Ft^2
Roll Stiffness	K_θ	-4×10^6	Ft.Lbs/Rad
Lateral Tire Stiffness	K_Y	-200 000	Lbs/Ft
Height of CG from Roll Axis	H	8	Ft
Change in Preferred Direction of Rolling	K_α	1	Rads/Ft
Roll Steer	K_ϕ	-.2	Rads/Rad

TABLE III

ROOTS FOR ROLLING MOTION OF SPECIMEN TRAILER

U Speed ft/sec	Roots for Roll Motion*		
	$K\alpha = .1$ $K_Y = 2 \times 10^4$	$K\alpha = 1$ $K_Y = 2 \times 10^5$	Slip Angle Model $K_Y = \infty$
0	±3.87 j	±6.6 j	±7.3 j
20	-.68 ±3.82 j	-1.9 ±6.5 j	-2.25 ±7.17 j
40	-1.3 ±3.6 j	-4.2 ±5.7 j	-5.5 ±6.47 j
60	-2.1 ±3.3 j	-7.1	-5 ±7.29 j
80	-2.8 ±2.75 j	-3.5	-3.14
100	-3.54 ±1.74 j	-2.4	-2.37

*When the mode has two real roots, the more positive one is shown.

These changes in roll frequency imply changes in the steady-state roll angle measured when cornering. The 10% error in frequency due to omission of tire lateral flexibility would lead to a 20% error in roll angle.

These results indicate the importance of including tire lateral flexibility when calculating roll behavior. In particular, the results show that the roll stability may be enhanced by proper tire selection.

CONCLUSIONS

It has been shown that the predicted vehicle rolling motion depends on the manner in which the tires are represented. Omission of tire flexibility introduced errors of 10-20% for the specimen vehicle. It must be concluded therefore that the approximations involved in the representation of tires solely in terms of slip angles can produce unacceptably large errors in the case of commercial vehicles.

REFERENCES

1. Dugoff, M. and Murphy, R.W., "The Dynamic Performance of Articulated Highway Vehicles: A Review of the State of the Art," SAE Paper No. 710223.

2. McHenry, R.R. and Deleys, N.J., Vehicle Dynamics in Single-Vehicle Accidents, Cornell Aeronautical Lab Report No. VJ-2251-V-3, 1968.

HANDLING DYNAMICS OF AN INTERCITY BUS

G. L. Teper
and
D. H. Weir
Systems Technology, Inc.

ABSTRACT

Recent applied research studies in vehicle handling have emphasized large commercial vehicles. Among the results to date are a set of nonlinear equations to model the lateral and longitudinal handling dynamics of an intercity bus. These equations were implemented as a digital simulation for analysis of vehicle response and performance with various steering and braking inputs. Concurrent full-scale tests with an instrumented vehicle served to verify the simulation results for both perturbation and large amplitude motions.

This paper describes the bus, the analytical model, and the simulation. Analytical and full-scale results are shown for various maneuvers to demonstrate the fidelity of the simulation, and to illustrate the nature of the limits of performance (spinout, plowout, and rollover).

INTRODUCTION

This paper summarizes an analytical investigation of bus handling (1)*[1] which emphasized the open loop dynamics of the vehicle related to directional (steering) control, with and without braking. The results represent an extension of work previously accomplished in the area of automobile handling (e.g., 2 and 3).

The overall objectives of the Reference 1 study were to:

- Develop performance parameters for evaluation of the road worthiness of selected commercial vehicles.
- Apply computer simulation programs to compile data on predicted behavior during vehicle operations in proximity to the limits of performance.
- Establish by full-scale testing the performance limits of such vehicles and verify the computer simulation.
- Furnish data on control inputs versus vehicle response characteristics.

The complete study is described in (1), and this paper emphasizes the simulation of an intercity bus. First, the physical aspects of the bus are described, followed

---

*Numbers in parentheses refer to similarly numbered references at end of paper.

[1]The applied research study described herein was accomplished in part for the National Highway Traffic Safety Administration under Contract DOT-HS-242-2-421. The findings and opinions expressed herein are those of the authors and not the NHTSA.

by a verbal description of the analytical model. The digital simulation which was used to implement the analytical model is also discussed. Finally, examples of full-scale data are compared with corresponding simulation validation runs. Limits of performance consisting of plowout, spinout, and rollover are demonstrated.

PHYSICAL DESCRIPTION OF BUS

The subject bus is a Motor Coach Industries Model MC-7, sketched in Figure 1. It has a solid I-beam front axle, a dual wheel rear axle, and a single rear trailing wheel (tag axle) on each side independently suspended from the coach body. It is diesel powered, with an automatic transmission and air-operated brakes on all wheels. The overall bus dimensions are 40 ft. long, 8 ft. wide, and 10.75 ft. high; and it has a wheelbase of 23.75 ft.

The coach has an air suspension system consisting of air beams, air bellows, height control valves, radius rods, and shock absorbers. The air beams are reservoirs at front and rear of the coach which improve ride characteristics. The bellows serve as springs on the front and rear axles, and carry the vertical load of the coach body. The height control valves operate on the front and rear axle air beams (bellows) to maintain the coach at a given trim height, regardless of load. These valves have a time constant in the range of 1 to 6 seconds, which means that the height control valve has little effect during normal transient maneuvers.

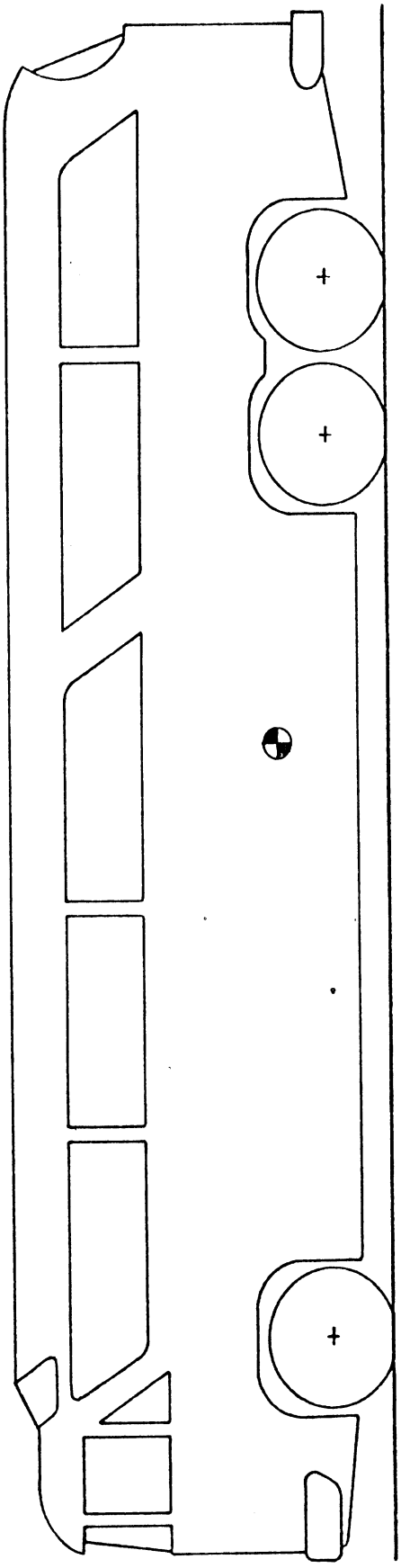

Figure 1. Overall Bus Geometry

The radius rods hold the axles in the proper transverse and longitudinal position. Four radius rods are used at the rear axle and five at the front axle, and they transmit driving and braking forces from the axles to the body. The shock absorbers are double acting, aircraft type. Two are used at the front axle, four at the rear axle and two at the tag axles.

The rear trailing wheels are carried on independent oscillating axle units, one for each wheel, attached to an axle tube located behind the rear driving axle. The rear trailing wheels use rolling-lobe bellows. Air pressure in these bellows is controlled by a pressure regulating valve which maintains constant pressure in the bellows, and uniform vertical loading of the rear trailing wheels, regardless of total vehicle loading. The time constant of the pressure regulating valves is assumed to be sufficiently large that the tag axle bellows behave like springs during maneuvers. More detailed physical descriptions of the bus are given in (4) and (5). The following section provides an analytical description.

ANALYTICAL MODEL

The handling dynamics of numerous land vehicles have been studied in the past via analytical models and computer simulation. These models and their status were reviewed at the outset of this program, and none was found to be fully applicable to the needed investigation of the subject vehicle. As a result, the equations of motion were rederived in a form suitable

to the study of the open-loop dynamics of the vehicle, with component elements of existing simulation models included when appropriate.

For purposes of modeling its handling dynamics, the bus was assumed to consist of the following interconnected rigid bodies:

- Coach body or sprung mass
- Front axle
- Rear axle
- 2 tag axles
- 2 front wheels
- 2 rear dual wheels
- 2 tag wheels

The drive line inertia was also included in the rear wheel torque dynamics. For analytical convenience these bodies were grouped as follows:

- Unsprung mass, comprising the front and rear axles and their wheels, which were interconnected by an analytical linkage whose motion was defined by a bus centerline axis system
- Sprung mass
- Tag axles and wheels

The motions of these groupings were defined according to the vector bases sketched in Figure 2. The analytical degrees of freedom which correspond to this physical description are summarized in Table 1. The motions directly related to handling response and

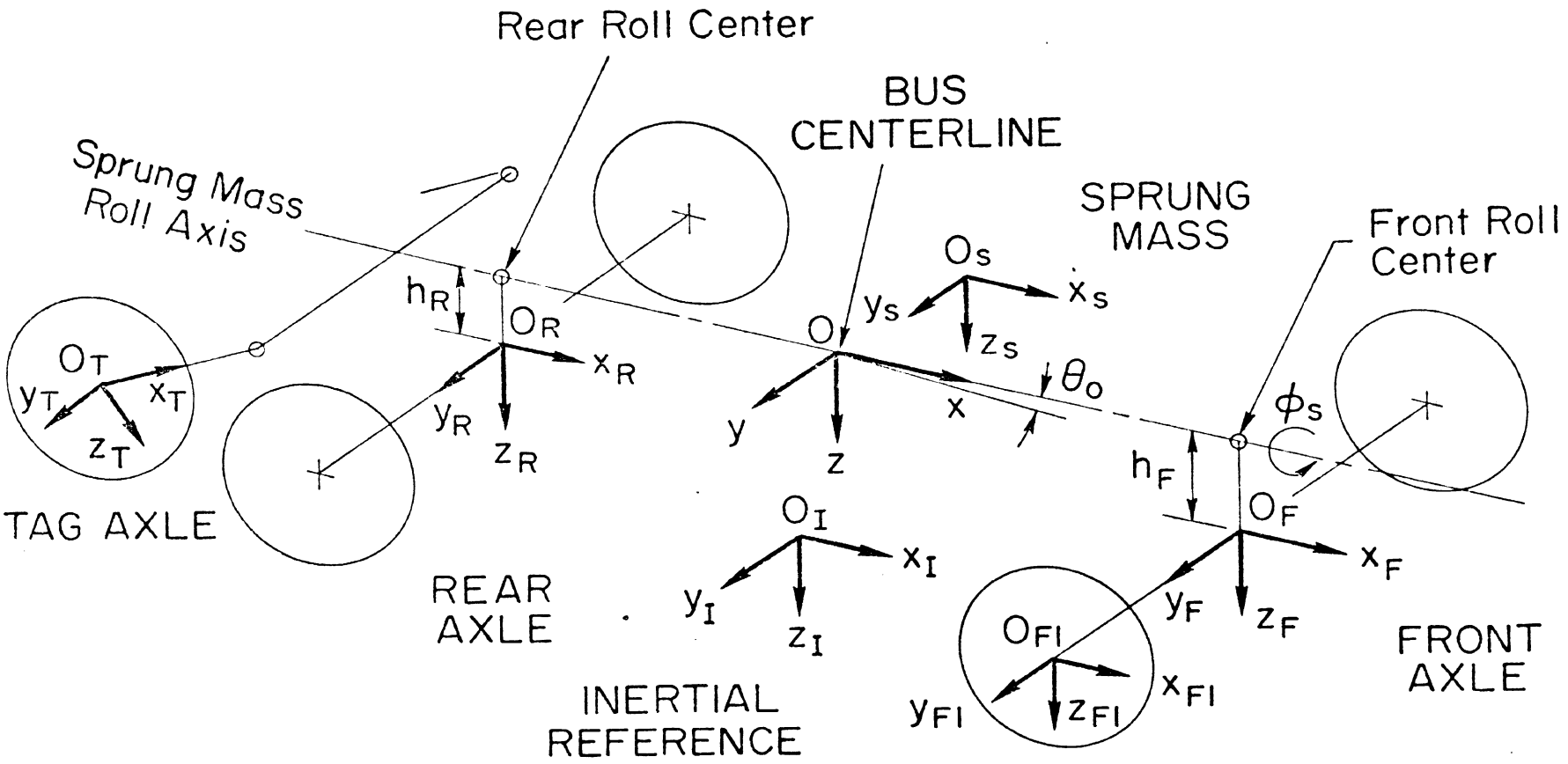

Figure 2. Definition of Component Body Motions

TABLE 1. DEGREES OF FREEDOM IN BUS DYNAMIC MODEL

ASSEMBLY	DEGREES OF FREEDOM	VARIABLES	ASSUMPTIONS
Unsprung Mass	Linear Velocities	u, v, w	
	Roll, pitch, and heading rates	p, q, r	
	Linear translation	x_I, y_I, z_I	
	Roll, pitch, and heading angles	φ, θ, ψ	Pitch angles are small
Sprung Mass	Vertical translation and velocity	$h_s, \dot{h}_s$	Sprung mass roll and pitch angles are small relative to unsprung mass
	Roll and pitch angles and rates	$\varphi_s, \theta_s, p_s, \dot{\theta}_s$	
Tag Axles and Tag Wheels	Trail angles and rates	$\theta_5, \theta_6, \dot{\theta}_5, \dot{\theta}_6$	
Front and Rear Axles	Roll angles and rates	$\varphi_F, \varphi_R, p_F, p_R$	Axle roll angles are small relative to unsprung mass
Wheel Rotation	Angular rates	$\Omega_1, \Omega_2, \Omega_3, \Omega_4, \Omega_5, \Omega_6$	
Front Wheel	Steer angle	δ_w	
Rear Wheels	Drive line torque	T_D	
Selected Wheels	Brake torque	T_B	

performance are those of the unsprung mass. The control variables (steer angle and wheel torque) comprise the system inputs. The remaining degrees of freedom in Table 1 are subsidiary in the overall performance sense, but they do have a direct influence via the dynamic coupling on the unsprung mass and total vehicle attitude and trajectory.

The more significant assumptions made in deriving the bus equations of motion can be summarized as follows. The bus height control valve was assumed to have a long time constant relative to the duration of the handling test maneuvers. The bus airbags were assumed to act like linear springs for purposes of modeling the lateral-directional motions. The pitch angles of the bus centerline relative to the ground (θ) and sprung mass relative to the bus centerline (θ_S) were assumed to be small angles. The roll angle of the sprung mass relative to the bus centerline (ϕ_S) was assumed to be small because of suspension constraints. The roll angles of the front (ϕ_F) and rear (ϕ_R) axles are relative to the bus centerline (and hence to each other) and were assumed to be small. The king pin camber and caster angles were assumed small. All other angles such as the vehicle heading angle and the body roll angle relative to the ground were assumed to be large, and were resolved into their trigonometric components. The following bodies were assumed to be symmetric about the x-z plane with respect to an axis system fixed at the corresponding body mass center: unsprung mass (bus centerline vector basis), sprung mass, front and rear axles, and tag axles.

The sprung mass was assumed to include the tag axles for purposes of writing the sprung mass equations of motion. Movement of the tag axles relative to the

sprung mass does not change the sprung mass inertial properties, significantly. The tag axle equations of motion assumed that the sprung mass is much larger than the tag axle mass. External forces and moments due to rolling resistance and aerodynamic effects were neglected, since these effects are relatveily insignificant for the types of handling maneuvers considered in this study.

For geometric and kinematic purposes, the wheels were assumed to be uniform circular discs, symmetrical about a plane which is normal to the spin axis and which bisects the tire. The tire width was assumed small. The rolling radius of the tire was assumed to vary with tire compression. The rear dual wheels were assumed to be an equivalent single wheel with the force and moment properties pertinent to two wheels. Despite these assumptions, the tire forces were treated in detail using an empirically based nonlinear tire model. This means that the actual width of the tire and the ground footprint geometry were accounted for empirically.

The modified friction ellipse tire model developed in (6), and used in (4), for example, was used to compute the forces on the tire at the ground contact point. This model takes into account the load normal to the ground (F_N), nonlinear side force (F_S) properties, circumferential forces (F_C) due to braking and acceleration, and the interaction of normal, circumferential, and side forces. The contact point geometry is shown in Figure 3. The model is empirical, and it uses test data for a tire towed at various lateral slip angles (α), braking torques resulting in fractional rotational slip (S), normal loads, and for selected pavement conditions. The required data includes

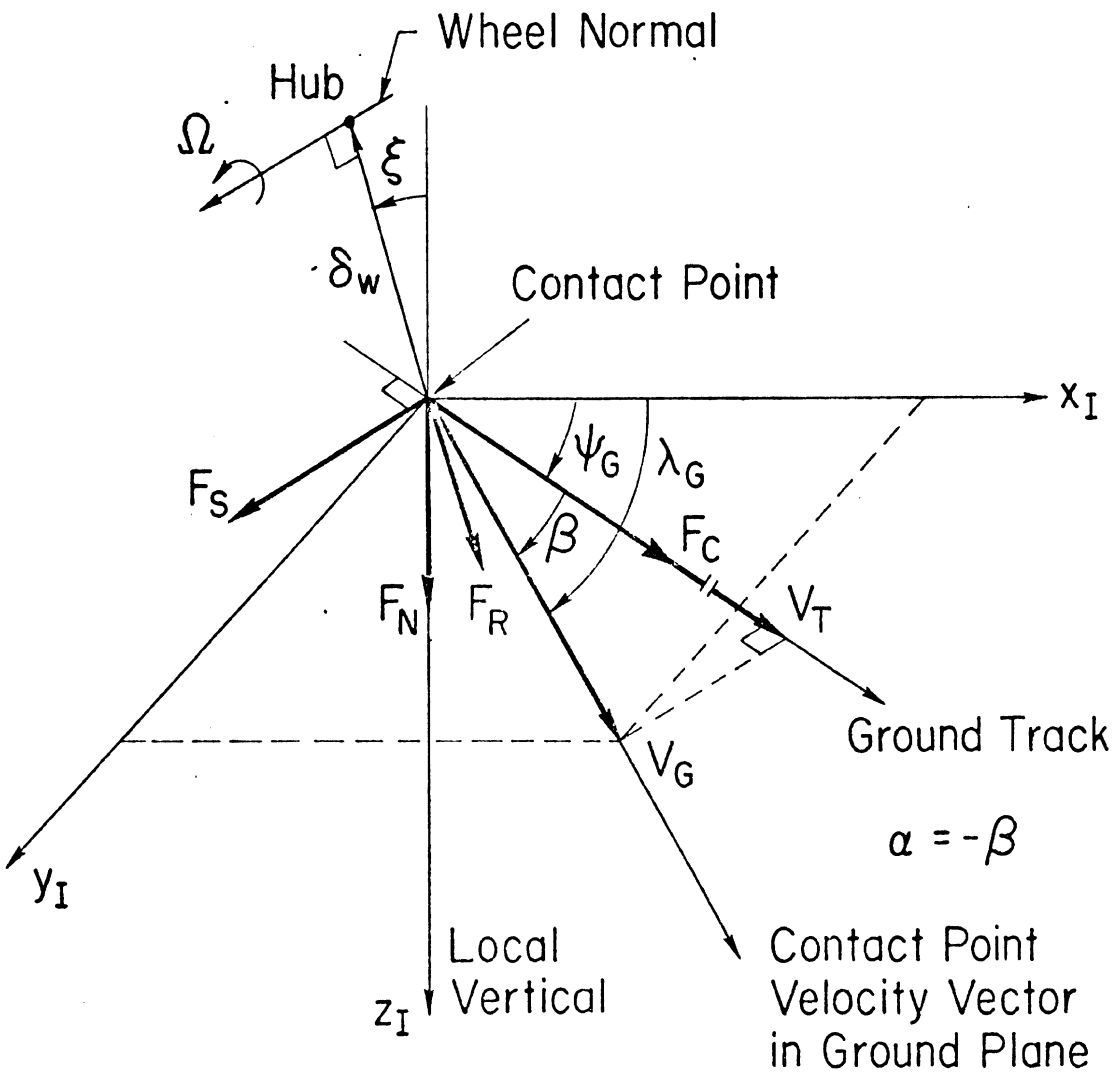

Figure 3. Contact Point Geometry

the tire load-deflection characteristics, the side force per unit slip angle (Y_α) vs. normal load, and the normalized maximum side force (μ_S) vs. normal load. Examples of these data for the MC-7 bus are given in Figures 4, 5, and 6. As indicated in the figures, these data were represented by analytical functions for use in the computer simulation.

The complete nonlinear equations for the bus and their derivation are given in (1). These equations were implemented in a digital computer simulation. The simulation and its use are described below.

COMPUTER SIMULATION

The complete model comprised 30 simultaneous first-order nonlinear differential equations. These were solved using a variable step size fourth-order Runge-Kutta method. A simplified 5 degree of freedom model was also simulated and used in parallel with the complete model.

The initial numerical values for the model parameters were either taken from (4), based on full-scale measurements, or based on ad hoc calculations, as appropriate.

The simulation programs were written in USA Standard FORTRAN IV, and they were implemented in a timesharing interactive computer system. This allowed ready access during the extensive checkout and development phase. It also permitted on-line operation of the simulation via a remote terminal at the full-scale test site which proved an invaluable aid in interpreting experimental results, refining the experimental design as the data were obtained, and probing potentially

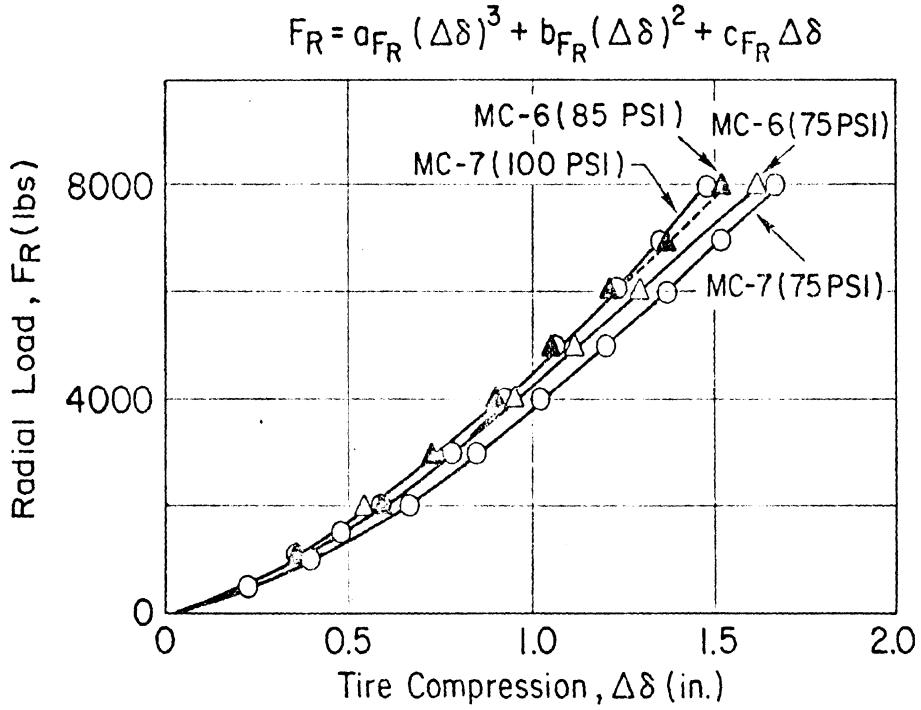

Figure 4. Tire Load Deflection Characteristics (4).

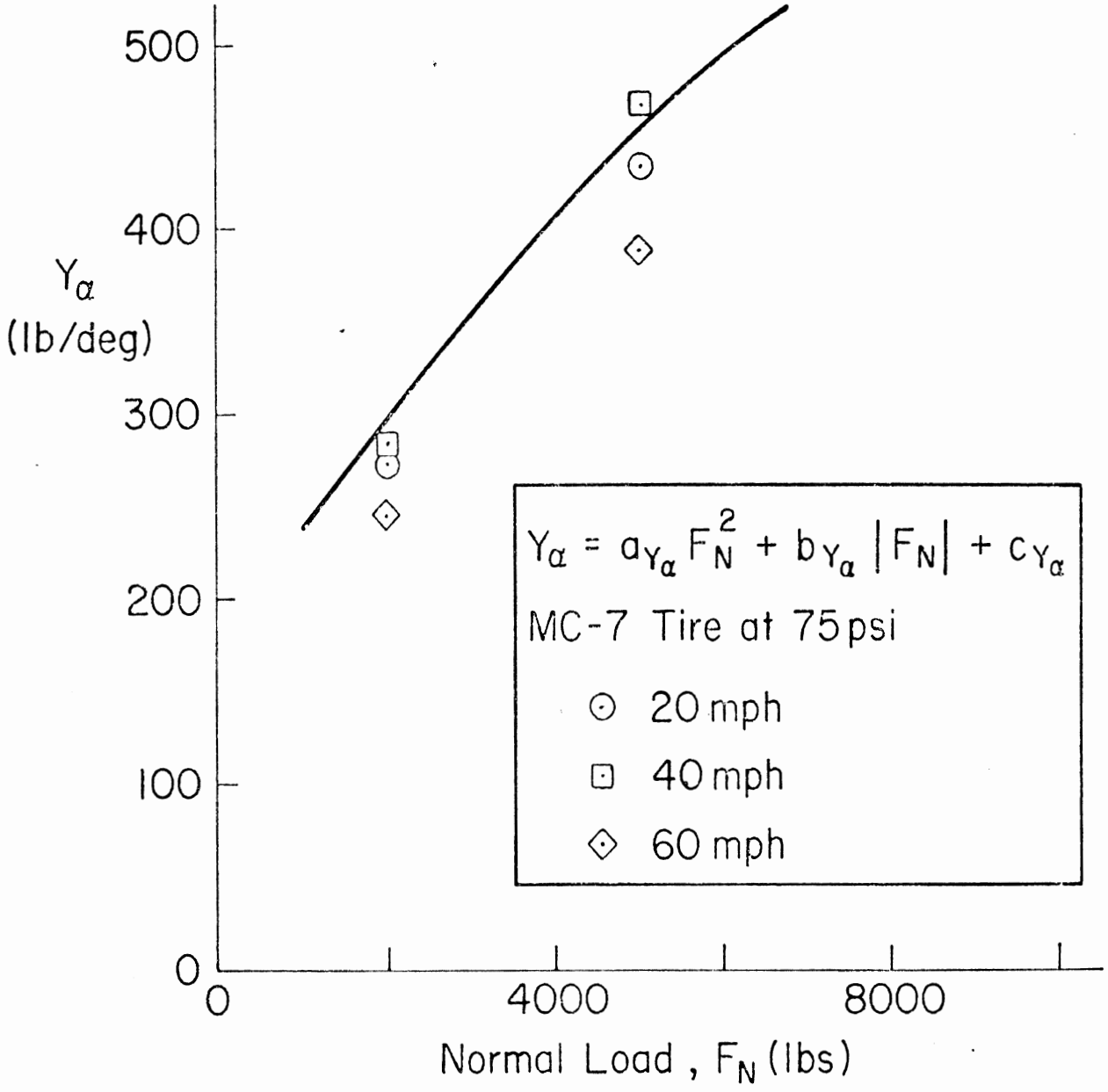

Figure 5. Bus Tire Cornering Stiffness (4).

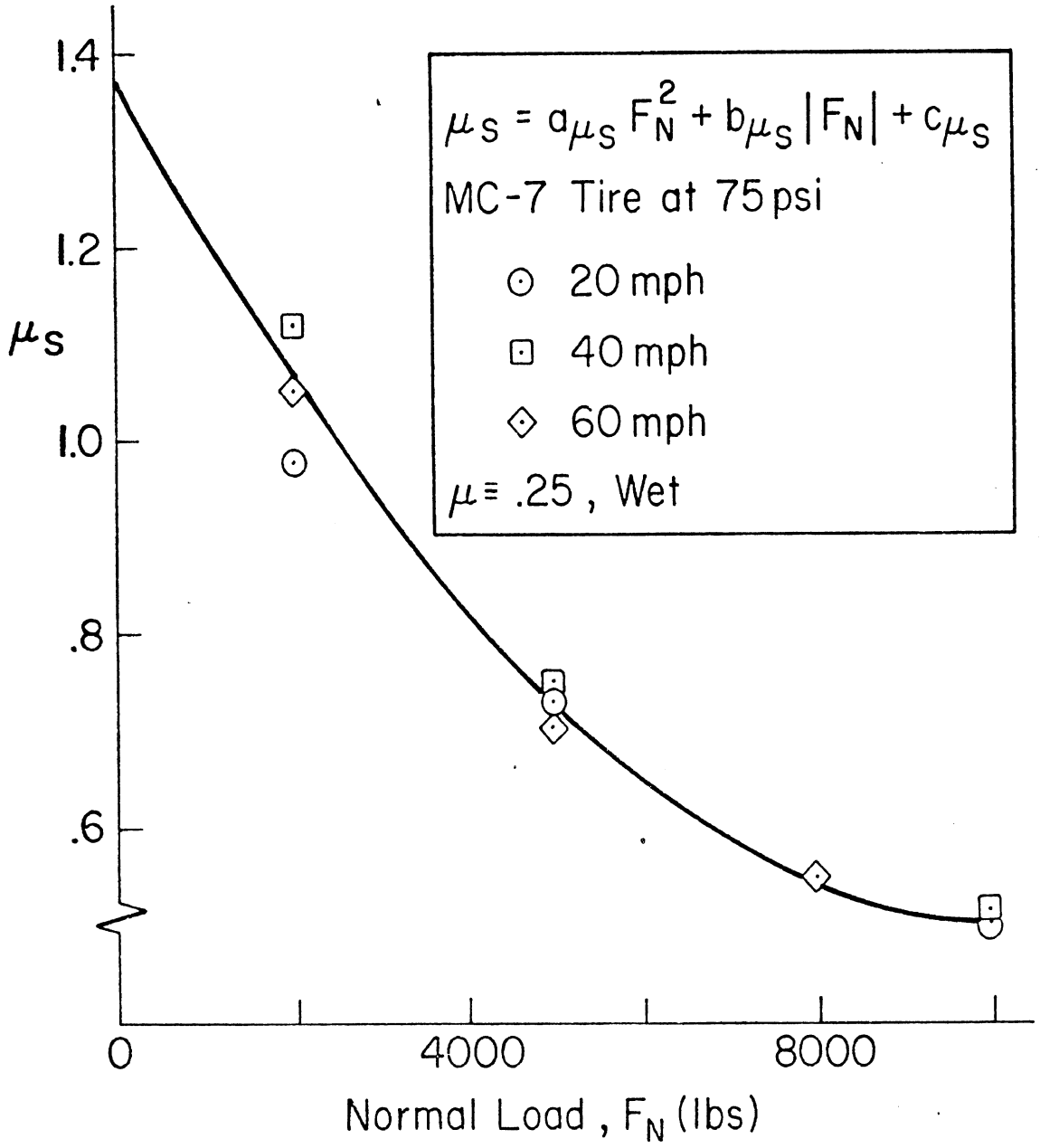

Figure 6. Normalized Maximum Tire Side Force Coefficient, Dry (4).

catastrophic performance limits such as rollovers. The primary computer used was a Digital Equipment Corp. PDP-10 computer, although some of the development work was done on a Control Data CDC 6400. The simulation has also been adapted to run in a batch mode on an IBM 370-91 at the Applied Physics Laboratory of Johns Hopkins University. The simulation costs per run varied somewhat with the type of maneuver, the nature of the response, and the amount of plotting desired.

SIMULATION VALIDATION

Full-scale handling tests comprised a significant part of the study. These were accomplished with several loading conditions, initial speeds, on high and low pavement surface coefficients, and with various control input amplitudes and timings. Selected examples provide comparison with the simulation results.

The bus was tested in three loading conditions: empty, nominal, and full. The total empty weight was 28,780 lb., including instrumentation. The bus tires were Goodyear tubeless 12.5-22.5 mounted on a 22.5 x 8.25 rim. They were in near new condition (not retreads) with several hundred miles of highway operation at the start of the tests. The bus tires were all operated at 75 psig. Two surface coefficients were used: wet with a nominal skid number (SN) of 25, and dry with a nominal skid number in excess of 70. The initial velocities were typically 30 and 50 mph. Various braking levels and configurations were used in the tests. The configurations included all axles braked and rear axles only braked, and this was accomplished via a brake selector panel which controlled solenoid valves in the air lines at each wheel. Brake levels corresponded to partial and full brake pedal deflection.

Oscillograph recordings were obtained for all of the test runs, and examples of these illustrate the nature of the full-scale responses and the degree to which the simulation corresponds to the real world. Runs selected to show the salient points include trapezoidal steer inputs on dry pavement, braking in a turn on the wet with all brakes (plowout), and braking in a turn on the wet with rear brakes only (spinout).

TRAPEZOIDAL STEER, DRY, NO BRAKING, 30 MPH

Full-scale response data for the empty bus with an 11 degree trapezoidal steer input (δ_w) are shown in Figure 7. This test was done on the high SN dry pavement at an initial speed of 30 mph. The corresponding simulation run is shown as dashed lines in Figure 7 for comparison.

The basic directional response (heading rate, r_G, and lateral acceleration, $a_{y_{acc}}$) of the simulation is seen to agree quite well with the full-scale results. The simulation values are slightly larger as steady state is reached, due in part to the more rapid speed reduction shown by the full-scale data (see the forward velocity as measured by the fifth wheel, u_{FW}). The latter is probably caused by rolling resistance and aerodynamic drag which were not included in the simulation (but could be added, readily). The heading angle (ψ_G), on the other hand, agrees quite closely.

The simulated sprung mass roll response (ϕ_G) shows only fair agreement with the full-scale data. The latter is more lightly damped with a smaller peak value. The simulation results shown correspond to the (4) values, and a reduction in the simulated spring

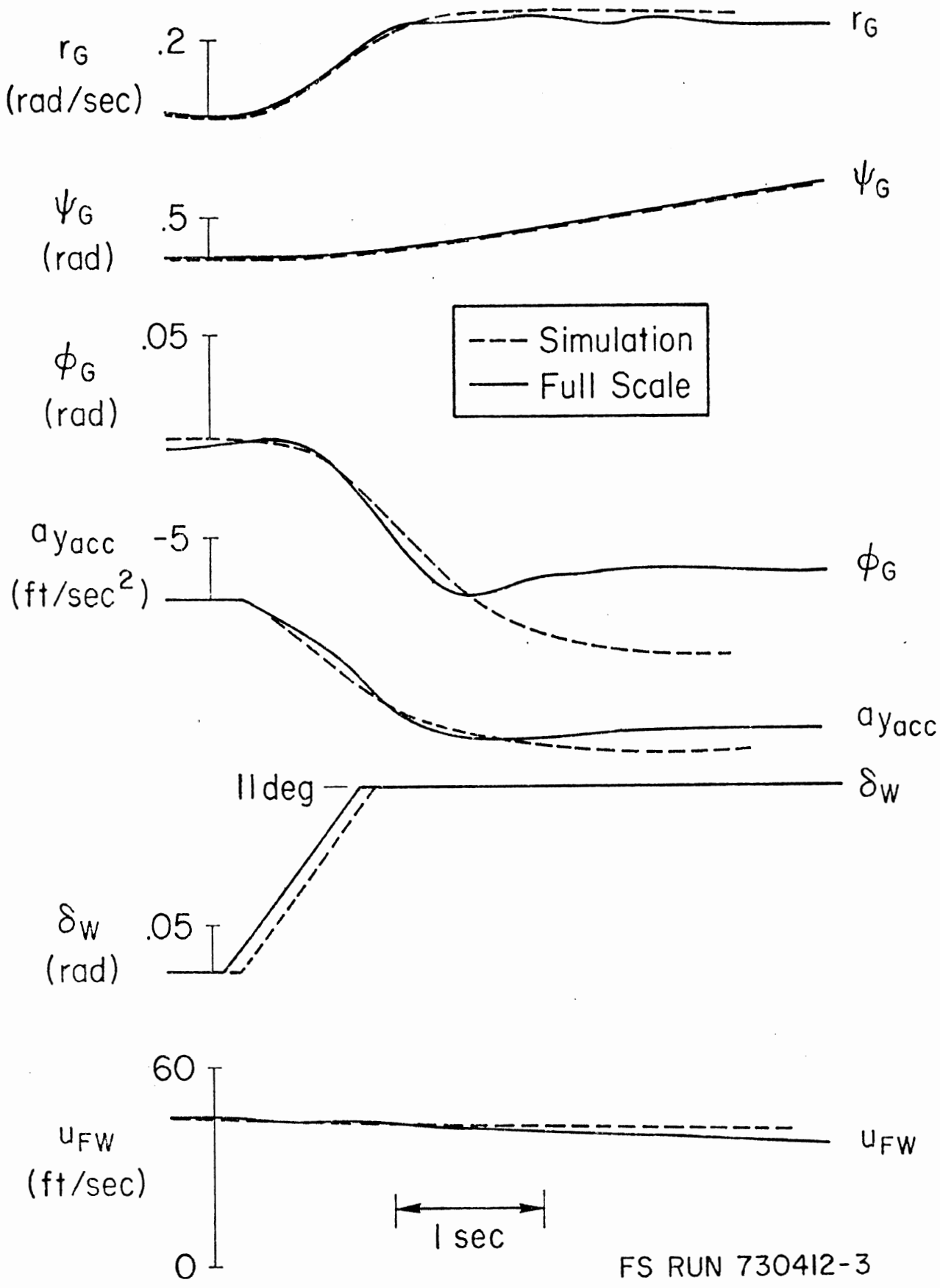

Figure 7. Empty Bus, Trapezoidal Steer, Dry, No Braking, 30 mph.

constants and damper values would bring the two traces into correspondence. Such adjustments were made during the data analysis to make the two roll traces match fairly closely, yet the heading rate and lateral acceleration responses were not affected. This illustrated the general lack of coupling between the rolling and directional modes of the commercial vehicles studied, due no doubt to the solid axle suspension geometry. The reduced steady-state, full-scale roll angle could also be due to the compensating effect of the load leveler valve in the pneumatic suspension. This nonlinear effect was assumed to be low frequency relative to the handling dynamics of interest and it was not included in the simulation.

Another effect illustrated in Figure 7 is the time delay between the simulated and actual vehicle responses. This is shown as a lag of about 0.1 second between the full-scale and simulated steer angle inputs, obtained by making the initial responses match to simplify the comparison of other factors. In other words, if the steer angle inputs were coincident, the full-scale response would lag the simulated response by about 0.1 second. This time delay probably reflects a combination of full-scale factors, e.g., steering system compliance, dead zone (free play) in the power steering unit, the tire relaxation time constant, and lags in the motion sensors (gyros, accelerometers).

BRAKING IN A TURN, WET, ALL WHEELS BRAKED, 30 MPH

Braking in a turn represents a much more complicated dynamic situation than a simple trapezoidal steer, particularly on a low SN surface which admits skidding and associated spinout or plowout. The simulation is

correspondingly more complex, also. Such a situation is shown in Figure 8 which presents full-scale and simulation results for the empty bus, braking in a turn on the wet, from an initial speed of 30 mph, with all wheels braked full. The steer angle input trapezoid has a rise time of 1 second to a maximum value of 7.4 degrees, and the brake pedal is fully depressed at the end of the 1 second rise. The wheel rotation data, not shown, indicate that all wheels did despin to zero within about 1 second after brake application. The overall result of this test is that the bus plows out, continuing tangent to its trajectory at the time braking becomes effective, with limit understeer. Despite the inherent complexities and nonlinearities of this test, the simulation does a good job of modeling the essential characteristics of the response.

The simulated longitudinal acceleration ($a_{x_{acc}}$) shows a similar response form to the full scale with a somewhat lower amplitude. The full-scale amplitude increases a little as the bus slows, while the simulation value remains more constant. The steady-state lateral acceleration ($a_{y_{acc}}$) is also less full scale. The reduced accelerations are probably caused by the actual test skid number being somewhat smaller than the $\mu_S = 0.25$ value used as nominal in the wet simulation runs. Of course, this simulation parameter could easily be adjusted to give a better match. The difference in longitudinal deceleration is reflected in the forward velocity traces (u_{FW}).

The general form of the simulated lateral acceleration ($a_{y_{acc}}$) is similar to the full scale—building initially, then dropping off sharply as braking

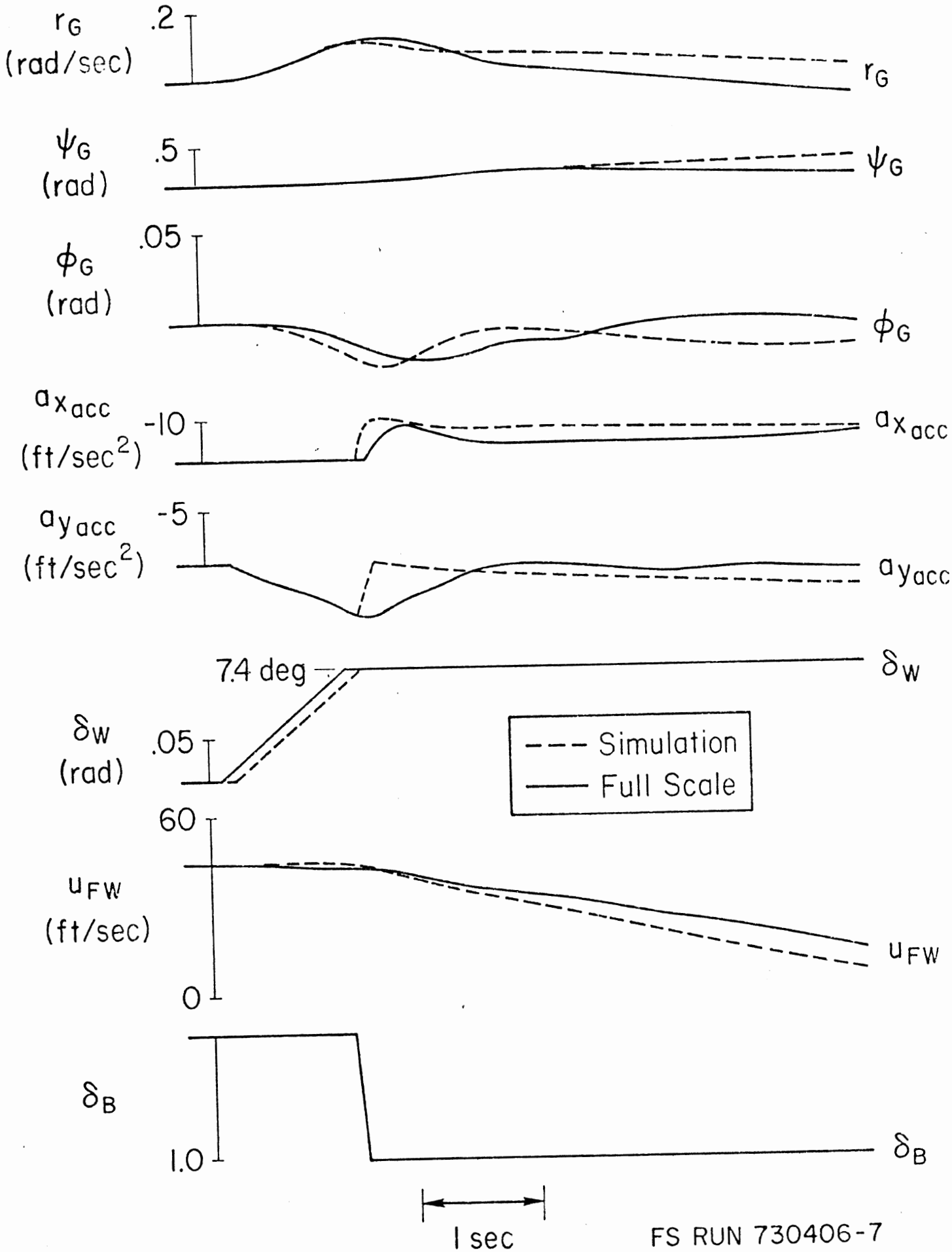

Figure 8. Empty Bus, Braking in a Turn, Wet, All Wheels Braked, 30 mph.

becomes effective. Most of the full-scale data for this test show a more rapid drop off of $a_{y_{acc}}$ than that shown in the Figure 7 example, but the effect on overall performance of such details is not important.

The heading rates (r_G) show initial buildups until brake application, then decay as the front wheels begin to skid and the steering moment reduces to a lower level. The simulated heading rate goes to zero monotonically, while the full-scale data show a decrease then a reversal of sign and an associated reduction in heading angle. These differences are minor and probably derive from some combination of unevenness in pavement frictional characteristics and asymmetry in brake torque application. Nevertheless, the essence of limit performance in this case is a straight ahead plowout, as noted.

The roll angle results (ϕ_G) show differences which in this case are readily attributable to the already noted differences in the lateral acceleration response. Dynamically, the roll angle lags the lateral acceleration response, and the more gradual full-scale $a_{y_{acc}}$ drop off after braking results in a delayed peaking of ϕ_G. This delayed ϕ_G peaking carries over as a phase shift between full scale and simulation in the latter part of the roll response.

BRAKING IN A TURN, WET, REAR BRAKES ONLY, 30 MPH

The two previous runs have demonstrated many of the features of the vehicle's dynamic response, including the plowout limit of performance with all wheels braked. The next example shows a limit of performance spinout

with rear braking only. Adding interest to this example is the terminal response which occurs when the brakes are released and the steer angle is centered at the conclusion of the run while the bus is still proceeding backwards. Remarkably enough, the simulation models all the salient aspects of this complex maneuver with reasonable fidelity.

The full-scale and simulated time responses are shown in Figure 9. The corresponding bus trajectory, obtained from the simulation, is shown in Figure 10; here the bus is shown at 1 second intervals. The steer input is a trapezoid with a peak value of 7.2 degrees. At the end of the 1 second rise, full brake torques are applied to the rear dual wheels and the tag wheels, which causes them to despin to zero within a second or so (see Ω_3-Ω_6). The right front wheel is not braked and does not despin (see Ω_1), and it shows the forward velocity (fifth wheel inoperative on this run). The simulated steer angle is shown lagging the full scale by about 0.1 second, for reasons discussed above. Similarly, the simulated brake torque application lags the full-scale pedal deflection by about 0.3 second, so that simulated wheel despin (Ω_3, Ω_5, etc.) corresponds to the data. As noted in Figure 9, some manual braking was used after the AVC input was removed to recover from the maneuver and halt the vehicle. This shows up as a difference in the longitudinal acceleration ($a_{x_{acc}}$) curves towards the end. Since this level of braking is undefined, the rotational velocity traces for the braked wheels have been truncated at the end of the basic input.

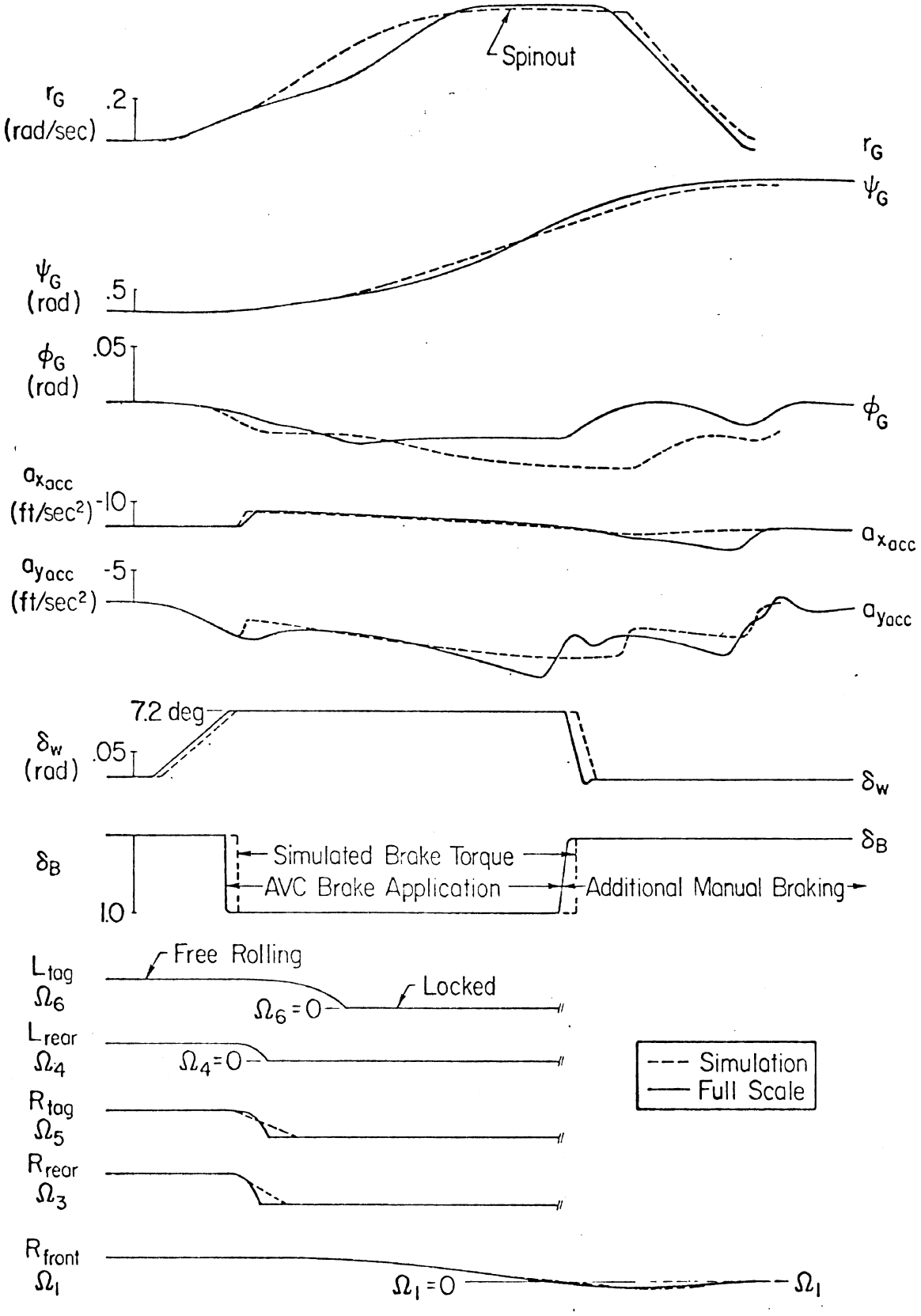

Figure 9. Empty Bus, Braking in a Turn, Wet, Rear Brakes Only, 30 mph

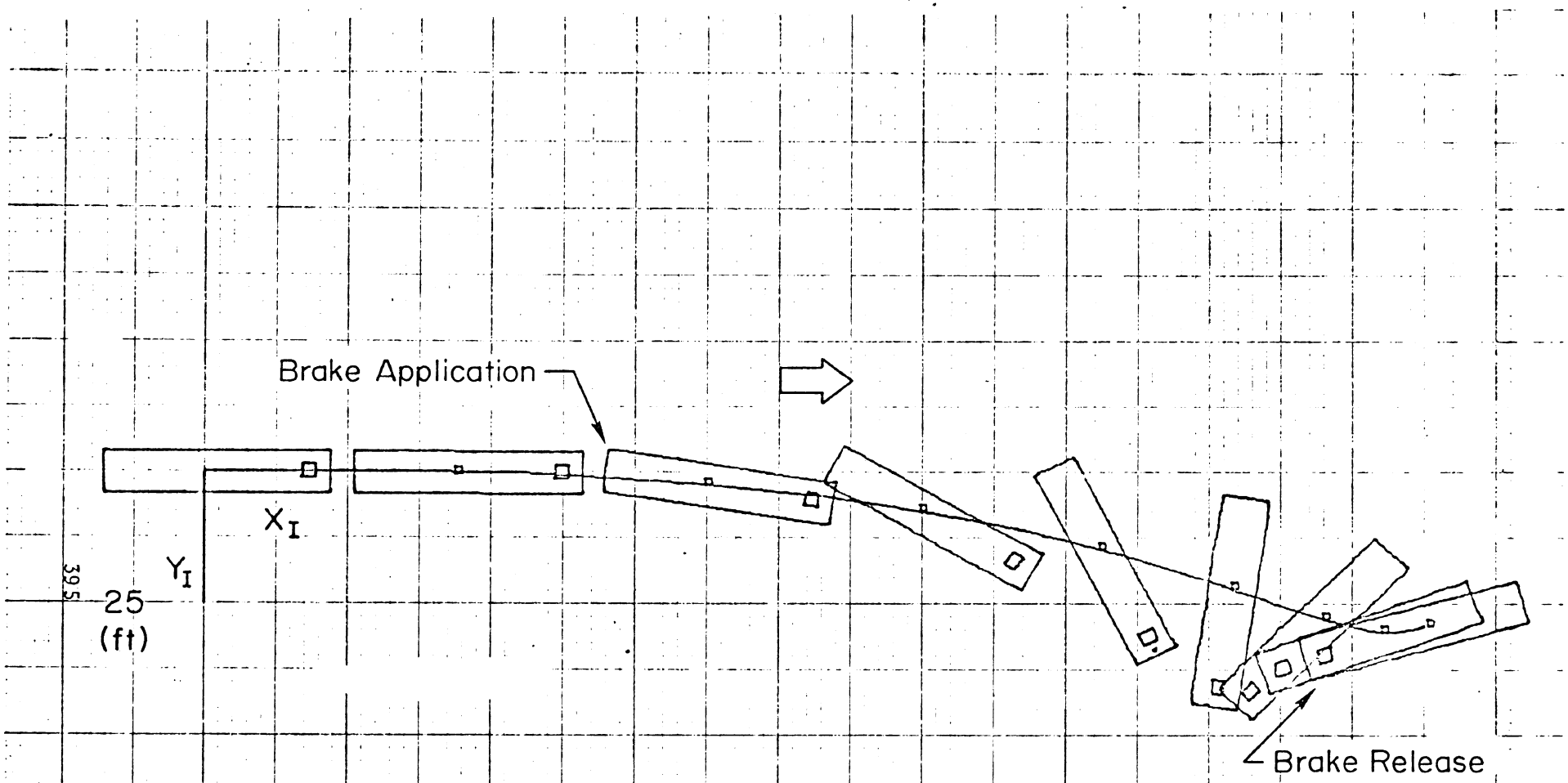

Figure 10. Empty Bus Trajectory, Braking in a Turn, Wet, Rear Brakes Only, 30 mph (from Simulation).

The waveforms of the simulated and full-scale response traces show good correspondence, with detail differences in amplitude and timing. For example, the simulation spins (r_G) a little more quickly, but the overall heading change (ψ_G) is about the same. The lateral acceleration ($a_{y_{acc}}$) peaks sooner and with higher amplitude in the data, but the form of the response is similar, including even the residual response at the end of the maneuver. The longitudinal acceleration ($a_{x_{acc}}$) agrees well until near the end, for reasons noted above. The simulated roll response (ϕ_G) is greater than the data, as it was in the simpler maneuvers (e.g., Fig. 7).

LARGE TRAPEZOIDAL STEER, DRY, NO BRAKING, 30 MPH

As the severity of the trapezoidal steer input increases, the bus will eventually roll over on dry pavement with no braking. This behavior was investigated with the simulation, but not in full scale. The results are illustrated in Figure 11 for an 18 degree peak steer angle, which is slightly more than the minimum input value needed for rollover. Here, the rapid trapezoidal input rate is a simulation convenience and it does not affect the longer term response.

The rollover is evident in the sprung mass roll angle relative to the ground (PHIG) which is shown going off scale at -23 degrees with a roll rate (PG) of about -26 deg/sec and increasing. Interestingly, the roll angle of the sprung mass relative to the unsprung mass (PHIS) peaks and then reduces as the inside wheels leave the ground during the rollover. The peak lateral acceleration (AY, $\hat{a}_y$) is about 15.1 ft/sec^2 (0.47 g), and this is one measure of the

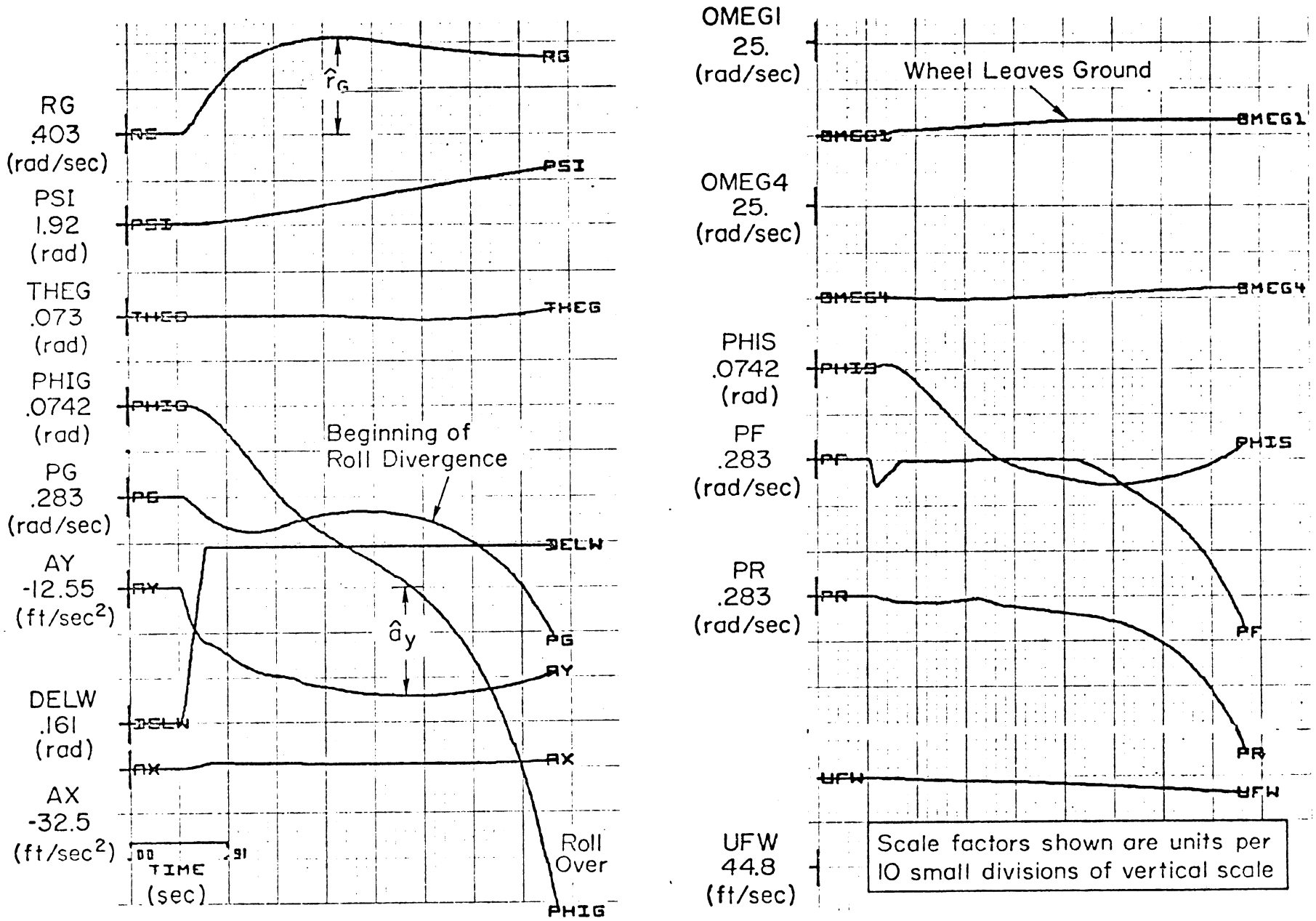

Figure 11. Empty Bus, Trapezoidal Steer, Dry, No Braking, 30 mph, Showing Rollover.

performance limit. Larger values of steer angle will not result in a greater lateral acceleration before rollover occurs. The right front wheel leaves the ground at the point where its velocity becomes constant, about 2.5 seconds after the start of the simulation run. This time is also seen as the beginning of the divergence in the front axle roll rate (PF). If desired, the simulation could have been run (about one more second) until the roll angle reached 90 degrees, which is the simulation limit in roll. This additional running time is unnecessary, since the roll divergence is clearly evident well before that point.

DISCUSSION

The results shown demonstrate that full-scale tests can be used to assess handling performance limits, and that the associated simulation provides an adequate model of the nominal handling and limit performance characteristics of the vehicle.

A readily interpreted overall handling parameter is the nature of the performance limit, and this varies with vehicle configuration and test condition. As illustrated in the paper, several kinds of performance limits result, i.e.,

- Rollover; which occurs on high coefficient pavement surfaces when the lateral acceleration exceeds a certain boundary and remains at that level for a short period of time.
- Spinout; which involves the limit oversteer and typically occurs on a low coefficient surface, particularly when the side force capability of the rear tires decreases

relative to that of the front tires, e.g., during braking in a turn with rear wheel brakes only.

- Plowout; which involves limit understeer and typically occurs on a low coefficient surface with a large front wheel steer input, with no braking or with moderate braking activity on all axles.

For turning and braking maneuvers on dry pavement the results are not clearcut, and the nature of the limit performance depends on the type and amount of braking effort. For example, with hard braking of the rear wheels only, the vehicle will spin out on a high coefficient surface. On the other hand, with hard braking of all wheels the vehicle may plow out, as it does on the low coefficient wet surface. For intermediate levels of braking of either the rear wheels or all wheels, the vehicle may roll over in a braking in a turn maneuver before plowout or spinout occurs.

The experiments and analyses show a dramatic difference in the limit performance between low (wet) and high (dry) coefficient surfaces. In the wet, rollovers are less likely, and the vehicle either spins or plows out. On a dry surface, the typical performance limit with a relatively topheavy commercial vehicle is rollover, if the lateral acceleration is sufficiently large. Further, the wet spinout situation is aggravated, if not initiated, by a relatively large braking effort on the rear wheels with minimal braking of the front. Such unbalanced braking causes the front wheels to retain a greater side force capability than the rear, which generates the large yawing moment leading to a spinout.

Although the existing simulation is extensive in its detail, there are several ways in which it might be usefully extended for certain applications. The front suspension currently comprises a solid axle and this could be replaced by independent suspension. Similarly, different rear axle geometries could be employed. The existing equations include a simple steering subsystem and this might be elaborated to include the dynamics and nonlinearities of a power steering box, tie rod ends, etc. Finally, aerodynamic terms could easily be added to permit study of the effects of crosswinds and aerodynamic disturbances.

SYMBOLS

a_{FR}, b_{FR}, c_{FR}	Coefficients of tire load-deflection characteristics
$a_{x_{acc}}$ AX	Longitudinal acceleration measured by vertical-gyro-stabilized accelerometer
$a_{y_{acc}}$ AY	Lateral acceleration measured by vertical-gyro-stabilized accelerometer
a_{Y_α}, b_{Y_α}, c_{Y_α}	Coefficients of tire cornering stiffness characteristics
F_C	Circumferential force at tire contact point
F_N	Vertical load on tire at contact point
F_R	Radial load on tire at contact point
F_S	Side force on tire at contact point
h_F	Distance from centerline x axis to front axle c.g., along z_F axis
h_R	Distance from centerline x axis to rear axle c.g., along z_F axis
h_s	Distance of sprung mass (including tags) c.g. above centerline axis
O	Origin of centerline axis system
O_F	Origin of front axle assembly axis system
O_{F1}	Origin of front (right) wheel axis system
O_I	Origin of inertial axis system

O_R		Origin of rear axle assembly axis system
O_S		Origin of sprung mass axis system
O_T		Geometric center of tank
p		Centerline axis system roll rate
p_F	PF	Front axle roll rate with respect to inertial frame
p_G	PG	Angular roll rate measured by rate gyro fixed in the sprung mass
p_R	PR	Roll rate of rear axle with respect to inertial frame
p_S		Roll rate of sprung mass with respect to inertial frame
q		Pitch rate of centerline axis system
r		Heading or yaw rate of centerline axis system
r_G	RG	Angular heading or yaw rate measured by rate gyro fixed in the sprung mass
T_B		Torque on wheel due to braking
T_D		Drive line torque
u		Forward velocity (of centerline origin) along x
u_{FW}	UFW	Forward velocity as measured by fifth wheel
v		Velocity of centerline origin along y
V_G		Total velocity of wheel contact point in ground plane measured in centerline axis system

V_T		Ground track velocity in plane of tire
w		Velocity of centerline origin along z
xyz		Vector basis fixed in the centerline
$x_F y_F z_F$		Vector basis fixed in front axle assembly
$x_{F1} y_{F1} z_{F1}$		Vector basis fixed in front (right) wheel
$x_I y_I z_I$		Vector basis fixed in inertial space
$x_R y_R z_R$		Vector basis fixed in rear axle assembly
$x_S y_S z_S$		Vector basis fixed in sprung mass
$x_T y_T z_T$		Vector basis fixed in tag axle assembly
Y_α		Cornering stiffness of tire
α		Slip angle of tire
β		Sideslip angle
δ_B		Brake pedal position
δ_w	DELW	Front wheel steer angle
$\Delta\delta$		Change in rolling radius (tire deflection) due to load
θ		Euler angle for (pitch) rotation of centerline axis system
θ_G	THEG	Pitch angle sensed by the vertical gyro fixed in the sprung mass
θ_o		Unperturbed value of θ
θ_s		Pitch angle of sprung mass relative to centerline axis system
θ_5		Pitch angle of right tag wheel trailing arm relative to sprung mass

θ_6		Pitch angle of left tag wheel trailing arm relative to sprung mass
λ_G		Lateral path angle of wheel
μ_s		Normalized maximum tire side force coefficient of tire
ξ		Camber angle of the king pin
ϕ		Euler angle for roll rotation of centerline axis system
ϕ_F		Roll angle of front axle relative to centerline axis system
ϕ_G	PHIG	Roll angle sensed by the vertical gyro fixed in the sprung mass
ϕ_R		Roll angle of rear axle relative to centerline axis system
ϕ_s	PHIS	Roll angle of sprung mass relative to centerline axis system
ψ	PSI	Euler angle for heading or yaw rotation of centerline axis system
ψ_G		Heading or yaw angle sensed by a directional gyro fixed in the sprung mass
Ω	OMEG	Rotation rate (angular velocity) of wheel

ACKNOWLEDGEMENTS

The authors would like to acknowledge the contribution of STI staff members Roger Hoh and James Nagy to the full-scale testing and of Calvin Sihilling to the preparation of the computer simulation program. Mr. Edward Kakaley was the NHTSA Contract Technical Manager, and his guidance and comments provided a valuable contribution throughout the contractual study.

REFERENCES

1. Weir, D.H., Teper, G.L., Hoh, R.H., Humes, R.W., et al., Analysis of Truck and Bus Handling, Systems Technology, Inc., Hawthorne, California, TR-1022-1, March 1974 (available from National Technical Information Service).

2. Dugoff, H., Ervin, R.D., and Segel, L., Vehicle Handling Test Procedures, Highway Safety Research Institute, University of Michigan, Final Report on Contract FH-11-7297, 2 Vols., November 1970 (also SAE Preprint 710080).

3. Ervin, R.D., Grote, P., Fancher, P.S., MacAdam, C.C., and Segel, L., Vehicle Handling Performance, Highway Safety Research Institute, University of Michigan, Final Report on Contract DOT-HS-031-1-159, 3 Vols., November 1972.

4. Wong, R.E., Seitzman, M., Chiang, S., and Matle, C.C., A Study of the Aerodynamic Effects and Stability Characteristics of Buses. Vol. II: Technical Report, Bendix Corp. Research Laboratories, Report No. 6451, November 1972.

5. Maintenance Manual: Challenger Model MC-7 Intercity Coach, Motor Coach Industries, Inc., Pembina, N.D., 1968.

6. McHenry, R.R., and Deleys, N.J., Vehicle Dynamics in Single-Vehicle Accidents: Validation and Extensions of a Computer Simulation, Cornell Aeronautical Laboratory, Inc., CAL Report VJ-2251-V-3, December 1968.

THE MODELLING AND TESTING OF ARTICULATED VEHICLES AT THE SCHOOL OF AUTOMOTIVE STUDIES, CRANFIELD

J.R. Ellis
and
P.L. Read
School of Automotive Studies
Cranfield Institute of Technology

ABSTRACT

The development of articulated vehicle studies at the School of Automotive Studies, Cranfield, is outlined. Reference is made to the various publications in this field originating at the School.

INTRODUCTION

The School of Automotive Studies at Cranfield Institute of Technology started work on the modelling of articulated vehicles to examine their handling qualities in the early nineteen sixties.

This initial work culminated in Ellis's paper, 'The Dynamics of Vehicles during Braking,' in 1963, Reference (1). This paper dealt with passenger cars and articulated vehicles. A model was developed for the passenger car and the technique was then applied to the articulated vehicle.

The vehicle modelled was a single drive-axle tractor with a single axle semi-trailer. The wheels on each axle are replaced by a single wheel on the vehicle centre line. These single wheels have the combined properties of the wheels they replaced. The equations of motion were obtained by using a body centred axes system. They were based on the use of equations of motion written for each body separately and with the bodies linked by the forces and geometry of the connection.

The model was simplified by neglecting pitch, roll, and bounce motions. The tractor and semi-trailer were considered separately and then linked by equating forces and velocities at the fifth wheel. The resulting equations were manipulated into the form of four non-linear simultaneous differential equations in terms of tractor forward speed, lateral and yaw velocities, and articulation angle between tractor and trailer. This method is sometimes known as the 'state variable' technique.

This model represented the first analysis of an articulated vehicle to incorporate variable forward speed and could accommodate large articulation and slip angles.

The paper also considered in some detail the representation of tyre lateral forces at large slip angles and the effect of tractive and braking forces on lateral force. The 'Friction Ellipse' concept was used to illustrate this last point.

As the equations of motion were not linear, it was not possible to use classical analytical techniques to examine the vehicle's stability. The equations were therefore solved for a hypothetical articulated vehicle by using a numerical integration routine executed by a digital computer.

Using this model, Ellis showed for the first time by simulation the phenomena of jack-knifing and trailer-swing of articulated vehicles. It was also employed to examine some features of the fifth wheel coupling. The effects of friction at the coupling were examined and extended to include such anti-jack-knife devices as fifth wheel disc brakes. The effect on jack-knifing and trailer-swing of moving the position of the fifth wheel on the tractor was also investigated.

Horn-Andrews, Reference (2) 1964, used the model to examine the effect of road camber on the braking performance of an articulated vehicle. Front wheel locking on an inclined surface was specifically investigated. It was shown that a situation similar to jack-knifing can result under these conditions.

In 1966 Ellis prepared a further paper on articulated vehicle studies, 'The Ride and Handling of Semi-Trailer Articulated Vehicles,' Reference (3). The handling section of this paper reviews the four degree of freedom, non-linear model discussed in (1). A linearized analysis of this model was then performed. The assumptions made were:

- Constant forward speed
- All products of variables are neglected
- Linear tyre data
- Articulation angle is small

By examining the roots of the characteristic frequency equation, the vehicle's stability at various configurations was examined.

The two features closely examined were the positions of the fifth wheel and the load on the trailer. It was shown that with a uniformly distributed load, movement of the fifth wheel towards the rear caused the vehicle to become less stable. The same effect was noted if, for a given fifth wheel position, the load was moved to the rear of the trailer.

A steady state analysis of an articulated vehicle's handling characteristics revealed features analogous to the understeer/oversteer characteristics often applied to passenger cars.

The work discussed in these two papers has been incorporated in a chapter of Ellis's book 'Vehicle Dynamics' Reference (4).

The next major piece of work was undertaken by Shapley. This involved extending the four degree of freedom model to examine the effects of pitch, roll and bounce and a series of vehicle tests to provide data to validate the simulation.

The model developed employed the six degrees of freedom of the tractor unit plus two for the trailer giving articulation and relative pitch angles. The equations of motion for each body were written separately with forces and geometric considerations at the joints providing extra constraints.

The equations were then manipulated, as in (1), to arrive at a set of equations which correspond to the degrees of freedom of the system.

Due to the size and complexity of these equations, a digital computer was employed to solve them. A matrix equation consisting of the equations of motion, the geometric constants, tyre forces, and fifth wheel forces was written. This equation was solved for accelerations. These accelerations were then operated on by a numerical integration routine to give velocities and displacements. The routine integrated over a real time step length determined by prescribed accuracy criterion. The velocities and displacements from one step served as initial conditions in the next solution of the matrix equation. The simulation proceeded in this fashion until a predetermined real time had been covered. Other important features of the model can be listed:

- Vertical and lateral compliance of all tyres; the tyre model is non-linear and forces are represented as functions of tyre deflection.
- Forces at the fifth wheel
- Non-linear representation of springs and dampers
- The simulation can represent the vehicle at standstill in addition to forward and reverse speeds.
- Any axle may be steered; roll steer is included.

With these features the vehicle can be represented in both ride and handling modes.

To provide experimental data to check the predictions of the simulation, an articulated vehicle was built. The dimensions of the vehicle had to be such that parameters could be measured on equipment available at the School. These parameters include vehicle mass, inertias about all three axes, positions of centres of gravity, suspension kinematics and force characteristics, rolling and static tyre data.

This limitation resulted in the construction of a 10000-pound gross weight vehicle. It was developed around a Ford Transit chassis-cab unit. The semi-trailer was built as a heavily triangulated tubular structure to give maximum torsional stiffness.

The design allowed a number of parameters to be easily changed. The major items were trailer mass, inertias and position of centre of gravity, position of rear axle and position and geometry of fifth wheel. The vehicle was instrumented to record a range of velocities, displacements, and forces.

To validate the simulation, tests were performed on this vehicle at the following operating conditions.

AT REST

The tests performed at rest were concerned with the geometry and axle loads of the vehicle. Measurements were taken of the angles of pitch and roll and of the height of the rear of the trailer over a range of articulation angles.

Using the simulation, the corresponding displacements were computed and showed satisfactory correlation with the measured values.

A similar routine was applied to axle loads.

RIDE MOTIONS AT ZERO FORWARD SPEED

A feature of this simulation was its ability to examine vehicle motions whilst at rest.

By exciting with a hydraulic vibrator, bounce, pitch, and roll frequencies and mode shapes of the vehicle riding on its springs and tyres were measured for a range of articulation angles.

These tests were then simulated using an eigenvalue extraction procedure. To determine natural frequencies and mode shapes from the non-linear model by normal running of the simulation proved prohibitive in computer time. It was therefore assumed that the vehicle motions under examination were 'small.' This enabled the model to be locally linearized, then eigenvalues extracted to give the natural frequencies.

Seven modes were identified by this procedure against three by experiment. This was attributed to limitations in the experimental equipment. The three modes compared well with the corresponding simulated values.

STEADY STATE TESTS

A 350-foot radius curve was available for these tests. The vehicle was held in a steady state on this curve over a range of speeds. Steer and articulation angles were monitored. Satisfactory correlation was achieved between these results and the simulated performance of the vehicle.

TRANSIENT TESTS

To examine the vehicle's transient response, a step input of steer was applied over a range of speeds. Good correlation was shown between measured and computed results.

A transient response to a small step input on an initial steady state turn was used to prove the accuracy of the eigenvalue extraction procedure.

Details of this work are given in a paper by Ellis and Shapley entitled 'Analysis and Testing of the Articulated Semi-Trailer Vehicle,' Reference (5).

Between 1970 and 1972, two pieces of work were carried out at the School on vehicles with articulated steering. The first by Jablonski, Reference (6), describes a six degree of freedom mathematical model developed to predict the steering responses of a vehicle with articulated steering. Novel features of the model were that the axis set was positioned at the steer pin axes and that motion on an inclined plane could be represented. Four models of tyre lateral force were simulated on the vehicle model: Linear rigid, non-linear rigid, linear laterally flexible, and non-linear laterally flexible. A two degree of freedom model was employed to compare the responses of an articulated steered vehicle with those of a conventionally steered vehicle.

The work illustrated a difference between the transient responses of articulated and conventionally steered vehicles. This was attributed to an initial negative yaw of the rear body. The responses of a vehicle while operating on an inclined plane were shown to depend on its orientation on the plane. Making a

turn when the vehicle is initially pointing down the plane was shown to be a particularly unstable condition.

The second piece of work, Vickers (7), extended this study by developing a more complex model including the six degrees of freedom for each of the three vehicle units: Main body, steered body, and rear axle. The tyre model included lateral and vertical flexibility. Undulating and inclined terrain was also modelled.

The simulation was employed to examine the vehicle's transient responses to terrain irregularities from both the vehicle handling aspect and vehicle riding quality. Conditions of static rollover were also investigated.

In 1972, Ben-Ari carried out a piece of work developing a mathematical model of a driver to control a vehicle model through a manoeuvre. The vehicle model chosen was the four degree of freedom, non-linear articulated vehicle. When the driver/vehicle system was performing satisfactorily in taking a standard vehicle through an S-bend, certain variations to vehicle parameters were made so that the 'driver's' reactions could be observed.

The parameters varied were:

a) Position of fifth wheel

b) Position of centre of gravity of trailer

c) Wheel base of trailer

Variations (a) and (b) confirmed the effects on vehicle stability examined in (3). Variation (c) indicated that semi-trailers below 20 feet might cause drivers some control problems.

The vehicle's responses to locked axles were also graphically illustrated by the use of computer graph plotting facilities. Details of this work are given in a paper by Ben-Ari and Ellis entitled 'Simulation of the Driver-Vehicle-Road System; An Initial Study,' Reference (8).

In April 1974, the School was awarded a contract by the Transport and Road Research Laboratory, Crowthorne, England, to examine various aspects of vehicle safety. One of these aspects was an examination of the handling characteristics of 'Double' outfits by simulation.

Vehicles towing two trailers, e.g., a semi-trailer and a full-trailer, are not permitted on British roads. However, their use on trunk roads and motorways for moving goods to distribution points outside cities is being considered.

Two models of this type of vehicle have been developed:

1) A linear, small angle model with constant forward speed

2) A non-linear, large angle model with variable forward speed

These models have been derived using the technique described by Ellis (1). The four portions of the vehicle: Tractor, semi-trailer, dolly axle, and second semi-trailer, are considered separately and linked by equating velocities and forces at the three joints. Both models neglect roll, pitch, and bounce. The non-linear model incorporates a braking model.

The linear model has been produced as both digital and analogue simulations. The non-linear model has only been produced in digital form.

Both models are now performing satisfactorily. The linear model will be used to examine handling characteristics of a 'double' outfit and such features as tracking or cut-in. The non-linear model will be employed to examine the unit's response to combinations of locked axles.

Vehicle data for these simulations is being derived from the only 'double' outfit in Britain. This has been produced as a demonstration unit jointly by Volvo and Crane-Fruehauf. It comprises a tractor and two 27-foot semi-trailers. Gross vehicle weight is 38 tons.

Work is in progress at the School to study the effects of multi-axle sets and steering axles on semi-trailers. A linear, small angle model of a single trailer vehicle with freedom to roll is also under development, along with a model of the car/trailer home combination.

The aim of the current work at the School is to produce a suite of programs of varying complexity to cover a wide range of vehicle configurations. It is planned that in the near future work will begin on an experimental vehicle, based on Shapley's unit, to provide performance data to validate these simulations.

REFERENCES

1. Ellis, J.R., "The Dynamics of Vehicles During Braking," I. Mech. E. Symposium on Control of Vehicles, 1963.

2. Horn-Andrews, B.W., "The Dynamics of an Articulated Vehicle During Braking," MSc Thesis, Cranfield Institute of Technology, 1964.

3. Ellis, J.R., "The Ride and Handling of Semi-Trailer Articulated Vehicles," Automobile Engineer Journal, December 1966, pp. 523-529.

4. Ellis, J.R., Vehicle Dynamics, London Business Books, 1969.

5. Ellis, J.R. and Shapley, C.G., "Analysis and Testing of the Articulated Semi-Trailer Vehicle," I. Mech. E./SAS Joint Symposium on Vehicle Safety Legislation, Cranfield, 1973.

6. Jablonski, J.E., "Simulation of the Steering Responses of a Vehicle with Articulated Steering," MSc Thesis, Cranfield Institute of Technology, 1971.

7. Vickers, A.G., "The Vibration Environment of a Vehicle with Articulated Steering," MSc Thesis, Cranfield Institute of Technology, 1972.

8. Ben-Ari, S. and Ellis, J.R., "Simulation of the Driver-Vehicle-Road System; An Initial Study," I. Mech. E./SAS Joint Symposium on Vehicle Safety Legislation, Cranfield, 1973.

THE ROLE OF ANALYTICAL TECHNIQUES IN THE FORMULATION OF VEHICLE SAFETY STANDARDS

Ronald L. Eshleman*
The Vibration Institute

* Formerly Science Advisor, IIT Research Institute, Chicago, Illinois.

INTRODUCTION

This paper briefly discusses the role of analytical techniques in the formulation of vehicle safety standards. The use of analytical techniques in the solution of vehicle handling and braking problems came of age with the digital computer in the era of the late fifties. Efficient use of the digital computer to solve numerical problems provided the engineer powerful tools for solving nonlinear differential equations. The present technology in this area is reviewed here along with the development criteria for safety standards. The paper also discusses the evaluation of response levels of general classes of vehicles and specific vehicle characteristics as they affect handling and braking capabilities. The emphasis in this paper is placed on actual maneuvers, roads, environments, and drivers. Separation of each of these effects is important in evaluations of braking and handling problems.

ANALYTICAL TECHNIQUES

Linear models have long been used to determine the stability and frequency response of vehicles. The use of these models in assessing stability leaves a lot to be desired, because in crucial maneuvers, the vehicle and its tires operate in the nonlinear regime. A case might be made for the use of linear models to evaluate the response of the vehicle in linear tire regimes during normal driving. However, safety criteria must be devveloped in nonlinear regimes of operation.

In this paper we are most interested in nonlinear response models. The only practical analytical method available today for the evaluation of nonlinear responses of a vehicle is direct integration of the equations of

motion. The equations can be integrated in one or two simple ways. The conventional control mode, where driver braking and steering are provided to the vehicle model and the vehicle response is assessed, can be used. The second method, called the trajectory mode, uses a maneuver input which constrains the c.g. of the vehicle to move through this maneuver. Figure 1 shows the scheme of computations for the trajectory mode. The left side of the figure indicates that any sort of maneuver may be put into the analytical model, which is a nonlinear model. This model, of course, takes care of all the properties of the vehicle, the road, and the environment. The model provides the response of the unconstrained variables, such as yaw, pitch, and roll. A check of the stability of the vehicle is obtained; and, finally, the response of the vehicle is generated.

Pure mathematical stability techniques--the solution of the equations of motion for asymptotic stability--have not been developed sufficiently for vehicles to provide practical results. To assess stability on a mathematical basis, the vehicle is operated on a prescribed trajectory, like those used in Figure 1, and the response of the vehicle is calculated as it moves through the trajectory. If the vehicle is perturbed due to environmental factors, vehicle error, or driver error, it may or may not return to its original trajectory. Whether it returns is a measure of its stability. A set of perturbation equations drived from the vehicle equations of motion is used to perturb the vehicle from its original or nominal trajectory. After the perturbation, which is just a slight motion off the trajectory, if the vehicle comes back to the trajectory, then it is assessed

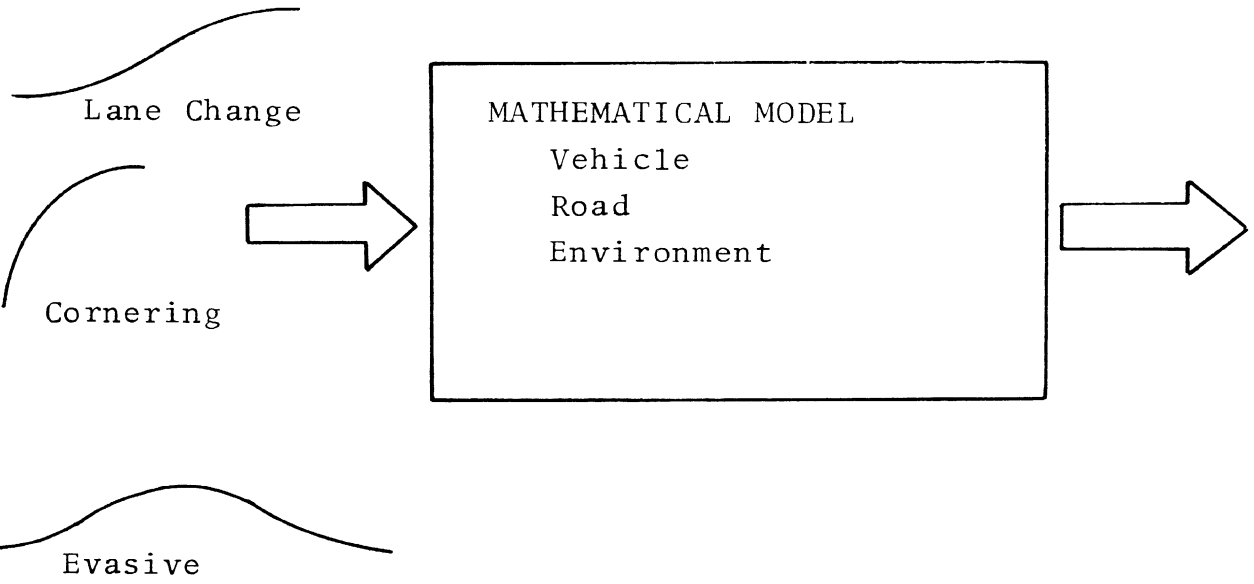

Figure 1. Articulated Vehicle Handling Methodology.

as being stable. If the vehicle departs from the trajectory, then it is unstable. Some people think this is a very restrictive theory, because it does not include provision for the vehicle's moving to an associated trajectory that may be stable. Figure 2 shows the relationship between mathematical stability and physical stability. Of course, physical stability is based on the slip angles and motions of the vehicle, whereas mathematical stability is a pure go/no-go type of assessment.

Several significant calculations using the trajectory mode have been made using the Articulated Vehicle Dynamic Simulation or so-called AVDS program. AVDS was developed at the Illinois Institute of Technology Research Institute in the early 1970's under federal sponsorship [1].

Some examples of work done with the AVDS simulation model using nonlinear differential equations are shown in Figure 3. Figure 3 shows the response of a tractor double semitrailer on a 14-ft. wide x 190-ft. long lane change at 40 miles per hour. The acceleration of the center of gravity of the vehicle is shown above the steering angle. The dotted lines on these figures represent simulation and the solid lines represent experimental results. Figure 4 shows the absolute yaw angles of the tractor and also the dolly. Finally, the relative yaw angles between the tractor trailer and the dolly, second semi-trailer are shown in Figure 5.

Figure 6 shows the results of some experiments involving steering response of drivers. It shows what they do with respect to the trajectory mode of computation. The trajectory mode of computation gives the response of

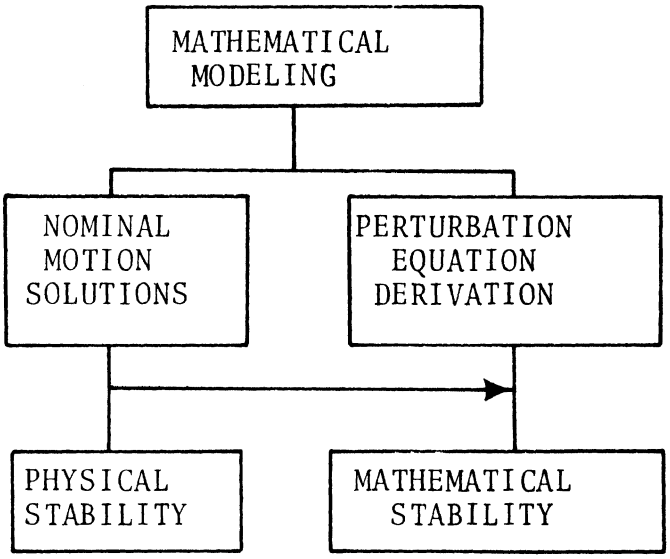

Figure 2. The Relationship Between Mathematical and Physical Stability.

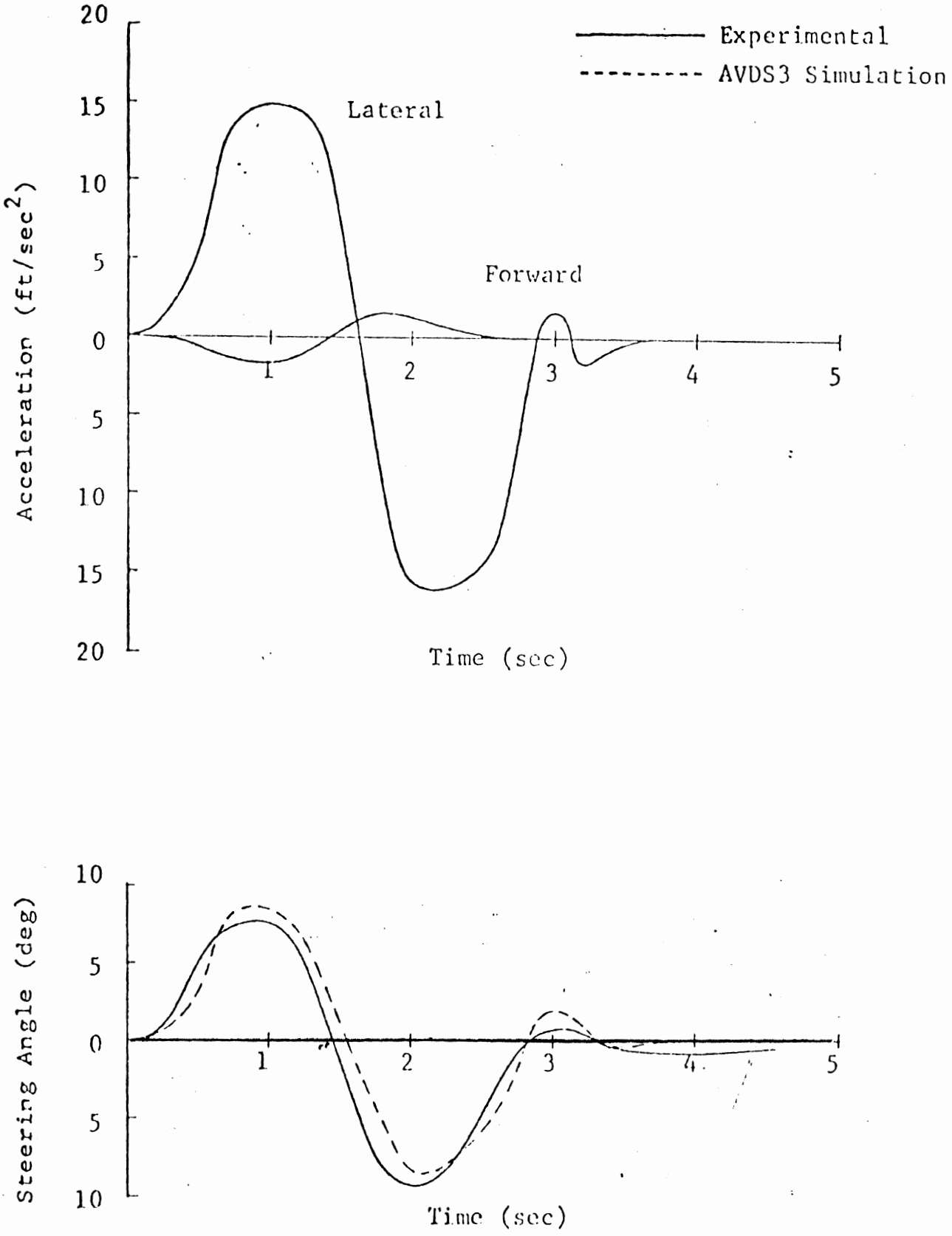

Figure 3. Analytical-Experimental Comparison of tractor double unloaded semitrailers (27 ft) response for lane change (14.4 ft x 191 ft) at 40 mph without braking. Steering angle vs. time

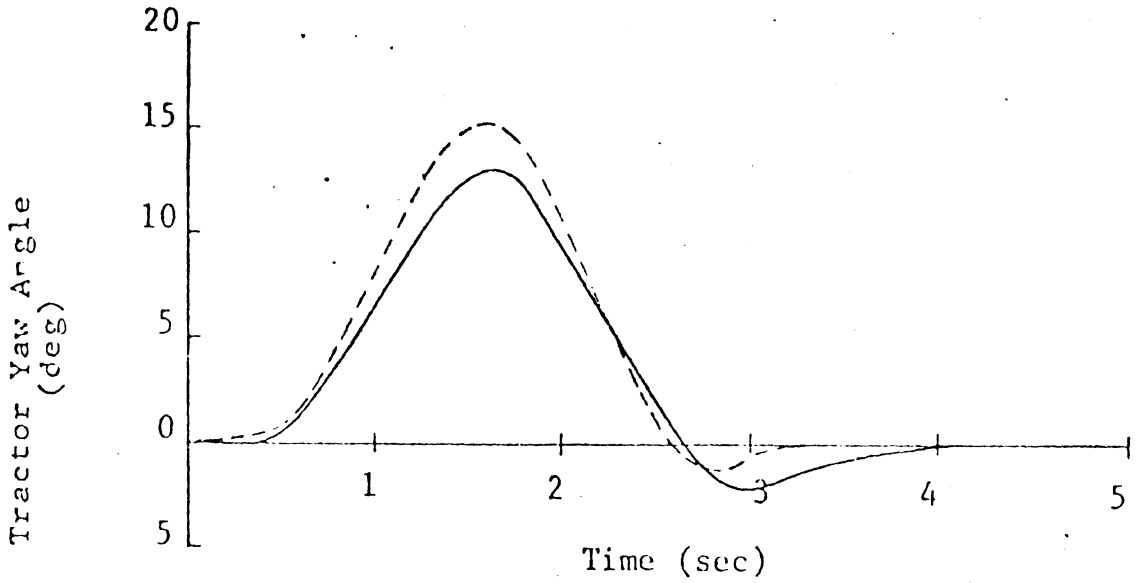

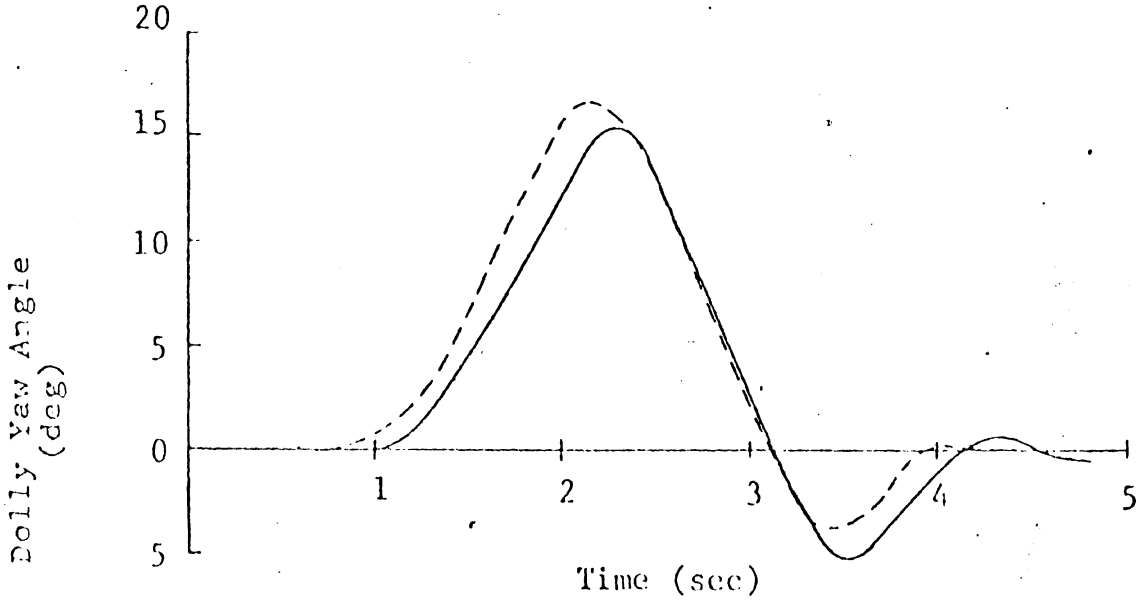

Figure 4. Analytical-Experimental Comparison of tractor double unloaded semitrailers (27 ft) response for lane change (14.4 ft x 191 ft) at 40 mph without braking. Tractor and dolly yaw angle vs. time.

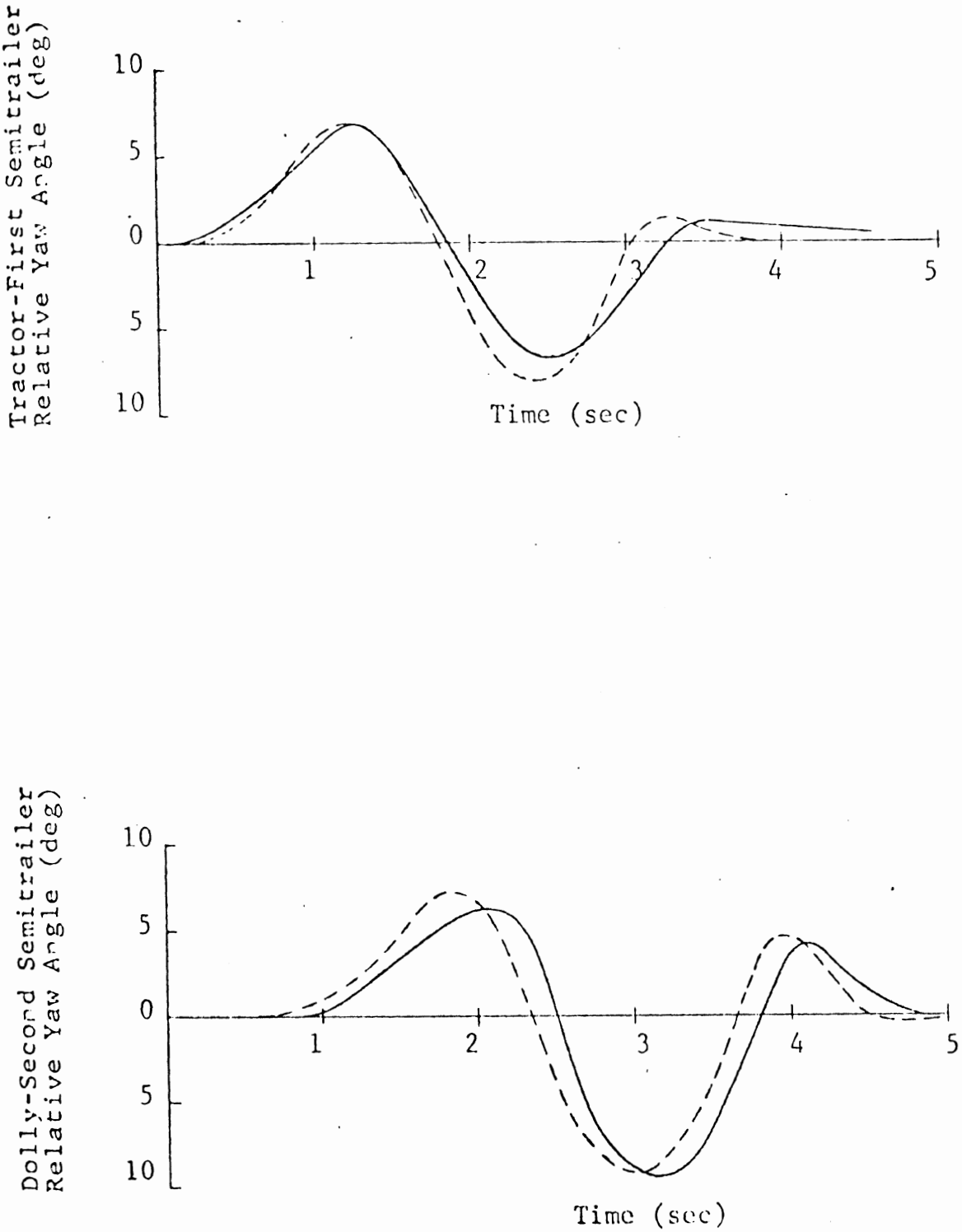

Figure 5. Analytical-Experimental Comparison of tractor double unloaded semitrailers (27 ft) response for lane change (14.4 ft x 191 ft) at 40 mph without braking. Relative yaw angle vs. time.

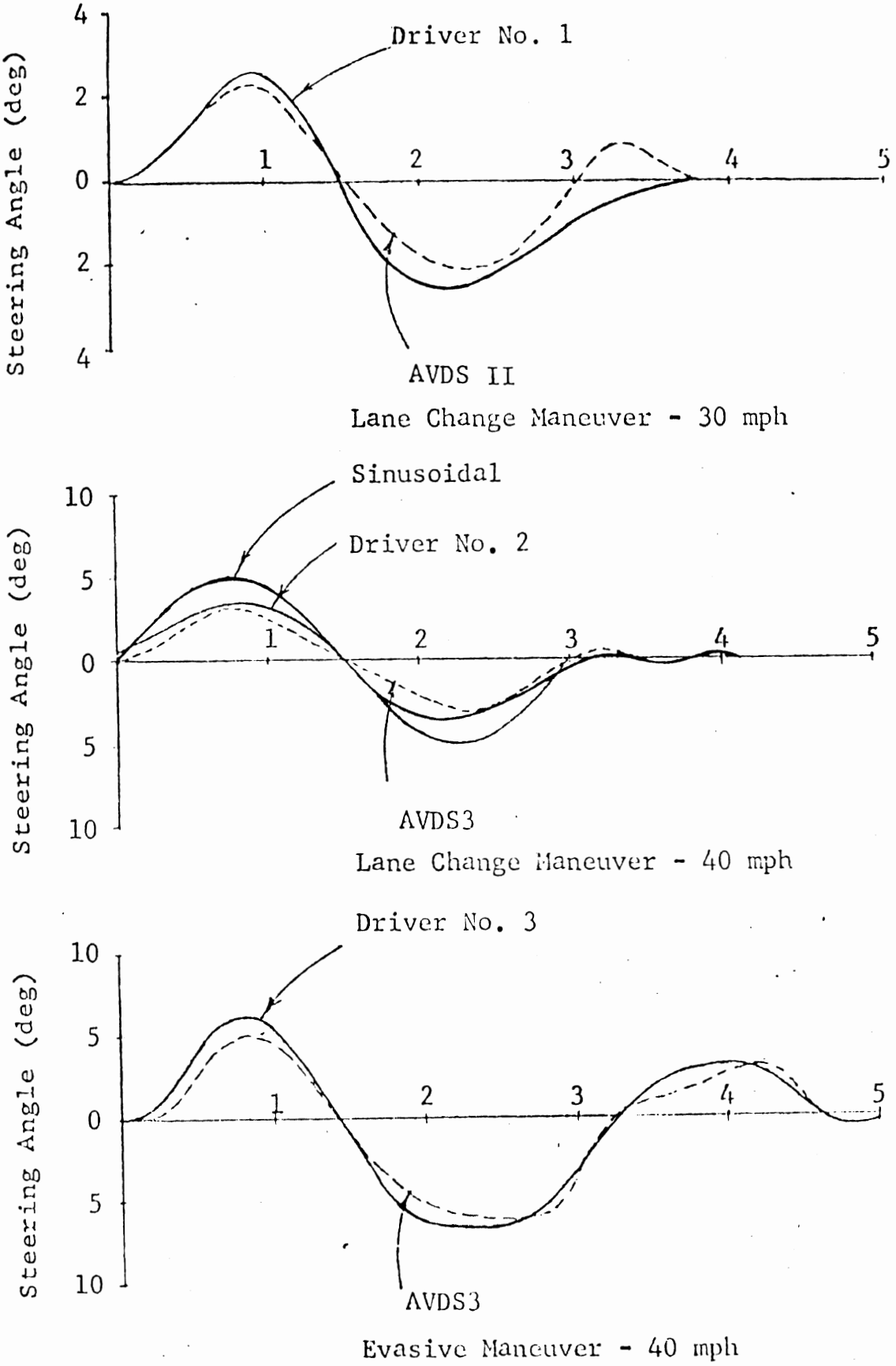

Figure 6. Driver characteristics

the optimum driver for that maneuver. Therefore these results show how the driver compares with the optimum driver. Having the optimum driver in a vehicle acts as a decoupling device for vehicle evaluation. These are some experiments taken at different times and compared to an optimum driver, as calculated by AVDS. This tells us something that we have known all along, that most drivers are pretty efficient; they do just about the best they can with the vehicle.

VALIDATION

Why do we validate? First, because there is a credibility problem with analytical techniques and simulation. To improve the credibility of these techniques, the results are compared with the results obtained from full-scale experiments. The second reason for validating concerns knowledge. Every time a valid experiment is conducted, data are obtained on how the simulation is working. Figure 7 shows a scheme used for validation with the trajectory mode; it shows the computer model obtaining test data from the real vehicle. The driver steers with light constraints through some maneuver. The vehicle responses and also the steering are measured and recorded. The actual measured trajectory that the driver went through is introduced to the analytical model, and the driver response obtained is one that would have resulted if the optimum driver had been used. The responses obtained are compared to full-scale tests on a one-to-one basis.

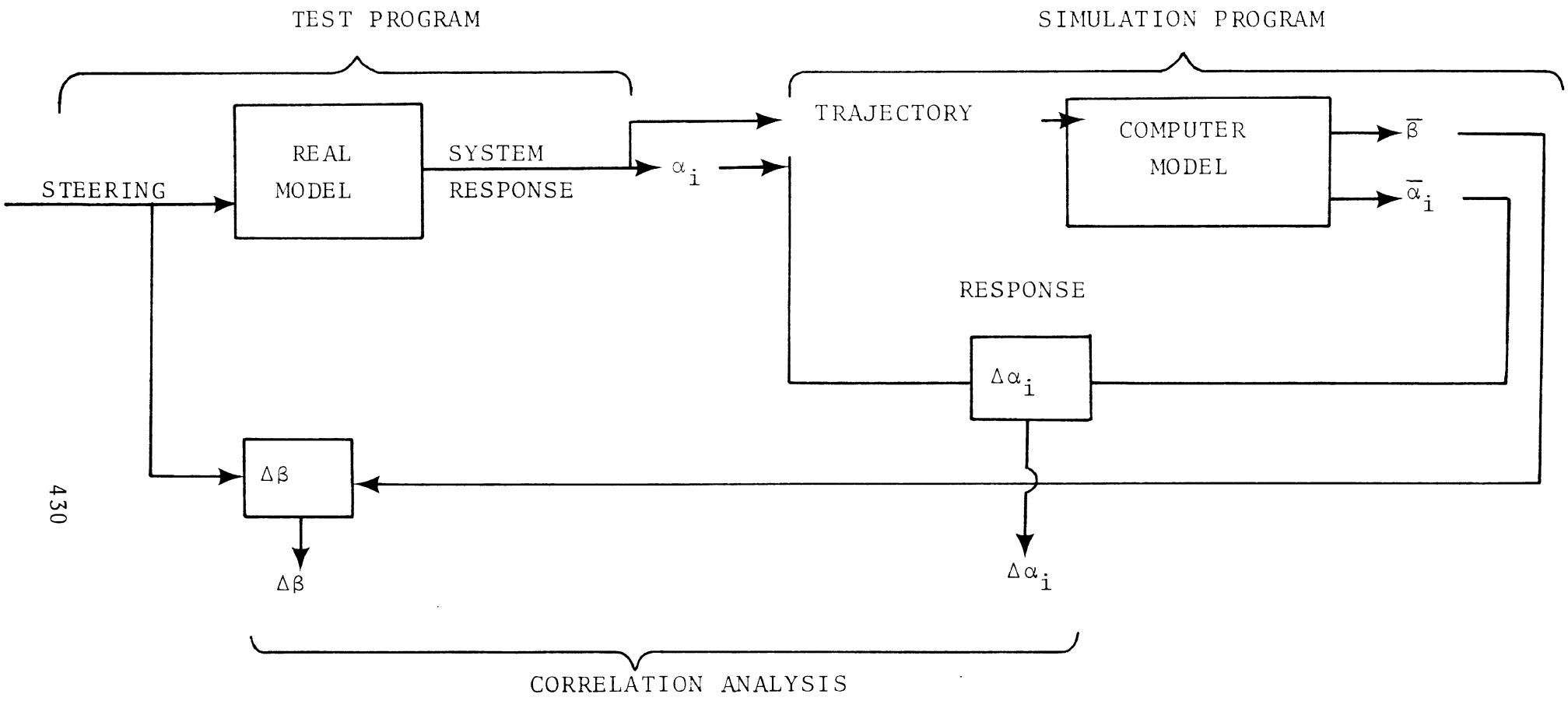

Figure 7. Analytical experimental validation

SAFETY STANDARDS DEVELOPMENT

What type of safety standard development can be done or has been done? Some work has been done on criteria development with respect to stability. Criteria development has been approached from the point of view of mathematical stability and physical stability. This relationship was shown in Figure 2. A second set of criteria could be concerned with the sensitivity of the vehicle to its environment. For instance, is it sensitive to a bad driver, or to wind, or to road perturbations? This set of criteria needs development. The third set of criteria is concerned with vehicle maneuverability and space considerations. How much space should be allowed for a vehicle to perform its maneuver? How does this affect traffic? Do you call a vehicle safe if it can perform the required maneuver but has taken up so much space that it causes an accident in heavy traffic conditions or in a traffic mix? These are questions that have to be answered technically under prescribed ground rules.

An example of a stability chart, showing limit maneuver speed versus road-tire coefficient, is shown in Figure 8. Some experimental results identified on this figure show the driver doing about what was expected. Figure 9 shows a stability chart based on peak lateral acceleration. This figure shows the variation of stability from vehicle to vehicle for lane changing. It shows the different stability levels obtained for a tractor-single, double, and triple semitrailer.

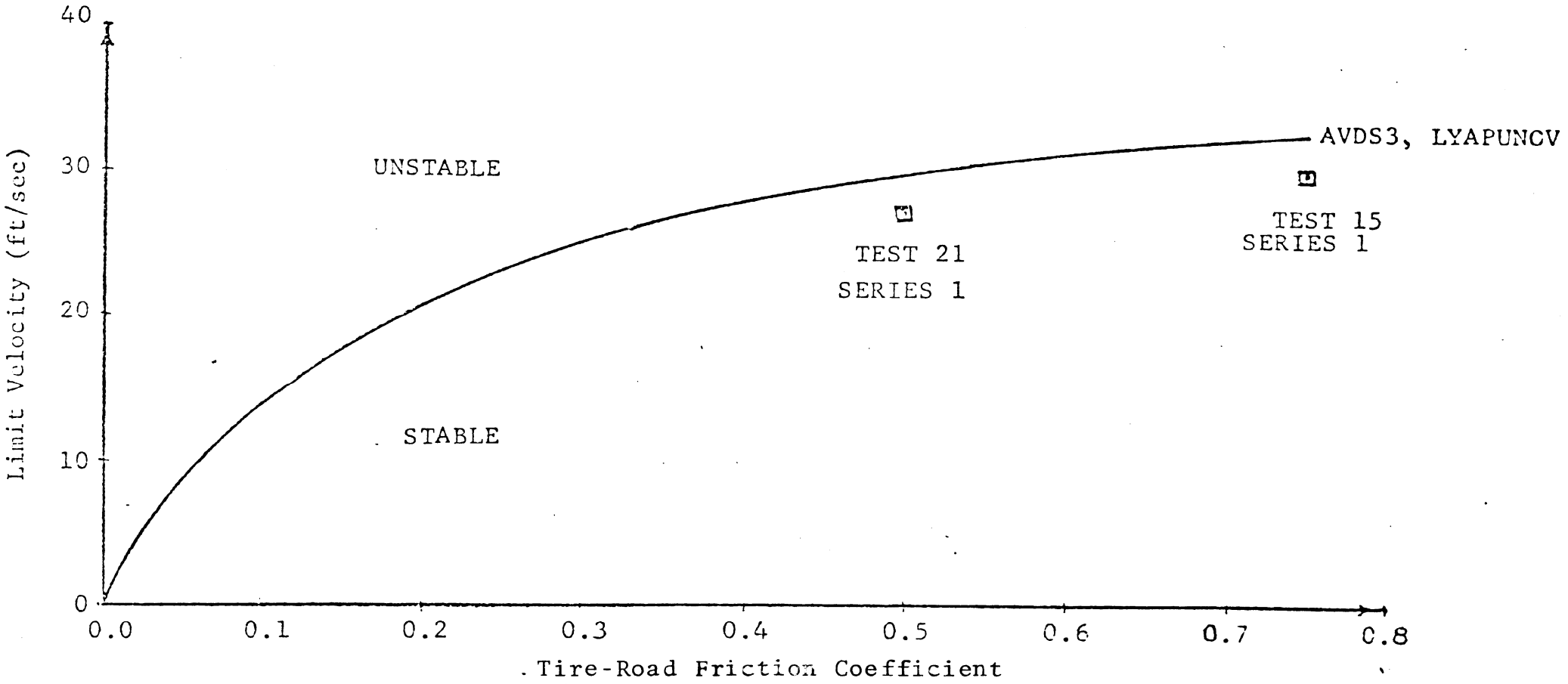

Figure 8. Tractor single-trailer (45 ft) vehicle stability limit for a 75-ft. radius circular maneuver without braking.

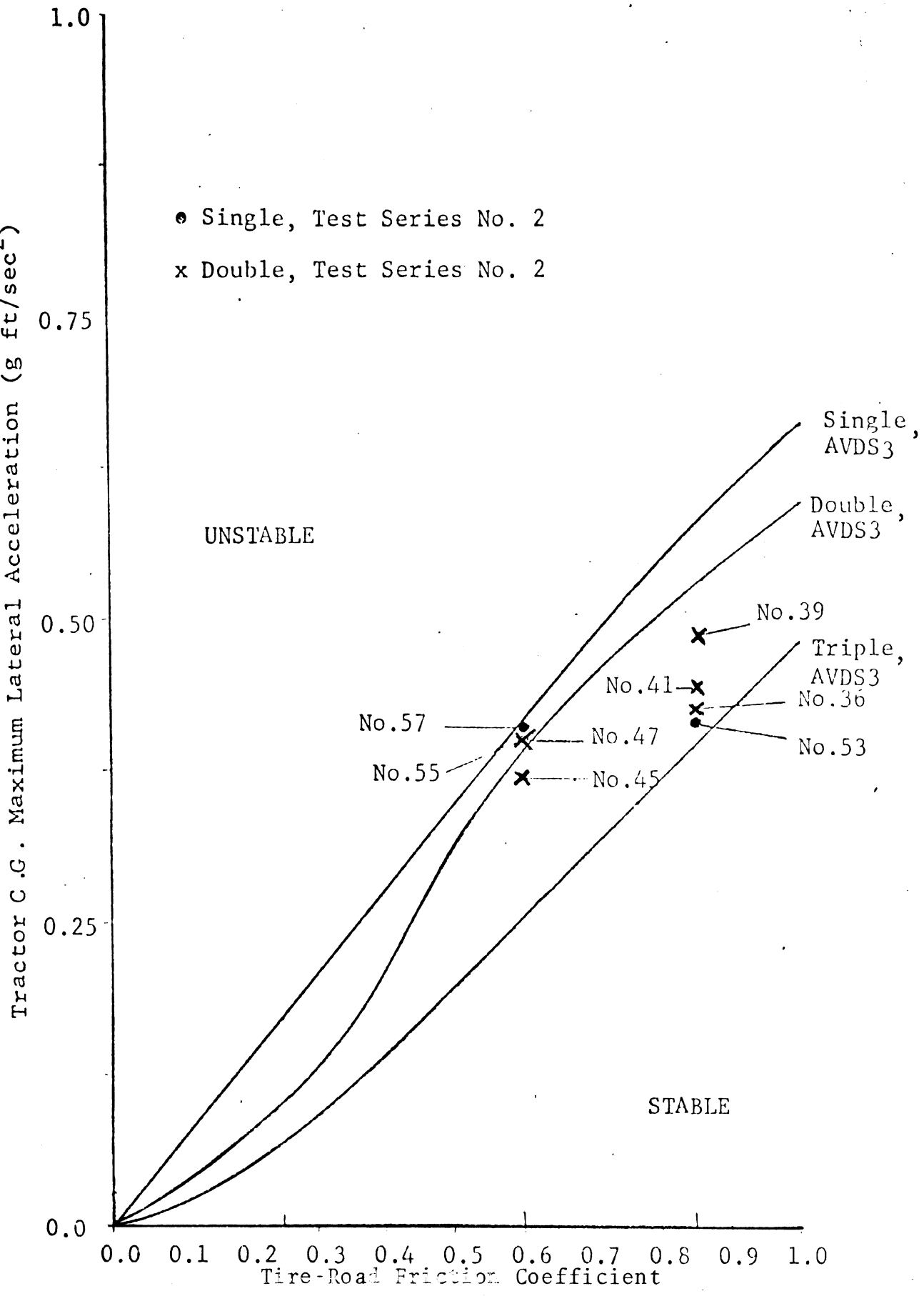

Figure 9. A comparison of stability limits for unloaded tractor single, double, and triple (27 ft) semitrailer systems performing 12-ft, evasive and lane changing maneuvers without braking.

EVALUATION OF LEVELS

Along with criteria development, some kind of an evaluation of levels is necessary. Two types of studies are conducted: sensitivity and parameter studies. Using sensitivity studies, different general classes of vehicles can be evaluated for the given environmental conditions. The effects of the road and of the driver—whether he is optimum or degraded—can be factored into this study. Using the analytical model, the driver can actually be degraded to see what effect he has on the vehicle performance. Figure 10 shows this type of information relating required steering to road condition.

Many of the vehicle parameters can be varied. These parameters include the vehicle geometry, tires, brakes, suspension, and loading. Figure 11 shows the type of chart that can be constructed to evaluate the vehicle characteristics. In essence this chart is the result of parameter variations.

CONCLUSIONS

Analytical techniques, available today, can be used as tools for the development of safety standards. These techniques have been validated and are ready to be used in the development of criteria and levels in safety standards. It must be understood, however, that the results of these techniques must be tempered by human judgment. Social and economic factors must be considered in the total development of safety standards.

The analytical techniques can be used to conduct sensitivity and parameter studies in vehicle design and evaluation. In addition, meaningful test programs can be developed with the aid of analytical techniques. These

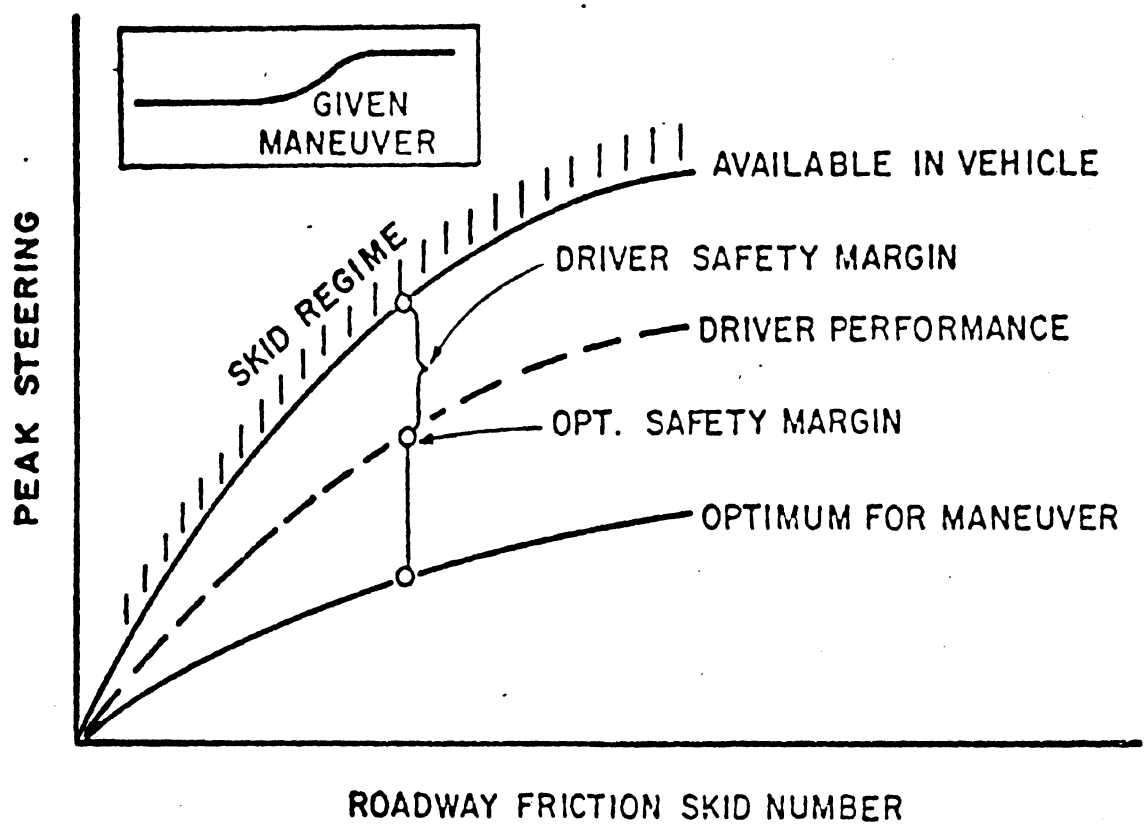

Figure 10. Driver friction demand index

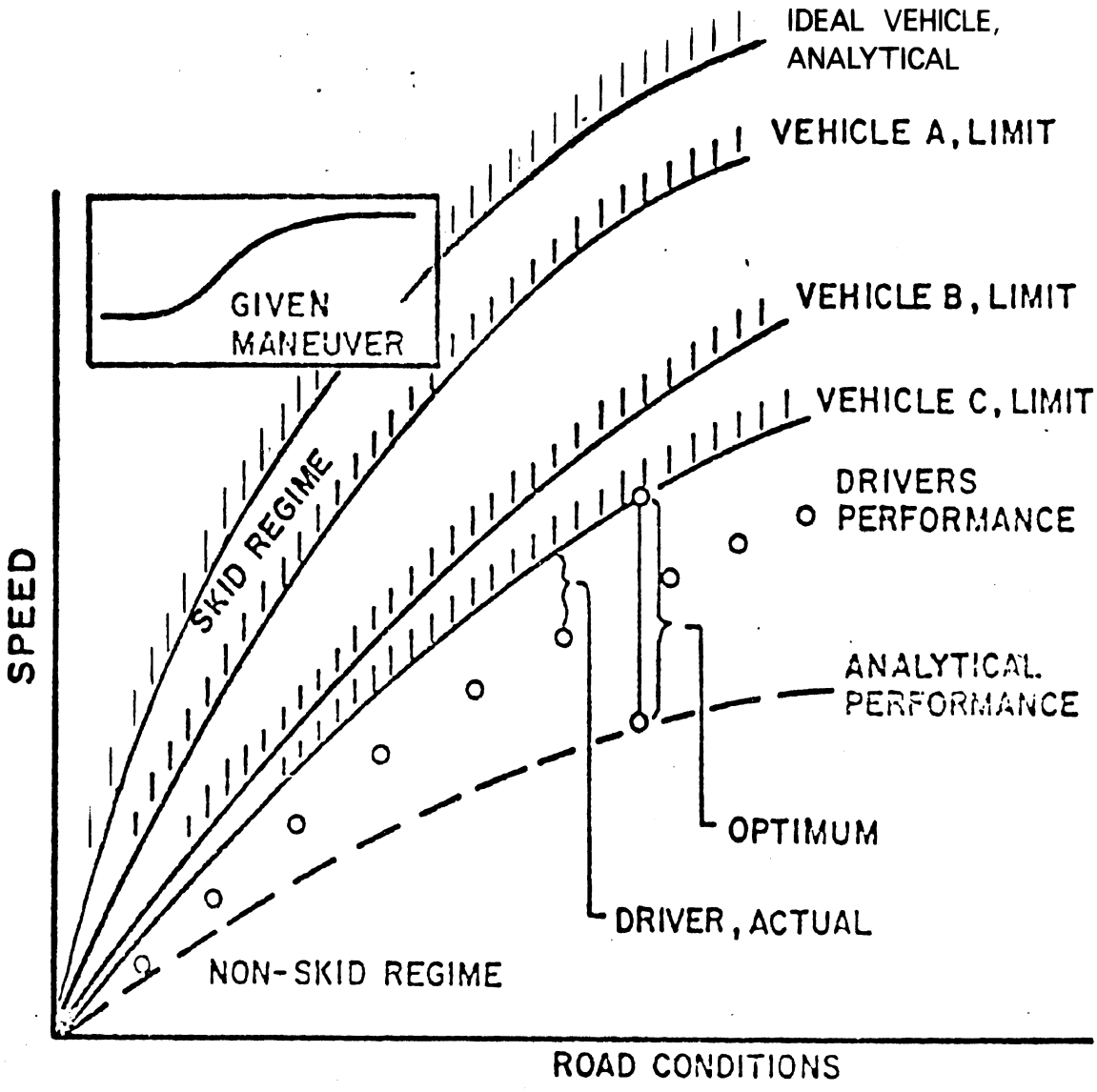

Figure 11. Vehicle maneuverability index

techniques should be used in the future, along with full-scale testing, to aid in the development of realistic safety standards based on present technology.

PREDICTION OF BRAKING AND DIRECTIONAL RESPONSES OF COMMERCIAL VEHICLES

P. S. Fancher, Jr.
Highway Safety Research Institute
The University of Michigan

INTRODUCTION

This paper provides an overview of the truck and tractor-trailer braking and handling project which the Highway Safety Research Institute (HSRI) has been conducting for the Motor Vehicle Manufacturers Association. The purpose of this research is to establish a digital computer-based mathematical method for predicting the longitudinal and directional responses of trucks and tractor-trailers.

In the context of this study, prediction involves the use of computer simulations to obtain numerical results that quantify the braking and steering responses of specific commercial vehicles (or projected vehicles). In addition to providing numerical results, the simulations can aid in developing an understanding of how changes in vehicle components and/or test conditions influence the response of a motor-truck system. Clearly, a basic understanding of the influence of changes in vehicle parameters and test conditions on vehicle response is fundamental to gaining confidence that the simulations are predicting valid and useful results.

Large-scale computer programs for predicting longitudinal and directional responses have been delivered to the vehicle manufacturers by HSRI. At the present time these programs are being applied and evaluated. The programs are intended to be useful for extrapolating from test results for a baseline vehicle configuration. After the simulation has been developed to the point where it accurately simulates the performance of a baseline vehicle, the values of parameters in the computer simulation can be changed to correspond to changes in vehicle configuration, and the simulation

will predict how the new vehicle configuration would perform. Experience will provide the basis for judging the accuracy and utility of this approach.

The body of this paper contains sections entitled:

- Objectives
- Elements of a Simulation Approach
- Accomplishments (A Historical Review)
- Future Developments
- Concluding Remarks

OBJECTIVES

The ultimate goal of the truck and tractor-trailer braking and handling project is to develop optimum means for predicting and evaluating the longitudinal and directional responses of commercial vehicles. The specific objectives are to ensure that industry and government will have available for use in their research

(1) appropriate computer software

(2) new techniques and equipment for parameter measurement, and

(3) meaningful response measures.

ELEMENTS OF A SIMULATION APPROACH

The turning and braking responses of highway vehicles are described by complex sets of non-linear differential equations. The state of knowledge concerning the performance of some vehicle components (for example, brakes, tandem suspensions, or tires) may necessitate using tables of empirical data rather than

analytical functions. In general, physical systems with these characteristics are intractable to closed-form solution. Consequently, computer simulation methods are used to develop means for predicting the braking and directional responses of commercial vehicles.

The general elements of a simulation approach are discussed here to provide a background for understanding the steps taken by HSRI to meet the objectives of this investigation.

A block diagram of the approach used by HSRI is shown in Figure 1. Clearly, the initial step in this approach is to describe the physical properties of commercial vehicles in mathematical terms. Once the equations are formulated and programmed on the computer,

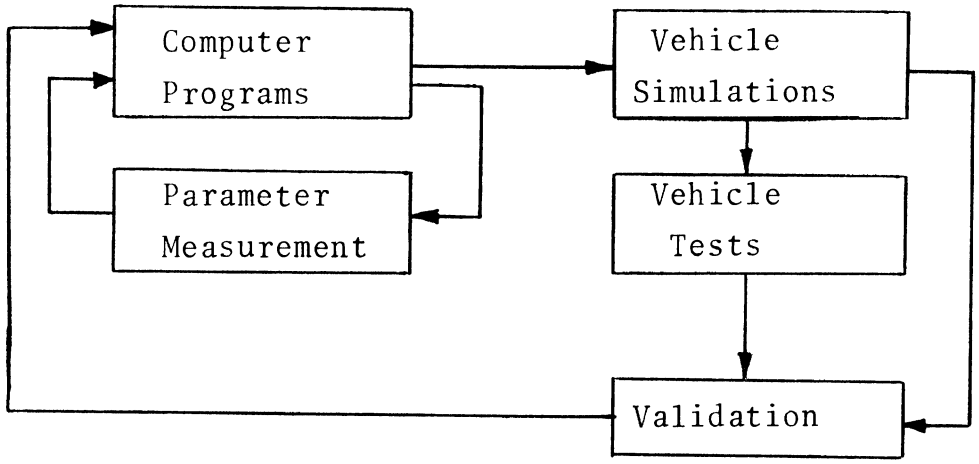

Figure 1. Development of a Computer-Based Prediction Capability Includes Parameter Measurement and Vehicle Test.

parametric values are needed before calculations can be made. For a complex vehicle model the parameter measurement activity can be difficult, costly, and time-consuming. To check whether the calculations are valid, vehicle test results are required to compare with simulated results. Thus the development of a computer simulation implies the development of parameter-measurement and vehicle-testing capabilities.

As indicated in Figure 1, the results of experimental activities (either parameter measurement or vehicle testing) influence the mathematical models. New information and ideas gained from experimental work are used to refine the model so that it becomes a better representation of the vehicle. Several iterations of parameter measurement, calculation, and vehicle testing may be needed to obtain confidence that (1) the vehicle system is adequately described by the equations (and empirical data), (2) the equations are programmed correctly, (3) the parameters are measured accurately, and (4) the vehicle response tests are conducted properly.

Once the original development cycle is completed and the simulation is operating, the user may find that he would like to extend the range of application of the computer program. The process of augmenting the program includes the elements of the original development cycle. Changes in the computer program to meet new requirements involve additional parameter measurement activity and further comparisons with vehicle test results. The process of extending the computer program is diagrammed in Figure 2.

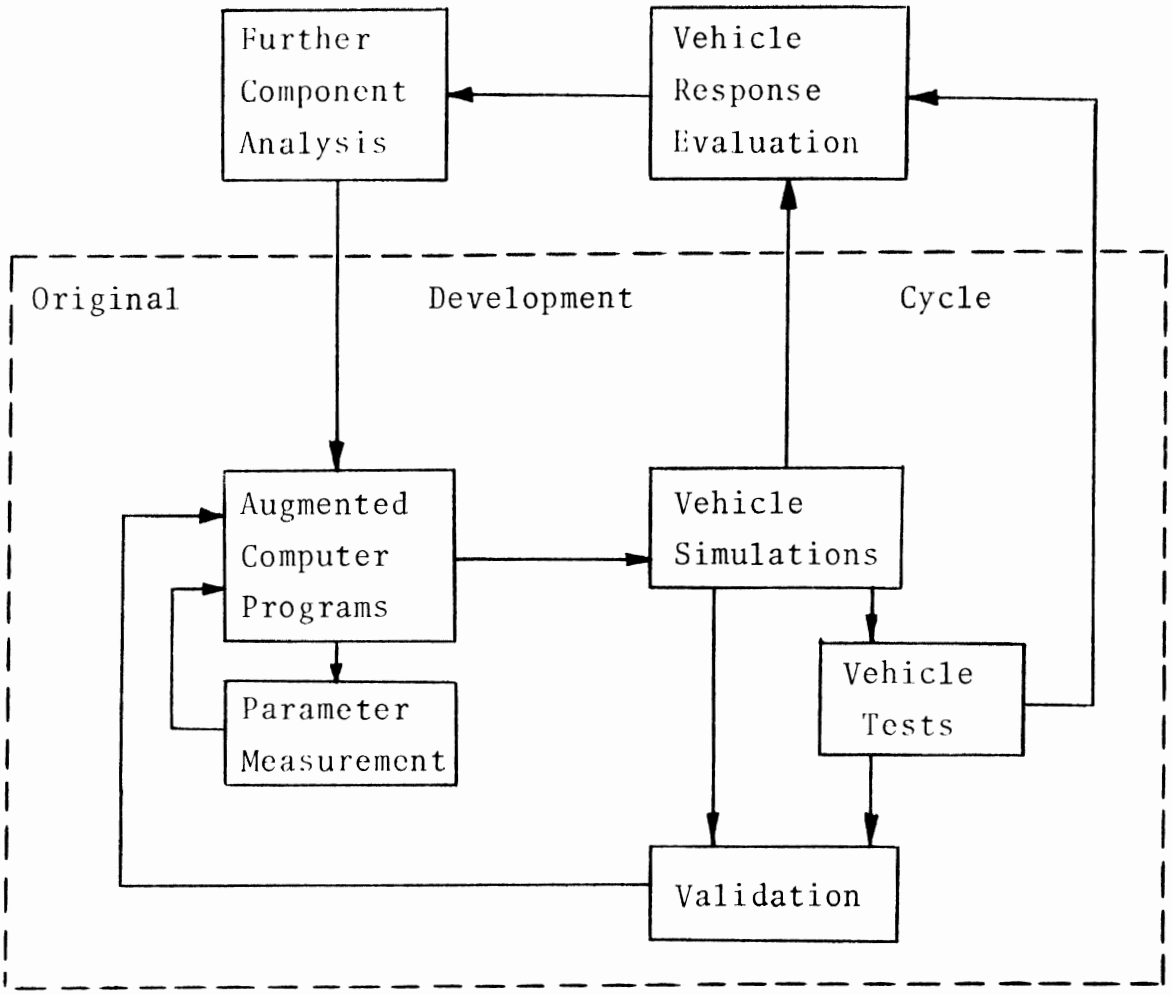

Figure 2. New Requirements Lead to Further Development

ACCOMPLISHMENTS (A HISTORICAL REVIEW)

The motor truck braking and handling project started in mid-1971. The major outputs from this project have been (1) comprehensive computer-based models for predicting the braking and directional response of trucks and tractor-trailers [1 through 5]* and (2) the development of test equipment and techniques for obtaining the parametric data needed in the computer models to simulate trucks and tractor-trailers [1, 3, 4, and 6 through 11].

From mid-1971 through mid-1973, the project was conducted in three phases. In Phase I, lasting from mid-1971 to mid-1972, a mathematical model of the straight-line braking performance of trucks and tractor-trailers was developed [1]. That model was constructed from mathematical representations of inertial properties, tandem suspension systems, tire-road interface forces, braking systems, and wheel rotational dynamics. The braking model contained 15 degrees of freedom for a tractor-semitrailer with five axles. The degrees of freedom included were (1) vertical motion of each axle, (2) rotational dynamics for the wheels on each axle, (3) vertical and pitch motions for the tractor and trailer sprung masses, and (4) a longitudinal degree of freedom for the entire vehicle.

The specific vehicles used by HSRI to validate the computer program constructed from this mathematical model were: a 50,000-lb GVW Diamond Reo straight truck, and a tractor-semitrailer consisting of a 6 x 4 COE White tractor and a 40-ft. Fruehauf trailer. The

---

*Numbers in brackets designate references.

straight-line braking performances of these vehicles were measured and compared with results obtained from computer simulations of the same tests (30 and 60 mph empty and loaded, dry and wet pavement). The simulated test results in general agreed closely with the results of the experimental braking tests for the Diamond Reo truck, which was equipped with a walking-beam tandem suspension. The simulated results for stopping distance versus brake pressure for the tractor-semitrailer vehicle also matched the test results. However, the simulation predicted wheel lock at a much lower level of brake pressure (and consequently, longer stopping distances) than the level of brake pressure which caused wheel lock in the vehicle tests. An improved model of the four-spring tandem suspension employed on the Fruehauf trailer and the White tractor was developed later (in Phase III) to correct this deficiency of the simulation.

In Phase II, conducted in 1972 and reported in 1973, the work focused on developing a computer program for simulating the directional response of trucks during combined steering-braking maneuvers [3]. This second computer program contains all of the brake, suspension, and tire modeling features contained in the straight-line braking performance simulation program plus the possibility for simulating the lateral, yaw, and roll motions of the vehicle. As with the first program, it was validated against experimental test results on both the straight and articulated vehicles.

Developing a simulation program to model the directional responses of an articulated vehicle was a complex undertaking. It was necessary to begin with the pitch plane model developed in Phase I and then

perform the following tasks:

1. Select appropriate axis systems and write equations describing the vehicle motion in terms of dynamic variables defined relative to these axis systems.
2. Program and refine a semi-empirical mathematical model for representing measured tire shear force characteristics.
3. Develop techniques for computing forces and moments of constraint between sprung and unsprung masses.
4. Model the fifth-wheel coupling between tractor and trailer.
5. Include deflection and compliance steer characteristics as well as side-to-side differences in steer angle.
6. Develop, refine, and use equipment and techniques for measuring vehicle inertial properties, axle roll steer, fifth-wheel roll spring rate, and tire shear force characteristics.
7. Perform full-scale vehicle tests consisting of steady turns, braking-in-a-turn maneuvers, and jackknife maneuvers.
8. Simulate the maneuvers listed in 7. and compare the predicted results with measured results to verify the validity of the simulations.

The computer program for simulating braking/steering responses has been written so as to be efficient and easy to use [12, 13]. However, users of this program must know a great deal about the components

of the vehicle (or projected vehicle) to be able to supply the needed parametric data.

Figure 3 presents a sample of simulation results that show very good correlation with test data. This level of agreement between simulation and test results requires that control input and parametric data describing the vehicle (including its tires) be extremely accurate.

In Phase III of the project, HSRI researchers refined and extended the work of Phases I and II in the following studies:

1. Development of a digital-computer-based method for predicting the moments of inertia and center-of-gravity locations along the principal axes for various truck, tractor, and trailer configurations.

2. Refinement of tandem-suspension models already developed, and formulation of models for five additional suspension types.

3. Development of over-the-road equipment for measuring the longitudinal shear force characteristics of truck tires.

4. Development of models for typical truck anti-lock braking systems to be used with Phase I (Braking Performance) and Phase II (Braking and Handling Performance) simulation programs.

5. Extension of the Phase I program to include provision for simulating a doubles (tractor-semitrailer-trailer) combination.

6. Development of a brake temperature model to be used for simulating the decrease in brake effectiveness as a result of fade.

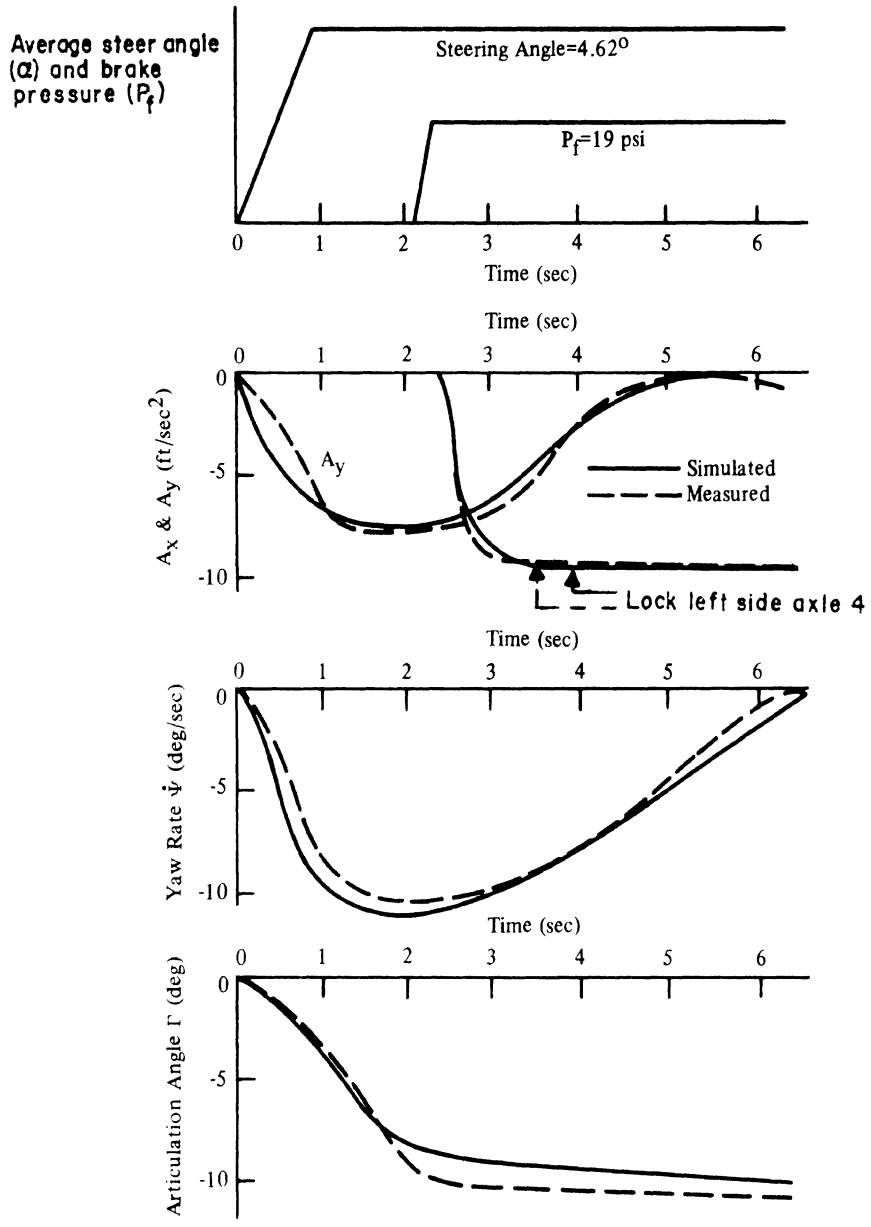

Figure 3. Validation of a braking-in-a-turn maneuver for a tractor-trailer.

7. Development of a computer-based mathematical model for evaluating the acceleration and handling performance of trucks and tractor-trailer combinations.

The results illustrated in Figure 4 show the improvement obtained with the refined four-spring tandem suspension model, which was developed in Phase III. As evidenced by the incipient wheel lock indicators in the figure, the initial model (Suspension Model I) predicted interaxle load transfer in excess of the levels that occurred in the vehicle tests. The second model (Suspension Model II) includes frictional forces at the points where the leaf springs contact the frame. These forces reduce the level of interaxle load transfer by contributing to the reaction of brake torque [8]. The data presented in Figure 4 demonstrate the increased accuracy of wheel lock prediction using the new model of the four-spring suspension.

At the end of Phase III the extended and refined braking performance program was operational on computers at several manufacturers of commercial vehicles. The simulation was used to aid in the development of vehicle systems intended to meet impending Federal motor vehicle safety standards pertaining to air brake systems for trucks, buses, and trailers [14].

During 1974, the straight-line and directional response programs were extended to allow simulation of campers and motor homes. This extension consisted of adding independently suspended front wheels to the set of available suspension options. (This option allows the possibility of simulating automobiles or light trucks and, since the fifth wheel connection is represented by force and moment characteristics in the

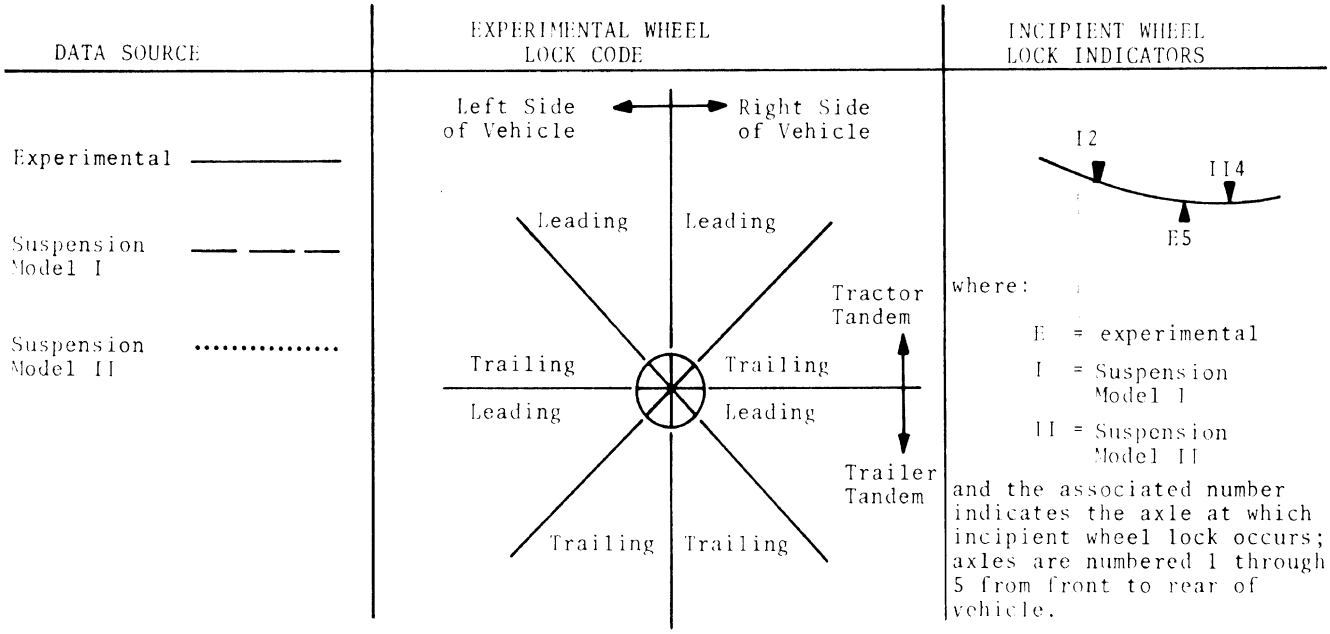

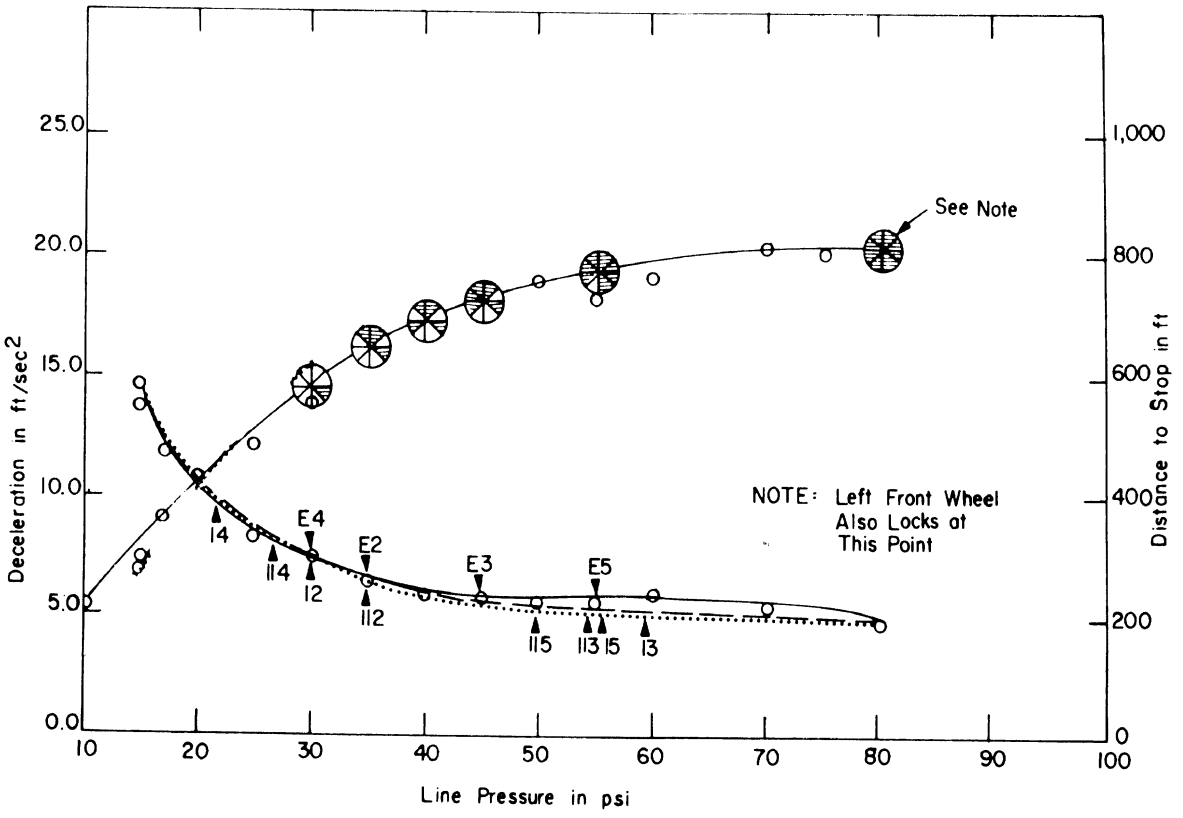

Figure 4. Braking Performance Validation - Empty Vehicle, 60 mph.

Phase II model, car-trailer and recreational vehicle-trailer combinations can be simulated using different types of hitch configurations.)

Major efforts during 1974 were directed towards developing a better understanding of truck-tire characteristics, brake fade, and antilock system performance. An over-the-road device for measuring the longitudinal force properties of truck tires was completed and two tire test programs were conducted [9, 11] (see Ervin's paper in these proceedings). In addition, construction was started on an over-the-road device for measuring the lateral force properties of truck tires. The device used to measure truck tire properties was modified to allow mounting of a number of different types of commercial vehicle brakes. The torque characteristics of a sample of different types of commercial vehicle brakes (S-cam and wedge) were measured, using the truck-tire dynamometer as a constant-speed brake tester [10] (see Post's contribution to these proceedings).

Figure 5 shows a recently obtained set of test data for a conventional truck tire. The solid line in this figure is the result of using a semi-empirical tire model [1] to match the test data obtained at 40 mph. The tire model includes a parameter, F_a, to represent the change in tire-road friction capability with sliding velocity.

The test data indicate that the peak longitudinal force is much higher than the locked-wheel (slip = 1.0) level of longitudinal force. To achieve the high "peak-to-slide" ratio exhibited by the truck tire data, it is necessary to make F_a large. However, as shown

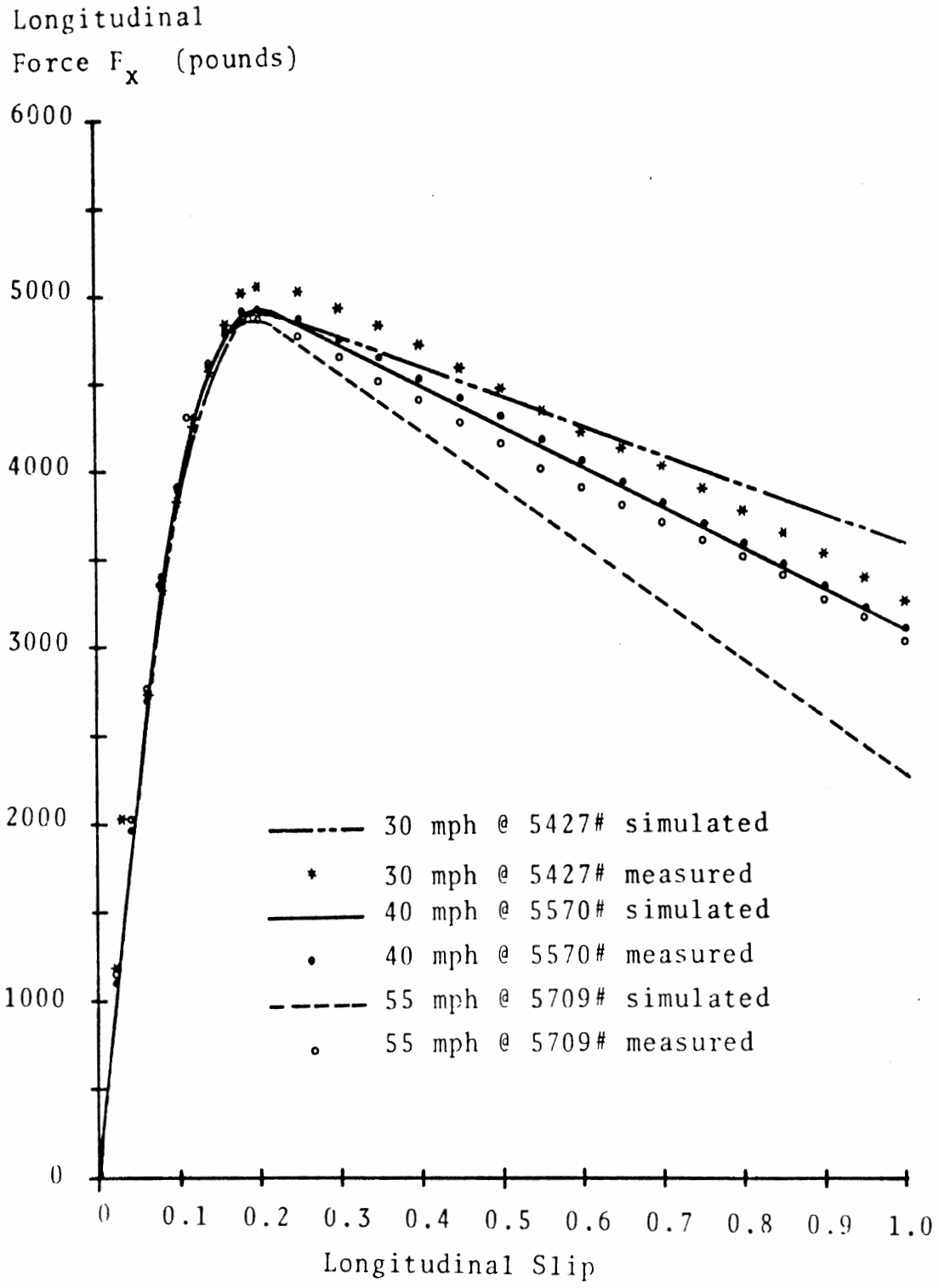

Figure 5. Effect of Speed on F_x-Slip Curve for Firestone Transport I (10.00 x 20/F) on a Dry Test Surface

in Figure 5, the longitudinal forces predicted by the tire model, using parameters evaluated at 40 mph, do not match the test data at 30 and 55 mph. These experimental results indicate the need for further tire model development to predict longitudinal force at high levels of longitudinal slip, and subsequent modifications to the simulation programs.

Descriptions of the operating characteristics of antilock braking systems are not readily available, especially in the form needed for computer simulation.* The algorithms written during Phase III had a general structure which allowed the user to construct a model of an antilock system using logical expressions and a variety of inequalities for determining how to apply or remove air pressure to the brake chamber. The users (the vehicle manufacturers) have received help from antilock manufacturers in programming the antilock algorithm in the simulation model to represent the performance of their antilock system. However, this information is not generally available in the public domain.

To aid in the procurement of descriptors to represent antilock systems, an analog computer circuit was developed to exercise antilock systems in the laboratory. The antilock system tests were made with the antilock hardware mounted on a vehicle and connected to the brake system. The brake pressure output was the input to the analog computer circuit, which computed the wheel-speed input signal to the antilock system hardware. From the time histories of simulated

*Both proprietary and technical reasons account for the difficulty in obtaining parameters for the simulation of commercial antilock systems.

wheel-speed input and brake pressure output a reasonable approximation to antilock system performance may be deduced (given some limited understanding of the principles of operation of the system) for a selected range of operating conditions. Thus the approximate input-output characteristics of a given antilock system can be represented in the computer program. (Examples of antilock modeling and testing results are given in MacAdam's paper in these proceedings.)

FUTURE DEVELOPMENTS

Plans for the near future call for assessing the state of the art in simulating the braking and handling performance of commercial vehicles. (This symposium represents the major part of that undertaking.) Simplified computer programs for straight-line braking and braking-in-a-turn will be developed to complement the complex computer models and to allow comparison between results from simple and complex analyses. A comprehensive document similar to the Phase I report [1] will be prepared to describe the current status of the computer models, including our latest work on representing different types of commercial vehicle suspensions, tire shear force characteristics, brake fade, and antilock system performance.

A new truck-tire lateral force measurement device will be operational in the near future at HSRI. An initial set of over-the-road tire data will be gathered as soon as possible. This data will complement the truck-tire lateral force data measured in the laboratory on the flat-bed machine [7, 3].

Because the original validation efforts conducted by HSRI did not include vehicles with antilock systems, vehicle tests are being planned to provide data for checking the accuracy of computed results for vehicles equipped with antilock systems.* This activity is extremely important because, in response to FMVSS 121, all (or nearly all) new commercial vehicles will be equipped with antilock systems. Thus, a useful simulation must be able to predict the influence of antilock system performance in maneuvers requiring vehicle braking.

In identifying long-range plans for conducting truck dynamics research, HSRI does not proceed on a unilateral basis. Accordingly, the conclusions reached in recent state-of-the-art reviews provide a suitable means for estimating the course of future research.

The specific reviews considered here are given in Table 1.

Table 1.

Recent State-of-the-Art Reviews

Authors	Dates
(1) Dugoff and Murphy [15]	January 1971
(2) Eshleman [16]	May 1973
(3) Smith and Barker [17]	August 1974
(4) Marples [18]	January 1975

*Vehicle manufacturers have achieved good success in specific instances [14].

Table 2 presents a summary of the areas for future research called for in these reviews.*

Table 2.

Agreement Within State-of-the-Art Reviews on Areas Where Research is Needed

		[15] DM	[16] E	[17] SB	[18] M
(1)	Experimental Validation	X	X	X	X
(2)	Truck Tire Traction	X	X	X	X
(3)	Loss-of-Control Potential	X	X		X
(4)	Stability Limits		X	X	X
(5)	Sensitivity Studies		X	X	X
(6)	Aerodynamic Effects		X		X
(7)	Road Geometrics		X		X
(8)	Normal Manuevering	X	X		

The reviewers are in total agreement in two areas: (1) the dearth of experimental work performed to validate predictive models, and (2) the need for accurately characterizing tire traction mechanics. It seems clear that more vehicle test programs are needed to verify that our understanding of truck mechanics (as represented by our simulation models) is sufficient to predict vehicle performance. Equally clear is the need to obtain truck-tire shear force performance data.

*Note that the particular interests of these reviewers are diverse and each uses his own terminology. Thus the condensation of their conclusions under a limited set of headings is the product of our interpretation of their remarks.

Further studies of truck tire mechanics will be stimulated as results from new tire testers become available.

Besides vehicle testing and tire measurement, other frequently mentioned areas are:

(1) potential for loss of control, including
    (a) the connection between vehicle response and the performance of the driver-vehicle system, and
    (b) the demands on driver skill
(2) the stability limits of commercial vehicle response in yaw or roll
(3) a large-scale parameter sensitivity study for
    (a) providing aids to vehicle design, and
    (b) studying the importance of simplifications and modeling assumptions.

Other items receiving more than a single mention are aerodynamic effects, roadway geometrics and conditions, and normal driving maneuverability and stability.

CONCLUDING REMARKS

The items mentioned in the state-of-the-art surveys cover a broad range of possibilities. A great deal of truck mechanics research is yet to be done.

We see the need for further tire studies and we are planning and building equipment to make truck tire measurements.

The mechanical friction brake does not appear to be well understood. Our test experience indicates that the performance of a given commercial vehicle brake varies with past work history during a series of repeated brake applications. This variability has not been explained but its presence can make it difficult to obtain repeatable vehicle test results. Clearly it will hinder any attempt to validate a simulation with a limited number of vehicle tests.

The use of antilock braking systems on commercial vehicles increases the complexity of the simulation problem considerably. Efficient, simple means for representing antilock systems are needed.

Thus in the future we expect to be involved in vehicle test activities, truck tire measurement programs, brake studies, and antilock performance studies aimed at improving our ability to predict the longitudinal and directional response of commercial vehicles.

REFERENCES

1. Murphy, R.W., Bernard, J.E., and Winkler, C.B., A Computer Based Mathematical Method for Predicting the Braking Performance of Trucks and Tractor-Trailers, Phase I Report, Motor Truck Braking and Handling Performance Study, Highway Safety Research Institute, University of Michigan, Ann Arbor, September 15, 1972. (Available from the National Technical Information Service, Springfield, Virginia, 22151; Report PB-212-805.)

2. Bernard, J.E., "A Digital Computer Method for the Prediction of Braking Performance of Trucks and Tractor-Trailers," presented at the International Automotive Engineering Congress, Detroit, Mich., January 8-12, 1973; SAE Paper No. 730181.

3. Bernard, J.E., Winkler, C.B., and Fancher, P.S., A Computer Based Mathematical Method for Predicting the Directional Response of Trucks and Tractor-Trailers, Phase II Technical Report, Motor Truck Braking and Handling Performance Study, Highway Safety Research Institute, University of Michigan, Ann Arbor, June 1, 1973. (Available from the National Technical Information Service, Springfield, Virginia, 22151; Report PB-221-630.)

4. Fancher, P.S., Winkler, C.B., and Bernard, J.E., "Computer Simulation of the Braking and Handling Performance of Trucks and Tractor-Trailers," HIT Lab Reports, Vol. 3, No. 5, January 1973.

5. Bernard, J.E., "A Digital Computer Method for the Prediction of the Directional Response of Trucks and Tractor-Trailers," presented at the Automotive Engineering Congress and Exposition, Detroit, Mich., February 25-March 1, 1973. SAE Paper No. 740138

6. Winkler, C.B., "Measurement of Inertial Properties and Suspension Parameters of Heavy Highway Vehicles," presented at the International Automotive Engineering Congress, Detroit, Mich., January 8-12, 1973; SAE Paper No. 730182.

7. Tielking, J.T., Fancher, P.S., and Wild, R.E., "Mechanical Properties of Truck Tires," presented at the International Automotive Engineering Congress, Detroit, Mich., January 8-12, 1973; SAE Paper No. 730183.

8. Winkler, C.B., "Analysis and Computer Simulation of the Four Elliptical Leaf Spring Tandem Suspension," presented at the Automotive Engineering Congress and Exposition, Detroit, Mich., February 25-March 1, 1974. SAE Paper No. 740136.

9. Ervin, R.D. and Fancher, P.S., "Preliminary Measurements of the Longitudinal Traction Properties of Truck Tires," presented at the Truck Meeting, Troy, Michigan, November 4-7, 1974, SAE Paper No. 741139.

10. Post, T.M., Fancher, P.S., and Bernard, J.E., "Torque Characteristics of Commercial Vehicle Brakes," presented at the Automotive Engineering Congress and Exposition, Detroit, Mich., February 24-28, 1975, SAE Paper No. 750210.

11. Ervin, R.D., MacAdam, C.C., and Fancher, P.S., The Longitudinal Traction Characteristics of Truck Tires as Measured on Dry Pavements, Highway Safety Research Institute Report No. UM-HSRI-PF-75-3, February 1975.

12. Bernard, J.E., "Some Time-Saving Methods for the Digital Simulation of Highway Vehicles," Simulation, Vol. 21, No. 6, December 1973.

13. Bernard, J.E., "Articulated Vehicle Simulation—A Fresh Approach to Some Recurring Problems," Proceedings of the 1974 Winter Simulation Conference, Washington, D.C., January 14-16, 1974.

14. Gurney, J.W. and Bernard, J.E., "Utilization of a Computer Simulation as an Aid to Predict Compliance with FMVSS 121," presented at the Automotive Engineering Congress and Exposition, Detroit, Mich., February 25-March 1, 1974. SAE Paper No. 740137.

15. Dugoff, H. and Murphy R.W., "The Dynamic Performance of Articulated Highway Vehicles—A Review of the State-of-the-Art," SAE Paper No. 710223, January 1971.

16. Eshleman, R.L., "Particular Handling Safety Problems of Trucks and Articulated Vehicles," Vehicle Safety Research Integration Symposium Proceedings, U.S. Dept. of Transportation, National Highway Traffic Safety Administration, DOT-HS-820-306, May 1973.

17. Smith, N.P. and Barker, D., The Operational Safety of Articulated Vehicles, First Report: Literature Survey on Articulated Vehicle Stability and Proposals for Further Research, Report No. AFC.9/1, Motor Industry Research Association, Lindley, England, August 1974.

18. Marples, V., Safety in Trucking Operations, Department of Mech. Eng., Report No. ME/A 75-1, Carleton University, Ottawa, Canada, January 1975.

SAFETY PROBLEMS IN COMMERCIAL VEHICLE HANDLING

L. Strandberg, O. Nordström,
and
S. Nordmark
The National Swedish Road and Traffic
Research Institute

ABSTRACT

Swedish research on the dynamic behaviour of heavy vehicle combinations and proposed regulations on handling performance are reviewed. Revealed safety problems are listed and some steps towards better safety are suggested.

The research was concentrated on the handling performance in a double lane change manoeuvre studied by means of digital computer simulation. The 10 degrees-of-freedom driver-vehicle simulation model used in these studies was validated by full scale tests.

Several studies on overturning stability were performed, such as: full scale static tests; lateral sloshing effects studied by means of servo-operated scale models connected to an analogue computer; studies of relations between driver estimated and calculated overturning risk in real traffic.

The low speed off-tracking problem was investigated separately and its interactions with high-speed behaviour is discussed.

Performance criteria were chosen in close relation to accident risk. Simulation results indicate that the rearmost unit of an articulated vehicle has the highest risk factors. Some important design parameters are: number of articulations, steered axle

location, tyre data, geometric configuration, load condition, and roll stiffness. For road tankers with laterally sloshing liquid the overturning risk can be more than twice the risk with corresponding rigid load.

Regulations were proposed on risk variable limits in different simulated manoeuvres. The steady-state overturning limit was proposed to be at least 4 m/s^2.

1. INTRODUCTION

At the moment no regulations concerning the dynamic behaviour of heavy vehicle combinations exist in Sweden. With increasing traffic density and the development of longer and heavier vehicle combinations, the need of such regulations has become more and more obvious.

In 1970 the Swedish Department of Transportation contracted the National Swedish Road and Traffic Research Institute to make investigations that have been reported earlier by Nordström et al. (1972), Backman et al. (1972), Strandberg (1974), and Nordström and Strandberg (1974). This work will be summarized in Chapters 2 and 3 with some comments for future discussion.

Later research is reviewed in Chapter 4 and will be fully reported by Nordmark (1975) and Strandberg (1975). Research within this problem area is still being done at the Institute, as indicated together with conclusions and suggestions for better safety in Chapter 5.

Today, Swedish regulations include some issues on brake design and the first research approach has been directed towards lateral dynamics and overturning stability. Therefore, no results from braking tests of commercial vehicles at the Institute are available by now.

It is well known that dynamic coupling exists between lateral and longitudinal vehicle motions, especially via tyre characteristics. Consequently, the lateral dynamics of a vehicle seems to be an important factor for braking performance and should be considered also in the design of antilock systems. In fact, the most urgent reason for antilock systems seems to be prevention of lateral and yaw motions induced by braking.

Anyhow, the behaviour of articulated vehicles during braking is a complicated and important safety problem and should have highest priority in future research.

2. SUMMARY OF PREVIOUS RESEARCH

2.1 DOUBLE LANE CHANGE TESTS

2.1.1 SCOPE OF THE MAIN INVESTIGATION. As mentioned above, the studies till now have been directed towards manoeuvres without braking. Three types of vehicle combinations (Figure 2.1) were taken into account, namely

- Tractor-semitrailer. One articulation
- Truck-full trailer. Two articulations
- Tractor-semitrailer-full trailer (double bottom). Three articulations

A double lane change manoeuvre (Figure 2.2) was chosen as most suitable for investigation of dynamic phenomena. Digital computer simulation was used as the primary test method, and full scale field tests were performed for validation purpose.

2.1.2. SIMULATION TECHNIQUE. The computer program simulated combinations with each vehicle unit rolling and yawing but not pitching. The road was assumed to be flat and horizontal. Thus the degrees-of-freedom were 4 for the leading vehicle sprung mass and 2 for each of the rear units. See Figure 2.3. The vehicle models were similar to the revised models described in Section 4.1 below.

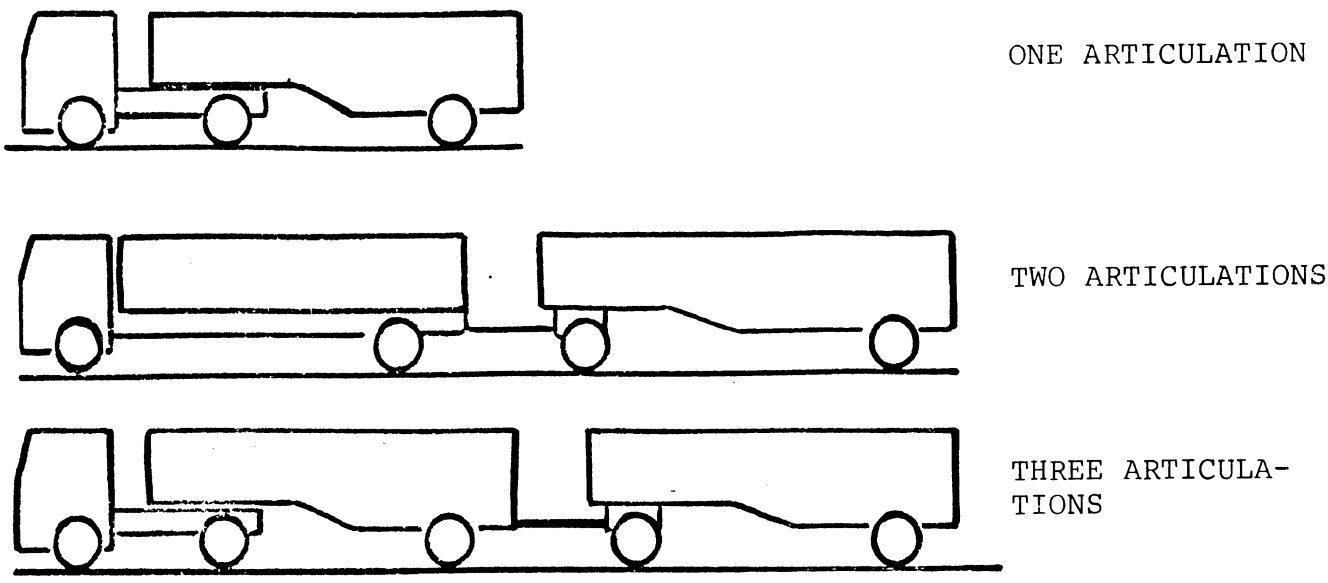

Figure 2.1. Studied vehicle combinations.

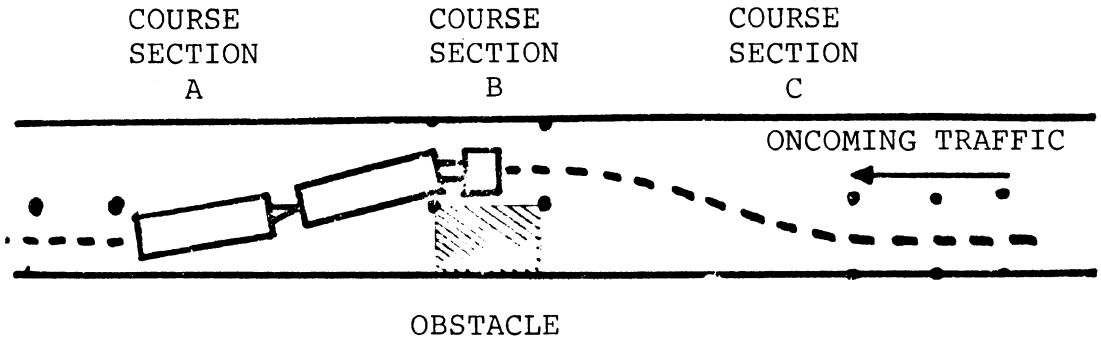

Figure 2.2. The double lane change manoeuvre.

VEHICLE MODEL

MAIN CONSIDERATIONS	MAIN NEGLECTIONS
ROLL AND YAW	PITCH
LONGITUDINAL MOTIONS	VERTICAL MOTIONS
LATERAL MOTIONS	
NONLINEAR TYRE CHARACTERISTICS	TYRE SIDE FORCES UNAFFECTED BY BRAKE OR TRACTIVE FORCES

VEHICLE COMBINATIONS	DEGREES OF FREEDOM	CONSTRAINT EQUATIONS
(TRUCK OR TRACTOR)	4	-
TRACTOR - SEMITRAILER	6	2
TRUCK - TRAILER	8	4
TRACTOR - SEMITRAILER - FULL TRAILER	10	6

Figure 2.3. Brief description of vehicle models for digital computer simulation used in the main investigation.

An inverse steering procedure called DAVIS—see Figure 2.4—was developed in order to get comparable simulation results for the investigated vehicle combinations. The procedure made the leading vehicle in every vehicle combination follow the same trajectory and lateral acceleration time history, independent of vehicle parameters, load or load distribution.

Other methods of steering along a predetermined path have been found in the literature before—Chiesa and Rinonapoli (1969)—and after—Eshleman and Desai (1972)—this investigation.

The test course illustrated in Figure 2.5 was selected as input for the inverse steering and has been used in all simulations except some validation runs. The acceleration peak values were 1.75 m/s^2 and its time history was composed by harmonic and linear functions of time. The lateral deviation peak value was 3.0 m. The tractive force was selected to maintain a constant speed of normally 70 km/h, i.e., 43 mph.

The validation tests showed that DAVIS and the mathematical vehicle model give simulation results well coinciding with field test results, see Figure 2.6. In order to get proper vehicle data, some methods and apparatus were developed by Nordström et al. (1972) for measurement of tyre characteristics, centre of gravity heights, yaw and roll moment of inertia, roll stiffness, roll damping, effective track width, etc.

2.1.3 ACCIDENT RISK CRITERIA. The double lane change manoeuvre (Figure 2.5) was considered to be sufficiently severe for the simulations and it is closely related to a real traffic situation (Figure 2.2). This connection to reality is important for valid results

D RIVER
A PPROXIMATION FOR
V EHICLE
I NVESTIGATION BY
S IMULATION

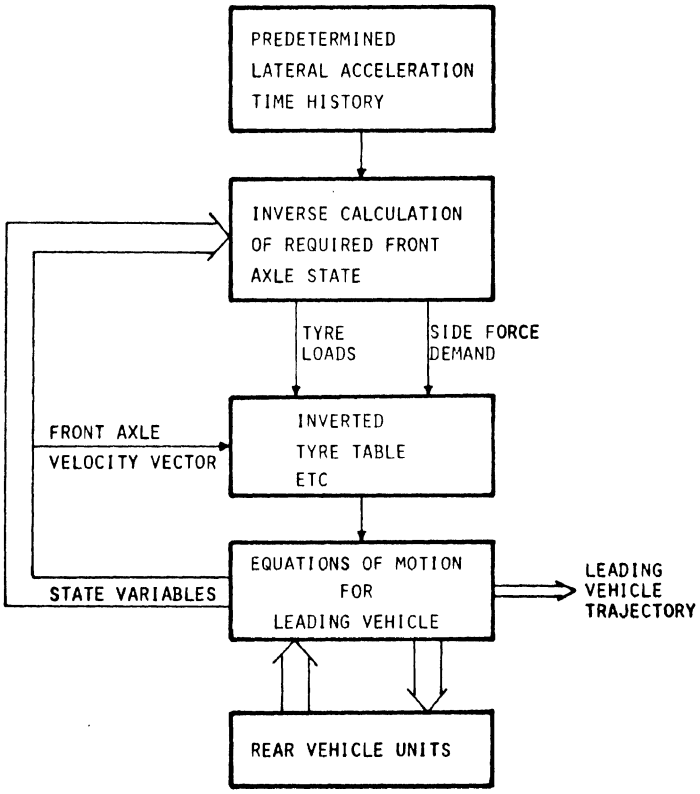

Figure 2.4. The "DAVIS" inverse steering procedure.

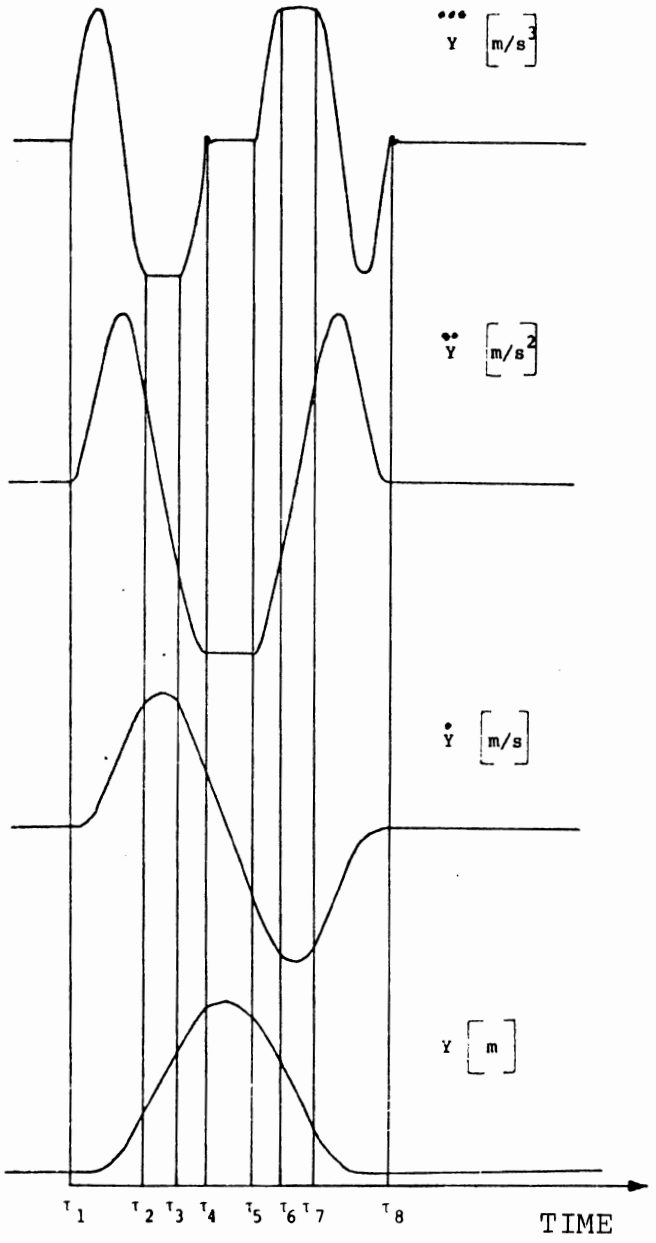

Figure 2.5. Lateral vehicle position (Y) and its time derivatives according to DAVIS' specification of a double lane change manoeuvre.

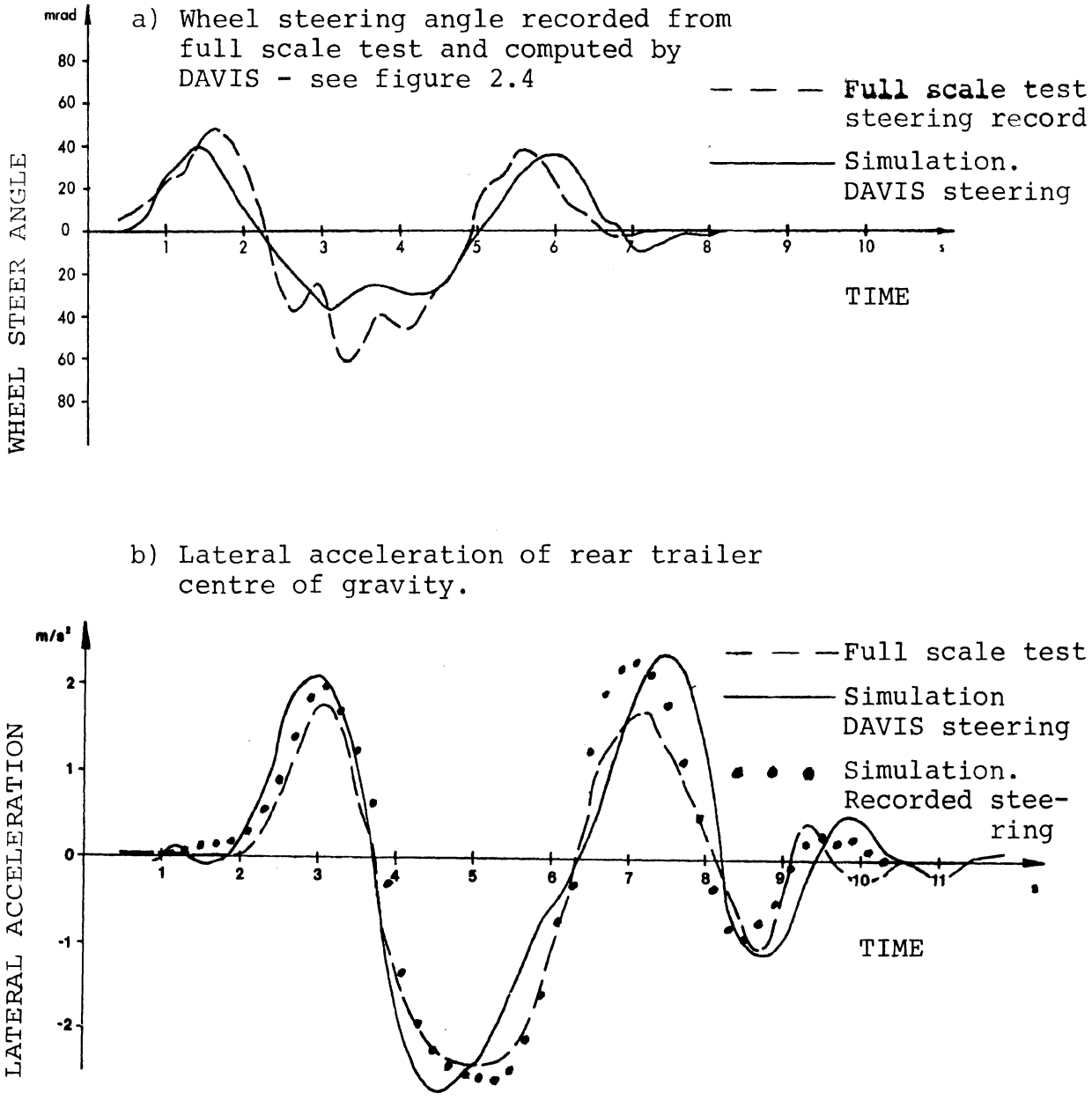

Figure 2.6. Comparison between simulations and full scale field test for a fully loaded tractor-semitrailer-full trailer combination.

as the stability of nonlinear systems depends on the input. Also, the figures of merit, or risk criteria, were selected in order to be closely related to the real accident risk. So, the comparisons between simulations with different vehicle combinations were based mainly on the so-called risk factors:

The lateral acceleration in the centre of gravity of each unit was a measure of the manoeuvre violence.

The sideslip angles acted as measures of friction utilization and skidding risk. They also indicated to what extent simultaneous braking would have been possible.

The overturning risk RV was calculated from the relative wheel loads. The formula shows that overturning has started when the risk factor value (RV) exceeds unity.

$$RV = \left| \frac{\text{Dynamic wheel load on left side}}{\text{Static wheel load on left side}} - 1 \right|$$

RV was always calculated for each axle. When appropriate, RV was also calculated for all axles together on a truck, on tractor+semitrailer, and on full trailer.

The lateral deviations of each axle indicated the necessary lateral space and if the simulated manoeuvre caused a collision or driving off the road.

To estimate the requirements on the driver, the time history of the steer angle was always examined and a quantity called the rearward risk factor amplification was introduced. It is defined as the ratio between the risk factor maximum of a rear unit and of the leading vehicle. If the rearward amplification exceeds unity,

the driver may perceive the manoeuvre as less risky than it really is. His sensory input comes mainly from the leading vehicle, due to the poor feedback from the rear units in an articulated combination.

2.1.4 COMPLETING INVESTIGATIONS ON VEHICLES DESIGNED FOR REDUCED OFF-TRACKING. Outwards off-tracking transients occurred in the double lane change tests at high speed. Corresponding steady-state phenomenon—see Section 5.3—has been described by Strandberg (1974) and no additional investigation on this specific subject was regarded as necessary.

However, awareness of this problem gave the impulse to a few full scale tests with three vehicle combinations equipped with different axle steering arrangements. (The axle steering is designed for reduction of kinematic, inwards off-tracking occurring at a low speed.) The subjective impressions from these dynamic tests were partly alarming and it was decided to expand the simulation model and computer program for a thorough investigation of similar vehicle configurations. The first results, presented in Section 4.2, coincide with the impressions mentioned above.

2.2 OVERTURNING LIMIT IN STEADY-STATE CORNERING

Empirical data on overturning limits were evaluated from full scale static tests. Steady-state cornering (Figure 2.7) was simulated by substitution of the resultant force (F) with the gravity force. The wheels of the full scale loaded vehicle were positioned on platforms, one for each axle. The platforms were inclined—by hydraulic actuators—the angle α to the

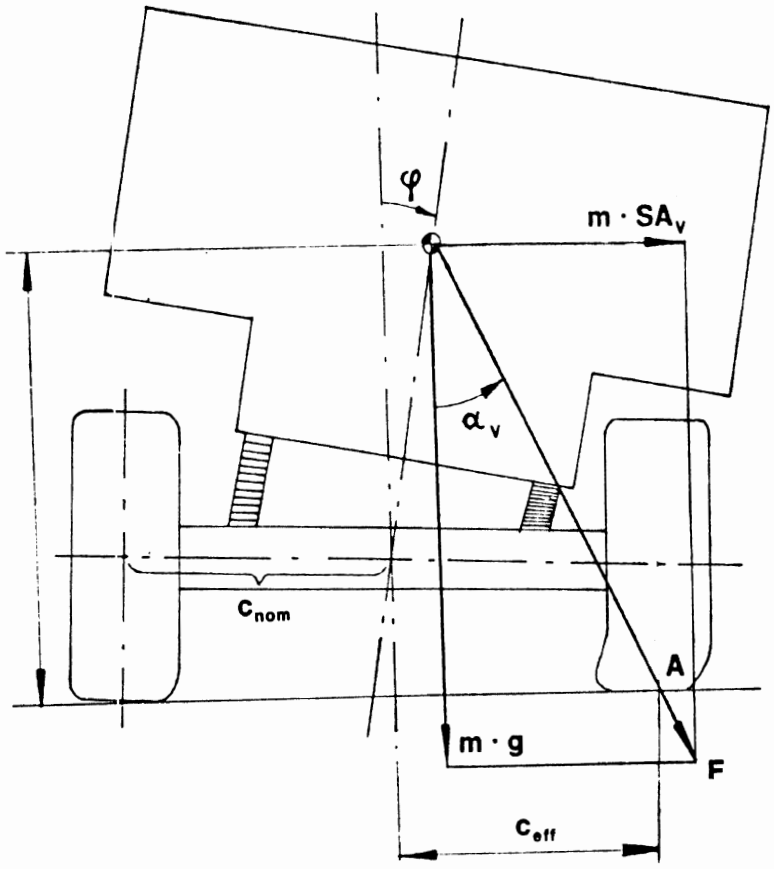

Figure 2.7. Overturning limit (SA_V) at steady-state cornering. The resultant (F) of the centrifugal force ($m \cdot SA_V$) and gravitation ($m \cdot g$) intersect the road surface at the point A.

horizontal plane around an axis perpendicular to the vehicle axles. See Figure 2.8. The inertia force, m · SA, was then simulated by the gravity force component, mg sin α. As the other component was mg cos α, the simulated mass of the vehicle was m cos α and the simulated lateral acceleration:

$$SA = \frac{mg \sin \alpha}{m \cos \alpha} = g \tan \alpha$$

When the upper wheels (corresponding to the inside of the bend) lost contact, the inclination, α_V, was measured and this gave the overturning limit, SA_V.

2.3 LOW SPEED OFF-TRACKING

The low speed off-tracking phenomenon was investigated separately by Nordström and Eldrot (1974). As this problem is of kinematic nature, it was decided to compare the space demand from different vehicle combinations with the aid of a simple scale model.

3. PROPOSED DEMANDS AND TEST METHODS

The aim for proposed demands and regulations were:

- as close connection to the actual safety problems as possible
- demands on driver-vehicle performance instead of restrictions on vehicle design that might prevent progress
- easy supervision of regulations assuming that today's technology (e.g., computer simulation) can be utilized.

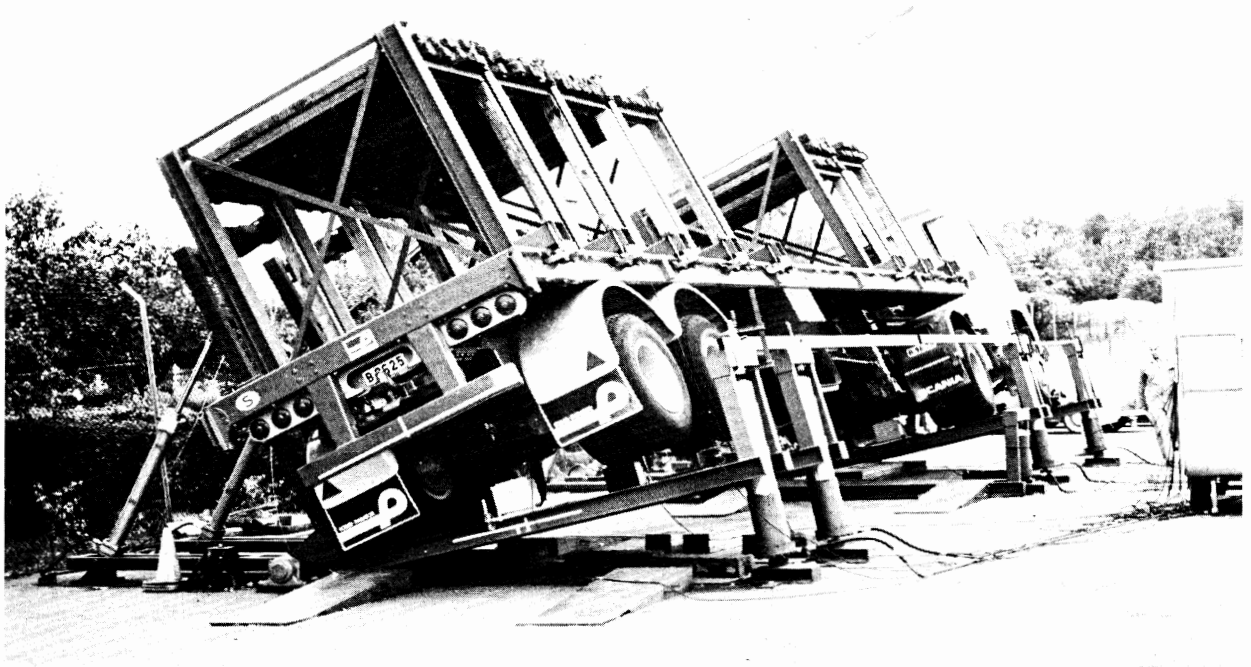

Figure 2.8. Measurement of overturning limit by static simulation of steady-state cornering. Maximum load height. Overturning has occurred and the platform inclination angle corresponds to the lateral acceleration 2.2 m/s^2.

3.1 DOUBLE LANE CHANGE MANOEUVRE BEHAVIOUR

For Swedish-type approval it was proposed that each vehicle combination must be able to make the manoeuvre according to Figure 2.2 and 2.5. The speed should be at least 70 km/h with the vehicle units fully loaded according to the steady-state overturning limit specifications—see next section.

The following demands were specified as minimum performance during non-braking conditions:

- No overturning risk is allowed to exceed unity.
- Sideslip angles must not exceed 150 milliradians (i.e., 8.6 degrees) at any moment.
- As a check on the oscillatory damping, all sideslip angles must be smaller than 20 m rad after passing the point where the front axle has maintained straight course for 75 metres.
- The rearwards amplification for the sideslip angles was suggested to be maximum 2.0. A much smaller value is desirable but it was regarded to be difficult to achieve without some years' research on new vehicle design principles.
- To assure that driving off the road or obstacle collision has not occurred, the axle centre trajectories must stay within certain limits demonstrated by Figure 3.1.

In the discussions subsequent to these demand proposals, it was concluded that the overturning risk limit should concern vehicle units instead of separate axles, see Section 2.1.3 (RV $\geq$ 1 for one axle only does not necessarily mean overturning).

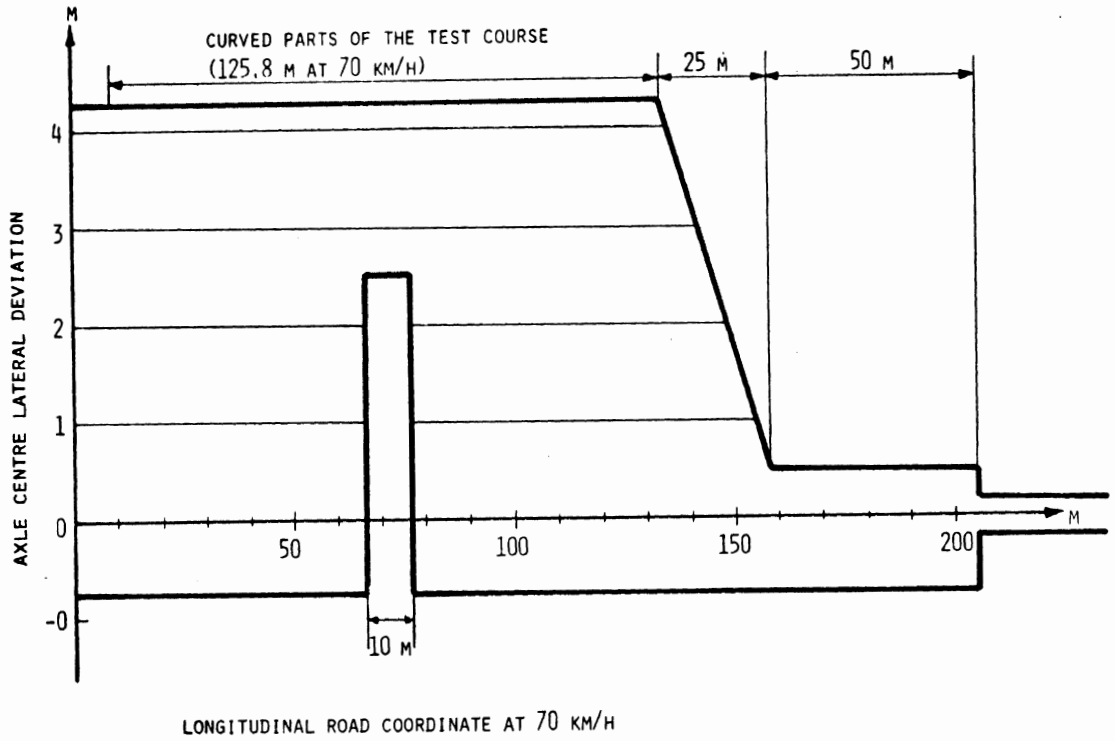

Figure 3.1. Proposed demands on lateral deviation limits for axle centres.

It was evident that the overturning risk rearwards amplification should have a limit in conformity with the sideslip angles.

The overturning risk in this manoeuvre is not neglectable even if the demand in the next section is fulfilled. This evidence and the variability of driver and road are serious drawbacks for full scale tests. Thus, computer simulation was regarded as the most reasonable test method. It will also allow tests of many vehicle combinations and of vehicles that are designed but not yet manufactured.

It has been questioned if it is satisfactory to use a more simple vehicle model compared to what has been used till now—see Sections 2.1.2 and 4.1. Excluding the roll degree-of-freedom will eliminate a large amount of data handling, schematic assumptions, and program modifications for new designs, without necessarily affecting the overall judgement—approval or not—on the tested combination. (The demands on maximum values and rearward amplification of the overturning risks might be substituted with corresponding demands on the lateral accelerations.) Then it is assumed that the risk variable limits are more restrictive and that the full scale steady-state cornering tests—see Sections 3.2 and 3.3—must be passed by each vehicle unit and combination. However, in order to put appropriate vehicle data into the computer, some schematic assumptions and approximations are necessary even after this simplification—mainly tyre characteristics and load configuration.

3.2 STEADY-STATE OVERTURNING LIMIT

According to the overturning limit measurements—see Section 2.2 and Figure 3.2—the limit 4 m/s^2 was regarded as a reasonable minimum, achievable with moderate limitations on design and load. So, it was proposed as a demand for type approval of load-carrying vehicle units. In practice, this demand will set an upper limit for the load (center of gravity) height to be specified for each vehicle and to be recorded in the inspection certificate.

The selection of this specific number as the limit can be, and has been, criticized. It may be too low to cause a noticeable decrease in overturning accidents and it may be so high that many existing vehicles will have a load limit too unfavourable for economical use. On the other hand, the technical conditions for a reduction of the overturning risk have been favourable for decades but has so far not been utilized to any further extent. Thus some kind of legislation seems necessary to make the out-of-date vehicle design principles out-of-use, as well.

Anyhow, an overturning limit must be set at some value to protect road users from vehicles designed and loaded in such a way that they will overturn for manoeuvres regarded as completely harmless by the average road user.

The test method used in the investigation (Figure 2.8) could not be substituted by theoretical calculations because of poor accuracy in preestimations of effective track width (see c_{eff} in Figure 2.7) and spring parameters. The method was recommended for future type tests.

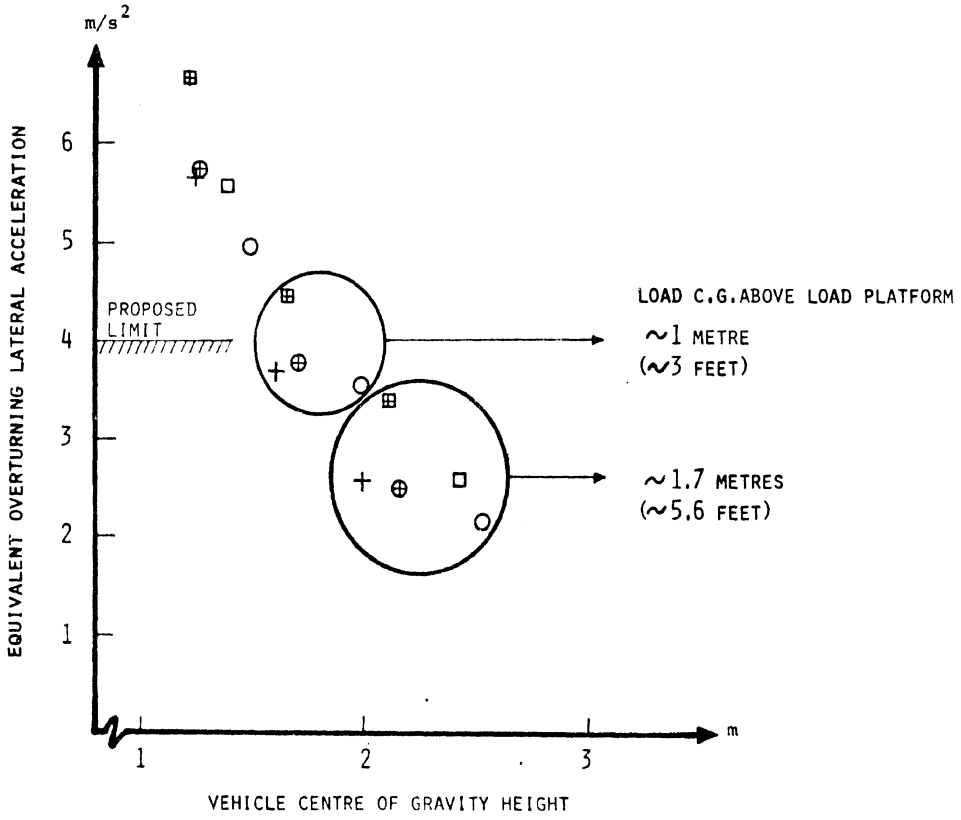

Figure 3.2 Full scale measurements on overturning limit related to centre of gravity height

3.3 LOW SPEED OFF-TRACKING

For reasons of simplicity and general conformity to regulations in other countries, a circle driving approval test was suggested.

The proposed demand requires the vehicle to be driven between two concentric circles defined by 15 m and 7.3 m radius. No part of the vehicle is allowed to exceed the circles. The circles shall be entered along a tangent and no part of the outer edge of the vehicle must offset more than 0.5 m from the tangent. The test has been designed under consideration of the Swedish 24 m length limit for vehicle combinations and of the results from model studies and mathematical calculations.

3.4 STEADY-STATE HIGH SPEED OFF-TRACKING

The proposed limitation of space requirement in the double lane change manoeuvre was completed by the following demand. Off-tracking towards the outside of the curve must not exceed 0.5 m in a curve defined by a speed of 70 km/h and a lateral acceleration 2 m/s^2. The lateral acceleration should be maintained during five seconds. The vehicles should carry maximum load with the centre of gravity at maximum height according to the overturning limit measurements.

Even the specific limits in this demand can be criticized in terms similar to those in Section 3.2. The most serious arbitrariness is not eliminated until the tyre-road characteristics have been specified.

If the road surface variability can be kept within a small region, full scale testing is a reasonable method in this case. To avoid expensive multiple tests, when the tested vehicle will be connected to several

others, the test could be performed with the worst combination—according to preceeding computer simulations with simplified vehicle models and schematic tyre characteristics.

4. LATE RESEARCH AND DEVELOPMENT

4.1 FURTHER DEVELOPMENT OF THE MATHEMATICAL MODEL AND COMPUTER PROGRAM

The mathematical model used in the earlier simulation has lately been slightly changed and expanded to permit studies of steerable axles. It is now possible to simulate heavy vehicle combinations with up to three articulation points. Double axles are allowed and these may be either axle- or parallel-steered.

To obtain a reasonably small number of equations several simplifications were introduced in the mathematical model and the most important of these are listed below.

1. Roll axes are assumed to be fixed and horizontal and run through the centres of gravity for the unsprung masses. Thus the mass centre of each vehicle does not move relatively to the sprung mass.
2. Pitch motion is neglected.
3. Roll angles are considered to be small.
4. Camber angles are neglected.
5. Roll and compliance steering effects are neglected.

6. The road is considered to be flat and horizontal, and no vertical movement is included.

7. The inertia tensor of the sprung mass is assumed to be diagonal at zero roll angle when computed in a system with origin at the sprung mass centre of gravity, vertical z-axis and horizontal x-axis pointing in the forward direction. A similar assumption is made for the unsprung mass.

8. The tyres are considered to be rigid. Consequently, the unsprung masses have no freedom to roll.

9. The sideslip angle for all wheels on one axle are regarded as equal and calculated at the axle centre.

For the vehicle combination with three articulation points the program is based upon 16 equations of motion. The corresponding numbers are 12 and 8 for combinations with two and one articulation points, respectively. The following variables are solved from these equations by an elimination method.

1. Longitudinal and lateral acceleration of the leading vehicle c.g.

2. Yaw angle acceleration for each unit in the vehicle combination.

3. Roll angle acceleration for each unit in the vehicle combination.

4. Horizontal coupling forces in each articulation point.

In order to avoid numerical instability due to high frequency components caused by small inertia and large spring constants when a dolly is present in the combination, the dolly roll angle is determined by the rear trailer roll angle via a simple geometric condition. Thus, the original number of equations might have been reduced by one, but this elimination is left to the computer. This approach is a compromise between two extreme possibilities, Mikulcik (1968) that eliminates all excessive variables and Shapley (1972) that leaves all the work to the computer.

The program structure is fairly conventional using a fourth-order Runge-Kutta method. To make it easier to use the program, in most computers the new and expanded version has been written in FORTRAN IV instead of IBM 360 CSMP that was used earlier. Computer cost is approximately 7 US dollars per real time second when about 70 variables are printed (5 times per real time second).

Due to difficulties to measure or obtain data from manufacturers concerning centre of gravity positions and inertia moments, a program has been developed which calculates these quantities approximately from more easily obtainable data, e.g., dimensions and weights of different parts of the vehicle.

The programs have been developed and run on an EAI PACER 100 and the simulation results are stored on disk. Risk factors and other relevant variables are then computed and plotted by an evaluation program utilizing the TEKPLOT subroutine package as supplied with the EAI/1415 Graphic Computer Terminal (Tektronix 4010).

4.2 SIMULATIONS OF VEHICLES DESIGNED FOR REDUCED OFF-TRACKING

4.2.1 VARIATION OF MIDDLE AXLE POSITION OF FULL TRAILER. As pointed out in Section 2.1.4, some of the full scale tests with vehicle combinations equipped with axle steering did give some bad results. The simulation program permits different kinds of steering (axle- and parallel-) and variation of axle positions. It was decided to study a 24 m truck-full trailer combination with double rear axles at both truck and trailer (Figure 4.1). The rearmost axle 78B is steerable and its steer angle is determined by the difference between dolly and trailer yaw angles. The trailer is designed for small sideslip angles at low speed, so the steer ratio depends on the position of axle 78 and can be computed with elementary geometry (Figure 5.3a). Three simulations were carried through:

I Middle axle positioned as in a conventional bogie.
$L78 = 0.86 \cdot LB\ 78$

II Middle axle moved forward to a position with
$L78 = 0.75 \cdot LB\ 78$

III Middle axle further advanced.
$L78 = 0.5 \cdot LB\ 78$

4.2.2 LIMITATIONS OF SIMULATION MODEL. The only vehicle parameters varied were middle axle position and steer ratio. Naturally, other parameters as well should have been changed, like centre of gravity position, yaw moment of inertia, and so on, but the influence of these changes were estimated as negligible.

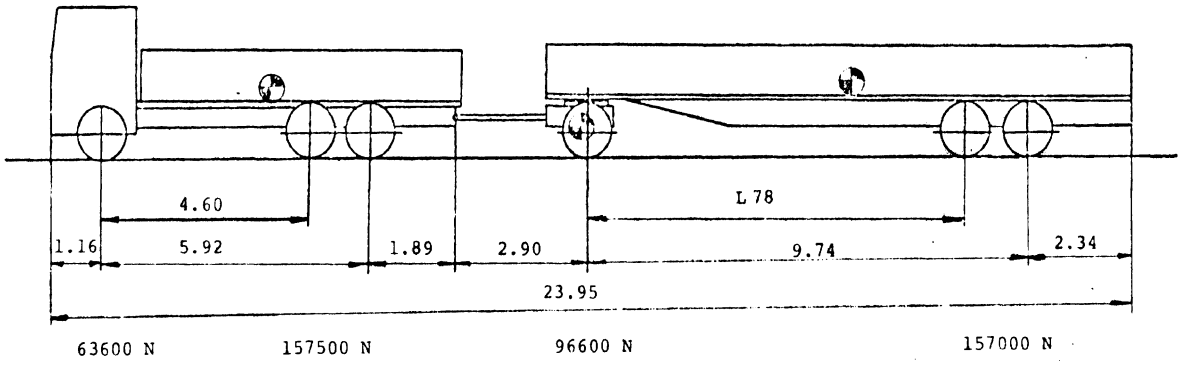

	Centre of gravity height (m)	Weight (kg)
Truck	1.42	22500
Dolly	0.63	1600
Trailer	1.63	24290

Simulation no	L 78
I	8.38
II	7.30
III	4.87

Figure 4.1 Measures, weights and axle loads for 24-m combination used in simulations according to section 4.2. The load masses are homogenous.

More important is that the same axle loads were used in all the three runs. That means that a construction, which distributes the loads evenly between the axles 78 and 78B is used on the trailer. For simplicity it was also assumed that no forces and torques were transmitted between the dolly and the steered axle via the steering arrangement, which implies some kind of servo assistance.

4.2.3 RESULTS FROM SIMULATIONS. The risk factors mentioned in Section 2.1.3 have been plotted in diagrams. The double lane change manoeuvre is divided in three parts:

A. the entry section
B. the middle section
C. the departure section

and in each of these the risk factor maxima are plotted. The results confirm qualitatively the earlier full scale tests. The performance of the full trailer becomes gradually worse as the middle axle is advanced, ending with very large lateral deviations of trailer in simulation III.

Notice the strikingly small influence from the different trailers on the truck, which behaves almost identically in all three runs. The driver will notice almost no difference between acceptable performance by the trailer in simulation I and the rather startling oscillations exhibited in simulation III. This can clearly be seen in Figure 4.5 where the overturning risks for the truck (RV14) and the full trailer (RV58) are plotted as functions of time. To demonstrate the magnitude of lateral oscillations, the trajectories of the centre of the rearmost axle have been plotted in Figure 4.7.

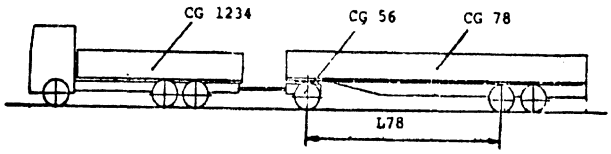

Course section A

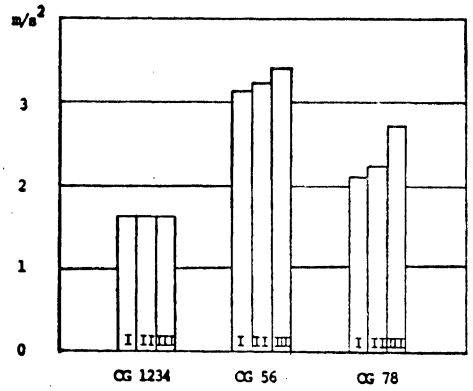

Course section B

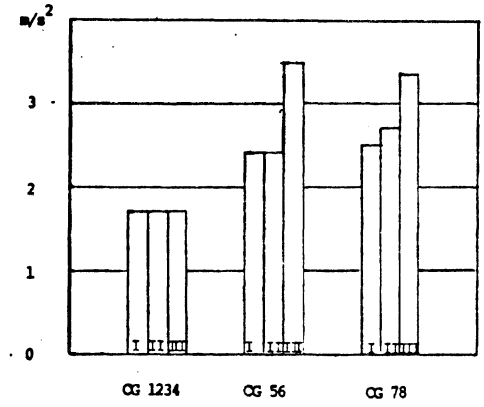

Course section C

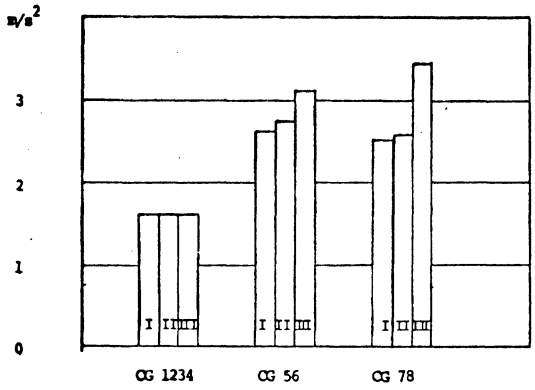

Figure 4.2 Maximum values of lateral accelerations in different parts of manoeuvre. 24 m-combination at a speed of 70 km/h and with different values of L78.

Course section A

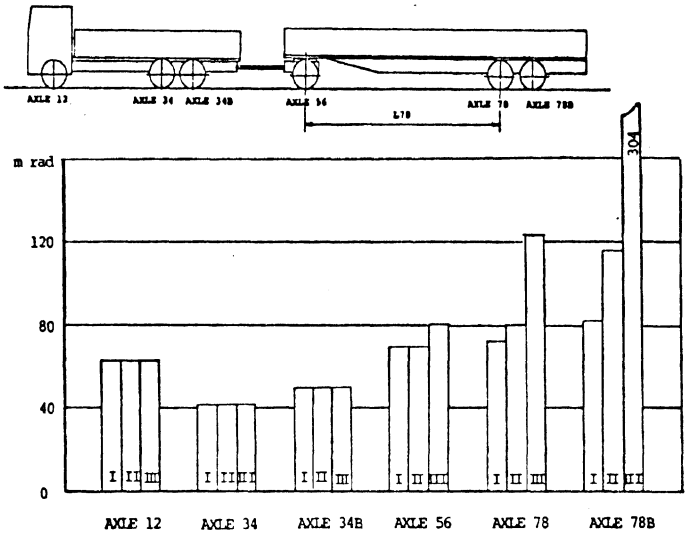

Course section B

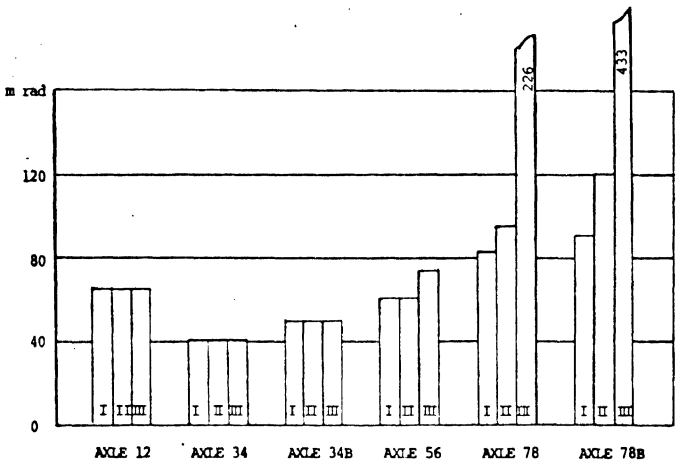

Course section C

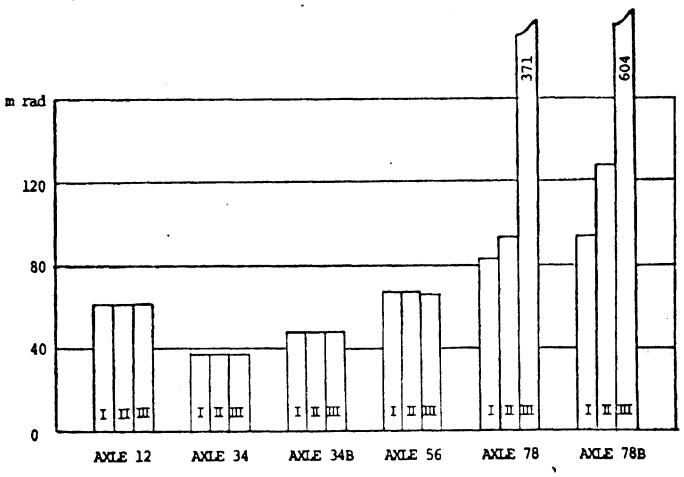

Figure 4.3 Maxima of side slip angles for the different axles. 24-m combination at a speed of 70 km/h and variation of L78.

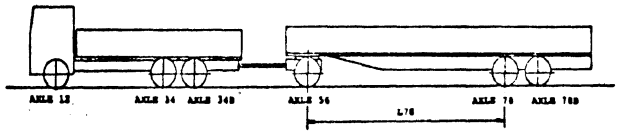

Course section A

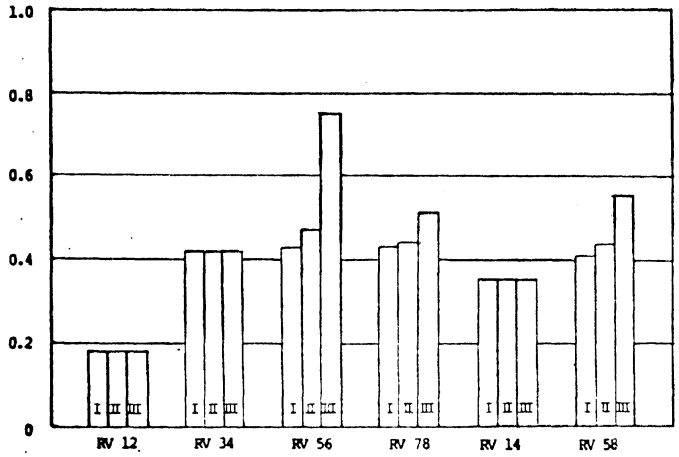

Course section B

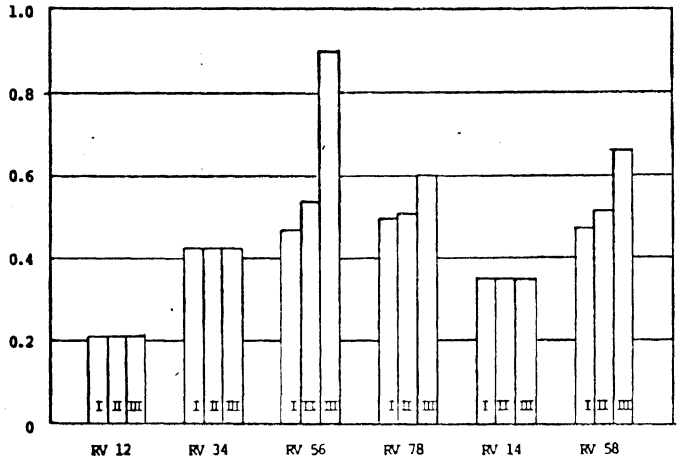

Course section C

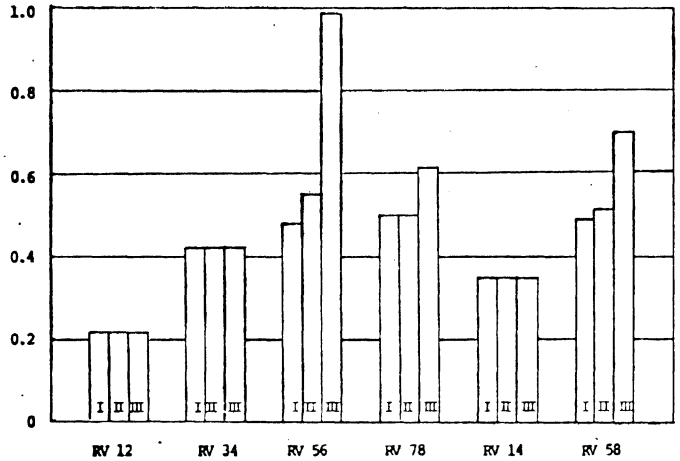

Figure 4.4 Maxima of overturning risks for the different axles (RV 12, RV 34, RV 56, RV 78), the truck (RV 14) and the full trailer (RV 58). 24-m combination at a speed of 70 km/h and variation of L78.

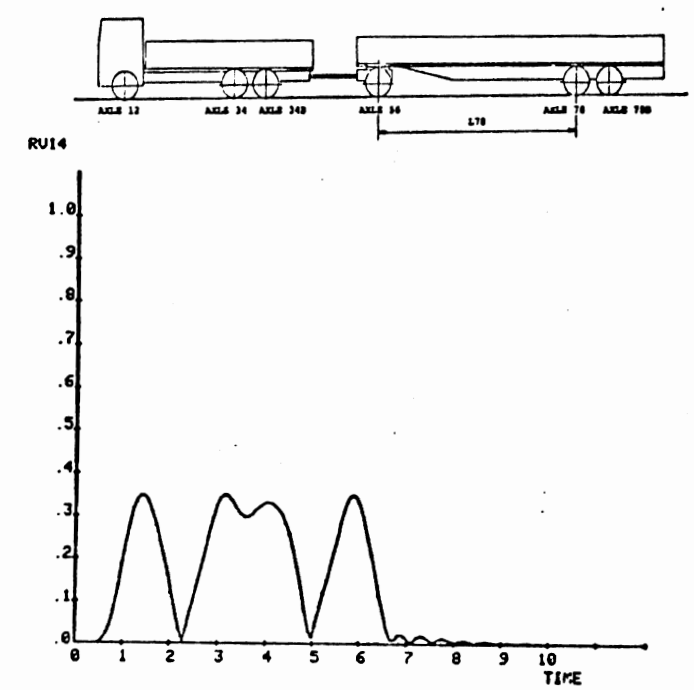

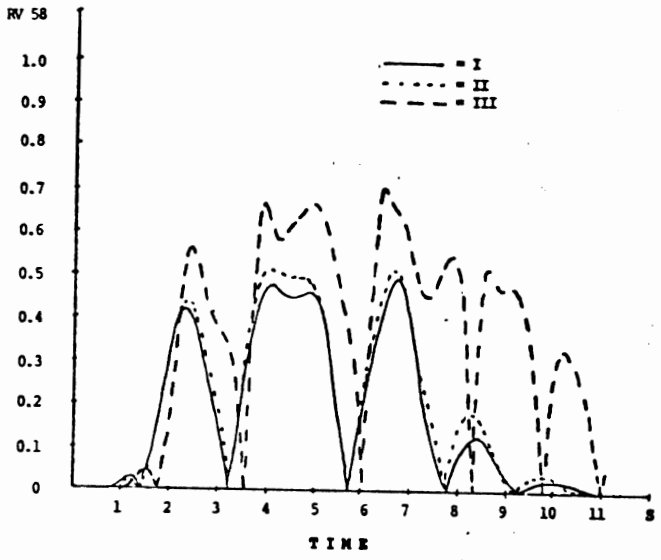

Figure 4.5 Overturning risk for truck (RV 14) and for full trailer (RV58) as functions of time. 24-m combination at a speed of 70 km/h and with different values of L78.

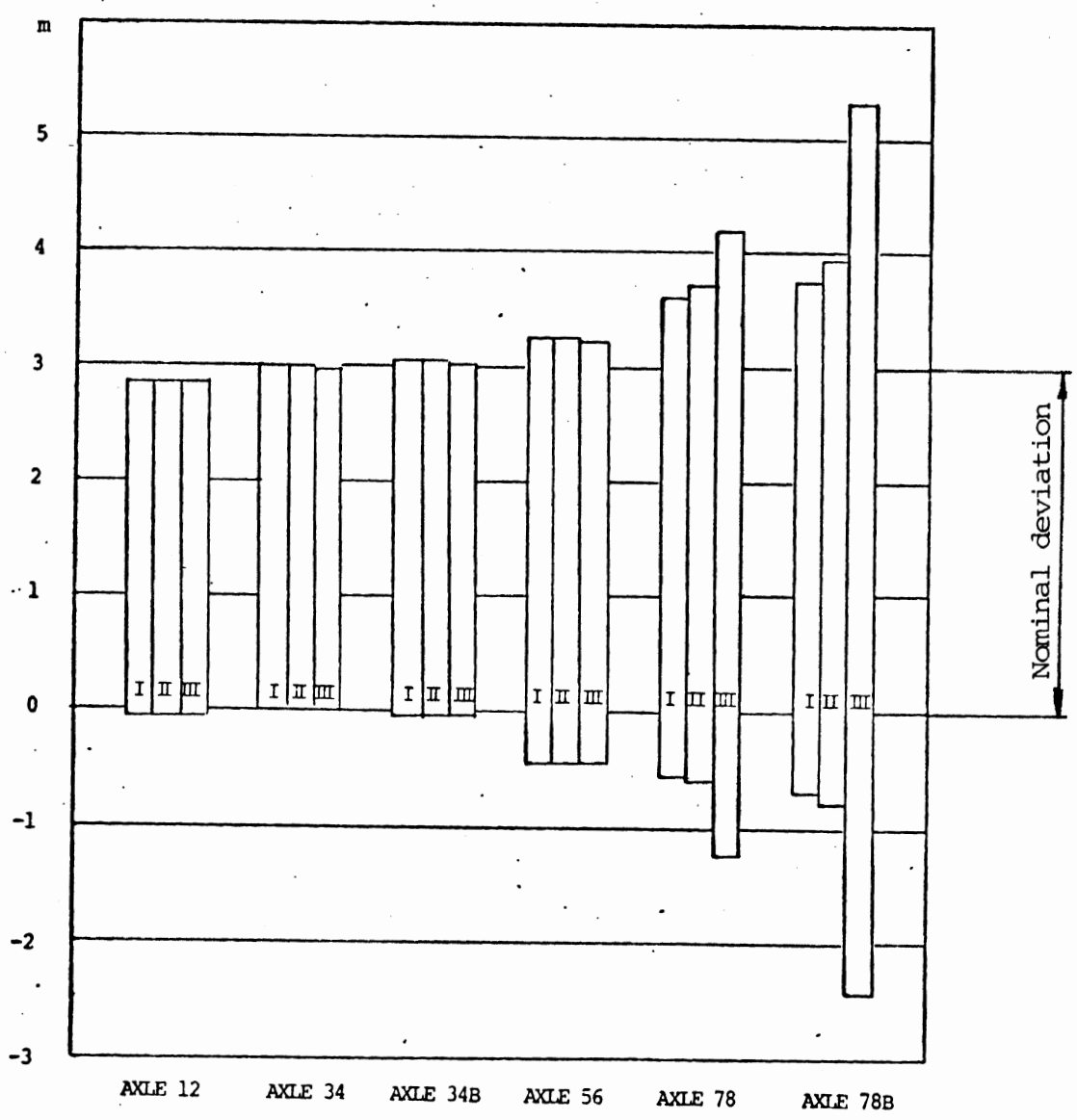

Figure 4.6 Maximum values of lateral deviation of axle centres during manoeuvre. 24-m combination at a speed of 70 km/h.

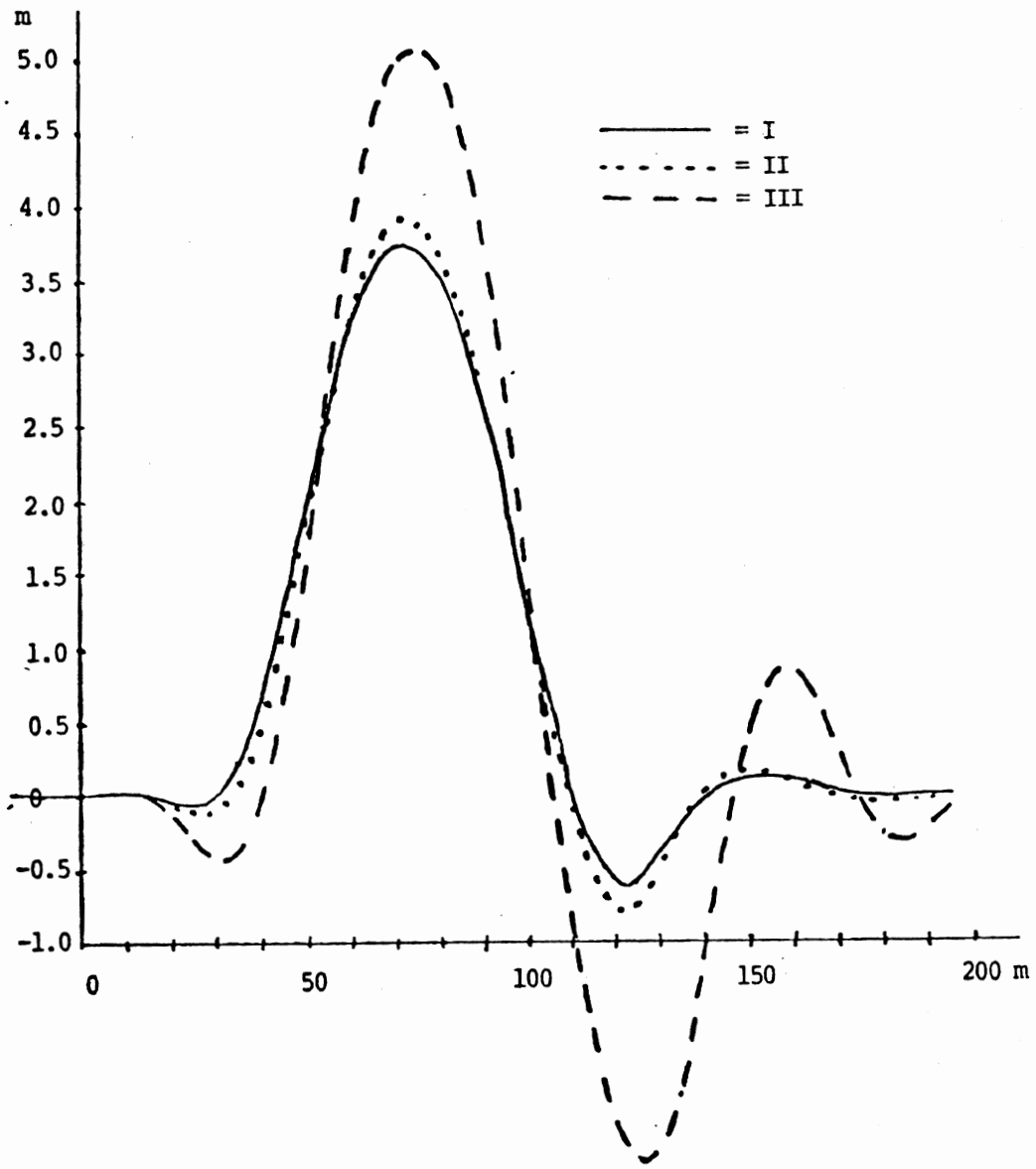

Figure 4.7 Trajectories of centre of axle 78B for different values of L78. 24-m combination at a speed of 70 km/h.

In terms of the demands described in Section 3.1, only the combination I will pass. Combination II does not satisfy the rearward amplification demand on sideslip angles. The remaining combination III does not pass in any respect except for the first demand on overturning risk and that is with a very small margin (see RV56, Figure 4.4, Course Section C).

The tendency revealed in these simulations can intuitively be attributed to two main reasons. First, steering of the rearmost axle will reduce the available side force from that axle and second, moving the middle axle forward will considerably shorten the distance between the dolly and this axle and thus reduce the stabilizing torque around the trailer king pin for given side forces. Corresponding phenomenon during steady-state can be explained in terms of sideslip angles (cf Section 5.3).

4.3 DRIVERS' ESTIMATION OF OVERTURNING RISKS RELATED TO COMPUTED RISK

The reason for proposing demands on overturning stability is to increase safety. If the drivers use this increased "technical" safety for higher cornering speeds the accidents might not decrease but just be more severe. In order to study if such a tendency could be expected, an investigation on drivers of road tankers has been made.

The investigation was made in real traffic during regular distribution trips. The vehicles were instrumented to record lateral acceleration, roll angle velocity of the driver's cabin, and driving speed. The measured data was stored in analogue form on magnetic tape for later A/D conversion and data processing. The

drivers were accompanied by a test leader who operated the instrumentation and made interviews with the drivers. Each vehicle was studied during a complete distribution trip. Data were recorded only in the curves. After each curve the driver was asked to estimate how much faster he could negotiate the curve without overturning. For each curve a number of road data were noted manually. Totally about 2500 curves have been examined.

About 50 different vehicles and vehicle combinations such as single vehicles, semitrailers and trucks with full trailers were studied under various conditions. The overturning stability of each vehicle has been calculated and several vehicles have undergone static overturning test in fully loaded condition.

Evaluation of the results is not yet completed, but it can already be said that the drivers tend to overestimate the possible cornering capacity of the vehicle at low speeds and underestimate it at high speeds irrespectively of loading condition. These results are illustrated in Figure 4.8. The results are consistent with earlier investigations—e.g., Ritchie et al. (1968).

In connection to these studies an inquiry has been made on a larger number of drivers of road tankers. The results show that the drivers regard braking and overturning as serious problems. Antilocking devices are expected to give considerable improvement in braking safety. The results have been reported by Tyden (1975).

4.4 OVERTURNING RISK DUE TO LATERAL SLOSHING IN ROAD TANKERS

4.4.1 REASONS AND NEEDS FOR RESEARCH. Regulations exist on the design and loading of road tankers to decrease longitudinal sloshing effects. Transversal

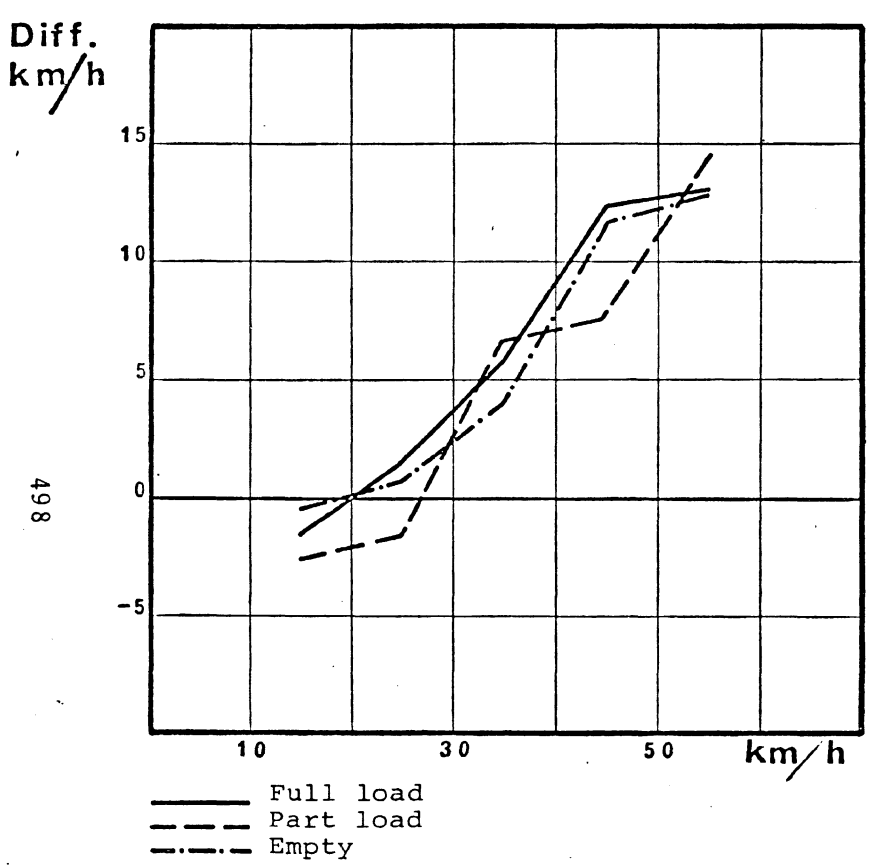

a) Tractor and semitrailer

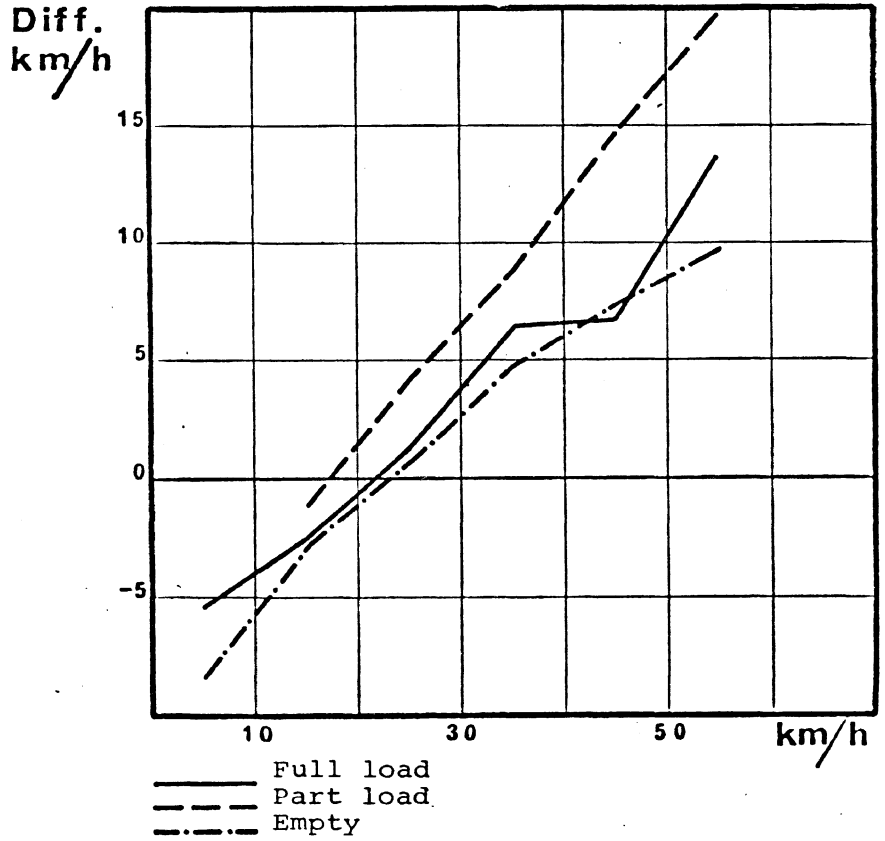

b) Truck and full trailer

Figure 4.8 Difference between calculated and driver estimated overturning speed in curves as function of actual driving speed

baffels and additional walls are conventional designs to keep the liquid motions within specified limits in a partially loaded tank. However, sloshing forces are not completely prevented and if the tank design is conventional—longitudinal cylinders with sharp corners at the transversal walls—sloshing is easily perceivable for the driver.

No regulations exist in Sweden to prevent or decrease lateral sloshing and its effect on the overturning tendency. Due to the conventional tank design—horizontal cylinders with smoothly rounded longitudinal walls—it is possible that drivers are less aware of this phenomenon than of longitudinal sloshing.

Full scale steady-state cornering simulations—method as in Section 2.2—have been reported by Isermann (1970). Tables from Isermann show that the overturning limit will increase from 3.2 m/s^2 to 3.6 m/s^2 only, when the liquid load is decreased from 100% to 50% of the volume.

Dynamic sloshing has been investigated analytically—see, e.g., Budiansky (1960), Dodge (1966), Roberts et al. (1966) and Bauer (1972)—where qualitative effects are revealed and explained. However, simulation with scale models is more straightforward and sometimes the only possible method for less simple tank boundaries.

Many dynamic sloshing experiments with scale models are reported—see, e.g., Silveira et al. (1961), Stofan and Sumner (1963), Sumner (1964), and Abramson (1966)—but only a few are known where the tanks are horizontal cylinders, see, e.g., McCarty and Stephens (1960). Not even these reports give data sufficient for calculation of corresponding overturning risks with the tanks mounted on conventional road vehicles. Thus it was decided to perform the experiments that are summarized in the following sections.

4.4.2 DYNAMIC FULL SCALE EXPERIMENTS. Full scale dynamic experiments were performed using a truck with outrigger in a double lane change manoeuvre. See Figure 4.9 from Jansson (1973). The purpose of the experiments was to investigate the overturning stabilizing effects from anti-roll bars compared to baffles. The results should contribute to the details of a legislation proposal in Norway.

The tests were performed with 6 m^3 and 8 m^3 water load occupying 50% and 75%, respectively, of the tank volume. The vertically mounted longitudinal baffles covered 50% of the longitudinal section area at both sides 0.4 m from the symmetry axis of the tank. The cross-section contour was similar to the tank model in Figure 4.11b. The roll stiffness without anti-roll bars was $1.1 \cdot 10^5$ Nm/rad in the front and $2.9 \cdot 10^5$ Nm/rad in the rear.

The trajectory was defined according to Figure 2.5 with the lateral translation peak 8.8 m and with the manoeuvre length 80 m. Thus variation of speed caused variations of lateral acceleration peaks and oscillation frequency. Unfortunately, the real manoeuvre frequencies seem to have been too low for liquid resonance and low enough to make high roll resistance and anti-roll bars favourable. This evidence is supported by the results from scale model simulations performed later and reviewed in the following sections.

These frequency relations and the uncertainty in optimal baffle design must be kept in mind when interpreting the results in the table below from Jansson (1973).

Figure 4.9. Full scale double lane change experiments. From Jansson (1973).

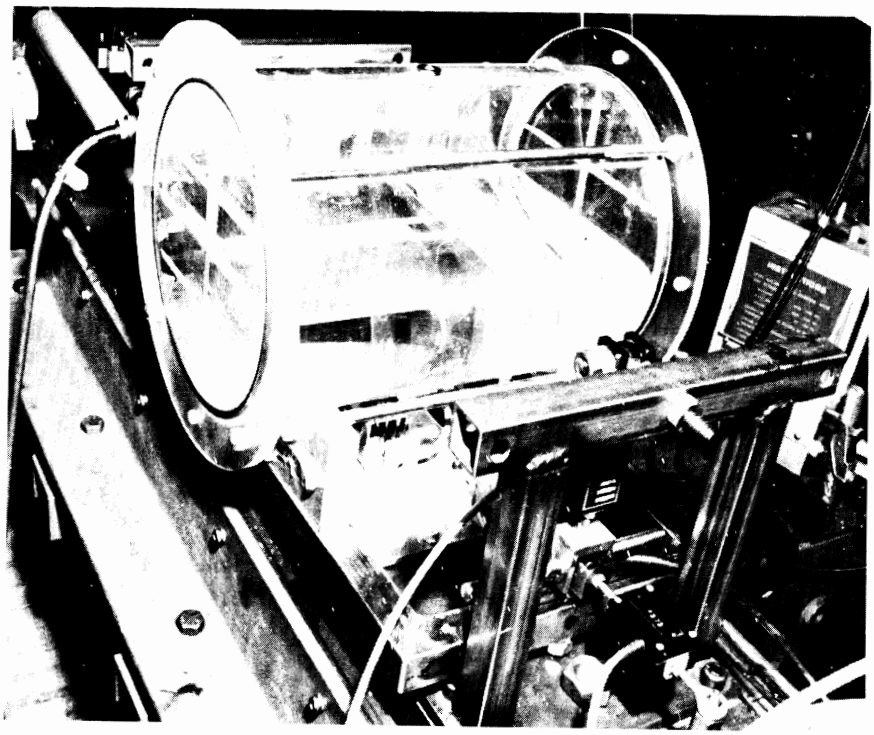

Figure 4.10. Laboratory equipment with circular tank model.

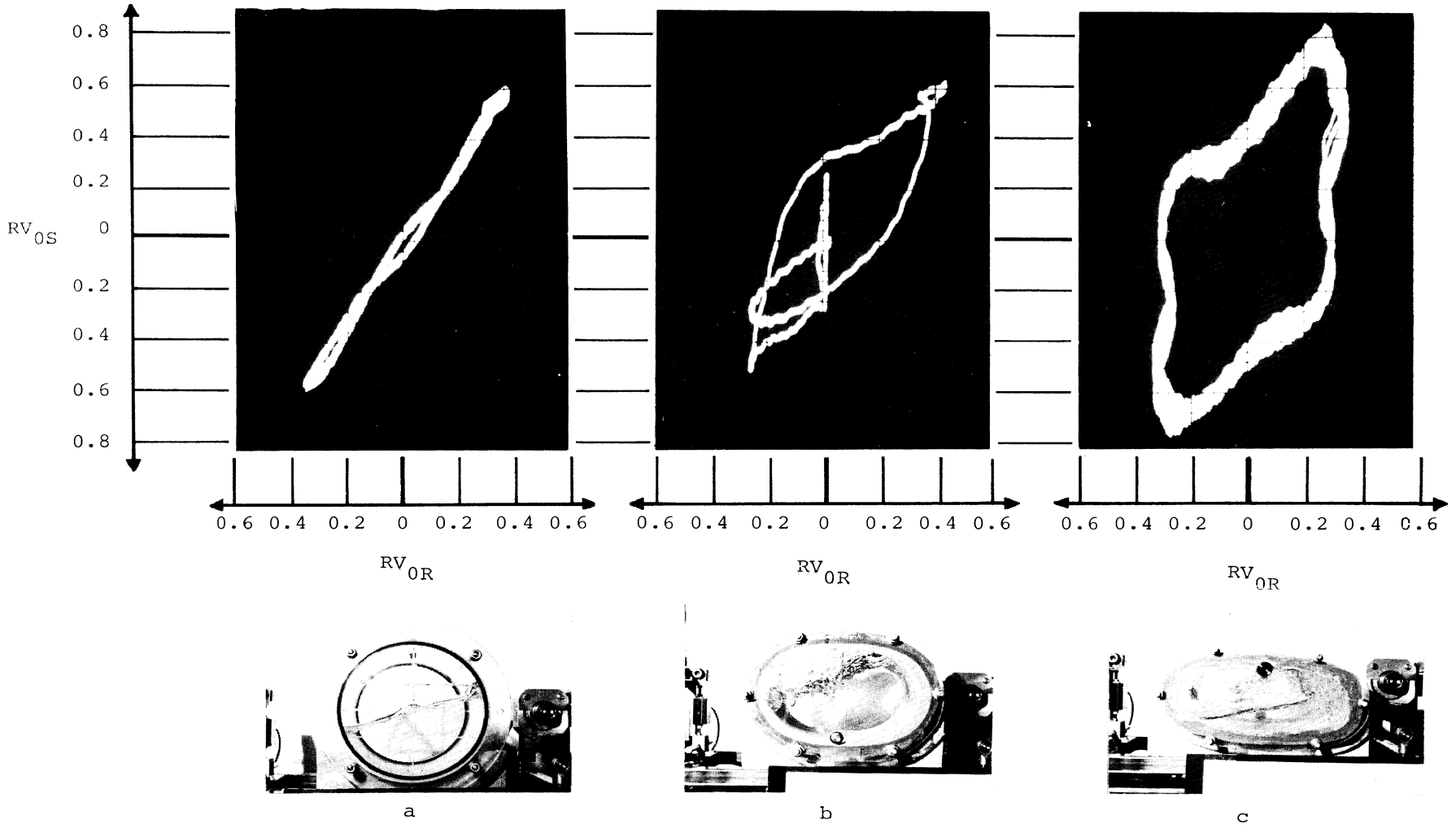

Figure 4.11. Overturning risk factor with sloshing load (R_{0S}) as a function of do. with corresponding rigid load (R_{0R}). Oscillation frequency 0.4 Hz.

a) 50 % circular tank, harmonic motion.
b) 75 % "Elliptic" tank, DAVIS motion.
c) 50 % "Superelliptic" tank, harmonic motion.

Load Volume %	Anti-Roll Bars	Overturning Speed km/h	
		No Baffles	With Baffles
50	No	33	38
50	Yes	45	Not tested
75	No	32	35
75	Yes	42	45

4.4.3 DYNAMIC SCALE MODEL - COMPUTER SIMULATION TECHNIQUE. The liquid forces from laterally moving tank models, scaled 1:10, together with its acceleration, were used as input signals to vehicle models in an analogue computer. See Figure 4.10 and 4.12. The tank motion was applied by a hydraulic servo as harmonic oscillations or double lane change manoeuvres. The main purpose was to investigate the influence from sloshing on the overturning risk with a few common tank types and within a relevant oscillation frequency range. The influence from baffles will be studied later.

Scaling rules—see, e.g., Dalzell (1966)—required time scaling of the analogue computer program. In order to maintain the proportion between inertia and viscous internal forces when the model liquid was water (kinematic viscosity 1 cSt = $1 \cdot 10^{-6}$ m^2/s) the full scale liquid was supposed to be combustible oil (~32 cSt). Corresponding densities were used when the liquid forces were scaled and put into the vehicle models. However, the large value of Reynolds number indicates that viscous forces are small compared to inertia forces. So, limited variations of the viscosity will not affect the results seriously.

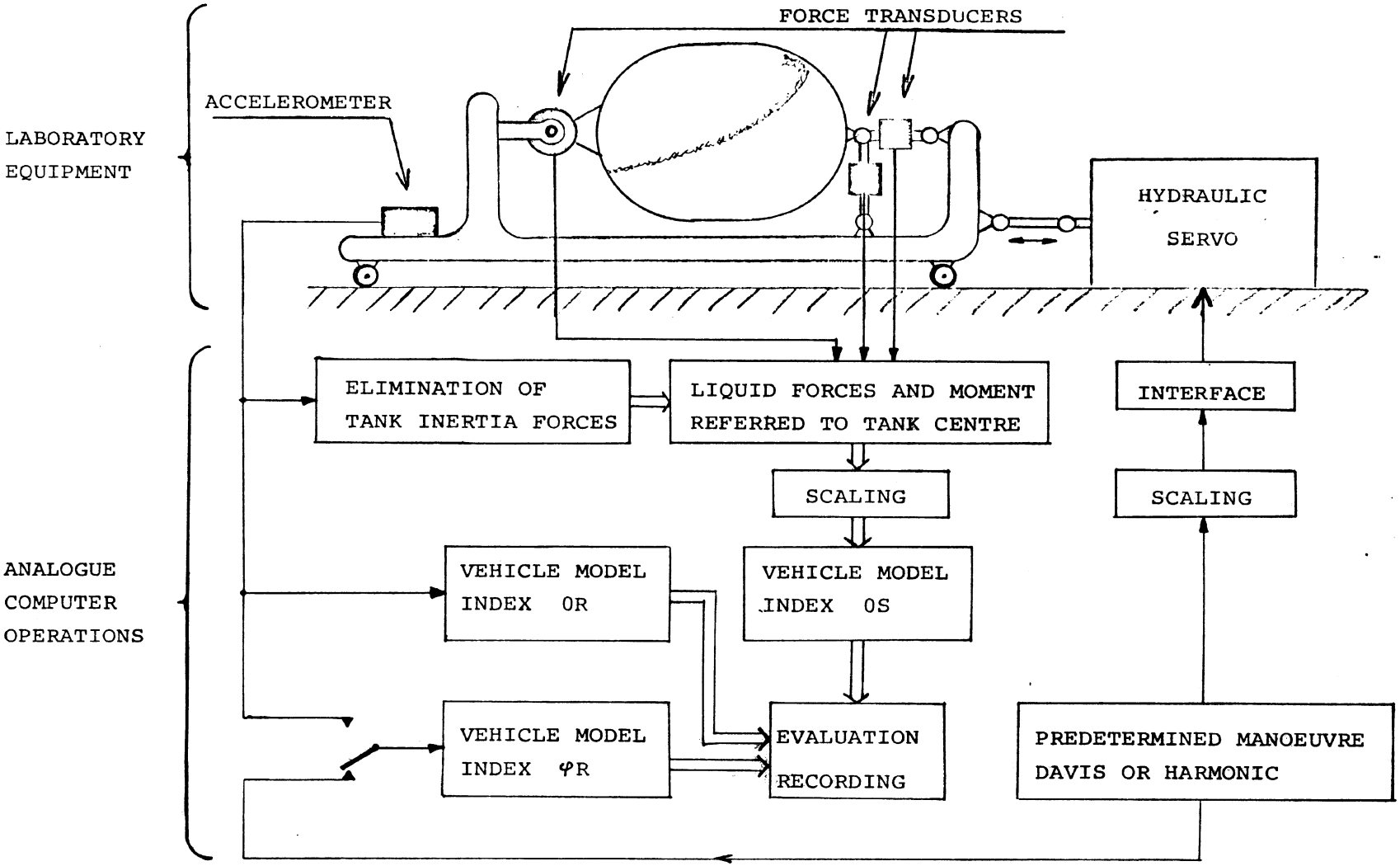

Figure 4.12. Experimental configuration and computing scheme.

The vehicle models were very simple with only one or two degrees-of-freedom. They were simultaneously simulated in the computer (refer to Figure 4.12) and differed in the following respects:

Index OR - Zero roll angle. Rigid load. All lateral forces computed from the accelerometer voltage. Force transducers neglected.

Index OS - Zero roll angle. Sloshing load. Liquid forces from the transducers' voltages.

Index ϕR - Rolling vehicle. Rigid load. Roll axis acceleration from the accelerometer or directly from the computer. Load forces computed from the sprung mass roll motion. Force transducers neglected.

Unfortunately, it was not possible to simulate a rolling vehicle with sloshing load. For comparability—and sometimes for computing stability—the predetermined lateral acceleration (SA_L in Figure 4.13) had to refer to a part of the vehicle that was not rolling. Then the lateral acceleration of the tank (SA_0)—which included a roll component—would not be independent of the vehicle model and the sloshing forces. This made closed-loop computation necessary. However, the accelerometer feedback to the hydraulic servo was not a successful strategy and these simulations had to be cancelled.

In simulations with ϕR-models, the peaks of SA_0 were sometimes more than twice as large compared to the SA_L peaks. Therefore, open-loop computation, based upon the approximation $SA \approx SA_L$, is not an acceptable way to simulate rolling vehicles with sloshing load.

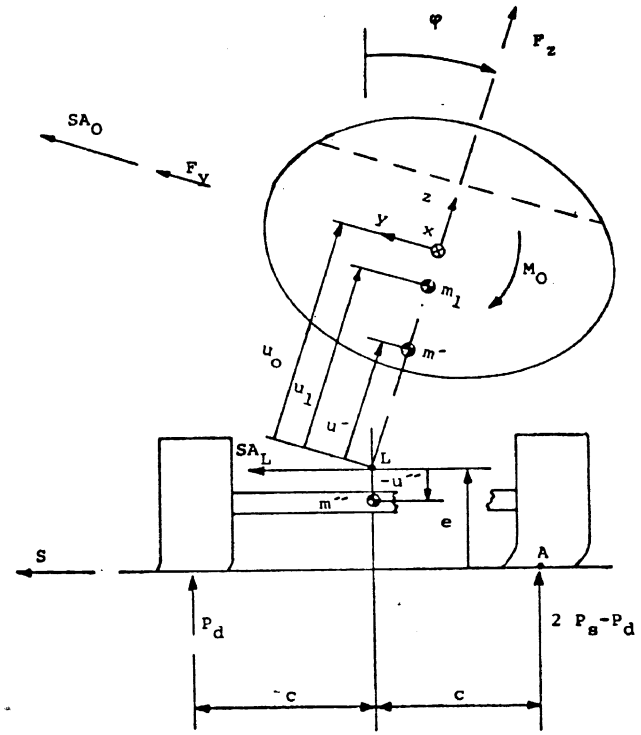

Figure 4.13a Rolling vehicle seen from the rear. For nonrolling vehicles φ=0 and the lateral acceleration SA is equal for all points ($SA=SA_L=SA_O$).

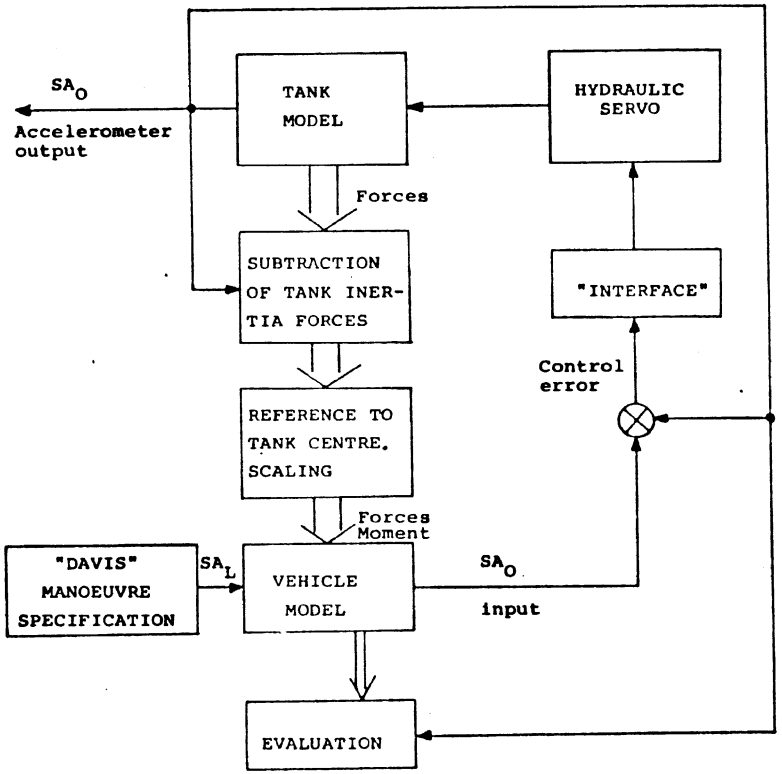

Figure 4.13b Experimental configuration proposed for investigation of the interaction between vehicle rolling and load sloshing.

The influence from sloshing on the overturning risk—computed like in Section 2.1.3—was evaluated from comparisons between the OR and the OS vehicle models. Model data and acceleration time histories were identical, except that the load of the OR model was assumed to be rigidly fixed to the tank. The ratio between the overturning risk peaks was called the sloshing factor:

$$SFAC = \frac{RV_{OS}\ peak}{RV_{OR}\ peak}$$

Corresponding evaluation of the influence from roll stiffness was performed by comparisons between the OR model (infinite roll stiffness) and each of the ϕR models (roll stiffness data in next section). The rolling factor was defined analogously by:

$$\phi FAC = \frac{RV_{\phi R}\ peak}{RV_{OR}\ peak}$$

4.4.4 SIMULATION DATA. Three tank cross-section configurations were used, see Figure 4.11. In the following they will be called C for "Circular," E for "Elliptic," and S for "Superelliptic" even if the E and S boundaries are not defined by mathematical expressions corresponding to their symbols. The liquid loads that were used occupied 0%, 50%, 75% or 100% of the tank volume. The simulation runs with 0% and 100% were made mainly for checking the experimental set-up.

Vehicle data were assessed with the aid of different manufactures and according to experience from previous measurements. The data were supposed to correspond to a trailer with two axles. Without load its gross weight was 5000 kg and with 75% load volume

the gross weight was 20000 kg. For the ϕR-model the roll stiffness constant was $0.6 \cdot 10^6$ Nm/rad (standard) or $1.2 \cdot 10^6$ Nm/rad (high).

The simulated manoeuvre in each run was either stationary harmonic oscillation (abbreviation H) or one double lane change (abbreviation D). The acceleration peaks were kept within the range 1.5 to 3.0 m/s^2. When oscillation frequency is mentioned it will always refer to full scale motion. (Due to insufficiencies in the hydraulic servo the motion was not exactly harmonic, which explains some irregularities in Figure 4.11.)

The spectral density of the acceleration time history in the double lane change manoeuvre (D as in DAVIS) has not been evaluated. The following expression—called the DAVIS-frequency in the text—has been used as a frequency label for the double lane change manoeuvre. The time when $\ddot{Y}<0$ is regarded as half a period, cf Figure 2.5.

$$f_D = \frac{1}{(\tau_6 + \tau_7) - (\tau_2 + \tau_3)}$$

4.4.5 SIMULATION RESULTS. With 50% load volume sloshing factors up to 2.3 were found for harmonic oscillation frequencies low enough to be likely to occur in normal driving. See Figure 4.14. Also, the double lane change (D) manoeuvre caused sloshing factors slightly above 2.0 for the S and E tanks. The C tank seems to be the most favourable because of its lower sloshing factors and higher resonance frequency. However, if some large longitudinal baffles are added, the S tank will probably represent the best contour

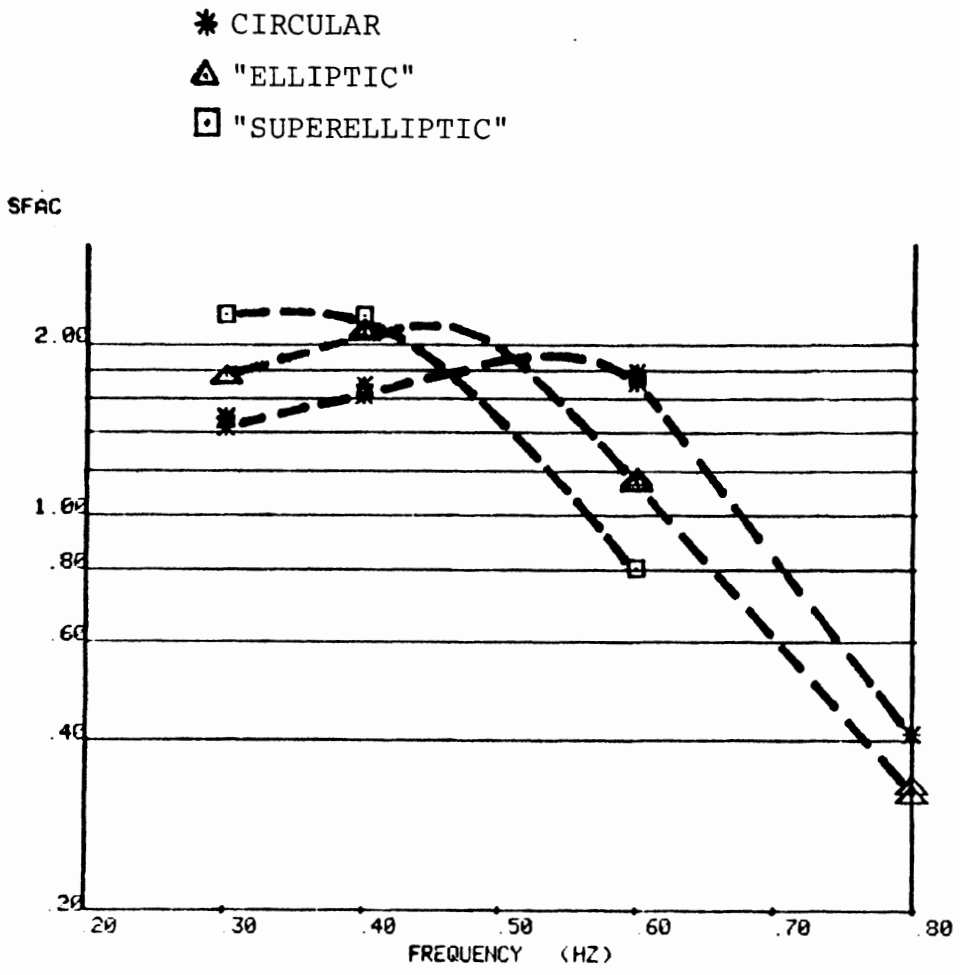

Figure 4.14. Sloshing factor (SFAC) as a function of the harmonic oscillation frequency. 50 % load volume in different tank shapes.

among these horizontal tank cylinders. This assumption is due to the lower centre of gravity with conventional vehicle designs.

The E tank was tested in 0.3 Hz and 0.4 Hz D manoeuvres with 75% load, as well. The sloshing factor varied between 1.4 and 1.6. Larger sloshing factors will probably be exhibited by the 75% S tank considering its cross-sectional shape and the results with 50% load.

The sloshing factors are supposed to indicate roughly the ratio between real and driver-estimated overturning risk. Of course, an experienced driver will be better aware of the problem. But if the sloshing occurs in a full trailer, much of the sloshing force feedback—that is important for learning and adaptation of steering behaviour—will never be perceived by the driver. It is easier for the driver to be aware of lateral sloshing effects if they occur in the truck itself. However, the irregular characteristics of sloshing and the phase shifts between acceleration and overturning risk—see Figure 4.11—will make adaptation of steering behaviour almost impossible.

In Figure 4.15a the overturning risk peak values with 0%, 50%, 75% and 100% load volume are related to each other. It is evident that unloading the vehicle may increase the dynamic overturning risk. This is even more alarming than Isermann's results for steady-state—see Section 4.4.1—although no rolling effects have been considered here.

Regarding rolling vehicles with rigid load—see Figure 4.15b—it is apparent that pure rolling may increase the overturning risk with the same ratio as pure sloshing. However, the rolling phenomenon in

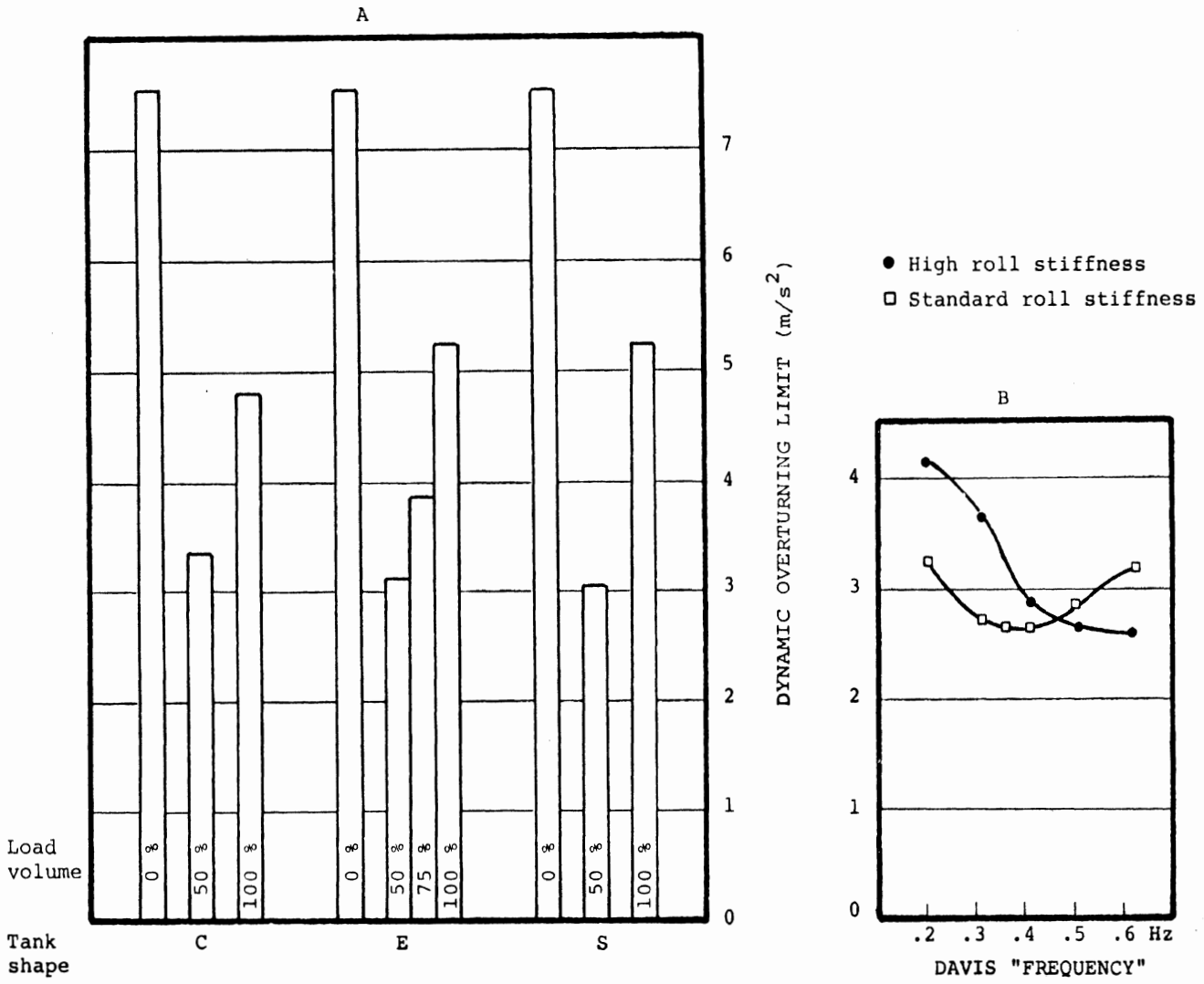

Figure 4.15. Overturning limits calculated as the ratio between the peaks of lateral acceleration and overturning risk in double lane change manoeuvres.

A) Comparisons between different sloshing load volumes and tank shapes. Vehicles without roll and 0.3 Hz DAVIS frequency - see section 4.4.4.

B) Comparisons between standard and high roll stiffness at different manoeuvre frequencies. Rolling vehicles with rigid load corresponding to 75 % volume.

itself is well-known to the driver, without irregular effects and hence easy to adapt the steering to.

Even if no simulations have been performed with simultaneous rolling and sloshing, it is evident that the risk factors due to sloshing effects will be further increased by the roll motions of the tank (see comments on the SA_0/SA_L ratio in Section 4.4.3).

5. SAFETY PROBLEMS AND SUGGESTIONS

5.1 ARTICULATION AND DRIVER-VEHICLE DYNAMICS

The possibility for vehicle movements that are uncontrollable for the driver, will increase with the number of articulations and degrees of freedom. In addition, the driver in an articulated vehicle combination has very small possibilities to judge and observe the dynamic state of the rear vehicles. Inertia and steering wheel forces (vestibular, kinesthetic, and tactile cues are often unaffected by the motions of the rear vehicles and the visual information via mirrors is unsatisfactory).

The dynamic controllability, observability, and the steady-state (see Section 5.3) evidence against articulation for high speed manoeuvres was reinforced by the dynamic behaviour in the double lane change simulations. All simulations at high speed showed the largest risk factor values for the rearmost vehicle unit and for the highest articulation number among comparable vehicle combinations. One example is found in Figure 5.1 where a truck-full trailer (two articulations) is compared with a tractor-semitrailer-full trailer (three articulations) in different speeds.

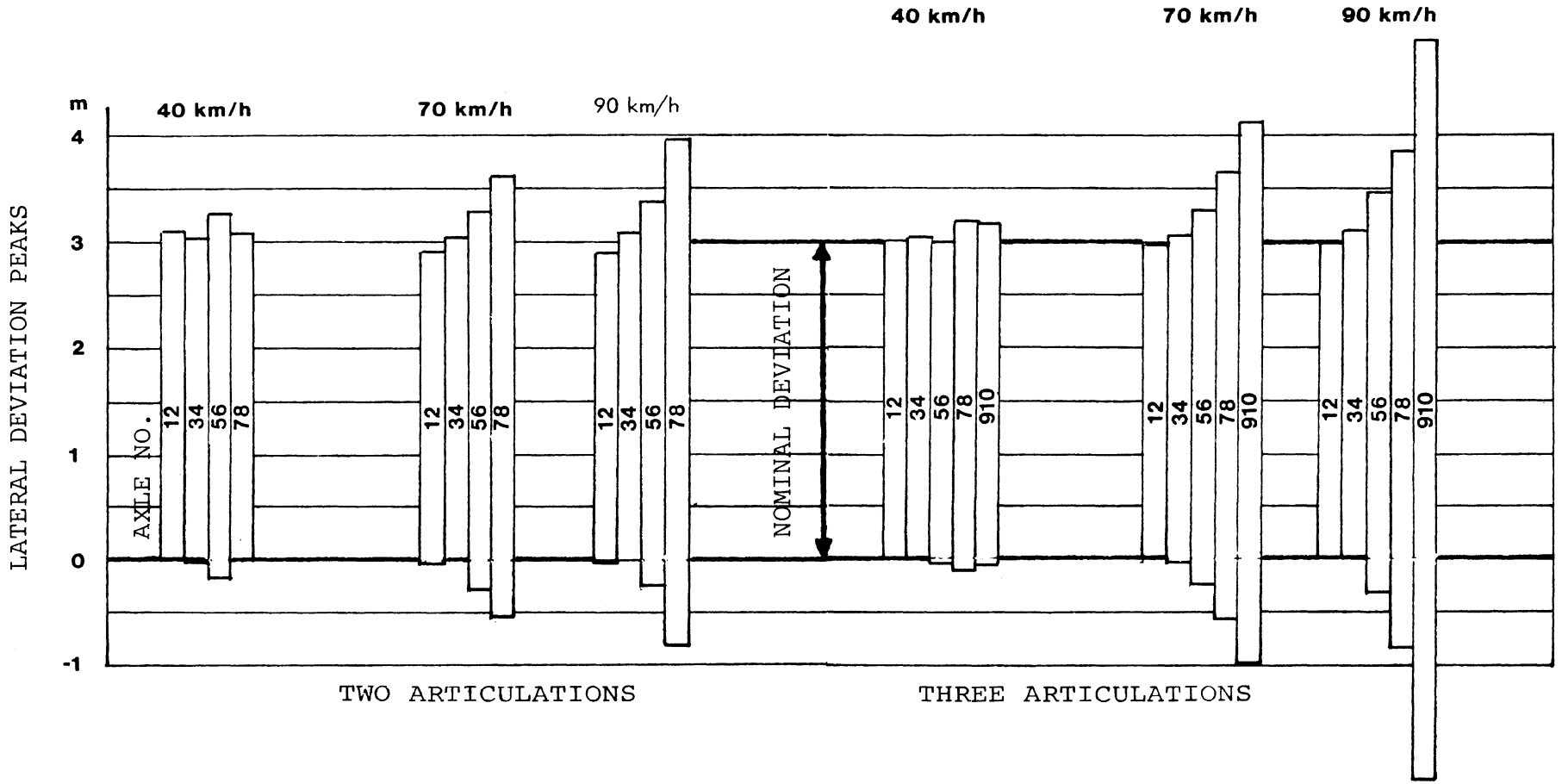

Figure 5.1. Speed influence on lateral deviation. Fully loaded 24 metre combinations and DAVIS manoeuvre, cf figure 2.5.

5.2 OVERTURNING - A PRIMARY RISK FOR COMMERCIAL VEHICLES

In many accidents commercial vehicles will overturn, without the primary cause being skidding and driving off the road. This is not surprising because commercial vehicles often have comparatively poor overturning stability. The accident accounts may be incorrect in many of these cases. When a vehicle is overturning the load is transferred to the outer wheels in the bend causing skidding tracks. Thus the skidding might be accounted for being the primary cause of the accident.

Because of the well-known nonlinearities of tyre characteristics, the skid tendency will decrease as a secondary effect, when the overturning stability is improved—see Strandberg (1974).

Due to the problems with driver perception, rearward risk factor amplification and driver training in control of irregular phenomena highest priority should be given to design, legislative and educational improvements for

- trailers and rear vehicle units more than for the leading vehicle in articulated combinations
- vehicles with liquid load

5.3 THE OFF-TRACKING DESIGN CONFLICT

Low speed off-tracking is a well-known problem for long vehicle combinations in sharp curves. At high speed and large sideslip angles off-tracking towards the outside of the curve will occur. This phenomenon is probably less known to the drivers than the "classic," low speed off-tracking. Furthermore,

it is often impossible for the driver to observe the outer track of the rear vehicle.

The outside off-tracking can be reduced by shortening the combination, reducing the number of free articulations, using tyres with high cornering stiffness, etc. Unfortunately, one common method to reduce low speed off-tracking (i.e., articulation) will also increase the high speed off-tracking. See Figure 5.2.

Another low-speed oriented design (spread and steered rear axles) is based mainly upon kinematics, as well. When cornering at a low speed the sideslip angles are small compared to relative yaw angles between vehicle units (Figure 5.3a). Then the conventional axle steering will work in the desired way. When cornering at a higher speed (Figure 5.3b) the rear axles of the trailer will deviate outwards instead of inwards compared to the truck. As the axle 9-10 is so steered that its extension will pass through A, its sideslip angle will be considerably smaller than for the other axles of the trailer. Therefore, the axles 5-6 and 7-8 will be subjected to an unreasonably large proportion of the inertia forces. So the outwards off-tracking will be larger than with a fixed bogie arrangement similar to that in Figure 5.2a. This tendency appears in dynamic manoeuvres as well—see Section 4.2.

The spreading of axles may cause other problems, too. If the vehicle frame is rigid and no pitch articulation is introduced between the spread axles, force distributions induced by road unevenness will stress the road and the vehicle abnormally.

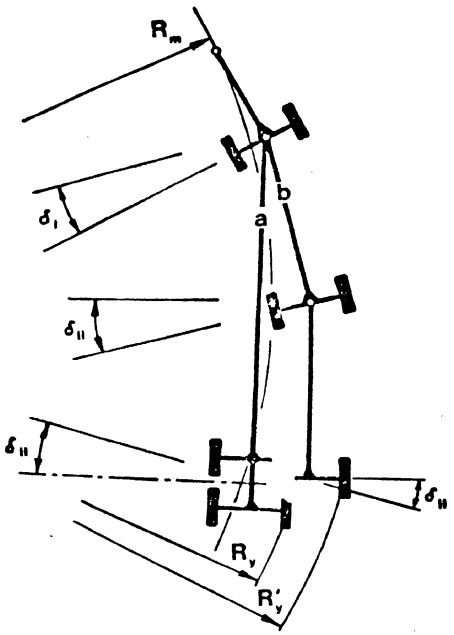

Figure 5.2 Increase in outwards off-tracking when a rigid vehicle unit (a) is replaced by an articulated unit (b). If side forces and side-slip angles for the rear axles (δ_{II}) are unaffected when one articulation is added, the outer wheel radius (Ry) will increase.

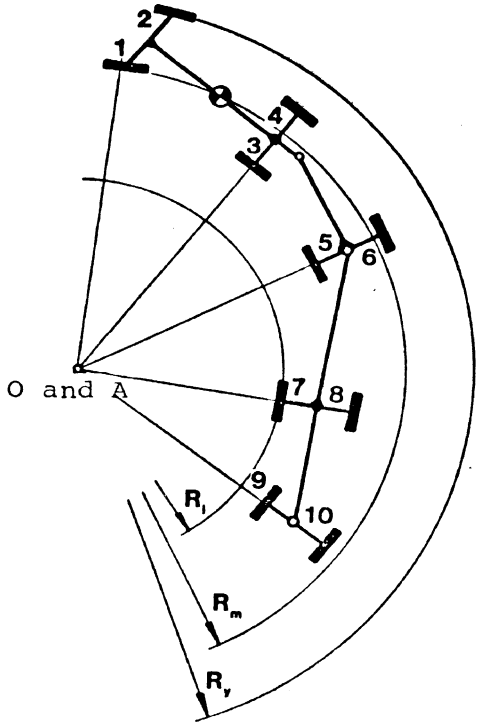

a)

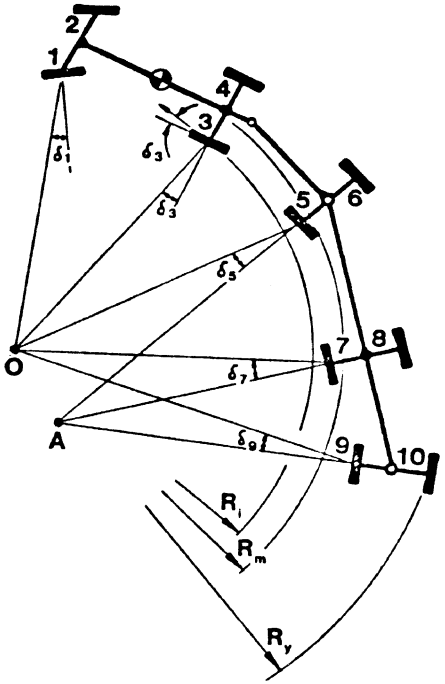

b)

Figure 5.3 The influence from speed and sideslip angles upon vehicle tracking. Steady-state cornering with centre of rotation at O.
The effect from conventionally steered trailer rear axle is also shown. The extension of the axle 9-10 joins the intersection of the axles 5-6 and 7-8 (point A).
a) very low speed
b) higher speed

5.4 BRAKING PERFORMANCE

The braking performance of heavy commercial vehicles has till now not been studied experimentally or theoretically to any greater extent at the Institute. The braking of heavy vehicles and heavy vehicle combinations in particular is regarded as an important problem though. Research in this field is planned to take place at the Institute in the near future. The performance of antilock brake systems seems to be the central problem.

The Swedish ESV-research program Steerability During Emergency Braking, which concerned passenger cars with antilock brakes, has pointed out three essential criteria which must be considered:

Stability
Steerability
Brakeability

Stability was defined as the ability to resist external disturbances and keep the deviation from the intended course at a minimum. It was studied by measurements of the vehicle sideslip angle.

Steerability was defined as the ratio between the lateral deviation from brake application to stand-still and the braking distance, see Figure 5.4.

Brakeability was based on the mean deceleration during braking in a curve

$$\bar{a}_{curve} = \frac{V_o^2}{2S}$$

V_o = velocity at brake application

S = braking distance

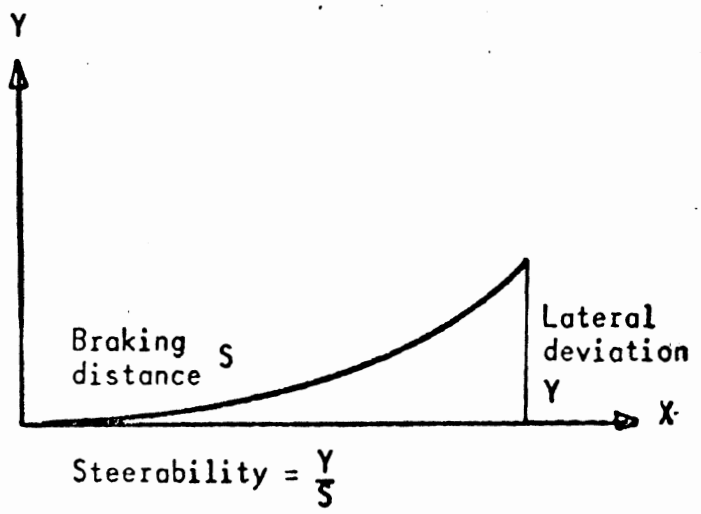

Figure 5.4 Definition of steerability

Brakeability was defined as $\frac{\bar{a}_{curve}}{\bar{a}_{locked\ wheels}}$ where

$\bar{a}_{locked\ wheels}$ = mean deceleration during braking straight ahead with locked wheels.

Braking in a curve with simultaneous brake application and step steering was recommended as test procedure. The steering input was defined to give minimum curve radius for the actual vehicle without brake application. The following test conditions were proposed:

Minimum and maximum vehicle load
Low friction surface at 50 km/h (studded winter tyres on ice)
High friction surface at 90 km/h (dry asphalt)

Stability performance on ice turned out to be critical even with studded tyres. So, it was concluded that tests on a low friction surface with properties similar to ice are important for the evaluation of antilocking brake systems.

Balancing of the rotational wheel slip percentage between the axles was shown to be of major importance for the stability during braking.

Similar performance criteria and recommendations might be used for commercial vehicles. However, the stability problems for vehicle combinations are more complicated than for single cars (the rotational wheel slip must be balanced between many axles mounted on different vehicle units).

Braking on ice is regarded as an essential problem in Sweden. Little seems to have been done to vehicle combinations in this problem area. So, the research at the Institute is intended to concentrate on low friction braking problems.

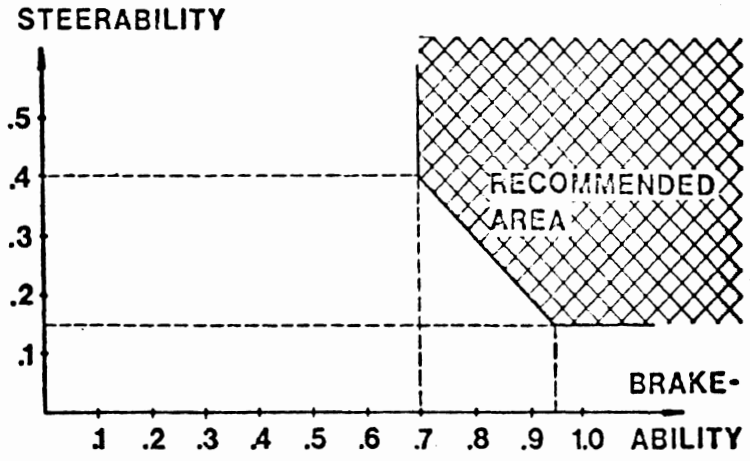

Figure 5.5 Steerability and brakeability performance recommended for cars with antilock brake systems. (Swedish ESV programme)

5.5 INTERDISCIPLINARY STEPS TOWARDS BETTER SAFETY

The nature of the revealed safety problems imply interdisciplinary solutions. Legislative measures seem to be necessary to achieve obvious safety improvements in commercial vehicle design. Total system improvements by vehicle design require knowledge on the sensory-motor characteristics of the driver, apart from knowledge on vehicle dynamics. Some problems cannot be solved quickly enough by technological measures and should be emphasized in road user education.

5.5.1 LEGISLATION AND TEST METHODS. A successful application of the major aims for regulations—listed below the headline of Chapter 3—will use proper performance (instead of design) demands to produce a spontaneous development towards vehicles with better safety/economy ratio. Certain improvements in vehicle design will allow more load to be carried, which seems to be the most important competition factor among commercial vehicle manufacturers and users.

Many times, finding relevant performance criteria is a research problem in itself, as for antilock systems in articulated vehicle combinations. Finding a reliable test method might be a problem, as well—e.g., how to make a suitable check on the overturning limit of certain road tankers.

Evidently the many possibilities to combine or connect commercial vehicles by articulations may cause paradoxical effects. Improvements in the leading vehicle handling performance may deteriorate the overall driver-vehicle safety due to the rearwards risk factor amplification, etc.

In checking the elementary dynamics of different vehicle combinations, computer simulation seems to be a reasonable method. Tables with permitted-or-not combinations will be more cumbersome to handle, and (again) it represents a demand on design—not on performance.

Full-scale tests are suggested for certain details of the demands where mathematical modeling is dubious or data collection is difficult. This is also preferable for type tests when corresponding checks will have to be repeated regularly because of fatigue and wear, e.g., in future antilock braking systems.

In order to reduce the number of overturning accidents it has been suggested to introduce different speed limits for different centre of gravity heights. Several investigations though—see Taragin (1954), Ritchie et al. (1968), and Herrin and Neuhardt (1974)—have shown that most drivers utilize larger lateral accelerations at low speeds than at high speeds. As many overturnings occur at a low speed, such limits would not be very effective. In addition, different speed limits for different types of vehicles will introduce new hazards due to disturbances in the traffic flow.

Independent of regulations and test methods, research must continue to reveal presently unknown problems and to continuously adapt legislation to the needs of community.

5.5.2 VEHICLE DESIGN. Even if it has not been in the line of the investigations to suggest suitable designs, this subject is often discussed. The regulation proposals must be realistic and the unspoken aim

is an increase in road safety with no evident deterioration of transport economics. Some suggestions are mentioned below without rank ordering. The effort should be concentrated on trailers and whole combinations, not primarily on trucks and tractors.

a) Use the space between axles and wheels to lower the center of gravity. Self-supporting containers, independent wheel suspension and modular tanks as vertical cylinders lowered between wheels and axles may help.

b) With the suggested road tanker design (vertical cylinders) sloshing could be completely eliminated by a piston arrangement in each tank that will be partially loaded.

c) Utilize as large a nominal and effective track as possible (super-single tyres may be favourable).

d) Utilize maximum lateral distance between adjacent springs and perhaps anti-roll bars to obtain better roll stiffness.

e) Avoid large overhangs and combinations with unsuitable length distribution.

f) Place the tow pin as far ahead as possible and be careful with long drawbars.

g) Minimize the risk for lateral oscillations at high speed having few articulations and dynamically acceptable control strategy for articulation yaw and steered axles. Maybe side force or speed could be used as input in such strategies.

Research will be performed on these questions at the Institute. As yet not tested, but perhaps a favourable solution is a double-articulated combination consisting of a tractor with two semi-trailers and appropriate control of articulation yaw movements, etc. An alternative might be a single-articulated combination consisting of a truck and semitrailer similarly controlled.

h) Develop well functioning brake control systems (load sensitive and anti-locking). Why not develop dynamic force transducers that can be used for brake systems as well as load indication and perhaps also for instruments or warning signals indicating the overturning risk?

i) Increase the continuous feedback of the vehicle's dynamic state to the driver. Modified servo assistance, seat movements, tactile displays, acoustic warnings and head up collimated visual displays may be used.

5.5.3 ROAD USER EDUCATION. In order to maximize the overall efficiency and safety, education and training are necessary complements to legislation and vehicle design. However, these steps should not be considered to be substitutes for immediate technological measures when they are possible.

Some vehicle dynamics phenomena are vaguely known and should be explained in driver education to make the requirements on the drivers more reasonable. Results

from research must be spread and used in education of other road users as well. This will contribute to a smaller number of accidents caused by—now understandable—overestimation of commercial vehicle handling and braking performance.

REFERENCES

1. Abramson, H.N., ed., The Dynamic Behavior of Liquids in Moving Containers, NASA SP-106, 1966.

2. Backman, G., Jönsson, C.A., Nordström, O., and Pelijeff, A., The Dynamic Stability of Heavy Vehicle Combinations, etc. (in Swedish), Swedish Department of Transportation, Ds K 1972:10, 1972.

3. Bauer, H.F., "On the Destabilizing Effect of Liquids in Various Vehicles," Vehicle System Dynamics 1, 1972.

4. Budiansky, B., "Sloshing of Liquids in Circular Canals and Spherical Tanks," Journal of the Aero/Space Sciences, No. 3, 1960.

5. Chiesa, A. and Rinonapoli, L., "A New Loose Inverse Procedure for Matching Tyres and Car Using a Mathematical Model," Proc. Instn. Mech. Engrs., Vol. 183, Part 3 H, 1969.

6. Dalzell, J.F., "Simulation and Experimental Techniques," in Abramson (ed.) The Dynamic Behavior of Liquids in Moving Containers, NASA SP-106, 1966.

7. Dodge, F.T., "Analytical Representation of Lateral Sloshing by Equivalent Mechanical Models," in Abramson (ed.) The Dynamic Behavior of Liquids in Moving Containers, NASA SP-106, 1966.

8. Eshleman, R.L. and Desai, S.D., Articulated Vehicle Handling, Final Report, DOT-HS-105-1-151, II TRI Project No. J6255, 1972.

9. Herrin, G.D. and Neuhardt, J.B., "An Empirical Model for Automobile Driver Horizontal Curve Negotiation," Human Factors, 16(2), 1974.

10. Isermann, H., Die Kippgrenze von Sattelkraftfahrzeugen mit fester und flüssiger Ladung, Deutsche Kraftfahrtforschung und Strassenverkehrstechnik, Heft 200, 1970.

11. Jansson, B., Rolling Test of Road Tanker (in Swedish) Report No. 665-2, AB Volvo, Gothenburg, Sweden, 1973.

12. McCarty, J.L. and Stephens, D.G., Investigation of the Natural Frequencies of Fluids in Spherical and Cylindrical Tanks, NASA TN D-252, 1960.

13. Mikulcik, E.C., The Dynamics of Tractor-Semi-trailer Vehicles: The Jackknifing Problem, Cornell University, 1968.

14. Nordström, O. and Eldrot, D., Space Demands in Manoeuvres with Long Vehicle Combinations, National Swedish Road and Traffic Research Institute, Report No. 51 (in Swedish), 1974.

15. Nordström, O., Magnusson, G., and Strandberg, L., The Dynamic Stability of Heavy Vehicle Combinations, (in Swedish), National Swedish Road and Traffic Research Institute, Report No. 9, 1972.

16. Nordström, O. and Strandberg, L., The Dynamic Stability of Heavy Vehicle Combinations, National Swedish Road and Traffic Research Institute, Publication, 1974.

17. Ritchie, M.L., McCoy, W.K., and Welde, W.L., "A Study of the Relation between Forward Velocity and Lateral Acceleration in Curves During Normal Driving," Human Factors, 10 (3), 1968.

18. Roberts, J.R., Basurto, R.B., and Chen, P.-Y., Slosh Design Handbook I, NASA CR-406, 1966.

19. Shapley, C.G., The Dynamic and Static Behaviour of Articulated Semi-Trailer Vehicles, Cranfield Institute of Technology, School of Automotive Studies, 1972.

20. Silveira, M.A., Stephens, D.G., and Leonard, H.W., An Experimental Investigation of the Damping of Liquid Oscillations in Cylindrical Tanks with Various Baffles, NASA TN D-715, 1961.

21. Stofan, A.J. and Sumner, I.E., Experimental Investigation of the Slosh-Damping Effectiveness of Positive-Expulsion Bags and Diaphragms in Spherical Tanks, NASA TN D-1712, 1963.

22. Strandberg, L., "The Dynamics of Heavy Vehicle Combinations," Teknisk Tidskrift, No. 3, 1974. Translated into English in Internal Report No. 172, National Swedish Road and Traffic Research Institute, 1974.

23. Sumner, I.E., Experimental Investigation of Slosh-Suppression Effectiveness of Annular-Ring Baffles in Spherical Tanks, NASA TN D-2519, 1964.

24. Taragin, A., "Driver Performance on Horizontal Curves," HRB Proceedings, Vol. 33, 1954.

25. Tyden, T., Driver Estimation of Overturning Risk in Road Tankers (in Swedish), Internal Report No. 197, National Swedish Road and Traffic Research Institute, 1975.

ARTICULATED VEHICLE RESEARCH IN ONTARIO

F. B. Snelgrove
Ministry of Transportation and Communications
Downsview, Ontario

ABSTRACT

An overview of the commercial vehicle research program undertaken by the Province of Ontario to improve the highway safety of articulated vehicles is presented. Accident statistics are examined to determine the extent of various causes of accidents—vehicle instability, mechanical deficiencies, or others. The research program is being developed around the need for safety regulations identified by accident data and vehicle inspections. The process of defining acceptable vehicle performance in terms which can be translated into realistic (enforceable) licensing regulations and inspection procedures is emphasized. A pragmatic approach is described, in which experimental results from vehicle tests and theoretical results from computer simulations will be used to predict acceptable performance criteria for a wide variety of conditions.

BACKGROUND

The Ontario Ministry of Transportation and Communications is responsible for the provision, maintenance, and safe keeping of the provincial highways. This responsibility includes the licensing of vehicles and drivers as well as the regulatory control of the type of vehicles, loads, and mechanical condition as they might affect safety on the highways.

Over the past few years, there has been a significant increase in the number and severity of accidents involving commercial articulated vehicles (CAV's) in Ontario. The especially severe accidents have notably involved the double articulated combinations (doubles) using convertor dollys and "pup" trailers. The initial public reaction to these large combinations and ensuing accidents demanded their being banned from the roads. As an alternative to this drastic solution, the Articulated Vehicle Research Program was initiated to examine the overall relative safety of these combinations, what safety measures should be instituted, and whether they are justified on a cost/benefit basis.

ACCIDENTS

Accident severity for "doubles" has initially been measured by the loss of life and high property damage involved. For the doubles, fatalities occurred 2.6 times more often, with 1.5 times more fatalities per fatal accident than for semi-trailer combinations. Property damage, as estimated from the accident reports, appears to substantiate this relative severity, with the doubles dollar loss 2.4 times greater than for semis. The average property damage in 1974 for doubles was about $7,000.

Many of the doubles' accidents have occurred under circumstances not particularly hazardous to other classes of commercial vehicles and have resulted in a serious questioning of the relative stability and handling characteristics of such combinations. The structural and mechanical integrity of these vehicles has also been questioned since mechanical failures, particularly with hitches common only to the doubles, have accounted for a number of accidents.

ONTARIO BRIDGE FORMULA

The variety of combinations currently seen on the highways of Ontario is generally attributed to the March, 1971, amendment to the Highway Traffic Act—commonly referred to as the Ontario Bridge Formula (OBF). Prior to 1971, only specific, predetermined configurations were permitted. The 1971 legislation, developed to take better advantage of the design capabilities of the highways and bridges of Ontario, defines the permissible weight of a given vehicle as a function of its individual axle weights and interaxle spacings. This progressive step towards the optimum usage of Ontario highways for shipping permits the highest vehicle loads in North America while at the same time maintaining damage to pavements and bridges within acceptable levels.

The OBF also provides the basis for optimizing heavy vehicle design. To maximize the load-carrying capacity of a vehicle, the number of axles and axle spacings must conform to the Formula. A highly-automated system is being implemented at the weigh stations to check vehicle conformance. Some possible configurations with various numbers of axles for the maximum

permissible vehicle weights and the shortest possible base length are shown in Figure 1. Figure 1 is taken from Research Report 186, "Proposed Ontario Bridge Design Load," by P.F. Csagoly and R.A. Dorton, published by the Ministry of Transportation and Communications, Ontario, November, 1973.

FUTURE CONSIDERATIONS

Many new, untried vehicle designs, based solely on the Ontario Bridge Formula, can be expected in the future. Some new combinations are already in operation and more are in the planning stage. A thorough understanding of what designs to expect and their potential impact on safety is required if provincial regulations are to be intelligently applied.

Many commercial vehicles are still operating well below the weight limitations imposed by the OBF so that future carrier shipping cost improvements are likely through greater volume allowances. Although this is not likely in the near future, it would certainly mean longer vehicles with more articulations. Information on the stability, braking and handling of these vehicles will be required before their cost/benefit to our society can be effectively evaluated.

The cost of fuel has certainly had an impact on the trucking industry, with many aerodynamic modifications and fuel saving devices being rapidly considered. One such device is self-steering trailer axles which are being prepared for fuel reductions as well as improved stability. While possibly improving vehicle stability under most conditions, they do not appear to have been proven for emergency maneuvers, adverse weather and road conditions, or even for all

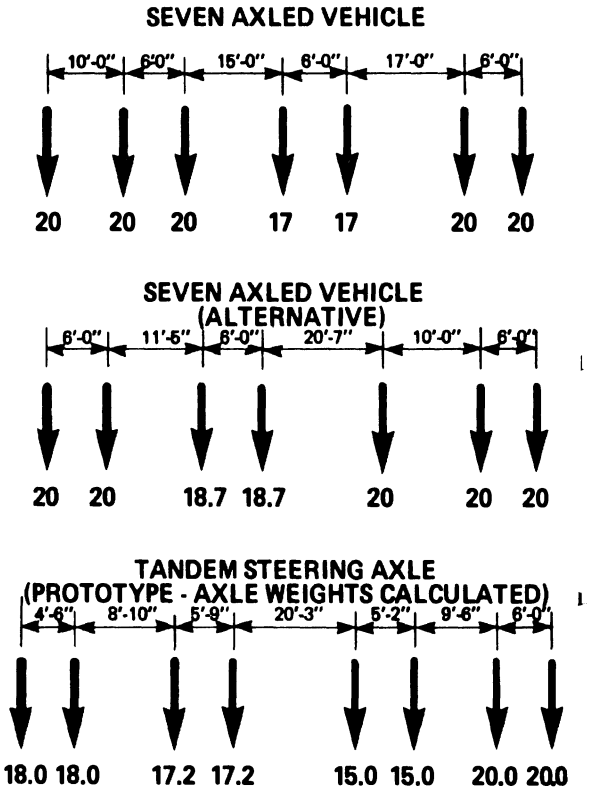

Heaviest Axle Combinations Permissible
by the Ontario Bridge Formula

Figure 1

vehicle configurations or load distributions under normal operating conditions.

The Articulated Vehicle Research Program, therefore, intends not only to evaluate the vehicle configurations currently operating on the highways of Ontario, but to provide a basis to better evaluate future configurations which might be proposed to fit within our present regulations.

PROJECT DESCRIPTIONS

While there are many good reasons for the Province of Ontario to undertake the study of articulated vehicles, the major concern is the basic stability and mechanical safety of these combinations already in use. The Articulated Vehicle Research project was initiated to study the present situation and to develop procedures or controls as required to ensure their operational safety.

Several intermediate measures have already been instituted by the Ministry to improve the overall safety of commercial vehicles. A driver licensing system requiring commercial vehicle operators to be licensed for each of several classes of vehicles has been introduced. Also, there has been an intensification of the roadside inspection program covering the mechanical condition of commercial vehicles.

The objective of the Articulated Vehicle Research Program is to provide the data and basic understanding of vehicles needed to support effective regulations and controls meeting the safety and cost/benefit requirements of our highway system.

Research activity (as shown in Figure 2) has followed three mainlines of research:

1. Accident Data and Statistics - a study to identify the main causes of CAV accidents and, thereby, guide vehicle research activity and to conduct a cost/benefit analysis of the need for additional regulations or controls.

2. CAV Research into

   a) Vehicle Dynamics - covering stability, performance braking and handling characteristics as they relate to safe highway operation, and

   b) Vehicle Structural and Mechanical Condition - covering the structural and mechanical integrity of such components as brakes, hitches, and load-retention devices.

3. Regulations - Ensuring that the output of the research (whether inspection or test procedures, vehicle licensing or operational regulations), fits within the framework of the Ontario Highway Traffic Act.

ACCIDENT DATA AND STATISTICS

The main question in a research project such as this is, "Where do you begin, and which of the many factors affecting vehicle safety should receive priority?" The answer can be found in accident statistics, accident investigations, and vehicle inspection statistics—three areas now under active consideration by the Ministry.

ARTICULATED VEHICLE RESEARCH - SYSTEM / PROCESS

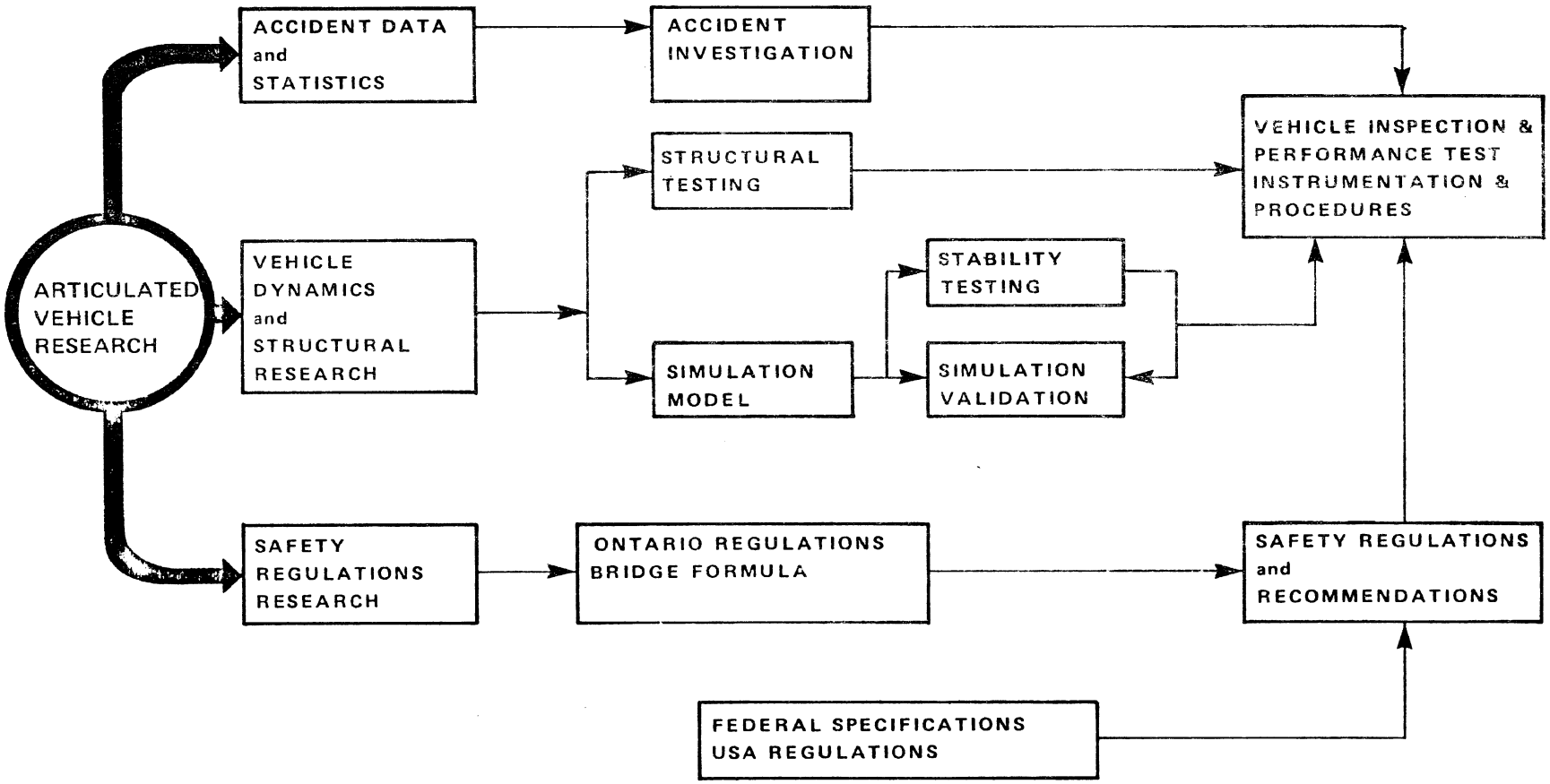

Figure 2

Accident data for the years 1972, 73, and 74 have been compiled for all of the CAV accidents recorded in Ontario. This has been an extensive compilation covering some 14,000 accidents. The data has been tabulated taking into account most of the available information recorded on the accident file. The data range from the time of day of occurrence, road condition and dollar-loss to the nature and circumstances of the collision. Although only a small portion of this data has been utilized to date, it has been fully tabulated to provide specific statistics when required.

The main emphasis of the statistical analysis thus far has been to provide direction for articulated vehicle research—to determine what emphasis should be placed on doubles research as compared to semis. In particular, analysis should indicate which accident causes would be the most cost/safety effective to research.

Accident Severity

Severity has been measured by frequency and number of fatalities, although property damage has also been used and generally supported the relative severity as indicated by fatalities. A summary of fatal accident data is shown in Table 1. These statistics clearly indicate that if a double is involved in an accident, the probability of a fatality is 2.6 times more than for a single. Also, the number of fatalities, once involved in a fatal accident, is greater by 58 percent. It is also clear that the accident frequency of doubles is increasing much more rapidly than that for singles. Although these statistics are indicative of the relative severity of CAV accidents, they do not give a

Table 1

CAV FATAL ACCIDENT SUMMARY, ONTARIO, 1972-74

	ACCIDENTS		FATAL ACCIDENTS		FATALITIES	
	SEMI	DOUBLE	SEMI	DOUBLE	SEMI	DOUBLE
1972	3840	61	84	7	100	12
1973	3806	125	103	5	127	17
1974	5271	228	87	10	115	12
TOTAL:	13,335		296		383	
% of TOT.:	96.9	3.1	92.6	7.4	89.3	10.7

	SEMI	DOUBLE
PERCENTAGE OF ACCIDENTS WITH FATALITIES :	2.1	5.3
AVERAGE No. OF FATALITIES PER FATAL ACCIDENT :	1.2	1.9

good indication of their relative significance in terms of cost/benefit factors such as the number of accidents or fatalities/pound/payload mile. This type of data is difficult to come by and it is generally biased since it usually represents only a few major companies and, in many cases, only specific routes or operating conditions. It is anticipated, however, that through the cooperation of the trucking industry and, in particular, the Ontario Trucking Association, that appropriate data may be made available in the future in a form that can be correlated with our accident data.

The Ontario Petroleum Association has been particularly cooperative in this regard, gathering accident data related to their truck fleets based on the payload-mile.

Accident Causes

Accident circumstances have been divided into four major categories—instability, mechanical deficiencies, driver oriented and other, a catch-all classification for those not readily identified with one of the other three. These categories were further subdivided to identify specific causes within the category as shown in Table 2. The distribution of accidents for both singles and doubles for the major classifications is shown in Figure 3. These distributions show that the majority of accidents (75%) fall into the categories of "Driver Oriented" or "Other," although 25 percent of all accidents (more than 4,000 accidents) could have been averted, in Ontario, over the past three years had vehicle instability and mechanical deficiencies been eliminated.

Table 2

COMMERCIAL ARTICULATED VEHICLE ACCIDENTS
ACCIDENT CIRCUMSTANCE CLASSIFICATION

INSTABILITY	PHYSICAL DEFICIENCY	DRIVER ORIENTED
1. Loss of Control in an Emergency	1. Brake Failure	1. Turning too sharply
2. Jack Knife due to Ice, Snow, etc.	2. Hitch Failure	2. Hitting Low Bridge
3. Fish Tail due to Ice, Snow, etc.	3. Tire Failure	3. Cutting-off a Passed Vehicle
4. Loss of Control due to Crosswing	4. Steering Failure	4. Driving into Another Vehicle
5. Jack Knife during Normal Manoeuver	5. Other Mechanical Failures	5. Hit While Turning
6. Fish Tail during Normal Manoeuver	6. Structural Failure	6. Stopped or Parked
	7. Runaway Trailer	7. Travelling in Reverse
	8. Runaway Truck	
	9. Fire	
	10. Load Shifting	
	11. Loss of Load	

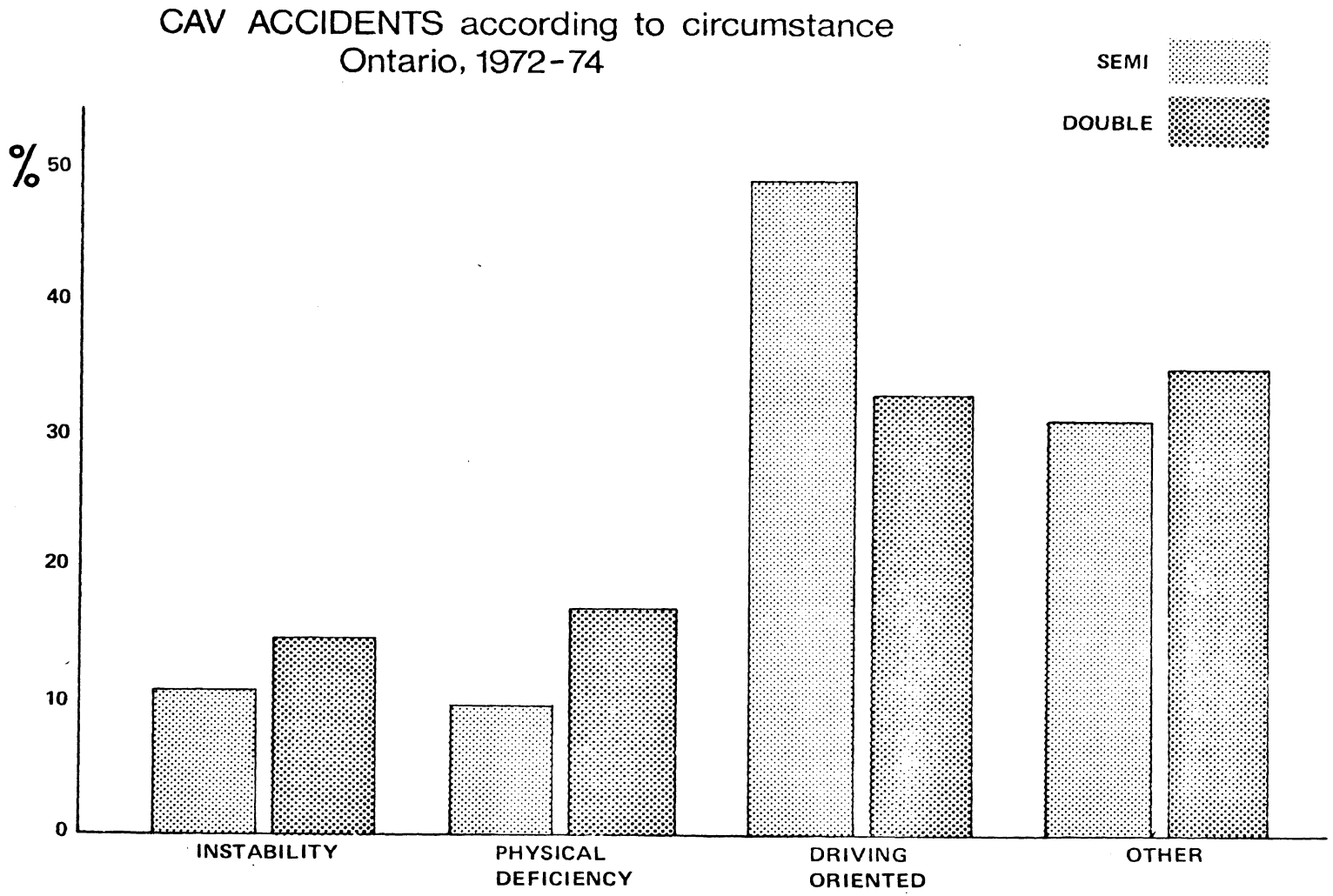
CAV ACCIDENTS according to circumstance
Ontario, 1972-74
SEMI
DOUBLE
%
50
40
30
20
10
0
INSTABILITY
PHYSICAL DEFICIENCY
DRIVING ORIENTED
OTHER

Figure 3

Instability

The distribution of causes of instability is shown in Figure 4. Very little statistical significance is attached to the differences between singles and doubles. Most of these accidents were apparently caused by emergency conditions with very few loss-of-control cases under normal conditions (normal operations on a good surface).

This data generally substantiates the requirements for dynamic and stability research oriented towards emergency maneuvers and poor weather and surface conditions.

Mechanical Deficiencies

The accident distribution for doubles according to mechanical deficiencies is shown in Figure 5. The most significant factor is that almost half of the accidents in this category could be attributed to hitch failures. Although the hitch classification included fifth wheels for the doubles, none of these accidents were identified as a fifth wheel failure. The remainder of this accident category was distributed proportionately with the mechanical failures for the tractor/semi-trailer. Coupling systems for doubles combinations have, therefore, been isolated as the major component for structural and mechanical research activity.

Driver Oriented

While this category constitutes a major portion of the accident causes, there are no immediate plans to include it in this phase of the research. It is, however, anticipated that certain results or observations derived from the vehicle test project will be

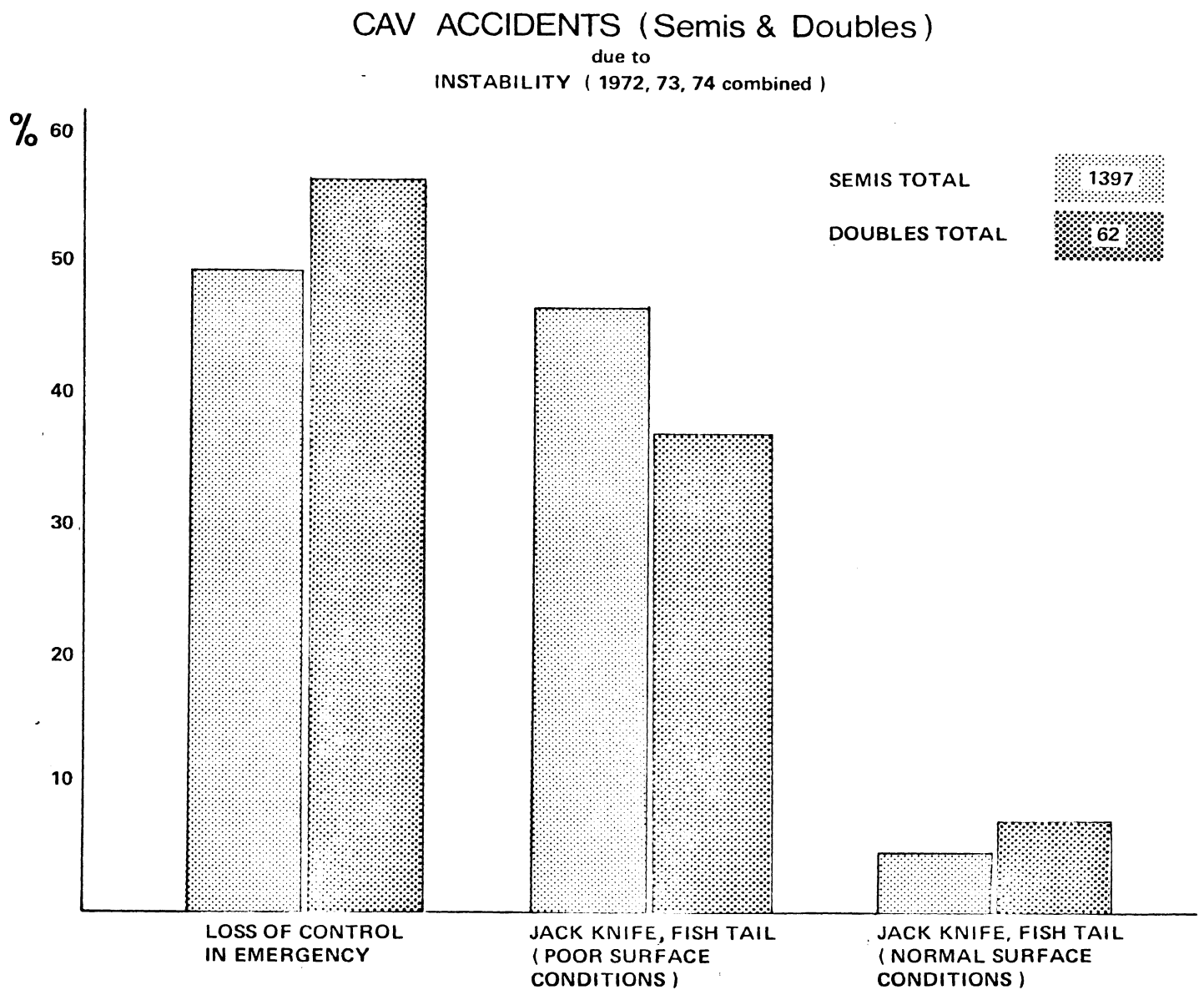
CAV ACCIDENTS (Semis & Doubles)
due to
INSTABILITY (1972, 73, 74 combined)
%
60
50
40
30
20
10
SEMIS TOTAL
1397
DOUBLES TOTAL
62
LOSS OF CONTROL IN EMERGENCY
JACK KNIFE, FISH TAIL (POOR SURFACE CONDITIONS)
JACK KNIFE, FISH TAIL (NORMAL SURFACE CONDITIONS)

Figure 4

CAV ACCIDENTS (doubles only)

due to

PHYSICAL DEFICIENCIES (1972, 73, 74 combined)

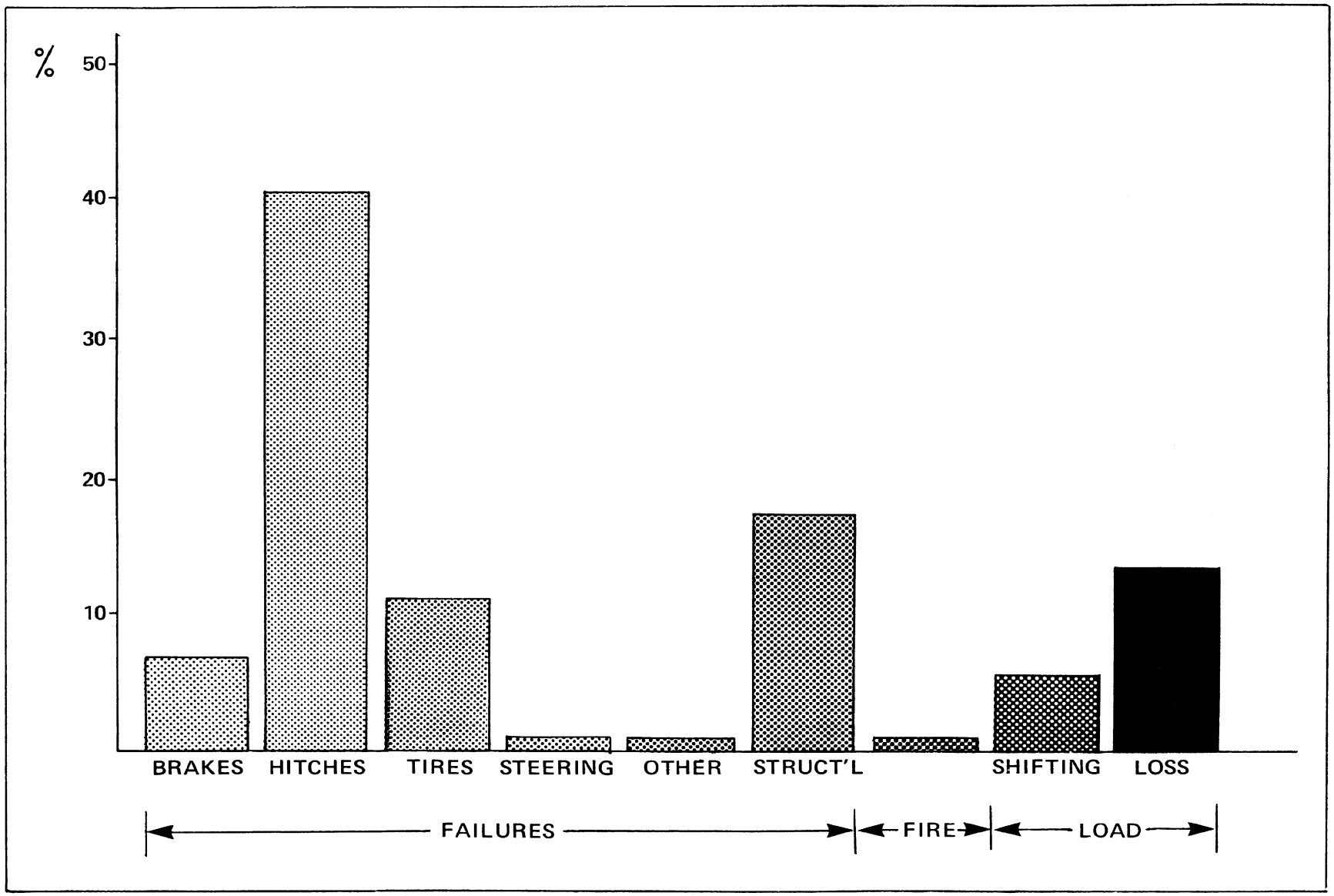

NUMBER OF ACCIDENTS=69

Figure 5

useful towards establishing a driver-oriented research activity possibly leading to recommendations for a driver training program.

Fleet Size Statistics

One additional classification was added to the 1974 statistical data. The accidents were identified according to whether the tractor involved belonged to a fleet of more than, or less than 100 tractors. Although greater resolution, such as identifying between fleets of 1, to 5, 6 to 25, 26 to 100 and more than 100, would have been preferred, it proved to be a much too laborious undertaking.

This one breakdown, however, proved to be quite informative, as seen from Figure 6, in which fleets of more than 100 tractors accounted for approximately 66 percent of the commercial tractors registered in Ontario but only 14 percent of the accidents. Fleets of less than 100 accounted for only 34 percent of the vehicles but were involved in 77 percent of the accidents. Nine percent of the accidents involved vehicles registered out of the province.

The tractor population given here excludes the private fleets not listed as commercial vehicles for hire whereas the accident data includes all tractor accidents in Ontario. These private fleets are estimated to account for no more than 25 percent of the tractor population. The accident data indicates that tractors belonging to fleets of more than 100 tractors are 10 times less likely to have an accident than tractors belonging to fleets of less than 100 tractors.

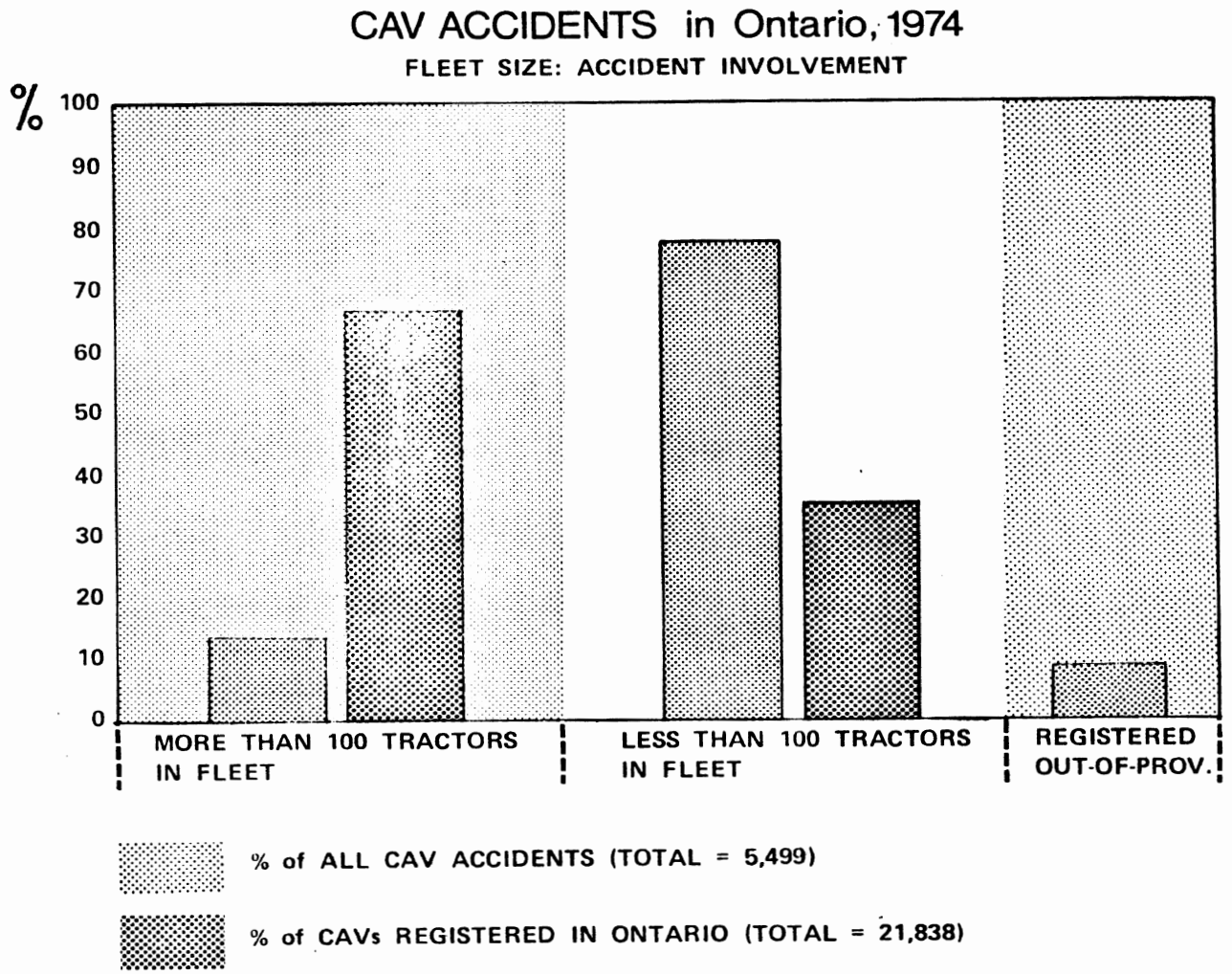
CAV ACCIDENTS in Ontario, 1974
FLEET SIZE: ACCIDENT INVOLVEMENT
%
100
90
80
70
60
50
40
30
20
10
0
MORE THAN 100 TRACTORS IN FLEET
LESS THAN 100 TRACTORS IN FLEET
REGISTERED OUT-OF-PROV.
% of ALL CAV ACCIDENTS (TOTAL = 5,499)
% of CAVs REGISTERED IN ONTARIO (TOTAL = 21,838)

Figure 6

Speculation as to whether the larger fleets have better driver training, or newer and better maintained vehicles cannot be supported from this preliminary analysis.

Vehicle Inspection Program

A pilot inspection program carried out by the Ministry in 1973, indicated that mechanical defects in large commercial vehicles had reached an unacceptable level for safety. It was, therefore, decided to intensify the inspection program with particular emphasis on the doubles combinations. This expanded inspection program is now being carried out with the capability of inspecting up to 60,000 vehicles per year. There are 75 vehicle inspectors (all certified mechanics) working out of 47 truck inspection stations across the province. As of mid-December, 1974 (9 months after the start of the program), almost 35,000 vehicles had been inspected.

The 59-point inspection covers most mechanical components affecting operational safety: air brakes, steering, fifth-wheel assemblies, pintle hooks, towbars, secondary safety attachments, suspensions, tires, and mufflers. Some of the more significant deficiencies are shown in Table 3.

Although the majority of vehicles inspected were selected at random, this data is somewhat biased since vehicles appearing to be defective received particular attention.

The principal aim of the vehicle inspection program is not just to compile statistics, but rather to persuade every fleet operator, truck owner and driver to accept the responsibility of having their vehicles

Table 3

COMMERCIAL VEHICLE INSPECTION PROGRAM, MECHANICAL DEFECTS*

COMPONENT or SYSTEM	% DEFECTIVE
SECONDARY SAFETY ATTACHMENTS	50.8
FIFTH WHEEL	24.9
BRAKES	24.8
SUSPENSION & FRAME	18.6
STEERING	17.2
PINTLE	6.2
TOW BAR	2.8

** TOTAL SAMPLE: 34,618 vehicles*

meet the safety standards of the province. Although the data obtained thus far is insufficient to provide a quantitative evaluation of the effect of the program, there are strong indications that the number of major mechanical defects are on the decline.

Accident Investigation

To further augment the accident data file, a more detailed accident investigation process at the second level is being considered. This is more detailed than the first level accident report, picking up many of the details of the circumstances, causes, and property damage not sufficiently covered by the police report. This would be carried out in cooperation with the federal Ministry of Transport in Ottawa, who have already initiated such a program.

ARTICULATED VEHICLE RESEARCH

The vehicle research has been divided into two separate areas: first, research into the vehicle dynamics and stability and second, the vehicle structural and mechanical integrity. The dynamics category will cover stability, handling, and performance characteristics of CAVs under normal and emergency operating conditions. This will later be expanded to include the effects of such mechanical deficiencies as uneven braking characteristics. Research into structural and mechanical integrity will cover a range of mechanical systems affecting vehicle safety, including hitches, safety attachments, strength and design load retention methods, and the effects of degraded brakes, steering and suspension systems.

Vehicle Dynamics

This research consists of both computer model simulation and full-scale field testing and will be used to determine analytical or test procedures to evaluate the relative operational safety of articulated vehicle configurations. Vehicle configuration variables of interest include trailer length, hitch length, load distribution, number of axles, and axle location.

Computer Simulation

The computer simulation is primarily intended to be an analytical tool with which a wide range of vehicle configurations and parameters can be modified and analysed—once it has been satisfactorily validated. A number of simulation models are available, with particular advantages for their specific applications. Their usefulness to the development of safety regulations will be fully evaluated. At present, we are adapting the HSRI Phase II computer simulation to meet these requirements by including a second trailer and super-elevated curves in the model. The second trailer has been modelled and is presently being integrated into the program, increasing the number of degrees of freedom from 32 to 60. The superelevated curves are being analysed to cover the range of turns in Ontario and will be included by either tabulated data or analytic functions.

As an analytical tool, the simulation will be used to:

a) Examine parameter sensitivity,

b) Select significant test conditions,

c) Extrapolate test data beyond the safety limits, and

d) Investigate stability and handling characteristics over a range of vehicle configurations.

Vehicle Dynamics Testing

The main objective of the vehicle testing is to examine the stability of the various combinations presently in use in Ontario and to obtain a better understanding of the factors affecting their stability and control. Additional testing is planned to include the effects of safety devices and mechanisms, such as the self-steering axles, not included in the simulation. The long-range test program will be used as the basis for the development of vehicle acceptability criteria, methods for vehicle performance testing, and licensing control.

The first phase of testing will be introductory in nature to gain the operational experience of running large vehicle field tests. During this phase we expect to:

1. Check out the test instrumentation and test operations procedures,

2. Validate the computer simulation, and

3. Derive stability data for some baseline reference configurations.

These tests will attempt to cover the basic maneuvers and some of the test conditions indicated in Table 4. The test runs will be selected on the basis of stability limits derived from pre-test simulations. The follow-on tests will be based on the success and extent of the test conditions covered during this first phase, and will include such variables as fifth-wheel location, towbar length, and hitch position.

Test Vehicles

We have a White Freightliner tractor on order and are preparing to purchase two trailers and a train dolly. One trailer will be extendable and the towbar will either be extendable or interchangeable. The bogie of the extendable vehicle will be moveable and it will have one axle air-lifted.

The range of vehicle configurations available with this combination is shown in Figure 7. The test vehicle can carry the maximum weight allowance in Ontario for a single steering axle configuration.

Test Instrumentation

The tractor and trailers will be fully instrumented to measure the vehicle parameters and dynamic variables needed to define the vehicle operational characteristics and dynamics during the test.

A preliminary list of 31 parameters required for the analysis and simulation is given in Table 5. Sensors or transducers for measurement of these parameters have not been selected at this time.

Table 4

VEHICLE TESTS, PHASE I

	MANOEUVER			
TEST VARIABLES	STRAIGHT LINE BRAKING	LANE CHANGE	EVASIVE	CORNERING
VEHICLES	• SEMIs & DOUBLES			
VEHICLE CONFIG.	• NOMINAL* & TOW BAR LENGTH			
TEST CONDITIONS:				
1. Load	• EMPTY to FULL			
2. Pavement	• DRY & WET ASPHALT			
3. Speed	• 50 to 100 km/hr			
4. Lateral Acceleration	• 0 to 0.5g			
5. Braking	• ZERO to FULL			

**NOMINAL CONFIGURATION FIXED -Fifth Wheel Position*
-Tow Bar Length
-Hitch Position
-Axle Location
-Trailer Lengths

TEST VEHICLE CONFIGURATIONS

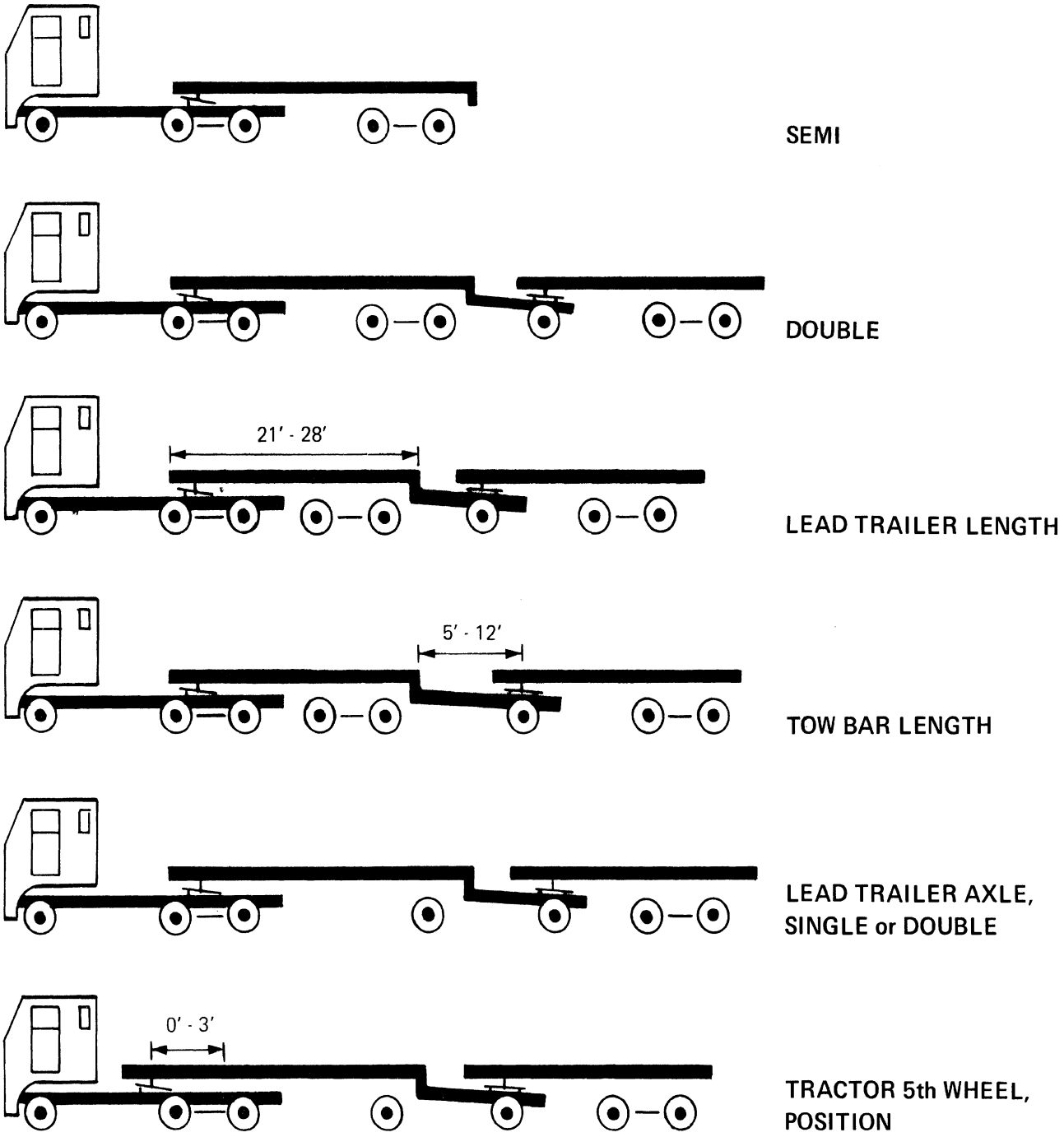

ADDITIONAL CONFIGURATION VARIABLES

1. Lead Trailer Bogie Configuration.
2. Pintle Hook Vertical Position.
3. Converter Dolly to replace Train Dolly.
4. Self-Steering Axles to replace Conventional Axles.

Figure 7

Table 5

Articulated Vehicle Parameters

TRACTOR	SEMI	PUP
Roll Angle	Roll Rate	Roll Rate
Yaw Angle	Yaw Rate	Yaw Rate
Roll Rate	Longitudinal Acceleration	Longitudinal Acceleration
Yaw Rate	Lateral Acceleration	Lateral Acceleration
Longitudinal Acceleration	Brake Pressure (2)	Brake Pressures (2)
Lateral Acceleration	Wheel Speeds (4)	Wheel Speeds (4)
Velocity	Articulation Angle	Hitch Angle
Steering Wheel Position		Articulation Angle
L. F. Wheel Position		
R. F. Wheel Position		
Brake Pedal		
Brake Pressure (each axle -3)		
Wheel Speeds (6)		

The main consideration so far, based on complexity, cost and lead time needed for delivery, has been to define the data acquisition system meeting the minimum system requirements listed in Table 6. A number of data acquisition systems were evaluated and the final selection of the system configuration is shown in Figures 8 and 9.

Based on the data acquisition requirements, cost, and delivery, this system can be of the FM multiplexed, pulse amplitude, or pulse duration modulation types. The system can be made fully self-contained and mounted in the tractor or it can be separated, with the tape recorder, oscillograph and demultiplexer maintained remotely in a mobile instrumentation van. An RF telemetry link is then required. Up to 12 of the most significant channels can be monitored and recorded directly on the oscillograph with the remaining channels available for playback after the test has been completed. Voice control will be maintained throughout the test.

REGULATIONS RESEARCH

The overall objective of this research program is to develop within the jurisdiction of the provincial government, regulations controlling the operational safety of the commercial articulated vehicles. These regulations, as provided for by the Highway Traffic Act of Ontario, can cover all operational aspects of the CAV ranging from the mechanical condition and state of maintenance through to the vehicle configuration and load distribution as it affects pavement and bridge loading factors.

Table 6

DATA ACQUISITION SYSTEM REQUIREMENTS

- RECORDING CAPACITY, 31 CHANNELS
- BANDWIDTH, DC to 50Hz
- ACCURACY, ± 1%
- WEIGHT (In Tractor) ≤ 200 lb.
- POWER (In Tractor) ≤ 500 watts
- ON-BOARD TAPE RECORDING or TELEMETRY
- ON-BOARD *QUICK LOOK* CAPABILITY
- ENVIRONMENTAL CONDITIONS:
  a. Temperature, -10°C to 50°C
  b. Shock & Vibration

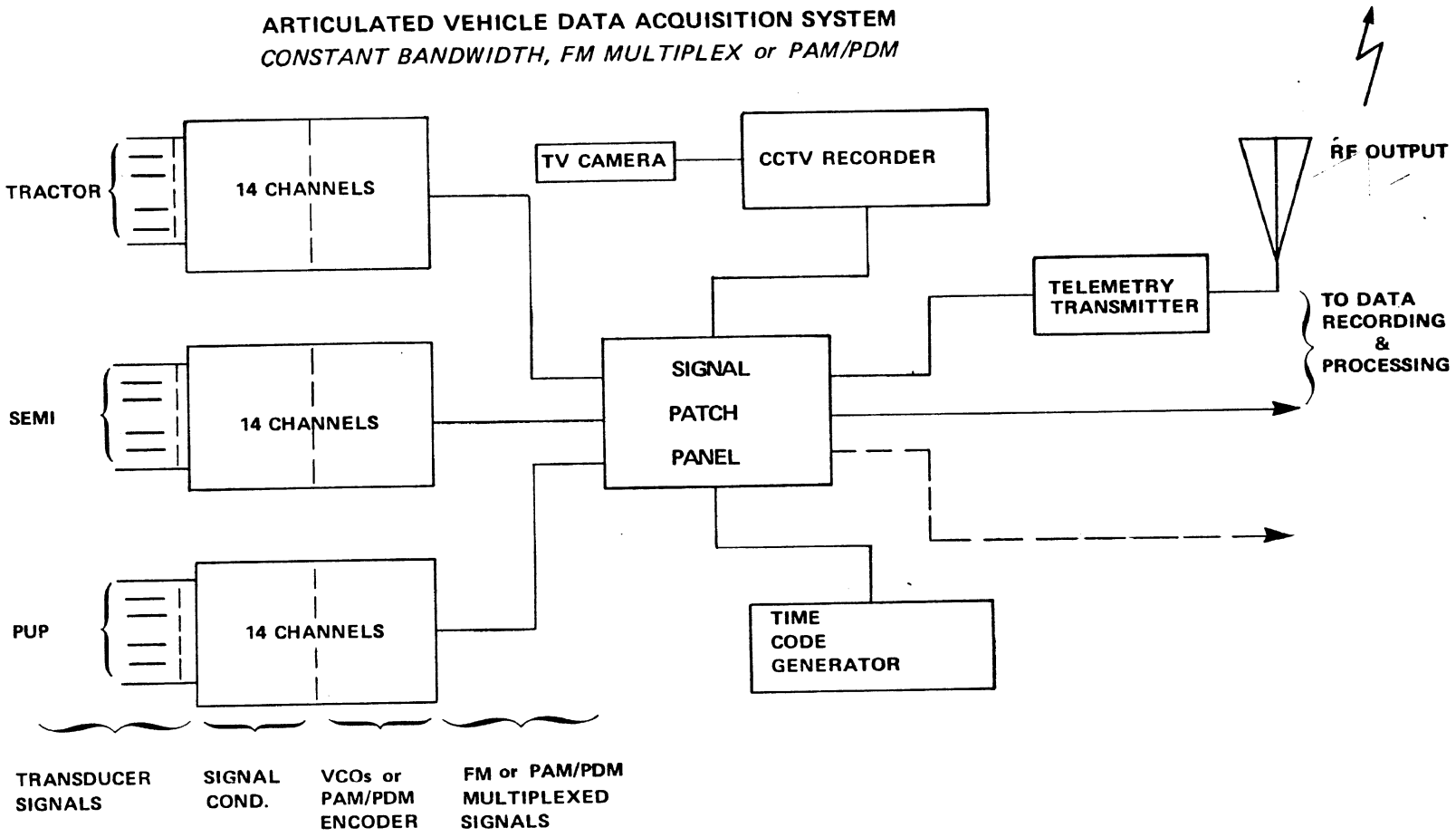
ARTICULATED VEHICLE DATA ACQUISITION SYSTEM
CONSTANT BANDWIDTH, FM MULTIPLEX or PAM/PDM
TRACTOR
14 CHANNELS
TV CAMERA
CCTV RECORDER
RF OUTPUT
TELEMETRY TRANSMITTER
TO DATA RECORDING & PROCESSING
SEMI
14 CHANNELS
SIGNAL PATCH PANEL
PUP
14 CHANNELS
TIME CODE GENERATOR
TRANSDUCER SIGNALS
SIGNAL COND.
VCOs or PAM/PDM ENCODER
FM or PAM/PDM MULTIPLEXED SIGNALS

Figure 8

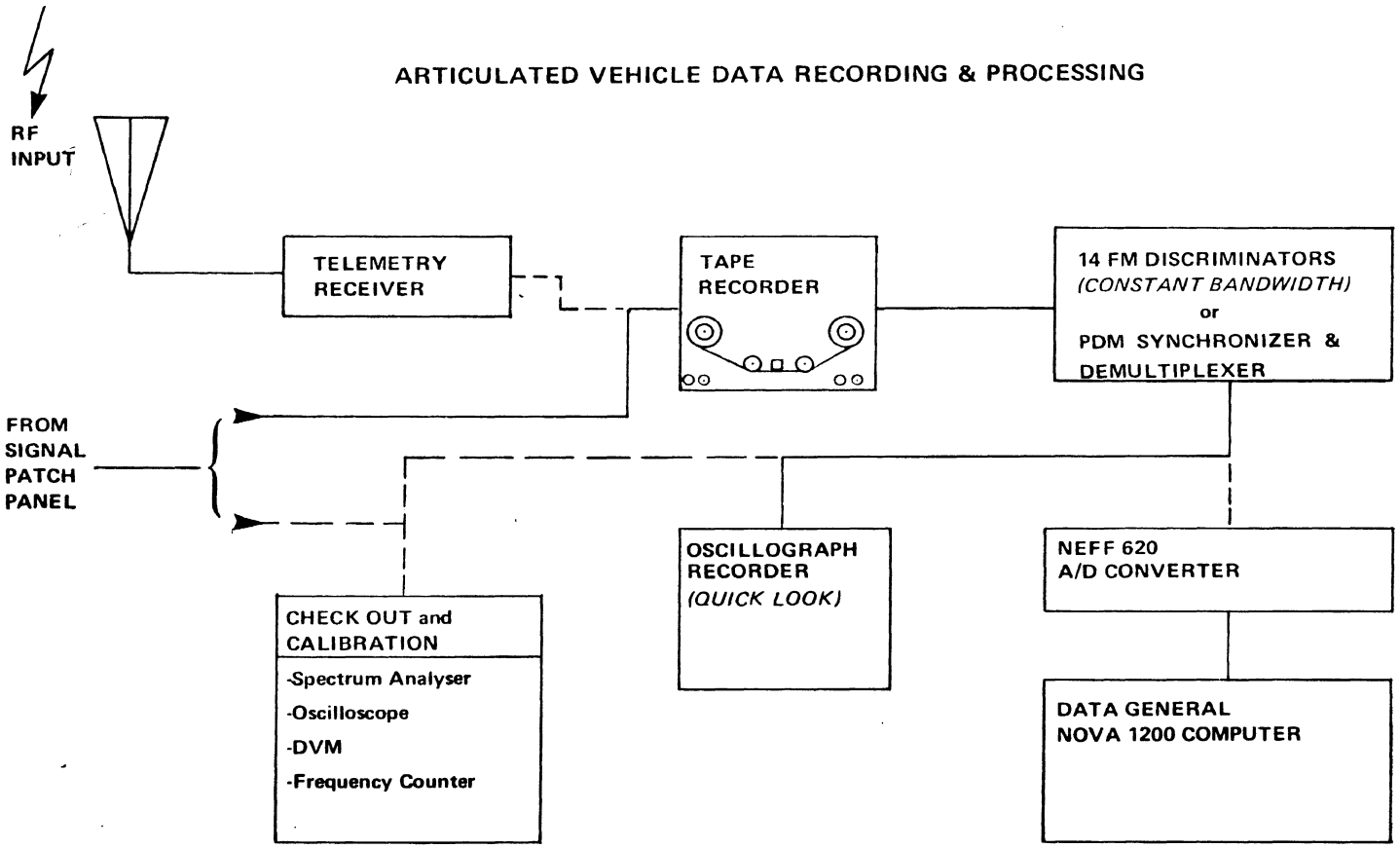
ARTICULATED VEHICLE DATA RECORDING & PROCESSING
RF INPUT
TELEMETRY RECEIVER
TAPE RECORDER
14 FM DISCRIMINATORS
(CONSTANT BANDWIDTH)
or
PDM SYNCHRONIZER & DEMULTIPLEXER
FROM SIGNAL PATCH PANEL
OSCILLOGRAPH RECORDER
(QUICK LOOK)
NEFF 620
A/D CONVERTER
CHECK OUT and CALIBRATION
-Spectrum Analyser
-Oscilloscope
-DVM
-Frequency Counter
DATA GENERAL
NOVA 1200 COMPUTER

Figure 9

Many of these conditions are inadequately covered to meet the safety requirements of the large articulated vehicles. Revisions or additions to the Highway Traffic Act of Ontario are being examined to bring these requirements up-to-date. Load retention methods and secondary safety attachments are being given major consideration in view of the impending FMVSS 121 braking specification.

Operational characteristics as defined by dynamic stability, maneuverability or handleability have generally not been controlled by regulation. These characteristics determine the extent to which safe operation can be expected within the boundaries of normal operating conditions—variable weather and road conditions, variable loads and distributions and a variety of normal and emergency maneuvers.

Within this phase of the research we intend to examine how these operational/performance factors can be controlled through regulations. The simulation model, when validated, will be used exclusively to determine the sensitivity of the CAVs' operational characteristics to variations in configuration—load distribution, axle location and loading, fifth wheel and hitch locations, and geometry. It is expected that performance will prove to be a more realistic criteria on which to develop safety standards.

CONCLUDING REMARKS

Articulated vehicle research at the Ministry is being pursued along two main lines:

a) mechanical and structural integrity of load attachment and articulation components,

b) vehicle dynamics and maneuverability as dependent on vehicle configuration.

Both of these will lead to the addition or revision of regulations upgrading the operational safety of CAVs.

The main emphasis of the research, however, is on the vehicle dynamics which should provide a more thorough understanding of the articulated vehicle as a complete operating system.

Safety standards based on performance are expected to significantly reduce the frequency and severity of accidents due to instability, loss of control and in some instances driver error.

The vehicle dynamics will provide for ongoing research—such as driver training requirements—to further improve the safety of the CAV as an operating system.

FEDERAL FOLLY--PUBLIC POLICY WITHOUT RESEARCH

by

William D. Eberle, President
Motor Vehicle Manufacturers Association

before the
Symposium on Commercial Vehicle
Braking and Handling
(AS DELIVERED)

University of Michigan
Ann Arbor, Michigan
May 7, 1975

Federal Folly--Public Policy Without Research

I was going to apologize for keeping you here with this lovely sun outside, but I was assured by the president of the University that this is a normal day, and that I didn't have to do that. I commend you for staying inside to listen to me.

The title I picked today--Federal Folly: Public Policy Without Research--I'm sure has stirred some thought in all of you, but I'm going to abandon that title. I picked up a Detroit paper this morning with a headline reading "Blame Yourself for Federal Rules, Automakers Are Told." I might suggest that that title might just as well have been the title of my speech.

Secretary of Transportation Bill Coleman recently made a very interesting comment in this regard. He said "We're in bad shape if a political official like me has to tell business what to do." I agree.

But I think this points up the problem that I'd like to talk to you about today, because I can think of no subject that will be more important to the public, the private enterprise system, and to the freedom of all of us as individuals, than the interface of a particular sector of industry with government, and the whole of private enterprise with all of government. If we are unable to find the kind of interface that will work, we're going to continue to have the kind of confrontation, the kind of misunderstanding, and the kind of "Federal Folly" of public policy without research that I think is leading this country into some very serious problems which will take a great deal of time to solve.

I could say, facetiously, that from the point of view of "pure" private enterprise, no regulations are any good. I can assure you, however, that I don't come

from that school. Having spent 3 1/2 years on the other side of the fence, I know there is a very important place for government regulation. There is going to be bigger business and there's going to be bigger government. But in saying that to you, I would also have to admit that the kind of government and the kind of business we're going to have will depend on the interface.

I might also comment today, again facetiously, that anything I say about government probably won't be true by the time I get through because somebody will have changed the rules. I didn't check to see what the Ways and Means Committee did before this meeting, but things are moving so fast that I'm certain something happened. We can't underestimate the speed of change in engineering--in technology--and, of equal importance, the speed with which government can move in and make regulations. This means we must learn to function in a world in which regulations are made with the kind of study, analysis, and research that will be sound, not only to solve the problem immediately at hand, but to anticipate the "ripple effects" resulting from a particular course of action.

Let's look at a few examples. And this is somewhat dangerous, because there are two sides to all these examples, although one usually stands out. Let me talk about these with you for just a few minutes, and focus on some of the things, some of the real problems, I think we face. Then I shall attempt to give you some suggestions as to where I think we must go from here if we're to have the kind of country that I think we all want.

In the mid-1950s one of the manufacturers of automobiles put seat belts into a car. They found that the public (a) didn't want it (b) it was noncompetitive.

The seat belts were taken out. It's very easy for people who are critical of the industry to suggest that the industry didn't try; that it was opposed to safety features. Obviously, if safety is a strong public policy, it takes the kind of cooperation and input, first from industry, and then a way to see that such a public policy is carried out.

Here was a chance of input that just didn't work. Then the other side--government--began to mandate certain safety features. Many were reasonably sound, and I think the give and take in that area was reasonably good.

At the time of the Clean Air Act, there were some very interesting preliminary--and I use that word somewhat with fear, being in academic circles--preliminary research findings which indicated air pollution problems nationally and some very serious problems in places like Los Angeles. But there was no serious consideration given at that time to conducting cost-benefit analyses of the proposed regulations. There was also no real consideration given in the mandating of specific standards in the legislation itself as to the overall impact and whether the technology was available to carry it out.

In no way did this mean that there wasn't a need for cleaner air, nor am I suggesting that there wasn't some technology and some evidence of how we might approach the problem. But I think the important thing that happened here was that Congress had many reasons for proceeding on the clean air issue and it went ahead because it was told that that was the important thing and not to worry about the ripple effects.

What has happened, of course, is we've built up in this country--within both industry and government--

a group of people who, from the government side in many cases, simply do not believe the industry anymore. And we've built up an antagonism within the industry that says all government is bad, and therefore we don't want any part of it.

There are two things, I think, that happened here. First, we got some standards too fast, and second, we created an atmosphere that contributes to a bad relationship between industry and government. This interface must be improved if we are to do a better job. Of course, all this came about at a time when energy was not considered such a high priority in public policy, although the Sierra Club and other concerned parties were talking about reducing the amount of energy consumed by this country at that time.

But if you look back at the impact that this has caused on increased use of energy, with 20-20 hindsight, you will see that the fuel economy reduction caused by these standards is something around 15-20%. In other words, federal policy has encouraged greater energy usage at a time when very clearly the production of oil is declining in the United States and energy for other purposes and the use of oil is rapidly increasing. All this contributed to a problem that was to appear in a very few years.

This was not a problem that any of us could say we didn't see coming, because it was clearly indicated that there was going to be an energy shortage. It just happened to come about in a different way than any of us anticipated.

We set our sights on one area without looking at the total impact. Proper research and analysis could well have allowed us to understand, or if we had not understood, at least we could have been alert to certain problems and made them part of the analysis to be done

as we moved down the road. Today we have an opportunity to reexamine the problems of emissions, and, with a 5-year standstill still making good progress toward clean air. And yet, we still face such problems as sulfate emissions from catalytic converters, for which at this time, to the best of my knowledge, and the best, I think, of the EPA's knowledge, there's no scientific basis to make a conclusion.

That does not mean that there isn't a worry or more research shouldn't be done. That't the very thing that should be done, without moving on new regulations.

There's the whole question of noise for example. It's interesting to me that last winter--Russ Train and I talked about this the other day--EPA proposed regulations on truck noise. At that same time, in January, EPA put out a proposal to evaluate the impact of community noise problems.

Does it make sense to start down the road of regulations again before we have completed the analysis and research that will give the backup for this? The reason I say this is that there is a real need here to get at the root causes of noise problems. And there is a need, probably, to have the kind of regulation that will move an industry toward a goal, because that's the way it should have to be done.

But to start down a road before we know precisely, or even generally, the direction in which we want to move, seems to me to create the kind of atmosphere that will not only make it worse for regulations further down the road, but will create problems, whether they be economic or noneconomic, in some ripple effects that we have not yet identified.

I also noted that a member of the Transportation Department recently said that heavy truck fuel economy

can definitely be improved by 12-18%. I would challenge anyone in this room to tell me where there is evidence to indicate that--knowing, as we do, that even emission testing on truck engines must be done in a way that recognizes the individual characteristics of most trucks. It's very difficult to identify a broad range of characteristics when you're talking about heavy trucks.

Despite the fact that, very often, trucks are one of a kind, we now are in the position where many Congressmen have picked this up and say we are now going to move on heavy trucks, because a transportation official says that it's clear this can be done.

Even research today--and I'm happy to say that I don't have any examples from this good institution--but research from various institutions has, itself, raised problems. But the kind of research that concludes that such-and-such is a problem when it may or may not be a final recommendation, but simply preliminary research findings, helps create the publicity which moves public policy forward and does not create proper academic discussion.

There was a marvelous article in the New York Times recently about well-known professor vs. unwell-known professors, and how, if you pick the right subject, and write a controversial article, you get to be a better-known professor than if you don't. The point here is that we're living in a world where the mass media helps determine public policy. What I'm suggesting here is that this is a world in which we have to find an interface; that there is a heavy responsibility on individuals--whether they be in business, in government, or the academic world--and recognizing, at the same time,the academic right of freedom to say what you want. When you say this, however, you must also recognize that you are participating in a very important program that moves this world one way or the

other, and that we have to be a lot closer to being right. The timing has got to be good, and we're playing for very big stakes.

We're playing for big stakes in the sense that the automobile industry is, as an example, of critical economic importance. We're talking today about a more efficient car. Now, more efficient cars mean different things to different people. To some Congressmen, this means elimination of gas guzzlers. Other people are talking about heavy cars. Others simply would like to eliminate all the limousines that drive government officials around. It all depends on whose ox is being gored.

The important thing here is that it isn't just a gas guzzling car or a limousine. What we're talking about here is an industry that represents 16% of the GNP of this economy. That doesn't mean that you shouldn't see it moving in the right direction, no matter where you are--government, academe, or industry. What is important is that you understand that there is much more to any given problem than just the specific area any one of us is charged with. Public policy must look not only at that area, but at the broad range of issues.

The proposed Ways and Means Committee bill that came out early this week and would put a heavy tax on so-called inefficient cars is a case in point.

This bill calls for a very high stakes game indeed. One of the automakers has estimated that if you miss the fuel-economy standard by one-tenth of one mile per gallon in one year, it could cost something in the neighborhood of 3-4 million dollars in penalties.

The reason you're playing for big stakes here is that if you assume that this is the penalty, then business must manage its affairs against this antici-

pation. If a manufacturer sees it's not going to make that average, it's very simple: They stop the production of the cars that will not meet the requirements. Or if you have a strike at your small car plant, you simply shut down the other one because you can't afford to do otherwise. What happens is that instead of having unemployment of around 110,000--as GM does today--there's another 100,000 people and $3 billion in investment idled.

How long does it take to turn that around? Can you reinvest in building a new plant, change this in two years with that much money and that many jobs at stake?

These are the kinds of questions that, when you start to regulate, I say we have to take a hard look at. It is federal folly to fool around with public policy unless you not only examine the particular problem that you're responsible for, but the ripple effect also, and be sure that we're moving down the right road at the right time.

It's easy for me to say that no regulation is better, and I've often jested, even in government, that I'm always happier the sooner Congress can go home because the less trouble the government and the country are in. But I don't mean it that way, and I don't want to leave that impression. What I do want to suggest to you is that there are some things that can be done, and I think the first thing that can be done is to see when we are making the right kind of statements, and doing the proper kind of analysis and in making recommendations we recognize not only the particular objective, but that we make responsible statements. That responsibility lies with each one of us as individuals.

It's nice to play the game of advocate. You have to be the advocate when you want to accomplish something, but you must be a responsible one. It would also be easy for me to suggest putting all of the regulations concerning motor vehicles into one government department. I'd be the last one to suggest that because I think that what we need here is responsible departments with their own expertise. But they've got to work together. I think that the suggestion of our former President of having various Cabinet people functionally responsible to coordinate general areas has a great deal of merit.

I very much liked the job of being functionally responsible for pulling together the Cabinet officers on international economic policy. I might just give you an interesting example. I was thrown the problem of what to do about Pan Am's flying rights and its bankruptcy potential last fall. Each department had a supremely simple solution. One department said, "we're for free enterprise, let them go broke." So I decided that what we really ought to do is call in a few people from the Federal Reserve and Treasury. They said, "My God, do you realize that we've got $1,400,000,000 of debt out to the banks?" What's the ripple effect there?

Then, we have 35,000 people employed, and we're getting an unacceptable unemployment rate. Then you ask, "If we let this go, what effect will it have on the Defense Department?" It was fascinating. By the time we got through, we came up with a solution which was again a private enterprise solution: a government policy that would force Pan Am, working with them, to tighten up their route structure,giving them fast withdrawal action, and taking a much tougher stance in

the regulatory landing rights of other airlines around the world. We, in turn, toughened up our negotiations on landing rights and numbers of flights across the Pacific and Atlantic. And then we said, "Given that commitment, what are the private bankers going to do for you?" They worked out the problem.

Which then leads me around to Secretary Coleman again. Having criticized him to start with, let me commend him, because he concludes his article by saying: --and here he was not talking about automobiles--"it disturbs me that the railroad leadership knows all this (the need for industry-government interface), but still doesn't come forward with an initial plan." I think here is a case where I'd like to make the plea for all of us--that it is up to all of us to share in the initial plan.

Industry must come forward, along with government and academe. It's not comfortable to come forward, because when you come forward someone's going to criticize you because you're now in the public policy arena. One thing you learn about public policy is that no matter what you propose, at least 40 percent of the people are going to be against you when you start. Because you're going to be in one party, and there happens to be at least one other party that doesn't believe in whatever you advanced. You must learn to deal with this criticism, but that should be no excuse for not sharing ideas, or trying to get together and understand problems before regulations are proposed.

I think here is where we have a major defect in our governmental system, which forces people to feel that they have dishonored themselves if they consult with industry before they put out a regulation. I think we have to have a great deal more discussion well ahead of time, because if we can have the right kind of impetus--

both ways, government to industry; industry to government--to find out where the problems are, then I think we'll have a much better chance of coming up with the kind of interface we want.

I guess I'd have to conclude that the United States can no longer afford, and we as individual members of this great country can no longer afford, the kind of approach and the kind of government that we have today--and the kind of attitudes that we have in industry--because we must find a way to build up an interface that will allow the exchange and the movement toward the public policy decisions that must be made, whether they be on clean air, or safety, or whatever the objective is, so that we know what the ripple effects are. We can take the time to move forward, and if we can have this kind of exchange, I think we will no longer have Federal folly. And I hope that's the road we're on. I think this is the kind of conference that will help achieve that.

Thank you for spending your time with me.

SYMPOSIUM ON COMMERCIAL VEHICLE BRAKING AND HANDLING

Formal Remarks

Panel Discussion

May 7, 1975

A. G. Beier
Chief Engineer
Brake Components Section
International Harvester

I appreciate the opportunity to be a member of this panel and participate in this worthwhile symposium. I'm firmly convinced the trucking industry and DOT needs to promote and support similar programs if we are to minimize our effort in upgrading trucks and trailers to realistic performance levels.

It's unfortunate that due to such things as consent decrees and their implication of collusion, criticism from consumer groups and industry workload generally, component suppliers, we truck and trailer manufacturers and DOT have attempted to resolve our problems separately. The time, money and manpower expenditures involved in individualistic solutions to problems of the air brake standards' magnitude is something our industry cannot afford. These resources are further diluted and inefficiently expended by the issuance of unrealistic performance requirements and time frames which ultimately results in a continually changing standard. The DOT must become familiar with our industry and the many vehicle manufacturers involved. The vast majority of these companies are small, with limited dollars and manpower to undertake development programs such as FMVSS 121. It must realize the great variety of options required in our business to provide customers with the specialized vehicles and components necessary to efficiently do their work. The regulations issued must fulfill a safety need and cost benefit justified by factual statistics.

We, on the other hand, must realize that government control of the truck industry is here to stay. We must react in a positive way to newly proposed rules, organize programs, set up and meet schedules to get the job done. Our responses to petitions must be specific and not general in nature,

providing data and other meaningful information which, hopefully, could be included in future upgradings. It takes time - a lot of time - to submit this type of response, but the consequence is one we all cannot tolerate. In my opinion, one company and man have really done an outstanding job - Wagner Electric and my fellow panelist, Jack Kourik.

As additional regulations are conceived or existing ones upgraded, I recommend forums or hearings be held with knowledgeable industry personnel before they're issued. Where necessary, I suggest government-sponsored test programs to analyze the practicality, necessity, effort, and potential conflicting overlap with other regulations. I question the validity of some government-sponsored test programs conducted by facilities with little or no knowledge of the vehicles and systems being evaluated. The results can be misleading. It is my personal opinion that our industry would support with manpower and equipment such cooperative, DOT-controlled programs. The cost of such investigations could be minimized, and the validity of results prove more realistic and readily available to all interested manufacturers. The DOT has previously indicated a willingness to become cooperatively involved in such mutually beneficial work. Do they really mean it?

If performance levels and time frames are not made more realistic, in the future, it will be extremely difficult to obtain the cooperation and support from our brake vendors regarding any upgrading of components because of the monetary losses experienced on FMVSS 121 and 105a to date.

In answer to the question, "What are the effects of government standards on commercial vehicle braking and handling?" I have the following comments:

FMVSS 121 has upgraded the performance of air brake systems on trucks and tractors 50%, and in some cases even more. What similar steps have been taken to insure that the loads these vehicles haul are adequately secured to absorb the resulting increased forces? I foresee future problems if improvements are not made in this area. As a cattle hauler told me recently, "Now that you've made these trucks stop much quicker, what have you done to keep the cow manure out of my neck?"

Everyone has been so busy qualifying vehicles to the air brake standard, and I don't think we've had sufficient time to take into consideration consumer-oriented requirements such as:

A. Tractor-trailer compatibility

B. Adequate lining life

C. Brake noise

D. Water recovery

E. Fade resistance

F. Drum capability, etc.

These aren't DOT requirements, but they're extremely important to our customers. In a number of cases today, we have no choice but to ignore these areas due to the difficulty in just meeting the regulation's performance requirements. This fact will be of little consolation to our customers or ourselves if problems do arise.

Some of the effects of FMVSS 121 have been beneficial. For example:

A. Both the vehicle manufacturers and their suppliers are beginning to realize improved Quality Control programs must be set up to insure uniform compliant components and

vehicles. The results of this effort will be an improved product for our customers.

B. Improved traceability has been achieved in the upgraded components used in DOT trucks. This will be extremely beneficial from a time and cost standpoint if a recall program is ever necessary.

C. To date, there has been only limited control of Body Builders and other installers of equipment before the customer receives his trucks. In many cases, the modifications made affect our ability to meet the air brake regulation. Now these installations must be tested and in addition to determining compliance, we will have the opportunity to review and approve such installations.

D. The vehicle manufacturers will also be expending additional effort in analyzing customer requests for optional equipment. Since many of these requests affect a vehicle's braking performance, they must be reviewed and in some cases tested to assure compliance. Customers today appear more receptive to acceptance of standard components due to the cost and delay which can result from compliance testing.

Thank you again for inviting me. I hope the results of this symposium are sufficiently fruitful to justify consideration of additional ventures.

Eugene Chosy
Director
Reliability and Quality Assurance
Fruehauf Corporation

These remarks will be confined to the general behavior of articulated vehicles more commonly known as Tractor-Trailer combinations. Whenever the safety aspect of these vehicles is discussed, the problem of jackknifing comes up. This is most often a result of the loss of lateral stability of the truck tractor rear wheels allowing the tractor and trailer to assume an angular position relative to one another. However, this condition can also occur if the trailer is initially at an angle with the tractor, and trailer wheels lose lateral stability; i.e., going around a sharp curve too fast on a slippery surface. The loss of lateral stability most generally occurs during braking with a lockup of wheels.

When an accident involving a tractor-trailer occurs, a jackknife is many times involved. It is pretty hard to determine after the accident, whether the jackknife is the result of or the cause of the accident. In my judgement it is usually the result of the accident.

Anything that can be done to improve lateral stability at the tire-to-road surface will reduce the possibility of jackknifing. In my opinion, the most common problem is over-braking for road and load conditions causing wheels to lock. Locked wheels will allow the vehicle to go in whatever direction external forces dictate; i.e., road slope-side wind, and imbalance in braking. It is difficult for a driver to control wheel lockup during braking; particularly, if he has unbalanced loading, as all he can feel is deceleration. Speed and direction he can control, although error in these areas can also contribute to vehicle instability. It is my judgement that the best cure for vehicle instability is to overcome the root causes of this instability. Anti-wheel-lockup for example to eliminate instability due to locked

wheels. Devices to compensate for this, such as so called anti-jackknife devices, in many cases can create worse problems than they cure. My limited experience indicates this to be true at least on some of these devices.

From a performance standpoint, we were happy to see an anti-wheel-lockup requirement in MVSS 121 as this would eliminate one of the root causes of vehicle instability, locked wheels due to braking. The driver no longer has to worry about brake balance, proper loading, and road surface conditions. He can now concentrate on the best deceleration rate and the control of the combination. It also relieves the designer and operator of these hard to control items. Our main objection to MVSS 121 was the relatively radical change in brake system and brake performance. The addition of anti-wheel-lockup to existing brakes and braking systems would have been a boon to safety on the highways and the debugging of a relatively new and sophisticated system could have been orderly accomplished under normal service operations. By the introduction of new braking systems including more powerful brakes, we have now introduced unknown factors which could adversely affect highway safety during the debugging of the anti-wheel-lockup systems.

Putting the industries "feet to the fire" may sound like an admirable way to achieve a radical goal, but from a practical standpoint does not really accomplish this objective in the best interest of the ultimate consumer. Forced development is not only extremely expensive, but arbitrary deadlines many times force decisions that are not the most cost effective. In addition, the initial maintenance costs many times are excessive. All these factors increase costs to the ultimate consumer. Government regulators just do not recognize the so called debugging requirements of new developments. It is hoped that this experience will be of benefit in future regulations.

To close, I believe we have to discard the adversary attitude that has been present in the past between Government regulators and the industry. We have much to offer in the cause of highway safety through genuine cooperative effort. We must also recognize that we all have a responsibility to the ultimate consumer, to give him the most cost effective package we possible can, as he ultimately ends up paying for all this.

John W. Kourik
Chief Engineer
Automotive Products
Wagner Electric Corporation

These opening remarks are intended to concentrate our attention on the NHTSA Safety Standards in this Panel discussion. The panel membership is oriented to that aspect of regulations. There is no new activity from the BMCS, the states are silent and the VESC has recently concentrated only on school bus system standards.

The revolutionary modifications in front axle and suspension design necessitated by FMVSS 121 suggests that there was little awareness of the consequences of requiring short stopping distances for trucks and tractors. These new distances made it essential to apply high levels of front axle brake torque to commercial vehicles in development programs initiated immediately after the first notices of the standard were issued. The status of FMVSS 105-75 was indeterminate at the time this manuscript was prepared. However, in its Notice 11 form it was even more intolerant of handling necessities; particularly on low friction road surfaces. We hope that the 105 interim non-passenger car standards will better address the issues of both braking and handling.

Commercial vehicle standards [FMVSS 121] were issued with proclamations of forthcoming safety benefits. However, the very act of mandating distances that necessitated front axle brakes on tractors that previously had none was foreboding. The companion action that necessitated 100% to 150% additional torque on the front axle of some trucks was ominous.

In the past, methods used in the sizing and selection of brakes for commercial vehicles were inherently entwined with all of the considerations required to achieve a safe, durable, economic stopping system within the framework of available, proven technology. Items such as steering control, vehicle stability, cargo retention, load variation, vehicle interchangeability, and reliability, were either knowingly or intuitively factored into the decisions relating to brakes and brake systems selection and design.[1]

The seriousness of brake system modifications can be simplified by a chart showing the effect on torque balance and magnitude for a typical 4x2 truck.

		TORQUE UNITS		CHANGE WITH 121 BRAKES
		Pre-121	121	
Axle	Front	30	70	+ 133%
	Rear	70	70	None
	Total	100	140	+ 40%

Note that the front axle retardation required is now 2-1/3 times the pre-121 level of effectiveness. This is a value well in excess of any reasonable "overdesign" or "safety factor" provision in pre-121 springs, suspensions, steering and structural considerations. The rear axle brake torque levels for pre-121 vehicles already had the capability of developing wheel lockup so no additional torque could be utilized on that axle.

[1]R.C. Bueler and E.J. Falk, A Practical Approach to the Selection and Sizing of Brakes to Meet FMVSS 121, SAE Paper No. 730198, Society of Automotive Engineers, January, 1973.

A similar chart for a typical 6x4 tractor reveals different modifications in torque balance that also affect the handling characteristics.

		TORQUE UNITS	
		Pre -121	121
Axle	Front	0	70
	Rear - Fwd.	70	70
	Rear - Rear	70	70
	Total	140	210

At the time FMVSS 121 issued in its basic form, tractors were known to have sufficient rear axle torque capability. The only way to "improve" braking, if in fact, the issue of shorter stopping distances is the proper choice for improvement, is the addition of torque to the front [steering] axle. Both of the previous charts illustrate this.

Vehicle stability, controllability, and stopping capability are mutually dependent and ultimately limited by the sum and the distribution of the tractive forces generated at each tire/road interface. Vehicle stability requires the presence of lateral force at the tire/road contact surface. Controllability requires preservation of both lateral and retarding forces, if simultaneous steering and braking maneuvers are to be realized.

At any given wheel, the total tractive force can be considered as the vector sum of the retarding force component and the lateral force component. Consideration of Fig. 1 reveals that for an unbraked wheel, the retarding component is essentially zero and, neglecting the effect of tread design, the lateral or stability component is a maximum approaching the value of the total tractive force. Conversely, for a braked wheel, as the retarding force component is maximized and approaches the value of total tractive force, the lateral component tends to disappear. This is the situation with a locked wheel.

Overall lateral stability is affected such that as total retarding force increases to the maximum attainable by any particular tire/road interface, the lateral force (stability) component is minimized, and, for practical purposes, approaches zero. The relationship, therefore, between required deceleration and attainable deceleration (as limited by skid number (SN)) is crucial for lock-free stopping, steering capability, and general stability.[2]

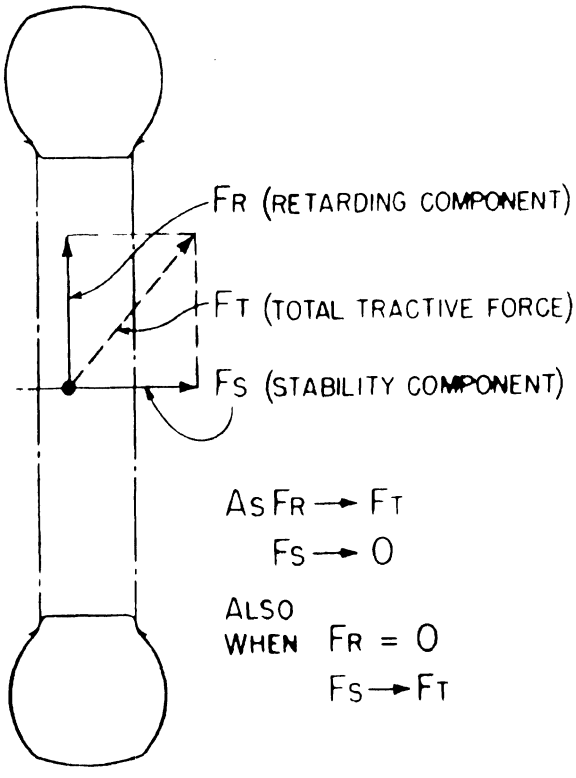

Fig. 1 - Retarding component for unbraked wheel

[2] Ibid

The NHTSA did not pursue the March, 1971 HSRI contract [DOT-HS-800-493] recommendations for a discrete 3-step sequence of improvements in bus, truck, tractor-trailer braking performance. The issuance of the proposed FMVSS 121 regulation in early 1972 forced the heavy vehicle manufacturer and equipment supplies into extensive design and development programs. The standard caused the industry to develop, invent and refine a multitude of products to achieve straight-line stops in remarkably short distances on wet and dry, flat and uniform surfaces. This goal apparently had to be achieved before the NHTSA would acknowledge the consequences of the standard on vehicle handling.

The practical evaluation of the various factors that influence handling could not be physically determined with 1972 chassis. The vehicle dynamics associated with brake torque, caster, steering linkage movement, suspension, structure, tire deflection, and driveability had to await new hardware development and procurement. To our knowledge none of the NHTSA responses have addressed the issue of practical handling for the driver's benefit of controlling the vehicle in normal driving activity.

The DOT has not responded to many open petitions asking for relief in stopping distances on Skid Number 75 surfaces. The vehicle manufacturers and the NHTSA have yet to fully address the issue of braking and handling under real-life conditions. The users are outspoken critics of this dilemma. We hope that panel discussions such as this will result in less aggressive performance standards for hydraulic brake systems and encourage further amendment to FMVSS 121 by the NHTSA in response to unanswered petitions.

The vehicle manufacturers and their suppliers have made these contributions available for ultimate resolution of a practical combination of regulations and good vehicle handling:

1. More Brake Torque
2. More Rugged Suspensions
3. Modified Steering
4. Skid Control Systems [Antilock]
5. Responsive Air Systems
6. Massive Amounts of Test Data.

The traditional, or pre-121, values for torque balance on commercial vehicles has proven satisfactory in both single-unit operation and a variety of vehicle combinations. The more sophisticated equipment [skid control, new valves, agressive lining] is now available from production tools. The evolution of 121 systems to provide braking "improvements" and "optimum" handling may progress at a less hectic pace, but it must evolve in an orderly manner.

LIST OF ATTENDEES

Tom Alexander
Eaton Research
26201 Northwestern
Southfield, Mi. 48024

Willard A. Alroth
Paul C. Box & Assoc.
Traffic Eng. Consultants
9933 Lawler
Skokie, Il. 60076

Bruce Anderson
Rockwell International
2445 W. Maple Road
Troy, Mi. 48084

John D. Andrus
General Motors Proving Ground
Tire and Wheel Systems
Milford, Mi. 48042

Richard C. Angelo
Dodge Truck Eng.
6565 E. Eight Mile Road
Warren, Mi. 48092

Gary Arnold
B.F. Goodrich Res. & Dev.
9921 Brecksville Road
Brecksville, Oh. 44141

Paul F. Aurand
Kelsey-Hayes
2260 Nixon Road
Ann Arbor, Mi. 48105

Les Austin
Dept. of State Police
3400 Cooper Street
P.O. Box 630
Jackson, Mi. 49204

James Avouris
Ford Motor Co.
Truck Eng. & Brake Dept.
20000 Rotunda Drive
Dearborn, Mi. 48121

James R. Baber
Delco Moraine Div. GMC
1420 Wisconsin Blvd.
Dayton, Oh. 45401

Kent C. Bates
Caterpillar Tractor Co.
Technical Center
Peoria, Il. 61629

James M. Beatty
Transportation Res. Center
of Ohio
P.O. Box
E. Liberty, Oh. 43319

Marcel Behar
Eaton Research
26201 Northwestern
Southfield, Mi. 48024

Al G. Beier
International Harvester
P.O. Box 1109
Fort Wayne, In. 46801

Jim Bernard
University of Michigan
Highway Safety Research Inst.
202 HSRI
Ann Arbor, Mi. 48104

David J. Bickerstaff
5779 Perrytown Dr.
W. Bloomfield, Mi. 48033

King Bird
Calspan Corp.
P.O. Box 235
Buffalo, N.Y. 14221

J.T. Blewett
Great Dane Trailers, Inc.
P.O. Box 67
Savannah, Ga. 31402

Paul Bohn
Johns Hopkins Univ.
8621 Georgia Avenue
Silver Springs, Md. 20910

William Booth
PACCAR, Inc.
790 Garden Avenue, N.
Renton, Wa. 98055

Jerry Boron
Motor Vehicle Manufacturers Assn.
320 New Center Building
Detroit, Mi. 48202

Donald E. Boyd
Oklahoma State Univ.
School of Mechanical &
Aerospace Eng.
Stillwater, Ok. 74074

Jerry L. Boyd
Chrysler Corp.
19945 W. Old U.S. 12
Chelsea, Mi. 48118

L. Earle Bretz
ABEX Corp.
1650 W. Big Beaver Road
Troy, Mi. 48033

H.G. Brilmyer
Ford Motor Co.
352 Belanger
Grosse Pointe Farms, Mi. 48236

W. Brintle
AC Delco Div., GMC
28318 Bayberry
Farmington Hills, Mi. 48024

J.H. Brown
Rockwell International
2445 W. Maple Road
Troy, Mi. 48084

Leonard Buckman
Ford Motor Co.
18215 Wayne Road
Livonia, Mi. 48152

R. Thomas Bundorf
Eng. Staff - North
GM Tech. Center
Warren, Mi. 48090

H. Burnham
Rockwell International
1000 W. Maple Road
Troy, Mi. 48084

John E. Byers
Bendix Corp.
401 N. Bendix Dr.
South Bend, In. 46620

E. Ryerson Case
Ministry of Transportation
and Communications
1201 Wilson Avenue
Downsview, Ontario, Canada
M3M 1J8

Shang-Li Chiang
Ford Motor Co.
P.O. Box 2053
Environmental and Safety
Research Office
Dearborn, Mi. 48121

Eugene Chosy
Fruehauf Corp.
10900 Harper Avenue
Detroit, Mi. 48232

Prof. S.K. Clark
Applied Mech. & Eng. Science
University of Michigan
201 W. Eng.
Ann Arbor, Mi. 48104

David R. Claydon
Kelsey Hayes
7300 Whitmore Lake Road
Brighton, Mi. 48116

William A. Cobb
General Motors Corp.
General Motors Proving Ground
Milford, Mi. 48042

G.A. Cornell
Bendix Res. Labs
20800 Civic Center Drive
Southfield, Mi. 48075

Byron A. Crampton
Truck Body & Equip. Assoc.
5530 Wisconsin Avenue, Suite 1220
Washington, D.C. 20015

Charles C. Custer
B.F. Goodrich Co.
2339 Averill Drive
Akron, Oh. 44313

Eugene Daniels
Iowa State University
329 East Seventh
Ames, Ia. 50010

W. Deibel
Rockwell International
1000 W. Maple Road
Troy, Mi. 48084

Richard A. Doversberger
WABCO
2300 Adams
Peoria, Il. 61639

Len Dozier
Rockwell Vnternational
2445 W. Maple Road
Troy, Mi. 48084

Gil Drutchas
TRW-Mich. Division
6794 Valley Sp. Drive
Birmingham, Mi.

Lewis Duff
B.F. Goodrich
900 Oak Lea Drive
Troy , Oh. 45373

Howard Dugoff
National Highway Traffic
Safety Admin.
400 Seventh St. S.W.
Washington, D.C. 20590

Robert Ervin
University of Michigan
Highway Safety Research Inst.
Room 203
Ann Arbor, Mi. 48104

Ronald Eshleman
IIT Res. Inst.
10 W. 35th Street
Chicago, Il. 60516

Richard T. Evans
Ford Motor Co.
12812 Crosley Avenue
Detroit, Mi. 48239

Paul Fancher, Jr.
University of Michigan
Highway Safety Research Inst.
Room 208
Ann Arbor, Mi. 48104

Eugene Farber
Ford Motor Co.
P.O. Box 2053
Environmental & Safety Res. Ofc.
Dearborn, Mi. 48121

T.R. Faucett
Mech. & Aerospace Eng.
University of Missouri
Rolla, Mo. 65401

David J. Foster
RMB 256
GM Tech. Center
12 Mile and Mound Roads
Warren, Mich. 48090

Wayne Garnet
Eaton Research
26201 Northwestern
Southfield, Mi. 48024

Tom Gee
Eaton Research
26201 Northwestern
Southfield, Mi. 48024

Gary E. Gibson
B.F. Goodrich Co.
500 S. Main Street
Akron, Oh. 44318

Gordon L. Gibson
Turner Quick Lift Corp.
P.O. Box 750
Canton, Oh. 44701

Andrew Gilberg
Ford Motor Co.
P.O. Box 2053
ESPRO
Dearborn, Mi. 48197

Tom Gillespie
Ford Motor Co.
20000 Rotunda Drive
Building 1
Dearborn, Mi. 48121

David Glemming
Goodyear Tire and Rubber Co.
3630 Portage Pt. Blvd.
Akron, Oh. 44319

D.E. Goss
GMC Truck & Coach Div.
GMC
660 South Blvd. E.
Pontiac, Mi.48053

Ronald N. Granning
Granning Suspensions, Inc.
3040 Wyoming
Dearborn, Mi. 48120

Raymond J. Green
46200 Pickford Avenue
Northville, Mi. 48167

R. Clay Green
Michelin Tire Corp.
24721 Michigan Avenue
Dearborn, Mi. 48124

Robert C. Greening
Michigan Trucking Assoc.
501 S. Capitol Ave., Suite 325
Lansing, Mi. 48933

Frank R. Grimaldi
Michelin Tire Corp.
24721 Michigan Ave.
Dearborn, Mi. 48124

Ann Grimm
University of Michigan
Highway Safety Research Inst.
134 HSRI
Ann Arbor, Mi. 48104

Robert Grimm
A.C. Spark Plug Div.
GMC
11420 Grand Oak Drive
Grand Blanc, Mi. 48439

Rajiv Gupta
University of Michigan
Highway Safety Research Inst.
Physical Factors
Ann Arbor, Mi. 48104

John W. Gurney
Truck Operations
Room 1015
Building 1
Ford Motor Co.
Dearborn, Mi. 48121

Ezzat A. Hammond
International Harvester
10400 W. North Avenue
Melrose Park, Il. 60160

Gerald A. Hartley
Truck Eng. & Brake Dept.
Ford Motor Co.
20000 Rotunda Dr.
Dearborn, Mi. 48121

R.H. Heinrich
U.S. Army Tank Auto Command
Warren, Mi. 48090

Robert Hess
University of Michigan
Highway Safety Research Inst.
Room 158
Ann Arbor, Michigan 48104

George B. Hickner
Bendix ACSG
P.O. Box 4001
South Bend, In. 46634

F. Hubert Ho
The B.F. Goodrich Co.
9921 Brecksville Road
Brecksville, Oh. 44141

Bryan Hood
Girling Ltd.
Oldwich Land East, Fen End
Goventry, Warks, England

Gard Hopkins
Eaton Corp. - Brake Div.
21220 W. Eight Mile Road
Southfield, Mi. 48075

Bruce Howard
1601 N. Averill Avenue
Flint, Mi. 48556

Richard F. Humphrey
GM Environmental Activities Staff
4798 Walnut Lake Road
Birmingham, Mi. 48010

Fulchand J. Jain
A.C. Spark Plug
5169 N. Georgetown
Grand Blanc, Mi. 48439

John Johnides
Motor Vehicle Mfg. Assoc.
Detroit, Michigan 48202

Gary W. Johnson
GMC Truck & Coach
4401 Charing Way
Bloomfield Hills, Mi. 48013

Richard Johnson
Kelsey-Hayes
2500 Green Road
Ann Arbor, Mi. 48105

Robert H. Keenan
Johns Hopkins Univ./APL
8621 Georgia Avenue
Silver Springs, Md. 20910

Christopher M. Kennedy
Chrysler Corp.
6561 Clarkston Road
Clarkston, Mi. 48016

Jay D. Kennedy
Michigan State Police
714 S. Harrison Road
E. Lansing, Mi. 48823

T.M. Kim
University of Michigan
Highway Safety Research Inst.
Physical Factors Group
Ann Arbor, Mi. 48104

Walter K. Klamp
Uniroyal Inc.
6600 E. Jefferson
Detroit, Mi.

Dan Kline
General Motors Corp.
660 S. Boulevard East
Pontiac, Mi. 48053

Milton G. Koenig
Wayne State University
46266 Pickford
Northville, Mi. 48167

John W. Kourik
Wagner Electric Corp.
11444 Lackland Road
St. Louis, Mo. 63141

Phillip L. Krahn
General Motors Corp.
18461 Jamestown Circle
Northville, Mi. 48167

A.I. Krauter
Shaker Res. Corp.
Northway 10 Exec. Park
Ballston Lake, N.Y. 12019

Alfred Kreis
Granning Suspensions, Inc.
3040 Wyoming
Dearborn, Mi. 48120

Dennis T. Kunkel
Calspan Corp.
P.O. Box 235
Buffalo, N.Y. 14221

N. Kurth
Rockwell International
1000 W. Maple Road
Troy, Mi. 48084

Svein I. Larsen
U.S. Dept. of Transportation
Rt. 5
Box 232 Forest Road
Annapolis, Md. 21401

B.E. Latvala
Bendix Heavy Vehicle
System Group
20800 Civic Center Dr.
Southfield, Mi. 48075

William Laule
Kelsey-Hayes
2500 Green
Ann Arbor, Mi. 48105

Noel Leitzman
I.H.C.
4430 Trier Road
Fort Wayne, In. 46805

Philip M. Leucht
General Motors Res. Labs
GM Tech Center, Room 256
12 Mile and Mound Road
Warren, Mi. 48090

Keith Lewis
Ford Motor Co.
20000 Rotunda Dr. Bldg. 1
Dearborn, Mi. 48121

Larry Louderback
Dept. of Education
1116 1/2 S. Washington Avenue
Lansing, Mi. 48902

John Luchini
Dept. of AMES
University of Michigan
201 W. Engineering
Ann Arbor, Mi. 48104

H. Lee McCord
Ford Motor Co.
23132 Heatherwoode
Novi, Mi. 48050

William McCormick
University of Michigan
Highway Safety Research Inst.
101 HSRI
Ann Arbor, Mi. 48104

Jack McIlroy
Conf. & Insts.
University of Michigan
Extension Service
350 S. Thayer
Ann Arbor, Mi. 48104

Joseph H. McNinch
Eaton Corporation
26201 Northwestern Highway
Southfield, Mi. 48076

Charles MacAdam
University of Michigan
Highway Safety Research Inst.
Room 206
Ann Arbor, Mi. 48104

Russell E. MacCleery
Motor Vehicle Manufacturers
Association
1909 K Street, N.W., Suite 300
Washington, D.C. 20006

R.H. Madison
RIVA
12814 Asbury Drive
Tantallon, Md. 20022

R.L. Marlowe
B.F. Goodrich Co.
500 S. Main Street
Akron, Oh. 44318

V. Marples
Dept. of Mechanical & Aero Eng.
Carleton University
Ottawa, Ontario Canada K1S 5B6

Peter Mate
University of Michigan
Highway Safety Research Inst.
Room 233
Ann Arbor, Mi. 48104

George Megginson
Kelsey-Hayes
2500 Green Road
Ann Arbor, Mi. 48105

David C. Merriman
International Harvester
Route 1
St. Joe, In. 46785

Edwin Mikulcik
Dept. of Mech. Eng.
University of Calgary
Calgary, Alberta, Canada
T2N 1N4

James W. Miller
Delco Moraine Div. GMC
1420 Wisconsin Blvd.
Dayton, Oh. 45401

William J. Milliken, Jr.
Calspan Corp.
4455 Genesee Street
Buffalo, N.Y. 14221

Richard Miernyk
International Harvester
960 Thomas Road
Ft. Wayne, In. 46808

Howard Moncarz
University of Michigan
Highway Safety Research Inst.
Room 233
Ann Arbor, Mi. 48104

M. Montie
Rockwell International
1000 W. Maple Road
Troy, Mi. 48084

Ray Murphy
Freightliner Corp.
2525 SW Third Ave.
Portland, Or. 97208

Aung S. Myint
Ford Motor Co.
5312 Provincial Dr.
Bloomfield Hills, Mi. 48013

Jeanette Nafe
University of Michigan
Highway Safety Research Inst.
Room 211
Ann Arbor, Mi. 48104

Sam Narayan
Rockwell International
2445 W. Maple Road
Troy, Mi. 48084

D. Neilson
Rockwell International
1000 W. Maple Road
Troy, Mi. 48084

Richard Neuman
Eaton Research
26201 Northwestern
Southfield, Mi. 48024

Russell Noble
Dodge Truck-Chrysler Corp.
P.O. Box 1283
Detroit, Mi. 48231

Conrad G. Noel
General Motors Corp.
3044 W. Grand Blvd, R. 10-117
Detroit, Mi. 48202

K.L. Oblizajek
Uniroyal
6600 E. Jefferson
Detroit, Mi. 48232

James V. O'Connell
Kelsey-Hayes
7272 Bentley Lake Road
Pinckney, Mi. 48169

Clifford Parton
Grirling Ltd.
Birmingham, England

Dan C. Pasma
White Motor Corp. Res. Center
34500 Grand River Avenue
Farmington, Mi. 48024

Thomas A. Peel
Peel Bros. Inc.
14375 172 nd. Avenue
Grand Haven, Mi. 49417

R.A. Pepoy
IHC
2615 Palisade
Fort Wayne, In. 46806

Duane A. Perrin
National Highway Traffic
Safety Admin.
Room 5307-A, Nassif Bldg.
400 7th Street, S.W.
Washington, D.C. 20590

Thomas Post
University of Michigan
Highway Safety Research Inst.
Room 205
Ann Arbor, Mi. 48105

Stan Powell
Iowa State Univ.
1024 Curtiss
Ames, Ia. 50010

Keith C. Pratt
Ford Motor Co.
Three Dover Court
Ann Arbor, Mi. 48103

W.H. Presley III
Engineering Building,
Veh. Dyn. Dept.
GMC Truck & Coach
660 S. Blvd. East
Pontiac, Mi. 48057

Y.V. Rajput
P.O. Box 340
Troy, Oh. 45373

Richard E. Rasmussen
General Motors Prov. Ground
Milford, Mi. 48042

Edmond J. Ray
Trans. Research Center of Ohio
E. Liberty, Oh. 43319

P.L. Read
Cranfield Inst. of Tech.
School of Auto. Studies
Cranfield, Bedford, England

Kenneth A. Reid
Uniroyal
6600 E. Jefferson
Detroit, Mi. 48232

Brian S. Repa
GM Res. Labs
12 Mile and Mound Roads
Warren, Mi. 48090

S.H. Reynolds
3919 Arroyo Dr. S.W.
Seattle, Wa. 98146

James Rickert
Chrysler Corp.
6565 East Eight Mile Road
Warren, Mi. 48090

J. Vernon Roberts
DOT, National Highway Traffic
Safety Administration
2130 Maleady Drive
Herndon, Va. 22070

Dove Rohrer
Eaton Research
26201 Northwestern
Southfield, Mi. 48024

David R. Samelak
Ford Motor Co.
20442 Charest
Detroit, Mi. 48234

O.R. Saunders
Uniroyal, Inc.
6600 E. Jefferson
Detroit, Mi. 48232

Paul Schenck
Trailer/Body Bldrs. Magazine
1602 Harold Street
Houston, Tx. 77006

Dieter Schuring
Calspan Corp.
P.O. Box 235
Buffalo, N.Y. 14221

T.V. Seshadri
Freuhauf Corp.
6500 French Road
Detroit, Mi. 48232

C.G. Shapley
Firestone Tire & Rubber
1200 Firestone Pkwy.
Akron, Oh. 44317

Thurman D. Sherard
Western Hwy. Inst.
333 Pine Street
San Francisco, Ca. 94104

William Sherman
Motor Vehicle Manufacture Assn.
320 New Center Building
Detroit, Mi. 48202

Sharad Sheth
Fruehauf Corp.
10900 Harper Avenue
Detroit, Mi. 48232

R. Sitler
Rockwell International
1000 W. Maple Road
Troy, Mi. 48084

Carl F. Smajd
Uniroyal Inc.
6600 E. Jefferson
Detroit, Mi. 48232

Joseph P. Smith
Motor Vehicle Manufacturers Assn.
1909 K Street, N.W., Suite 300
Washington, D.C. 20006

Russell A. Smith
Catholic Univ. of America
Washington, D.C. 20017

Franklin Snelgrove
Ministry of Transportation
1201 Wilson Avenue
Downsview, Ontario, Canada
M3M 1J8

John J. Stansbrey
White Motor Corp.
35129 Curtis Blvd.
Eastlake, Oh. 44094

John Storz
Great Dane Trailers, Inc.
P.O. Box 67
Savannah, Ga. 31402

Don S. Strader
Neway Division, L.S.I.
P.O. Box 425
Muskegon, Mi. 49443

Lennart Strandberg
National Swedish Road &
Traffic Research Institute
Drottning Kirstinas vag 25
11428 Stockholm, Sweden

W.B. Straub
Firestone Tire and Rubber Co.
1200 Firestone Parkway
Akron, Oh. 44301

George B. Stroh
Eaton Corp.
26201 Northwestern Highway
Southfield, Mi. 48076

Glenn W. Tannahill
Chrysler Corp.
P.O. Box 1283 (CIMS 425-11-08)
Detroit, Mi. 48231

G.L. Teper
Systems Tech., Inc.
13766 S. Hawthorne Blvd.
Hawthorne, Ca. 90250

Paul Terrano
White Truck Division
842 East 79th Street
Cleveland, Ohio 44101

C. Thomas Terry
General Motors Tech. Center
Auto Safety Engineering
Warren, Mi. 48090

Ken Thorp
Detroit Automotive
11445 Stephens Drive
Warren, Mi. 48090

A.J. Thrower
P.O. Box 340
Troy, Oh. 45373

John Tielking
University of Michigan
Highway Safety Research Inst.
Room 210
Ann Arbor, Mi. 48104

W.E. Tobler
Sibley School of Mech. &
Aerospace Engineering
Cornell University
Ithaca, N.Y. 14850

John Urban
Eaton Corp. - Brake Division
21220 West Eight Mile
Southfield, Mi. 48075

Dusan Vacval
International Harvester Co.
1810 S. 59th Avenue
Cicero, Il. 60650

Gary VanOverschelde
Kelsey-Hayes
2500 Green Road
Ann Arbor, Mi. 48105

Edward L. Volker
Ford Motor Co.
2089 Traneck Circle
Wixom, Mi. 48096

Richard L. VonLehman
Rockwell International
1000 W. Maple Road
Troy, Mi. 48084

Donald A. Vorwerk
Eaton Corp. - Brake Div.
21220 West Eight Mile
Southfield, Mi. 48075

James D. Walden
GMC Truck & Coach
660 S. Blvd. East
Pontiac, Michigan

Kathleen Weber
University of Michigan
Highway Safety Research Inst.
Room 137
Ann Arbor, Mi. 48104

C. Thornton
Rockwell International
1000 W. Maple Road
Troy, Mi. 48084

James White
Ministry of Transport
27th Floor
Transport Canada Bldg.
Ottawa, Ontario, Canada K1A ON5

Robert Wild
University of Michigan
Highway Safety Research Inst.
Room 209
Ann Arbor, Mi. 48104

James T. Wilson
University of Michigan
6117 IST
Ann Arbor, Mi. 48104

Lee Wilson
International Harvester
9741 St. Joe Road
Fort Wayne, Ind. 46815

Christopher Winkler
University of Michigan
Highway Safety Research Inst.
Room 207
Ann Arbor, Mi. 48104

Frederick J. Winsor
Chrysler Corp.
69 Winona Avenue
Highland Park, Mi. 48203

Ronald T. Wong
Ford Motor Co.
2173 Lakeview Dr.
Ypsilanti, Mi. 48197

Edward L.J. Young
Neway Div., L.S.I.
P.O. Box 425
Muskegon, Mi. 49443

SYMPOSIUM ON COMMERCIAL VEHICLE BRAKING AND HANDLING

MAY 5-7, 1975

PROGRAM

(All sessions will be held in the Auditorium of the Chrysler Center unless otherwise indicated.)

MONDAY, MAY 5

Morning

Display of Commercial Vehicle Test Equipment
Highway Safety Research Institute

Afternoon

12:30-3:30 **Symposium Registration**
Chrysler Center Lobby

2:00 **Welcoming Remarks**
Dr. Robert L. Hess, Director, Highway Safety Research Institute

2:30 **Technical Session: The Measurement of Commercial Vehicle Tire Properties**

Chairman: S. K. Clark, The University of Michigan

Truck Tire Testing at the TIRF Facility
King Bird and Dieter Schuring, Calspan Corporation

Mobile Measurements of Truck Tire Traction
Robert Ervin, Highway Safety Research Institute

Traction Characteristics of Truck Tires
W. B. Straub, Firestone Tire and Rubber Company

TUESDAY, MAY 6

8:15 a.m.-3:30 p.m. **Registration and Coffee** (Chrysler Center Lobby)

Morning

9:00 **Technical Session: Brake and Antilock System Performance**

Chairman: V. Marples, Carleton University

Torque Characteristics of Commercial Vehicle Brakes
Thomas Post, Highway Safety Research Institute

Simulation in Antilock System Development
G. A. Cornell and B. E. Latvala, Bendix Corporation

A General Purpose Simulation for Antiskid Braking Systems
Charles MacAdam, Highway Safety Research Institute

Testing for FMVSS 121—A Discussion of Results
William Booth, PACCAR, Inc.

Evaluation of Antilock System Performance on an Air-Braked Commercial Vehicle
James Ehlbeck, Freightliner Corporation

Afternoon

2:00 **Technical Session: Topics in Computer Simulation**

Chairman: Dan Klein, General Motors Truck and Coach

NHTSA/APL Hybrid Vehicle Simulation
P. Bohn, Johns Hopkins University Applied Physics Laboratory

Tire Friction Models and Their Effect on Vehicle Dynamics Simulation Accuracy
P. K. Nguyen and E. R. Case, Ontario Ministry of Transportation and Communications

Application of General Rigid Body Dynamics to Vehicle Behavior
A. I. Krauter, Shaker Research Corporation and W. E. Tobler, Cornell University

The Rolling Motions of Road Vehicles
C. G. Shapley, Firestone Tire and Rubber Company

Handling Dynamics of an Intercity Bus
G. L. Teper and D. H. Weir, Systems Technology, Inc.

WEDNESDAY, MAY 7

Morning

8:15-11:30 **Registration and Coffee**
Chrysler Center Lobby

9:00 **Technical Session: An Overview of Simulation and Testing**

Chairman: John W. Gurney, Ford Truck and Recreation Products Operations

The Modeling and Testing of Commercial Vehicles at the School of Automotive Studies, Cranfield
J. R. Ellis and P. L. Read, School of Automotive Studies

The Role of Analytical Techniques in the Formulation of Vehicle Safety Standards
R. L. Eshleman, Illinois Institute of Technology Research Institute

Prediction of Braking and Directional Response of Commercial Vehicles
P. S. Fancher, Highway Safety Research Institute

Stability and Handling of Commercial Vehicles (Overview of Research Work at the National Swedish Road and Traffic Research Institute)
Olle Nordstrom and Lennart Strandberg, National Swedish Road and Traffic Research Institute

Commercial Vehicle Braking and Handling Research in Ontario
F. B. Snelgrove, Ontario Ministry of Transportation and Communications

12:00 **Luncheon**
North Campus Commons

Federal Folly—Public Policy without Research
W. D. Eberle, President and Chief Executive Officer, Motor Vehicle Manufacturers Association

Afternoon

2:00 **Panel Discussion: The Effects of Government Standards on Commercial Vehicle Braking and Handling**

Moderator: Paul Fancher, Research Scientist, Highway Safety Research Institute

Panelists:

Al Beier, Chief Engineer, Brake Group, Truck Division Engineering, International Harvester

Gene Chosy, Director, Reliability and Quality Assurance, Fruehauff Corporation

Howard Dugoff, Chief, Handling and Stability Division, National Highway Traffic Safety Administration

John Kourik, Chief Engineer, Automotive Products, Wagner Electric Corporation

Ray Murphy, Director, Research and Development, Freightliner Corporation

Paul Terrano, Chief Engineer, Engineering Services, Truck Group, White Motor Corporation

GENERAL INFORMATION

LOCATION—All sessions will be held at the Chrysler Center for Continuing Engineering Education, Bonisteel Boulevard near Murfin, on the North Campus of The University of Michigan, Ann Arbor, Michigan.

REGISTRATION—To ensure enrollment, your registration card should be received **no later than Monday, April 28, 1975.** Please complete and mail the enclosed card, accompanied by payment, to the U-M Extension Service, Conferences & Institutes, 412 Maynard St., Ann Arbor, MI 48104. Name badges and meal tickets should be called for on arrival at the Symposium registration desk, which will be located in the Lobby of the Chrysler Center. Hours: May 5—12:30-3:30 p.m.; May 6—8:15 a.m.-3:30 p.m.; and May 7—8:15-11:30 a.m. **Only one person may register per card; duplicate if necessary or request additional cards.**

FEE—The registration fee for the entire Symposium or any part of it is $5.00 per person and includes the cost of a parking permit for North Campus University Staff parking lots. The fee, payable in advance, should be mailed with the enclosed registration card. Please indicate on the registration card if you desire a parking permit.

MEALS—A luncheon is planned for 12:00 noon May 7 at the North Campus Commons at a cost of $5.00 per person. Meal tickets should be ordered in advance on the enclosed registration card. Other meals are on your own at area restaurants.

HOUSING—To arrange for your housing requirements, please complete and mail the enclosed Housing Request Form to the Conference Housing Information Office, 350 South Thayer, Ann Arbor, Michigan 48104; Telephone (313) 764-2584 no later than Monday, April 21, 1975. Please indicate your preference from the following facilities:

Ann Arbor Inn, corner S. Fourth Ave. and Huron in downtown Ann Arbor and about a 10-minute drive to North Campus. Rates: Single $18-22, Double and Twin $24-29.

Campus Inn, near the corner of State St. and Huron in downtown Ann Arbor and about a 10-minute drive to North Campus. Rates: Single $19-22, Double and Twin $25-28.

Marriott Inn, located near the intersection of US-23 and Plymouth Road, about a 5-minute drive to North Campus. Rates: Single $22, Double and Twin $27.

Michigan Union, located on the U-M central campus on State St. and about a 10-minute drive to North Campus. Rates: Single $13.50-15, Double $18, Twin $20.50-27.50.

PARKING—Limited public parking and University Staff parking are available in a lot north of the North Campus Commons at the corner of Herbert and Murfin. University Staff parking is also available in a lot east of the Chrysler Center. Guest permits for University Staff parking should be ordered in advance on the enclosed registration card and will be mailed with acknowledgement of registration.

TRANSPORTATION—Ann Arbor may be reached by auto via US-23 from the north and south and via I-94 from the east and west. Air transportation is available at Detroit Metropolitan Airport, about a 30-minute drive east of Ann Arbor on I-94. Limousine service at $5.50 per person, one way and bus transportation at $2.50 per person, one way are available to and from the airport at regularly scheduled intervals. The limousine makes stops in major area hotels and motels and the bus stops at the downtown depot and the Michigan Union. Ann Arbor is also served by Greyhound Bus Lines and Amtrak train service. Please check with local offices for current bus and train schedules.

FOR FURTHER INFORMATION—The University of Michigan Extension Service, Department of Conferences and Institutes, 412 Maynard Street, Ann Arbor, Michigan 48104; Telephone (313) 764-5304.

NORTH CAMPUS AREA

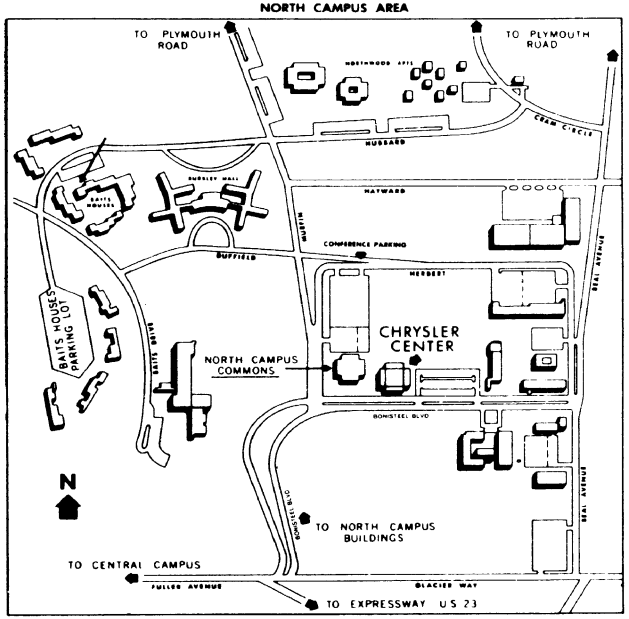

COVER PHOTOGRAPH—The H.S.R.I. Mobile Dynamometer outfitted for measuring the longitudinal traction properties of a truck tire. The Dynamometer incorporates a strain gaged transducer for measuring the traction performance of heavy truck tires on actual test pavements at speeds up to 70 mph.

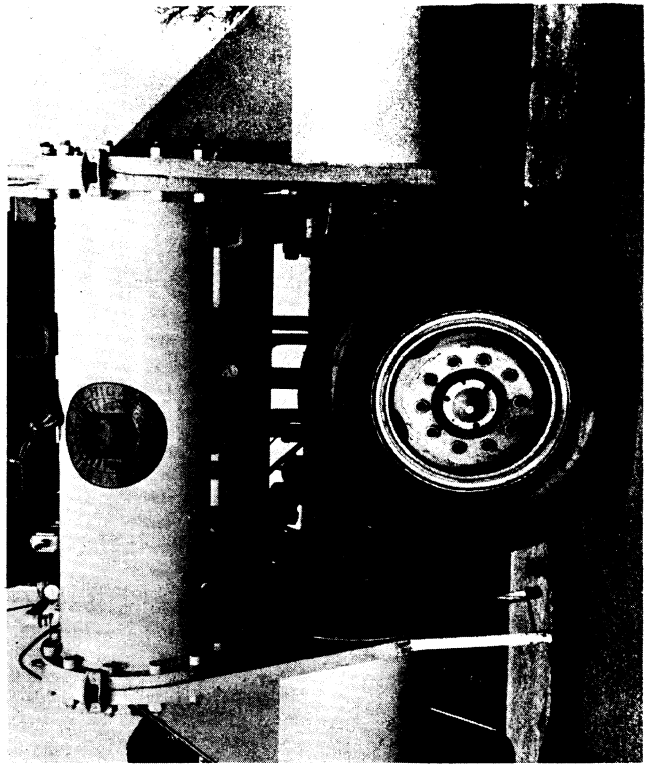

SYMPOSIUM ON COMMERCIAL VEHICLE BRAKING AND HANDLING

MAY 5-7, 1975

CHRYSLER CENTER FOR CONTINUING ENGINEERING EDUCATION

NORTH CAMPUS, THE UNIVERSITY OF MICHIGAN, ANN ARBOR, MICHIGAN

Sponsored by The University of Michigan Highway Safety Research Institute In cooperation with The University of Michigan Extension Service